EARTHQUAKE ENGINEERING RESEARCH CENTER
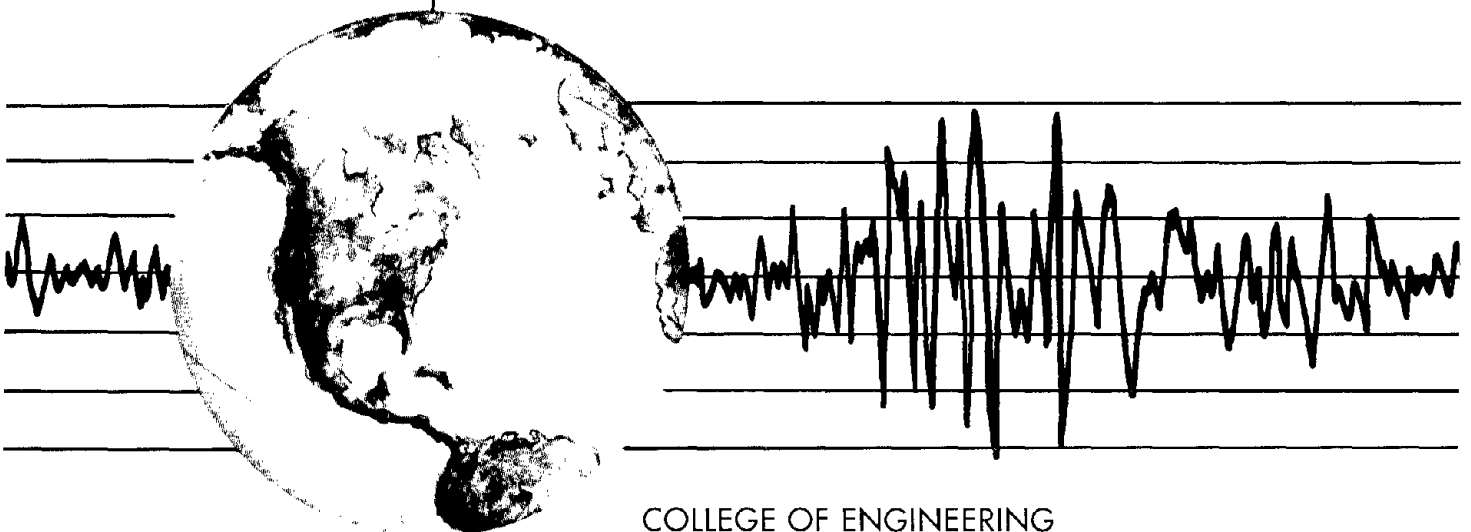
SECOND U.S.-JAPAN WORKSHOP ON SEISMIC RETROFIT OF BRIDGES

edited by

KAZUHIKO KAWASHIMA
STEPHEN A. MAHIN

COLLEGE OF ENGINEERING

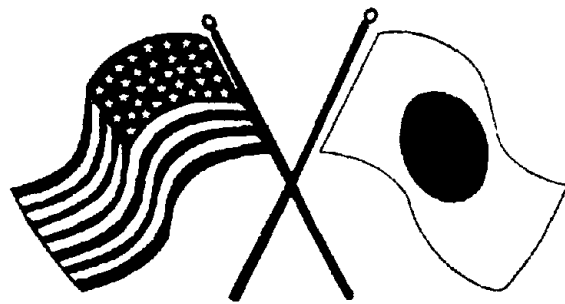UNIVERSITY OF CALIFORNIA AT BERKELEY

SECOND U.S.-JAPAN WORKSHOP ON SEISMIC RETROFIT OF BRIDGES

January 20 and 21, 1994
Berkeley Marina Marriott Hotel
Berkeley, California

ORGANIZERS

Kazuhiko Kawashima
Public Works Research Institute
Japan Ministry of Construction

Stephen Mahin
Earthquake Engineering Research Center
University of California at Berkeley

SPONSORS

Public Works Research Institute

Japan Ministry of Construction

U.S. National Institute of Standards
and Technology

Federal Highway Administration

National Science Foundation

Waterways Experimental Station

Preface

THE SECOND U.S.-JAPAN WORKSHOP ON SEISMIC RETROFIT OF BRIDGES

BACKGROUND

Considerable research is underway throughout the world to identify effective, practical and reliable methods for evaluating the seismic safety of existing bridges and for reducing their vulnerability through retrofit. The U.S. and Japan are at the forefront of these activities, as well as of their practical implementation. Because of the importance of this issue, it is especially desirable for researchers and practitioners from the U.S. and Japan to meet to exchange technical data as well as to identify issues of mutual concern and opportunities for cooperative study.

The first cooperative U.S.-Japan Workshop on Seismic Retrofit of Bridges was held in Tsukuba Science City, Japan, on December 17 and 18, 1990. The meeting was attended by 40 Japanese and six U.S. participants. The workshop provided a forum for discussions and technology-sharing on a wide range of topics, including: the history of seismic damage in both countries and the development of seismic design codes, damage to San Francisco area bridges during the Loma Prieta earthquake, assessment and prioritization of techniques for seismically vulnerable bridges, application of inspection and strengthening methods to mitigate hazards in reinforced concrete bridges, and research on seismic retrofitting and strengthening of reinforced concrete and steel bridges. In conjunction with the workshop, a study tour of bridge retrofit projects in Japan was undertaken by the U.S. participants.

The first seismic retrofit workshop was held under the auspices of Task Committee J, "Wind and Earthquake Engineering for Transportation Systems," of the UJNR Panel on Wind and Seismic Effects. Funding for the U.S. participants was provided by the National Institute for Standards and Technology.

At the conclusion of the workshop, the participants unanimously resolved that a similar workshop should be held after a one or two year period in order to share new research data as well as experiences with field retrofits.

The second U.S.-Japan Workshop on Seismic Retrofit of Bridges was held on January 20 and 21, 1994, at the Berkeley Marina Marriott Hotel. It focussed on recent research and application of retrofit technology, rather than state-of-the-art reviews, in response to the rapid development of technology and the tremendous amount of research underway in both countries. Topics covered during the workshop include: (1) assessment and prioritization techniques, (2) design methods for seismic retrofit of bridges, (3) issues related to foundation evaluation and retrofit, (4) case studies of bridge assessment and retrofit, and (5) recent research. Both steel and reinforced concrete bridges were covered, and issues related to the broad spectrum of bridges found throughout the U.S. and Japan were addressed.

The second U.S.-Japan Workshop on Seismic Retrofit of Bridges was attended by 19 Japanese and 55 U.S. participants. Several observers from the U.S. and other countries also participated.

HOST ORGANIZATIONS AND SPONSORS

The workshop was again held under the auspices of Task Committee J of the UJNR panel on Wind and Seismic Effects. The host institutions for the workshop on this panel were the Public Works Research Institute (PWRI) in Japan and the National Institute of Science and Technology in the U.S. The Workshop was organized by the Public Works Research Institute and the Earthquake Engineering Research Center (EERC) of the University of California at Berkeley.

The Program Coordinators for the Workshop were Dr. Kazuhiko Kawashima, Head of the Earthquake Engineering Division at the PWRI and Dr. Stephen A. Mahin, Nishkian Professor of Structural Engineering at the University of California at Berkeley. A Steering Committee consisting of Dr. Ian Buckle, Mr. Ian Friedland, Dr. Stephen Mahin and Dr. Nigel Priestley developed the program on the U.S. side.

Financial support was provided on the Japanese side by the PWRI of the Ministry of Construction. On the U.S. side, funding was provided by the National Institute of Standards and Technology, the Federal Highway Administration (through the research program at the National Center for Earthquake Engineering Research, State University of New York at Buffalo), the National Science Foundation, and the Waterways Experimental Stations the U.S. Army Corps of Engineers. Special thanks is owed to H. S. Lew, James Cooper, S. C. Liu and James Ray of these organizations for their encouragement and support.

The efforts of Parshaw Vaziri of the Earthquake Engineering Research Center in making local arrangements and contacting U.S. participants are especially appreciated. Ian Friedland and Debbie O'Rourke of the National Center for Earthquake Engineering Research were especially helpful in coordinating the activities of the U.S.-Japan workshops of seismic retrofit and protective systems. The effort of the staff of the Public Works Research Institute in facilitating the efforts of the Japan side is similarly appreciated.

TECHNICAL STUDY TOUR

A two day technical tour followed the workshop (Saturday and Sunday, January 22 and 23, 1994). The tour included several major retrofit sites in the San Francisco-Oakland area as well as a new seismically isolated bridge under construction in Walnut Creek, CA. Both U.S. and Japanese participants participated in the study tour.

Because the Workshop immediately followed the January 17, 1994, Northridge earthquake, several Japanese and U.S. participants visited the Los Angeles area to inspect bridge performance immediately before or after the Workshop. A special presentation on bridge damage was made by Prof. Gregory Fenves of the University of California at Berkeley.

U.S.-JAPAN WORKSHOP ON EARTHQUAKE PROTECTIVE SYSTEMS FOR BRIDGES

The U.S.-Japan Workshop on Seismic Retrofit was coordinated and held in conjunction with the U.S.-Japan Workshop on Earthquake Protective Systems for Bridges. This Workshop was organized by Dr. K. Kawashima of the Public Works Research Institute and Dr. Ian Buckle of the State University of New York at Buffalo.

RESOLUTIONS

Recent earthquakes have caused significant damages to bridges in both Japan and the U.S. This was evidenced in the U.S. during the 1989 Loma Prieta and 1994 Northridge earthquakes. In Japan, bridge distress was observed during the Kushiro-oki and Hokkaido Nansei-oki earthquakes of 1993. These and other earthquakes point out the need for reliable methods for evaluating the earthquake vulnerability of bridges and for effective and practical methods for seismic retrofit.

Papers presented at the Workshop indicate that there is considerable activity in the U.S. and Japan directed at developing assessment and prioritization procedures and seismic retrofit technologies. In addition, presentations at the workshop illustrated many interesting cases of applications of these procedures to actual bridges. These case studies provided important insight into many practical problems in seismic evaluation and retrofit. Discussion by participants at the Workshop indicated that there are many problems in the U.S. and Japan of mutual interest and concern.

The participants agree that the workshop was successful and led to greater understanding to the issues related to seismic hazard mitigation for existing bridges. While much information has been developed on these important issues, the participants agree that many problems remain unresolved and that additional studies and research are needed.

The participants expressed interest in technology and applications related to new materials, new construction procedures, verification tests in the field and laboratory, and development of reliable and efficient analysis tools. Previous activities tended to focus on the behavior of materials and components. It was recommended that increasing attention be placed on seismic response of bridge systems.

The participants suggest that increased cooperation between the U.S. and Japan would be beneficial to improve seismic evaluation and retrofit technologies. As a first stage, the following recommendations are offered:

1. Because of the rapid rate at which new information and applications are being achieved, and the importance of these problems to Japan and the U.S., the participants recommend that a third U.S.-Japan workshop on seismic retrofit of bridges be held in Japan in about two years time.

2. One or more example bridge structures be identified. These structures can provide a basis for comparing the analysis and retrofit procedures, standards and guidelines used by investigators and practitioners in both countries. Systematic studies of these example structures by researchers, practitioners and consultants in both countries are recommended.

3. Cooperative activities between the U.S. and Japan should be encouraged to address problems of mutual concern. Participants recommend that as a start efforts be undertaken to facilitate exchange of personnel as well as of information on technical issues and applications. Opportunities to share unique laboratory and other facilities available in each country should be explored.

4. Specific areas for cooperative research between the U.S. and Japan should be identified, and initiated, as appropriate.

TABLE OF CONTENTS

SECOND U.S.-JAPAN WORKSHOP ON SEISMIC RETROFIT OF BRIDGES

Papers

January 20 and 21, 1994
Berkeley Marina Marriott Hotel
Berkeley, California

Seismic Strengthening of Highway Bridges

K. Kawashima, S. Unjoh and H. Mukai

SEISMIC STRENGTHENING OF HIGHWAY BRIDGES

Kazuhiko KAWASHIMA[1], Shigeki UNJOH[2] and Hidetoshi MUKAI[3]

1) Head, Earthquake Engineering Division, Public Works Research Institute, Ministry of Construction, Tsukuba Science City, Japan
2) Senior Research Engineer, ditto
3) Assistant Research Engineer, ditto

ABSTRACT

This paper presents current technical developments for seismic strengthening of existing highway bridges in Japan. Seismic strengthening for substructures is described based on the past practice. Emphasis is placed on the example of implementation.

INTRODUCTION

Japan is one of the most seismically disastrous countries in the world and has often suffered significant damage from large earthquakes. More than 3,000 highway bridges suffered damage in the past earthquakes since the Kanto Earthquake in 1923. The damage to highway bridges caused serious loss of function of road as an emergency evacuation route and a transportation route for emergency relief goods. Since repair of bridges damaged by an earthquake takes a long time, it significantly affects social and economical activities in the area. Therefore, it is important to provide appropriate seismic resistance for existing highway bridges.

This paper presents the seismic strengthening methods for substructures based on the case study of 121 examples of seismic strengthening.

HISTORY OF PROVISIONS OF SEISMIC DESIGN CODES
FOR HIGHWAY BRIDGES

One year after the 1923 Kanto Earthquake, it was initiated to consider the seismic effect in design of highway bridges. The Civil Engineering Bureau of the Ministry of Interior notified "the method of seismic design of abutments and piers" in 1924. The seismic design method has been developed and improved through bitter experience in the number of past earthquakes and with progress of technical development in earthquake engineering. Table 1 shows the history of provisions in seismic design for highway bridges.

1

In particular, the seismic design method was integrated and upgraded by compiling the "Specifications for Seismic Design of Highway Bridges" in 1971, which exclusively provided issues related to seismic design. It was revised in 1980 and integrated as "Part V : Seismic Design" in "Design Specifications of Highway Bridges". It was further revised in 1990 and has been in practice for all highway bridges with span length shorter than 200m. In the latest Specifications, design seismic force, bearing capacity of reinforced concrete piers for lateral force, soil liquefaction, dynamic response analysis, and design detailings are prescribed.

HISTORY OF SEISMIC EVALUATION AND SEISMIC STRENGTHENING OF HIGHWAY BRIDGES

The Ministry of Construction made seismic evaluation of highway bridges 5 times throughout the country since 1971 as a part of the comprehensive earthquake disaster prevention measures for highway facilities. Seismic strengthening for vulnerable highway bridges has been successively made based on the seismic evaluations. **Table 2** shows the history of past seismic evaluations[1]−[8].

The first seismic evaluation was made in 1971 to promote earthquake disaster prevention measures for highway facilities. The significant damage of highway bridges caused by the San Fernando Earthquake, U.S.A. in February 1971 triggered the seismic evaluation. Highway bridges with span length longer than or equal to 5m on all sections of national expressways and national highways, and sections of the others were evaluated. Attention was paid to detect deterioration such as cracks of reinforced concrete structures, tilting, sliding, settlement and scouring of foundations. Approximately 18,000 highway bridges in total were evaluated and approximately 3,200 bridges were found to require strengthening.

Following the first seismic evaluation, it has been subsequently made in 1976, 1979, 1986 and 1991 with gradually expanding highways and evaluation items. The seismic evaluation in 1986 was made with the increase of social needs to insure seismic safety of highway traffic after the damage caused by the Urakawa−oki Earthquake in 1982 and the Nihon−kai−chubu Earthquake in 1983. The highway bridges with span length longer than or equal to 15m on all sections of national expressways, national highways and principal local highways, and sections of the others, and overpasses were evaluated. The evaluation items included deterioration, devices for preventing falling−off of superstructure, strength of substructures and stability of foundations. Approximately 40,000 bridges in total were evaluated and approximately 11,800 bridges were found to require strengthening. Through a series of seismic strengthening works, approximately 25,000 bridges were strengthened by the end of 1991 fiscal year. Latest seismic evaluation was made in 1991. The results are being compiled.

In the seismic evaluation in 1986 and 1991, the evaluation was made based on a statistical

analysis of bridges damaged and undamaged in the past earthquakes[9]. Factors which affect seismic vulnerablity were detected as shown in **Table 3**. **Table 4** shows the inspection sheet proposed to evaluate the seismic vulnerability. Because collapse of bridges tends to be developed due to the excessive relative movement between the superstructure and the substructures, and failure of substructures associated with inadequate strength, the evaluation is made in **Table 4** based on both the relative movement and the strength of substructure.

Table 5 shows the feasibility of seismic strengthening against the 16 factors which would affect the seismic vulnerability of highway bridges as shown in **Table 3**. Among the 16 factors, ⑥ devices for preventing falling−off of superstructure, ⑦ type of substructures, ⑩ effect of soil liquefaction, ⑫ effect of scouring, ⑬ materials of substructures, ⑭ type of foundation, and ⑯ termination of main reinforcement at mid−height with inadequate anchoring length are the factors for which countermeasures are feasible. Countermeasures for other factors may not be feasible unless the whole bridge be replaced.

Fig. 1 shows how the countermeasures can be made for the above 7 factors. Installation of the devices for preventing falling−off of superstructure, strengthening of foundations, and strengthening of piers and abutments are the measures which are most often adopted for seismic strengthening.

Emphasis has been placed to install the falling−off prevention devices in the past seismic strengthening. Because the installation of the falling−off prevention devices is being completed, it now becomes important to promote the strengthening of substructures with inadequate strength and lateral stiffness.

SEISMIC STRENGTHENING FOR SUBSTRUCTURES

Practices of Strengthening

The Public Works Research Institute collected the data on the highway bridges in which substructures were strengthened based on the seismic evaluation in 1979 and 1986.[10]−[12] The first survey was made in 1987 to collect the data of seismic strengthening due to the seismic evaluation in 1979 and the second survey was made in 1991 to collect the data of seismic strengthening due to the seismic evaluation in 1986. Although the data base covers only a few bridges, it provides the most reliable information for seismic evaluation and strengthening.

The data base includes the year of construction, design specifications referred to, type of structures, results of the seismic evaluation, selection and comparison of seismic strengthening methods, design of strengthening, and construction method. In total the data for 121 bridges were collected.

3

Fig. 2(a) shows the year of construction of the bridges surveyed. About 70% of the strengthened bridges were constructed from 1950s to 1960s. The rate of bridges constructed before 1950 is only 22%. For such old bridges, replacement rather than the seismic strengthening has been made. Fig. 1(b) shows the design specifications referred to for the bridges surveyed. About 93% of the bridges strengthened were designed according to the pre−1971 specifications.

Reasons to Require Strengthening

Fig. 3 shows the number of bridges strengthened classified in terms of requirements for seismic strengthening. The requirements for strengthening, i.e., the reason for requiring the seismic strengthening, were classified from **Table 3** into 10 as
·scouring around foundation
·abnormal displacement of foundation
·apparent deterioration of reinforced concrete structure
·weak reinforced concrete frame
·substructure placed on two independent caisson foundations
·bent piles with inadequate strength and lateral stiffness
·pier with inadequate strength
·soil liquefaction
·inadequate bearing capacity of piles
·inadequate bearing capacity of soil/foundation

The seismic strengthening was required mostly because of the inadequate bearing capacity of foundations associated with scouring, inadequate strength of reinforced concrete frame structure, and inadequate bearing capacity of piles. Forty bridges were strengthened because problem arose due to the scouring. Because the vulnerability of foundations due to scouring can be reliably evaluated, the strengthening has been made successively. Sixteen bridges were strengthened due to the weakness of reinforced concrete frame structure and inadequate bearing capacity of piles, respectively.

Strengthening Methods

Fig. 4 shows the methods adopted for seismic strengthening. They are presented for the 10 requirements presented above. Various methods were adopted depending on site conditions and other restrictions and requirements. Increase of number of piles, enlargement of footing, placing of new reinforced concrete section surrounding the existing structure, and construction of new lateral beams for increasing strength and lateral stiffness are the major methods.

IMPLEMENTATION OF SEISMIC STRENGTHENING

Seismic Strengthening of Weak Reinforced Concrete Frame Structures

Fig. 5 shows an implementation of seismic strengthening of a reinforced concrete frame. This bridge was constructed in 1959 and has a 5—span simply—supported steel plate girder with length of 176m. The substructures were of reinforced concrete frame structures with reinforced concrete piles.

Based on the 1979 seismic evaluation, an increase of the lateral strength of substructures in transverse direction was detected to be required. It was decided to place a new reinforced concrete wall to strengthen the substructures. Thickness of the wall was designed as 40cm, and it was assumed that the seismic lateral force is supported by the integrated structure consisting of the new and the existing reinforce concrete members. Therefore, the most crucial point of the design and construction was how reliably the integration between the new and the existing structures be made. To assure the reliable integration, the cover concrete of exciting substructures was chipped—out by about 1cm and anchor bars were installed with 30cm pitch at the columns. The anchor bars with diameter of 16mm (D16) were inserted in the drilled holes with diameter of 26mm and depth of 24cm. The spaces between the holes the and the anchor bars were filled with epoxy resin.

Seismic Strengthening of Bent Piles with Inadequate Lateral Stiffness

Fig. 6 and Photo 1 show a seismic strengthening for bent piles with inadequate lateral stiffness. This bridge was constructed in 1960 and has a 9—span simply—supported prestressed concrete slab with length of 54m. The substructures were of bent piles with 7 reinforced concrete piles with length of 12m and diameter of either 30cm or 50cm.

Based on the 1979 seismic evaluation, an increase of the lateral strength of the bent piles in longitudinal direction was detected to be required. It was decided to place a new reinforced concrete surrounding the piles at the river bottom level and to connect each bent pile by reinforced concrete slabs. The reinforced concrete slabs were placed to decrease the lateral displacement of bent piles at the river bottom level. This method was selected because the span length was short and the effectiveness of strengthening was apparent. Design was made assuming that the lateral force is supported by a new integrated structure.

Seismic Strengthening of Bent Piles in Liquefaiable Sandy Soils

Fig. 7, Photos 2 and 3 show a seismic strengthening of 11—span simply—supported pre—tensioned concrete slab bridge. It was constructed in 1959. Reinforced concrete bent plies were used for piers and abutments. The diameter and length of reinforced concrete piles were 60cm and 12m for piers and 50cm and 8m for abutments, respectively.

5

Based on the 1986 seismic evaluation, it was found that the bent piles were vulnerable to soil liquefaction. The Liquefaction Resistance Factor F_L at the sandy layer with thickness of 3.2m below the river bed was less than 1.0. The length of the part of piles which were supported by stable soil was only 1/3 of the total pile length of 12m. Based on the stability analysis of piles, the stress induced in concrete and reinforcing bars of piles significantly exceeded the allowable stresses. The displacement predicted at piles was 4.6cm at the design ground level and 12.8cm at the crest. Those were much larger than the allowable displacement.

Five strengthening measures were proposed. Those were ① to strengthen all 12 substructures, ② to strengthen one substructure per two spans, ③ to strengthen both abutments and connect all pier crests by continuous beams, ④ to replace liquefiable soil layer by stable soils, and ⑤ to increase soil strength by chemical grouting. Because the methods ④ and ⑤ were expensive in spite of unreliable effectiveness, they were decided to be not appropriate at this site. Among the three strengthening methods, ③ was adopted because cost performance was the most superior. Because strengthening of the substructures was required at only two end abutments, it was less expensive. It was decided that the seismic safety can be increased to the level required if the lateral displacement induced at pier crest was controlled by the continuous beams.

In the design, it was assumed that the lateral force in longitudinal direction is supported by both the new piles and the existing piles. Since the pier crests of bent piles are strengthened by the connecting beams, it was required to insure enough strength for the connecting beams and fix bearing set between the pier crests and the connecting beams. Therefore, they were designed adopting two times larger design lateral force. It should be noted that the connecting beams were also used as the girders for supporting a pedestrian deck installed to the bridge.

Seismic Strengthening of Weak Bent Piles

Fig. 8 and **Photo 4** show strengthening of 3−span continuous steel plate girder bridge with deck length of 75m. Steel pipe bent plies were used for piers. The diameters and length of the piles were 1m and 45.2m, respectively. The bridge was constructed in 1969.

Based on the 1986 seismic evaluation, it was found that the stress induced in the reinforced concrete lateral beam significantly exceeded the allowable stress when the seismic lateral force was applied in transverse direction. The stress induced in the steel−pipe piles is smaller than the allowable stress. Because it was not easy to strengthen the lateral beam, it was decided to place a new reinforced concrete wall surrounding the existing bent piles. Hollow section was adopted to mitigate the increase of the weight. The construction was made by drying−up the water using the steel sheet piles.

Seismic Strengthening of Foundations with Inadequate Soil Bearing Capacity

Fig. 9 shows seismic strengthening of foundations by increasing number of piles and enlarging footing. The bridge was constructed in 1960 and consisted of 14−span simply−supported prestressed concrete girder with length of 238m. The abutments were of a gravity type with wooden piles. Piers were of reinforced concrete frames with wooden piles.

Based on the 1979 seismic evaluation, the bearing capacity of soils around foundations was found to be insufficient. Two strengthening methods were proposed. The first was to increase number of piles and the second was to improve soils. Since it is reliable and the construction cost was cheaper in the first method, it was adopted as a principal countermeasure. However, since the construction space was very limited to place the new piles, the soil improvement as well as enlargement of the existing footing was adopted for some foundations.

In increasing number of new piles, the existing wooden piles were neglected and it was assumed that the lateral force is supported by only new piles. On the other hand, in the design of soil improvement and enlargement of footings, it was assumed that the lateral force is supported by shear force at the bottom of the new and the existing footings. Because the soil was improved so as to increase the N−value to 30, the bearing capacity of the soil could be increased. When the new footing was placed on the existing footing, the surface of existing footing was chipped−out by 2cm, and anchor bars with diameter of 22mm (D22) were installed with epoxy resin injection. The cement milk was injected to improve soil up to 3m deep below the bottom of the footing.

Seismic Strengthening of a Pile Foundation Vulnerable to Liquefaction

Fig. 10 shows seismic strengthening of pile foundations in liquefiable soil layers. This bridge was constructed in 1952 and consisted of a Langer girder and 15−span simply−supported plate girder with length of 575m. Abutments were of gravity type foundations and piers were of reinforced concrete walls. Foundations were of open caisson for the Langer girder and pile foundations for the others.

Based on the 1979 seismic evaluation, it was detected that the bearing capacity of soils at the pier foundations was inadequate, because the soil was vulnerable to liquefaction.

Three strengthening methods were proposed. They were ① to improve the ground by soil cement, ② to increase number of piles, and ③ to surround the existing foundations by steel sheet piles. Since ① was expensive, ② and ③ were investigated precisely, and ② was finally adopted. Effectiveness of strengthening was reliable and cost performance was

7

superior.

In the design, it was assumed that the existing piles would resist to the lateral seismic force up to the design level and that the lateral force beyond the design level be supported by the new piles. Since the piers were in the high water channel, a temporary road was constructed to the piers during the construction. The steel—pipe piles were placed using a vibro hammer. The new footing was constructed by drying—up water by steel sheet piles. Integration between the new and the existing footings was made by anchor bars with injection of resin mortar. **Photo 5** shows the construction of new piles. **Photos 6** and **7** show the connection of the new and the existing footings.

Seismic Strengthening of a Pile Foundation by Enlarging Footing and Increasing Number of Piles

Fig. 11 and **Photo 8** show Akisato Bridge on National Highway No.9 in Tottori City.[13] It was planned to be of two bridges in parallel with length of 264m. Because number of traffic was small at the construction stage, only one bridge was completed in 1975 with the substructures being completed so as to support the two bridges. Since number of traffic increased in recent years, it became required to construct one more bridge on the existing substructure. The existing bridge is of 7—span simply—supported steel plate girder and a simple prestressed concrete hollow slab. The substructures consist of reinforced concrete frame structures and wall type reinforced concrete piers. All substructures are supported by steel pipe piles with length of 40m. The ground is of very soft clay with thickness of about 30m.

Associate with the revision of the seismic map and the lateral force coefficient, it was required to increase the design lateral force coefficient from 0.2 to 0.3 to meet with the current design requirements. Some deterioration is also found at the substructures,

For the 50% increase of the lateral force, the superstructure was made continuous so as to distribute the lateral force to as many substructures as possible. The substructures required to increase number of piles, thickness and size of footing and strength of piers. Because the space on the footing was limited, the thickness of the footing was required to be increased not only on the footing but also at the bottom. An unique method with high fluid concrete was adopted.

Fig. 13 shows the construction procedure. After excavating the bottom of the existing footings, new piles were placed and the new footing was constructed. The high fluid concrete was placed from one side of the footing. It was placed from the other side. The new footing was completed by placing the concrete on the existing footing. It is very unique to place the new reinforced concrete under the existing footing and to adopt the high fluid concrete. The strengthening was completed in 1993. **Photo 9** shows the excavation at the

bottom of the existing footing. Although mini—back—hoes were used to excavate the soil under the footing, manpower was also required as shown in the **Photo 10**. **Photos 11** and **12** show the reinforcement at the top of new piles and the new footing. **Photo 13** shows the seismic strengthening of piers.

Fig. 14 shows the strengthening of the abutments. Instead of increasing the strength of the abutments, expanded polystyrene (EPS) was used behind the abutments to decrease the earth pressure on the abutments. Expanded polystyrene was placed with height of 1.75m and length of 13m.

CONCLUSIONS

This paper presented seismic strengthening of existing highway bridges with emphasis on case study of implementation. Emphasis has been placed by now to install the falling—off prevention devices. Because the installation of the falling—off prevention devices is being almost completed, it is now required to further promote the seismic strengthening of substructures. As described in this paper, the past strengthening of substructures has been made case by case basis.

Being different from the installation of the falling—off prevention devices, the seismic strengthening of substructures requires more cost. Because most of the substructures designed and constructed before 1971 do not meet with the current seismic requirements, it is urgently needed to study the level of seismic vulnerability requiring the strengthening. Upgrading of the reliability to predict the possible failure modes in the future earthquakes is also very important.

REFERENCES

1) Headquarters Office for Earthquake Disaster prevention Countermeasures, Ministry of Construction : Countermeasures against Large—scale Earthquakes, Monthly Journal of Construction, Vol.25, No.1, January, 1972 (in Japanese)
2) Fujii, T. : Road Disaster Prevention Measures, Journal of Road, September, 1978 (in Japanese)
3) Fujii, T. : Road Service and Road Disaster Prevention Measures, Journal of Road, June, 1980 (in Japanese)
4) Yamauchi, Y. : Present Status of Road Disaster Prevention Measures, Journal of Road, December, 1980 (in Japanese)
5) Yoshikoshi, H. : Present Status and Subjects of Road Disaster Prevention Measures, Journal of Road, September, 1982 (in Japanese)
6) Miyaji, A. : Road Disaster Prevention Measures, Journal of Road, September, 1990 (in Japanese)
7) Edited by Road Bureau, Ministry of Construction : Road Traffic and Economy Survey,

1992 Version, December, 1990 (in Japanese)

8) Kawashima, K. : Seismic Design and Earthquake Disaster Countermeasures for Highway Bridges, Journal of Road, September, 1990 (in Japanese)

9) Kawashima, K. and Unjoh, S. : An Inspection Method of Seismically Vulnerable Existing Highway Bridges, Structural Eng./Earthquake Eng., Vol.7, No.7, Proc. JSCE, April 1990

10) Kawashima, K., Unjoh, S. and Azuta, Y. : Case Survey of Seismic Strengthening Practices of Existing Highway Bridges Based on Seismic Inspection of 1979, Technical Memorandum of Public Works Research Institute, No.2674, October, 1989 (in Japanese)

11) Kawashima, K., Unjoh, S. and Iida, H. : Case Survey of Seismic Strengthening Practices of Existing Highway Bridges Based on Seismic Inspection of 1986, Technical Memorandum of PWRI, No. 69, 1990 (in Japanese)

12) Kawashima, K. and Unjoh, S. : Seismic Strengthening and Retrofitting of Highway Bridges in Japan, Proc. the 5th U.S.–Japan Workshop on Earthquake Disaster Prevention for Lifeline Systems, 1992, Technical Memorandum of PWRI, No.3198, 1992

13) Kaneyama, T., Suzuki, H. and Hashimoto, T. : Seismic Strengthening and Construction of Akisato Bridges, Proc. of the 20th Road Conference, 1993 (in Japanese)

14) Suzuki, H. and Kanoh, S. : Seismic Strengthening of an Existing Bridge Foundation — Akisato Bridge at Tottori New National Highway —, Seminar on Construction Technology, Shikoku Regional Office of Japan Construction Technology Association, October, 1993 (in Japanese)

Table 1 Development of Seismic Design Methods for Highway Bridges

11

		1926 Details of Road Structure (draft), Road Law, MIA	1939 Design Specifications of Steel Highway Bridges (draft), MIA	1956 Design Specifications of Steel Highway Bridges, MOC	1964 Design Specifications of Substructures (Pile Foundations), MOC	1964 Design Specifications of Steel Highway Bridges, MOC	1966 Design Specifications of Substructures (Survey and Design), MOC	1968 Design Specifications of Substructures (Piers and Direct Foundations), MOC	1970 Design Specifications of Substructures (Caisson Foundations), MOC	1971 Specifications for Seismic Design of Highway Bridges, MOC	1972 Design Specifications of Substructures (Cast-in-Piles), MOC	1975 Design Specifications of Substructures (Pile Foundations), MOC	1980 Design Specifications of Highway Bridges, MOC	1990 Design Specifications of Highway Bridges, MOC
Seismic Loads	Seismic Coefficient	Largest Seismic Loads, k_h =0.2	k_h =0.1 ~ 0.35 varied dependent on the site	varied dependent on the site and ground Condition						k_h =0.1 ~ 0.3 Standardization of Seismic Coefficient Provision of Modified Seismic Coefficient Method			Revision of Application range of Modified Seismic Coefficient Method	k_h =0.1 ~ 0.3 Integration of Seismic Coefficient Method and Modified one.
	Dynamic Earth Pressure	Epuations proposed by Mononobe and Okabe were supposed to be used.					Provision of Dynamic Earth Pressure							
	Dynamic Hydraulic Pressure	Less Effect on Piers except High Piers in Deep Water.					Provision of Hydraulic Pressure		Provision of Dynamic Hydraulic Pressure.					
Reinforced Concrete Column	Bending at Bottom	Supposed to be designed in a similar way provided in current Design Specifications					Provisions of Definite Design Method							
	Shear	Less Effect on RC Piers except those with Smaller section area such as RC Frame and Hollow Section					Check of Shear Strength					Provision of Definite Design Method, Decreasing of Allowable Shear Stress		
	Termination of Main Reiforement at Mid-Hieght											Elongation of Anchorage Length of Terminated Reinforcement at Mid-Height		
	Bearing Capacity for Lateral Fore							Less Effect on RC Piers with Larger Section Area				Ductility Check Check of Bearing Capacity for Lateral Force		
Footing							Provisions of Definite Design Method (Designed as a Cantilever Plate)					Provisions of Effective width and Check of Shear Strength		
Pile Foundation			Bearing Capacity in vertical direction was supposed to be checked.		Provisions of Definite Design Method (Bearing Capacity in vertical and horizontal directions)					Special Condition (Foundation on Slope, Consolidation Settlement, Lateral Movement)		Provisions of Design Details for Pile Head		
Direct Foundation			Stability (Overturning and Slip) was supposed to be checked.				Provisions of Definite Design Method (Bearing Capacity, Stability Analysis)							
Caisson Foundation					Supposed to be designed in a similar way provided in Design Specification of Caisson Foundation of 1969			Provisions of Definite Design Method						
Soil Liquefaction								Provisions of Soil Layers of which Bearing Capacity shall be Ignored in seismic design				Provisions of Evaluation Method of Soil Liquefaction and the treatment in seismic design	Consideration of effect of fine sand content	
Bearing Support	Bearing Support			Provisions of Design Methods for Steel Bearing Supports (Bearing, Roller, Anchor Bolt)					Provision of Transmitting Method of Seismic Load at Bearing					
	Devices Preventing Falling-off of Superstructure							Provision of Bearing Seat Length S	Provisions of Stopper at Movable Bearings, Devices for Preventing Superstructure from Falling (Seat Length S, Connection of Adjacent Decks)				Provisions of Stopper at Movavle Bearings, Devices for Preventing Superstructure from Falling (Seat Length S_L, Devices)	

Table 2 Past Seismic Evaluations of Highway Bridges

Year	Highways Inspected	Inspection Items	Number of Bridges		
			Inspected	Require Strengthening	Strengthened
1971	All Sections of National Expressways and National Highways, and Sections of the Others (Bridge Length ≧ 5m)	① Deterioration ② Bearing Seat Length S for Bridges supported by Bent Piles	18,000	3,200	1,500
1976	All Sections of National Expressways and National Highways, and Sections of the Others (Bridge Length ≧ 15m or Overpass Bridges)	① Deterioration of Substructures, Bearing Supports and Girders/Slabs ② Bearing Seat Length S and Devices for Preventing Falling-off of Superstructure	25,000	7,000	2,500
1979	All Sections of National Expressways, National Highways and Principal Local Highways, and Sections of the Others (Bridge Length ≧ 15m or Overpass Bridges)	① Deterioration of Substructures and Bearing Supports ② Devices for Preventing Falling-off of Superstructure ③ Effect of Soil Liquefaction ④ Bearing Capacity of Soils and Piles ⑤ Strength of RC Piers ⑥ Vulnerable Foundations (Bent Pile and RC Frame on Two Independent Caisson Foundation)	35,000	16,000	13,000
1986	All Sections of National Expressways, National Highways and Principal Local Highways, and Sections of the Others (Bridge Length ≧ 15m or Overpass Bridges)	① Deterioration of Substructures, Bearing Supports and Concrete Girders ② Devices for Preventing Falling-off of Superstructure ③ Effect of Soil Liquefaction ④ Strength of RC Piers (Bottom of Piers and Termination Zone of Main Reinforcement) ⑤ Bearing Capacity of Piles ⑥ Vulnerable Foundations (Bent Piles and RC Frame on Two Independent Caisson Foundation)	40,000	11,800	8,000 (As of the End of 1991 Fiscal Year)
1991	All Sections of National Expressways, National Highways and Principal Local Highways, and Sections of the Others (Bridge Length ≧ 15m or Overpass Bridges)	① Deterioration of Substructures, Bearing Supports and Concrete Girders ② Devices for Preventing Falling-off of Superstructure ③ Effect of Soil Liquefaction ④ Strength of RC Piers (Piers and Termination Zone of Main Reinforcement) ⑤ Vulnerable Foundations (Bent Piles and RC Frame on Two Independent Caisson Foundation)	60,000	——	——

Note) Number of bridges inspected, number of bridges that required strengthening and number of bridges strengthened are approximate numbers.

12

Table 3 Factors which Affect Seismic Vulnerability of Highway Bridges

Items	Seismic Vulnerability
① Design Specifications	Those designed in accordance with 1926 or 1939 Specifications have higher vulnerability
② Type of Superstructure	• Gerber or simply supported girders with 2 or more spans have higher vulnerability • Arch, frame, continuous girders, cable-stayed bridges or suspension bridges have lower vulnerability
③ Shape of Superstructure	Skewed or curved bridges do not necessarily have higher vulnerability than straight bridges
④ Materisls of Superstructure	Reinforced concrete bridges or prestressed concrete bridges have lower vulnerability than steel bridges although the difference is small
⑤ Slope in Bridge Axis	Bridges with slope in bridge axis have higher vulnerability
⑥ Device for Preventing Falling-off of Superstructure	Bridges with devices for preventing falling-off of superstructure have lower vulnerability
⑦ Type of Substructure	Bridges supported by single-line bent piles or by reinforced concrete frame placed on two separate caisson foundations have higher vulnerability
⑧ Height of Piers	Bridges supported by higher piers have higher vulnerability
⑨ Ground Condition	Bridges constructed on soft soil have higher vulnerability
⑩ Effect of Soil Liquefaction	Bridges constructed on sandy soil layers susceptible to liquefaction have higher vulnerability
⑪ Irregularity of Supporting Soil Condition	Bridges constructed on soils with irregularity of supporting conditions have higher vulnerability
⑫ Effect of Scouring	Bridges where the surface soils are scoured have higher vulnerability
⑬ Materials of Substructures	Bridges supported by plane-concrete substructures designed in accordance with 1926 or 1939 specifications have higher vulnerability
⑭ Type of Foundation	Bridges supported by timber, brick, masonry or other old unknown type substructures have higher vulnerability
⑮ Intensity of Ground Motion	Bridges subjected to higher intensity of ground acceleration have higher vulnerability. In particular, vulnerability becomes quite high when the bridges are subjected to peak ground acceleration larger than 400 gal (0.4g)

13

Table 4 Inspection Sheet to Evaluate Seismic Vulnerability of Highway Bridges

Point of Inspection			Factors of Inspection	Evaluation
Inspection for Vulnerability to Develop Excessive Deformation	Inspection Format (A) Inspection for Deformation of Superstructure		① Design Specifications	4.0: 1926 Specs. or 1939 Specs. 2.0: 1956 Specs. or 1964 Specs. 1.0: 1971 Specs. or 1980 Specs.
			② Superstructure Type	3.0: Gerber Girder or Simply-supported Girders with Two Spans or More 1.5: Simply-supported Girder or Continuous Girders Consisting of Two Spans or More 1.0: Arch, Flame, Continuous Girder (One Span), Cable-stayed Bridge, Suspension Bridge
			③ Shape of Superstructure	1.2: Skewed or Curved Bridge 1:0: Straight Bridge
			④ Materials of Superstructure	1.2: Rc or PC 1.0: Steel
			⑤ Gradient	1.2: 6% or Steeper 1.0: Less Than 6%
			⑥ Falling-off Prevention Device	2.0: None 1.0: One Device
			$P_A = ① \times ② \times ③ \times ④ \times ⑤ \times ⑥$	$P_A =$
	Inspection Format (B) Inspection for Deformation of Substructure		⑦ Type of Substructure	2.0: Single-line Bent Pile Foundation 1.0: Others
			⑧ Height of Pier H	2.0: $H \geqq 10m$ 1.5: $5 \leqq H < 10m$ 1.0: $H < 5m$
			⑨ Ground Condition	5.0: Extremely Soft in Group 4 2.5: Group 4 2.0: Group 3 1.2: Group 2 1.0: Group 1
			⑩ Effects of Liquefaction	2.0: Liquefiable 1.0: Non-liquefiable
			⑪ Supporting Ground Condition	1.2: Irregular 1.0: Almost Uniform
			⑫ Scouring	1.5: Recognized 1.0: None
			$P_B = ⑦ \times ⑧ \times ⑨ \times ⑩ \times ⑪ \times ⑫$	$P_B =$
Inspection for Vulnerability to Develop Failure Due to Inadequate Strength of Substructure	Inspection Format (C) Inspection for Strength of RC Pier at Termination of Reinforcement		⑬ Shear Span Ratio (h/D)	2.0: $1 < h/D < 4$ 1.0: $h/D \geqq 4$ 0.5: $h/D \leqq 1$
			⑭ Tension Cracks in Flexure at Terminated Point of Main Reinforcement	2.0: Cracks Will Occur 1.0: Cracks Will Possibly Occur 0.3: Cracks will Not Occur
		⑮ Safety Factor for Yield Strength at Terminated Section of Main Reinforcement (15-1) S_{tn}	3.0: $S_{tn} \leqq 1.1$ 2.0: $1.1 < S_{tn} < 1.5$ 0.5: $S_{tn} \geqq 1.5$
			(15-2) S_{mn}	3.0: $S_{mn} \leqq 1.1$ 2.0: $1.1 < S_{mn} \leqq 1.3$ 1.0: $1.3 < S_{mn} < 1.5$ 0.5: $S \geqq 1.5$
			⑯ Shear Stress σ (tf/m^2)	3.0: $\sigma \geqq 45$ 2.0: $30 \leqq \sigma < 45$ 1.0: $15 \leqq \sigma < 30$ 0.5: $\sigma < 15$
			$P_C = ⑬ \times ⑭ \times$ (15-1) $\times$ (15-2) $\times ⑯$	$P_C =$
	Inspection Format (D) Inspection for Strength of Substructure		⑰ Failure of Fixed Supports and Proximity	5.0: Extensive Failure 2.0: Small Failure 1.0: None
			⑱ Extraordinary Damage of Pier	5.0: Extensive Damage 2.0: Small Damage 1.0: None
			⑲ Materials of Substructure	2.0: Plane Concrete Older Than 1926 Excluding Gravity-type Abutment 1.0: Others
			⑳ Construction method of Foundation	2.0: Timer Pile, Masonry, Brick, Other Old Construction Methods 1.5: RC Piles, Pedestal Piles, Pier Supported by Two Independent Caissons 1.0: Foundation Designed by 1971 Specs. and Other Later Specs.
			㉑ Foundation Type	1.5: RC Flame Supported by Two Independent Caisson Foundations 1.0: Others
			㉒ Extraordinary Failure of Foundation	2.0: Recognized 1.0: None
			$P_D = ⑰ \times ⑱ \times ⑲ \times ⑳ \times ㉑ \times ㉒$	$P_D =$
Evaluation of Deformation and Strength				$X = P_A \times P_B =$ and $Y = P_C \times P_D =$

14

Table 5 Feasibility of Seismic Strengthening for
16 Factors Which Affect Seismic Vulnerability of Highway Bridges

Items	Feasibility of Seismic Strengthening	Principles of Countermeasures
① Design Specifications	×	————
② Type of Superstructure	×	————
③ Shape of Superstructure	×	————
④ Materials of Superstructure	×	————
⑤ Slope in Bridge Axis	×	————
⑥ Device for Preventing Falling-off of Superstructure	○	Installation of Devices
⑦ Type of Substructure	○	Strengthening of Substructures
⑧ Height of Piers	×	————
⑨ Ground Condition	×	————
⑩ Effect of Soil Liquefaction	○	Strengthening of Fundations or Strengthening of Surrounding Soils
⑪ Irregularity of Supporting Soil Condition	×	————
⑫ Effect of Scouring	○	Treatment for Prevention of Scouring, or Strengthening of Foundations
⑬ Materials of Substructures	○	Strengthening of Substructures
⑭ Type of Foundation	○	Strengthening of Foundations
⑮ Intensity of Ground Motion	×	————
⑯ Effect of Termination of Main Reinforcement at Mid-height	○	Strengthening of Substructures

Note ○ Items for which seismic strengthening is feasible
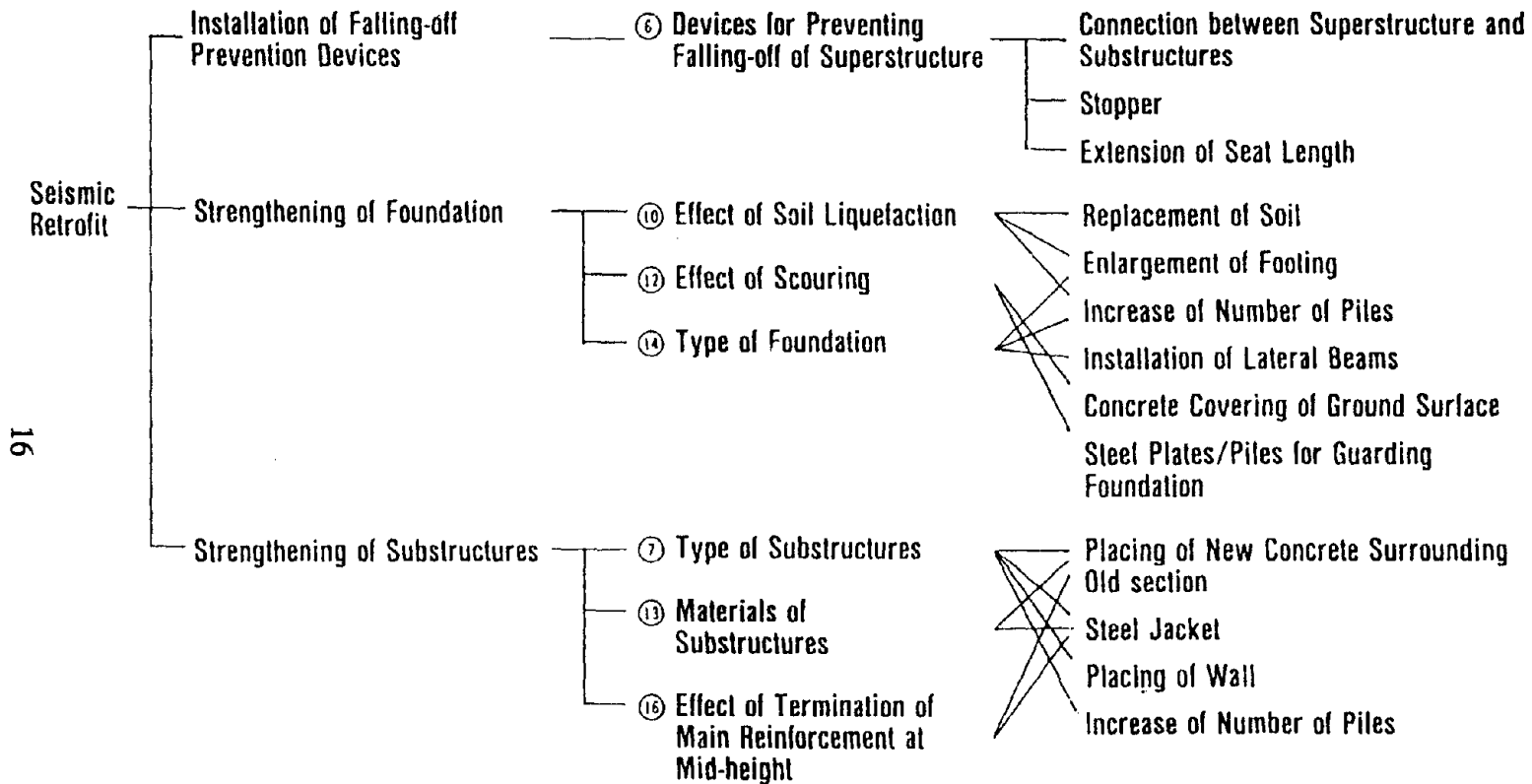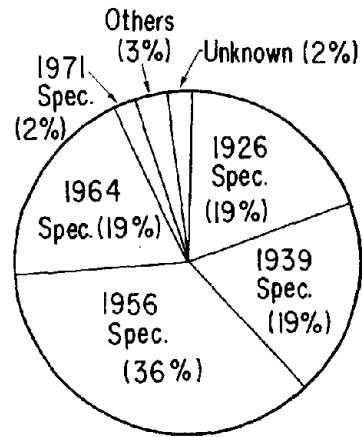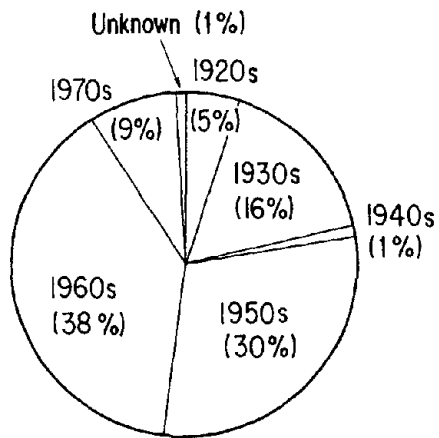   × Items for which seismic strengthening is not feasible

15

16

Installation of Falling-off Prevention Devices ──── ⑥ Devices for Preventing Falling-off of Superstructure ─── Connection between Superstructure and Substructures

── Stopper

└── Extension of Seat Length

Seismic Retrofit

Strengthening of Foundation ──┬── ⑩ Effect of Soil Liquefaction ── Replacement of Soil

Enlargement of Footing

├── ⑫ Effect of Scouring ── Increase of Number of Piles

Installation of Lateral Beams

└── ⑭ Type of Foundation ── Concrete Covering of Ground Surface

Steel Plates/Piles for Guarding Foundation

Strengthening of Substructures ──┬── ⑦ Type of Substructures ── Placing of New Concrete Surrounding Old section

├── ⑬ Materials of Substructures ── Steel Jacket

Placing of Wall

└── ⑯ Effect of Termination of Main Reinforcement at Mid-height ── Increase of Number of Piles

Fig. 1 Methods Adopted for Seismic Strengthening

(a) Year of Construction

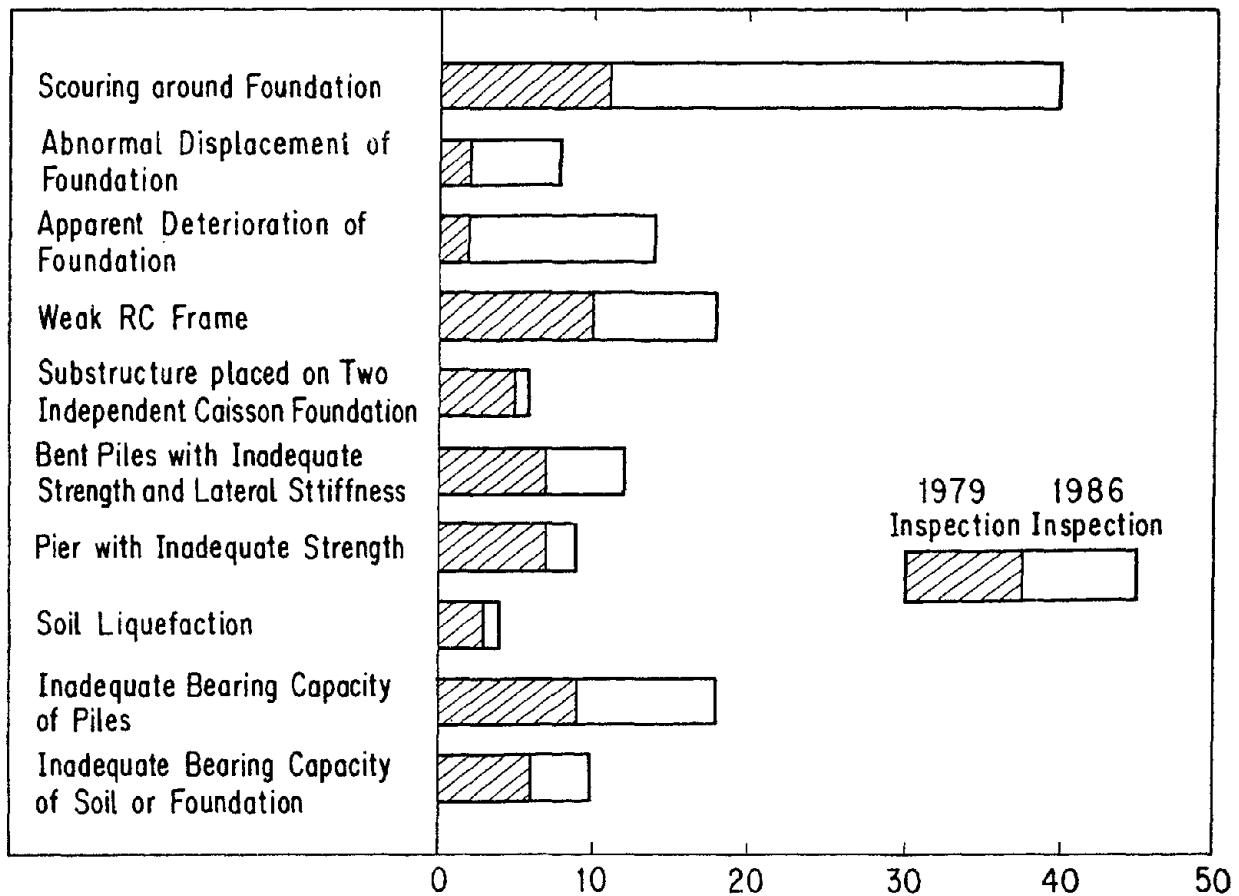(b) Design Specifications Referred to
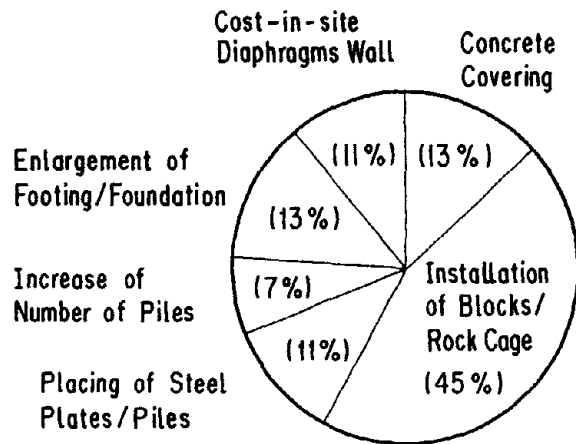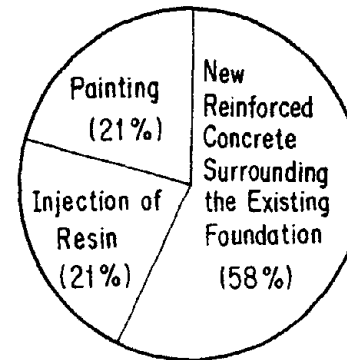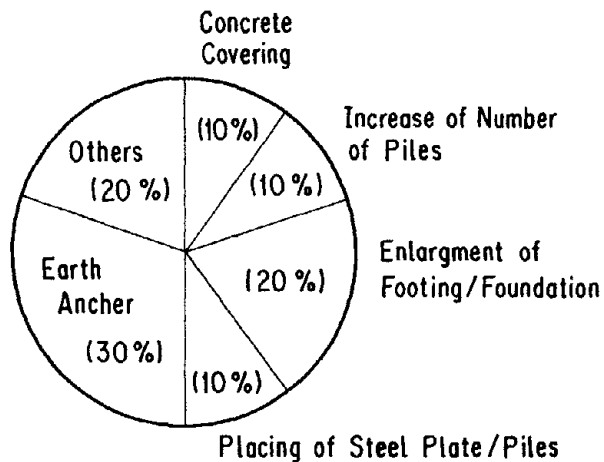
Fig. 2 Bridges Surveyed

Fig. 3 Number of Bridges Strengthened Classified by Requirement
for Seismic Strengthening

(a) Scouring around Foundation

(b) Abnormal Displacement of Foundation

(c) Apparent Deterioration of Reinforced Concrete Structure
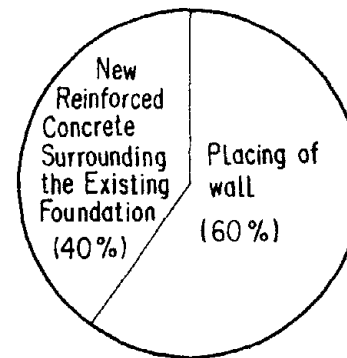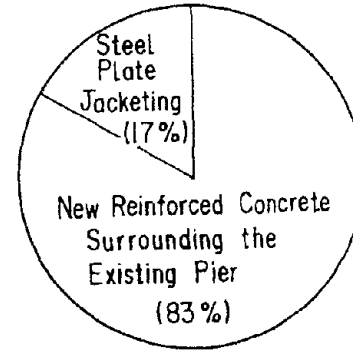
(d) Weak Reinforced Concrete Frame

Fig. 4 Methods Adopted for Strengthening
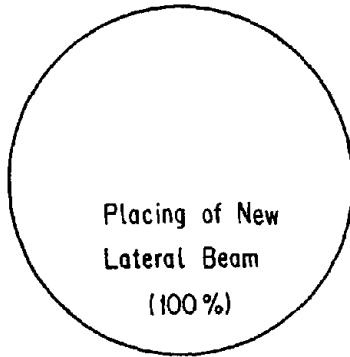
(e) Substructure Placed on Two Independent Caisson Foundations

(g) Pier with Inadequate Strength
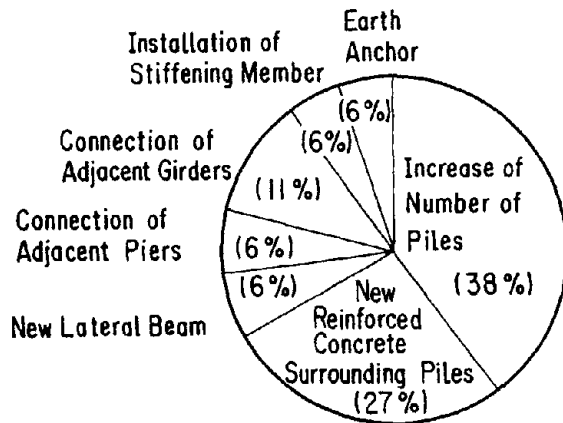
(f) Bent Piles with Inadequate Strength and Lateral Stiffness
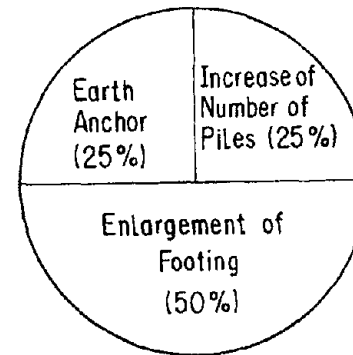
(h) Soil Liquefaction

Fig. 4 Methods Adopted for Strengthening
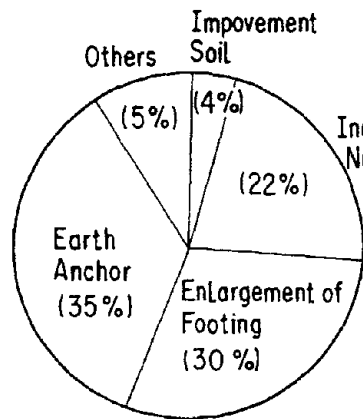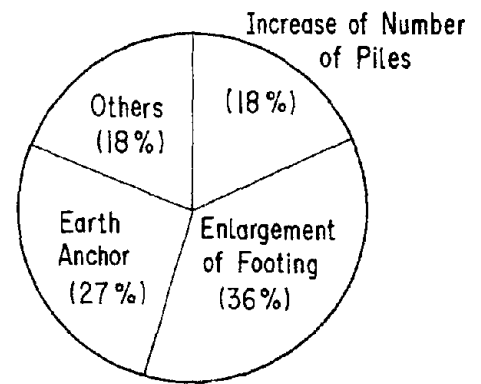
(i) Inadequate Bearing Capacity of Piles   (j) Inadequate Bearing Capacity of Soil/Foundation

Fig. 4 Methods Adopted for Strengthening
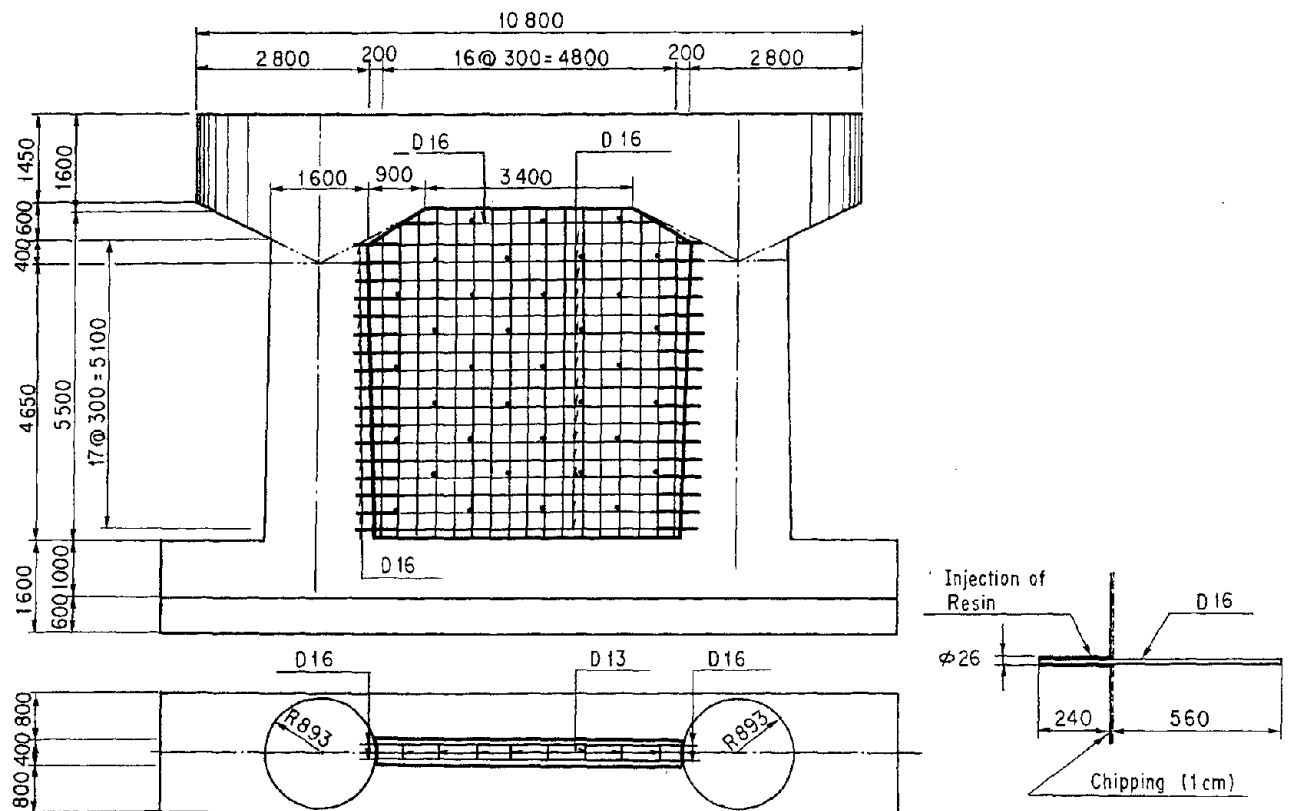
Fig. 5 Seismic Strengthening of A Reinforced Concrete Frame
by Placing A New Reinforced Concrete Wall

20
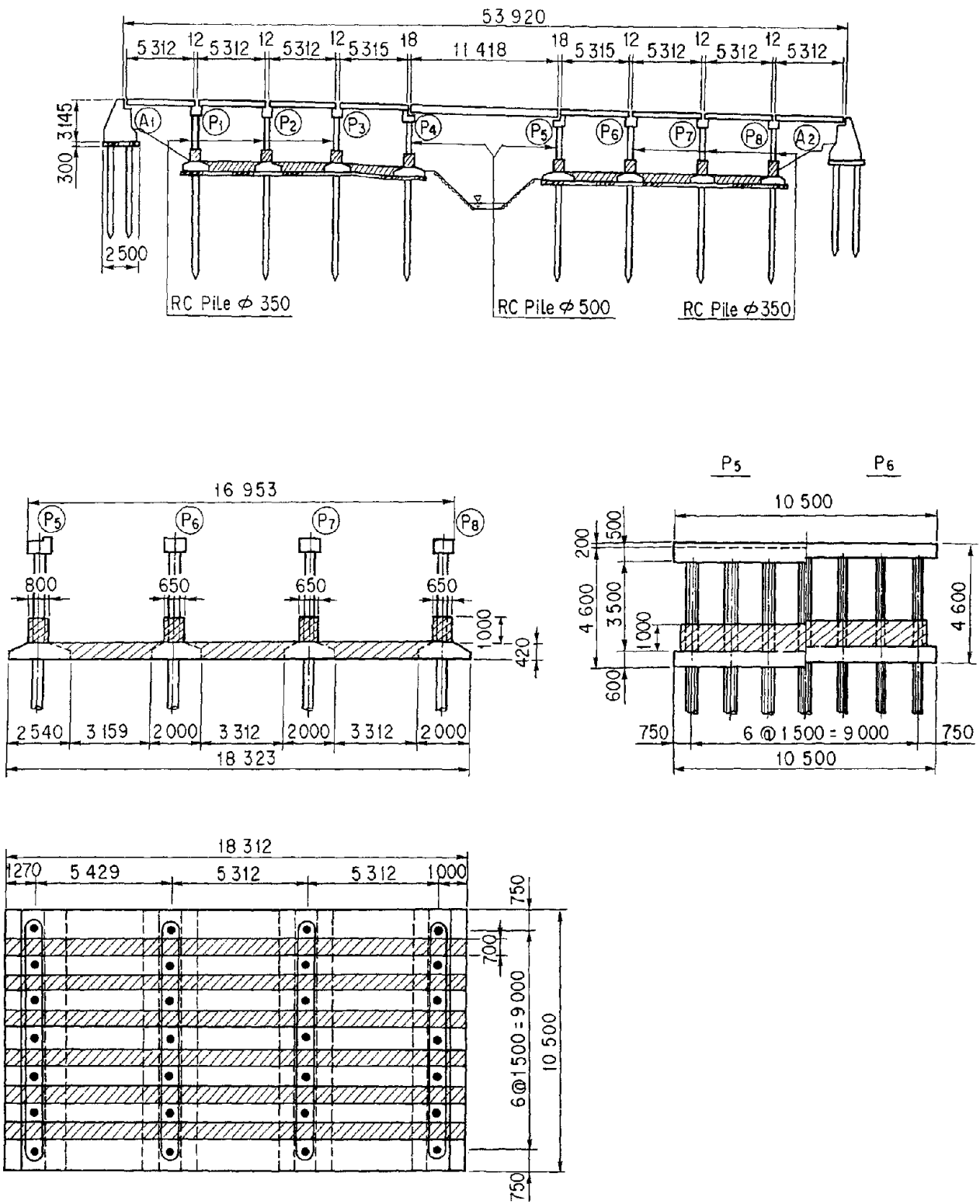
Fig. 6 Seismic Strengthening of Bent Piles by New Concrete Walls and New Connection Slabs

21
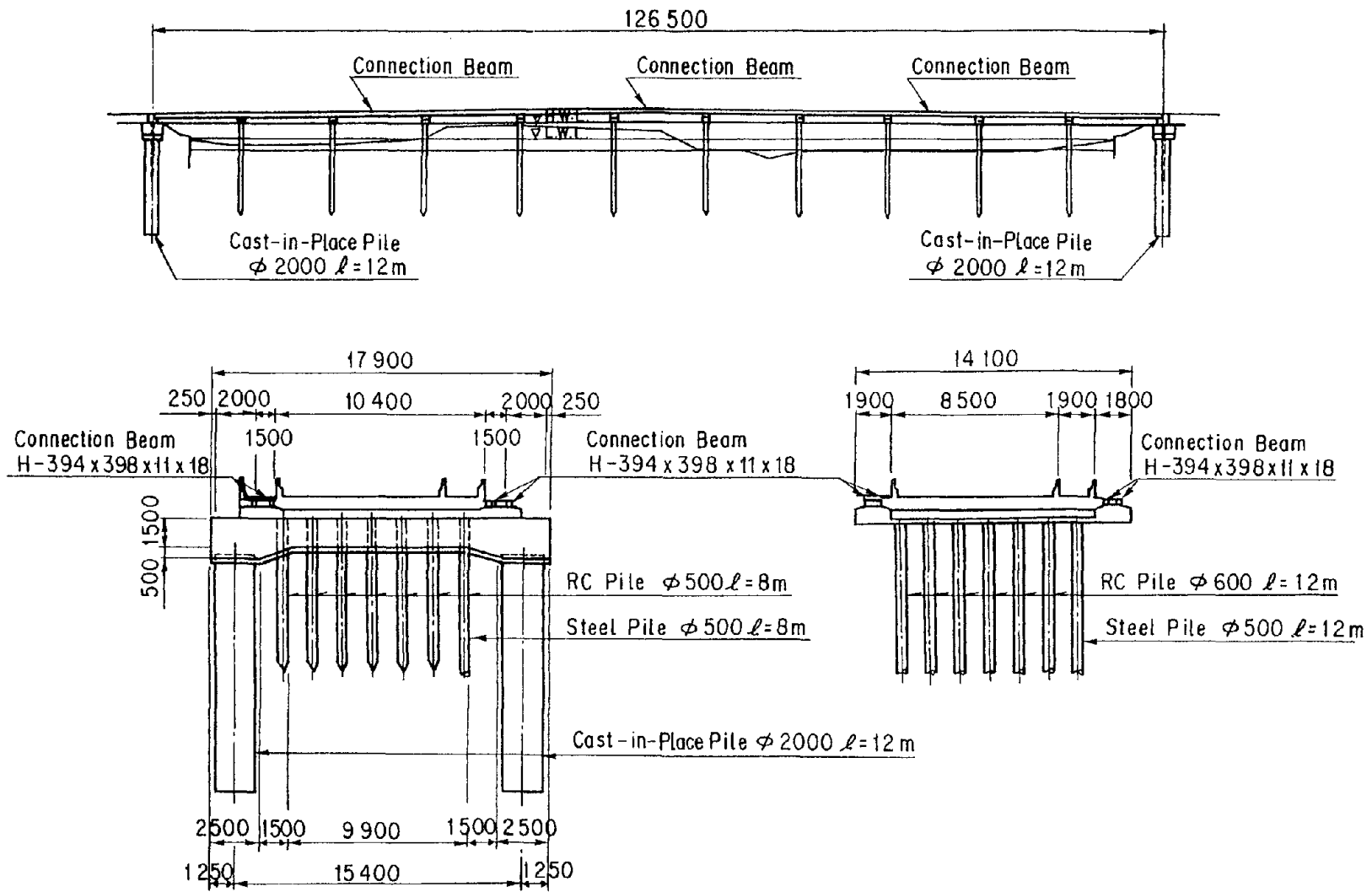
Fig. 7 Seismic Strengthening of Bent Piles in Liquefiable Sandy Soils by Connecting Beams
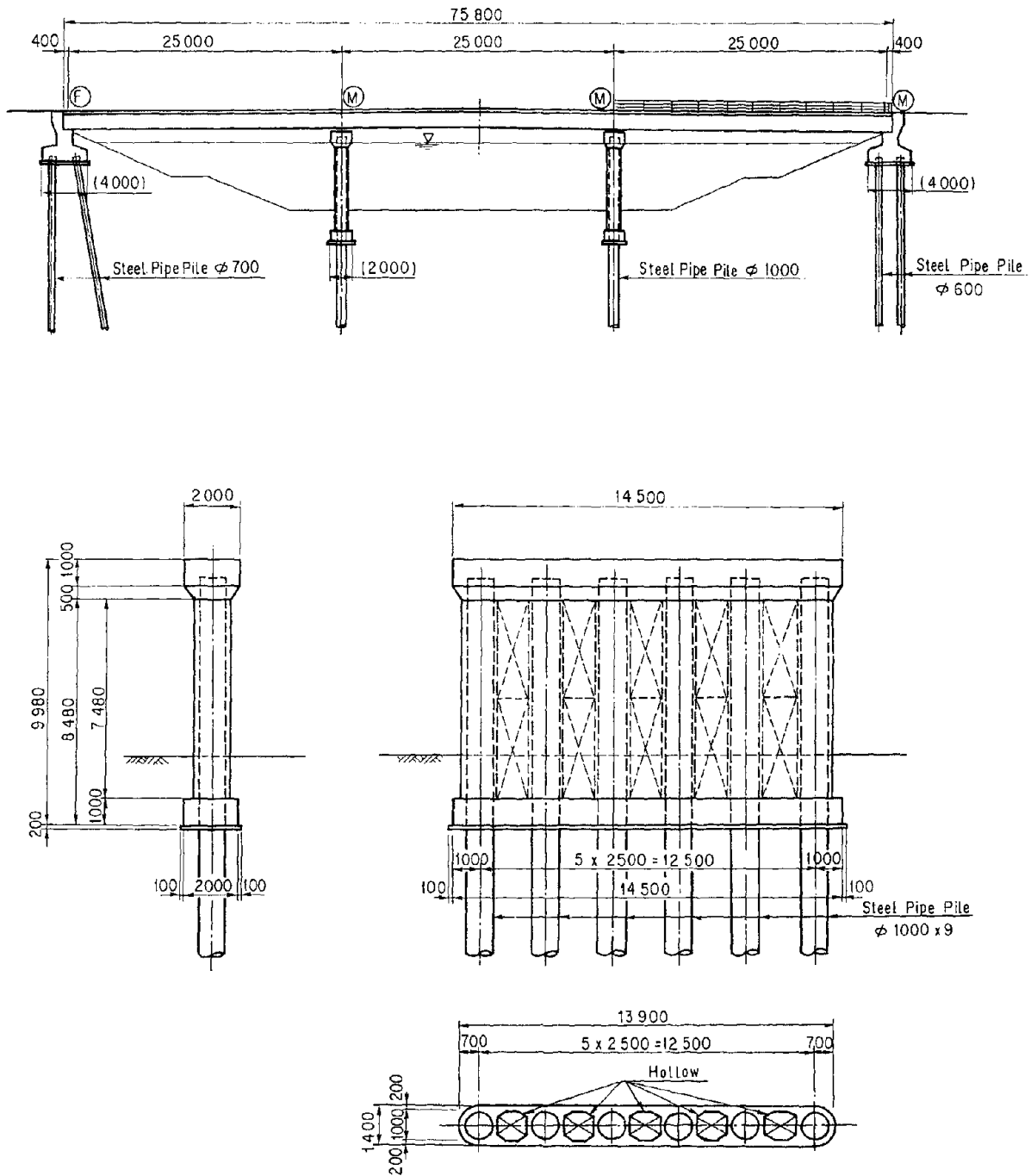
Fig. 8 Seismic Strengthening of Bent Piles by Placing A New Reinforced Concrete Wall

23
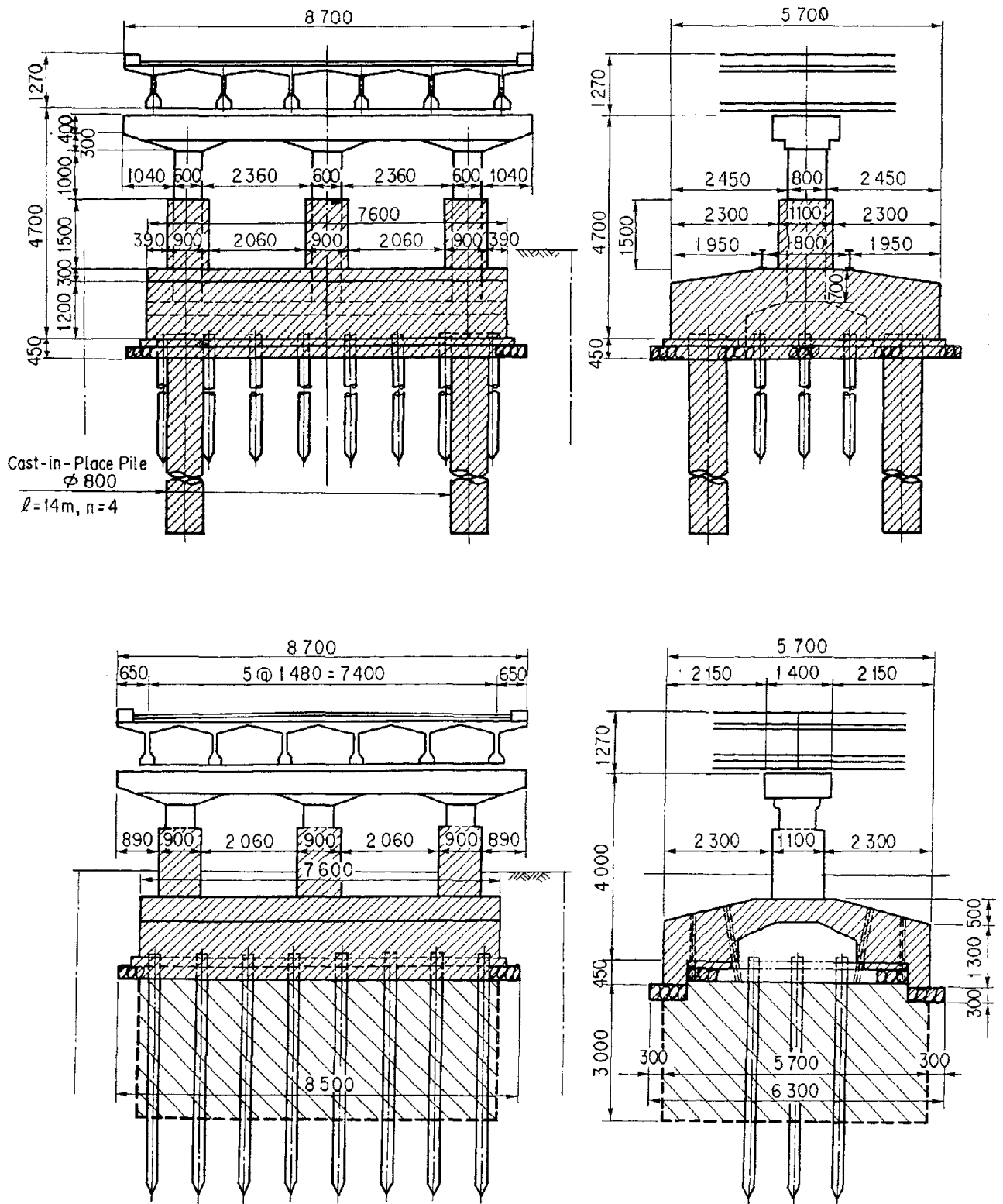
Fig. 9 Seismic Strengthening of Foundations by Increasing Number of Piles and by Enlarging Footing

24
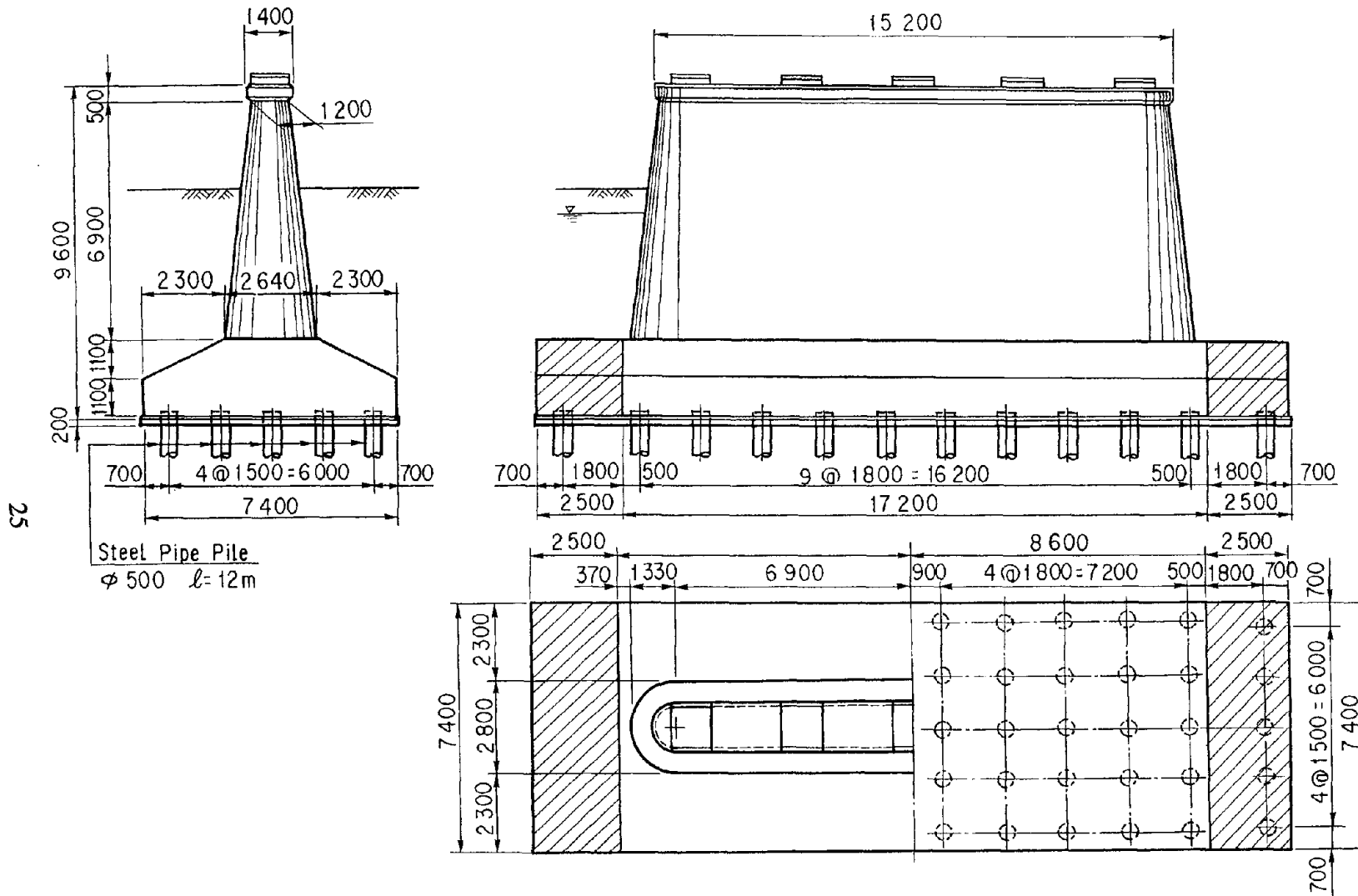
Fig. 10 Seismic Strengthening of A Pile Foundation in Liquefiable Soils
by Increasing Number of Piles

5-Span Continuous Steel Plate Girder
172.9

2-Span Continuous
Steel Plate Girder
70.6

PC Girder
17.7

Matsue

Kyoto

Fukuro River

New Bridge

Existing Bridge

Matsue

Koyto

New Bridge   Existing Bridge

Fig. 11 General View of Akisato Bridge

10.6

1.25 4.0 1.25

High Fluid
Concrete

7.5

2.0

9.5

3.4

1.5

Existing
Footing

1.3

1.5

4.3

1.5

2.0

New Footing

New Pile

9.0
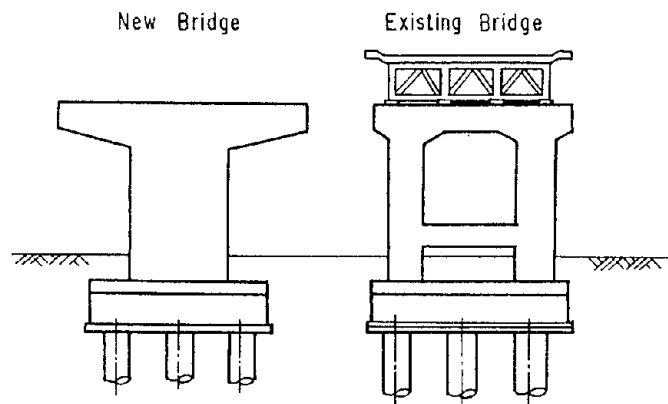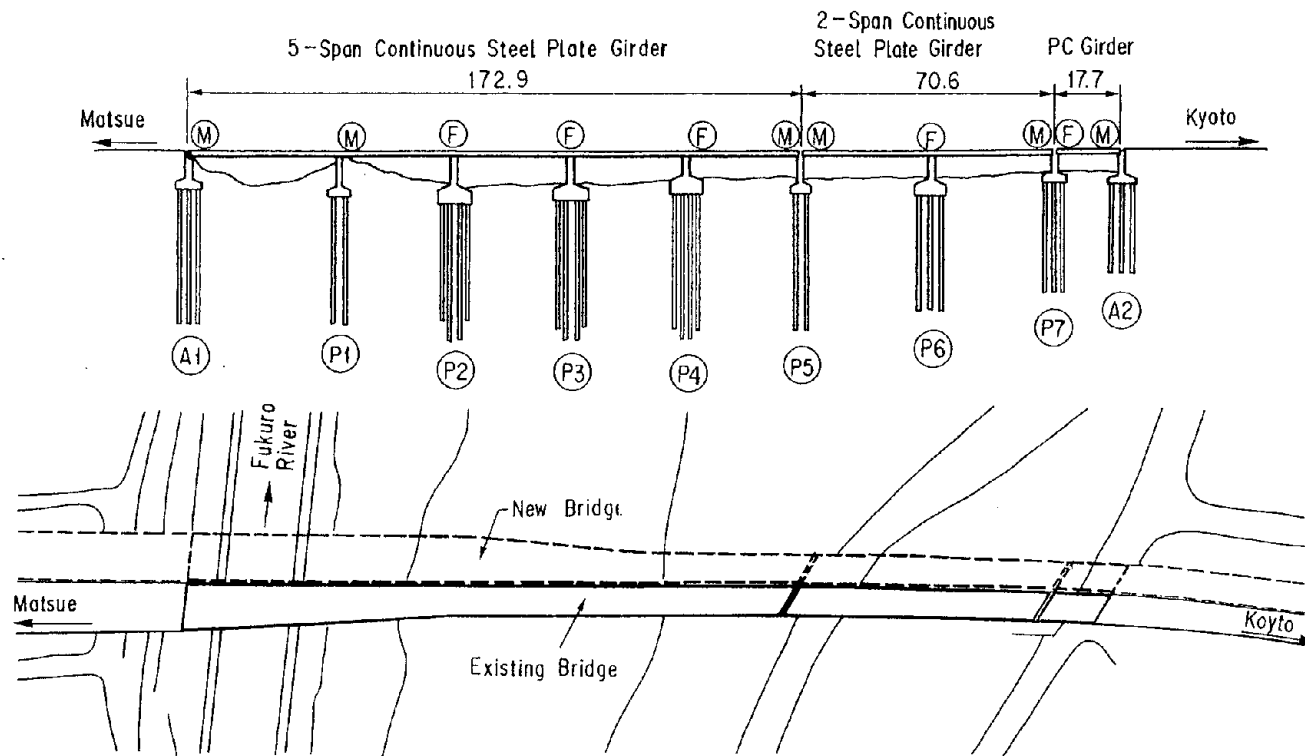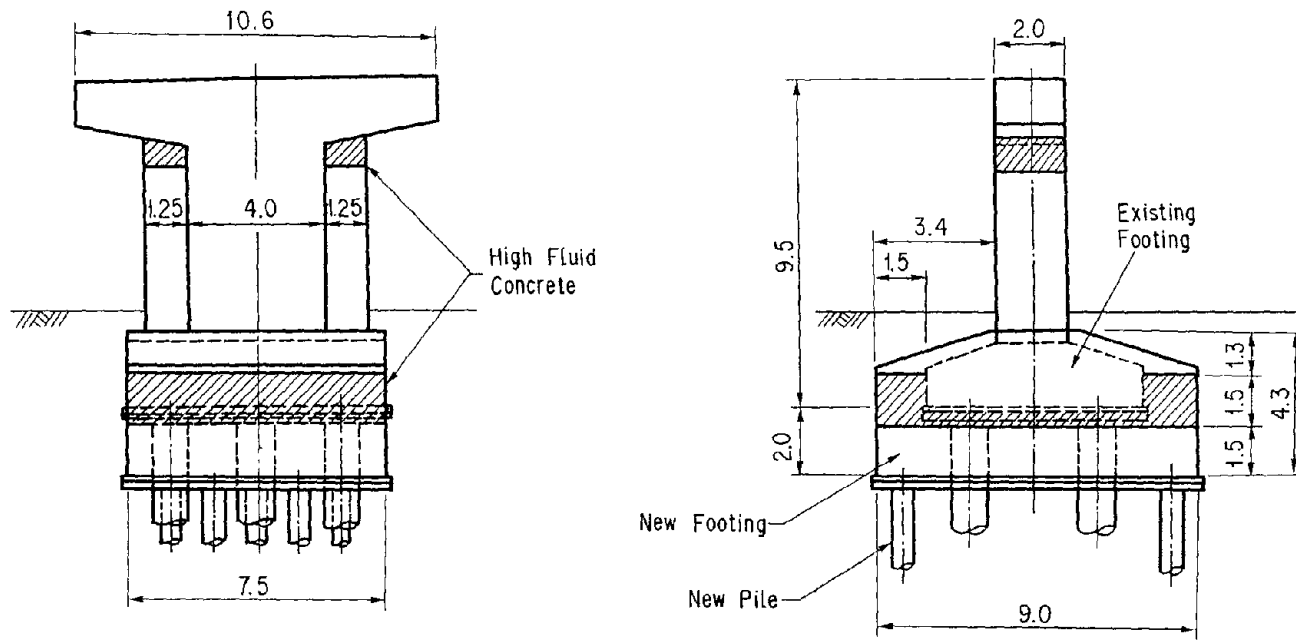
Fig. 12 Seismic Strengthening Method of Substructures (Akisato Bridge, Pier P4)

New
Footing

Existing
Footing

New
Piles

Excavate soil at the bottom of
existing footing, place new piles
and construct new footing

High Fluid
Concrete

Place high fluid
concrete from one side

High Fluid
Concrete

Add high fluid
concrete at the other side

Normal Concrete

Complete new footing by
placing normal concrete
on the existing footing
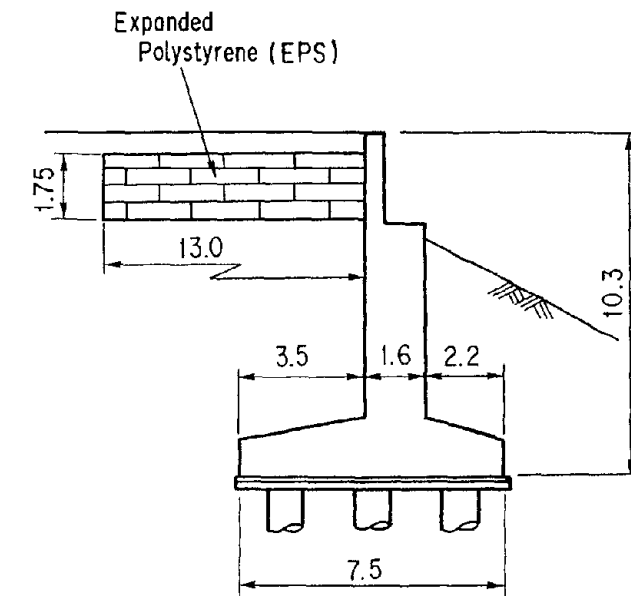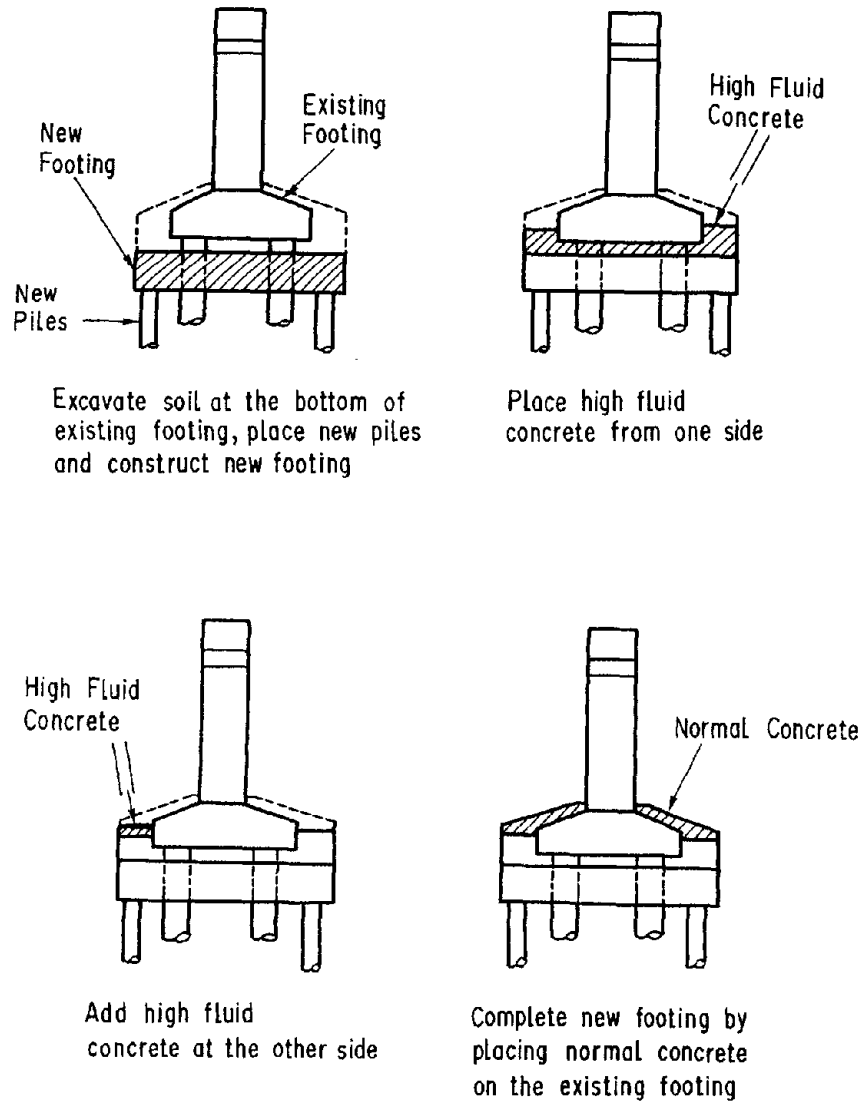
Fig. 13 Construction Procedure of Strengthening of Substructures

Expanded
Polystyrene (EPS)

1.75

13.0

3.5 1.6 2.2

10.3

7.5

Fig. 14 Seismic Strengthening of Abutment
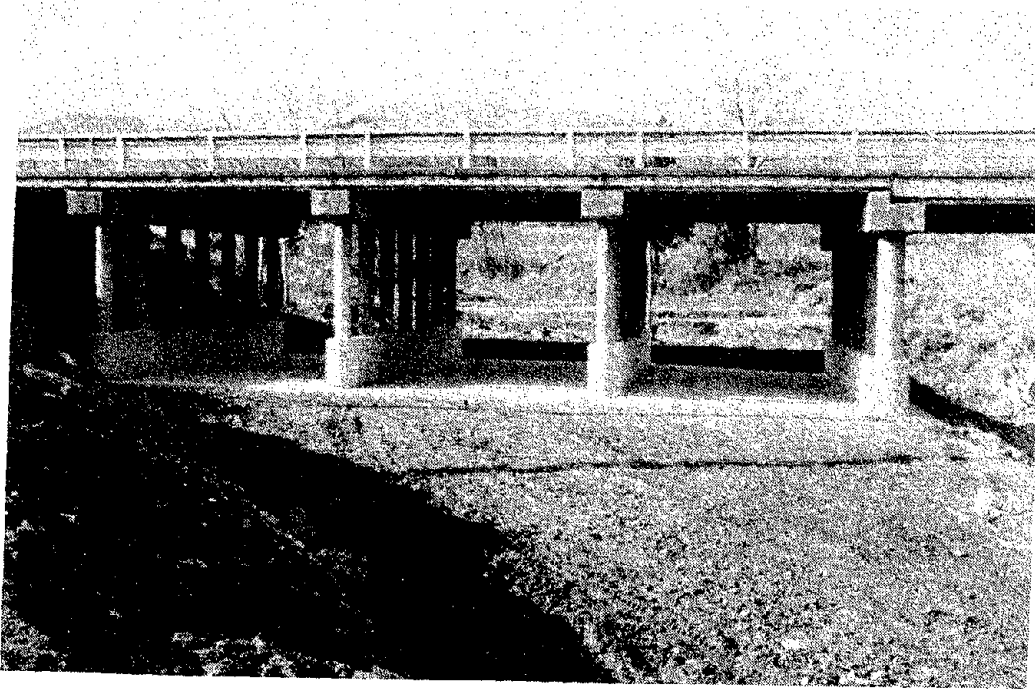
Photo 1 Seismic Strengthening of Bent Piles by New Concrete Walls and New Connection Slabs
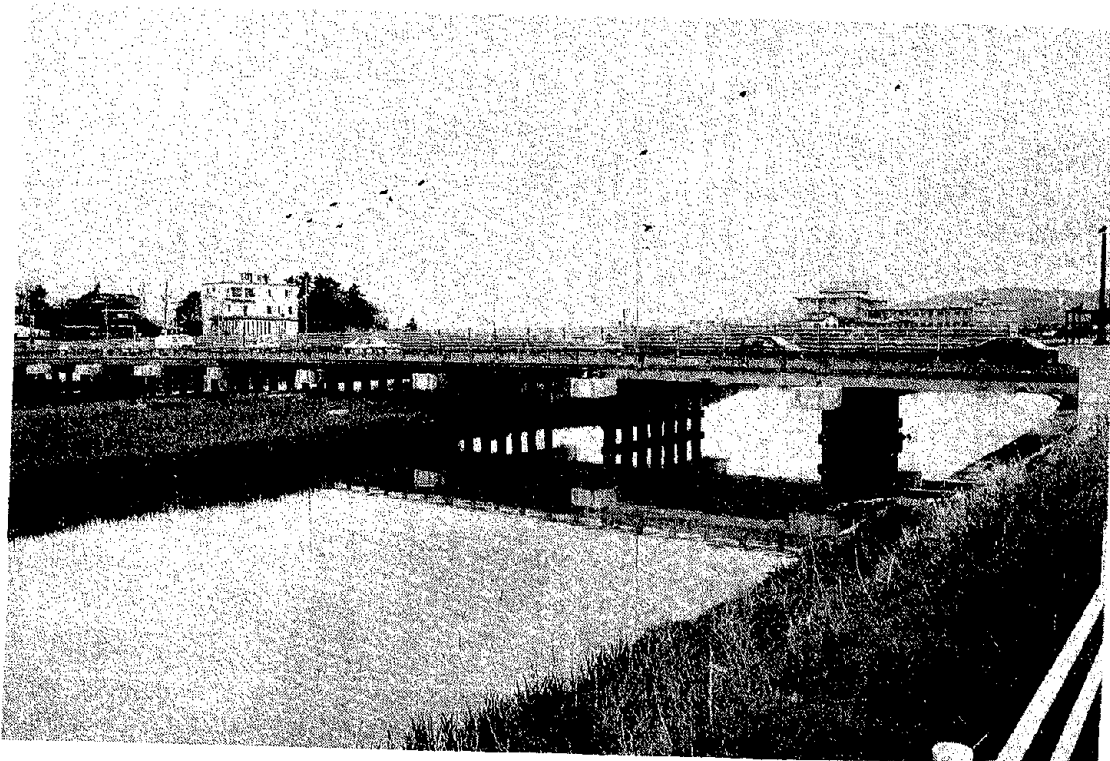
Photo 2 Seismic Strengthening by Connecting Beams

29
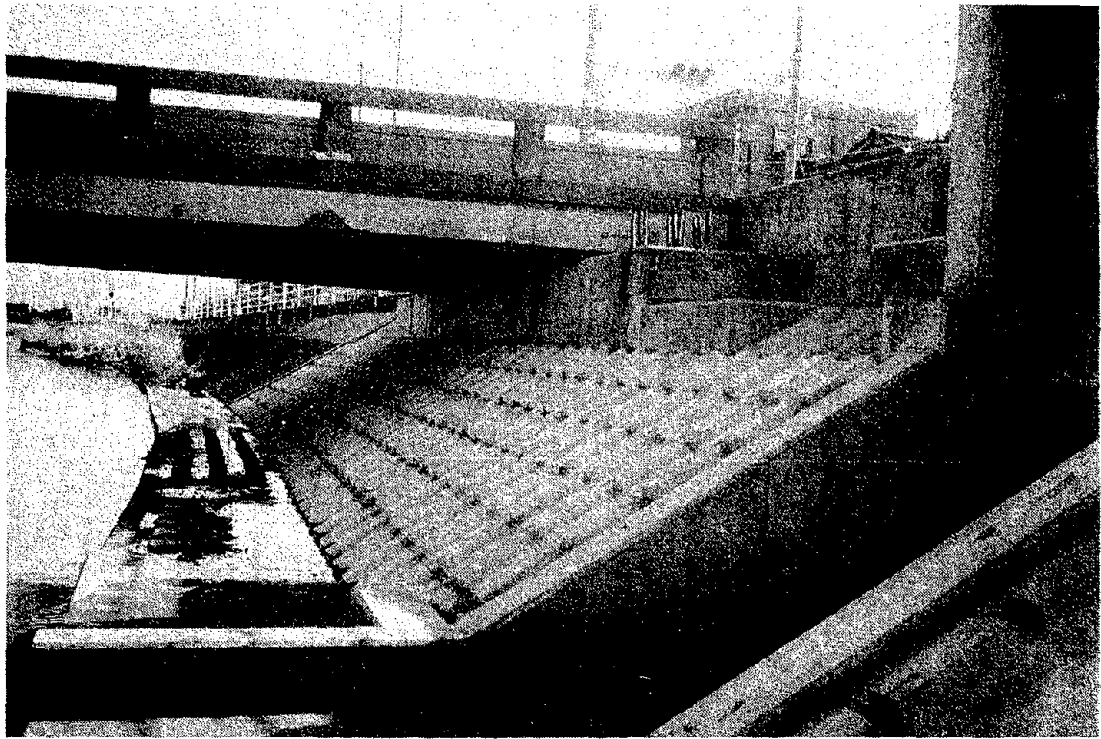
Photo 3 Seismic Strengthening of Abutment by Increasing Number of Piles

(a) Before the Seismic Strengthening

Photo 4 Seismic Strengthening by A New Reinforced Concrete Wall

30
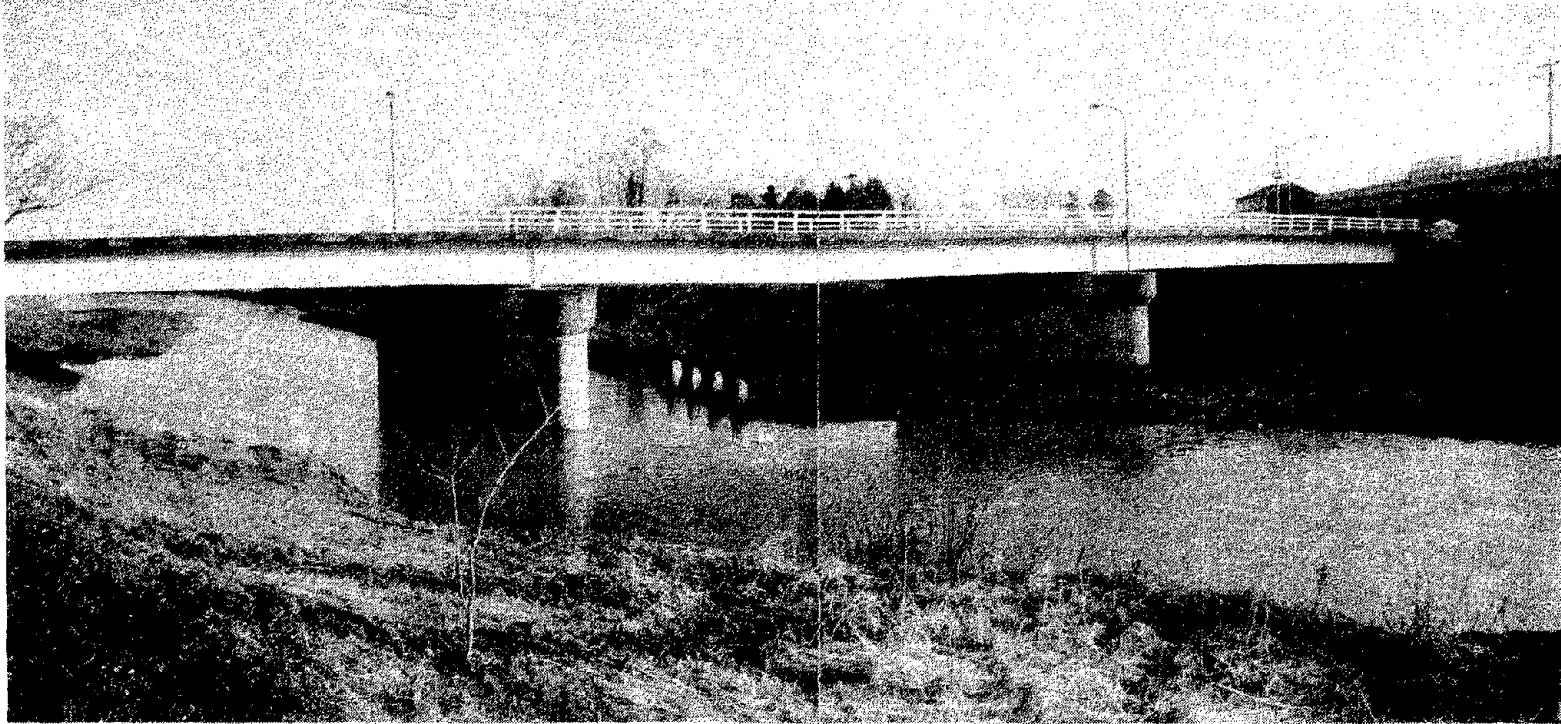
(b) After the Seismic Strengthening

Photo 4 Seismic Strengthening by A New Reinforced Concrete Wall
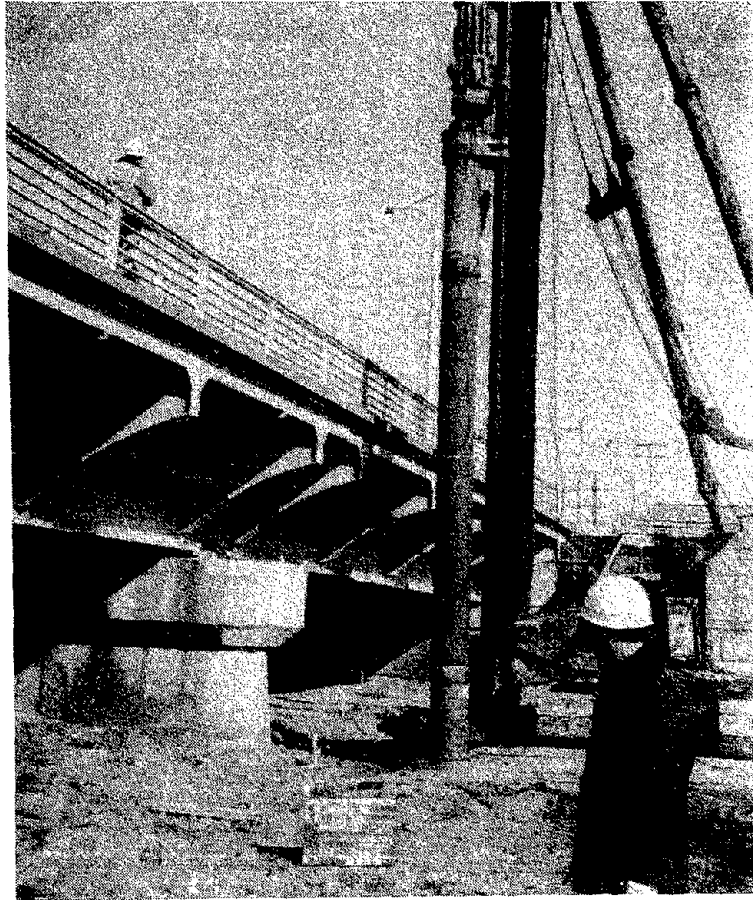
Photo 5 Construction of the New Piles

Photo 6 Reinforcement of at the New Footing

Photo 7 New Footing
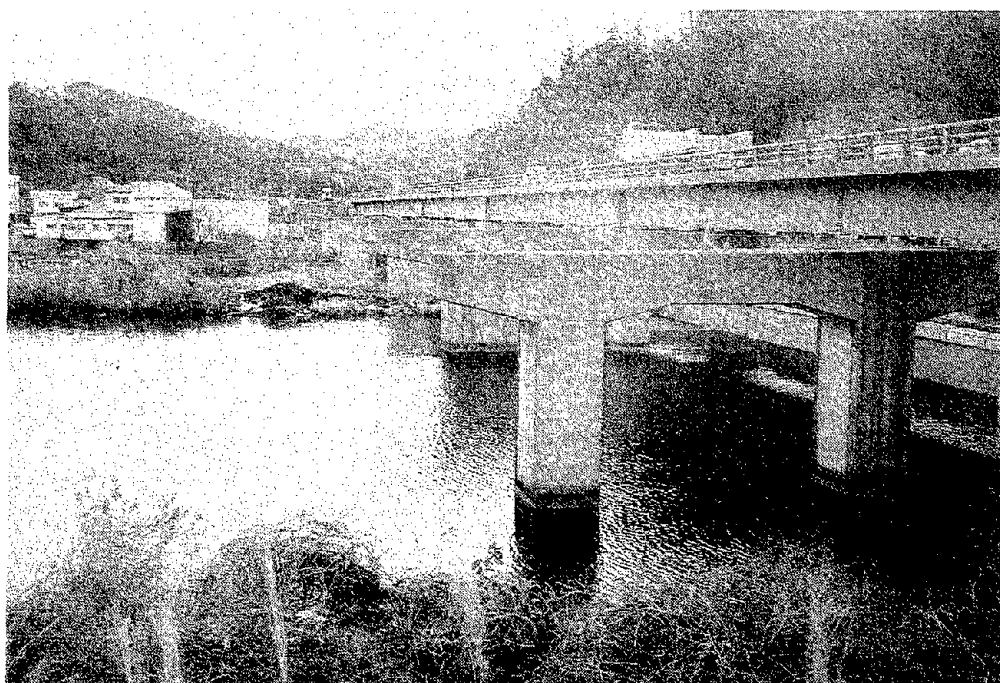
Photo 8 General View of Akisato Bridge and Existing Piers
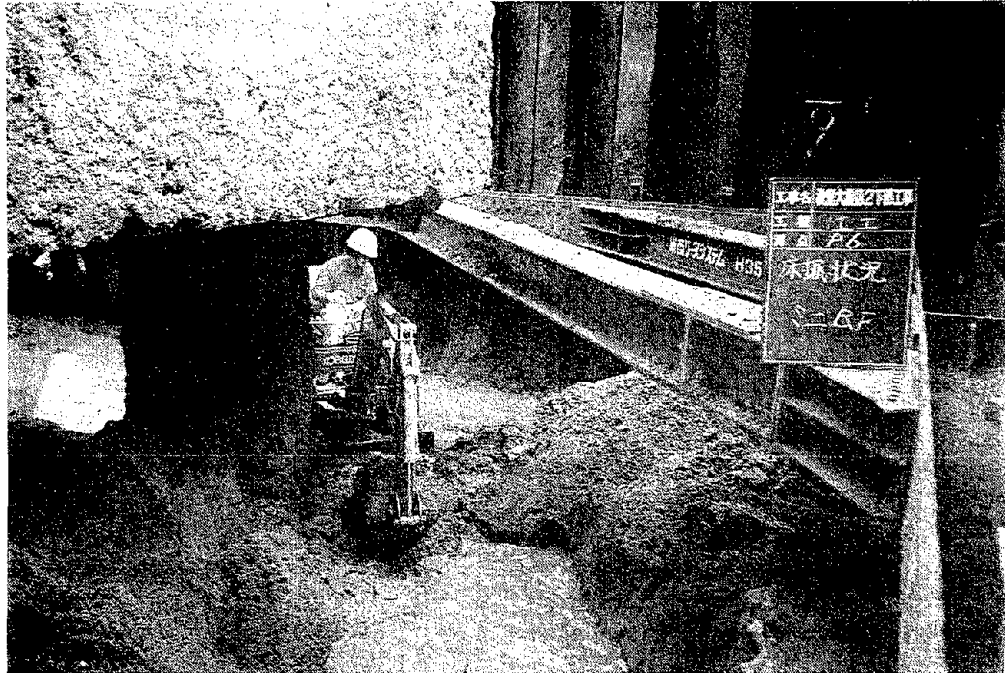
Photo 9 Excavation below the Bottom of Existing Footing

Photo 10 Excavation by Manpower and the Head of New Pile

34
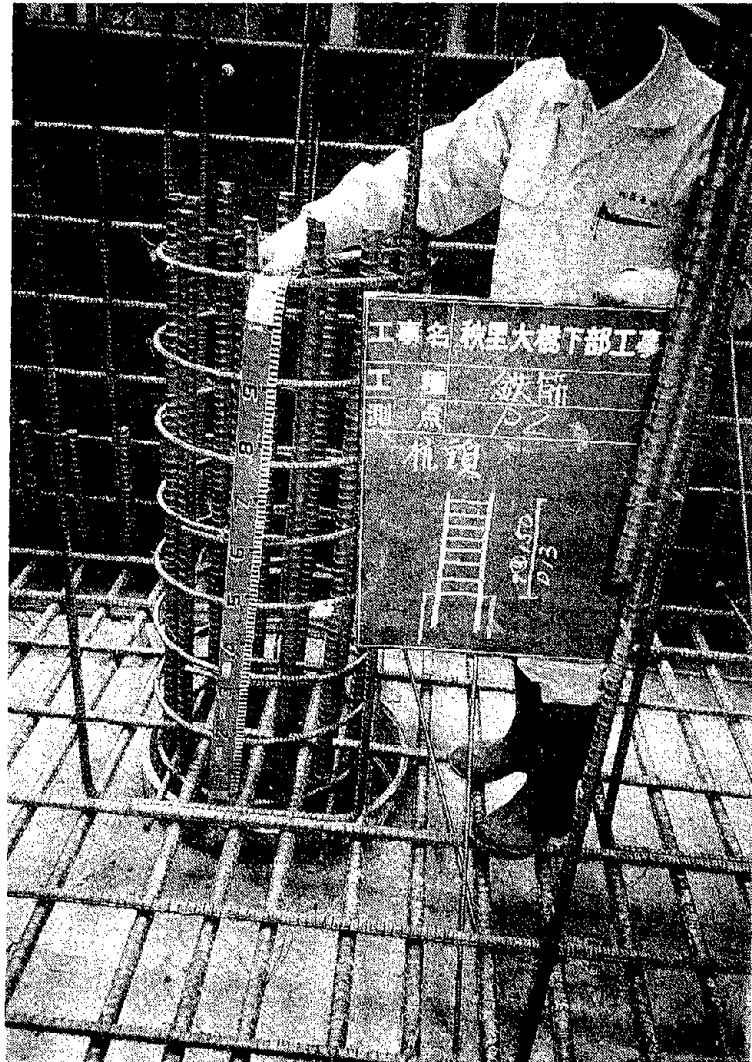
Photo 11 Reinforcement around the New Pile
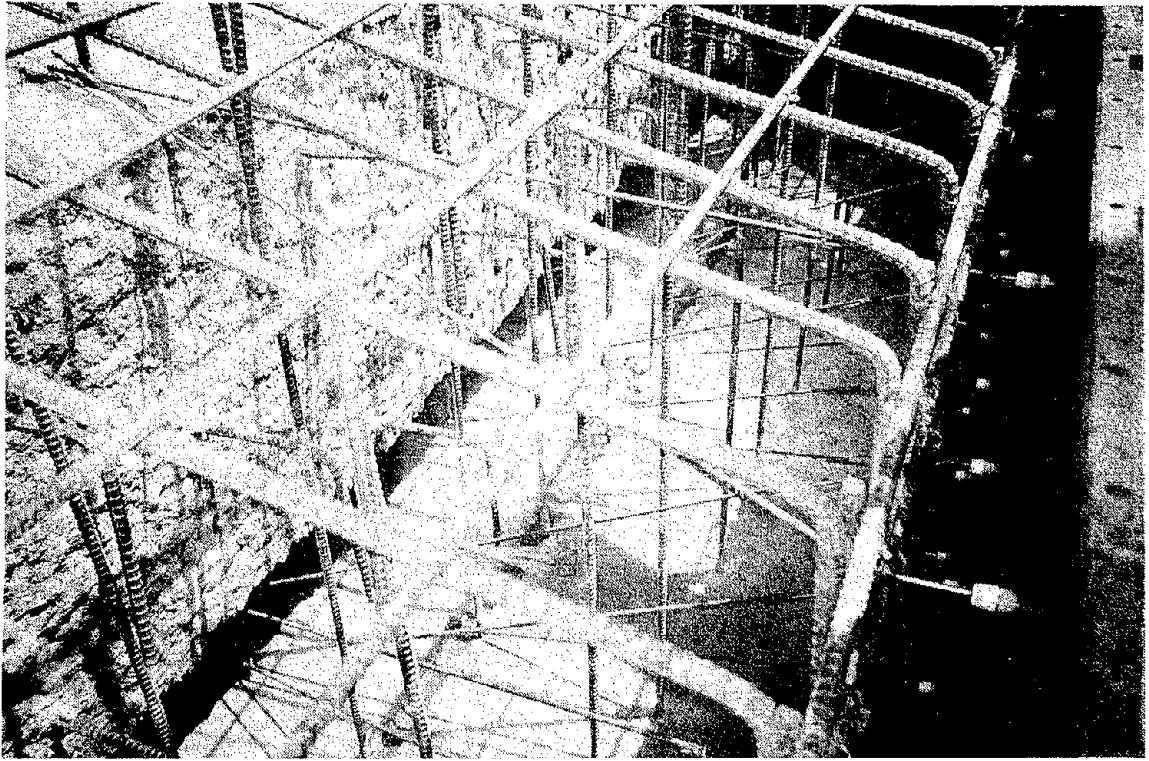
Photo 12 Reinforcement at the New Footing
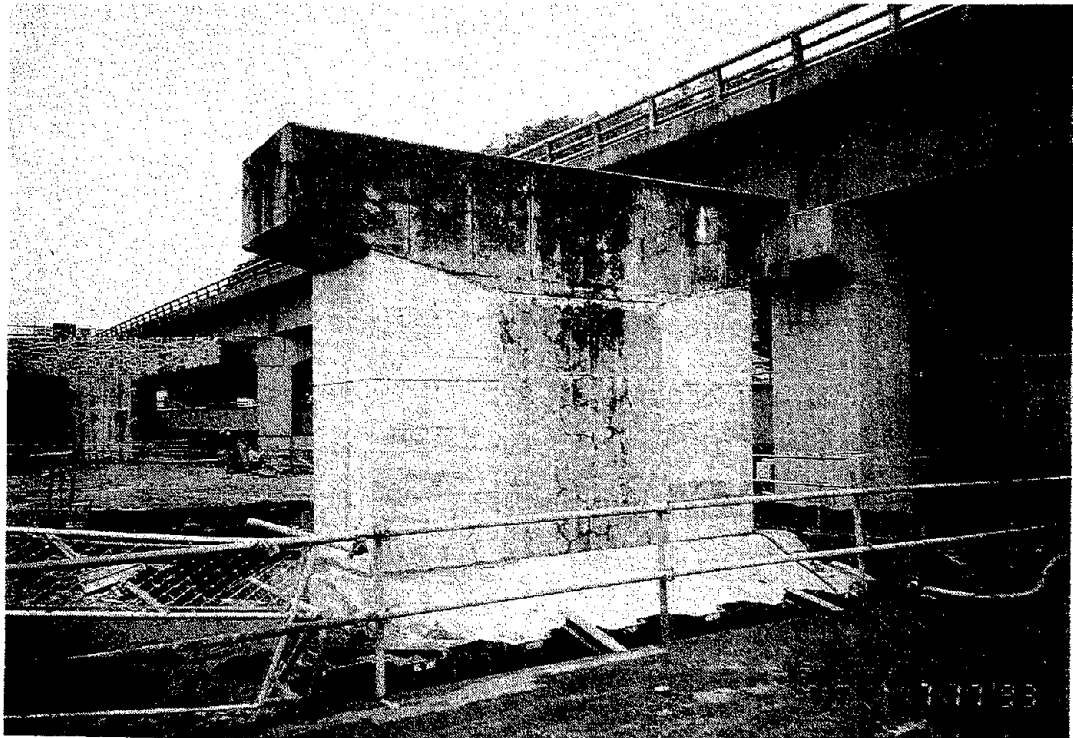
Photo 13 Seismic Strengthening of the Piers

SECOND U.S.-JAPAN WORKSHOP ON SEISMIC RETROFIT OF BRIDGES

Caltrans' Bridge Restrainer Retrofit Program
Y. Yashinsky
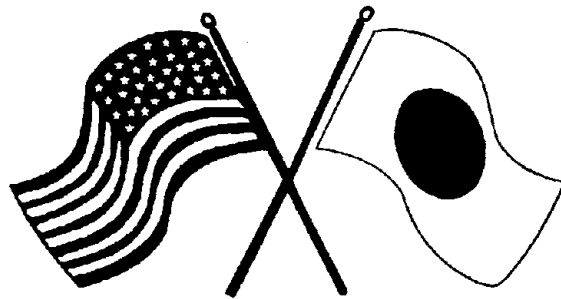
Caltran's Bridge Restrainer Retrofit Program
Mark Yashinsky
California Department of Transportation

Introduction

Caltrans has pursued a seismic retrofit program since the 1971 San Fernando Earthquake. Damage from that earthquake showed that bridges were vulnerable to collapse if their joints were free to move apart. To prevent reoccurrence of such failures, Caltrans began the first major seismic retrofit program for bridges. Bridges were selected for retrofitting after examining the 15,000 bridge inventory for poor expansion joint details such as narrow seats and weak bearings. Since then, 1261 bridges have been retrofit at a cost of 54.2 million dollars as part of the Phase One Retrofit Program. This program addressed several issues. To prevent simply supported spans from falling off their supports, they were tied together (and sometimes tied to the substructure) with cable restrainers. To prevent bridge frames from becoming unseated, restrainers were added at hinges. Poor bearings were replaced and shear keys were provided to prevent transverse motion. Finally, for new bridges the seat width was increased. Other retrofit programs were begun after the Whittier and Loma Prieta Earthquakes to address other bridge vulnerabilities. However, this paper focuses on the role that cable restrainers play during large earthquakes.
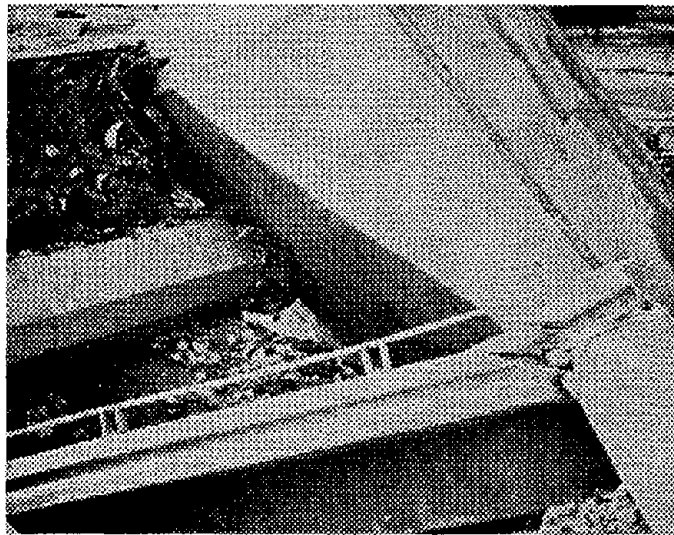
Figure 1. San Fernando Earthquake Bridge Damage
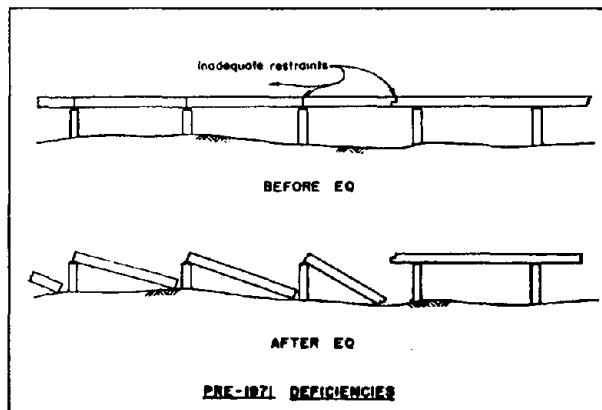
Figure 2. Damage Prevented by Cable Restrainers

Caltrans' Cable Restrainer Design Procedure

As previously discussed, cable restrainers join bridge decks together at expansion joints. After the San Fernando earthquake, Caltrans' policy was to design earthquake restrainers to yield at a force equal to 25% of the weight of the lighter adjacent frame. Later, this force was increased to 35%. At one point, a multimodal dynamic analysis was performed to determine the number of restrainers needed at a joint. Caltrans' current cable restrainer design procedure is to determine the equivalent linear stiffness and the mass of the frames on each side of the joint (see figure 3). This stiffness includes any change in column stiffness during the maximum credible earthquake. Then the displacement of the restrained system for the maximum credible earth-
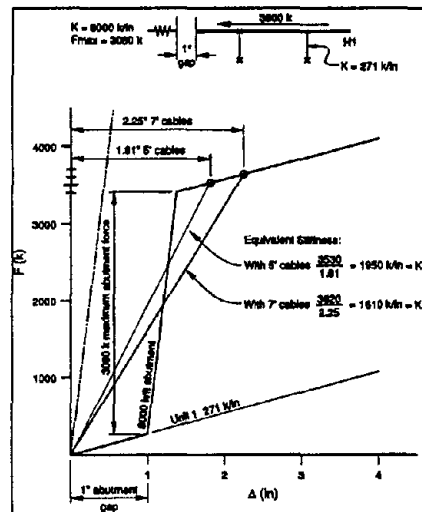
Figure 3. Equivalent Static Analysis

39

quake is calculated using the appropriate response spectra. If the displacement is too large, enough restrainers are added to equal the force of the excessive displacement times the frame's stiffness. Then, the earthquake displacement of the more flexible frame attached to the restrainers is calculated. If the displacement is too large, the number of restrainers is increased and the displacement for the maximum earthquake is recalculated. This procedure is
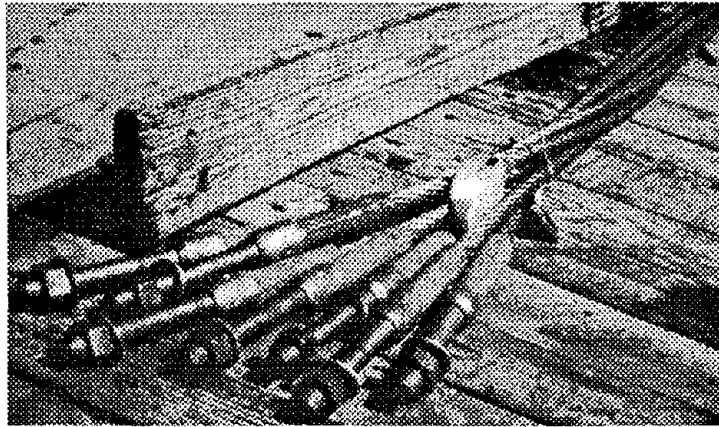
Figure 4. Cable Restrainers

repeated until the number of restrainers remains constant. If the displacement is large enough to impact the next frame, its stiffness should be included in the analysis. For a detailed description of Caltrans' restrainer design procedure, see Caltrans' Bridge Design Aids Section 14. Also, a procedure for calculating the number of restrainers needed to prevent unseating of curved bridges for transverse motion is provided.

The actual behavior of bridges during earthquakes is considerably more complicated than this procedure indicates. The role of pounding, soil-structure interaction, and out of phase motion is not included in our analysis and may increase the amount of displacement at expansion joints. For this reason, new bridges are designed with a minimum 24 inch hinge seat to insure that the allowable displacement is always larger than the earthquake displacement. Also, 2 restrainers per hinge are included to provide continuity.

Properties of Cable Restrainer Assemblies

Restrainer Cables have a 3/4 inch diameter and a 0.22 square inch steel area. They are preformed of 6 x 19 strands, galvanized, with a wire strand core or independent wire rope core, a right regular lay, and made of improved plow steel with a minimum breaking strength of 23 tons. Cable assemblies consist of cables, swaged fittings, studs, nuts, and sometimes turnbuckles, all of which should be 25% stronger than the cable. For more information on restrainers see California's Standard Specifications (Section 75-1.035). Figure 6 shows the behavior of restrainer rods and cables for a cyclic load. The cables (shown at the bottom) have a yield strength of 39.1 kips. This equals a yield stress of 176.1 ksi. They have an initial modulus of elasticity of 10,000 ksi. Note that the post yield strength of the cables increases to an ultimate of about 53 kips. Therefore, connecting elements should be designed for 1.25 x 53 = 66.2 kips. The figure shows that restrainers have a large post yield ductility. This gives the bridge some added protection. See Caltrans' Memos to Designers Section 20-3 for a detailed description of bridge restrainers.
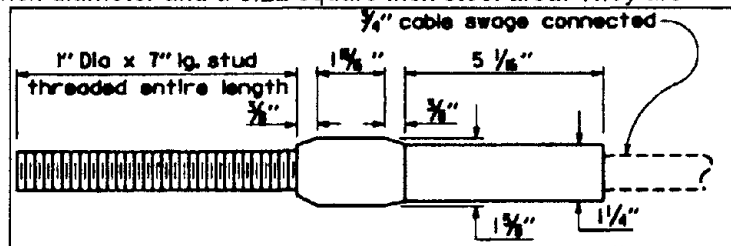
Figure 5. Typical Cable Restrainer
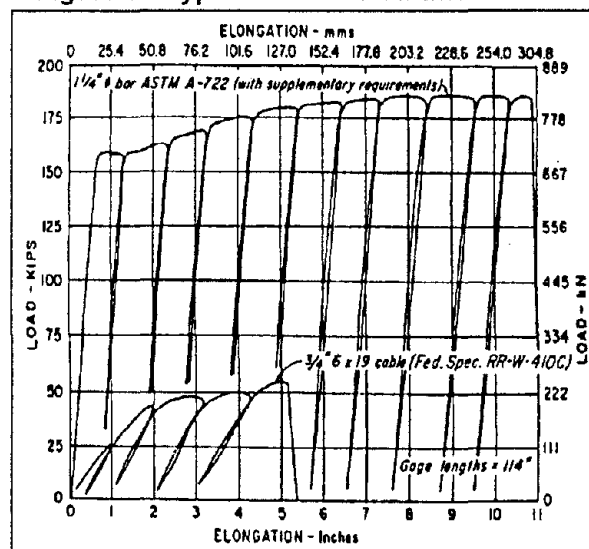
Figure 6. Restrainer Load-Elongation Diagram

40

Typical Cable Restrainer Configurations

There are many different ways that restrainers are installed on bridges. The most common configuration for new and retrofit concrete box girder bridges with adequate hinge seat widths is the Type C1 Restrainer Unit (see figure 7). The Type C1 has 5 cables wrapped around a drum and threaded through holes in the hinge diaphragms. Bolsters are provided on each side of the hinge to distribute the restrainer force into the superstructure. The restrainer units are bolted to metal plates on the other side of the hinge. The nuts are tightened and then backed off a certain amount depending on the ambient temperature. This is to provide temperature movement at the joints without putting the restrainers into tension. Another problem is that the restrainers can

Figure 7. Type C1 Cable Restrainer Unit

go into tension and even fail due to the creep and shortening of prestressed bridges. The restrainer tightening procedure should address all these problems. The information on how much to tighten the restrainers should be included with the plans. Vertical restrainer cables must also be provided at hinges where the vertical seismic force exceeds 50% of the dead load reaction (see figure 8). This is to provide additional protection against the bridge unseating during a large earthquake. These restrainers are to be designed for the larger of 10% of the dead load or 1.2 times the uplift force. For more information, see Caltrans' Bridge Design Specifications Section 3.21.

For concrete box girder bridges where the hinge seat is too small, Caltrans has begun using pipe seat extenders. A hole is cored through the hinge and an 8 inch double strong pipe is inserted in the hole. Then a new bolster anchors the pipe at one end. Cable restrainers are then placed below the pipe (see figure 9). Enough pipe extenders are added to the hinge to support the

Fig. 8 Vertical Restrainer

Figure 9. Typical Pipe Extender Configuration
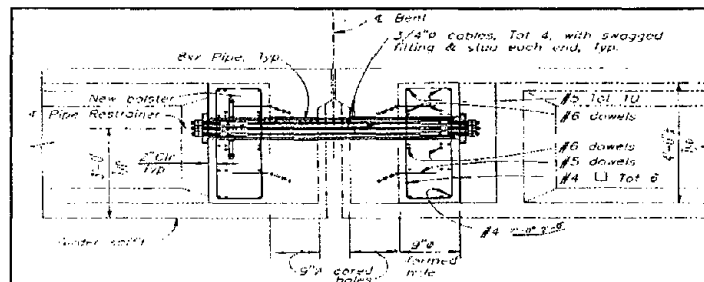
Figure 10. New Pipe Extender Configuration

superstructure if it becomes unseated during the earthquake. A newer design places the cable restrainers inside the pipe to limit coring of the diaphragms (see figure 10). These are the typical restrainer configurations for new concrete box girder bridges and box girder retrofits. For steel and precast girder bridges and retrofits there are a variety of configurations depending on the specific strategy. If the column bents can handle the force, the restrainers are wrapped

41

around the girders and the bent cap. This provides additional restraint to the superstructure. However, if the goal is to isolate vulnerable columns from the superstructure, the steel girders are tied together with cable restrainers or steel plates and the force is resisted at the abutments. Some of these design and retrofit strategies will be shown when the performance of restrained bridges is examined in this paper.
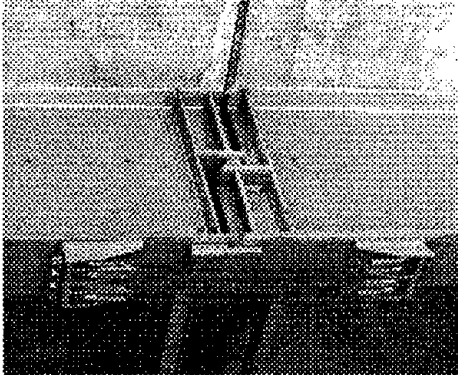
Figure 11. Restrained Steel Bridge at Hinge
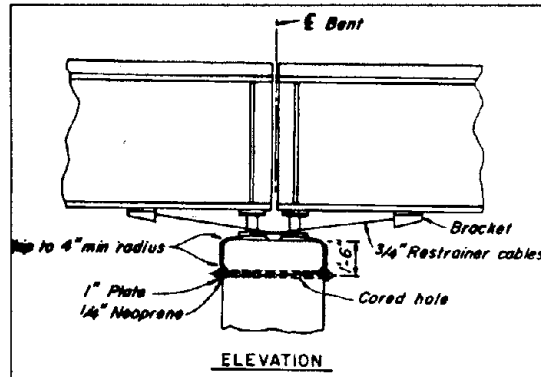
Figure 12. Restrained Steel Bridge at Bent

Bridge Cable Restrainer Research

There has been quite a bit of research done on cable restrainers. Over the years, Dr. Roy Imbsen has written several papers that include studies on the role restrainers play during earthquakes (Penzien and Imbsen 1986). He developed the first bridge expansion joint element that included restrainers in the nonlinear structural analysis computer program NEABS. His studies showed that if enough restrainers were placed at the joints, they helped the separate frames move in phase during earthquakes.

Another study, by UCLA Professor Lawrence Selna was a full scale test of restrainer units attached to concrete anchorages (Selna and Malvar 1987). Among his findings was that there was a potential for the restrainers to puncture the diaphragms. In response, Caltrans limited the number of restrainers to no more than 5 per unit to insure that a ductile failure of the cables occurs rather than a brittle failure of the concrete diaphragm.

After the Loma Prieta earthquake, 2 studies were begun that examined the role of cable restrainers. The results of those studies have recently been presented. The first was an examination of parameters influencing the dynamic behavior of long double deck viaducts by Professor Fenves of UC Berkeley. He found that restrainers were good at limiting displacement, particularly of frames moving out of phase to each other due to differences in stiffness or soil characteristics. However, he found that the current design procedure couldn't predict the maximum displacement very well and could underestimate displacements of end spans. Finally, a 3 year study of the role played by restrainers during the Loma Prieta Earthquake has just been completed by Professors Saiidi and Maragakis of the University of Nevada at Reno. It includes an examination of affected bridges and a computer simulation of their behavior during the Loma Prieta Earthquake. They found that Caltrans' Restrainer Design Procedure leads to a conservative design in terms of the number of restrainers, but that a more refined analysis procedure could result in savings and the elimination of restrainers on some bridges.

Figure 13. U of N Researchers

All of the completed research suggests that cable restrainers do a good job of reducing hinge displacements. The only criticism has been that the design procedure does not accurately calculate the actual displacement when changes in the soil, pounding of the hinge, or other nonlinear and dynamic effects modify the response of the structure.

42

I) The Whitewater Overcrossing (Bridge # 56-0571) During the Palm Springs Earthquake.
This bridge was the first test of the Phase 1 Seismic Retrofit Program. The Whitewater O.C. is a
two simple span, steel girder bridge with a composite concrete deck. It crosses Interstate 10
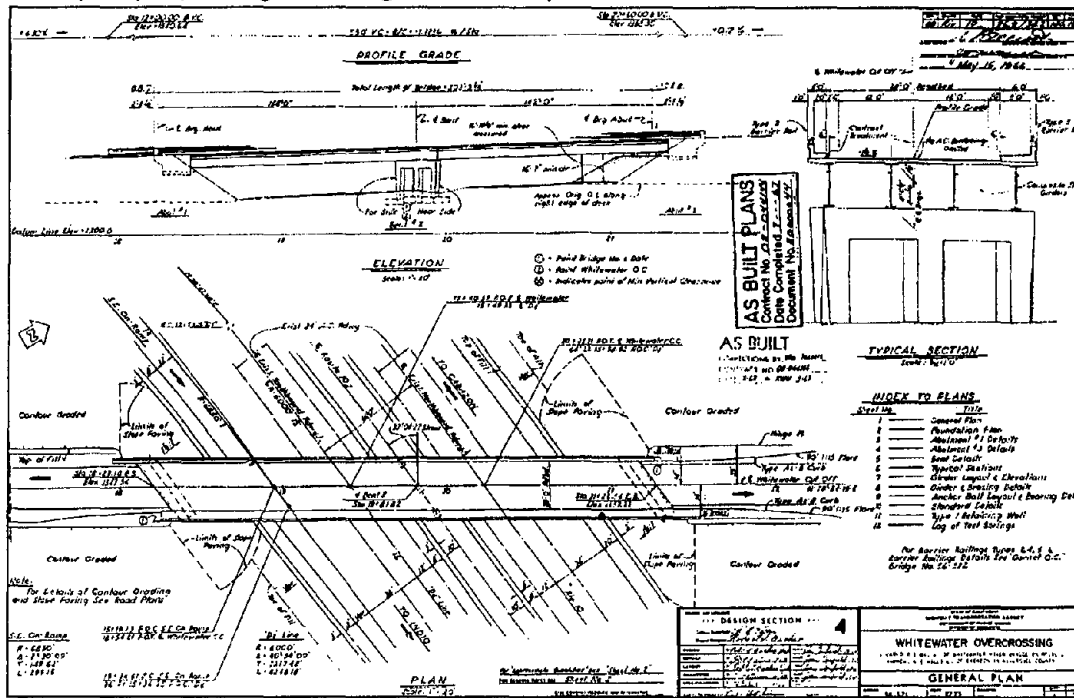
Figure 14. General Plan of Whitewater Overcrossing

about 8 miles northwest of Palm Springs. It has a single 3 column bent, a 37 degree skew, and
seat-type abutments with pedestals. The girders were set on elastomeric pads and were bolted
at the far ends. Keeper angles were used to restrain the girders transversely at the free ends.
This bridge was seismically retrofitted with longitudinal and transverse cable restrainers in 1981.
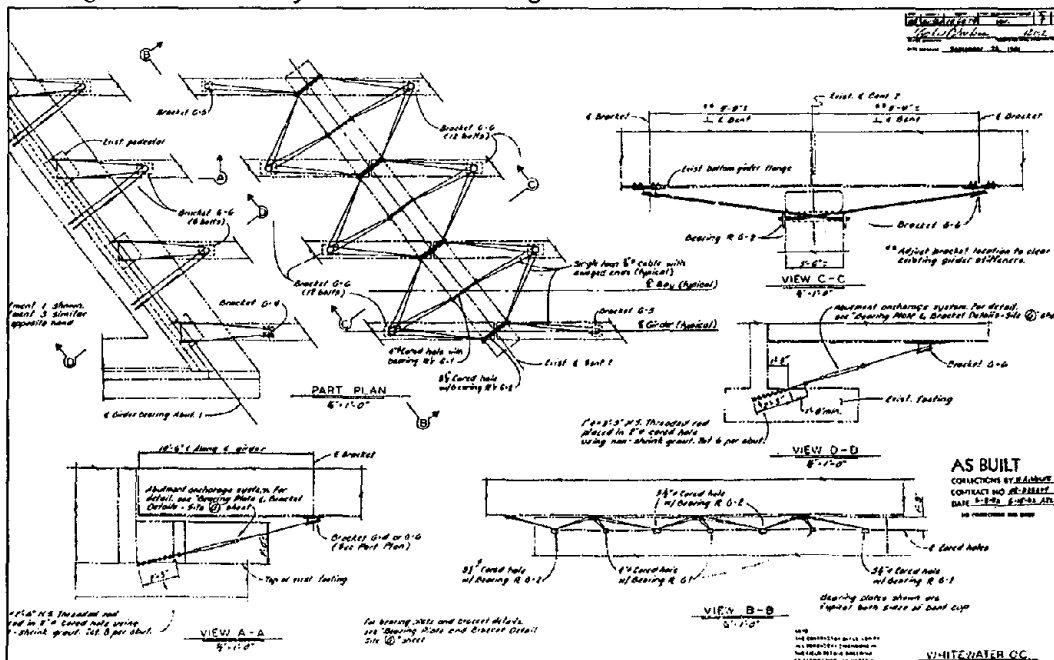
Figure 15. Seismic Retrofit Plan for Whitewater Overcrossing

43

Cable restrainers on steel bridges are usually connected with a turnbuckle that is torqued to a nominal level and locked with jam nuts. In this case the restrainers were wrapped around brackets that were bolted to the bottom girder flanges. The restrainer ends were swaged onto rods that were embedded into concrete at the abutments and were swaged and bolted to bearing plates at the bent cap. The tension could be adjusted by a pipe turnbuckle at the abutments and with a nut at the bent cap.

The Palm Springs earthquake measured 5.9 M_L on the Richter Scale. The Whitewater O. C. was about 6 miles south of the earthquake epicenter and less than 2 miles from the fault. We estimate a maximum ground acceleration of .6g from stations near the bridge.

During the earthquake the superstructure moved in a mainly transverse direction. At Abutment 1 the superstructure came to rest 7 inches west of its original position. All three of the transverse restrainers failed. A turnbuckle broke on one

Figure 16. CSMIP Map and Strong Motion Record for Station 149 Located near Whitewater Overcrossing

restrainer due to an installation error followed by two cable failures. All the keeper angles broke. The abutment pedestals and backwall were heavily fractured. At Bent 2 there was cracking of the bent cap by the inside face of both exterior columns and the metal expansion sleeve pulled apart. At Abutment 3 a restrainer turnbuckle failed and there was concrete cracking around the expansion joint. It appears that at Abutment #1, the keeper angles immediately failed due to lack of confinement at the pedestal corners. Then the force was taken by the restrainers. Unfortunately one of the turnbuckles wasn't tightened all the way and the threads failed.

44

After the initial failure the remaining restrainers couldn't take the load and failed. A restrainer at Abutment 3 also failed by stripping of the turnbuckle threads. However this occurred later during the earthquake and without the large movement that occurred at Abutment #1.

There are several lessons to be learned from this bridges' behavior during the Palm Springs Earthquake. The most obvious point is that simply supported spans are extremely lively during earthquakes. Caltrans' revisited this bridge after the Joshua Tree, Landers, and Big Bear Earthquakes. It had been thoroughly repaired with better restrainers and keeper plates and yet evidence suggests that it still jumped around. Less damage was done during these other earthquakes and no restrainers failed, however, the steel girders did manage to slam into the abutments smashing up some concrete.

For moderate earthquakes, these loose structures with several expansion joints rack up more damage than monolithic bridges with diaphragm type abutments. Which kind of bridge does a better job during a very large earthquake remains to be seen. However, Caltrans' general view is that many of our problems are a result of expansion joints on the structure (and the rest of our problems come from nonductile details and poor soil).

The second lesson is that restrainers may not be necessary on this bridge. For a short, 2 span bridge, where is it going to go? The spans just banged against the abutments and then banged together until the earthquake ended. All the damage was spalling of concrete. Restrainers probably play a bigger role on long, tall bridges where there's some chance of the superstructure falling off the substructure. Even though all the restrainers and keeper angles failed at Abutment #1, no collapse occurred.

However, the third lesson is that its reassuring to have restrainers on bridges. A little added insurance is always welcome. Restrainers do limit large displacements (although they don't seem to control minor banging) A little redundancy is a good thing. And the lack of redundancy was the major problem with this bridge. There were
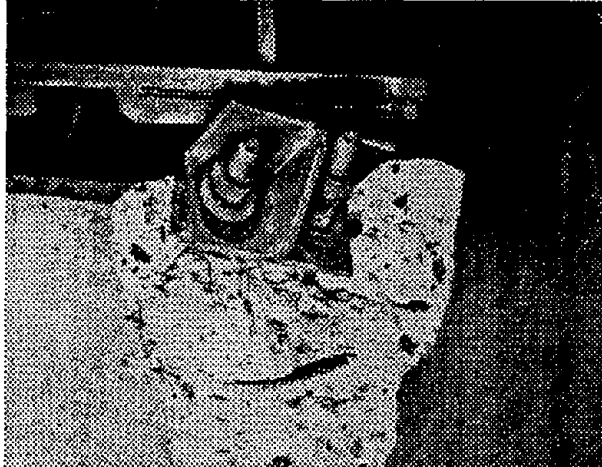
Figure 17. Keeper Angle Failure at Whitewater O.C. Abut. 1 During the Palm Springs Earthquake.
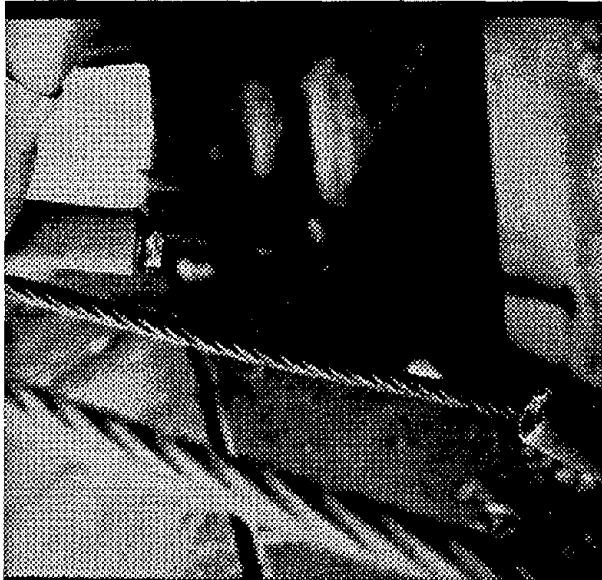
Figure 18. Broken Restrainer Turnbuckle at Abut. 1
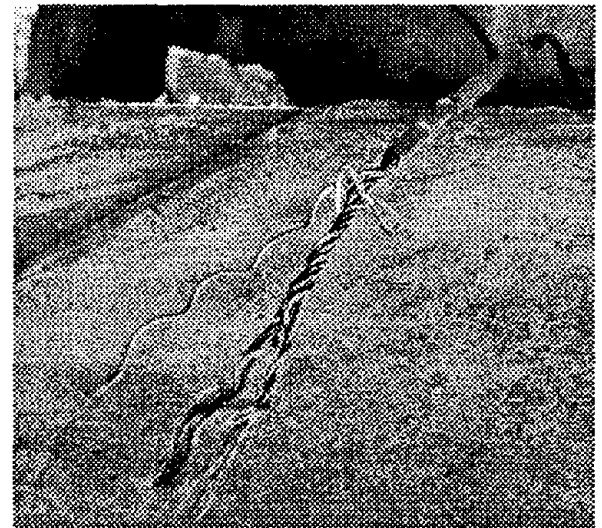
Figure 19. Cable Restrainer Failure at Abut. 1

45

not enough restrainers installed to handle the acceleration of the deck after the first restrainer failed. A little redundancy would have resulted in far less damage. Every seismic device adds another layer of protection to the structural system. If the keeper angles break, the transverse restrainers can hold the structure. If one restrainer breaks, there are others to take the load.

Another problem with this bridge is the high skew of the expansion joints. The large movements may be partially the result of the ease with which the superstructure can come off a skewed abutment seat.

Figure 20. Damage at Whitewater O.C. Abutment 1 Expansion Joint

A final lesson can be gained from the way the restrainers failed. Good construction practices would prevent such damage from occurring. All too often we've seen restrainers on bridges that are hanging loose or with some hardware left unattached. Familiarity with the plans and the purpose of these devices by construction personnel will result in better performance of seismic controls during earthquakes.

The premier performance of a seismically retrofitted bridge during a moderately strong earthquake gave an ambivalent message about cable restrainers. No catastrophic damage occurred but probably more than we would have liked. This was the result of poor construction and poor details. With better restrainers the results are as shown in figure 21 during the 6.1 M_l Joshua Tree Earthquake. The results of that earthquake show that when the restrainers are properly designed much less damage occurs.

A more detailed study of this bridge can be obtained from a paper by Professor Maragakis of the University of Nevada that analyzes this bridge's behavior for the Palm Springs Earthquake (Maragakis 1992).

Figure 21. Damage at Abutment #3 from the April 1992 Joshua Tree Earthquake

46

II) The Port of Oakland Overcrossing (West Grand Blvd. Viaduct)

This steel girder bridge was built in 1937 and was modified in 1964. The main structure is 5445' long. It spans highway 80, railroad tracks, city streets, and an army base in the City of Oakland.
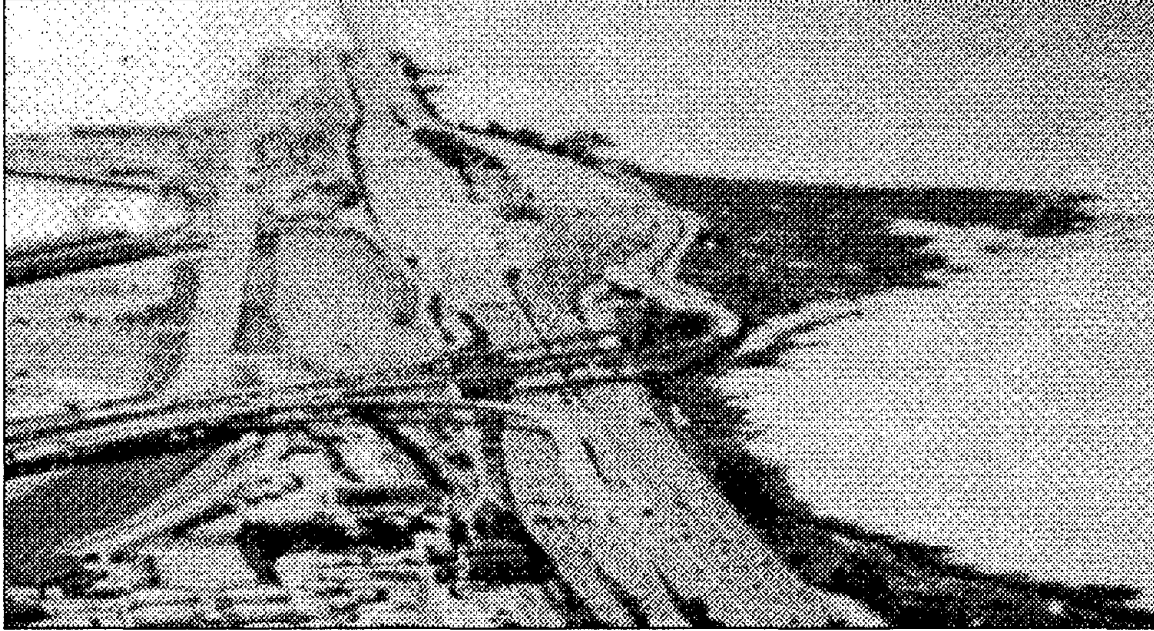
Figure 22. Aerial View of the north end of the Port of Oakland Overcrossing going over I-80

The bridge is mostly simple spans on roller bearings and some cantilever spans with drop in spans on roller bearings.
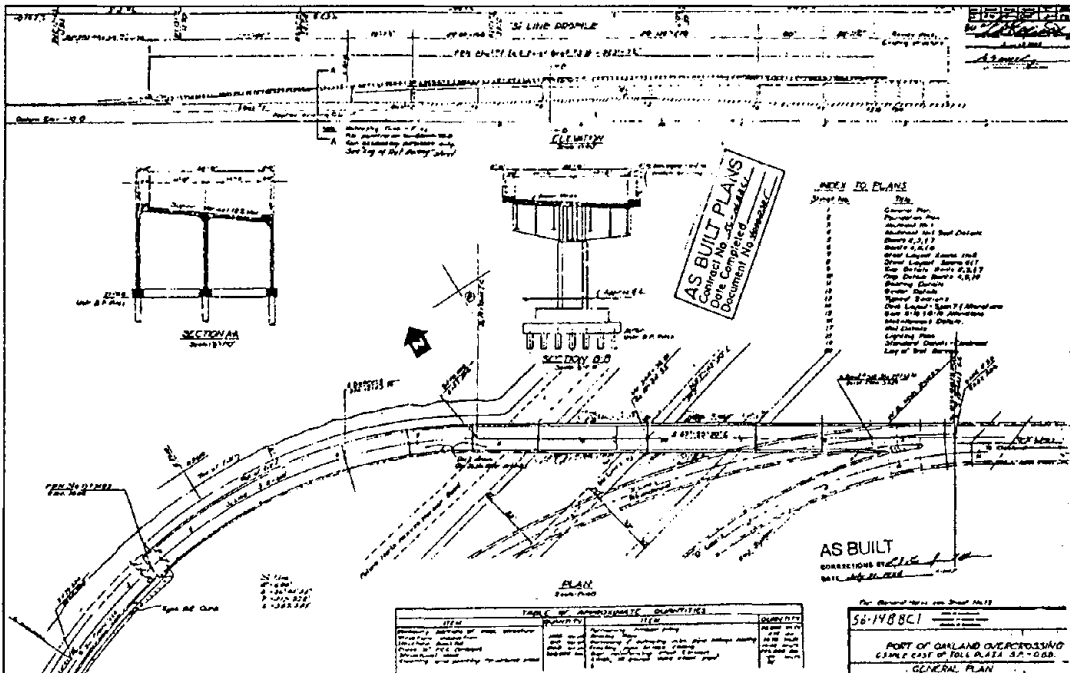
Figure 23. General Plan of the Port of Oakland Overcrossing

47

This bridge was seismically retrofitted in 1976. The retrofit consisted of longitudinal restrainers at each joint connected by steel brackets to the bottom girder flange or web on each side of the web.
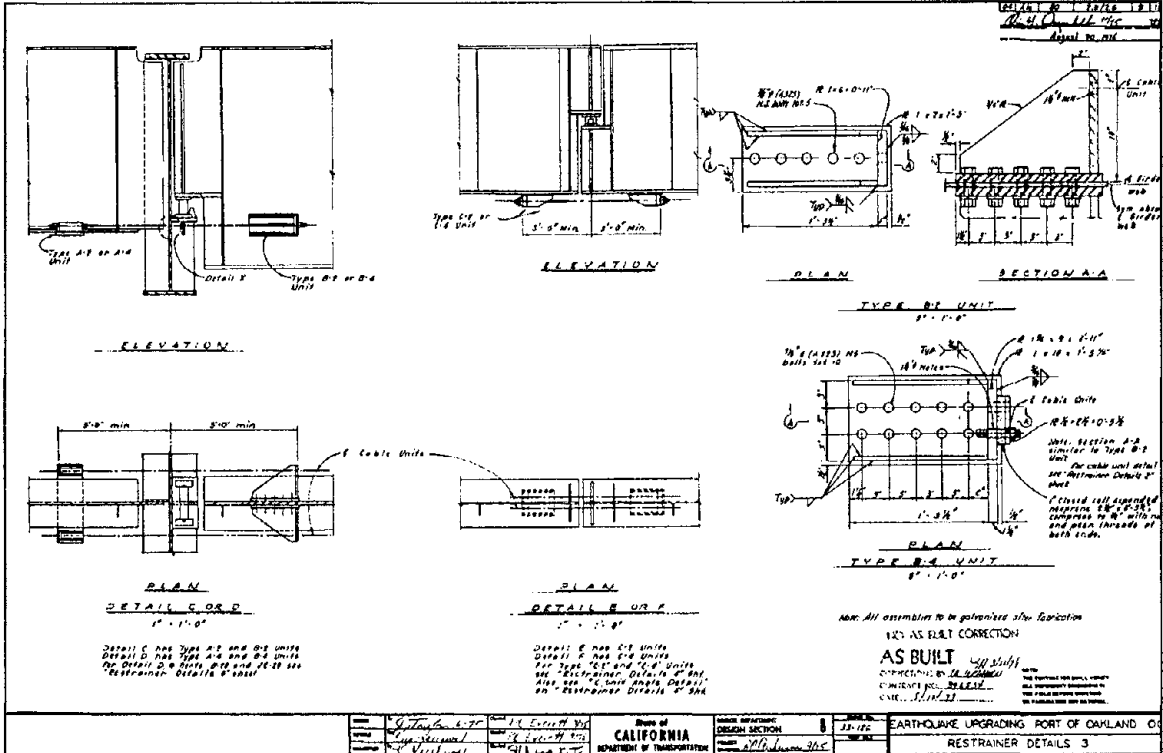
Figure 24. Port of Oakland Seismic Retrofit Details

At a couple of locations the bent cap was widened to provide a seat to catch the girder ends.
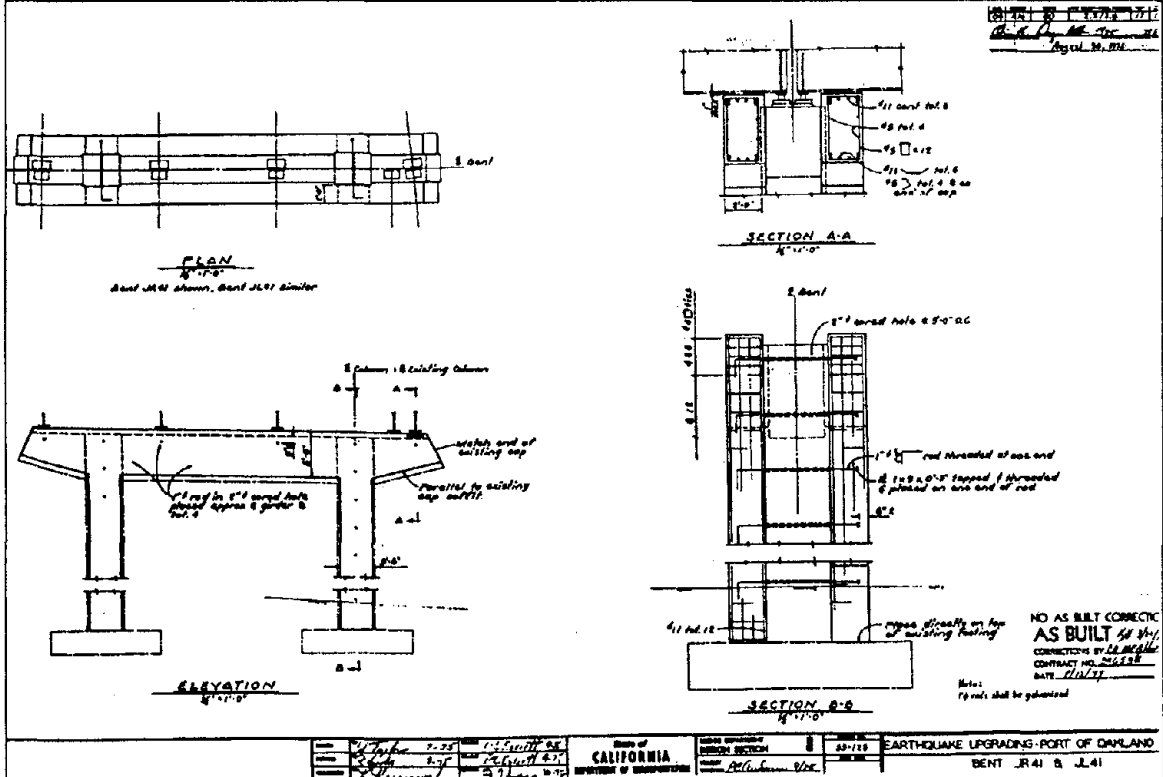
Figure 25. Port of Oakland Seismic Retrofit Details

48

Although this bridge is about 80 miles north of the epicenter of the Loma Prieta Earthquake, the soft sediments of this area seem to have accentuated shaking of this bridge. We estimate a maximum ground acceleration for the area of about 0.30g. However, cable restrainers were routinely designed for 0.25g in the mid 70's. During the earthquake the girders moved diagonally up to 14 inches with most anchor bolts and keeper plates broken, buckled cross-bracing, and many cable restrainers broken or overstressed. There was also some spalling at a few columns.
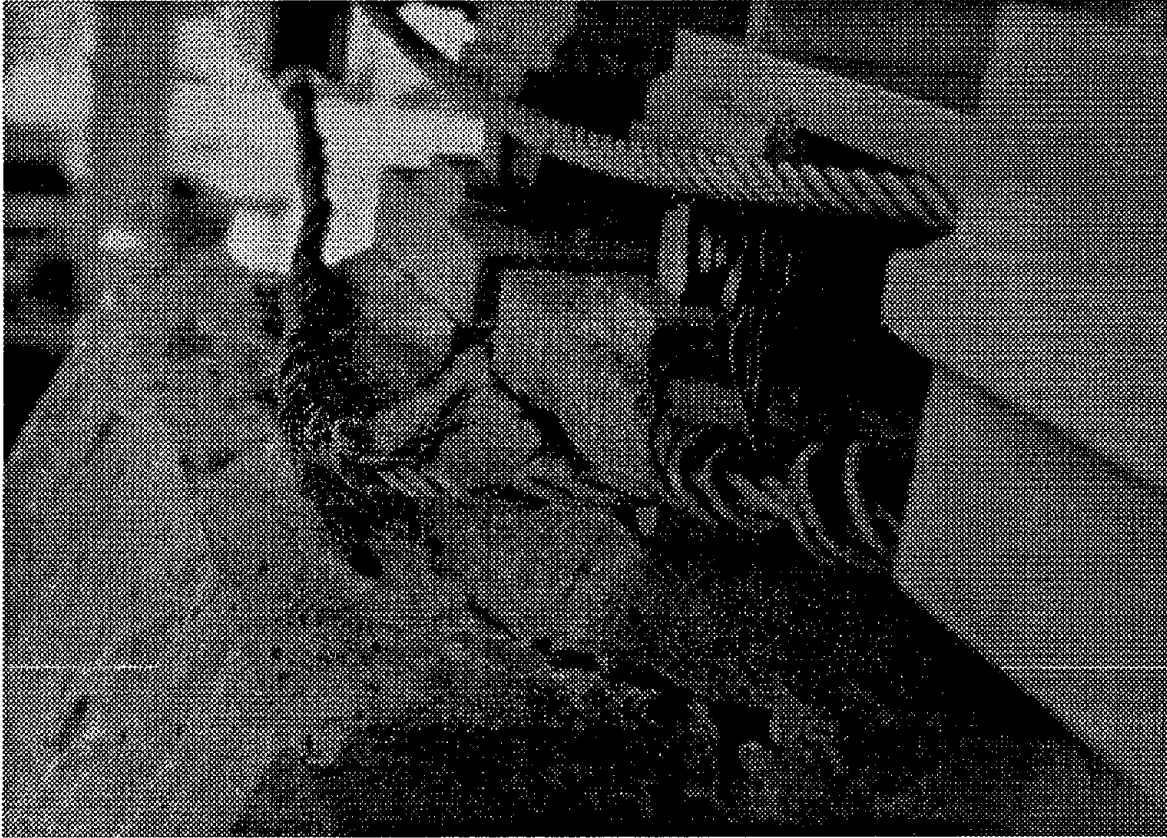
Figure 26. Loma Prieta Earthquake Damage to Port of Oakland Overcrossing

However, this bridge remained open for a while after the earthquake and was even used to carry timber shoring to a more severely distressed structures in the area. Considering the soft soil conditions in this area and the damage to nearby structures this retrofit appears to be a success. The restrainers were all activated holding the structure together. Research would give a better picture of how the restrainers performed for this long, steel structure.

III) Napa River Bridge (Br. # 23-64) During the Loma Prieta Earthquake

This 3280 foot structure crosses the Napa River on State Route 37 in Solano County. It was built in 1966. It is a 25 span precast prestressed I girder bridge. As the bridge climbs over the river it rises to over 100 feet in the air. The supports alternate between 3 or 4 flexible piers and a more rigid tower. The bridge is mostly simple spans with 2 cantilever spans and a drop in hinge span at the main river span of the bridge.
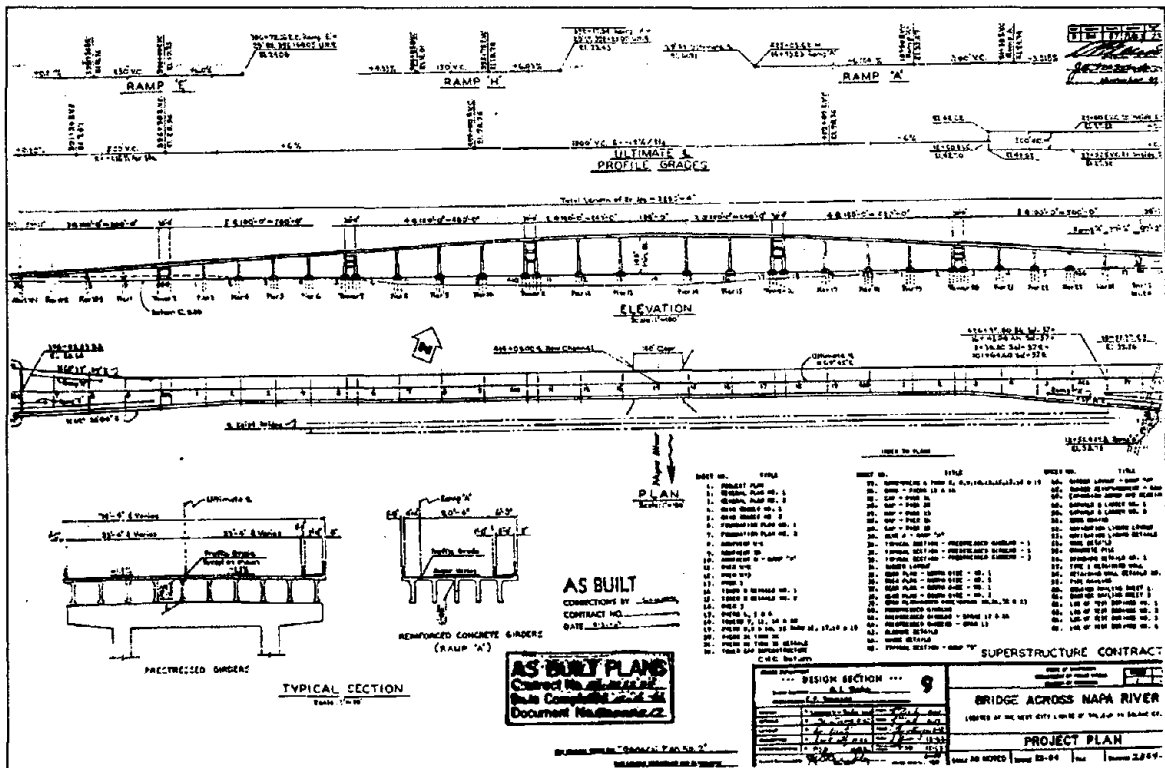
Figure 27. General Plan of the Napa River Bridge

During construction two inch cored holes were drilled at the ends of the precast I girders and #6 bars were inserted. Then the bent caps were poured. At 8 locations an expansion joint was placed between the I girder spans. In these locations one of the girder end spans rests on a rocker bearing and 1-1/2" bolts were placed in each bay to hold the spans together.

50
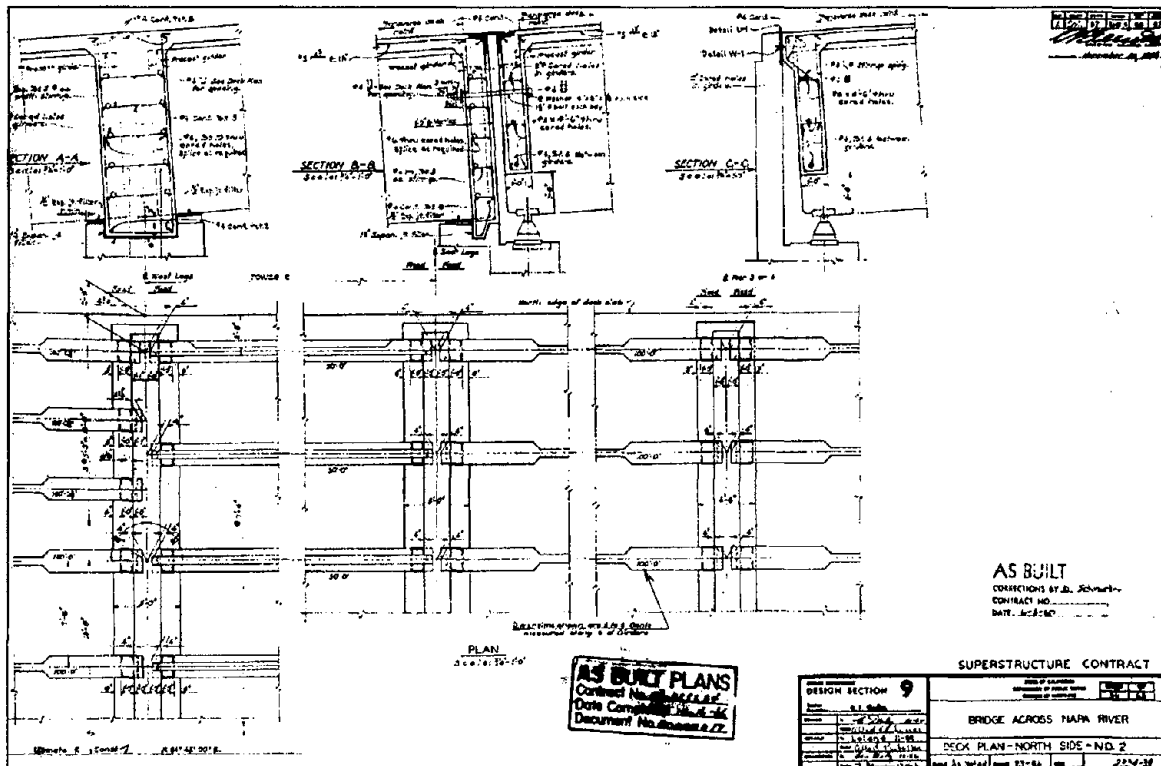
Figure 28. Precast Girder End Details for the Napa River Bridge

This bridge was seismically retrofitted in 1983. The retrofit consisted of restrainers at the expansion joints and the two hinges. Rocker bearings at abutments were replaced with concrete blocks that also acted as shear keys.
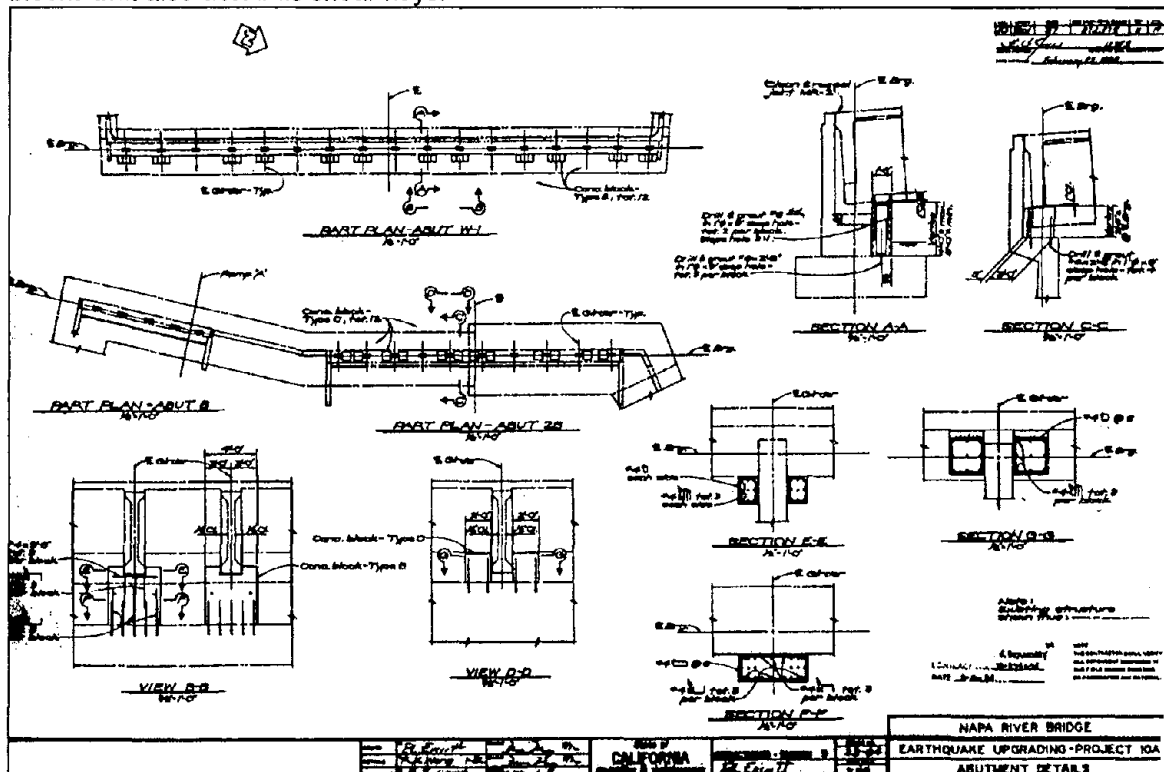
Figure 29 Napa River Bridge Earthquake Retrofit Details at Abutments

The rocker bearings at the piers were replaced with elastomeric pads on new concrete pads doweled into the cap. Longitudinal and transverse cable restrainers were wrapped through cored holes in girders and diaphragms at expansion joints and hinges.
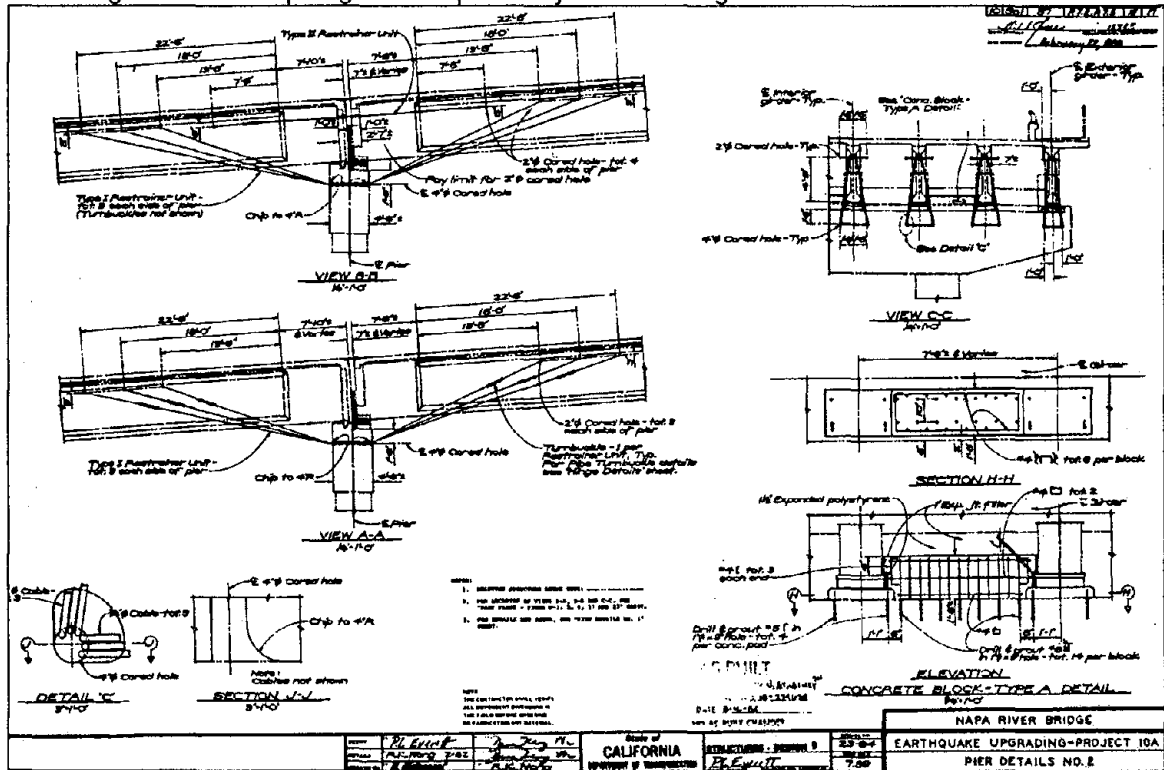
Figure 30. Napa River Bridge Cable Restrainer Details

This bridge is located approximately 110 miles north of the epicenter of the Loma Prieta Earthquake. The accelerations from the CSMIP strong motion records in this area were only about 0.lg. However, this tall, flexible structure was strongly shaken by the October 17th earthquake. The girders pulled out of their diaphragms at piers 12 and 15. These were at fixed locations without earthquake restrainers. Five inches of the girder ends sheared off along the horizontal holes provided for the continuous horizontal reinforcement in the diaphragms. This turned the fixed joints into expansion joints. However, the girders still retained about 12" of seat. There was major concrete spalling between girders and diaphragms at many other locations. The hinge at span 13 closed an additional 4". The earthquake restrainers at this hinge were slack with a great deal of spalling around the bent cap and appear damaged. The transverse earthquake restrainers and shear keys were damaged at piers 9 and 17. Quoting from the maintenance report; "...This structure has sustained much damage from the October 1989 earthquake. The EQ restrainers were damaged, however, catastrophic failure of the structure was prevented by their presence."

A thorough analysis of this structure will explain why so much damage occurred to a structure so far away from the epicenter of the earthquake. Like the Whitewater O.C. and the Port of Oakland O.C., the precast I girders jumped around during the earthquake. Moreover, the peirs are on long piles that are unsupported for the 30 feet to the river bottom. Below that is soft soil. We know that as an earthquake travels farther from the epicenter the high frequency waves fade and the long frequency waves dominate. Apparently, the long frequency content of the waves closely matched the natural frequency of this very flexible structure. Caltrans' Structural Design Section 8 is currently analysing this structure as part of the seismic retrofit for this bridge. This analysis should provide insight into Napa Rivers' behavior during the Loma Prieta Earthquake.
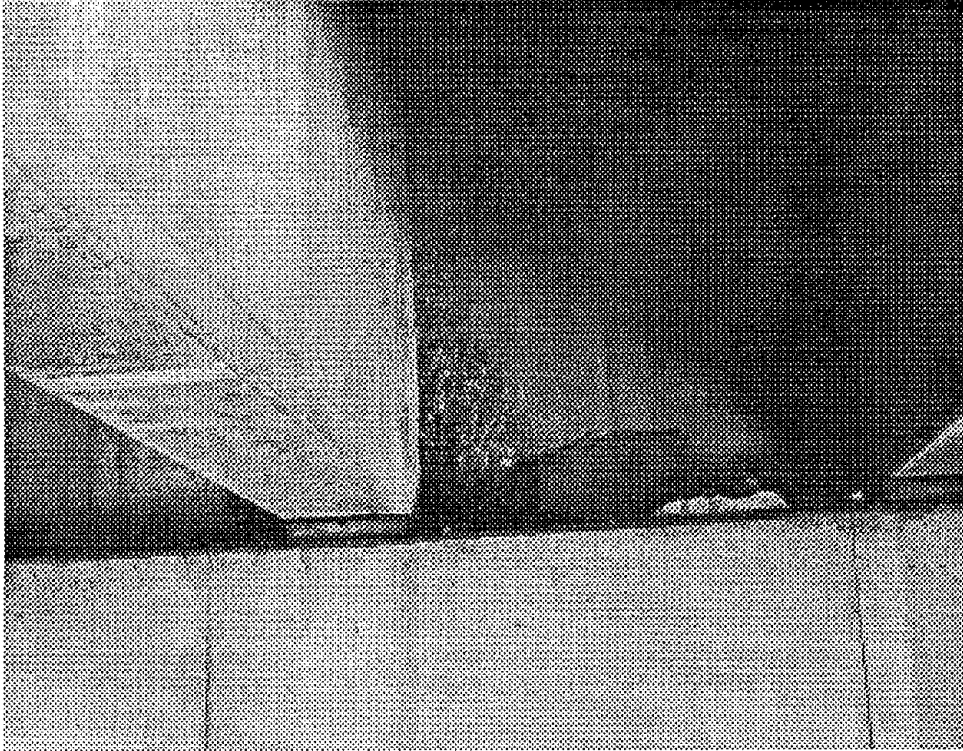
Figure 31. Napa River Bridge Earthquake Damage at Fixed Joint

Figure 32. Napa River Bridge Earthquake Damage at Fixed Joint

53
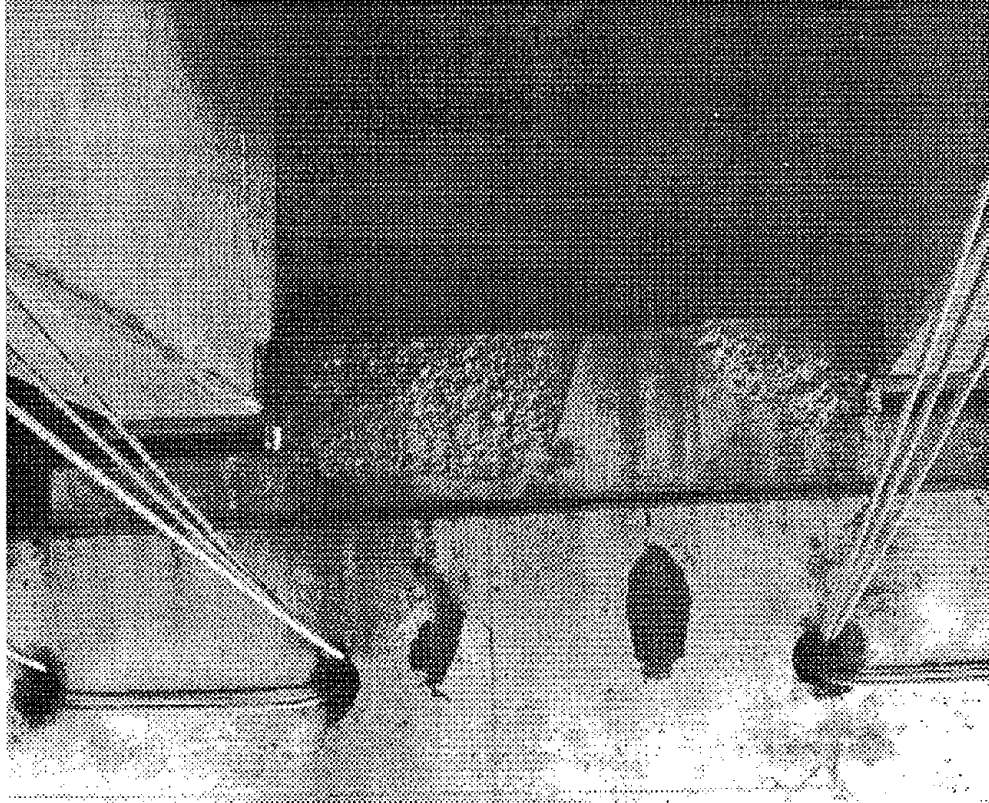
Figure 33. Napa River Bridge Earthquake Damage at Expansion Joint
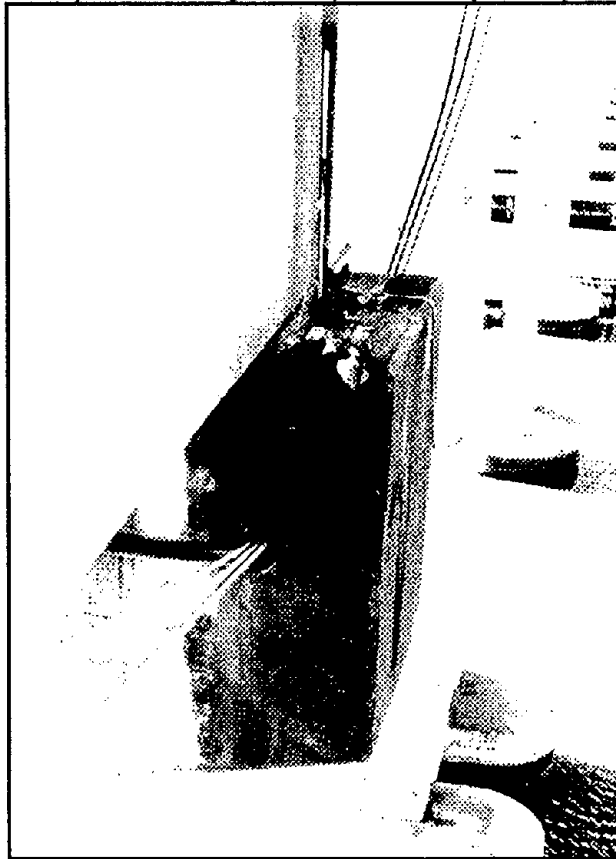
Figure 34. Napa River Bridge Earthquake Damage at Expansion Joint

IV) Route 24/580/980 Interchange North and East Connectors (Br. #33-302H & 33-304G)

These are long, tall, curved, box girder bridges on 460 feet of firm alluvium. All of these conditions cause the bridges to have a lot of displacement during earthquakes. The bridges were originally constructed in 1970 and were retrofit with Cable restrainers and 1-1/2" high strength rod restrainers in 1980. As can be seen from figures 1 and 2, the structures' elaborate geometry makes portions of it particularly sensitive to the direction of the earthquake. During the Loma Prieta Earthquake the North and East Connectors experienced punching shear failures in hinge diaphragms. This was caused by the rod restrainers overstressing the diaphragm during the earthquake. The damage in the North Connector occurred at hinge #33 and in the East Connector at hinge #20. We estimate a peak lateral acceleration of 0.25g at the base of these structures during the earthquake from instruments near the site. As mentioned previously, research by Professor Selna of UCLA identified that failure should occur in the ductile restrainers rather than in the brittle diaphragm and made specific recommendations such as using bolsters and spacing the restrainers to avoid overstressing the concrete. In many locations this was done. However, at these 2 locations bolsters were not provided and too many high strength rods were placed together. Two research studies examined these structures. An analysis of the structures was performed by Dr. David Liu and the results are to be summarized in a paper for the Fifth U.S. Earthquake Engineering Conference in 1994. A field investigation was also performed by Professors Saiidi and Maragakis of the University of Nevada at Reno as part of their restrainer research project. Both studies concur that failure was a result of placing too many restrainers too close together and without sufficient shear strength in the diaphragms. This situation is exacerbated by the use of high strength rods with
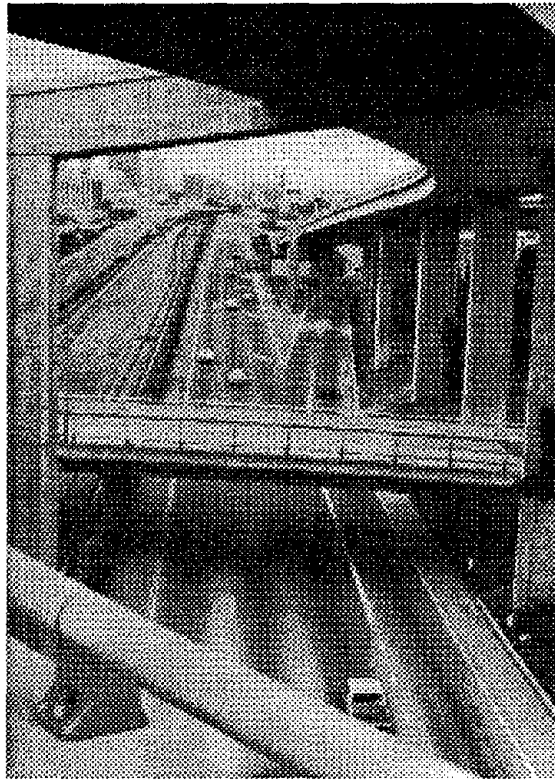
Figure 35. Part of 24/580/980 Facing Oakland
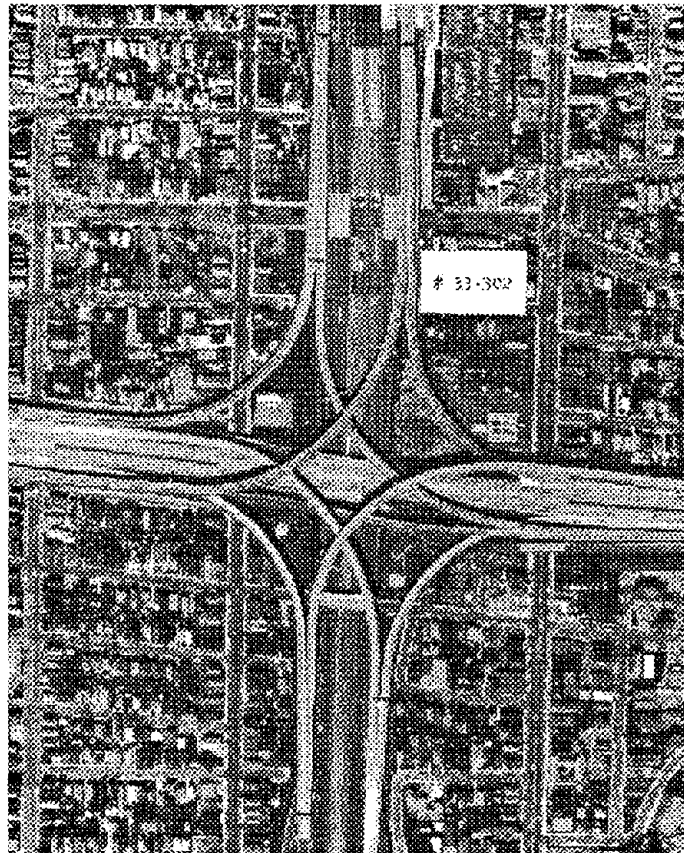
Figure 36. Plan View of Route 24/580/980

their significantly higher yield strength. Therefore it is recommended that all connections to restrainers be designed to handle 25% more force to assure yielding of the restrainers.
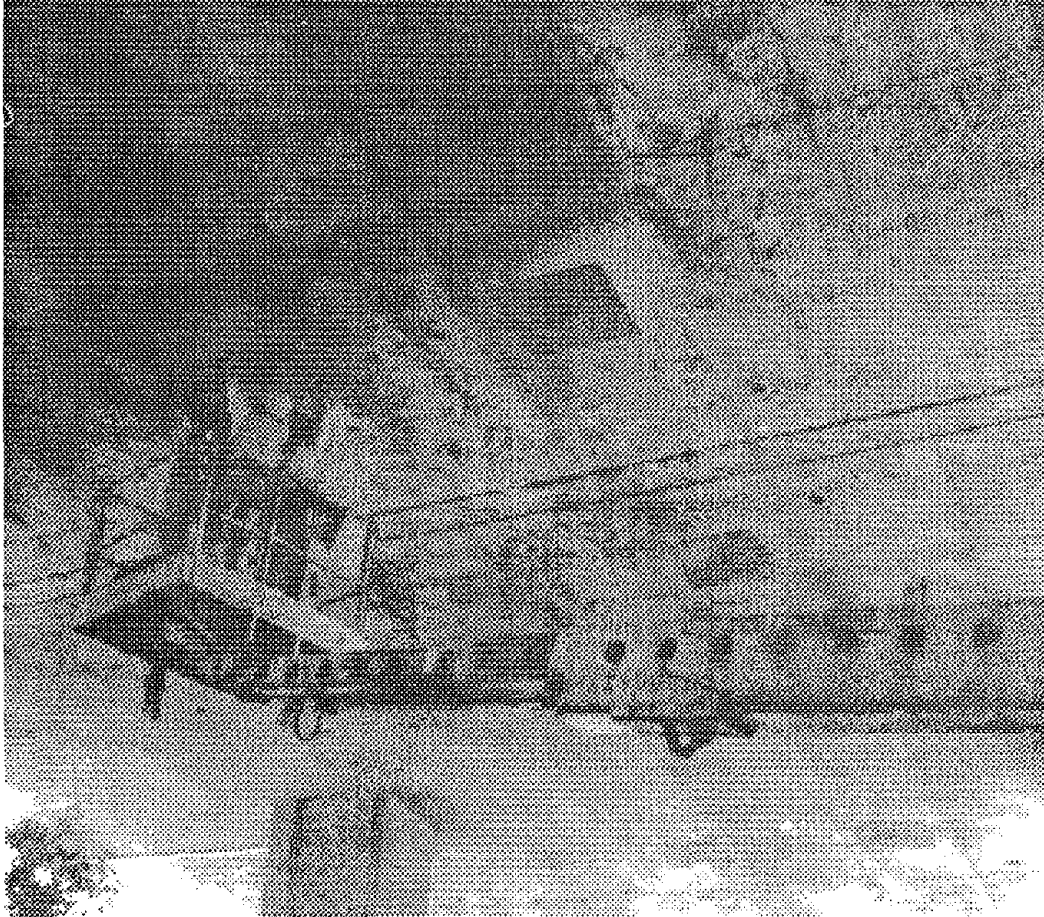
Figure 37. Access into Box Gider Bays for Studying Restrainers at Damaged Hinges
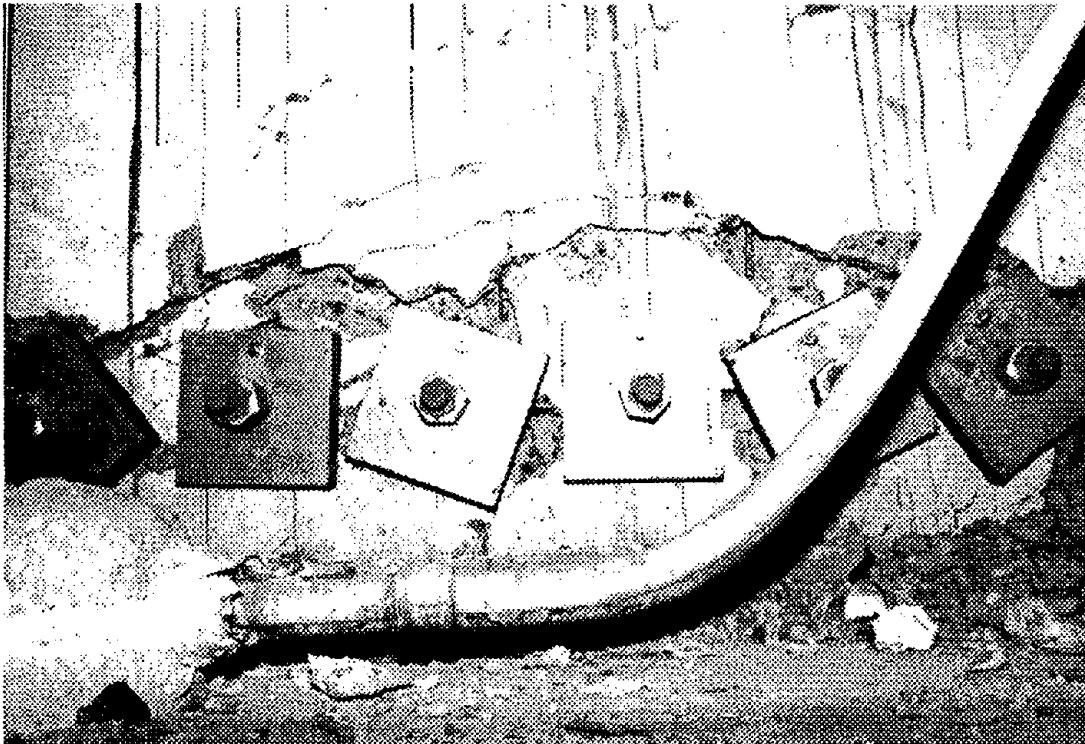
Figure 38. Punching Shear Failure of Hinge Diaphragm

Figure 39. Looking up at Bridge Soffit Damage from Hinge Diaphragm Punching Shear Failure
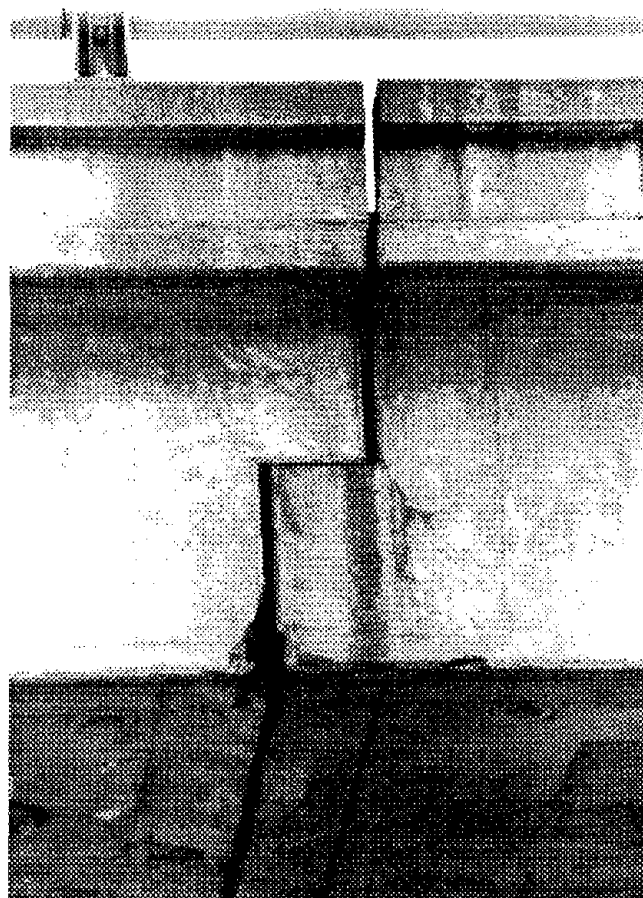
Figure 40. Elevation View of Hinge Damage

V) Strouve Slough Bridges (Br. #36-88L&R) During the Loma Prieta Earthquake

These are 2 long reinforced concrete T-beam bridges supported by long pile shafts in a very soft soil. During the Loma Prieta Earthquake the soil moved like jello taking the pile shafts for a ride. The tops of the shafts sheared through the drop bent caps and drove through the bridge deck causing a collapse of both bridges. This caused a closure of this portion of Interstate 1 near Santa Cruz for several months after the earthquake. Amazingly, the restrainer cables at all hinges held the superstructure together even as it fell to the ground.

Figure 41. Elevation View of Damaged Bridge with Cable Restrainer Holding Hinge Together.

58
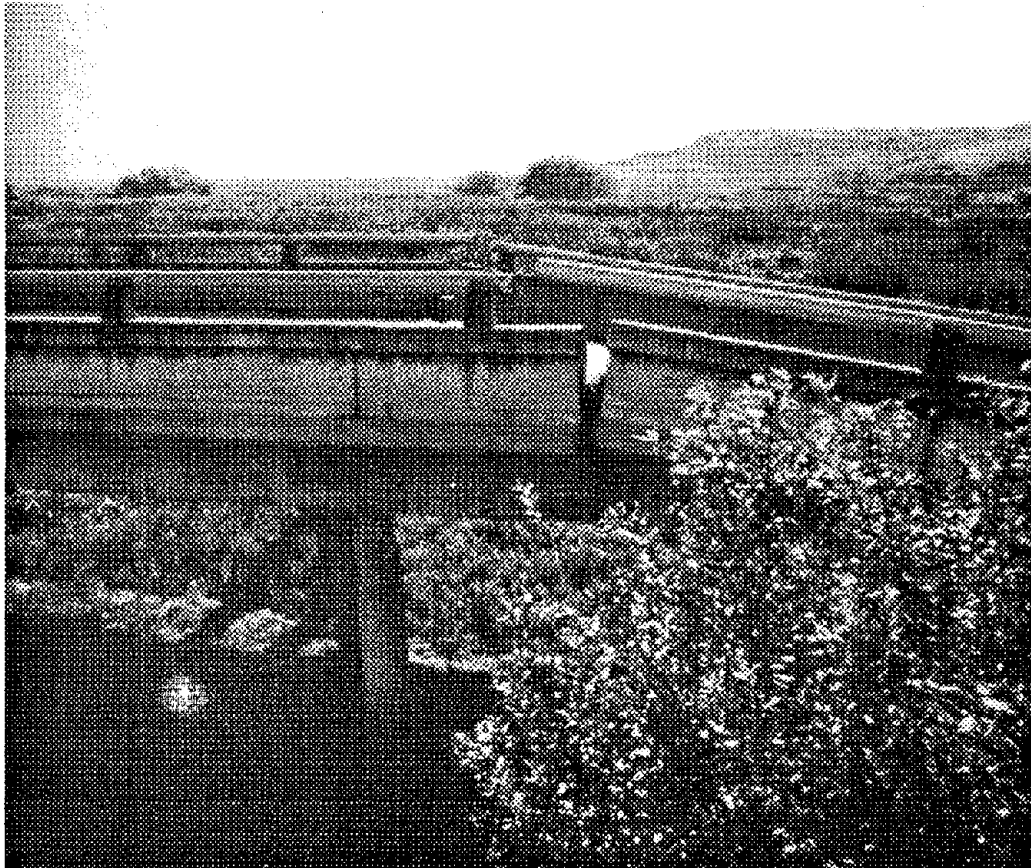
Figure 42. Elevation View of Damaged Bridge with Hinge Remaining Closed

Figure 43. Damage occurring at Strouve Slough during the Loma Prieta Earthquake

Conclusions

This paper gives an overview of Caltrans' use of restrainers to prevent bridge damage during earthquakes. Restrainer properties, restrainer research, and performance of restrainers during earthquakes are shown.

Over 200 bridges with restrainers were shaken by the Loma Prieta Earthquake and performed well. Restrainers also performed well during the recent Landers and Cape Mendocino Events. All the research conducted so far suggests that cable restrainers are an effective method of reducing seismic motion at hinges. However, recent research also points out that the actual displacement during a major earthquake is hard to predict with our current method of analysis. That is why new bridges are designed with sufficient seat to handle the maximum credible event. That is also why seismic retrofits are typically provided with seat extenders. However, research also shows that the current design procedure for restrainers is conservative for all but a few cases. This could be where the dynamic properties of the system change dramatically between 2 frames, or where the soil and stiffness of the structure abruptly changes or near the end of a long bridge where there's a sudden change of stiffness. Also, research and experience show that the restrainer connections must be significantly stronger than the restrainer yield strength to allow the restrainers to function properly.

The examples shown give evidence that restrainers are capable of preventing significant damage for large earthquakes. However, more research is needed. Restrainers are typically used between adjacent frames and also to hold simple spans together. More research and better analytical tools are needed to simulate each of these conditions. As mentioned previously, better methods of calculating the maximum displacement are needed. Analysis that consider all nonlinearities of the system including banging of different parts of the hinge, soil behavior, column steel pulling out and yielding, as well as better time histories will result in better predictions of displacement. Also the design of restrainers for curved and skewed bridges where transverse movement can activate the longitudinal restrainers needs refinement. Current research by Dr. Roupen Donikian of Cygna Engineers on the behavior of the five mile long concrete trestle portion of the San Mateo Bridge will give insight on how the gradual change of soil conditions affects a very long cable restrained structure. Current work by Professor Greg Fenves of U.C. Berkeley into the behavior of the Northwest Connector of the Colton Interchange will help our understanding of how curved bridges with many restrained hinges performs for large earthquakes. Work by Dr. David Liu of Imbsen and Associates on the 24/580/980 Interchange on the sensitivity of long tall Y Connectors having many restrained hinges to the direction of the earthquake force should provide useful information.

We have seen that restrainers can limit the earthquake damage for bridges like Whitewater Overcrossing. We have seen that they can keep a superstructure together even if the substructure fails as in Strouve Slough. They can perform a role both to prevent catastrophic damage and to maintain serviceability of the structure. More knowledge on how their role changes for stiff and flexible structures, for curved and straight structures, for long and short structures, for simply supported and continuous structures will provide more efficient seismic designs in the future.

References

Imbsen, Roy, Richard Nutt, and Joseph Penzien. "Seismic Response of Bridges-Case Studies." University of California Earthquake Engineering Research Center 78-14 (1978)

Imbsen, Roy, and Joseph Penzien. "Evaluation of Energy Absorption Characteristics of Highway Bridges Under Seismic Conditions." University of California Earthquake Engineering Research Center 84-17 (1986)

Selna, Lawrence G.and L. Javier Malvar. "Full Scale Experimental Testing of Retrofit Devices Used for Reinforced Concrete Bridges." University of California Earthquake Engineering Structural Laboratory 87-01 (1987)

Maragakis, E., M. Saiidi, and S.M. Abdel Ghaffar. "Evaluation of the Response of the Whitewater River Bridge During the 1986 Palm Springs Earthquake." U.S.-Japan Conference on Bridge Behavior (1992)

Liu, W.D., et al. "Seismic Performance Assessment of a Highly Curved Interchange Structure During the Loma Prieta Earthquake." Fifth U.S. National Conference on Earthquake Engineering (1994)

Caltrans. "Bridge Memos to Designers" California Department of Transportation -Division of Structures (1992)

Caltrans. "Bridge Design Specifications" California Department of Transportation -Division of Structures (1986)

Caltrans. "Bridge Design Aids" California Department of Transportation -Division of Structures (1992)

Caltrans. "Standard Specifications" California Department of Transportation (1992)

Fung, George, et al. "Field Investigation of Bridge Damage in the San Fernando Earthquake." California Department of Transportation -Division of Structures (1971)

Mellon, Steve "Highway Bridge Damage from the Palm Springs Earthquake." California Department of Transportation -Division of Structures (1986)

SECOND U.S.-JAPAN WORKSHOP
ON SEISMIC RETROFIT OF BRIDGES
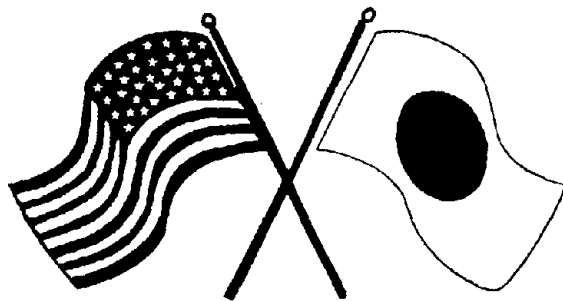
Seismic Retrofit of Bridges in Northern Nevada

M. Saiidi, E. Maragakis, D. Sanders
and D. O'Connor

SEISMIC RETROFIT OF BRIDGES IN NORTHERN NEVADA

M. Saiidi, E. Maragakis, D. Sanders, and D. O'Connor

Civil Engineering Department
University of Nevada
Reno, Nevada 89557, USA

ABSTRACT

This study was undertaken to evaluate the highway bridges on I-80 in the Reno-Sparks area for their damage potential during strong earthquakes. A data base consisting of a total of 26 bridges was formed. The focus of the study was on bridges with relatively thin, tapered columns. Three representative bridges were analyzed to determine their displacement histories, abutment force histories, and column forces and displacement ductility demands in response to a suite of representative earthquake acceleration. The nonlinear analyses were conducted using computer program NEABS. Results of the nonlinear analyses indicated that in bridges with one or two columns per piers, abutment soil yielding may occur and that the column shear forces and moments may exceed permissible values.

INTRODUCTION

The October 1989 earthquake in Loma Prieta, California renewed the interest in a careful re-evaluation of existing bridges which were designed based on codes developed before 1971, particularly those in areas with the expected peak bedrock acceleration of 30 percent of gravity or higher. Many of the highway bridges in the northwest part of the State of Nevada fall in this category. These bridges were designed prior to the development of extensive modern codes on seismic design of bridges, and hence are likely to be vulnerable.

To determine the degree of seismic vulnerability, guidelines developed by the American Association of State and Transportation Officials (AASHTO) may be used. The guidelines may be supplemented by detailed response history analyses of the bridge for earthquake records which are representative of the historical ground motions at the bridge site. The inadequate bridge components need to be strengthened to improve their seismic performance to the level anticipated during the expected earthquakes.

More than 25 bridges located in the Reno-Sparks area in Northwestern Nevada have been targeted for seismic retrofit in the next few years. A study is in progress at the University of Nevada, Reno, to (1) estimate the degree of seismic vulnerability of these bridges based on response history analyses of representative bridges and (2) develop and test retrofit details for bridge components which are found to be most vulnerable. The first part of the study was

completed in September 1993. Test specimens which model typical bridge components are currently being designed and constructed. The purpose of this paper is to present the first part of the study and discuss some of the work which is in progress.

DESCRIPTION OF BRIDGES

The bridges considered in this study are listed in Table 1. The table includes the structures that compose the Interstate 80/U.S. 395 interchange as well as 13 other bridges located in the Reno-Sparks area. Some bridges consist of two structures, bringing the total number of structures considered in the study to 26. Because of the large number of bridges involved, an attempt was made to limit the number of structures to analyze by selecting bridges which are representative of several bridges. Selection criteria included the number of spans, bridge skew angle, number of columns per bent, and column dimensions, aspect ratios, and base details. The column dimensions are in terms of feet. The column ties in all columns were spaced at 12 in. which are considered to be inadequate by current standards for bridges in earthquake-prone areas. Other typical deficiencies included a lack of top mat in the footings, lap-spliced column dowels, inadequate anchorage length for column bars, and inadequate steel in pier cap beams. All the bridges are supported on spread footings.

Of particular interest to the Nevada Department of Transportation (NDOT) were bridges with tapered columns. These structures are those with different column dimensions at the base and the top. It can be seen that four bridges, P-1177, G-996, I-1010, and I-1006, had columns with constant column sections. One of these bridges was a pedestrian and another was a rail road bridge used by the Western Pacific Rail Road (WPRR). None of these four bridges were selected for detailed study because they did not represent a significant number of structures.

Three bridges were selected for this study: (1) I-1000, representing bridges with a small skew angle, a single column per bent, and rigid column base details; (2) I-1086N, representing structures with a small skew angle, two columns per bent, and one-way hinge column base details; and (3) I-1171, representing structures with a large skew angle, more than two columns per bent, and rigid column bases.

All the selected structures were designed according to the 1964 interim American Association of State Highway Officials (AASHO) bridge specifications to support a live load of HS-20. Construction records indicate that the concrete had an average compressive strength, f'_c, of approximately 4800 psi, while the reinforcing steel had an average yield stress of approximately 47,000 psi.

Bridge I-1000

This bridge, shown in Fig. 1, carries southbound U.S. 395 to eastbound Interstate 80 ramp traffic over the Interstate. The bridge is a four-span, continuous, conventionally reinforced concrete, multi-cell box girder structure which is supported on single-column piers. The cross section of the bridge is shown in Fig. 2. The column sections are round at the ends with a

diameter of one foot. The columns have rigid connections at both ends. Thermal movement of the bridge is accommodated at the "rocking backwall"-type abutments (Figure 7.a).

Bridge I-1086N

Dimensions of this bridge are shown in Figs. 3 and 4. The bridge carries northbound U.S. 395 traffic over Interstate 80. This structure is paired with I-1086S, but because the median slab is only nominally connected to the two bridges, the slab connections could be expected to fail during an earthquake, any rigid link effect between the two bridges could be ignored, resulting in no interaction between the two structures. The bridge is a four-span conventionally reinforced concrete, multi-cell, box girder structure. The abutment connection detail is shown in Fig. 7. The deck is continuous over the three double-column bents. Each of the bents is composed of two tapered columns, the sections of which are round at the ends with a diameter of one foot. The column to footing connections consist of one-way hinges, hinged about the transverse axis of the bridge.

Bridge I-1171

This structure, shown in Fig. 5, carries southbound U.S. 395 to westbound and eastbound Interstate 80 ramp traffic over 9th Street. The bridge is a three-span reinforced concrete box girder structure. The superstructure section (Fig. 6) is a continuous box girder. Each of the bents is composed of three tapered columns. The columns are round at the edges with a diameter of one foot and are rigidly connected to the footings. The abutment detail is shown in Fig. 7.b.

ANALYTICAL STUDIES

To determine the effects of an earthquake on the columns of the selected bridges, three types of computer analysis were performed: (1) a modal analysis to determine the periods of vibration for the first two modes in each structure; (2) an earthquake analysis with linear columns; and (3) an earthquake analysis with nonlinear columns.

The modal analysis was performed to obtain each structure's mass-proportional and stiffness-proportional damping factors, which are required as input values for the earthquake analyses. The modal analysis was performed using *Images-3D* from Celestial Software [1]. *Images-3D* is a three-dimensional general-purpose finite element analysis package for IBM-compatible personal computers. The modal analysis feature of *Images-3D* can calculate the frequencies, mode shapes, modal weights, and participation factors for a given structure.

The earthquake analyses were performed using the software package *NEABS* (*N*onlinear *E*arthquake *A*nalysis of *B*ridge *S*ystems) [2]. *NEABS* is a mainframe-based program written in FORTRAN IV (converted to FORTRAN 77 for this study) that was developed specifically for

performing non-linear dynamic analysis of bridges. *NEABS* evaluates the response history to either applied dynamic loadings or to uniform support excitations.

Two sets of response history analyses were carried out. In all of these analyses, the abutments were modeled by nonlinear springs using the hinge restrainer element in NEABS. The springs representing the abutments were active when the bridge moved toward the abutment, but were inactive when the bridge moved away. The columns, however, were treated as linear elements in one set of analyses and nonlinear elements in the other. For the earthquake analysis with nonlinear columns, biaxial bending elements, known as "five-spring elements," were employed at the base of each column. Five-spring elements (FSE) were added to the *NEABS* program in the course of an earlier study conducted at the University of Nevada [3]. Each element represents a column as a group of five axial springs, with each spring representing the properties of concrete and reinforcing steel. When used in regions of column plastic hinging, FSE's account for stiffness degradation which is typically seen in the response of reinforced concrete elements. Compared to the non-degrading bilinear models, the FSE provides a more realistic response during yielding, which, in turn, provides more accurate structural response. The properties of the FSE's were based on the measured steel and concrete properties.

The modified NEABS model has produced satisfactory results for a variety of bridge structures. In the study presented in this report, however, it was found that when relatively soft horizontal translational foundation springs are utilized, the model would not work properly and would become unstable. The foundation stiffness values for these springs determined based on the method supplied by the NDOT Geotechnical Section were relatively small. Because of time limitations, it was not possible to conduct a comprehensive review and modification of the algorithm in NEABS to solve the numerical instability problem. Furthermore, it was observed that, because of inadequate steel reinforcement anchorage lengths and due to a lack of concrete confinement, even the FSE would not be able to accurately model the actual behavior of the piers. No other bridge seismic analysis model is available that accounts for these effects.

The foundation stiffness values for horizontal springs had to be increased to 1.5×10^6 kips/foot to obtain stable results. This value is approximately ten times higher than the upper bound stiffnesses. The factor of ten may appear to be large. However, it is noted that the upper bound stiffness values are higher than the lower bound values by a factor ranging from approximately 10 to over 60 [6]. Considering the approximate nature of the soil stiffness calculations and the wide range in the values, the increased stiffness may be acceptable in determining an estimate of the ductilities. Nonetheless, in order to observe the effects of the realistic foundation stiffnesses, an earthquake analysis with non-yielding columns, without the use of five-spring elements, was also conducted.

Bridge Models

Figure 8 shows the finite element model for bridge I-1086. The number and location of the nodes represent those of the other two bridges. For the non-linear earthquake analysis, *x*-and *z*-direction translational foundation spring stiffnesses were artificially increased to the level

necessary for *NEABS* to yield stable results. The column foundations were modeled using spring-to-ground elements. Upper- and lower-bound soil stiffness values were calculated using the NDOT method [4] which is based on the half-space method and the measured soil properties at or near the site of the bridges. The computer runs were made using the mean stiffness value for each of the six spring components. The stiffness values for bridge I-1086 are shown in Table 2.

The abutment soil stiffness and yielding values were determined based on the NDOT method [1]. To simulate the one-way action and yielding characteristics of the abutment soil, *NEABS* expansion joint elements were used. The expansion joint was assumed to have no internal stiffness; only the restrainer cable feature was employed. Six equally-spaced restrainer cables were used to simultaneously simulate the stiffness for the *x*-translation and *y*-rotation degrees-of-freedom. At the abutments, *z*-direction translation was restrained. In addition, *x*-rotation and *y*-translation were restrained, but *z*-rotation was left unrestrained.

Input Ground Motion

Each of the three bridges selected for study was subjected to five different earthquake acceleration records, based on five well-known historical earthquake records: Castaic, El Centro, Lake Hughes, Loma Prieta, and Parkfield [5]. These records were selected and recommended by the Geotechnical Section of the Nevada Department of Transportation, based on soil depth to the bedrock, soil types at the site, and historical earthquake data. The records represented the expected earthquake records at the level of footings and the abutments of the bridges in the area.

The five records form a "suite" of standard acceleration records designed to produce a range of results the envelope of which present critical forces and displacements. Each of the original acceleration records has been scaled to a rock acceleration of 0.4-g, then modified to represent the ground acceleration at the level of the bridge footings and the abutments. For this analysis, the five records were convoluted through the soil profile at the Sparks I-80 viaduct, approximately three miles east of the Interstate 80/U.S. 395 interchange. The same record was applied simultaneously in the longitudinal and the transverse direction of the bridge in each analysis. Samples of the earthquake records are shown in Figs. 9 and 10.

ANALYTICAL RESULTS

Typical response histories are shown in Figs. 11 and 12. It can be seen that both abutments "yielded". This was typically the case in bridges I-1000 and I-1086 but not in I-1171. The maximum abutment force in this bridge was less than sixty percent of the yield force.

Tables 3 to 5 show the peak responses for different earthquakes when the columns were linear. The table also lists the nominal shear and moment capacities. The permissible shear values are the column shear strengths based on the AASHTO Specifications multiplied by the shear strength reduction factor of 0.85. The moment capacities were determined from a

69

moment-curvature analysis. Because the anchorage lengths for the column longitudinal bars were inadequate at both the top and bottom, the nominal moments correspond to the moments that can be developed with the short anchorage lengths. The nominal moments listed were obtained by reducing the steel stress by a factor equal to the ratio of the available to the required embedment lengths. The required lengths were calculated using the current AASHTO Specifications. The 25 percent increase in the yield stress which is specified in AASHTO to compute the required embedment of the column bars was not taken into account.

The columns labeled "λ" are the ratios of the *NEABS* results to the permissible values. Values of λ greater than 1.0, shown shaded in the table, indicate a possible yielding condition. The magnitude of λ values greater than 1.0 are artificially high because the model had linear columns. When yielding is permitted, the force values cannot be significantly higher than the yield forces. No shear capacities are listed for one-way hinges. This is because recent studies have shown that the failure of one-way hinges for loading in the strong direction is controlled by flexure and not shear [7].

The Parkfield earthquake record was found to be the most critical record for I-1000 and I-1086 and was thus chosen for further study in the analysis with non-linear columns. In bridge I-1171, the El Centro record was the most critical record.

Ductility in this study is defined as the ratio of the maximum displacement at the inflection point of a column divided by the displacement corresponding to the flexural yielding of the column at its end. The effects of foundation flexibility and rigid-body movement of the column are subtracted from the displacements to obtain a direct index for the level of yielding in the column itself.

Table 6 lists the estimates of the column ductility demands in all bridges for the "critical earthquakes." It should be noted that program NEABS assumes that the columns are well confined and that sufficient anchorage is provided for all the bars. It also assumes that sufficient shear strength exists at all the elements and joints. The program does not incorporate any strength degradation effects that may result from the lack of confinement, short anchorage lengths, or insufficient shear strength. The bridges which are analyzed in this study, however, are inadequately detailed based on current standards for seismic design. Therefore, the actual displacements may be considerably higher than those calculated. The loss of anchorage may result in structural instability, a phenomenon that is not accounted for in NEABS.

Highlighted in the table are ductility demand values of 0.7 or higher. In bridge I-1000, only the base of the column is likely to yield because of the fact that the bents consist of single columns in this bridge. No numbers are shown for the base of I-1086 in the longitudinal direction because the column bases are one-way hinges detailed to be moment-free in the longitudinal direction.

It can be seen that the results of the analysis with nonlinear columns are in line with the results with linear columns in that they point out potential for plastic hinging of the columns. Similar to what was observed in the linear column analyses, bridge I-1171 appears to be less critical than others. The fact that the maximum ductility demand in this bridge is 0.7 or less and

that the elastic column moment ratios (Table 5) were also 0.7 or less suggests that the bridge columns could perform adequately when subjected to earthquakes.

EXPERIMENTAL PROGRAM

Nearly two-thirds of the bridges included in the data base of Table 1 showed some deficiencies in the substructure. An analysis of the pier cap to column connections has also shown that the cap beams are inadequately reinforced. Four sets of test specimens are being designed currently to determine the as-built strength and ductility capacity of typical substructure components. The scale of these specimens is 0.417 with respect to the geometry of the elements. The steel reinforcement area and details are being designed to represent the majority of the bridges. Column ties are being selected so that the degree of confinement provided in the specimens is close to the prototype. Anchorage lengths of column bars are short by the same ratio of the actual to required embedment lengths in the actual bridges. Specimens representing the bridge column to footing connections are shown in Figs. 13 and 14. Other specimens which are being designed are a footing specimen and a column to pier cap connection. The specimens will be subjected to constant loads representing the dead load effect and will be subjected to cyclic loads to determine the strength and ductility of the as-built details. Once these limits are established, identical specimens will be built and retrofitted to determine the adequacy of retrofit details.

CONCLUSIONS

Results of the nonlinear analysis with linear columns indicated that in bridges with one or two columns per bent, abutment soil yielding may occur and that shear forces and moments may exceed permissible values. In the case of the bridge with three columns per bent, the abutment soil did not yield and shear forces and moments did not exceed the permissible values.

Results of the analysis with non-linear columns showed that column displacements may exceed the yield value in single-column per bent structures. In structures with two columns per bent, ductility demands were close to one, but did not exceed the yield value of 1.0. In the bridge with three-column per bents, an even lower ductility demand was found. The high skew angle in this bridge did not seem to lead to excessive forces or displacements. These ductility demands should be viewed with caution because computer program NEABS (and no other available bridge seismic analysis programs) account for strength and stiffness degradations that are expected in unconfined reinforced concrete members with inadequate embedment length for the reinforcing bars. The results suggest that, should the confinement and anchorage problems be resolved through retrofitting, a maximum displacement of the order of 1.5 in. would be expected in bridges considered in this study. The results also indicate strongly that bridges with single-column piers are the most susceptible structures to seismic damage, while multi-column structures are much less susceptible.

71

ACKNOWLEDGEMENTS

REFERENCES

1. *Images-3D*. 1985. Berkeley, Calif.: Celestial Software.

2. Imbsen, R. A., and R. A. Schamber. 1983. "Earthquake resistant bridge bearings." *Report No. FHWA/RD-82/166*. Vol. 2. Washington, D.C.: U.S. Department of Transportation, Federal Highway Administration.

3. Ghusn, G. E., and M. Saiidi. 1986. "A simple hysteretic element for biaxial bending of R/C columns and implementation in NEABS-86." *Report No. CCEER-86-1*. Reno: University of Nevada, Department of Civil Engineering.

4. Beaston, Ted. 1993. Column footing- and abutment-soil spring stiffness notes. Carson City: Nevada Department of Transportation, Geotechnical Section.

5. Beaston, Ted. 1993. Seismic design acceleration records. Carson City: Nevada Department of Transportation, Geotechnical Section.

6. Saiidi, M., D.N. O'Connor, and E. A. Maragakis. 1993. "A Study of Seismic Damage Susceptibility in Bridges in Northwest Nevada." Report number CCEER-93-10. Reno: University of Nevada, Department of Civil Engineering.

7. Saiidi, M. and D. Straw. 1993. "Monotonic and Cyclic Response of One-Way R/C Bridge Pier Hinges in the Strong Direction," American Concrete Institute, <u>Structural Engineering Journal</u>, Vol. 90, No. 5, September-October 1993, pp. 568-573.

Table 1 - General Information for Bridges Included in the Study

BRDG.	NO. OF SPANS	SKEW	COL. DIM AT BASE	COL. DIM AT TOP	AVG. COL. ASP. RTO	BASE DETAIL	NO. OF COL/BNT	COMMENTS
I-1000	4	10	2 BY 6	2 BY 9	3.75	RIGID	1	
I-1001	4	14	2 BY 6	2 BY 9	3.75	RIGID	1	
I-1086	4	7	2 BY 4	2 BY 8	3	1-WAY HINGE	2	TWO PARALLEL BRIDGES
I-1087	4	VAR.	2 BY 6	2 BY 9	3.75	RIGID	1	
I-1088	4	9	2 BY 3.5	2 BY 7.5	2.75	1-WAY HINGE	2	
I-1149	3	32	2.5 BY 4	2.5 BY 6	2	RIGID	3	TWO PARALLEL BRIDGES W/ DIFF. COL. SPACING
I-1171	3	39	2 BY 3.5	2 BY 5.5	2.25	RIGID	3	VARIABLE WIDTH
I-1172	4	12	2 BY 4	2 BY 8	3	1-WAY HINGE	2	TWO PARALLEL BRIDGES
I-1173	3	39	2 BY 3.5	2 BY 5	2.13	RIGID	2	
H-991	4	16	2 BY 5	2 BY 9	3.5	1-WAY HINGE	2	RALSTON- 2-FT PEDESTAL @ BASE
P-1177	4	16	2.5X4.25	2.5X4.25	1.7	RIGID	1	PEDESTRIAN; ARLINGTON
I-994	4	0	2 BY 5	2 BY 9	3.5	1-WAY HINGE	2	CENTER; 2-FT. PEDESTAL @ BASE
H-995	5	11	2 BY 5	2 BY 9	3.5	1-WAY HINGE	2	EVANS; 2-FT. PEDESTAL @ BASE
G-996	4	9	2.5 BY 10	2.5 BY 10	4	RIGID	1	WPRR
I-992	4	0	2 BY 5	2 BY 9	3.5	1-WAY HINGE	2	SIERRA; 2-FT. PEDESTAL @ BASE
H-990	4	10	2 BY 5	2 BY 9	3.5	1-WAY HINGE	2	WASHINGTON; 2-FT. PEDESTAL @ BASE
H-993	4	0	2 BY 4.5	2 BY 6	2.68	1-WAY HINGE	3	VIRGINIA; 2-FT. PEDESTAL @ BASE
H-997	4	6	2 BY 5	2 BY 9	3.5	1-WAY HINGE	2	VALLEY; 2-FT. PEDESTAL @ BASE
I-1002	3	47	3 BY 4	3 BY 6.25	1.71	RIGID	3	US-40 INT; 1.5' COL. PED.; 2 PARALLEL BRIDGES
H-1003	3	33	3 BY 4	3 BY 6	1.67	RIGID	3	KIETZKE; 2 PARALLEL BRIDGES
I-1010	4	33	2 BY 9	2 BY 9	4.5	RIGID	1	RAMP NO. 24;
I-1006	3	0	2.83DIAM	2.83DIAM	NA	1-WAY HINGE	3	PYRAMID WAY; CIRC. COLS.

Table 2 - Column Footing Spring Properties for Bridge I-1086

Spring Component	Upper Bound	Lower Bound	Average
K_r, k/ft	1.56×10^5	2.53×10^3	7.91×10^4
K_v, k/ft	1.33×10^5	2.16×10^3	6.76×10^4
K_z, k/ft	1.51×10^5	2.46×10^3	7.69×10^4
K_{rr}, k-ft/rad	1.20×10^7	1.95×10^5	6.11×10^6
K_{ry}, k-ft/rad	1.30×10^7	2.12×10^5	6.62×10^6
K_{rz}, k-ft/rad	8.79×10^6	1.43×10^5	4.47×10^6

Table 3 - Maximum Shears and Moments in Bridge I-1000

Column	Component	Nominal	Permissible	Castaic Calc.	λ	El Centro Calc.	λ	Lake Hughes Calc.	λ	Loma Prieta Calc.	λ	Parkfield Calc.	λ
1 Top	Vx (kips)	310	264	51.2	0.19	72.9	0.28	90.0	0.34	85.3	0.32	112.9	0.43
	Vz (kips)	395	336	82.7	0.25	88.9	0.26	124.7	0.37	89.5	0.27	118.3	0.35
	Mx (k-ft)	6708	6037	383.3	0.06	375.1	0.06	535.8	0.09	378.1	0.06	509.7	0.08
	Mz (k-ft)	1867	1680	542.0	0.32	756.0	0.45	943.6	0.56	890.5	0.53	1180.0	0.70
1 Base	Vx (kips)	236	201	59.8	0.30	79.7	0.40	103.6	0.52	95.4	0.48	126.8	0.63
	Vz (kips)	280	238	89.6	0.38	92.4	0.39	127.0	0.53	94.2	0.40	117.8	0.49
	Mx (k-ft)	2683	2415	2020.0	0.84	2142.0	0.89	2990.0	1.24	2169.0	0.90	2811.0	1.16
	Mz (k-ft)	1317	1185	539.7	0.46	731.2	0.62	936.2	0.79	871.0	0.73	1158.0	0.98
2 Top	Vx (kips)	310	264	49.6	0.19	73.2	0.28	99.0	0.38	92.7	0.35	123.6	0.47
	Vz (kips)	395	336	169.0	0.50	186.0	0.55	254.6	0.76	186.9	0.56	244.2	0.73
	Mx (k-ft)	6708	6037	713.3	0.12	797.7	0.13	1097.0	0.18	801.4	0.13	1033.0	0.17
	Mz (k-ft)	1867	1680	528.0	0.31	769.3	0.46	1039.0	0.62	969.7	0.58	1282.0	0.76
2 Base	Vx (kips)	236	201	58.3	0.29	83.0	0.41	111.7	0.56	103.7	0.52	133.8	0.67
	Vz (kips)	280	238	177.5	0.75	190.5	0.80	261.5	1.10	193.8	0.81	247.0	1.04
	Mx (k-ft)	2683	2415	4087.0	1.69	4469.0	1.85	6122.0	2.54	4513.0	1.87	5809.0	2.41
	Mz (k-ft)	1317	1185	523.9	0.44	753.4	0.64	1013.0	0.85	944.5	0.80	1227.0	1.04
3 Top	Vx (kips)	310	264	45.9	0.17	77.7	0.29	102.6	0.39	96.4	0.37	127.0	0.48
	Vz (kips)	395	336	85.1	0.25	94.8	0.28	132.8	0.40	94.1	0.28	119.5	0.36
	Mx (k-ft)	6708	6037	347.3	0.06	399.0	0.07	553.1	0.09	390.7	0.06	535.8	0.09
	Mz (k-ft)	1867	1680	490.3	0.29	802.1	0.48	1077.0	0.64	1009.0	0.60	1311.0	0.78
3 Base	Vx (kips)	236	201	54.5	0.27	82.7	0.41	116.4	0.58	107.5	0.54	135.3	0.67
	Vz (kips)	280	238	92.3	0.39	98.9	0.42	140.1	0.59	99.9	0.42	117.1	0.49
	Mx (k-ft)	2683	2415	2077.0	0.86	2288.0	0.95	3203.0	1.33	2282.0	0.95	2843.0	1.18
	Mz (k-ft)	1317	1185	488.4	0.41	760.7	0.64	1054.0	0.89	977.7	0.82	1246.0	1.05
Max. Longitudinal Displacement (in.)				0.22		0.31		0.42		0.40		0.52	
Max. Transverse Displacement (in.)				0.73		0.80		1.09		0.81		1.04	

Table 4 - Maximum Shears and Moments in Bridge I-1086

Column		Component	Nominal	Permissible	Castaic Calc.	λ	El Centro Calc.	λ	Lake Hughes Calc.	λ	Loma Prieta Calc.	λ	Parkfield Calc.	λ
1	Top	Vx (kips)	254	216	8.8	0.04	11.4	0.05	26.1	0.12	11.5	0.05	53.0	0.25
		Vz (kips)	372	316	69.6	0.22	96.7	0.31	134.2	0.42	84.7	0.27	184.8	0.58
		Mx (k-ft)	3508	3157	1229.0	0.39	1709.0	0.54	2373.0	0.75	1496.0	0.47	3268.0	1.04
		Mz (k-ft)	1407	1266	244.4	0.19	317.7	0.25	731.6	0.58	319.1	0.25	1482.0	1.17
	Base	Vx (kips)	n/a	—	8.8	—	11.4	—	26.1	—	11.5	—	53.0	—
		Vz (kips)	n/a	—	69.5	—	96.7	—	134.2	—	84.7	—	184.8	—
		Mx (k-ft)	1061	955	719.3	0.75	998.2	1.05	1385.0	1.45	874.5	0.92	1906.0	2.00
		Mz (k-ft)	n/a	—	0	—	0	—	0	—	0	—	0	—
3	Top	Vx (kips)	254	216	12.5	0.06	17.8	0.08	39.3	0.18	17.0	0.08	80.5	0.37
		Vz (kips)	372	316	157.9	0.50	213.5	0.68	318.5	1.01	185.3	0.59	420.0	1.33
		Mx (k-ft)	3508	3157	2393.0	0.76	3237.0	1.03	4830.0	1.53	2809.0	0.89	6367.0	2.02
		Mz (k-ft)	1407	1266	301.3	0.24	428.7	0.34	944.9	0.75	408.4	0.32	1937.0	1.53
	Base	Vx (kips)	n/a	—	12.5	—	17.8	—	39.3	—	17.0	—	80.5	—
		Vz (kips)	n/a	—	157.9	—	213.5	—	318.5	—	185.3	—	420.0	—
		Mx (k-ft)	1061	955	1409.0	1.48	1906.0	2.00	2840.0	2.97	1654.0	1.73	3749.0	3.93
		Mz (k-ft)	n/a	—	0	—	0	—	0	—	0	—	0	—
5	Top	Vx (kips)	254	216	12.8	0.06	17.3	0.08	38.4	0.18	16.4	0.08	80.1	0.37
		Vz (kips)	372	316	92.3	0.29	107.3	0.34	161.1	0.51	96.2	0.30	213.9	0.68
		Mx (k-ft)	3508	3157	1398.0	0.44	1627.0	0.52	2440.0	0.77	1457.0	0.46	3244.0	1.03
		Mz (k-ft)	1407	1266	307.6	0.24	414.8	0.33	924.7	0.73	394.1	0.31	1928.0	1.52
	Base	Vx (kips)	n/a	—	12.8	—	17.3	—	38.4	—	16.4	—	80.1	—
		Vz (kips)	n/a	—	92.3	—	107.3	—	161.1	—	96.2	—	213.9	—
		Mx (k-ft)	1061	955	823.2	0.86	957.9	1.00	1440.0	1.51	858.9	0.90	1906.0	2.00
		Mz (k-ft)	n/a	—	0	—	0	—	0	—	0	—	0	—
Max. Longitudinal Displacement (in.)					0.34		0.56		1.30		0.39		0.88	
Max. Transverse Displacement (in.)					0.32		0.43		0.64		0.38		0.72	

Table 5 - Maximum Shears and Moments in Bridge I-1171

Column		Component	Nominal	Permissible	Castaic Calc.	λ	El Centro Calc.	λ	Lake Hughes Calc.	λ	Loma Prieta Calc.	λ	Parkfield Calc.	λ
1	Top	Vx (kips)	187	158.95	14.1	0.09	9.3	0.06	9.5	0.06	10.4	0.07	14.3	0.09
		Vz (kips)	261	221.85	53.5	0.24	54.2	0.24	46.0	0.21	47.9	0.22	50.7	0.23
		Mx (k-ft)	2083	1874.7	727.9	0.39	748.7	0.40	596.7	0.32	626.0	0.33	669.9	0.36
		Mz (k-ft)	929	836.1	116.8	0.14	91.3	0.11	73.8	0.09	112.6	0.13	94.0	0.11
	Base	Vx (kips)	140	119	14.6	0.12	12.1	0.10	10.8	0.09	11.9	0.10	12.7	0.11
		Vz (kips)	161	136.85	63.4	0.46	65.2	0.48	49.6	0.36	51.2	0.37	55.5	0.41
		Mx (k-ft)	1000	900	521.6	0.58	536.2	0.60	401.5	0.45	425.0	0.47	460.8	0.51
		Mz (k-ft)	750	675	133.7	0.20	116.9	0.17	73.8	0.11	120.0	0.18	103.4	0.15
4	Top	Vx (kips)	187	158.95	12.2	0.08	14.9	0.09	9.8	0.06	16.7	0.11	10.3	0.06
		Vz (kips)	261	221.85	74.4	0.34	74.4	0.34	55.9	0.25	66.2	0.30	62.1	0.28
		Mx (k-ft)	2083	1874.7	905.5	0.48	888.6	0.47	697.2	0.37	787.4	0.42	761.9	0.41
		Mz (k-ft)	929	836.1	119.9	0.14	137.5	0.16	75.3	0.09	147.7	0.18	87.9	0.11
	Base	Vx (kips)	140	119	16.2	0.14	17.6	0.15	12.4	0.10	17.5	0.15	13.8	0.12
		Vz (kips)	161	136.85	84.7	0.62	80.6	0.59	68.7	0.50	70.1	0.51	72.1	0.53
		Mx (k-ft)	1000	900	642.1	0.71	613.1	0.68	512.9	0.57	537.3	0.60	543.1	0.60
		Mz (k-ft)	750	675	151.8	0.22	157.0	0.23	99.4	0.15	164.7	0.24	98.5	0.15
Max. Longitudinal Displacement (in.)					0.17		0.21		0.15		0.17		0.16	
Max. Transverse Displacement (in.)					0.18		0.14		0.12		0.11		0.15	

Table 6 - Estimates of Maximum Ductility Demands

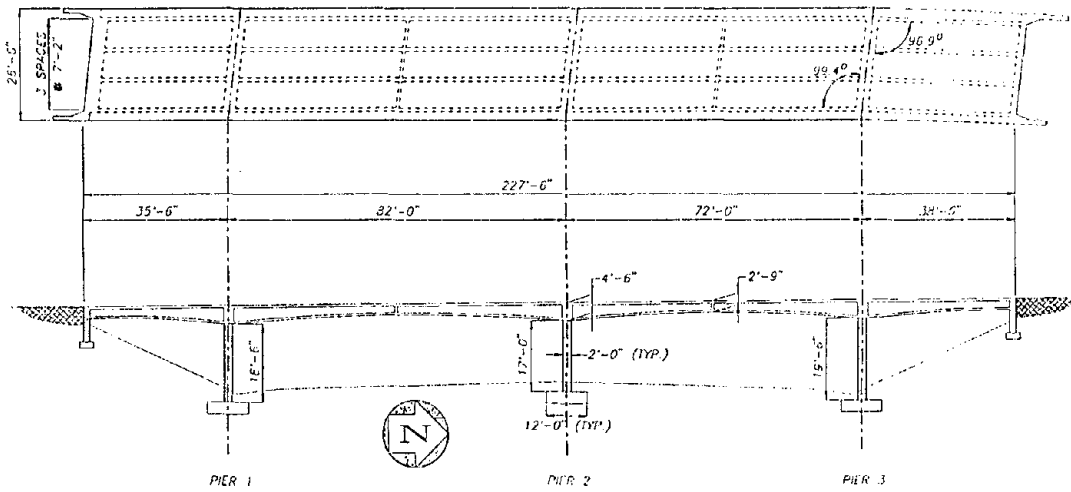| Bridge Number	Columns per Bent	Skew (deg)	Direction of Displacement	Type of Curvature		Arm (in.)	Yield Displacement (in.)	Maximum Displacement (in.)	Calculated Ductility Demand
I-1000	1	0	Longitudinal (Weak Axis)	Double	Top	137	0.570	0.238	0.42
					Base	97	0.240	0.160	0.67
			Transverse (Strong Axis)	Single	Top	—	—	—	—
					Base	234	0.420	0.510	1.21
I-1086	2	0	Longitudinal (Weak Axis)	Single	Top	288	3.318	0.561	0.17
					Base	—	—	—	—
			Transverse (Strong Axis)	Double	Top	221	0.306	0.047	0.15
					Base	67	0.044	0.042	0.95
I-1171	3	46	Longitudinal (Weak Axis)	Double	Top	129	0.394	0.082	0.21
					Base	104	0.245	0.100	0.41
			Transverse (Strong Axis)	Double	Top	157	0.190	0.081	0.43
					Base	76	0.076	0.055	0.72

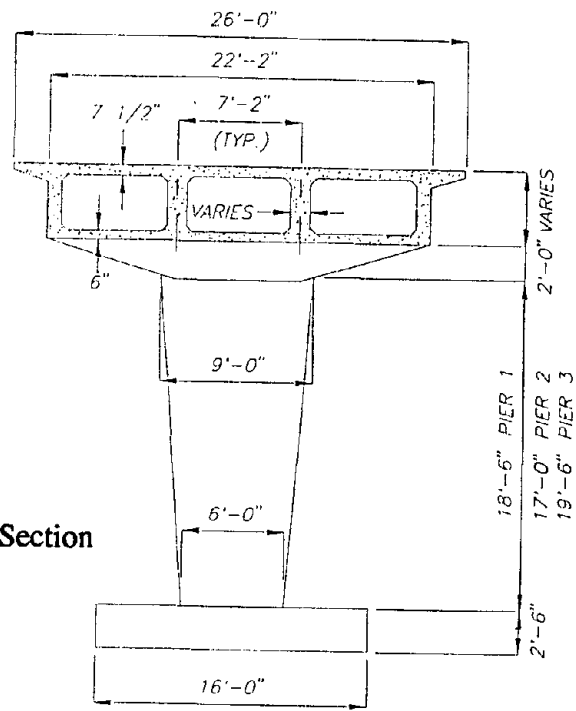**Fig. 1 - I-1000 Plan and Elevation**
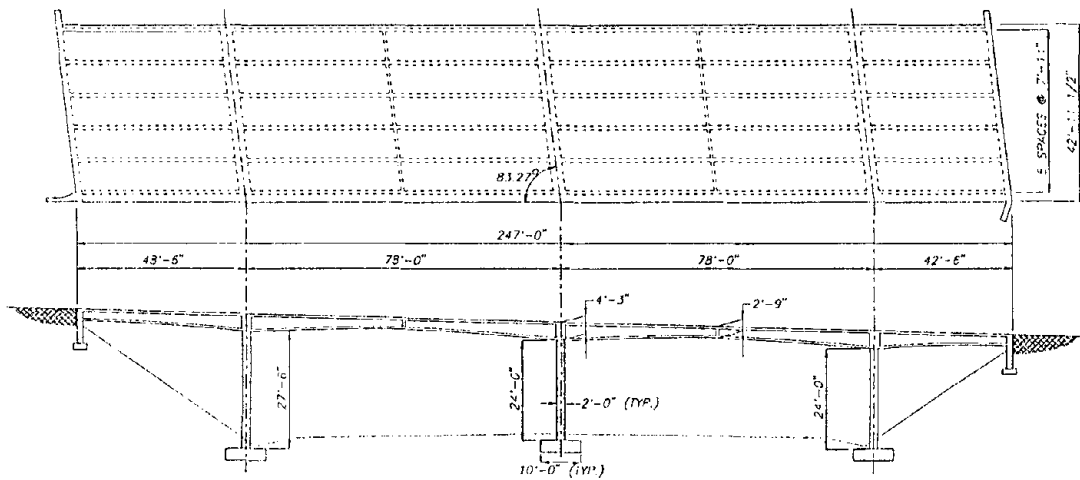

Fig. 2 - I-1000 Deck Section

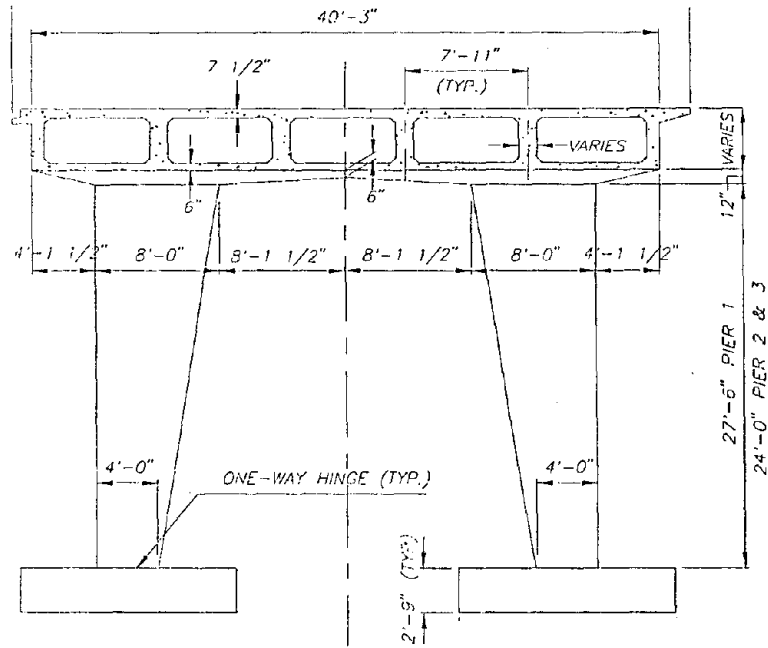**Fig. 3 - I-1086N Plan and Elevation**

Fig. 4 - I-1086N Deck Section and Column Elevation
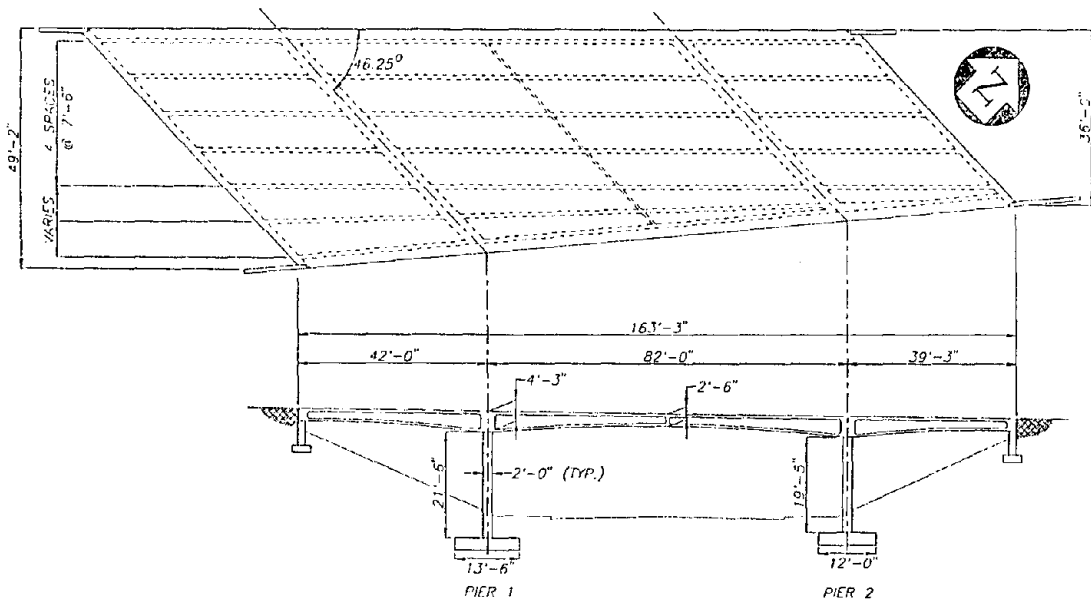

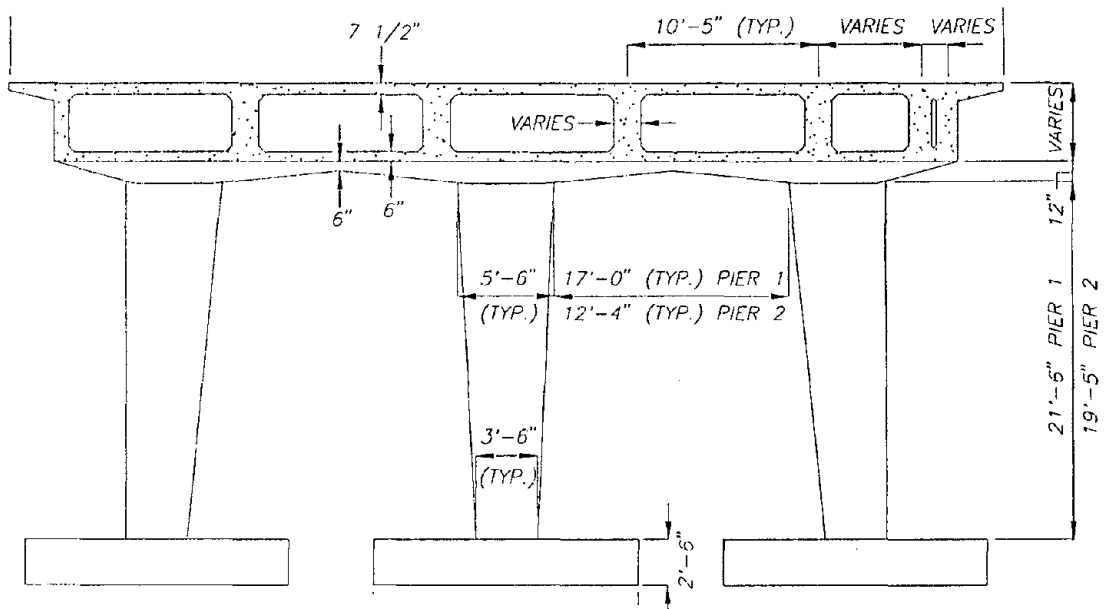**Fig. 5 - I-1171 Plan and Elevation**

76

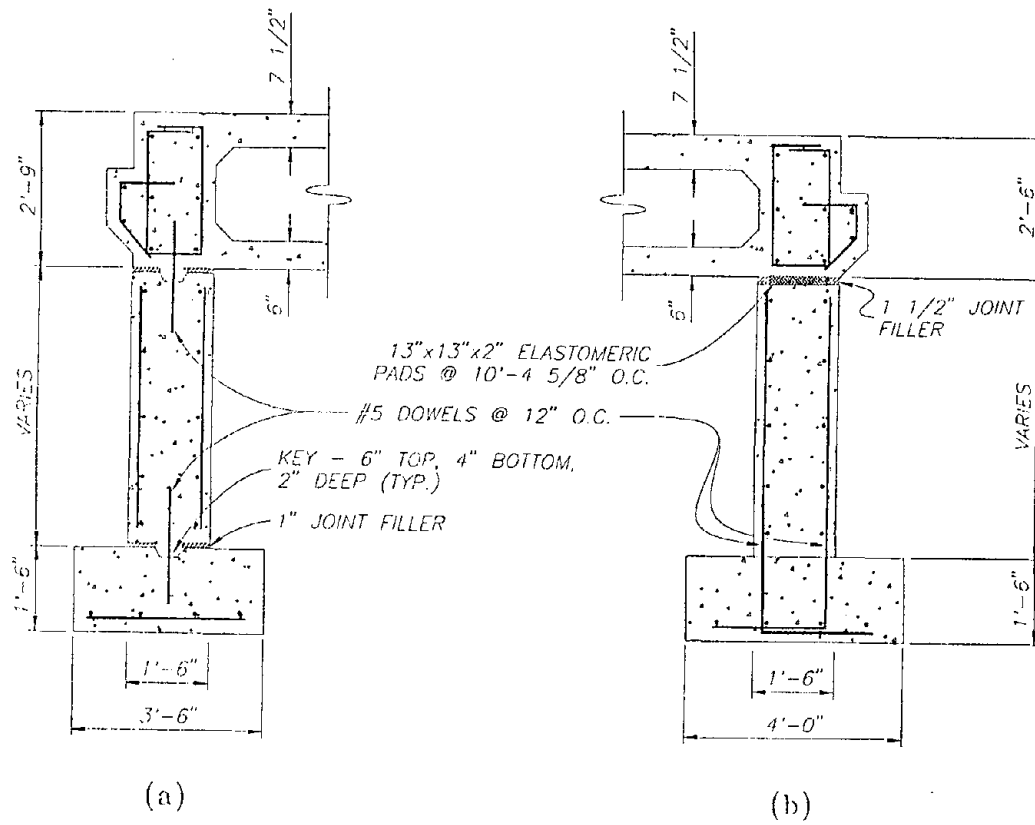Fig. 6 - I-1171 Deck Section and Column Elevation

(a) (b)

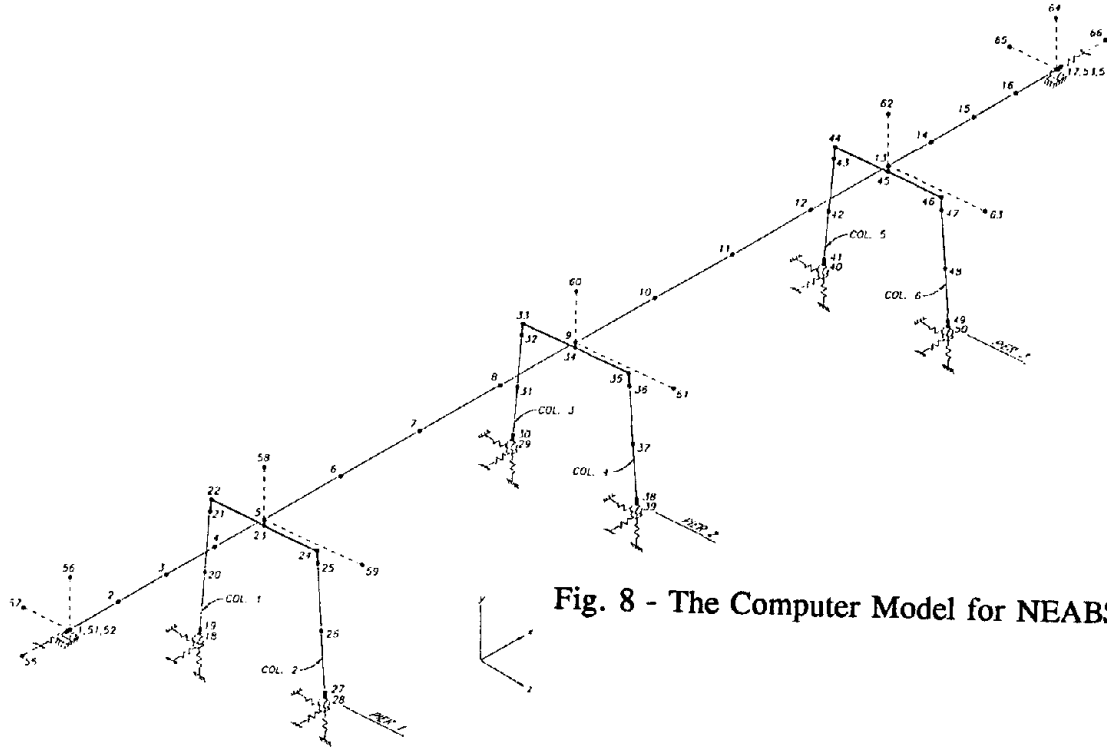Fig. 7 - Abutment Sections: (a) I-1000 and I-1086N; (b) I-1171

77

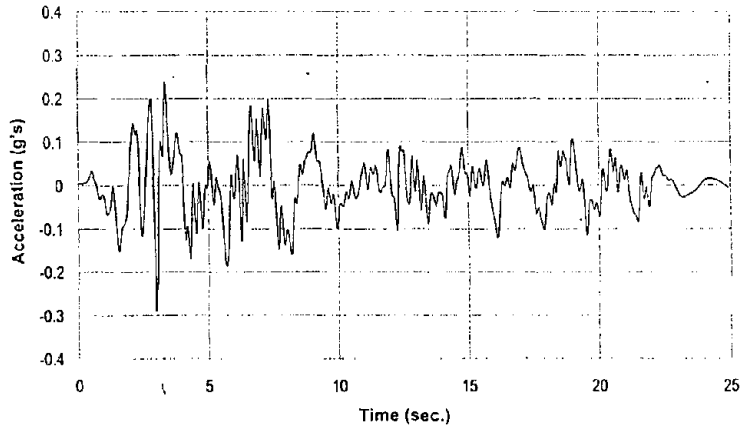Fig. 8 - The Computer Model for NEABS Analysis of I-1086N
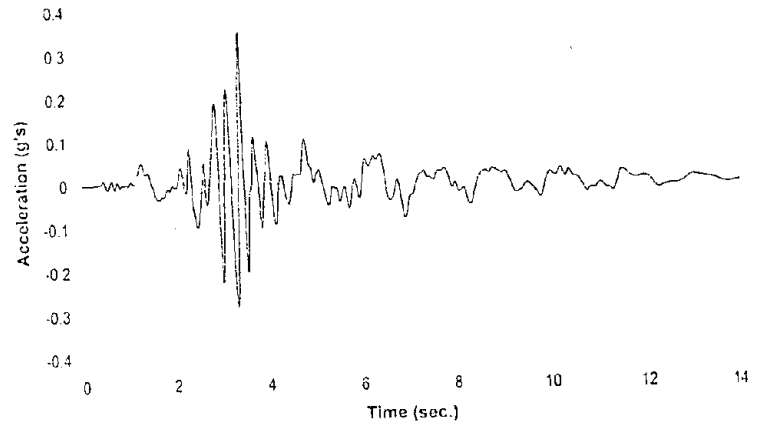

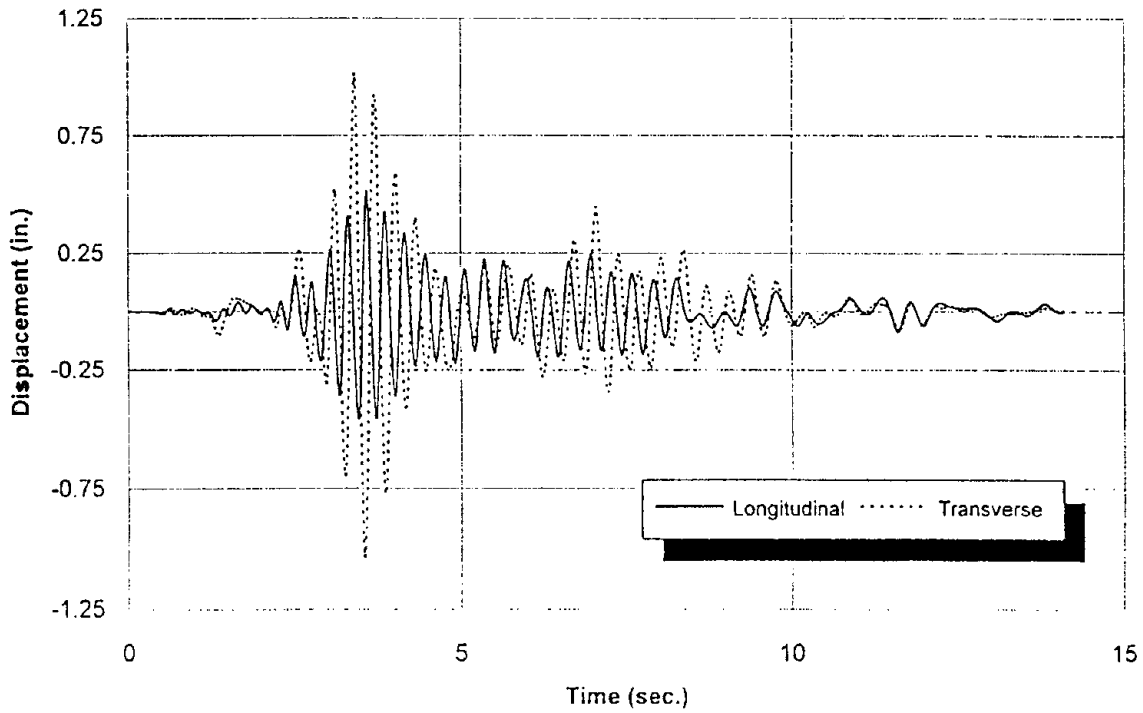Fig. 9 - The Modified El Centro Record

Fig. 10 - The Modified Parkfield Record

Fig. 11 - Response of Superstructure Center in Bridge I-1000 for the Parkfield Record
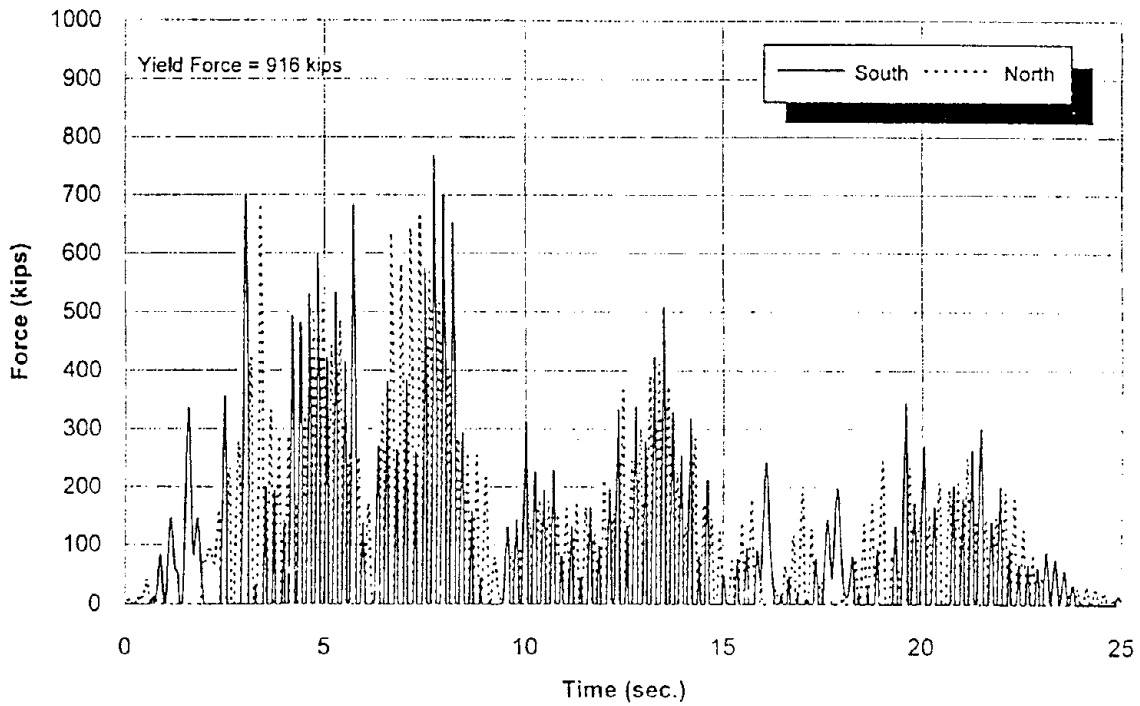
Fig. 12 - Abutment Response in Bridge I-1000 for the Parkfield Record

79

Fig. 13 - Details of Column-Footing Rigid Connection

Fig. 14 - Details of Column-Footing One-Way Hinge Connection

80
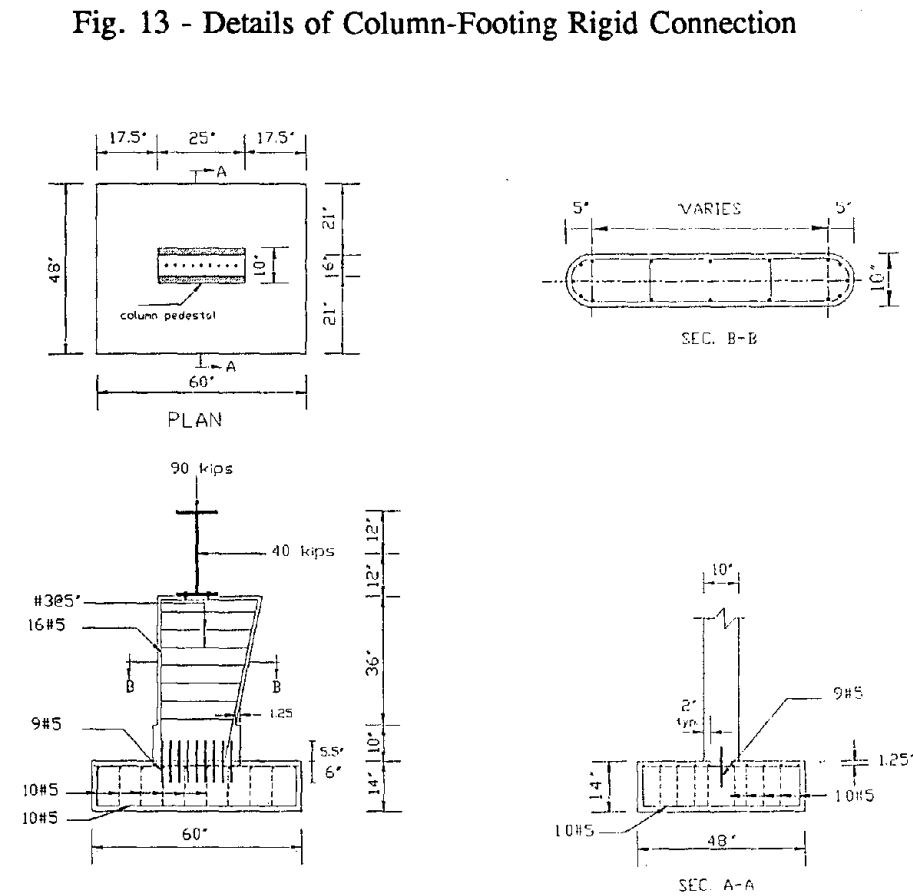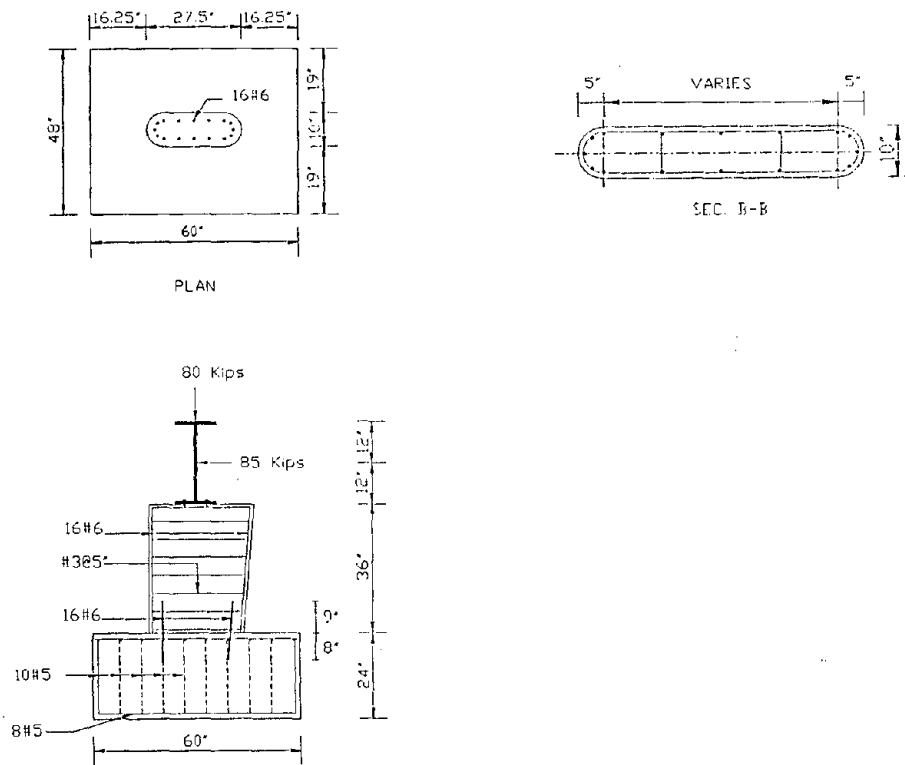
SECOND U.S.-JAPAN WORKSHOP ON SEISMIC RETROFIT OF BRIDGES

Damage of Bridges by Kushiro-oki Earthquake, January 1993, and Hokkaido nansei-oki Earthquake, July 1993

K. Kawashima, S. Unjoh, T. Nakajima and J. Hoshikuma
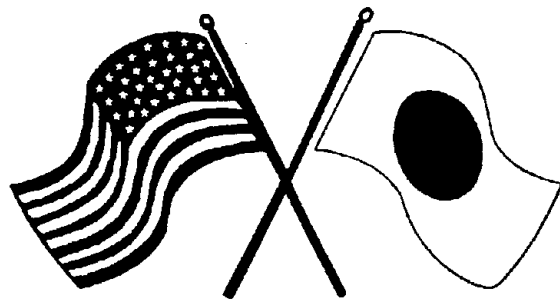
January 20 and 21, 1994
Berkeley Marina Marriott Hotel
Berkeley, California

DAMAGE OF BRIDGES BY KUSHIRO-OKI EARTHQUAKE, JANUARY 1993, AND HOKKAIDO NANSEI-OKI EARTHQUAKE, JULY 1993

Kazuhiko KAWASHIMA[1], Shigeki UNJOH[2], Tomoru NAKAJIMA[3]
and Junichi HOSHIKUMA[3]

1) Head, Earthquake Engineering Division, Public Works Research Institute, Ministry of Construction, Tsukuba Science City, Japan
2) Senior Research Engineer, ditto
3) Research Engineer, ditto

ABSTRACT

This paper presents the damage to bridges caused by the recent earthquakes occurred in Japan. Sixty-two bridges were damaged by the Kushiro-oki Earthquake of January 15, 1993, and twenty-four bridges by the Hokkaido-nansei-oki Earthquake of July, 12, 1993 including slight damage which did not affect the trafficability of bridges.

INTRODUCTION

The Kushiro-oki Earthquake occurred on January 15, 1993, and Hokkaido-nansei-oki Earthquake occurred on July 12, 1993 both in Hokkaido island. They caused a lot of damages to highway, river and port facilities and buildings.

The Kushiro-oki-Earthquake with magnitude of 7.8 on the Richiter scale occurred approximately 15km from the Kushiro city. The Hokkaido-nansei-oki Earthquake with the magnitude of 7.8 occurred approximately 60km north-west from the Okushiri Island. Hokkaido-nansei-oki Earthquake caused heavy damage to Okushiri island by the Tsunami and the Fire. Although two earthquakes were a large-scale earthquake with the magnitude of 7.8, structural damages were not so heavy because the earthquakes hitted rural area with low population density and there are not large scale structures in the affected area.

Figs. 1 and 2 show the location of the damaged structures. On the highway bridges, large damage such as falling-off of superstructures was not found. However, based on the investigation of the damaged bridges important lessons on the seismic design of highway bridges and countermeasures to highway systems in the future were found. This paper presents damages to highway bridges caused by the Kushiro-oki Earthquake and Hokkaido-nansei-oki Earthquake.

DAMAGE TO REINFORCED CONCRETE BRIDGE PIERS WITH TERMINATION OF LONGITUDINAL REINFORCEMENT AT MID—HEIGHT

Common damage to bridges in the two earthquakes was damage to the reinforced concrete bridge piers where the longitudinal reinforcement was terminated at mid—height. This type damage was recognized by the heavy damage to the piers of Shizunai Bridge during the Urakawa—oki Earthquake of 1982. Shizunai bridge was damaged as almost falling—off of superstructure.

The damage to reinforced concrete piers were found for six bridges by the Kushiro—oki Earthquake and three bridges by the Hokkaido—nansei—oki Earthquake. All of eight bridges were constructed in 1960s to early 1970s and the bridges were designed according to the specifications before the revision of design details on the anchorage of reinforcement in 1980.

The followings show the interesting damage in which some spans were designed according to the older specifications and damaged by the Hokkaido—nansei—oki Earthquake, and the other designed according to the revised specifications was not damaged.

Photo 1 shows the Shin—Shiriuchi bridge on the municipal highway of Motomachi No.1. It is a 7 span simple post—tension T shaped girder bridge with length of 214m and width of 6m. Although the original bridge was constructed in 1970, the right side two spans with length of 66m were newly constructed in 1989 because of the river reconstruction. Existing piers have the height of 6.8mm for Piers P1 and P4, that of 7.04m for Piers P3 and P4. They all have the circular section with diameter of 1.8m. Newly constructed Pier P1 has the oval section of 3×1.8m, and P2 has that of 3m $\times 1.5$m. The foundations are caisson type for all piers except that the new Pier P1 has a direct type foundation.

Sixty—four reinforcing bars with diameter 22mm (D22) were arranged for existing piers. In which, 32 reinforcing bars are terminated at the height of 2.47m from the bottom of piers and then 16 reinforcing bars are terminated at the height of 3.67m. On the other hand, for new Pier P2, 56 reinforcing bars are arranged at the bottom and 28 bars are terminated at the height of 3m from the bottom. No termination of the reinforcing bars for new pier P1 are made.

The damage was found at the termination section of all of the existing piers. **Photo 2** and 3 shows the damage situation. Cracks and spalling—off of cover concrete was found and the buckling and the deformation of reinforcing bars towards the outside of the piers were occurred.

Heaviest damage was found at Pier P3 and the pier was damaged with the height about 1m at the lower termination section. It was caused by the response in the transverse direction because the damage was found at the both side of the pier in the upper and lower stream sides of the river.

The judgement methods of the damage degree in terms of residual strength and

ductility characteristics of reinforced concrete piers are shown in the Manual of the Earthquake Disaster Prevention for Highways. The damage degree can be estimated according to **Table 1**. The damage to Pier P3 is estimated as "heavy damage" with requirement to close the traffic. The strength of the pier is estimated under the yielding strength.

It is interesting that the damage was found at the exciting piers but no damage was found newly constructed Pier P2 which also has the termination of main reinforcement. It is proved that this type damage was prevented by providing an enough anchorage length for the terminated reinforcing bars according to the 1980 specifications.

The strong motion records was obtained at the Shichihou Bridge (no damage) which is located about 10km form the Shin—Shiriuchi Bridge by the Hokkaido Development Bureau. Peak acceleration on the ground surface was about 200cm/sec^2. The wooden house is located at the just side of the bridge and the owner said that the house was excited heavily during the earthquake but the vibration was not so large and a cup was dropped from the case. It is an important damage to learn even if the excitation is not so heavy heavy damage will occurred if the anchorage length is not enough.

The same type damage was found at five bridges during the Kushiro—oki Earthquake, i.e., Matsnoe Bridge on national highway No.240 (**Photo 4**), Gojukkoku Bridge on national highway No.391 (**Photo 5**), Shin—tawa bridge on regional highway Nakashibetsu—Shibetya (**Photo 6**), Hatsune Bridge on regional highway Onbetsu—Teishajo (**Photo 7**), Akangawa Bridge on the regional highway of Akan—Shibetya (**Photo 8**), Yoda Bridge on the regional highway Horokayanto (**Photo 9**). And 2 bridges during the Hokkaido—nansei—oki Earthquake, i.e., Motoe Bridge on the municipal highway Motoebashi (**Photo 10**), and Motouriya Bridge on the municipal highway Uriya No.2 (**Photo 11**).

DAMAGES TO ABUTMENT AND BEARING SUPPORTS

Kamiisoshin Bridge is located on the National Highway No.228 at the Kamiiso in Hakodate city. **Photo 12** shows the bridge with bridge length of 53.1m and the width of 8m. The bridge constructed in 1961 and was a three span simply supported steel plate girder bridge. The foundations are a caisson type.

Photo 13 shows the damage found at the A1 abutment (fixed bearing). The girder moved by about 5cm in the longitudinal direction and crashed into the parapet of the abutment. The web of the steel plate deformed and the crack was found at the parapet. The bearing supports were rotated with displacement of 5cm as shown in **Photo 14**. The bearing was damaged because the bearing was one anchor type bearing. This type bearing was easily rotated by the longitudinal lateral force. After and the bearing concrete was damaged, the anchorage was dislodged and then the bearing was floated up.

Although this type damage was commonly found in the past earthquakes, it is difficult

to repair this type damage. Generally, the parapet is reconstructed after the displacement of the girder was fixed. However, the repair work significantly affects the traffic. This type damage is easy to be developed during earthquakes, therefore, it is required to develop the structural details which is not affected by the earthquakes and also is easy to repair.

DAMAGE CAUSED BY SOIL LIQUEFACTION

During the both earthquakes, the effect of soil liquefaction was found in a wide area of Hokkaido especially in Kushiro area and south—west area of the Hokkaido. Many damages were found at the road embankment, submerged structures, port facilities and buildings. Although the bridge was not affected by the soil liquefaction, Oshamanbe bridge is an only bridge clearly damaged by the soil liquefaction.

Photo 15 shows the Osyamanbe bridge in the Oshamanbe on the National highway No.37. It is 5 span simply supported post tension T shaped girder bridge with bridge length of 150.1m and deck width of 7m. The foundations are a caisson type. The bridge was constructed in 1960 and the pedestrian bridge was added at the upper stream in 1976.

The bridge pier was inclined in the direction of upper stream of the river as shown in Photo 16 resulting in the displacement of 42cm on the deck level. No inclination was found at the abutments. Since inclination angle is larger at the center of the bridge and smaller at the abutments, the bridge looks like a curved bridge as shown in Photo 17. The largest inclination of pier was found at the Pier P2, the height level at the bearing support in the upper stream side is higher by 38.6cm than that in the lower stream side. The inclination angle was about 0.035 radian.

Several boiling holes caused by the soil liquefaction were found around the bridge. Fig. 3 shows the ground condition around piers. Gravel, fine sand, and gravel sand layers are around caisson foundation, it is estimated that the these layers in particular fine sand layer was liquefied. Fig. 4 represent the liquefaction resistance factor, F_L , of the pier P2. In the computation of the liquefaction resistance factor, the seismic lateral force coefficient was assumed as 0.15 which is the design lateral force coefficient.

It should be noted here that the evaluation method for soil liquefaction was introduced in the design specification of highway bridges in 1971. And the evaluation method and treatment method which is almost the same method as a current design method for the design of highway bridges was revised in 1980. The bridge was constructed in 1960 and the effect of soil liquefaction was not considered in the design of the bridge.

DAMAGE TO FALLING—OFF PREVENTION DEVICES

Although damage to the stoppers which were installed at the bearings was found in the past earthquakes, there has been very few damage to the falling—off prevention devices because the large—scale earthquakes has not occurred recently. The bolts of the connection

devices between adjacent girders of Hatsune Bridge on the regional highway Onbetsu—teisyajo were failed during the Kushiro—oki Earthquake. On the other hand, the steel links connecting between girder and substructure were buckled at the Yanagisaki bridge on the national highway No.229 during the Hokkaido—nansei—oki Earthquake.

Hatsune Bridge as shown in **Photo 18** is 6 span simply supported steel plate girder bridge with bridge length of 172m. The bridge was constructed in 1969. **Photo 19** shows the connection devices between adjacent girders used for the Hatsune Bridge. The steel plate (SS400) with height of 68cm, width of 34.5cm and thickness of 9mm was connected by 7 bolts in one side, total 14 bolts for both sides. The bridge has 3 steel plate girders and one connection plate was installed for each steel plate girder. The one side of the connection plate was fixed to the plate girder and the other side had the oval holes so as to be movable in the longitudinal direction by ±20mm.

During the earthquake, the 3 to 10 bolts were cut by shear for 10 connection plates in the total 15 plates as shown in **Fig. 5**. **Photo 20** shows the connection plate at which 10 bolts in 14 were cut and all bolts of one side were cut resulting that the connection function was lost. All bolts at one side were cut at 7 connection plates of ten damaged plates.

Photo 21 shows the cutting surface of the bolts. **Photo 22** shows the 2000 times magnifications. According to the photos, the cutting surface shows the typical stretch failure type shape. The origin of the cut was estimated to occur from the thread of the screw at the B side as shown in **Fig. 5**, and the failure was occurred only in one direction. Therefore, the bolts were cut by the relative displacement between the adjacent girders during the earthquake. The damaged bolts with shear deformation were also found other than cut bolts and it was found that the reversed force was estimated to act the bolts.

The objective of the falling—off prevention devices is a fail—safe function to prevent destructive damage such as falling—off of superstructure when the main members are damaged during earthquake. Hatsune bridge was damaged at the reinforced concrete pier with termination of longitudinal reinforcement as shown in **Photo 7**.

Although the devices were functioned, the damage was found at Yanagisaki bridge on the national highway 229 as shown in **Photo 23**. The bridge is 5 span simply supported steel plate girder bridge. The connection devices using a steel link between girders and abutment were buckled as shown in **Photo 24**. Although the connection portion at the girder had the oval shape to release some amount of movement, the larger displacement was developed during the earthquake. The stoppers installed at the bearings at the other side abutment to prevent an excessive displacement were damaged as shown in **Photo 25**.

This type of falling—off prevention devices functions as a tension member when the girder moves in the center of the bridge, on the other hand, in the opposite direction it works as a compression member resulting in buckling of the devices.

Although this type of devices is recommended for the installation to the existing bridges in the current design specifications, the device should be designed so as to release the relative displacement between the girder and abutment. The appropriate design

displacement of the devices is necessary to be investigated.

CONCLUSIONS

This paper presents the typical damage of highway bridges caused by the recent earthquakes occurred in Japan. The following conclusions may be deduced :

1) The bending failure to shear failure of the reinforced concrete bridges were found at the section of the longitudinal reinforcement were terminated at mid—height. Six bridges during the Kushiro—oki Earthquake and three bridges during the Hokkaido—nansei—oki Earthquake were found. These bridges were designed according to the specifications of highway bridges before 1980 version and they all have RC piers with the circular section. The damage to Shinshiriuchi bridge showed that piers the bridge designed according to the specifications after 1980 were not damaged at the termination section of main reinforcement at mid—height. Since this type of damage tends to develop a brittle shear failure from the bending failure, the countermeasures to the vulnerable bridge piers is required to be promoted.

2) Although the damage to the parapet of abutment is not a destructive one, it is difficult to repair without closing of the exciting traffic. The structure of the abutments which is not damaged and is easy to repair should be investigated.

3) The damage to falling—off prevention devices were found at two bridges. Since the devices are to prevent a destructive damage such as falling—off of superstructure, the improvement of the devices should be investigated.

ACKNOWLEDGEMENT
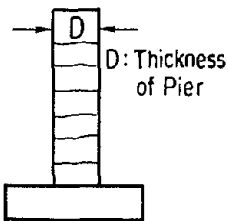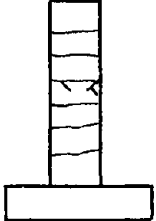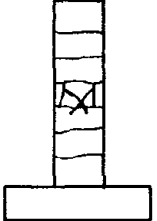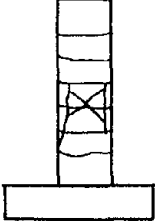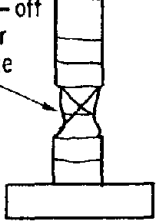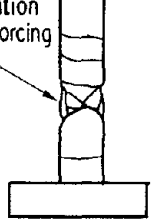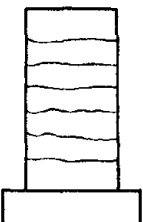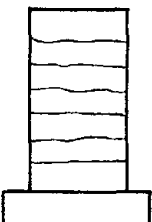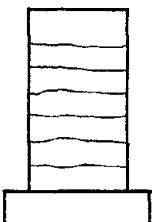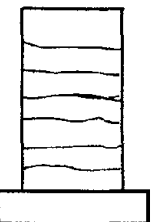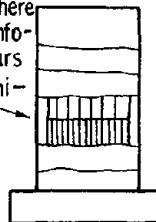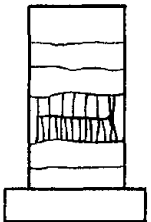
REFERENCES

1) Kushiro Development Department of Hokkaido Development Bureau : Prompt Report (Road Facilities) of the Kushiro—oki Earthquake of January 15, 1993, 1993 (in Japanese)

2) The First Investigation Team of the Public Works Research Institute : Prompt Report of the Kushiro—oki Earthquake of 1993, Civil Engineering Journal, Vol.35, No.4, 1993 (in Japanese)

3) Hakodate Development Department of Hokkaido Development Bureau : Prompt Report

(Road Facilities) of the Hokkaido—nansei—oki Earthquake of 1993, 1993 (in Japanese)

4) The First Investigation Team of the Public Works Research Institute : Prompt Report of the Hokkaido—nansei—oki Earthquake of 1993, Civil Engineering Journal, Vol.35, No.10, 1993 (in Japanese)

5) Kawashima, K., Unjoh, S. and Nakajima, T. : Prompt Report of the Hokkaido—nansei—oki Earthquake of July, 1993, Technical Memorandum of PWRI, No.3204, 1993 (in Japanese)

6) Narita, N., Murakami, P. and Asanuma, H. : Report of the Damage to Shizunai Bridge during the Urakawa—oki Earthquake of 1982, The 15th Joint Meeting of the Panel on Wind and Seismic Effects, UJNR, Tsukuba, 1983

7) Kawashima, K., Unjoh, S., Sugita, H. and Nakajima, T. : Damage to Bridges caused by the Kushiro—oki Earthquake, Bridges and Foundations, Vol.93, No.6, 1993 (in Japanese)

8) Kawashima, K., Unjoh, S. and Iida, H. : Damage to Reinforced Concrete Bridge Piers with Termination of Longitudinal Reinforcement at Mid—height and the Analysis, Civil Engineering Journal, Vol.34, No.5, 1992 (in Japanese)

9) Japan Road Association : Part IV, Substructures of Design Specifications of Highway bridges, 1980 (in Japanese)

10) Japan Road Association : Manual for Earthquake Disaster Prevention Measures of Road Facilities (Post Earthquake), 1988 (in Japanese)

11) Kawashima, K. and Nishikawa, K. : Damage to Bearings of Highway Bridges during the Miyagi—ken—oki Earthquake, Civil Engineering Journal, Vol.21, No.4, 1979 (in Japanese)

12) Japan Road Association : Seismic Design of Design Specifications of Highway bridges, 1971 (in Japanese)

13) Japan Road Association : Part V, Seismic Design of Design Specifications of Highway bridges, 1980 (in Japanese)

Table 1 Estimation Meshod of Damage Degree of Reinforced Concrete Piers at the Termination Section of Main Reinforcement

Observed Damage		① Horizontal Crack	② Diagonal Crack (Less Than the Width of D/2)	③ Diagonal Crack (More Than the Width of D/2)	④ Diagonal Crack (Vertical Crack)	⑤ Spalling-off of Cover Concrete	⑥ Deformation of Reinforcing Bars
Damage	Side View	D: Thickness of Pier				Spalling-off of Cover Concrete	Deformation of Reinforcing Bars
	Front View					Height where main reinforcing bars are Terminated	
Damage Degree		C : Small	C : Small	C : Small	B : Medium	B : Medium	A : Large
Residual Strength		P_u $(1.05\,P_y \sim 1.1 P_y)$	P_u $(1.05 P_y \sim 1.1 P_y)$	$1.0\,P_y$	$1.0\,P_y$	Less Than P_y	Less Than P_y
Residual Ductility $\dfrac{\delta u - \delta}{\delta u - \delta y} \times 100\ (\%)$		100 %	70 %	40 %	10 %	0 %	0 %

P_y : Yielding Strength P_u : Ultimate Strength δy : Yielding Displacement δu : Ultimate Displacement, δ : Peak Displacement

Nate) D : Thickness Pier
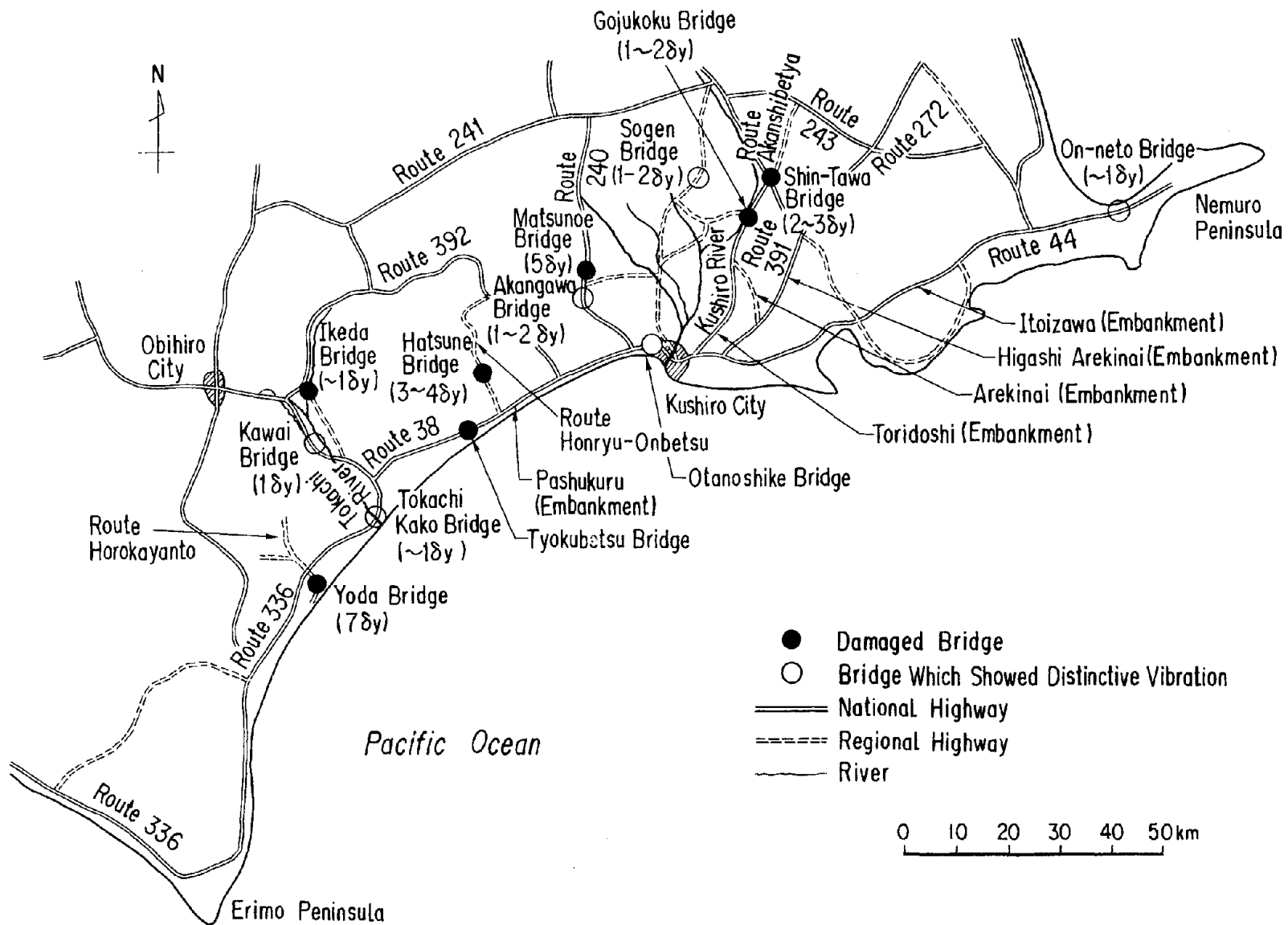
Fig. 1 Location of Damaged Bridges and Damage Degree of Piers caused by the Kushiro—oki Earthquake
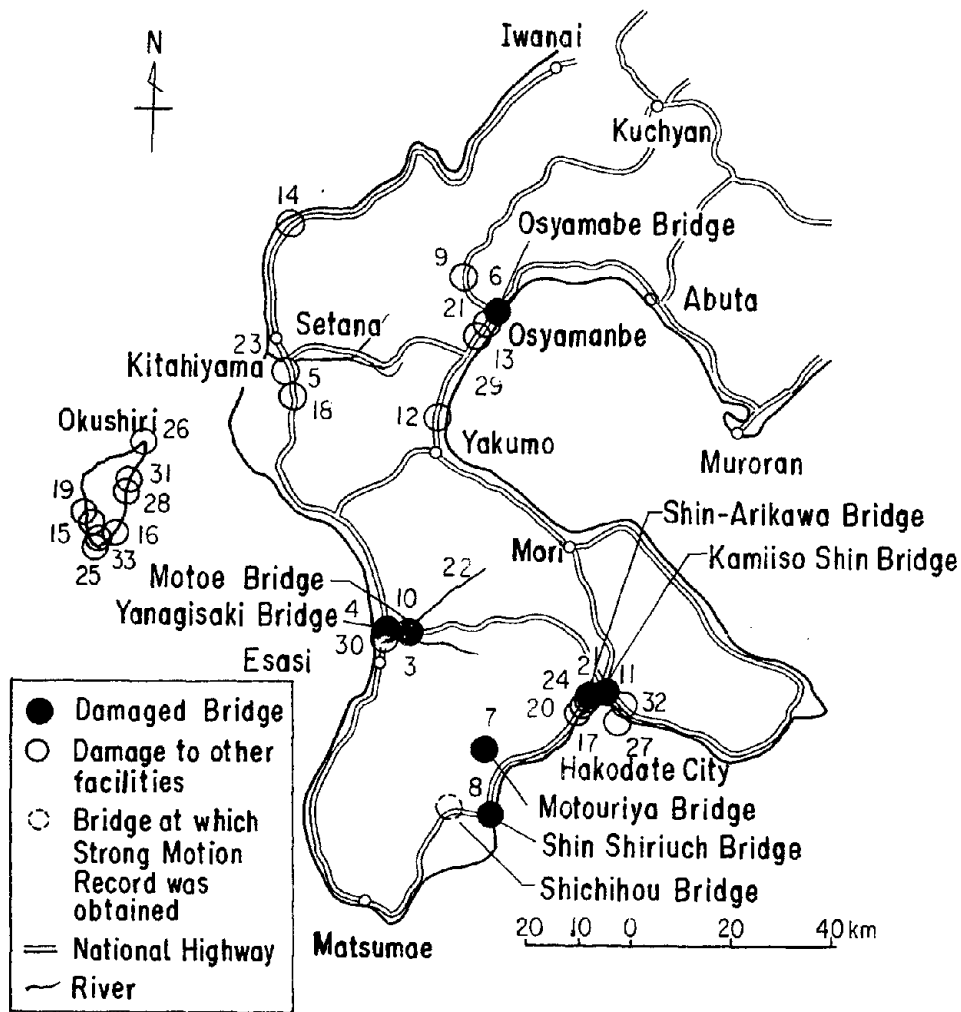
Fig. 2 Location of Damaged Bridges caused by the Hokkaido—nansei—oki Earthquake
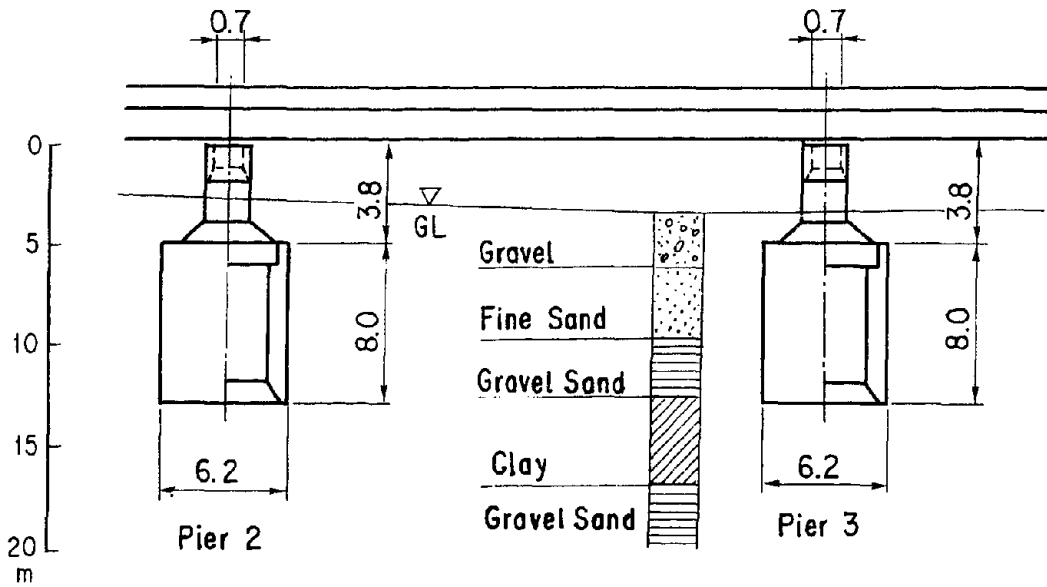
Fig. 3 Ground Condition of Osyamanbe Bridge (by Hokkaido Development Bureau)
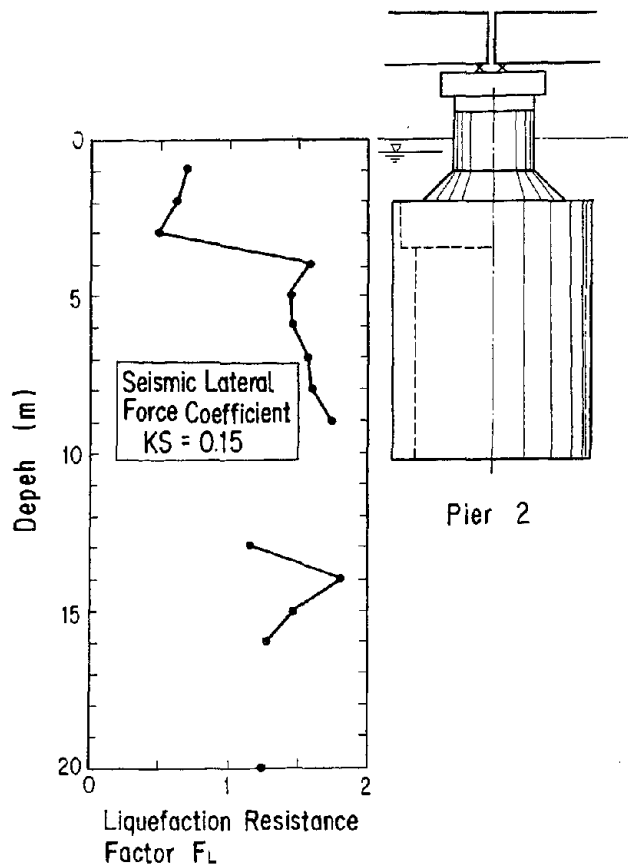
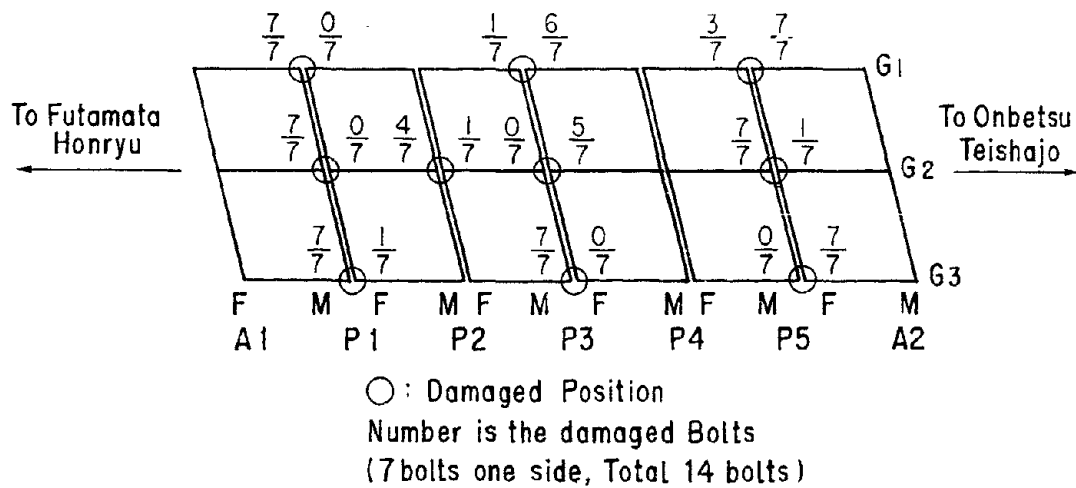**Fig. 4** Liquefaction Resistance Factor, F_L (Pire P2, Osyamanbe Bridge)

$$\frac{7}{7} \quad \frac{0}{7} \qquad \frac{1}{7} \quad \frac{6}{7} \qquad \frac{3}{7} \quad \frac{7}{7}$$

To Futamata
Honryu

$$\frac{7}{7} \quad \frac{0}{7} \quad \frac{4}{7} \quad \frac{1}{7} \quad \frac{0}{7} \quad \frac{5}{7} \qquad \frac{7}{7} \quad \frac{1}{7}$$

To Onbetsu
Teishajo

$$\frac{7}{7} \quad \frac{1}{7} \qquad \frac{7}{7} \quad \frac{0}{7} \qquad \frac{0}{7} \quad \frac{7}{7}$$

F   M   F   M F   M   F   M F   M   F   M
A1   P1   P2   P3   P4   P5   A2

◯ : Damaged Position
Number is the damaged Bolts
(7 bolts one side, Total 14 bolts)

Fig. 5 Location of damage to the connection devices between adjacent girders
(Hatsune Bridge)

O Magnified Position
→ Estimated Direction
   of failure
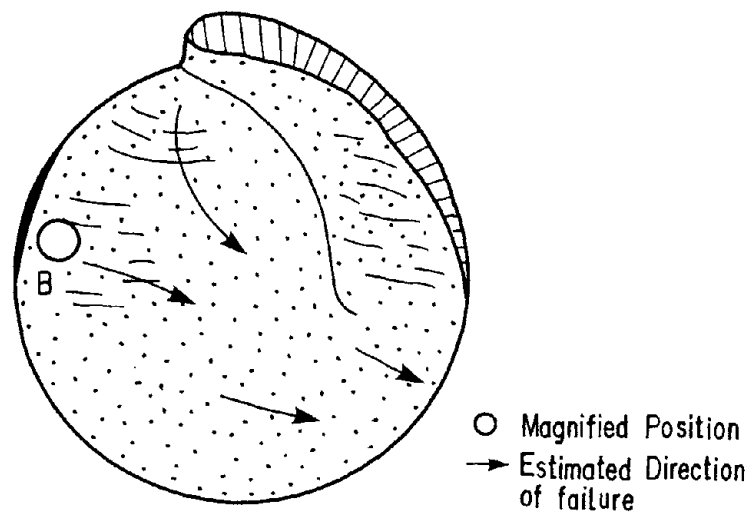
Fig. 6 Direction of Failure of Bolts (Hatsune Bridge)
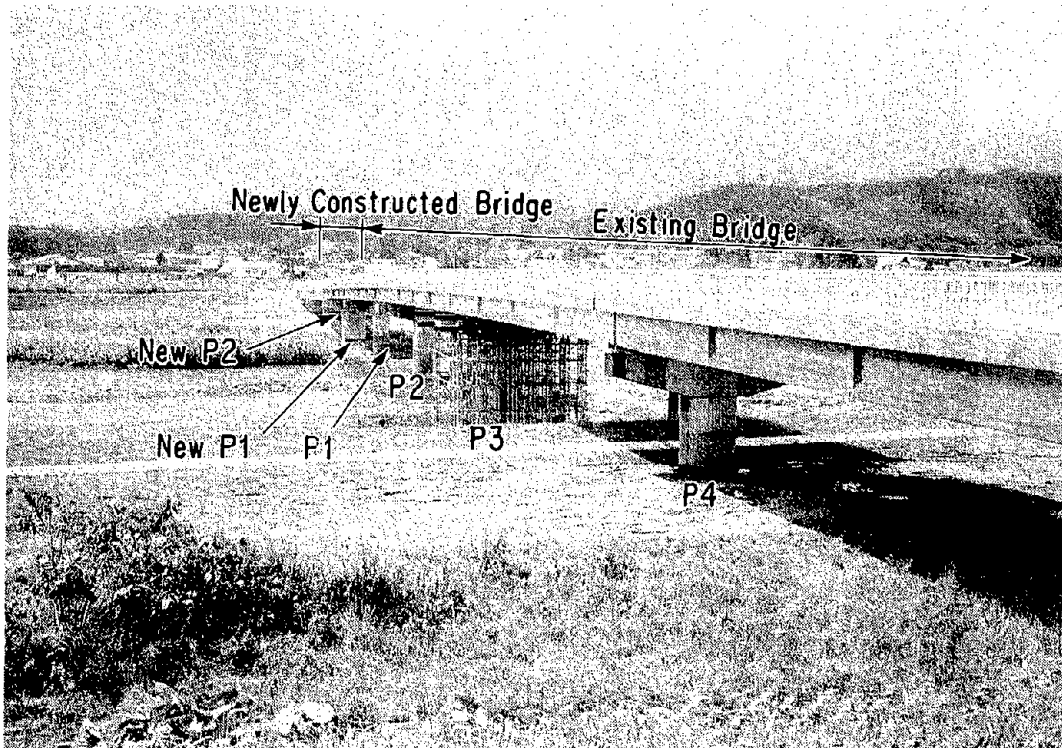
Photo 1 Shin–Shiriuchi Bridge
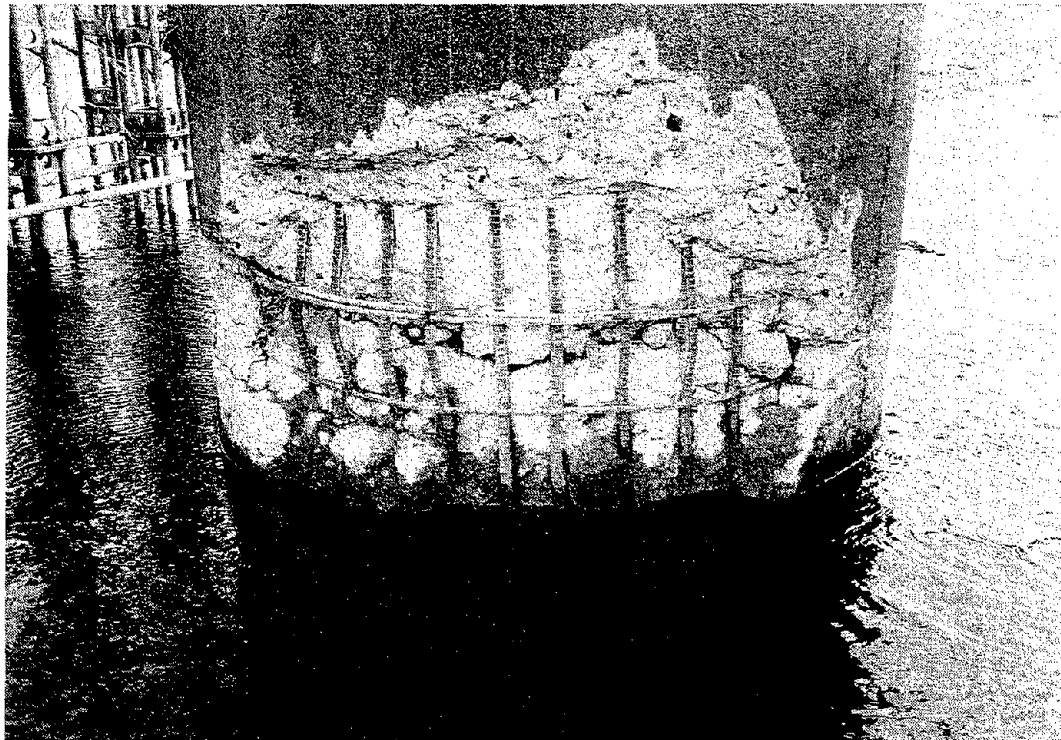
Photo 2 Damage of Pier P3 (from the lower stream side)
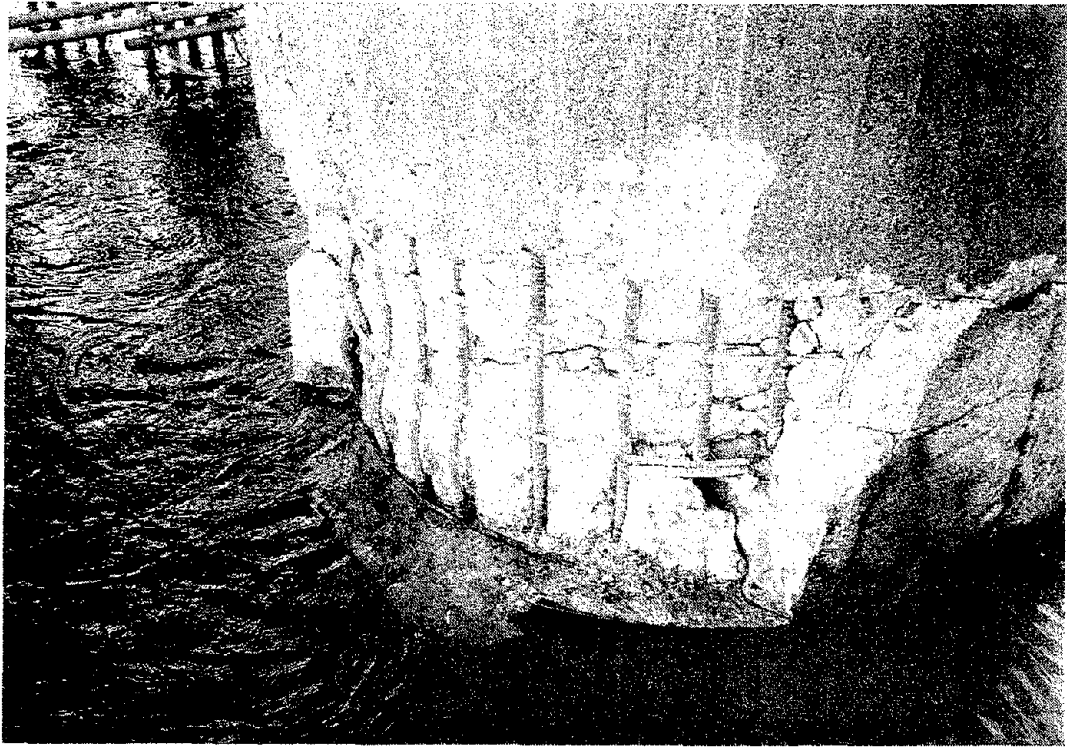
Photo 3 Damage of Pier P3 (from the upper stream side)

Photo 4 Spalling—off of Cover Concrete and the Bucking
of Main Reinforcement of Matsunoe Bridge (Pier P4)

Photo 5 Cracks of Gojukkoku Bridge
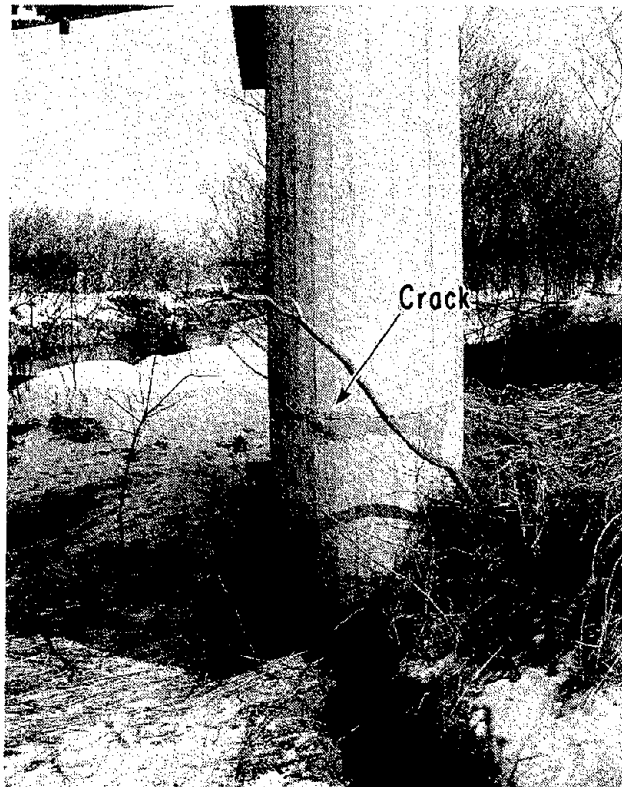
Photo 6 Cracks of Shin−Tawa Bridge (Pire P1)

Photo 7 Diagonal Cracks of Hatsune Bridge (Pire P4)

Photo 8 Cracks of Akagawa Bridge (Pire P2)

98

Photo 9 Damage to Pire P2 of Yoda Bridge
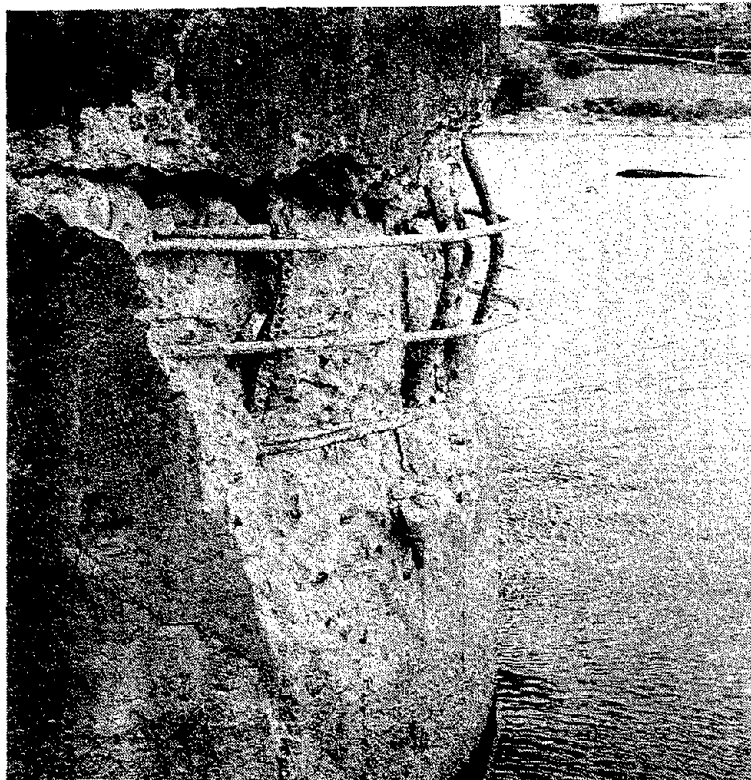
Photo 10 Damage to Pire P3 of Motoe Bridge

99

Photo 11 Damage to Pire of Motouriya Bridge
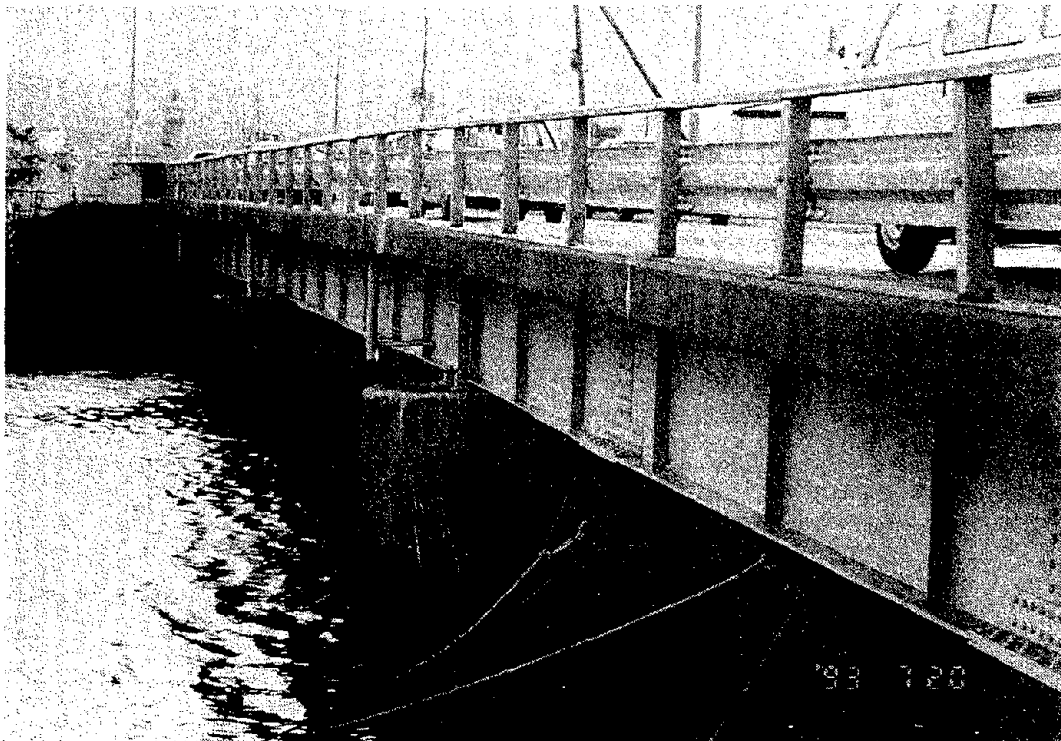
Photo 12 Kamiisoshin Bridge
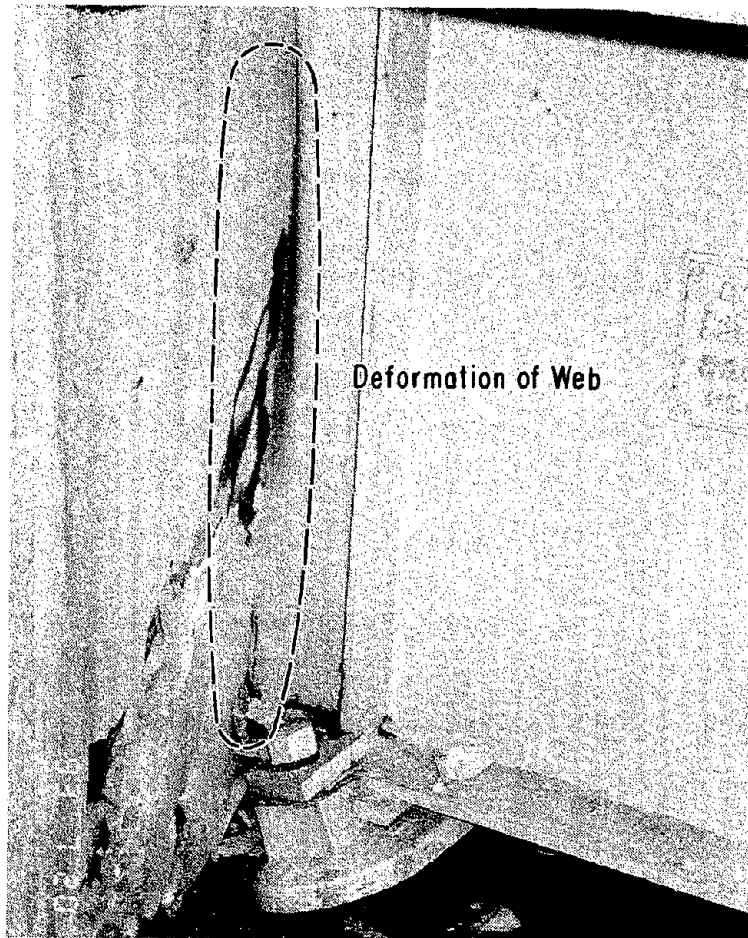
Photo 13 Crash of Girder to Parapet and Deformation of Web and Rotation of Bearings (Kamiisoshin Bridge)
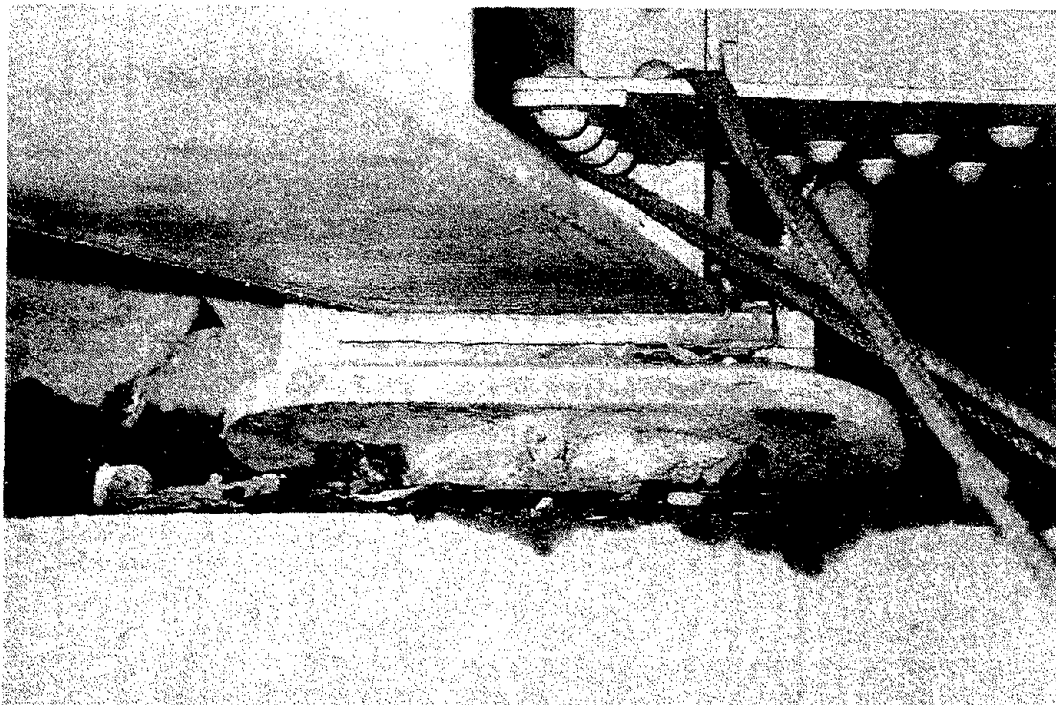
Photo 14 Rotation of Bearing (Kamiisoshin Bridge)
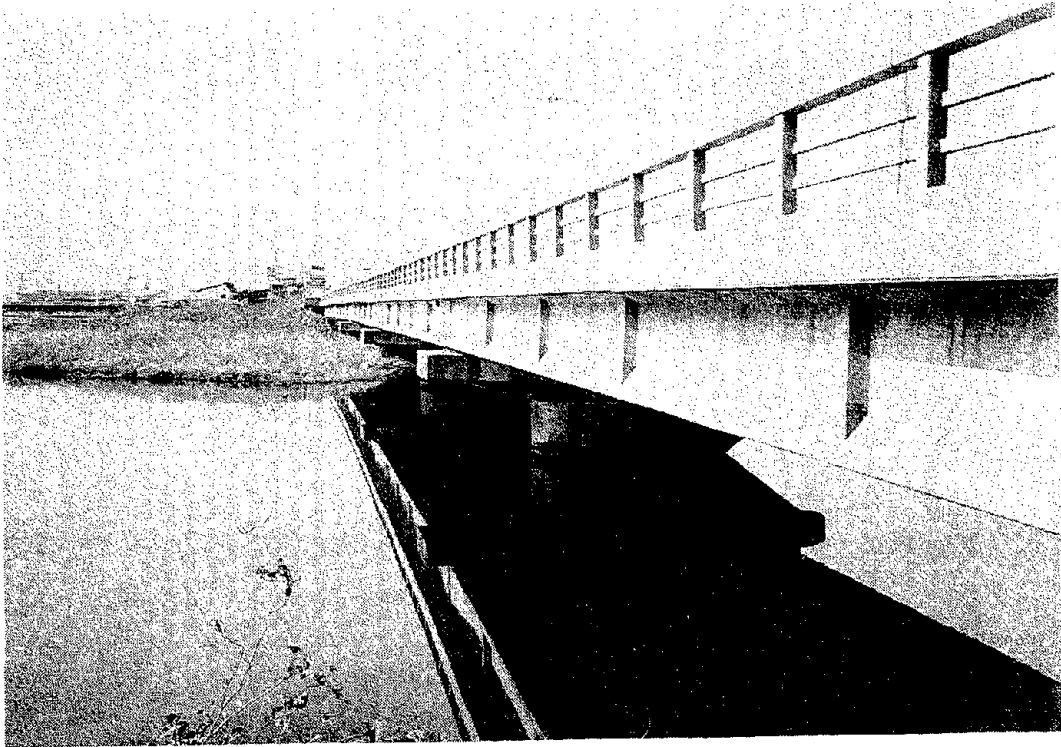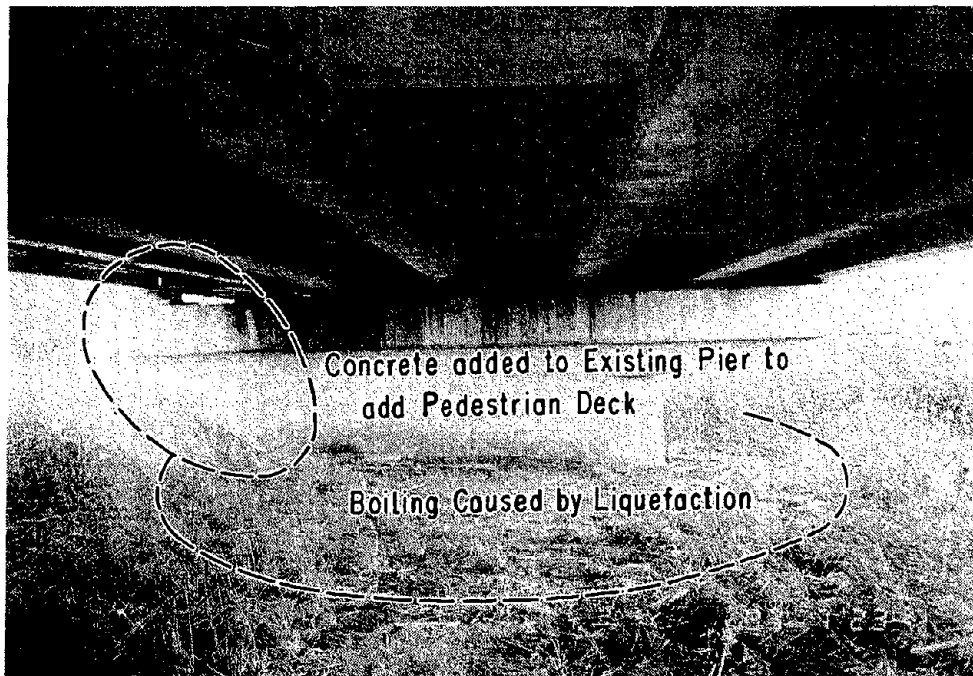
Photo 15 Osyamanbe Bridge

Concrete added to Existing Pier to add Pedestrian Deck

Boiling Caused by Liquefaction

Photo 16 Inclination of Pire and soil Liquefaction (Osyamanbe Bridge, Pier P2)

Photo 17 Residual Displacement found at the Deck caused by
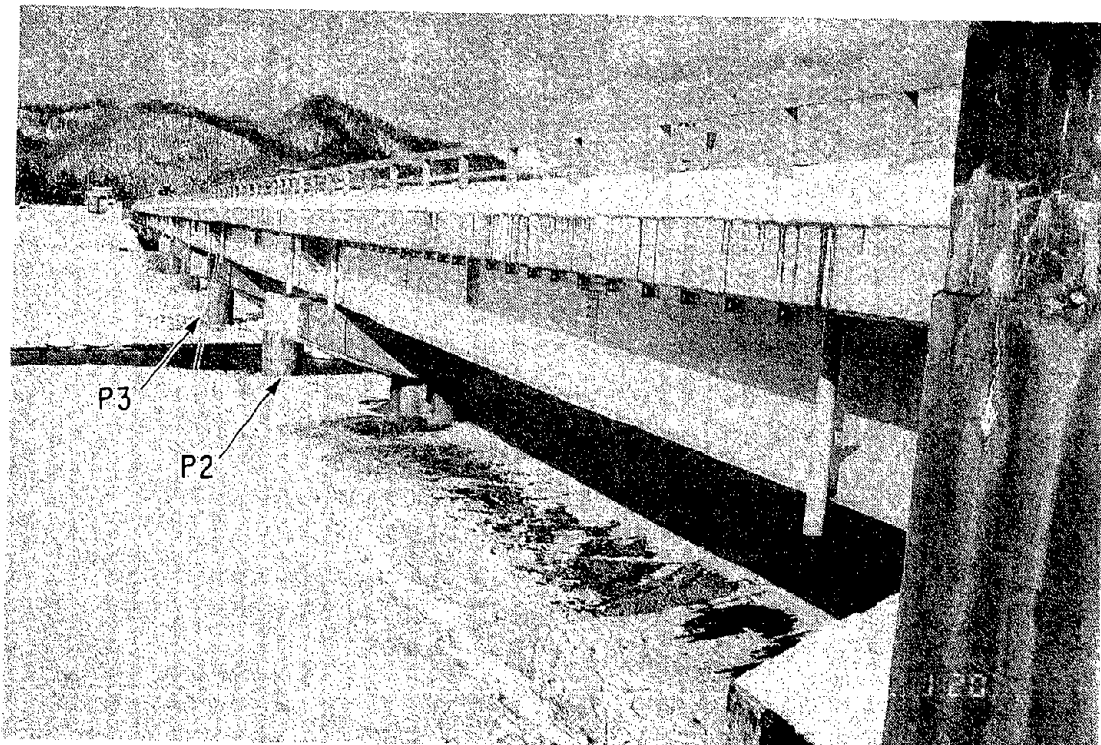the Inclination of Piers (Osyamanbe Bridge)

P3

P2
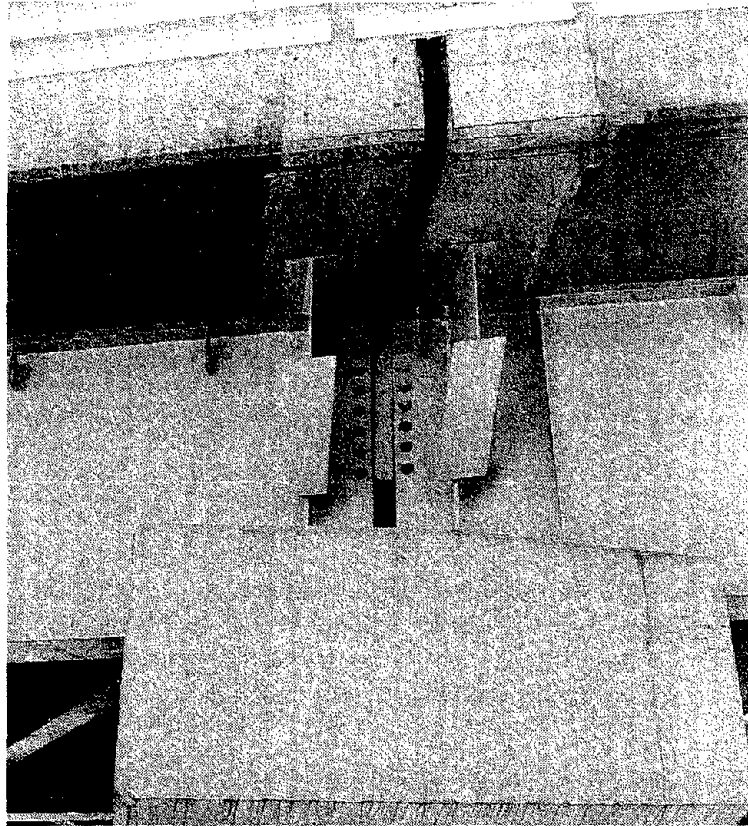
Photo 18 Hatsune Bridge
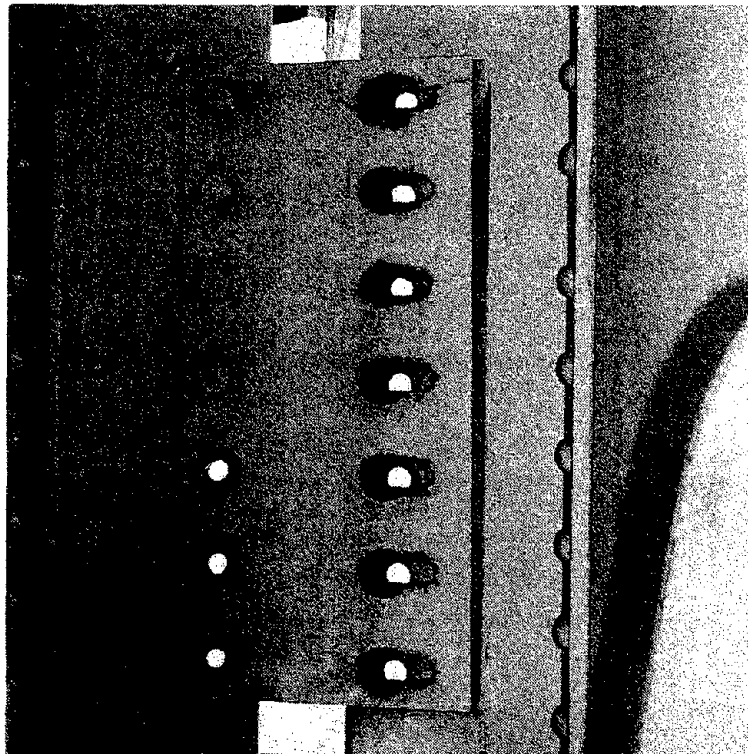
Photo 19 Damage of the Connection Devices (Hatsune Bridge)

Photo 20 Device where all bolts were cut in one side (Hatsune Bridge)
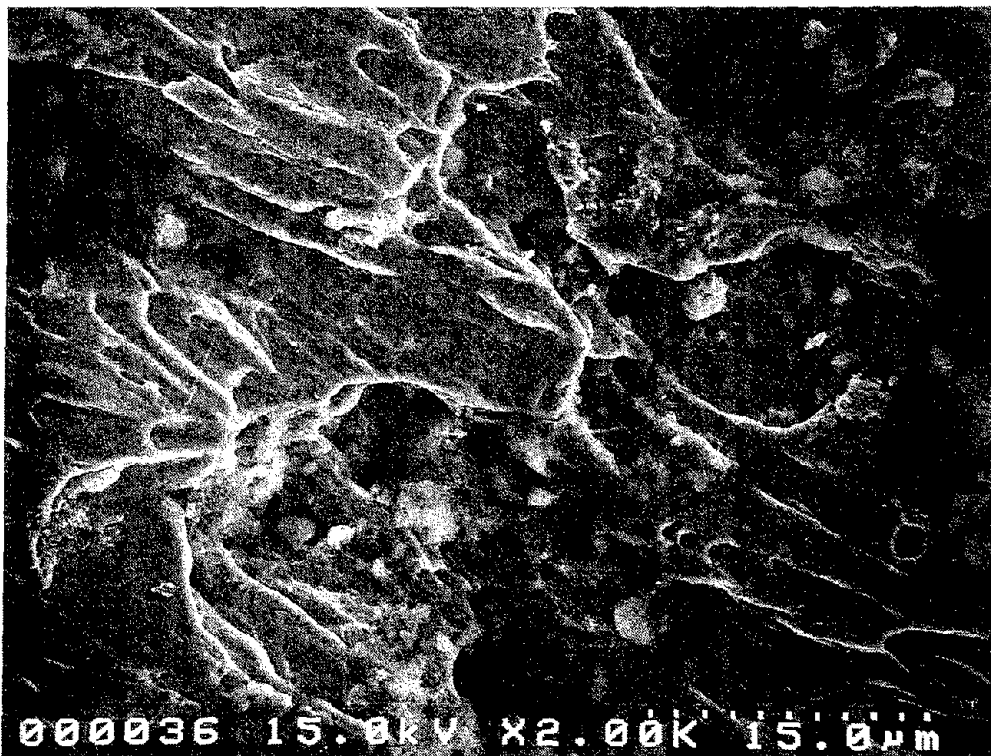
Photo 21 Cutting Surface of Bolts (Hatsune Bridge)

000036 15.0kV X2.00K 15.0μm

Photo 22 Magnification of Cutting Surface (Hatsune Bridge, Position B in **Fig. 6**)
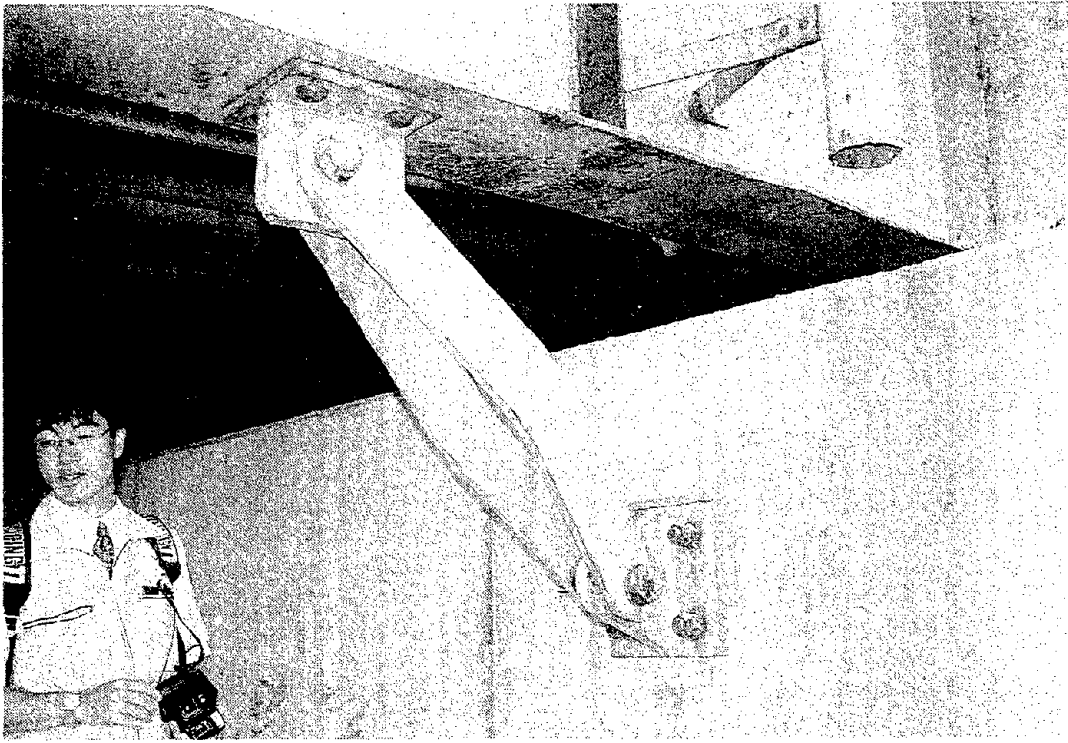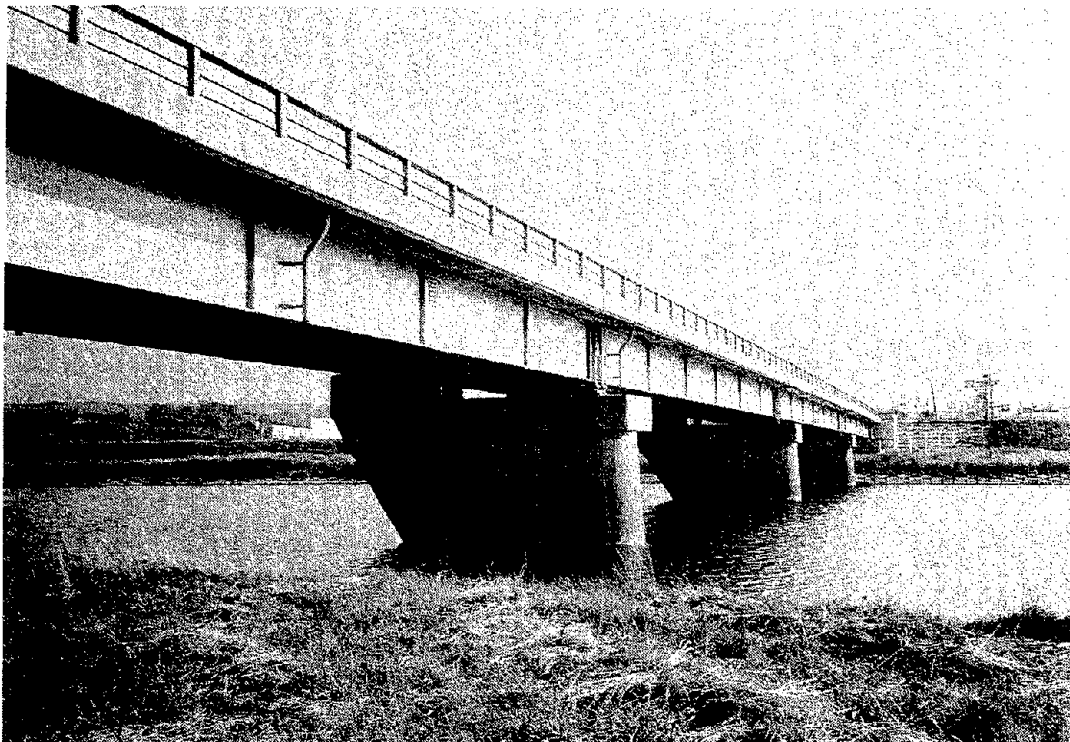
Photo 23 Yanagisaki Bridge

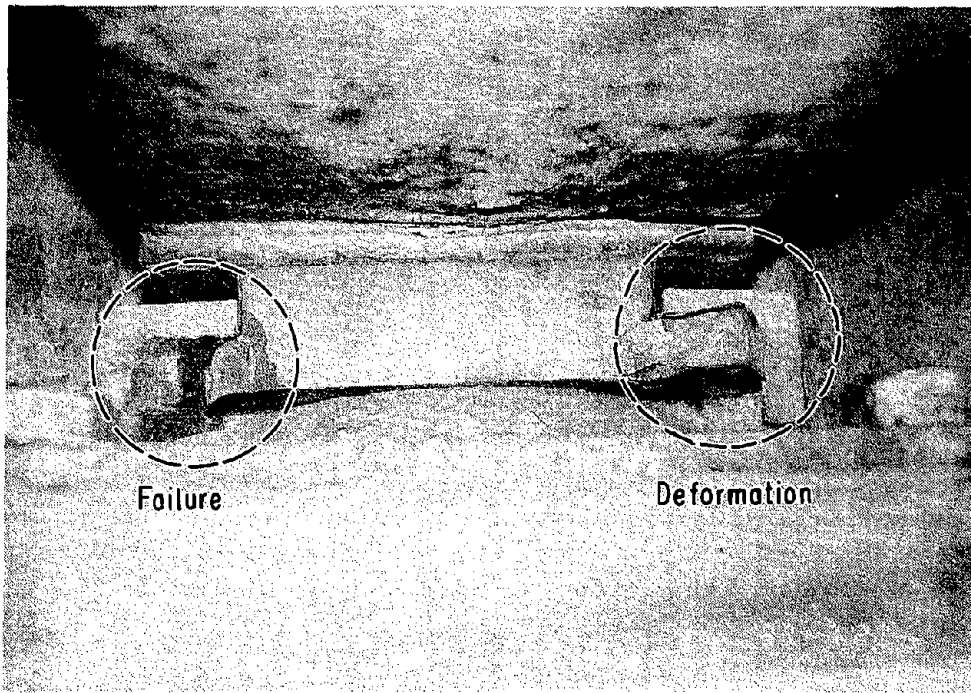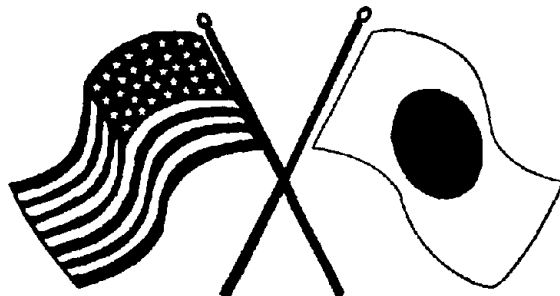**Photo 24** Buckling of Falling−off Devices (Yanagisaki Bridge)

Photo 25 Damage of Stoppers (Bearing at Abutment, Yanagisaki Bridge)

SECOND U.S.-JAPAN WORKSHOP ON SEISMIC RETROFIT OF BRIDGES

Damage Analysis of Reinforced Concrete Bridge Piers by Kushiro-oki Earthquake, January 1993, and Hokkaido nansei-oki Earthquake, July 1993

K. Kawashima, J. Hoshikuma and S. Unjoh

DAMAGE ANALYSIS OF REINFORCED CONCRETE BRIDGE PIERS BY KUSHIRO-OKI EARTHQUAKE, JANUARY, 1993 AND HOKKAIDO NANSEI-OKI EARTHQUAKE, JULY, 1993

K. Kawashima[1], J. Hoshikuma[2] and S. Unjoh[3]

1) Head, Earthquake Engineering Division, Public Works Research Institute, Ministry of Construction, Tsukuba Science City, Japan
2) Research Engineer, ditto
3) Senior Research Engineer, ditto

ABSTRACT

This paper presents the effectiveness of a seismic evaluation method for reinforced concrete bridge piers with termination of longitudinal reinforcement at mid-height based on the damage due to the Kushiro-oki Earthquake and the Hokkaido Nansei-oki Earthquake. During these earthquakes, several reinforced concrete bridge piers with circular cross section suffered significant damage at mid-height. The piers were designed and constructed prior to 1980, when the Design Specifications of Highway Bridges was revised. The seismic vulnerability of damaged and undamaged piers was evaluated.

INTRODUCTION

During the Kushiro-oki Earthquake in January, 1993 and the Hokkaido Nansei-oki Earthquake in July, 1993, many bridges were damaged[1]. In particular, reinforced concrete piers suffered damage at mid-height, where the longitudinal reinforcement was terminated with inadequate anchorage length. The importance for this type of damage was firstly pointed out when Shizunai bridge was critically damaged during the Urakawa-oki Earthquake in 1982[2]. The damage causes a brittle shear failure and may result in a collapse of substructures.

Before 1980, an anchorage length of terminated reinforcement was stipulated as[3]

$$l = \frac{\phi \, \sigma_{sa}}{6 \tau_{0a}} \tag{1}$$

where

l : anchorage length (cm)

σ_{sa} : allowable tensile stress of reinforcement (kgf/cm^2)

τ_{0a} : allowable adhesion stress of concrete (kgf/cm^2)

ϕ : diameter of reinforcement (cm)

In the revision of the Design Specifications of Highway Bridges in 1980[4], the anchorage length was increased as

$$l = \frac{\phi \, \sigma_{sa}}{4 \tau_{0a}} \tag{2}$$

and the allowable shear stress of concrete in anchorage zone was reduced to two thirds of the shear stress at the normal zone. Therefore, reinforced concrete piers designed and constructed in accordance with the Specifications after 1980 are redundant at the termination zone, however, the others require to be adequately evaluated and strengthened at need. To identify the seismic vulnerability at the termination point, a seismic evaluation method was proposed based on the study at PWRI and has been applied to the seismic evaluation in 1991 throughout the country.

This paper presents a result of seismic evaluation of piers which were damaged and undamaged during the Kushiro–oki Earthquake and the Hokkaido Nansei–oki Earthquake, and describes an application of the seismic evaluation method at the termination of longitudinal reinforcements.

SEISMIC EVALUATION METHOD FOR THE TERMINATION OF LONGITUDINAL REINFORCEMENT

The seismic evaluation method for the termination of longitudinal reinforcement was already reported[5][6], hence a summary of the evaluation method is described here briefly.

Fig. 1 shows a flow chart of the seismic evaluation for reinforced concrete piers with termination of longitudinal reinforcement. According to the evaluation method, the seismic vulnerability at the termination point is evaluated by two parameters, i.e., failure mode factor and safety factor. The safety factor is defined as a ratio of the yielding bending moment to the bending moment due to the lateral force for design as shown in Fig. 2 and is given as

$$F_y^T = \frac{M_y^T}{M^T} \tag{3}$$

$$F_y^B = \frac{M_y^B}{M^B} \tag{4}$$

where

F_y^T and F_y^B : safety factor at the termination point and base, respectively

M_y^T and M_y^B : yielding bending moment at the termination point and base, respectively

M^T and M^B : bending moment at the termination point and base, respectively, due to the lateral force for design

In this evaluation, the termination point is defined as the point with anchorage length below
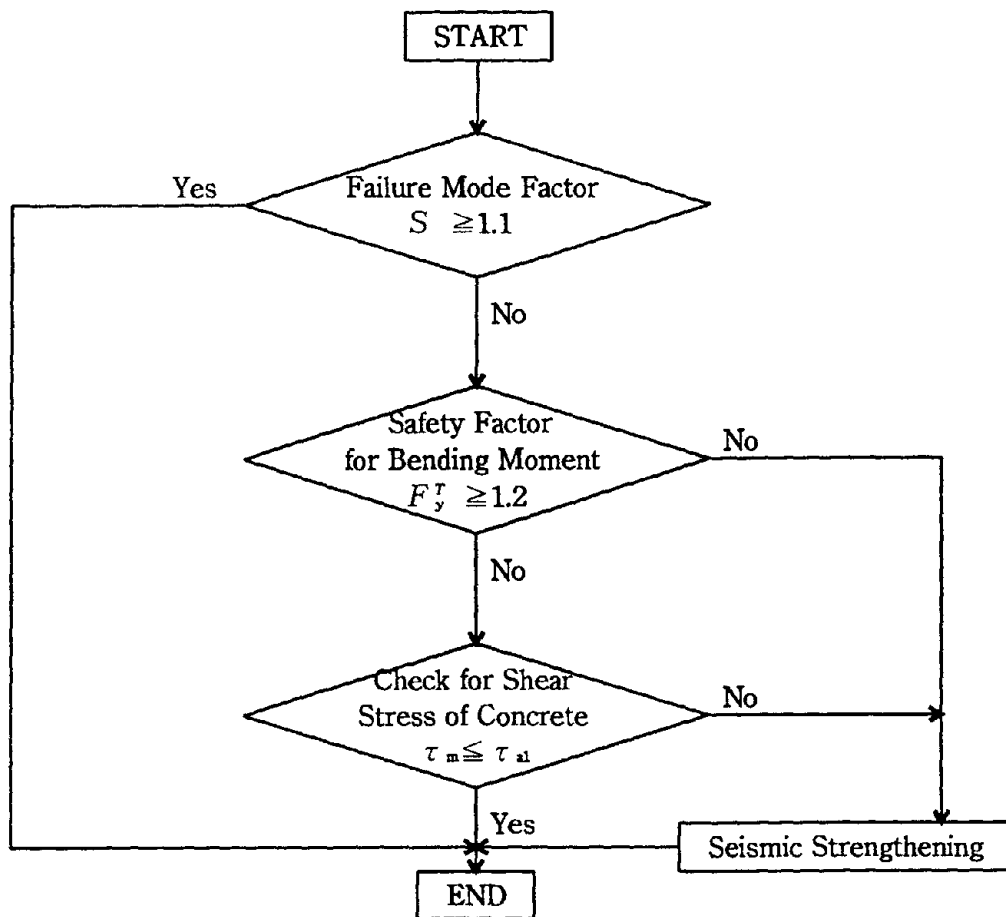
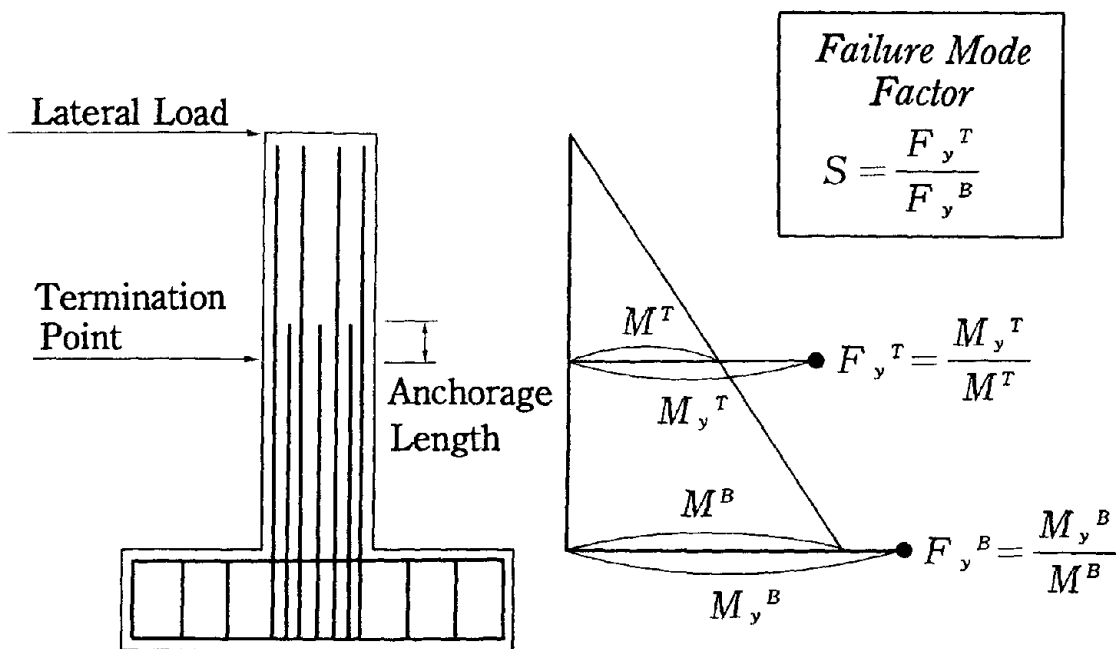Fig. 1 Seismic Evaluation for Reinforced Concrete Bridge Piers with Termination

Fig. 2 Definition of Failure Mode Factor

the actual point of terminations.

To identify which zone the initial damage would be developed, the failure mode factor S is defined as

$$S = \frac{F_y{}^T}{F_y{}^B}$$
(5)

Based on a series of loading test results at PWRI, the seismic vulnerability at the termination point was evaluated by means of the failure mode factor S and the safety factor $F_y{}^T$ as shown in **Table 1**. The piers which are evaluated S as larger than 1.1 are not damaged at the termination point, while the others are predicted the damage degree by **Table 1(b)**. **Fig. 3** summarizes the damage degree at the termination point predicted by **Table 1**. The seismic strengthening is required for the piers evaluated S as less than 1.1 and $F_y{}^T$ as less than 1.2.

DAMAGE OF REINFORCED CONCRETE PIERS
AT MID–HEIGHT DUE TO RECENT EARTHQUAKES

General

During the Kushiro–oki Earthquake and the Hokkaido Nansei–oki Earthquake, nine bridges suffered damage at mid–height. **Fig. 4** and **Table 2** show the locations and damage of the bridges. The remarkable points of damage are as follows.

  a) All bridges damaged were designed and constructed prior to 198ṳ. Therefore, the anchorage length of the terminated longitudinal reinforcement was inadequate.

  b) Most of piers damaged have a circular cross section with smaller concrete area.

  c) The damage was developed by the lateral force in transverse direction.

In this paper, the damage of Yoda bridge, Motoe bridge, Shin–shiriuchi bridge and Motouriya bridge, which are evaluated as the "Critical Damage" based on the Guide Specifications for Earthquake Hazard Mitigation for Transportation Facilities[7], is described below.

Damage of Yoda Bridge

The pier of Yoda bridge has a circular cross section with 1.4m diameter and 4.1m height. As shown in **Fig. 5**, forty eight D19 bars (deformed bars with diameter of 19mm) were used as the longitudinal reinforcement at the base. Twenty four bars were terminated at 0.78m above the base, and twelve bars were terminated at 1.58m above the base. The hoop reinforcement (D13) was placed every 20cm around the termination points. The P2 pier suffered the spalling–off of concrete and serious buckling of longitudinal reinforcement at the second termination point as shown in **Photos 1 and 2**. Among twelve bars above the second termination point, six bars were ruptured. Judging from such failure, almost no residual strength was left at the pier.

Table 1 Evaluation of Seismic Vulnerability

(a) Evaluation in terms of Failure Mode Factors S

Failure Mode Factor S	Failure Mode
$S \geq 1.1$	Flexural Failure at Base
$S < 1.1$	Vulnerable to Failure at Termination Zone

(b) Evaluation in terms of Safety Factors F_y^T

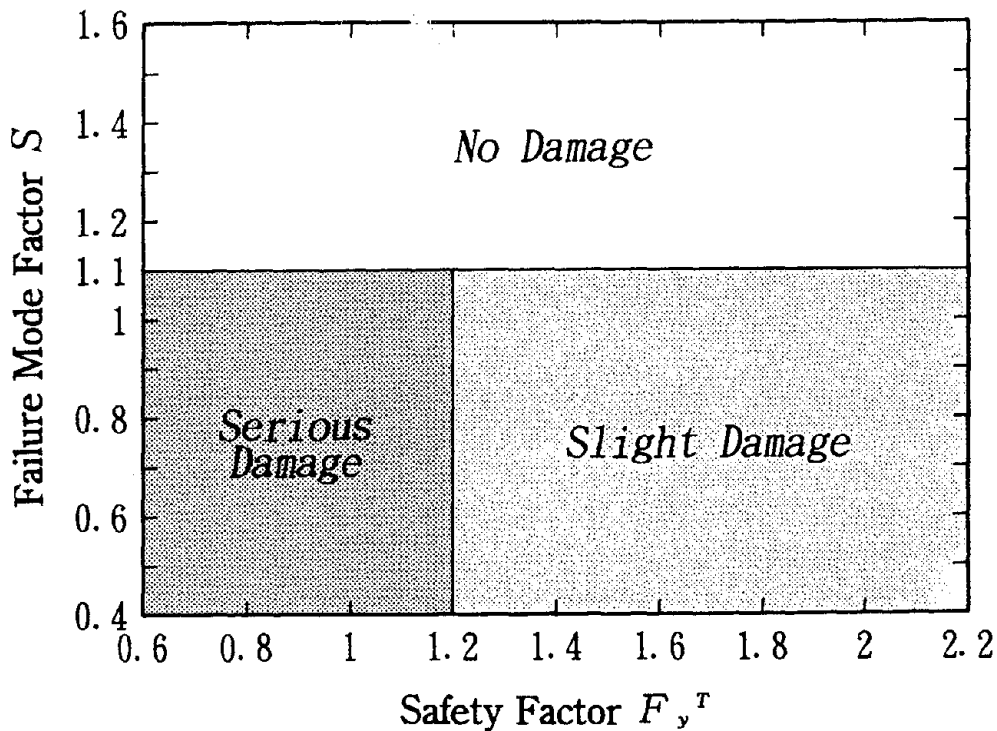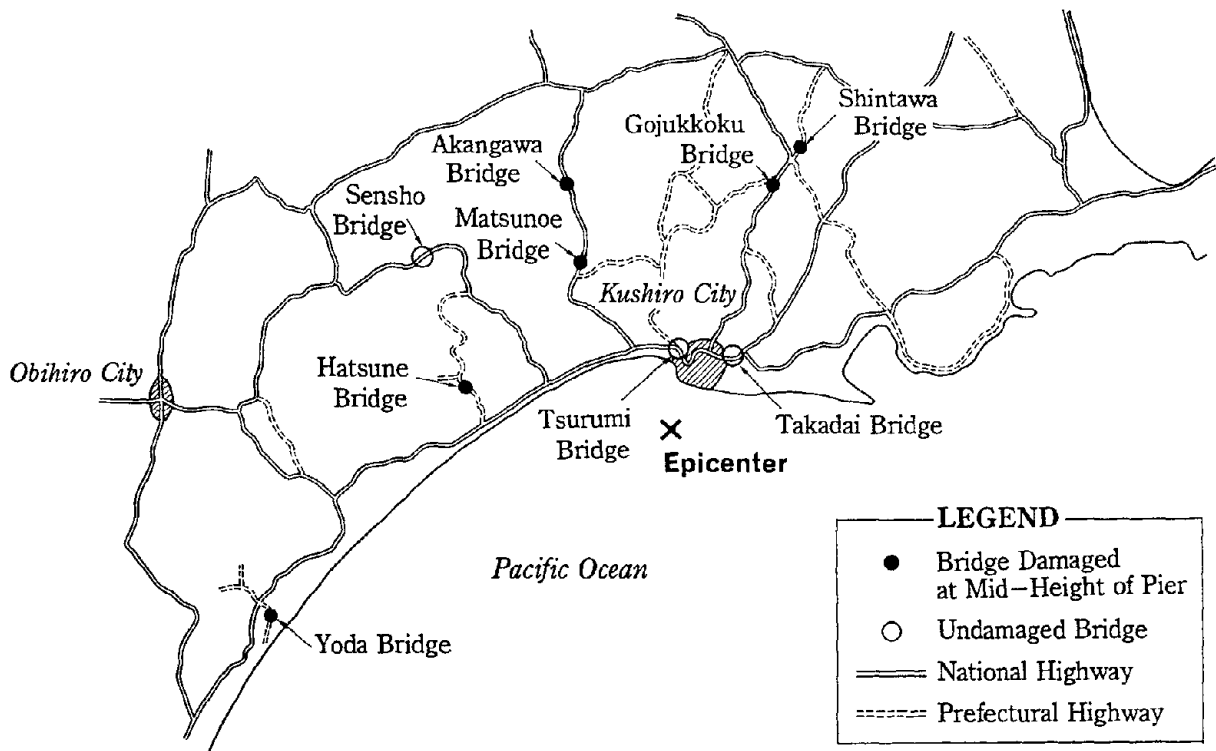| Safety Factor F_y^T	Damage Degree at Termination Zone at the Loading Displacement of $5\delta_y$
$F_y^T < 1.2$	Rupture and serious buckling of longitudinal reinforcement are developed.
$F_y^T \geq 1.2$	Diagonal racks, spalling−off of cover concrete, and slight buckling of longitudinal reinforcement are developed.

Fig. 3 Evaluation of Damage Degree

115

(a) Bridges Damaged Due to Kushiro–oki Earthquake
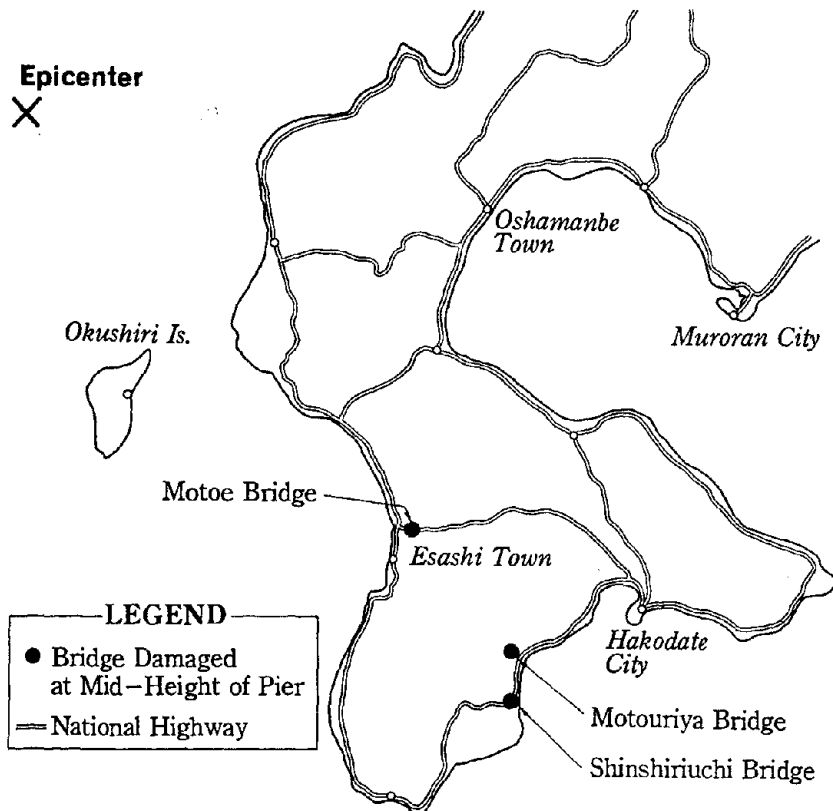
(b) Bridges Damaged Due to Hokkaido Nansei–oki Earthquake

Fig. 4 Location of Bridges

116

Table 2 Summary of Bridge Damaged

| Earthquake	Bridge	Year of Design	Length(m)	Superstructure Type	Cross Section		Damage Degree
					Shape	Dimension(m)	
Kushiro—oki Earthquake	Yoda Br.	1969	70	3−Span Simple Supported Steel Girder Bridge	Circular	ϕ 1.4	Critical Damage
	Matsunoe Br.	1962	157	5−Span Simple Supported PC Girder Bridge	Circular	ϕ 2.5	Medium Damage
	Hatsune Br.	1967	172	6−Span Simple Supported Steel Girder Bridge	Circular	ϕ 1.8	Medium Damage
	Shintawa Br.	1974	60.3	3−Span Simple Supported Steel Girder Bridge	Oval	7.9 × 1.0	Slight Damage
	Gojukkoku Br.	1966	249	7−Span Simple Supported PC Girder Bridge	Circular	ϕ 2.2	Slight Damage
	Akangawa Br.	1973	126.5	4−Span Simple Supported PC Girder Bridge	Circular	ϕ 2.0	Slight Damage
Hokkaido Nansei—oki Earthquake	Motoe Br.	1968	165.7	7−Span Simple Supported Steel Girder Bridge	Circular	ϕ 1.8	Critical Damage
	Shinshiriuchi Br.	1970	214	7−Span Simple Supported PC Girder Bridge	Circular	ϕ 1.8	Critical Damage
	Motouriya Br.	1964	63	2−Span Simple Supported PC Girder Bridge	Circular	ϕ 1.5	Critical Damage

117
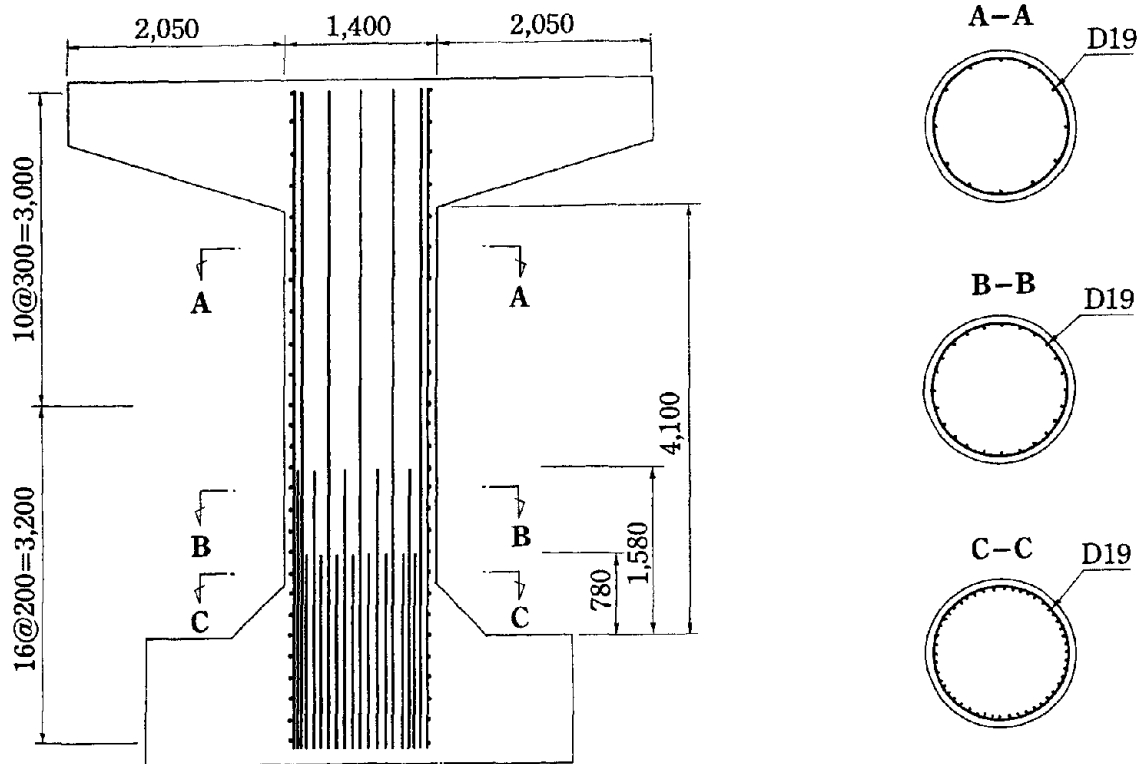
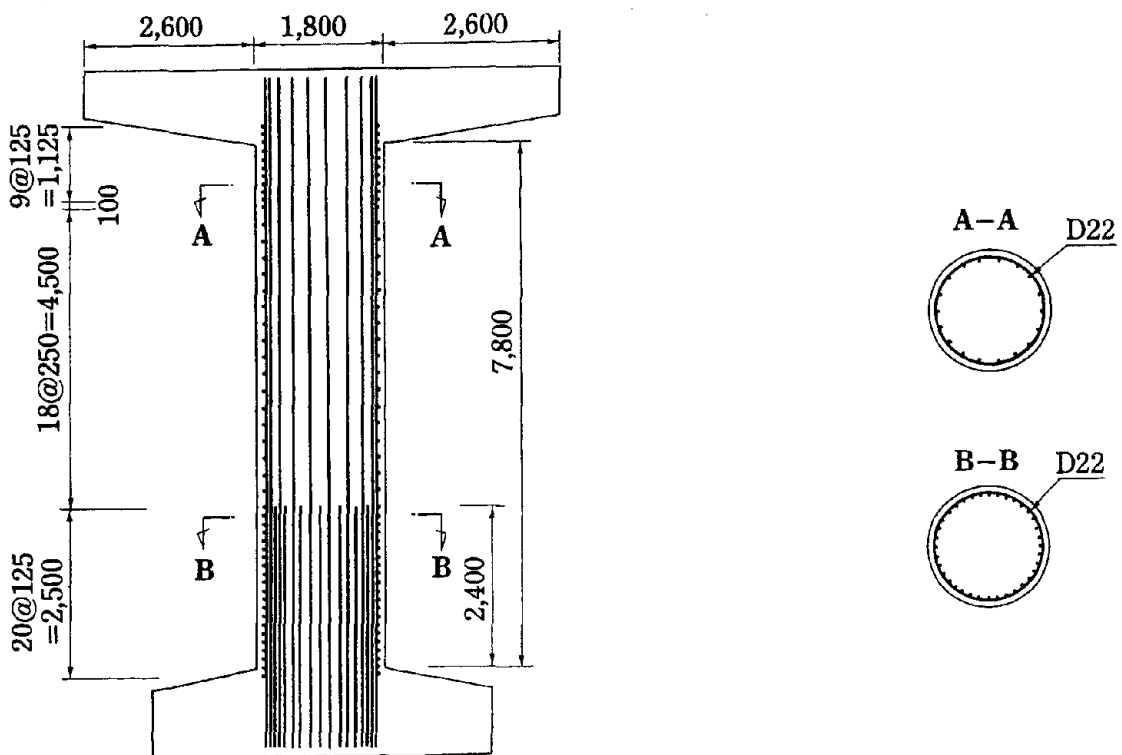**Fig. 5** Layout of Longitudinal Reinforcement in Yoda Bridge Pier

Fig. 6 Layout of Longitudinal Reinforcement in Motoe Bridge Pier

Photo 1 Damage of Yoda Bridge

Photo 2 Failure at Termination Point

Damage of Motoe Bridge

The pier of Motoe bridge has a circular cross section with 1.8m diameter and 7.8m height. As shown in **Fig. 6**, thirty six D22 bars were placed as the longitudinal reinforcement at the base, and eighteen bars were terminated at 2.4m above the base. The hoop reinforcement (D13) was placed every 12.5cm between the base and the termination point. The P3 pier suffered the most serious damage as shown in **Photos 3** and **4**. The spalling—off of concrete and the buckling of longitudinal reinforcement were developed at the termination point. This was developed due to the lateral force in transeverse direction.

Damage of Shin—shiriuchi Bridge

Shin—shiriuchi bridge consists of seven simply supported girders as shown in **Fig. 7**. After the five spans at the left bank side were constructed in 1969, the other two spans were extended associated with the extension of Shiriuchi River in 1989. Among six piers, only new P1 pier did not have the termination of the longitudinal reinforcement. It was interesting that the old piers were damaged at the termination point, while the new piers were not damaged.

The old P3 pier has a circular cross section with 1.8m diameter and 7.04m height. As shown in **Fig. 8**, sixty four D22 bars were double—placed as the longitudinal reinforcement at the base. Thirty two inside bars were terminated at 2.47m above the base, and sixteen outside bars were terminated at 3.67m above the base. The hoop reinforcement (D13) was placed every 12.5cm at base and every 25cm around the termination points. Failure of concrete and buckling of longitudinal reinforcement were developed at the first termination point as shown in **Photo 5**. In the old P2 pier, the horizontal and diagonal cracks were developed at the second termination point as shown in **Photo 6**.

The new P2 pier has an oval cross section of 3m × 1.5m with 6.1m height. The cross sectional area of the new P2 pier is approximately 1.6 times larger than that of the old P3 pier. As shown in **Fig. 9**, fifty six D22 bars were placed as the longitudinal reinforcement at the base, and twenty eight bars were terminated at 3m above the base. The hoop reinforcement (D16) was placed every 10cm. The structure is quite different between the old pier and the new pier. It was proved that the damage at the termination point can be prevented by taking the anchorage length long enough in accordance with the current Specifications.

Damage of Motouriya Bridge

The pier of Motouriya bridge has a circular cross section with 1.5m diameter and 3.05m height. As shown in **Fig. 10**, thirty six ϕ 16 round bars were placed as the longitudinal reinforcement below the termination point, and eighteen ϕ 13 round bars were placed above it. These bars were spliced with lap length of 50cm. Two thirds of longitudinal reinforcement in terms of the gross area were terminated. The round hoop reinforcement
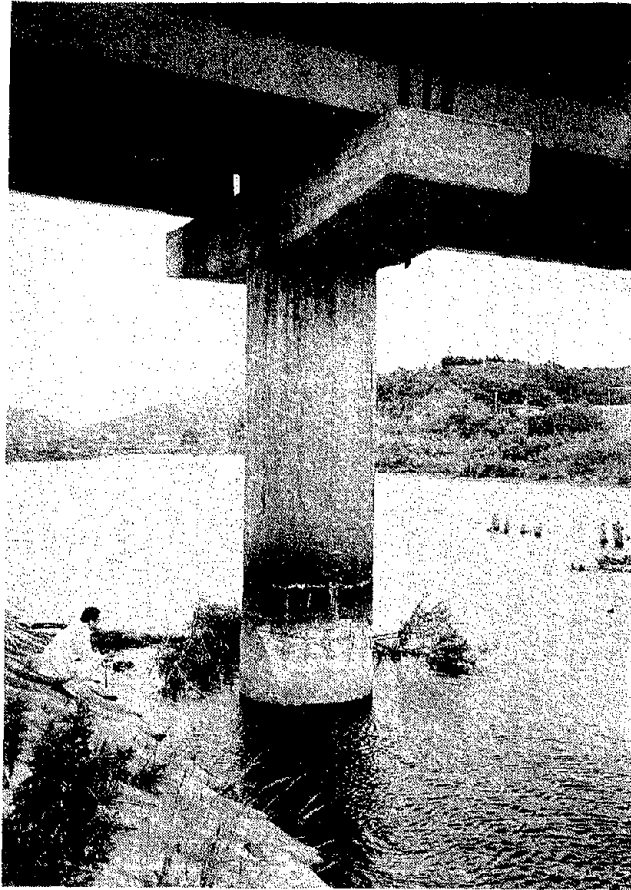
Photo 3 Damage of Motoe Bridge
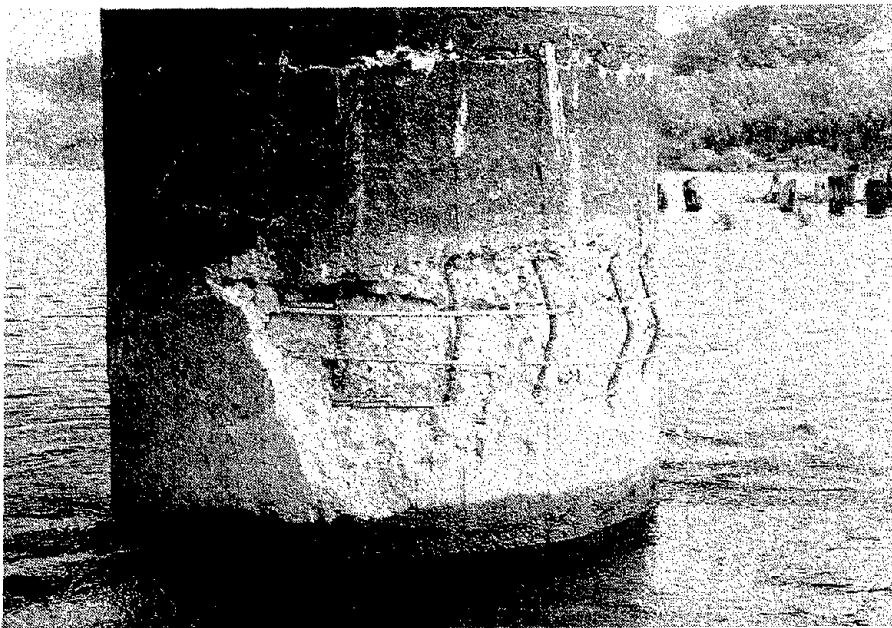
Photo 4 Failure at Termination Point

Old Bridge

Left Bank

F M M F M F M

P 4
No Damage

P 3
Critical Damage at
The 1st Termination

P 2
Slight Damage at
The 2nd Termination

New Bridge

122

F M F M F M F

Right Bank

New P 2
No Damage

P 1
Slight Damage at
The 2nd Termination

New P 1
No Damage
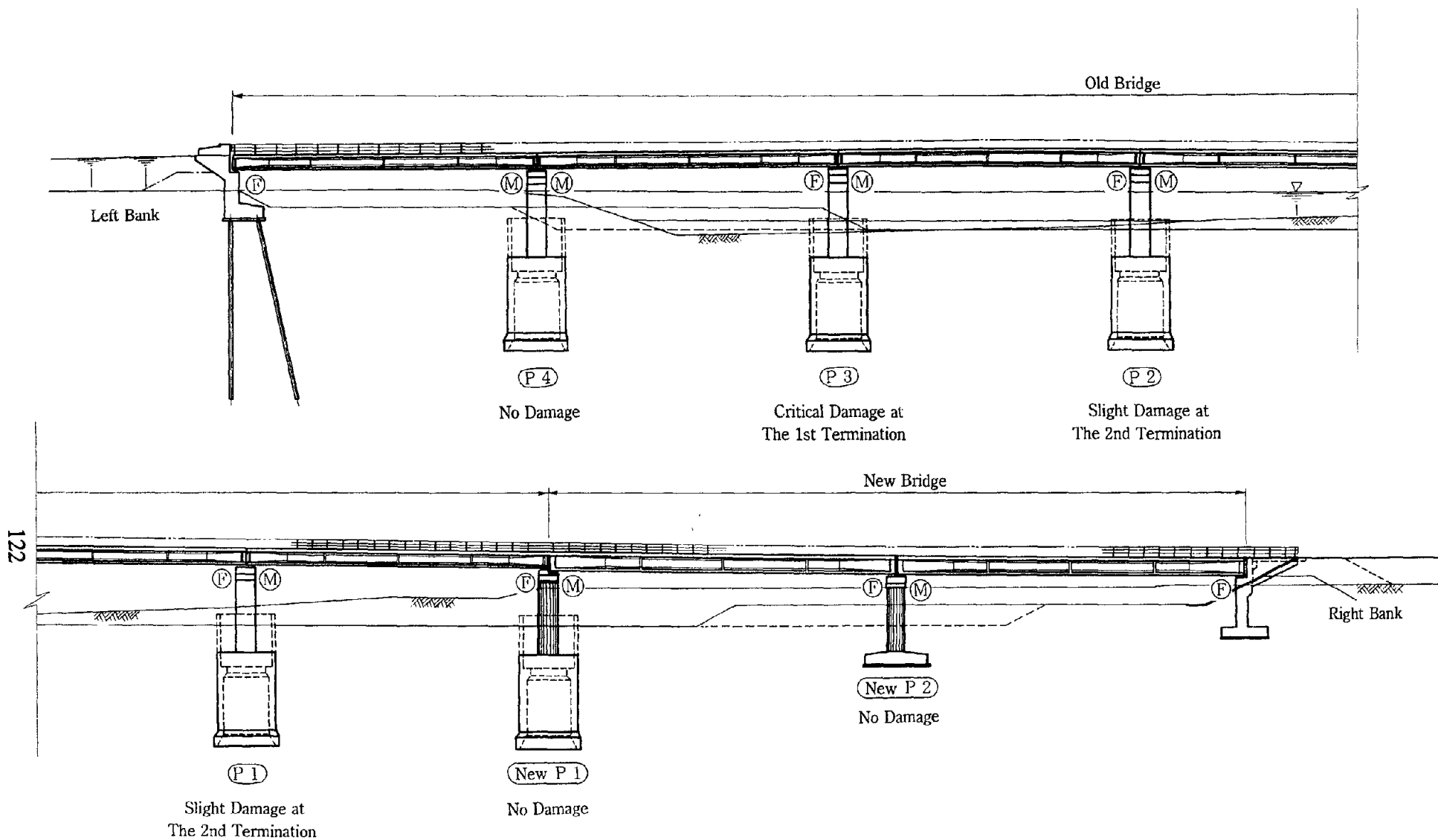
Fig. 7 General Schematic View of Shin—shiriuchi Bridge
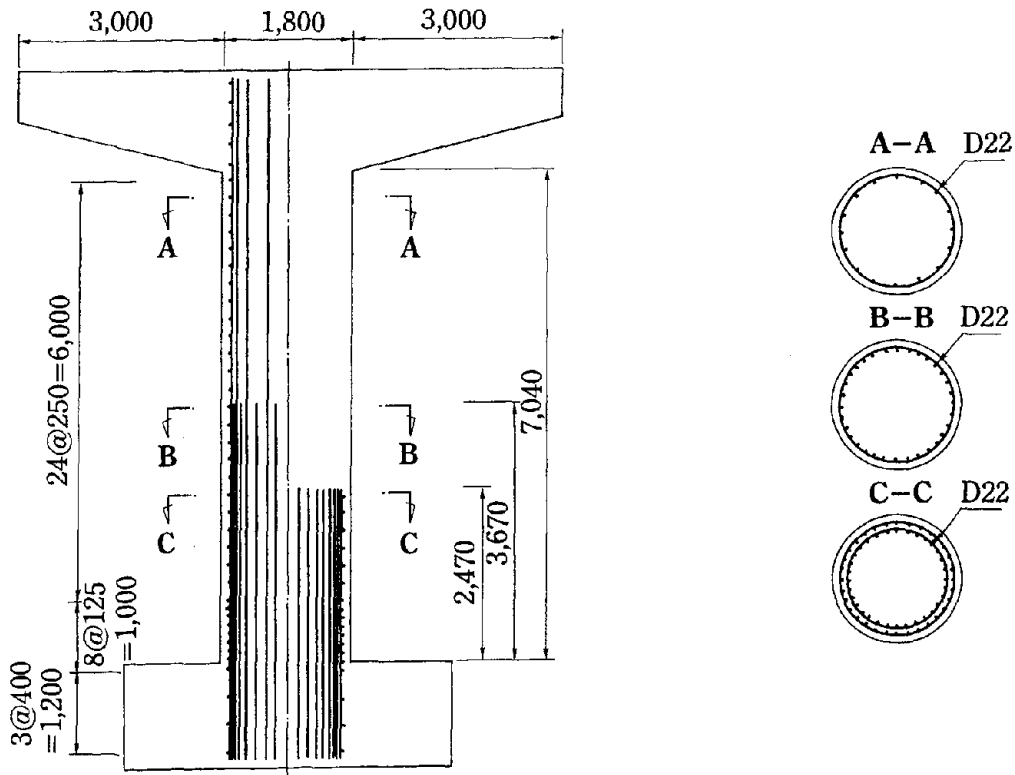
Fig. 8 Layout of Longitudinal Reinforcement in Shin—shiriuchi Bridge Pier (Old P3)

Fig. 9 Layout of Longitudinal Reinforcement in Shin—shiriuchi Bridge Pier (New P2)

Photo 5 Damage of Shin—shiriuchi Bridge at The First Termination Point (Old P3)

Photo 6 Damage of Shin—shiriuchi Bridge at The Second Termination Point (Old P2)

124

Fig. 10 Layout of Longitudinal Reinforcement in Motouriya Bridge Pier

Photo 7 Damage of Motouriya Bridge at Splicing Zone

125

(ϕ 13) was placed every 40cm.

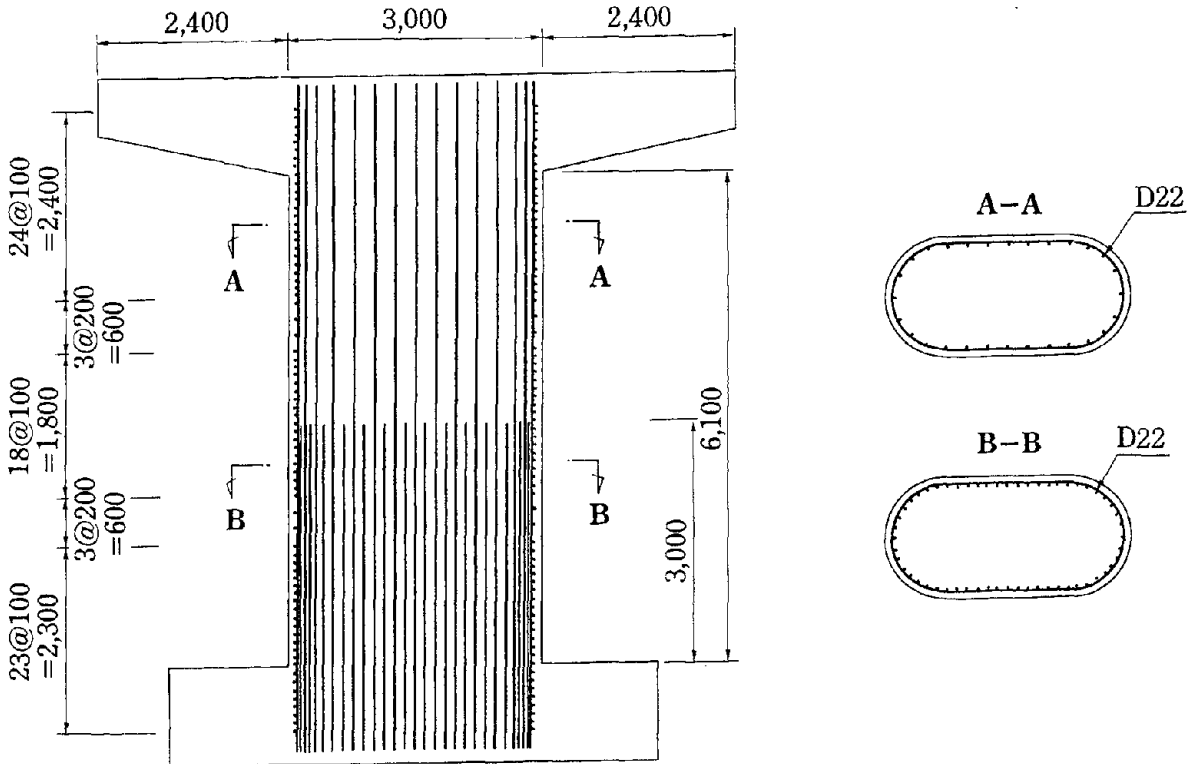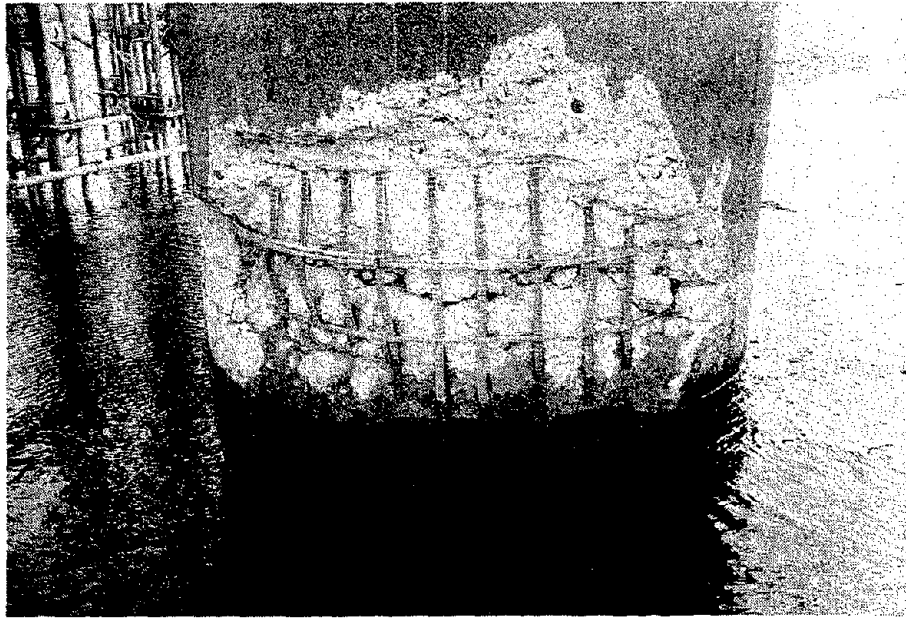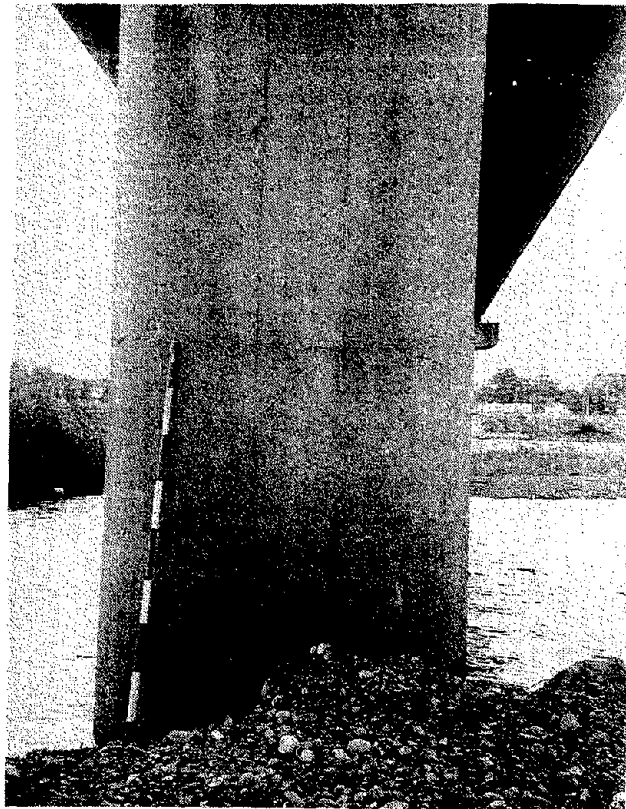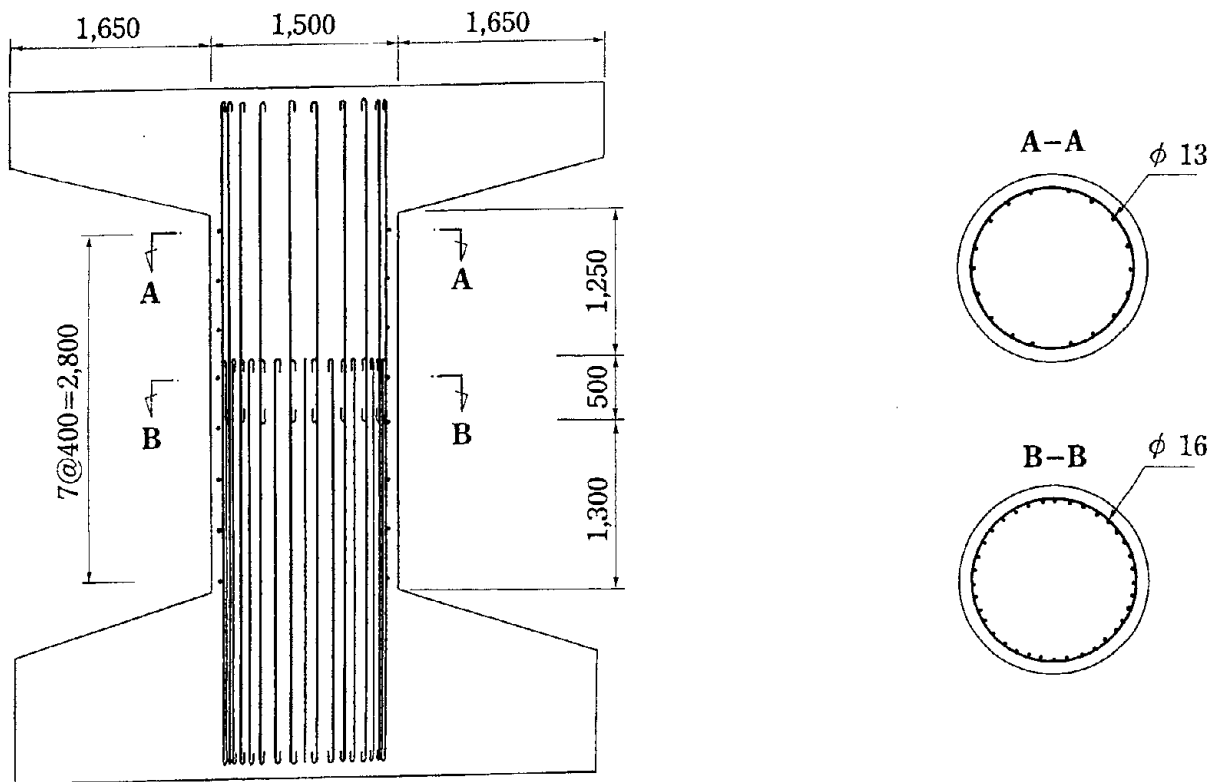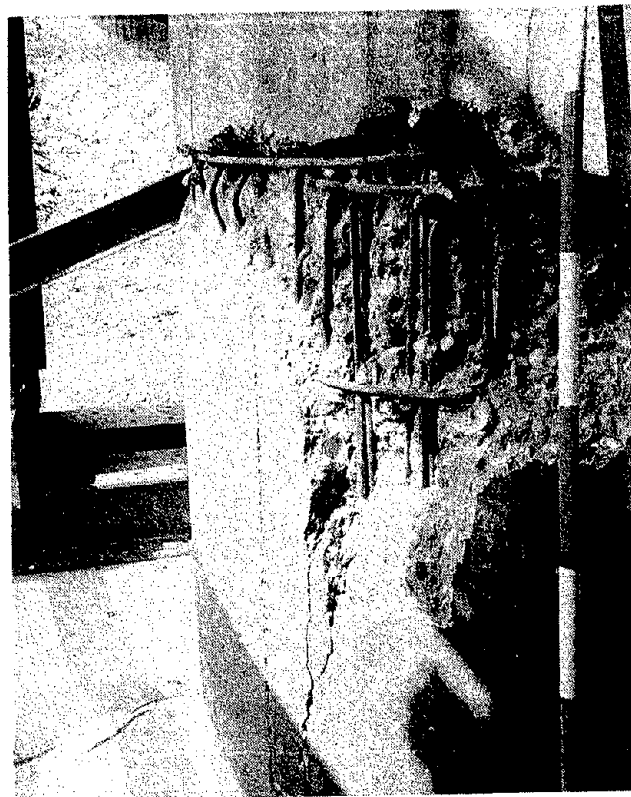Spalling—off of concrete and buckling of longitudinal reinforcement were developed at the splicing zone as shown in **Photo 7**. The lap length of this pier is estimated as 53cm by Eq.(1) and as 80cm by Eq.(2). Because the actual lap length is only 50cm, it was inadequate.

ANALYSIS OF SEISMIC VULNERABILITY
AT THE TERMINATION POINTS

Reinforced Concrete Piers Analyzed

Fourteen reinforced concrete piers were analyzed. They were selected from nine piers which suffered damage at the termination point due to the Kushiro—oki Earthquake and the Hokkaido Nansei—oki Earthquake, and five piers which were undamaged and located close to the fault zone. All piers undamaged were constructed after 1980. **Table 3** summarizes the bridges analyzed, and the analytical parameters required for the analysis, i.e. seismic coefficient, concrete strength and the material of reinforcement, are shown in **Table 4**. Because there were a few uncertain parameters, these were assumed from the past records.

Results of Analysis

Table 5 summarizes the failure mode factor S and the safety factor $F_y{}^T$ at the termination points. **Fig. 11** shows the failure mode factor S vs. the damage degree. It is clearly observed that the serious damage is developed as the failure mode factor S becomes smaller. The failure mode factor S of the piers which were damaged is less than 1.1. This very much matches with **Table 1(a)**. The failure at the termination point can be predicted quite well by the failure mode factor S .

Fig. 12 shows the safety factor $F_y{}^T$ vs. the damage degree. It is also observed that the serious damage is developed as the safety factor becomes smaller. Matsunoe bridge is an only exception, in which the safety factor is evaluated as 2.01, while it suffered significant damage at the termination point. The reason for this is not clear. Lager lateral force than expected would be developed due to the response of adjacent decks. The safety factor $F_y{}^T$ of the piers which were damaged is less than 1.1 except Matsunoe bridge. This also matches with **Table 1(b)**, in which 1.2 was proposed as the critical $F_y{}^T$.

Fig. 13 compares the predicted damage (refer to **Fig. 3**) with the actual damage at the termination points (refer to **Table 2**). The piers predicted by **Fig. 3** as "Serious Damage" suffered at least horizontal cracks. Most of them suffered diagonal cracks, buckling of and rupture of longitudinal reinforcements. On the other bend, the piers predicted by **Fig. 3** as "No Damage" were not damaged during the two earthquakes. Therefore the damage degree predicted by **Fig. 3** provides reasonable estimation. As described previously, Matsuuoe bridge suffered slight buckling of longitudinal reinforcement, although it is predicted by **Fig. 3** to develop only slight damage.

126

Table 3 Bridge Piers Analyzed

Cross Sectional Shape	Circular		Oval	
	Damaged	Undamaged	Damaged	Undamaged
Kushiro—oki Earthquake	Yoda Br. Matsunoe Br. Hatsune Br. Gojukkoku Br. Akangawa Br.	Sensho Br.	Shintawa Br.	Takadai Br. Tsurumi Br.
Hokkaido Nansei—oki Earthquake	Motoe Br. Shin—shiriuchi Br. (Old Pier) Motouriya Br.	—	—	Shin—shiriuchi Br. (New Pier)

Table 4 Analytical Parameters

Bridge	Pier	Analytic Direction	Seismic Coefficient k_h	Concrete Strength (kgf/cm^2)	Material of Longitudinal Reinforcement
Yoda Br.	P1	Transversal	0.20*)	210	SD295
Matsunoe Br.	P3	Transversal	0.20	180	SD235
Hatsune Br.	P4	Transversal	0.20	210	SDC390
Shintawa Br.	P2	Longitudinal	0.20	210	SD295
Gojukkoku Br.	P1	Transversal	0.20	210	SDC390
Akangawa Br.	P1	Transversal	0.20*)	210	SD345
Sensho Br.	P4	Longitudinal	0.18	210	SD295
	P5	Transversal	0.18	210	SD295
Takadai Br.	P2	Longitudinal	0.24	210	SD295
Tsurumi Br.	P5	Longitudinal	0.24	210	SD295
Motoe Br.	P3	Transversal	0.20	210	SDC390
Shinshiriuchi Br.	P3	Transversal	0.15	210	SD295
	New P2	Longitudinal	0.14	210	SD295
Motouriya Br.	P1	Transversal	0.15*)	210	SR235*)

*) assumed from the past records

127

Table 5 Analytical Results

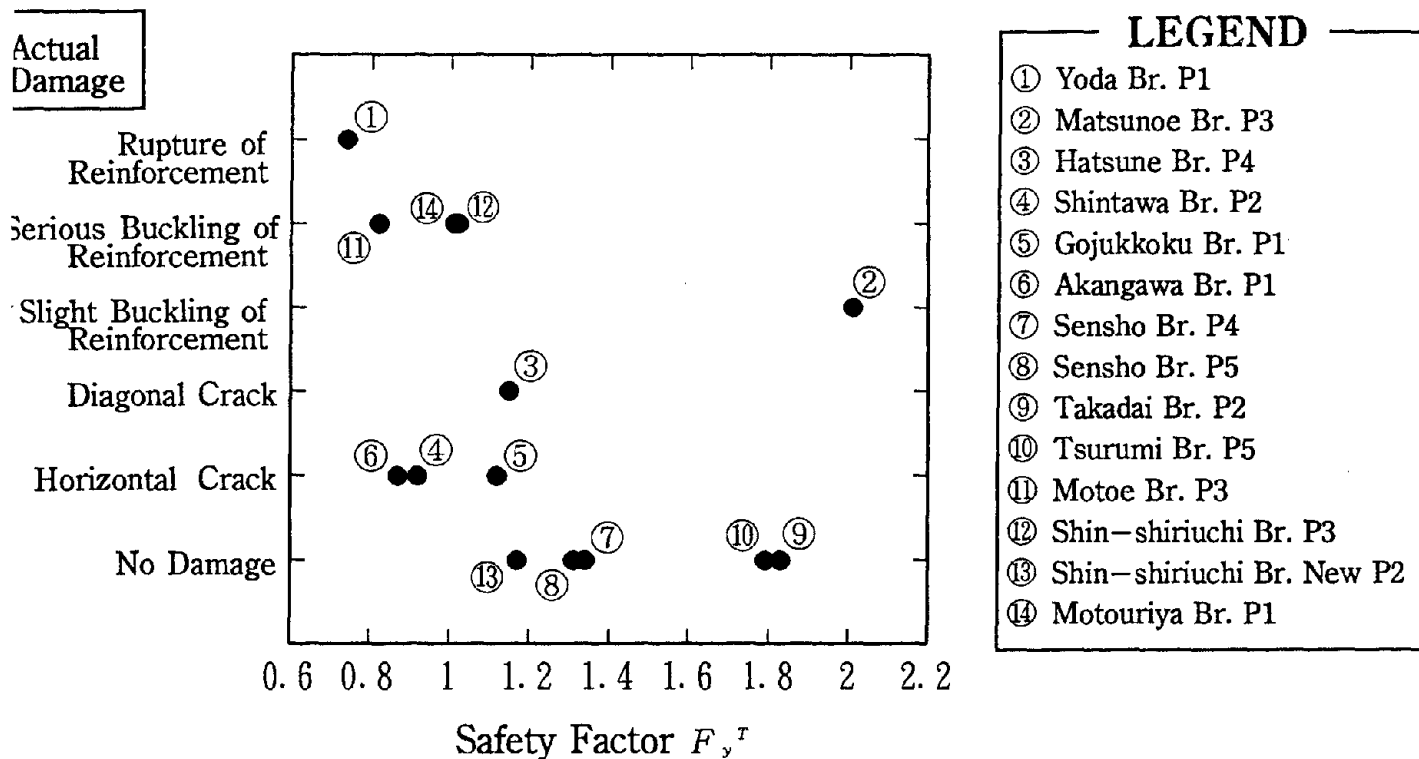| Bridge	Pier (Termination)		Yielding Bending Moment (tf·m)		Safety Factor		Failure Mode Factor S	Damage Degree Predicted at Termination Zone	Damage
			Base M_y^B	Termination M_y^T	Base F_y^B	Termination F_y^T			
Yoda Br.	P1	1st	218.3	148.9	1.24	0.87	0.70	Serious	No Damage
		2nd		111.9		0.74	0.60		Rupture and Serious Buckling of Longitudinal Reinforcement
Matsunoe Br.	P3		962.4	760.7	1.96	2.01	1.03	Slight	Slight Buckling of Longitudinal Reinforcement
Hatsune Br.	P4		657.4	433.8	1.51	1.15	0.76	Serious	Diagonal Crack
Shintawa Br.	P2		358.6	201.3	1.02	0.92	0.90	Serious	Horizontal Crack
Gojukkoku Br.	P1		915.8	634.4	1.26	1.12	0.89	Serious	Slight Horizontal Crack
Akangawa Br.	P1	1st	1161.1	772.9	1.30	1.00	0.77	Serious	No Damage
		2nd		551.5		0.87	0.67		Slight Horizontal Crack
Sensho Br.	P4		2193.8	1387.6	1.09	1.34	1.23	No Damage	No Damage
	P5		1174.6	790.3	1.08	1.31	1.21	No Damage	No Damage
Takadai Br.	P2		1179.8	599.9	1.33	1.83	1.38	No Damage	No Damage
Tsurumi Br.	P5		11113.8	6089.5	1.59	1.79	1.13	No Damage	No Damage
Motoe Br.	P3		425.1	294.9	1.00	0.82	0.82	Serious	Serious Buckling of Longitudinal Reinforcement
Shinshiriuchi Br.	P3	1st	562.2	408.7	1.19	1.02	0.86	Serious	Serious Buckling of Longitudinal Reinforcement
		2nd		325.6		0.96	0.81		No Damage
	New P2		530.2	407.5	1.02	1.17	1.15	No Damage	No Damage
Motouriya Br.	P1		184.7	141.0	1.08	1.01	0.94	Serious	Serious Buckling of Longitudinal Reinforcement
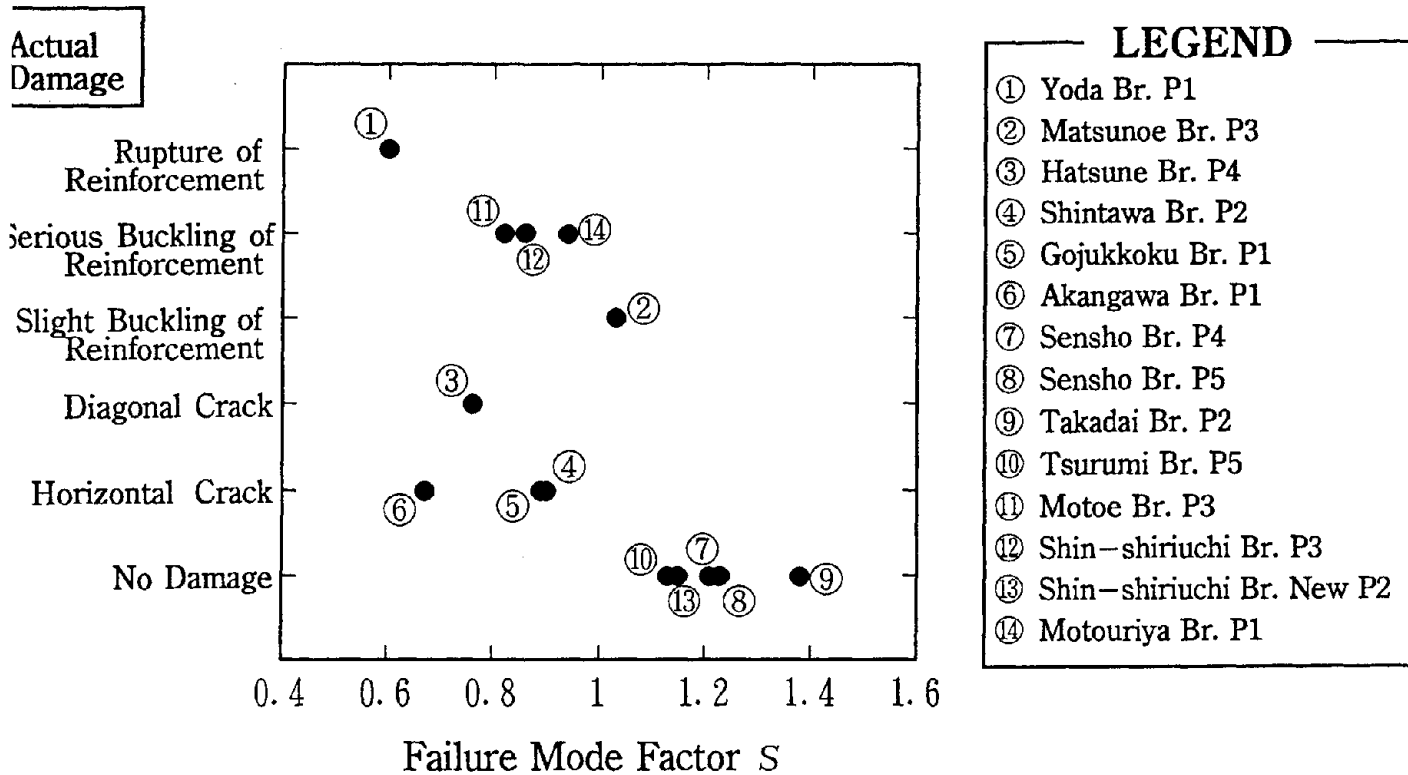
Fig. 11 Failure Mode Factor and Actual Damage

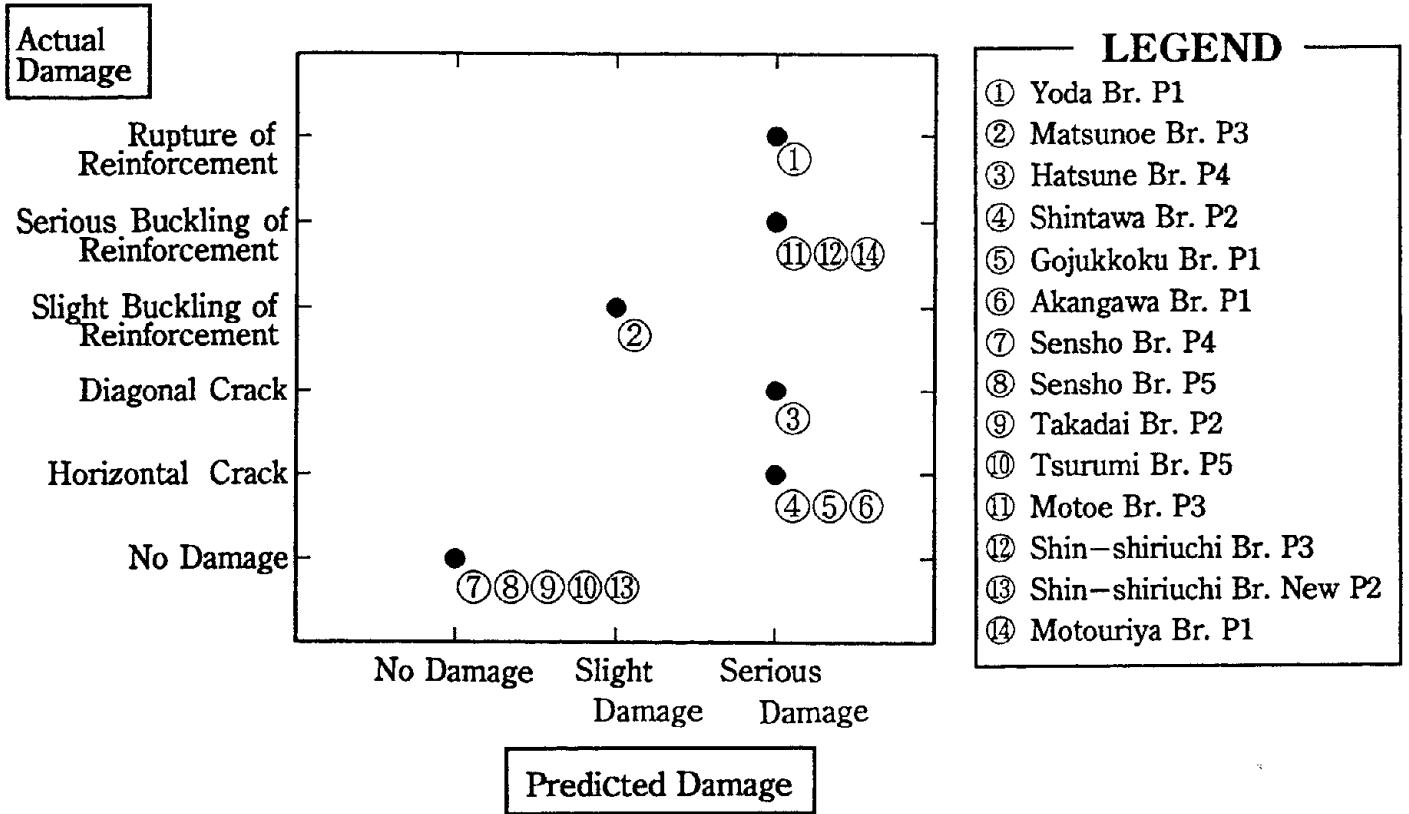Actual Damage (y-axis, top to bottom): Rupture of Reinforcement, Serious Buckling of Reinforcement, Slight Buckling of Reinforcement, Diagonal Crack, Horizontal Crack, No Damage

Failure Mode Factor S (x-axis): 0.4, 0.6, 0.8, 1, 1.2, 1.4, 1.6

LEGEND
① Yoda Br. P1
② Matsunoe Br. P3
③ Hatsune Br. P4
④ Shintawa Br. P2
⑤ Gojukkoku Br. P1
⑥ Akangawa Br. P1
⑦ Sensho Br. P4
⑧ Sensho Br. P5
⑨ Takadai Br. P2
⑩ Tsurumi Br. P5
⑪ Motoe Br. P3
⑫ Shin−shiriuchi Br. P3
⑬ Shin−shiriuchi Br. New P2
⑭ Motouriya Br. P1

Fig. 12 Safety Factor and Actual Damage

Actual Damage (y-axis, top to bottom): Rupture of Reinforcement, Serious Buckling of Reinforcement, Slight Buckling of Reinforcement, Diagonal Crack, Horizontal Crack, No Damage

Safety Factor $F_y{}^r$ (x-axis): 0.6, 0.8, 1, 1.2, 1.4, 1.6, 1.8, 2, 2.2

LEGEND
① Yoda Br. P1
② Matsunoe Br. P3
③ Hatsune Br. P4
④ Shintawa Br. P2
⑤ Gojukkoku Br. P1
⑥ Akangawa Br. P1
⑦ Sensho Br. P4
⑧ Sensho Br. P5
⑨ Takadai Br. P2
⑩ Tsurumi Br. P5
⑪ Motoe Br. P3
⑫ Shin−shiriuchi Br. P3
⑬ Shin−shiriuchi Br. New P2
⑭ Motouriya Br. P1

129

Fig. 13 Predicted Damage and Actual Damage

Actual Damage

Rupture of Reinforcement
Serious Buckling of Reinforcement
Slight Buckling of Reinforcement
Diagonal Crack
Horizontal Crack
No Damage

No Damage　Slight Damage　Serious Damage

Predicted Damage

LEGEND

① Yoda Br. P1
② Matsunoe Br. P3
③ Hatsune Br. P4
④ Shintawa Br. P2
⑤ Gojukkoku Br. P1
⑥ Akangawa Br. P1
⑦ Sensho Br. P4
⑧ Sensho Br. P5
⑨ Takadai Br. P2
⑩ Tsurumi Br. P5
⑪ Motoe Br. P3
⑫ Shin−shiriuchi Br. P3
⑬ Shin−shiriuchi Br. New P2
⑭ Motouriya Br. P1

Zone Required for Seismic Strengthening

LEGEND
● Critical Damaged
● Medium Damaged
● Slight Damaged
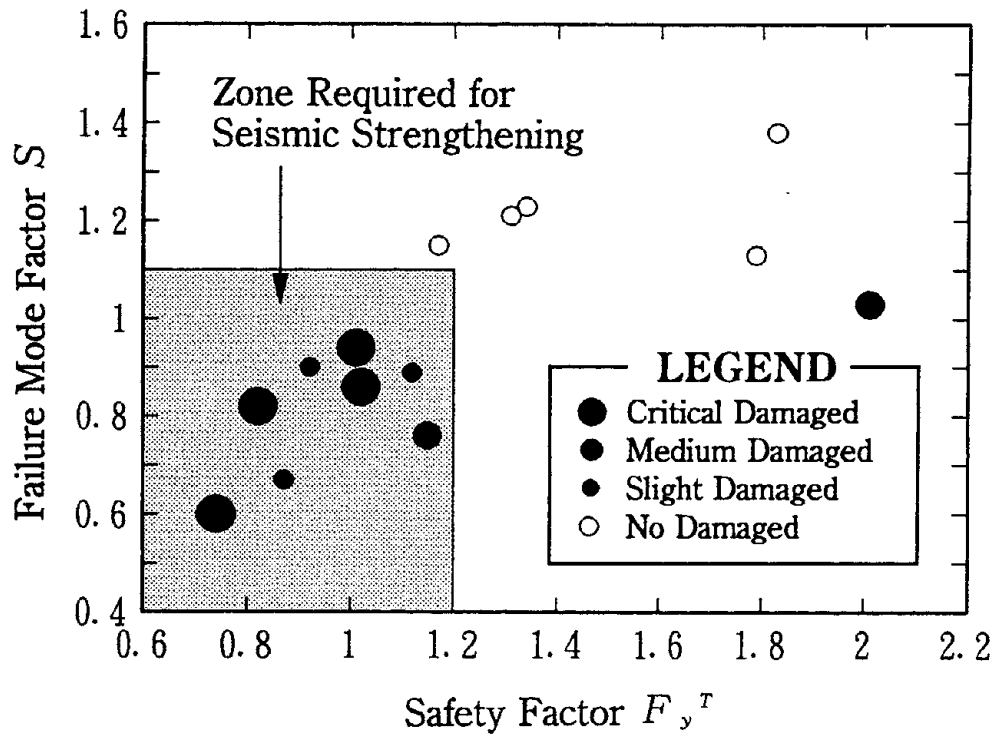○ No Damaged

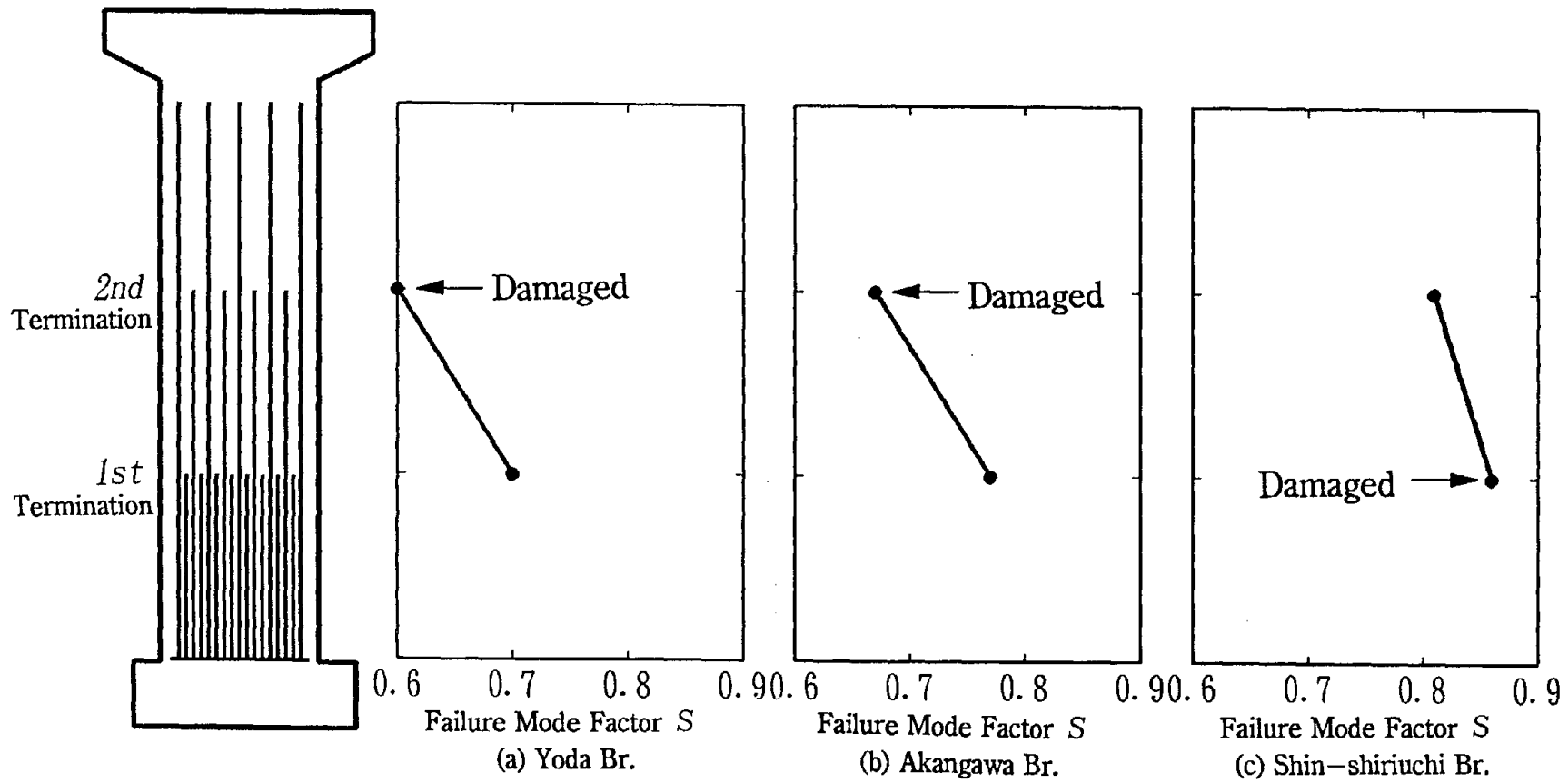**Fig. 14** Relation between Failure Mode Factor and Safety Factor

130

Fig. 15 Two Inadequate Terminations and Actual Damage

Fig. 14 summarizes the evaluation of damage degree in terms of S and $F_y{}^T$. Excluding only Matsunoe bridge, the damage degree developed during the two earthquakes agree quite well with the prediction by **Fig. 3.**

There were three bridges in which the longitudinal reinforcement were terminated at two different heights. It is interesting to clarify at which termination point the failure was developed between the two.

Fig. 15 compares the failure mode factors S at the two heights. At Yoda bridge and Akangawa bridge, the failure occurred at the 2nd (higher) termination point. Because the failure mode factor S is smaller at the 2nd termination point, the prediction by S is quite well. At Shin−shiriuchi bridge, on the other hand, the damage was developed at the first termination point, while S is smaller at the 2nd termination point. Because the difference of S between the 1st and the 2nd termination points is only 0.05 at Shin−shiriuchi bridge, this may be the reason for wrong prediction. But it should be noted that, at some other piers of Shin−shiriuchi bridge, cracks were developed not at the 1st termination point but at the 2nd termination point.

CONCLUDING REMARKS

This paper presented the damage of reinforced concrete bridge piers at the termination point of longitudinal reinforcements with inadequate anchorage length due to the Kushiro−oki Earthquake and the Hokkaido Nansei−oki Earthquake, and the applicafion of the seismic evaluation method proposed by PWRI. The conclusions derived from the study presented herein are the following;

1) The reinforced concrete bridge piers which were designed and constructed in accordance with the Specification prior to 1980 suffered damage at the termination points. They had a circular cross section.

2) The damage degree becomes serious as the failure mode factor S by Eq.(5) becomes smaller. The failure mode factor S of the piers which were damaged is less than 1.1. This is quite close with **Table 1(a)** which was proposed based on the loadng tests.

3) The serious damage is developed as the safety factor $F_y{}^T$ becomes smaller. The safety factor $F_y{}^T$ of the piers which were damaged is less than 1.1 except Matsunoe bridge. This is also very closed with Table 1(b) which was proposed by the loading tests.

4) Based on this study, the seismic evaluation at the termination point by means of the failure mode factors and the safety factor $F_y{}^T$ is appropriate.

REFERENCES

1) Kawashima, K., Unjoh, S., Nakajima, T. and Hoshikuma, J. : Damage of Bridges by Kushiro−oki Earthquake, January, 1993 and Hokkaido Nansei−oki Earthquake, July, 1993, 2nd U.S.−Japan Workshop on Seismic Retrofit of Bridges, Berkeley, USA, January
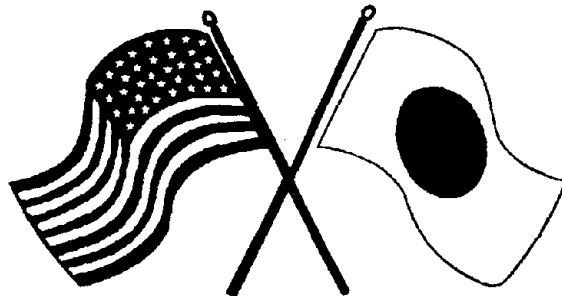
1994

2) Narita, N., Murakami, M. and Asanuma, H. : Report of the Investigation on Earthquake Damage to Shizunai Bridge, 15th Joint Meeting, U.S.–Japan Panel on Wind and Seismic Effects, UJNR, Tsukuba, Japan, May 1983

3) Japan Society of Civil Engineering : Standard Specifications for Concrete, December 1958

4) Japan Road Association : Part IV Design of Foudations, Design Specifications of Road Bridges, Feb. 1991

5) Kawashima, K., Unjoh, S. and Iida, H. : Seismic Inspection and Seismic Strengthening of Reinforced Concrete Bridge Piers with Termination of Main Reinforcement at Mid–Height, 1st U.S.–Japan Workshop on Seismic Retrofit of Bridges, Tsukuba, Japan, December 1990

6) Kawashima, K., Unjoh, S. and Iida, H. : Seismic Inspection and Seismic Strengthening of Highway Bridges in Japan, 4th U.S.–Japan Workshop on Earthquake Disaster Prevention for Lifeline Systems, Los Angeles, USA, August 1992

7) Japan Road Association : Guide Specifications for Earthquake Hazard Mitigation for Transportation Facilities – Post–Earthquake Countermeasures –, 1987

SECOND U.S.-JAPAN WORKSHOP
ON SEISMIC RETROFIT OF BRIDGES

Methods of Restoring Bridges Damaged in the Kushiro Offshore Earthquake of January 1993 and the Southwest Hokkaido Offshore Earthquake of July 1993

Y. Ono, M. Kaneko, T. Shirono, M. Sato and T. Yamauchi

METHODS OF RESTORING BRIDGES DAMAGED IN THE KUSHIRO OFFSHORE EARTHQUAKE OF JANUARY 1993 AND THE SOUTHWEST HOKKAIDO OFFSHORE EARTHQUAKE OF JULY 1993

Yuji Ono, Manabu Kaneko, Tadayuki Shirono, Masashi Sato and Toshio Yamauchi

Structures Section, Civil Engineering Research Institute

OUTLINE

The Kushiro Offshore Earthquake of January 1993 damaged many roads, bridges and other structures primarily in eastern Hokkaido. In addition, the Southwest Hokkaido Offshore Earthquake of July 1993 damaged many structures in southwestern Hokkaido.

The Southwest Hokkaido Offshore Earthquake caused a tsunami tidal wave and resulted in particularly great disaster, with over 200 fatalities. **Table 1** indicates the epicenters, scales and maximum seismic intensities of the 2 earthquakes. **Table 2 and 3** indicate the conditions of bridges damaged in the Kushiro Offshore Earthquake and Southwest Hokkaido Offshore Earthquake, respectively.

Most damage to bridges was slight, such as collapse of areas around supports or subsidence of access roads. However, some, such as broken piers and inclined foundations, necessitated urgent countermeasures. This paper reports the damage conditions and repair methods of cases of severe damage.

Table 1 Epicenter, Mgunitude and Maximum seismic Intensity(JMA)

		Kushiro-oki earthqake	Hokkaido Nansei-oki Earthquake
Epicenter	North	42.85 deg.	42.78 deg.
	East	144.38 deg.	139.20 deg.
	Depth	107 km	34 km
Magunitude		6 in Kushiro city	5 or 6 in Okushiri island
Maximum Seismic Intensity		7.8	7.8
number of Damaged bridges	national road	20	17
	prefectual road	89	2
	other road	33	3

OUTLINE OF DAMAGE CAUSED BY JAN. 1993 KUSHIRO OFFSHORE EARTHQUAKE, AND REPAIR CONDITIONS

The Kushiro Offshore Earthquake, occurring at 20:06, January 15, 1993, did conspicuous damage to areas around supports. Also, columnar piers were seriously broken

table.2 Outline of damaged bridges by Kushiro-oki earthquake in 1993, Jan.

Bridge name	road line name	const. year	bridge length	Bridge type superstructure	substructure	foundation	Damaged points	Outlook of damage
Chokubetsu bridge	route 38	1966	41.6m	single span plate garder	RC wall abuts	piles	Abuts & foundations	moved by a land slip
							in and around supports	cracked, buckling and broken
							palapet & wing wall	cracked
							joints, back-fill, river wall	broken
Matsunoe bridge	route 240	1963	157m	5 spans PC garders	RC round shape piers (diameter of 2.5m)	piles	cover concrete of piers	cracked & peeling off
							main reinforcements of No.2 pier	buckling
Yoda bridge	No.881 prefectural road Horokayanto line	1968	70m	3 spans plate garders	RC rour shape piers (diameter of 1.4m)	piles	cover concrete of piers	cracked & peeling off
							main reinforcements of No.2 pier	buckling & broken
Hatsune bridge	prefectural road Honryu-Onbetsu st. line	1969	172m	6 spans plate garders	RC round shape piers (diameter of 1.8m)	piles	cover concrete of piers	shear cracked

table.3 Outline of damaged bridges by Hokkaido nansei-oki earthquake in 1993, July

Bridge name	line number (line name)	const. year	bridge length	Bridge type superstructure	substructure	foundation	Damaged points	Outlook of damage
OSHAMANBE bridge	route 37	1960	150m	5 spans PC garders	RC round shape piers (diameter of 2.5m)	caisson	piers & caissons	inclined (and moved)
							in and around supports	broken
YANAGISAKI bridge	route 229	1961	181m	5 spans plate garders	RC abuts and piers	piles	stopper to fall out	buckling & broken
MOTOEI bridge	Esashi town road	1970	165.7m	7 spans plate garders	RC round shape piers (diameter of 1.8m)	piles	cover concrete of piers	cracked
							cover concrete of No.4 pier	cracked & peeling off
				RC abuts	piles	main reinforcements of No.4 pier	buckling & bent to outside
MOTOURIYA bridge	Kikonai town road (Uriya 2nd line)	1964	63m	2 spans PC garders	RC round shape piers (diameter of 1.5m)	piles	cover concrete of pier	cracked & peeling off
							main reinforcements of pier	buckling & bent to outside
SHIN-SHIRIUCHI bridge	Kikonai town road (Motomachi 1st line)	1970	214m	7 spans PC garders	RC round shape piers (diameter of 1.8m(old))	piles	cover concrete of old piers	cracked & peeling off
							main reinforcements of No.3 pier	buckling & bent to outside

outward of the damaged bridges shown in **Table 2**, we report the damage conditions and restoration measures for those in the "severe damage" (and some in the "medium damage") category as defined by the Handbook of Measures for Earthquake—Damaged Roads (Earthquake Damage—Restoration Edition).

YODA BRIDGE

The Yoda Bridge, constructed in 1968 as a second—class bridge, is a 70—m—long, 3—span, simple steel plate girder bridge on the Horokayanto section of Prefectural Route 881. It has 1.4—m—dia. columnar piers, designed with 36 D19 main reinforcements distributed in each pier footing. The number of reinforcements was designed to be 2/3 and 1/3 at points 30cm and 1m above the footing surface (**Fig. 1**).
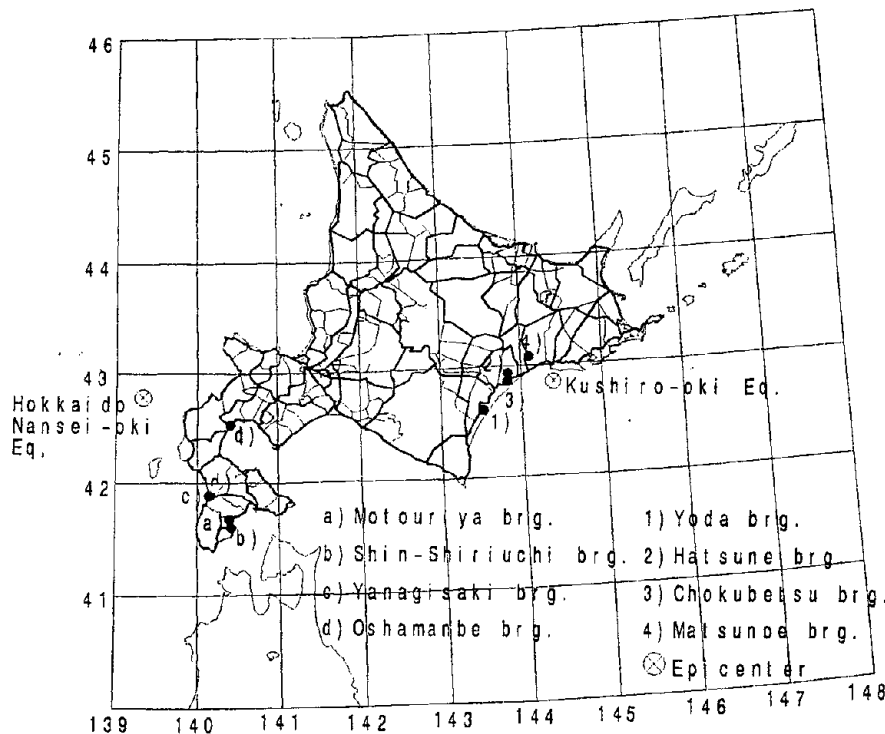
Fig. 1 Epicenter and location of Damaged bridges

In Pier 2, great amounts of concrete cover were exfoliated at the second point of decreasing number of reinforcements, and main reinforcements were buckled and swollen outward. Furthermore, of 12 main reinforcements above the point of decreasing number of reinforcements, 6 main reinforcements had broken. In Pier 1, although these points had been buried by ground, horizontal and oblique cracks and exfoliation of concrete cover were observed. Such damage was also noted in the Shizunai Bridge after the 1982 Urakawa Offshore Earthquake.

To repair the Yoda Bridge, we reconstructed the piers. For P1, the cable we used
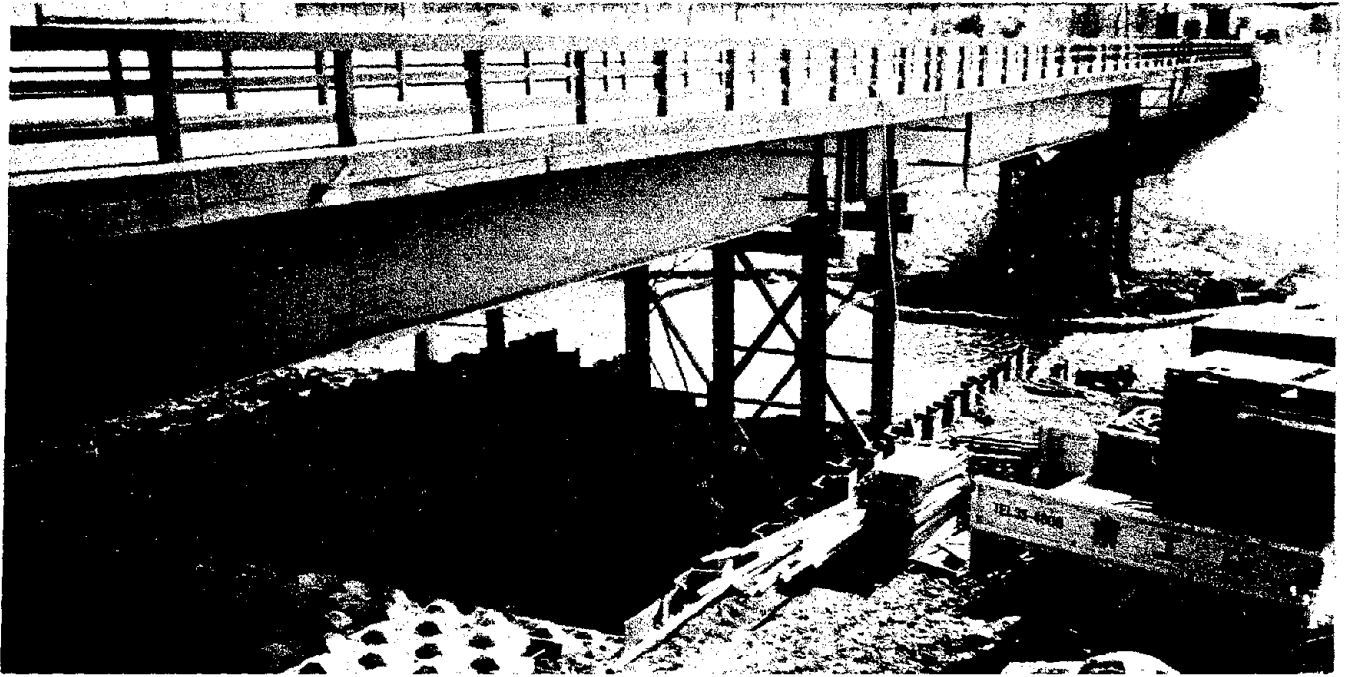
139

Photo 1 Repairing piers at Yoda Bridge

Photo 2 Repaired at Yoda Bridge

was not one with decreasing numbers of reinforcements, and we increased the number of distributing bars to prevent main reinforcements from swelling out. For P2, in addition to applying the same methods as we did for P1, we added 12 pieces of D19 main reinforcements inside the existing main reinforcements from the footing surface to 3m above. The new reinforcements were fixed with epoxy resins into $\phi 25 \times 655$—mm holes which we newly drilled in the footing (Photo 1, 2).
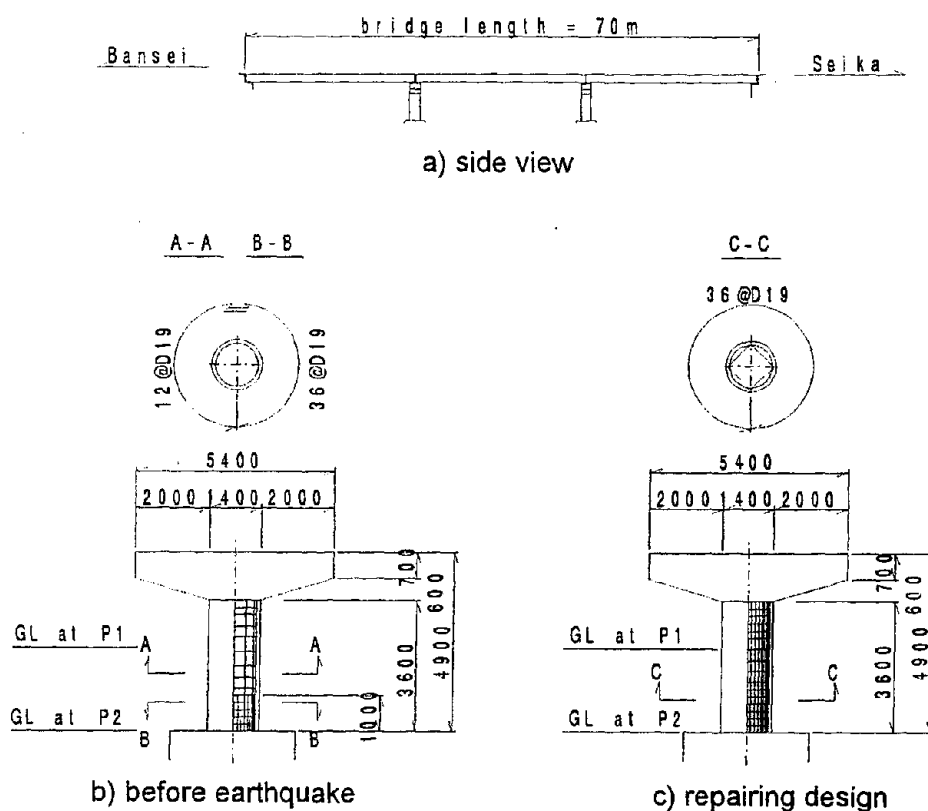
Fig. 2 Yoda Bridge

HATSUNE BRIDGE

The Hatsune Bridge, constructed in 1969 as a first—class bridge, is a 172—m—long, 6—span, simple steel plate girder bridge on the Honryu Ombetsu Teishajo section of a general prefectural road. In each of its 1.8—m—dia. columnar piers, main reinforcements had been designed with numbers decreasing at about 4m below the top (Fig. 3).

In every pier, horizontal cracks occurred around points of decreasing number of reinforcements. Oblique cracks also occurred in P4, which proves the shift from the fracture by bending to fracture by shearing.

To prevent bridge parts from falling, a girder—coupling device was installed on each of the 3 main girders. It was a 68—cm—high, 34.5—cm—wide and 9—mm—thick steel plate,

141

fixed with 7 bolts on each side. For 10 out of the 15 coupling plates, 3 to 10 of each one's 14 bolts were sheared.

To repair P3 and P4, we chipped and lined the existing 1.8−m−dia. columnar piers with 200−mm−thick concrete in the longitudinal direction and with 20−30−mm−thick concrete in other directions, thus changing their forms to 1.8m × 3.6m elliptical cylinders (**Photo 3**). The cable we used was not one with points of decreasing number of reinforcements, and we drilled $\phi 38 \times 1100$−mm holes in the footings to fix main reinforcements with capsulated resin adhesive. To repair other piers, resin mortar was injected into cracks.

The anti−fall devices were restored to their original forms except for the holes of the movable sections, whose diameters we expanded from about ±20mm to about ± 30mm. Because bolts were sheared by the earthquake, we may have to change the coupling plates to multiple plates to reduce the shearing stress on the bolts.
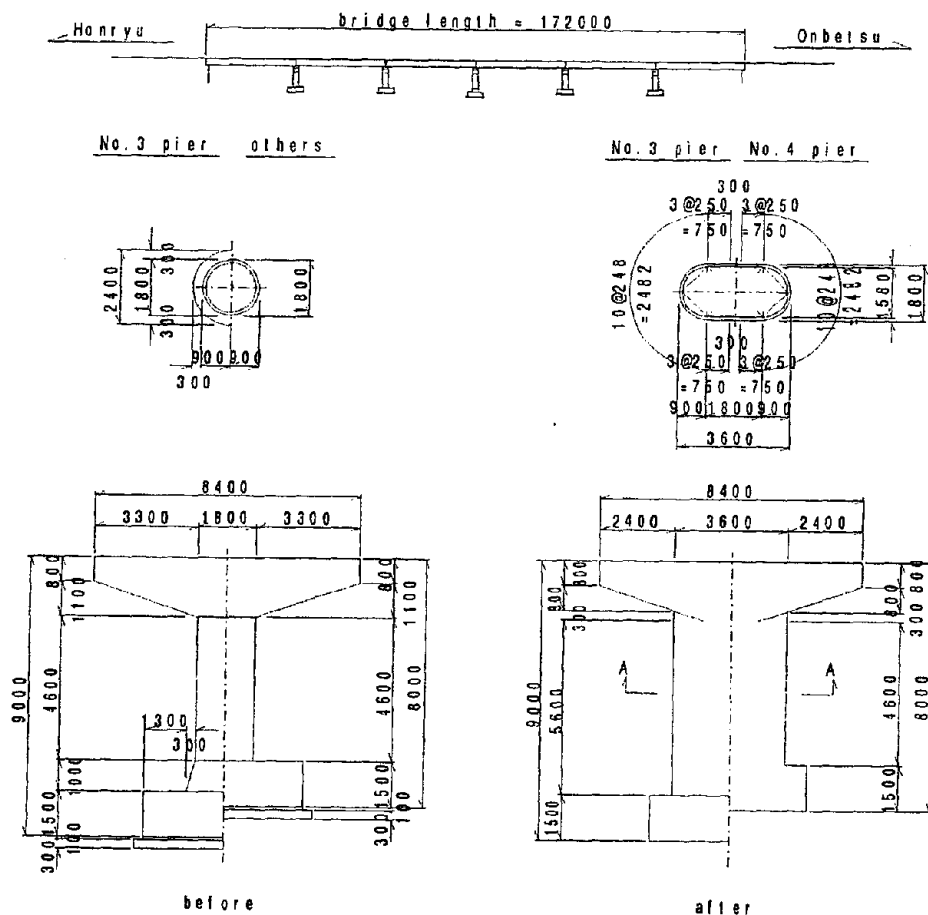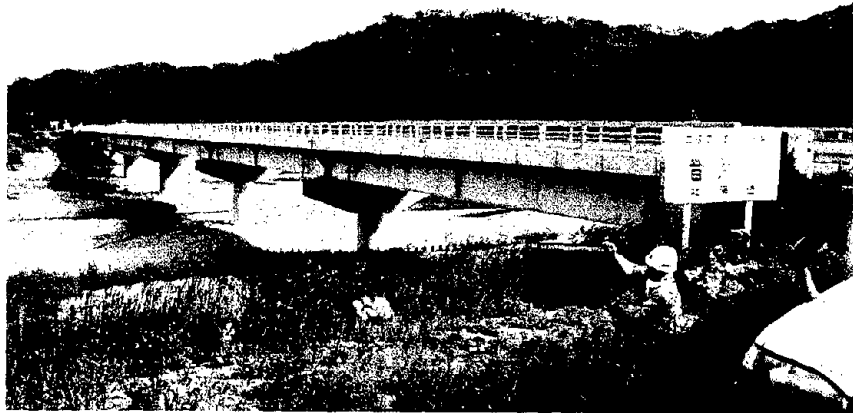

Fig. 3 Hatsune bridge

142

Photo 3 Reaired at Hatsune Bridge

MATSUNOE BRIDGE

The Matsunoe Bridge, constructed in 1963 as a first-class bridge, is a 157-m-long, 5-span, simple PC-girder bridge, built where National Route 240 crosses the Class-A Akan River. Each pier is 2.5-m-dia. columnar and each pier foundation is an open caisson (Fig. 4).

The earthquake caused horizontal cracks in the piers' point of decreasing number of reinforcements 2.25m above the footing surface. In P3, the most damaged, x-shaped shear cracks also occurred, and main reinforcements and tie hoops were exposed as the concrete cover exfoliated (Photo 4). Since main reinforcements swelled out, the residual strength already may have been less than the yield strength. Regarding abutments, the mortar of the bridge seat at the points of movable supports was damaged, concrete of the bridge seat was cracked and girder edges were damaged.

To repair the greatly damaged P2 and P3, we used steel bents to support the main girder temporarily. After chipping damaged sections and injecting resins, we reinforced these sections with 50-cm-thick concrete lining (Photo 5). For other piers, we injected resins and then reinforced them with 50-cm-thick concrete lining. This operation changed the cross sectional diameter of the piers from ϕ 2.5m to ϕ 3.5m (Photo 6). We installed 14 layers of 8 anchors to connect the concrete linings with the old body. 40 D22 main reinforcements were placed with a 105-mm-deep concrete cover and were fixed with capsulated adhesive into ϕ 35 × 700-mm holes which we newly drilled in the footing. The main reinforcements had not been constructed with points of decreasing number of reinforcements.
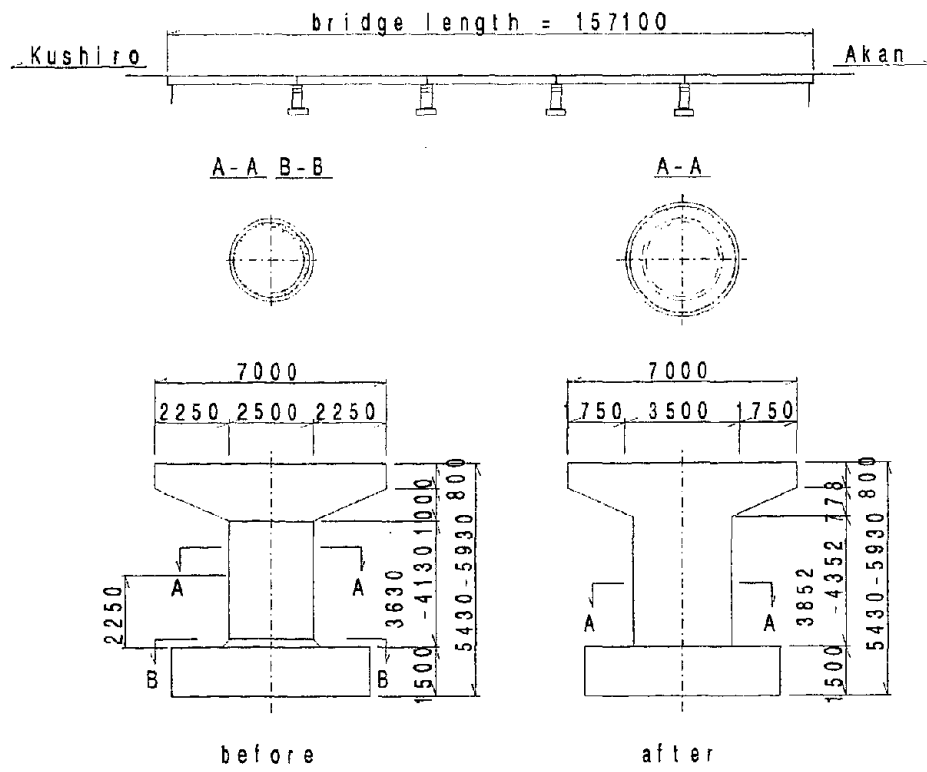
143

bridge length = 157100

Kushiro | | Akan

A-A B-B   A-A

before

7000
2250 2500 2250

after

7000
750 3500 1750
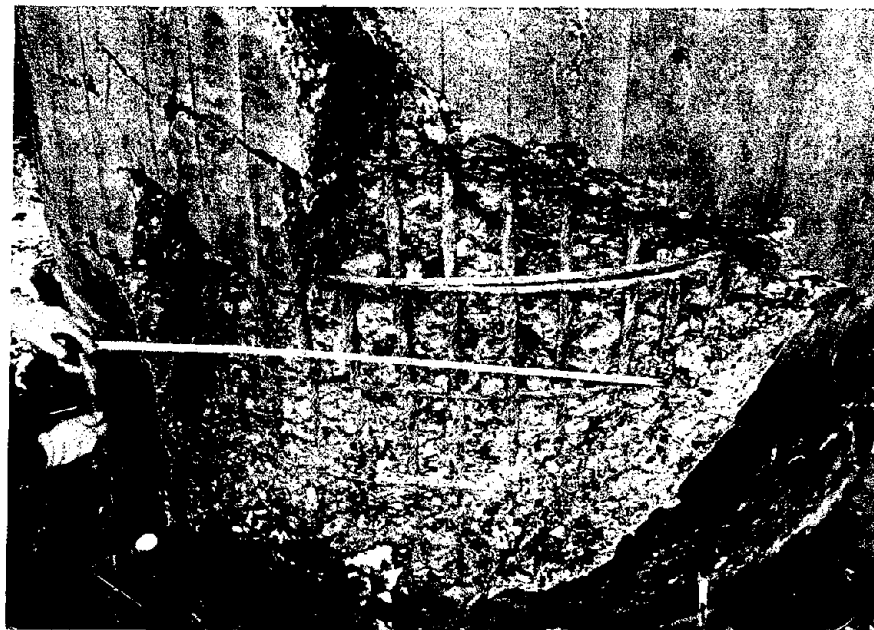
Fig. 4 Matsunoe Bridge

Photo 4 Damaged conditin of 3 Pier at Matsunoe Bridge
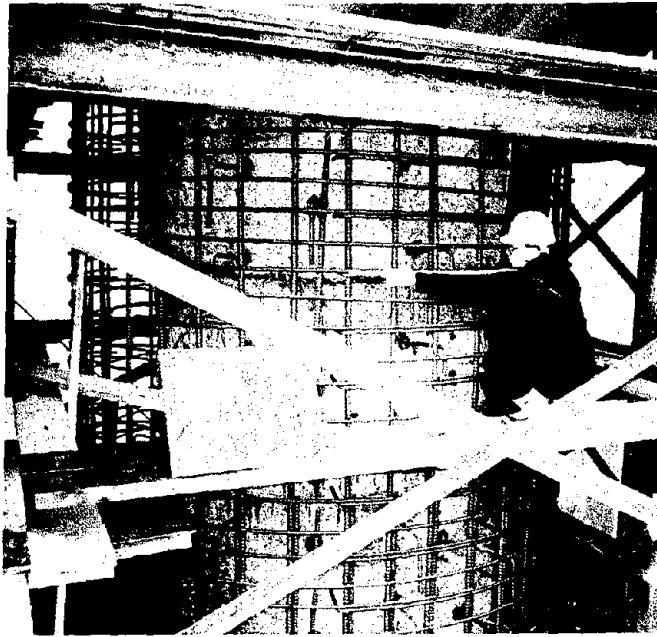
Photo 5 Repairing of 2 Pier at Matsunoe Bridge

Photo 6 Repaired at 3 Pier of Matsunoe

CHOKUBETSU BRIDGE

The Chokubetsu Bridge, constructed in 1966 as a first—class bridge, is a 41.6—m—long, simple steel—plate girder bridge on National Route 38. It has RC—wall—type abutments and pile foundations (Fig. 5).

Ground sliding toward the river center caused the abutments to move horizontally and incline. While the upper part of the Obihiro—side abutment inclined toward girders by the pressure of back—filling soil, the Kushiro—side abutments moved toward the river center as if carried off their feet. As a result, the upper part of the Kushiro—side abutment inclined toward the back—filling soil. Consequently, girders touched abutment parapets and the mortar of supports cracked.

Such damage has often occurred in past earthquakes, and we have accomplished restoration by reconstructing abutment parapets, which is the generally accepted method. Because the positions of supports changed with abutment movement, we also reconstructed the support sections of abutments (Photo 7, 8).
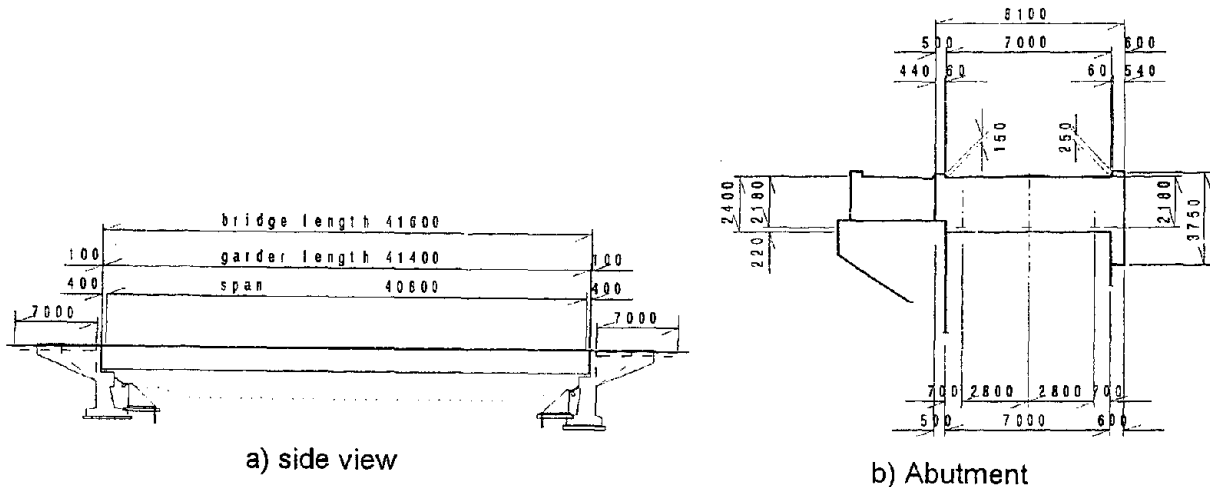
a) side view

b) Abutment

Fig. 5 Chokubetsu Bridge

Photo 7 pulling down Abutment of
Chokubetsu Bridge

146

Photo 8 Repairing Abutment of Chokubetsu

OUTLINE OF DAMAGE CAUSED BY JULY 1993 SOUTHWEST HOKKAIDO OFFSHORE EARTHQUAKE, AND REPAIR CONDITIONS

The Southwest Hokkaido Offshore Earthquake, occurring at 22:17, July 12, 1993, damaged areas around supports, broke columnar piers outward, and moved abutments—damage types also seen in the Kushiro Offshore Earthquake. Moreover, the earthquake inclined pier foundations and cracked girders, the latter of which pheno—menon seems to have occurred by the clashing of girders. Of the damaged bridges shown in **Table 3**, we report the damage conditions and restoration measures for those in the "severe damage" category as defined by the Handbook of Measures for Earthquake—Damaged Roads (Earthquake Damage—Restoration Edition).

MOTOURIYA BRIDGE

The Motouriya Bridge, constructed in 1964 as a second—class bridge, is a 63—m—long, 4—m—wide, 2—span simple post—tension PCT—girder bridge, built where the Uriya Nisen section of Kikonai Town Road crosses the Uriya River. It has RC inverted—T—type abutments, 1.5—m—dia. columnar RC piers, and pile foundations (**Fig. 6**).

At the middle height of the piers, concrete cover was exfoliated, and main reinforcements were buckled and swollen outward. As in the Kushiro Offshore Earthquake, damage was great in the direction at a right—angle to bridges' longitudinal direction (**Photo 9**).

In this pier, ϕ 16mm round bars were used as main reinforcements, and there were
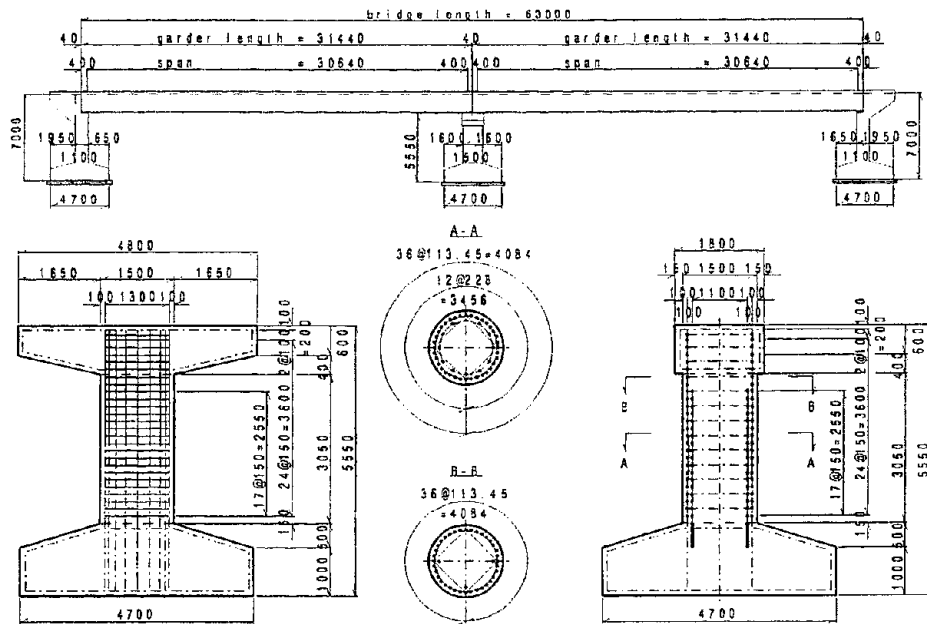
147

Fig. 6 Motouriya Bridge

Photo 9 Damage condition of pier at
Motouriya Bridge

148

lap joints at damaged sections. The joints were about 50cm long, and at the end of the bars were U—shaped hooks for anchoring. These hook joints were weak points which compounded the damage.

To restore the bridge, we reconstructed pier bodies as we did for the Yoda Bridge after the Kushiro Offshore Earthquake. We changed main reinforcements to 2 layers of D16. We drilled $\phi 28 \times 500$—mm holes in the footings and fixed the second—layer reinforcements into the holes with capsulated adhesive.

SHIN—SHIRIUCHI BRIDGE

The old Shiriuchi Bridge was constructed in 1970 as a second—class bridge where the Motomachi Nakanogawa section of Shiriuchi Town Road 1 crosses the Shiriuchi River. In 1989 when river improvement was conducted, 2 spans were added to the right—bank side and the entire bridge was renamed the Shin—Shiriuchi Bridge. It is a 214—m—long, 6—m—wide, 7—span simple post—tension PCT—girder bridge. Columnar piers at points connecting the old pier part with the new bridge part are 1.8m wide, and columnar Pier 2 of the new bridge part is 1.5m wide. As main reinforcements, 2 layers of D22, 64 bars in total, had been distributed in the old piers. At 3.8m above the footings, the number of main reinforcements was designed to be half, and at 5m above, to be 1/4 (Fig. 7).
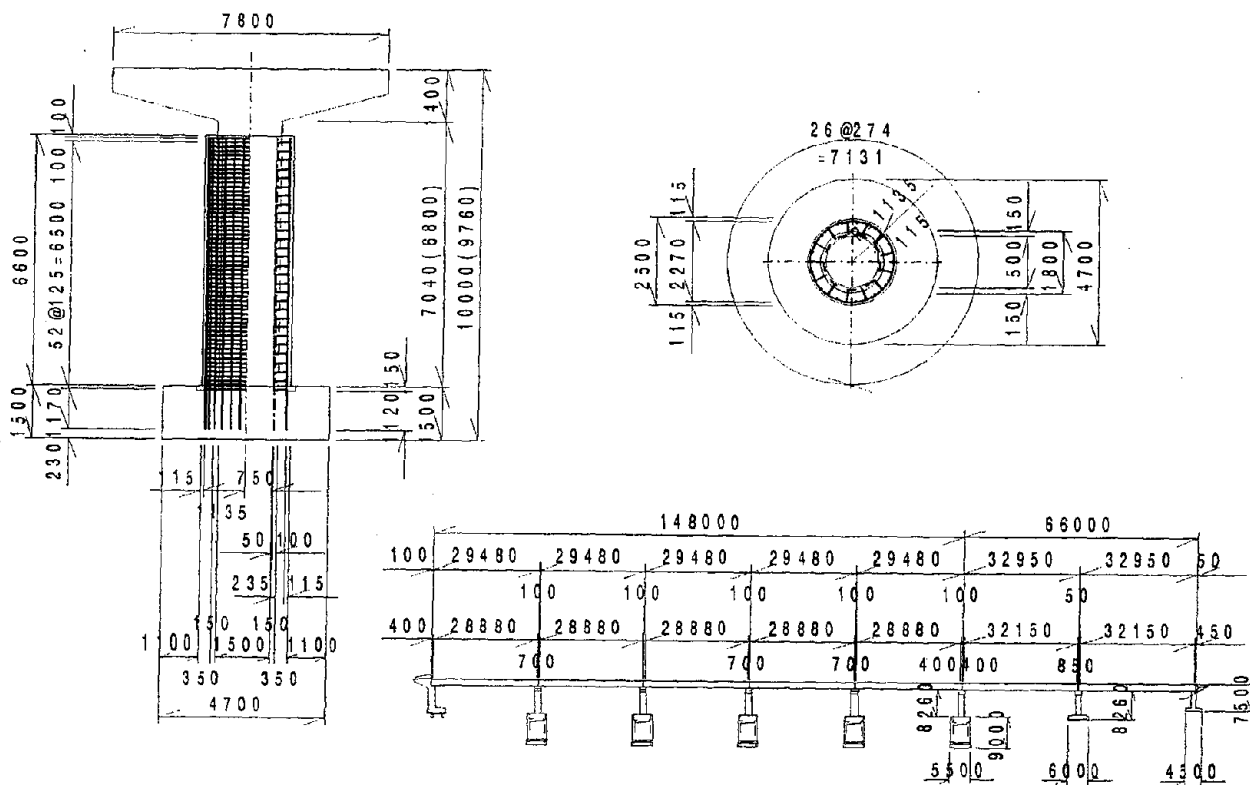

Fig. 7 Shin Shiriuchi Bridge

149

Although all piers of the old part, P1−4, were damaged, the newly constructed piers were completely undamaged. P3 received the greatest damage: At its point of decreasing number of reinforcements 3.8m above the footing surface, the concrete cover was exfoliated over a vertical length of about 1m, and main reinforcements were buckled and swollen outward. The damage was caused by short fixing areas of main reinforcements, which similarly had caused great damage in the aforementioned Kushiro Offshore Earthquake. The damage to the other old piers was less serious, limited to cracks at the point of decreasing number of reinforcements and slight exfoliation of concrete cover in the direction at a right−angle to the bridges' longitudinal direction.

To repair piers, we lined them with 35−cm−thick concrete from the footings to 6.6m above and changed the cross sectional diameter from ϕ 1.8m to ϕ 2.5m. As main reinforcements, we placed 25 D32 main reinforcements with a 115−mm−deep concrete cover and fixed them with PC grouting into newly drilled, ϕ 40 × 1.5−m holes.

YANAGISAKI BRIDGE

The Yanagisaki Bridge, constructed in 1961 as a first−class bridge, is a 181−m−long, 5−span simple steel composite−girder bridge, built where National Route 229 crosses the estuary of the Assabu River.

Apart from damage at its support sections, anti−fall devices were buckled. The design of the devices is shown in Road & Bridge Specifications V, Earthquake−proof Design Edition as a device to prevent already−constructed bridge parts from falling (Fig. 8).
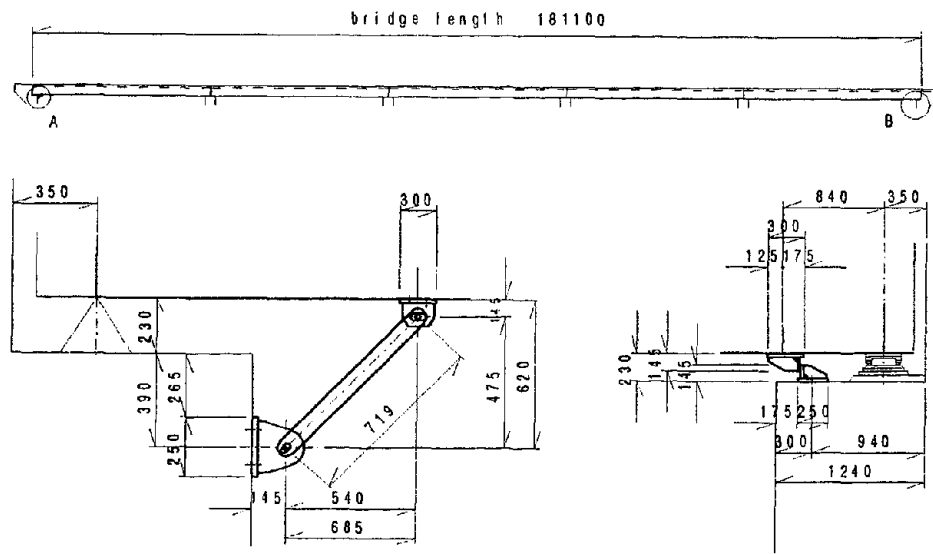

Fig. 8 Yanagisaki Bridge

150

However, when girders move to the abutment side, they become compressed and are apt to receive such buckling damage. Regarding the anti–fall devices on the other side, concrete of fixing sections exfoliated partly, and anchor bolts bent slightly downward (Photo 10).

To restore them, the anti–fall devices at the movable ends were replaced and their moving ranges widened by changing the hole diameter from 60mm to 80mm. We installed movement limiters at the fixed ends in order to prevent the devices from bumping against the bridge wall.
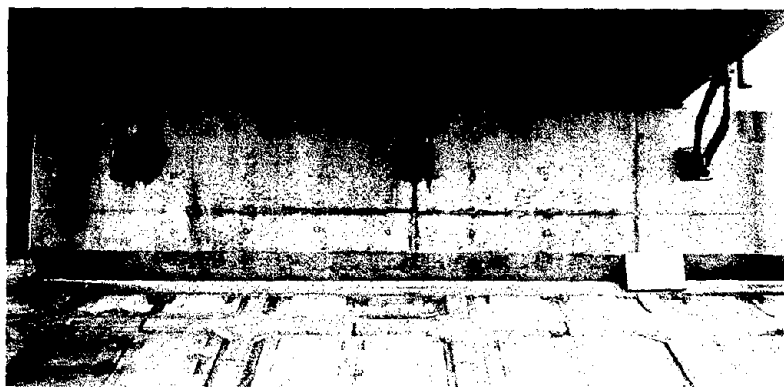

Photo 10 Ynagisaki Bridge

OSHAMAMBE BRIDGE

The Oshamambe Bridge, constructed in 1960 as a first–class bridge, is a 150.1–m–long, 7–m–wide, 5–span simple post–tension PCT–girder bridge, built where National Route 37 crosses the Oshamambe River. In 1976, piers were added on the upstream side to attach a pedestrian bridge.

Ground liquefying around the bridge caused the caisson foundations to incline to the upstream side. Inclination of P2 was great, and the upstream edge of its support bridge seat was 386mm lower than the downstream one. Consequently, the road surface on P2 moved 420mm upstream. From the displacement, the gradient of the caisson and the pier was calculated to be about 2 degrees. Piers closer to abutments had smaller inclinations, and abutments themselves did not incline at all.

As the initial restoration of foundations, we improved the ground near the caissons' pedestrian bridge–side walls and bases by using cement hardeners. Subsequent restoration (permanent measures) is now under review.

CONCLUSION

The Kushiro Offshore Earthquake and the Southwest Hokkaido Offshore Earthquake of 1993 damaged many bridge structures. Of these, we have explained the restoration of greatly damaged ones.
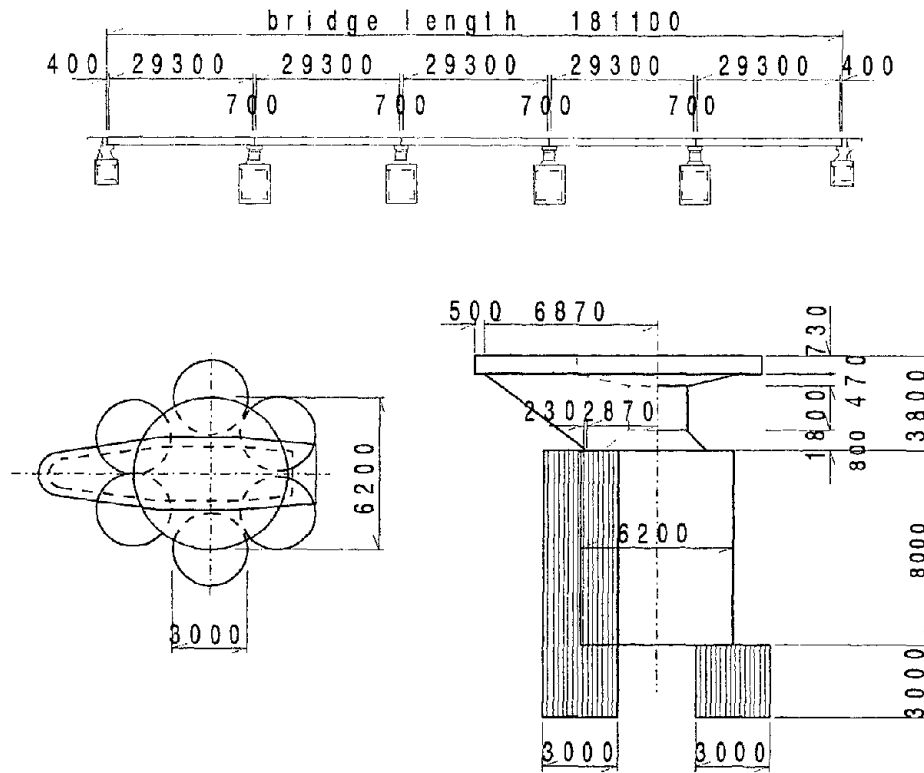
Fig. 9 Oshamambe Bridge

The major damage to bridges by the 2 earthquakes was seen in columnar piers constructed before 1980. These piers received conspicuous damage in the direction at a right—angle to the bridges' longitudinal direction. We may have to carefully watch the piers which are similar but which were not damaged in these earthquakes. The systems which had fail—safe functions such as anti—fall devices and support stoppers broke before bridge parts fall. We must take this into consideration from the standpoint of future earthquake—proof technology development.

REFERENCES

1) "1993 Kushiro Offshore Earthquake Damage Investigation Report": Civil Engineering Research Institute Report; Hokkaido Development Bureau, Civil Engineering Research Institute Vol. 100, September 1993

2) "Civil Engineering Technical Material" Vol. 35—4: Public Works Research Institute of the Ministry of Construction, April 1993

3) Kazuhiko Kawashima, Hideki Sugita, Shigeki Unjo and Tomoru Nakajima: "Characteristics of Road Bridges Damage Caused by the Kushiro Offshore Earthquake," Bridges and Foundations, June 1993

4) Shosuke Toki, Kinya Miura, Satoshi Yamashita and Migitoshi Nishimura: "Damage

Outline of 1993 Southwest Hokkaido Offshore Earthquake," Earth and Foundations, November 1993

5) "General Investigative Report of Damage Caused by July 1993 Southwest Hokkaido Offshore Earthquake": Laboratory of Aseismatic Structures, Earthquake Disaster Prevention Division, Public Works Research Institute, Ministry of Construction; Public Works Research Institute Material No. 3204, August 1993

6) "Southwest Hokkaido Offshore Earthquake of July 12, 1993": Severe Earthquake Observation Project Promotion Liaison Council, Research Institute for Disaster Prevention of the Science and Technology Agency; Severe-Earthquake Preliminary Report No.43, August 1993

SECOND U.S.-JAPAN WORKSHOP
ON SEISMIC RETROFIT OF BRIDGES

An Experimental Study on the Behavior of a Large Model Pier After Repair
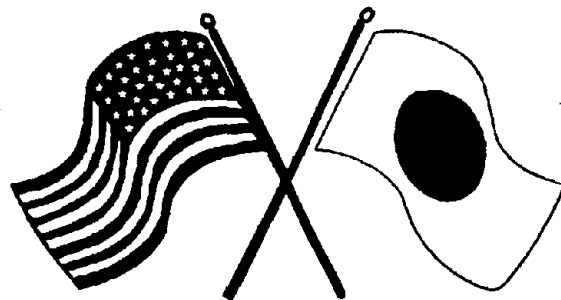
Y. Adachi, K. Kousa and Y. Murayama

AN EXPERIMENTAL STUDY ON THE BEHAVIOR OF A LARGE MODEL PIER AFTER REPAIR

Yukio Adachi[1], Kenji Kosa[2], Yasuo Murayama[3]

1) Engineer, Design Section, Engineering Department, Hanshin Expressway Public Corporation.
2) Senior Engineer, Design Section, Engineering Department, Hanshin Expressway Public Corporation.
3) Chief Research Engineer, Kajima Corporation Research Institute

SUMMARY

In order to grasp the load resistance characteristics of a real structure designed according to the old design code in which fracture occurs at the cut-off point, an experimental test was carried out using a relatively large-sized RC bridge pier model.

Then, the damaged specimen was repaired and the load bearing capacity was investigated.

The test results show that the repaired specimen presented the similar load-deformation relationship as that of the normal one after the crack occurrence. The welding of new reinforcing bars can be an effective repairing method for bridge piers damaged by earthquakes.

INTRODUCTION

The sectional area of urban-type elevated RC bridge piers is generally made small because of restricted conditions around the piers. For this reason, main reinforcements are usually multi-layers, and numerous reinforcements cross hoop reinforcements vertically. In a real bridge pier, shearing type fracture is liable to be induced by the presence of cut-off point if the pier was designed according to the old design code of highway bridges. Shear strength is greatly affected by the dimension of a structural member and reinforcement arrangement. Since most of the experiments were performed using small specimens, the derived results were deviated from those obtained from real structures. Consequently, the behavior of real structures, particularly the shear strength of cut-off area, are yet to be made clear. Significant damage, such as the failure of the cut-off section, is likely to be caused by seismic load of a greater magnitude than design seismic load, or when a pier was designed according to the old design code. Basically it is desirable that such a damaged bridge pier is replaced with a new one immediately. However, from the point of view of restoring its function as soon as possible, repairing only damaged section and bringing the pier back into service is considered to be an alternative. In order to grasp the load resistance characteristics of a real structure designed according to the old design code in which fracture occurs at the cut-off point, an experimental test was carried out using a relatively large-sized RC bridge pier models containing the similar reinforcement arrangement as that of real structures. The damaged model was repaired by cutting fractured steel bars and welding new reinforcing bars, and finally by the replacement of concrete. Then the load bearing capacity of this repaired model was investigated. To be more specific, the effectiveness of this preparing work was evaluated through the comparison of the load bearing capacity of the repaired model and that of the normal model.

OUTLINE OF EXPERIMENT USING A NORMAL SPECIMEN

Form of the specimen

A 1/3 scale model of RC single-column, T-Type standard bridge pier containing the same urban-type multi-layered reinforcement arrangement as that of a real structure, was fabricated in accordance with the Hanshin Expressway standard design code. To let its cut-off area fracture, the cut-off point in the axial direction was positioned to be lower by 1d (d: effective width), and the reinforcement of the cut-off point was changed to 55% of that of basement (normal: 70%). The specifications for the RC bridge pier specimen is presented in Table 1, and its sectional form in Fig. 1. The sectional form and shear span / depth ratio of the specimen were almost the same as those of a real structure. The cement used was high-early-strength Portland cement. The design concrete strength of the specimen (270 kgf/cm^2) was employed as a target strength in the experiment. Microconcrete whose maximum coarse aggregate size was 10 mm was used. Reinforcements in the axial direction with a diameter of 13 mm (deformed), and lateral ties with a diameter of 6 mm (deformed) were used. The yield strength of the former and the latter is 38 kgf/mm^2 and 32 kgf/mm^2, respectively. The reinforcement ratio of the column reinforcement was 2.28% (at the lower end area of the pier), that of the lateral ties (at the lower end area of the pier), 0.22%, and that of the overall lateral ties, 0.11%. The intermediate lateral ties were not taken into account.

Method of load application

As is shown in Fig. 2 Loading Arrangements, the specimen was bound to the reaction floor with steel bars at positions away from the column area of the footing. Axial force equivalent to the dead load in the superstructure was introduced by means of an unbonded prestressing steel inserted in the sheath having relatively large inner space with its axial center set on the column's center. To be more specific, the end of the steel bars was anchored to the bottom of the footing, and axial force was applied under control so that the load could be maintained constant. Using a two-way actuator installed on the reaction wall, horizontal load was applied at the top of the specimen. For this purpose, a steel jacket was placed on the top of the specimen, and the tip of the jack was bound to the specimen with PC steel. Horizontal load was applied alternately under the load control until the outer-most reinforcement in the axial direction reaches a little before the yield point, and from that point on, with displacement being controlled. As is shown in the loading pattern in Fig 3, 6-step loading was carried out until the yield point was reached. From that point on, the specimen was subjected to a series of step-wise increasing symmetric displacement cycles at δ_y, $2\delta_y$, $3\delta_y$, and $4\delta_y$. At each step, 10 cycles of loading with the same displacement amplitude were applied.

The experiment was continued until load being applied dropped to either the yield point or 0.7 times of maximum load. Fig. 4 shows measurement locations of typical items, such as load (load cell), displacement, and strain.

Experimental results of the normal specimen

A load-displacement curve is shown in Fig. 5, the development of cracks, in Fig. 6 and its picture, in Fig. 7. Distinctive behaviors observed in the course of load application were as follow:

(1) Cracks occurred in the corner area. (13.3 t)
(2) Flexural cracks that appeared in the cut-off area shifted to diagonal cracks. (expected yield load: 75.2 t)
(3) Spalling-off of cover concrete increased at the cut-off area and its range enlarged. ($3\delta_y$, n (loading cycle) =3)
(4) The buckling of column reinforcement ($3\delta_y$, n=6)

(5) Marked drop of load at the p-δ envelopment line and the progress of damage ($4\delta_y$, n=1)

As apparent from the above, flexural cracks occurred in the first place. However, the hoop reinforcements reached the yield point at the cut-off point (104.7 t) and the members fractured (shear failure) in the same section. Although maximum load and ductility decreased compared to the standard specimen (fractural failure type), the specimen still retained toughness ratio 4 ($\delta u/\delta_y=4\delta_y/\delta_y$)) and did not bring a brittle failure.

OUTLINE OF THE EXPERIMENT USING A REPAIRED SPECIMEN

Preparation of the specimen

As has been described in the preceding section, fracture occurred in the specimen, mainly in its area of approximately 80 cm around the cut-off point located 1.23 m above the footing. This fractured section was repaired following the procedure shown below:

1) Concrete chipping

Chipping was carried out to such a depth that the main reinforcement in the second row from the concrete surface became completely exposed. Damaged concrete was completely removed.

2) Cutting and welding of the main reinforcements and hoop reinforcements

All the main reinforcements and hoop reinforcements at the fractured zone were cut with a gas burner. In order to maintain the stability of the specimen, cutting and welding were carried out alternately with a unit of approximately 10 steels at a time. A weld length of 150 mm and 70 mm was secured for the main reinforcement with a diameter of 13 mm and hoop reinforcement with a diameter of 6 mm, respectively, according to the results of weldability test conducted to find required weld lengths. As with the welding of hoop reinforcements, the reinforcements processed into U-shape were jointed together, and a lapped section of 70 mm was welded. Fig. 8 shows the cutting and welding of the reinforcements.

3) Formwork installation and cement paste placement

Two-step formwork was constructed. After the first-step formwork was installed, coarse aggregate was placed, followed by the installation of the second-step formwork and the placement of the rest of coarse aggregate. Finally, cement paste was placed over the entire formwork.

4) Epoxy resin grouting

Cracks remained after concrete chipping were repaired by means of epoxy resin grouting. Prior to grouting, several tubes were inserted for grouting and venting purposes. Epoxy resin grouting was carried out after prepacked concrete placement.

Experimental results of the repaired specimen

The load application method employed for the repaired specimen were the same as that used for the normal specimen. The yield load obtained from calculations for the normal specimen was 75.2 t, and displacement resulting from the calculated yield load was 26 mm, which was employed for the experiment as δ_y. A load-displacement curve for the repaired specimen is shown in Fig. 9, and the development of cracks, in Fig. 10. Distinctive behaviors observed during load application were summarized below:
(1) Cracks occurred in the corner area. (6.7 t)
(2) Flexural cracks that appeared in the cut-off area shifted to diagonal cracks. (71.0 t)
(3) The range of spalling-off of cover concrete enlarged. ($3\delta_y$)
(4) Marked drop of load at the p-δ envelopment line. ($4\delta_y$, n=1)

159

(5) The drop of load at the p-δ envelopment line became even more conspicuous. (5δ$_y$)

Comparison of experimental results

1) Load-displacement curve

The typical results obtained from the experiments of the normal and repaired specimens were compared. The comparison between Fig 5 and Fig. 9 shows that the load-displacement relationships almost coincide, except for those before crack occurrence. However, at around the first two cycles of loading, a marked drop in load was observed in the repaired specimen. Furthermore, the maximum load of the repaired specimen exceeded that of the normal specimen by nearly 8%. This is considered to be due to the increase in the amount of lateral ties at the lapped section.

2) Cracking pattern

The cracking pattern of the repaired and normal specimens almost coincide, except that cracking occurs more frequently near the cut-off point in the former. One of the possible reasons is that in the upper part of the repaired section, placing aggregate near the formwork was difficult, and so a greater amount of cement paste was eventually placed near the surface.

3) Horizontal displacement distribution

Fig. 11 shows the relationship between horizontal displacement and the different height levels of the specimen. The horizontal deformation distributions of the repaired specimen at different loading levels are almost identical with that of the normal specimen. From this, it can be concluded that the repair was effective and the area subjected to the repair was appropriate.

4) Strain distribution of the main reinforcement

As is shown in Fig. 12, strain distributions at different loading levels are almost identical. Strain decreased at around the upper and lower ends of the repaired section. This is considered to be due to the reasons that welding was carried out at these areas and that the amount of reinforcements was increased.

The above comparisons revealed that there were some differences between the repaired specimen and the normal specimen, namely, the cracking pattern of the former and that of the latter differ particularly in the repaired section, and the initial rigidity curve for the former was more moderate than that for the latter. On the whole, however, the two are almost identical in terms of their load-deflection curves and deformation characteristics.

CONCLUSION

The results obtained from the comparative tests using the large-sized specimens (the repaired and normal models) can be summarized as follows:

(1) Before cracking occurred at the cut-off section, the deformation of the repaired specimen was relatively larger compared to that of the normal specimen under the same loading conditions.

(2) However, the repaired specimen presented the similar load-deformation relationship as that of the normal one after the crack occurrence.

(3) From the above, it can be concluded that welding of new reinforcing bars is an effective repairing method for bridge piers damaged by earthquakes.

REFERENCES

1) Hanshin Expressway Public Corporation, "Standard design code and figures on Hanshin Expressway", 1991.
2) Nakabayashi, S.; Hamada, K. and Hayashi, H., "An Experimental Study on the Displacement Performance of RC Bridge Piers", Technical Report of Hanshin Expressway, Vol. 11, March, 1991.
3) Ozaka, Y.; Suzuki, M.; Kuwasawa, S. and Ishibashi, T., "Load-Deflection Characteristics of Reinforced Concrete Columns under Static Alternating Cyclic Loads", Proceedings of JSCE, No. 372, Vol. 5, Feb., 1988, pp. 45–54.

Table 1 Shape and mix proportions of the specimen.

| Dimension B×H (mm) | Longitudinal reinforcement | | | | Transverse reinforcement | | | | |
| | Cut-Off point (m) | Dia. | Steel ratio | | Dia. | Column base | | General part | |
			Column base $\rho_\ell(\%)$	Cut-Off $\rho_{cut}(\%)$		Spacing (cm)	Steel ratio $\rho_w(\%)$	Spacing (cm)	Steel ratio $\rho_w(\%)$
1167 × 1000	1.233	D13	2.28	1.26	D6	5	0.22	10	0.11

| Max. size coarse agg. (mm) | Slump (cm) | Water-cement ratio W/C (%) | Sand-agg. ratio S/a (%) | Unit content(kg/m^3) | | | | Admixture (kg/m^3) | Air (%) |
				Water W	Cement C	Sand S	Gravel G		
10	18	62.0	46.0	200	323	785	951	0.808	4
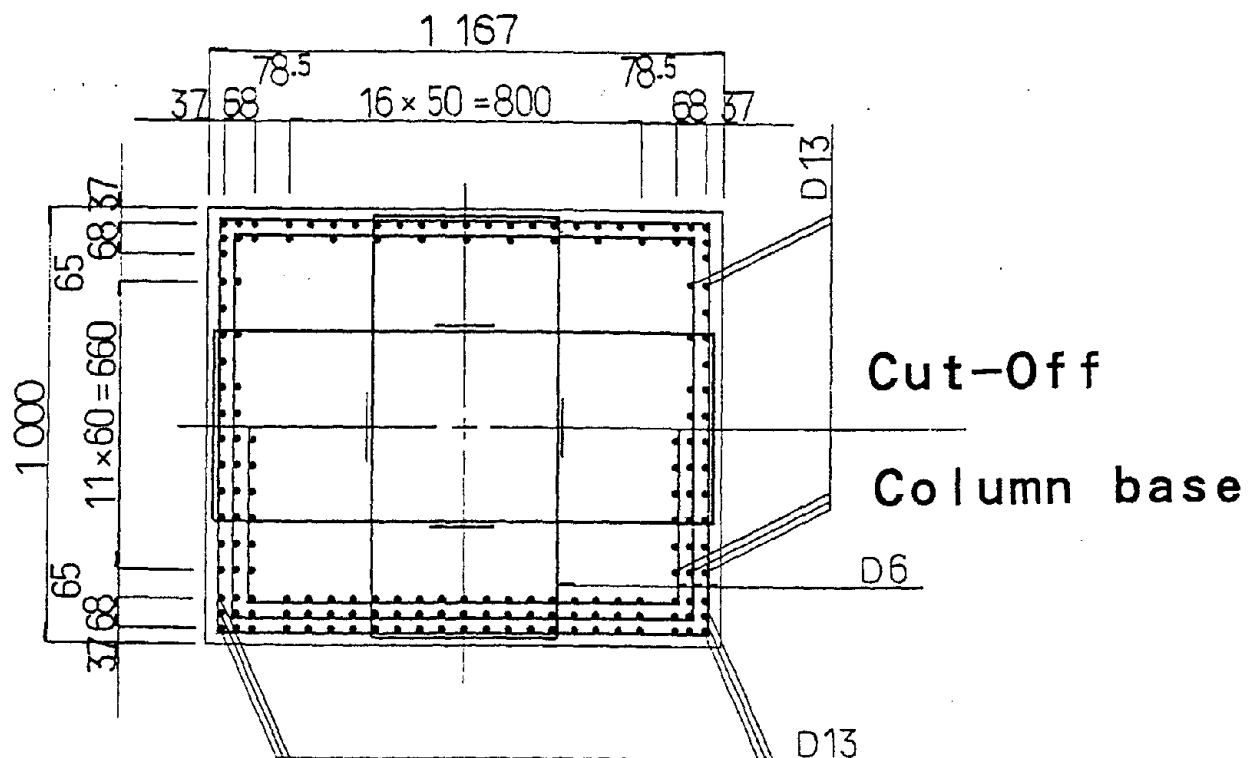
Fig. 1 Cross section of the specimen.
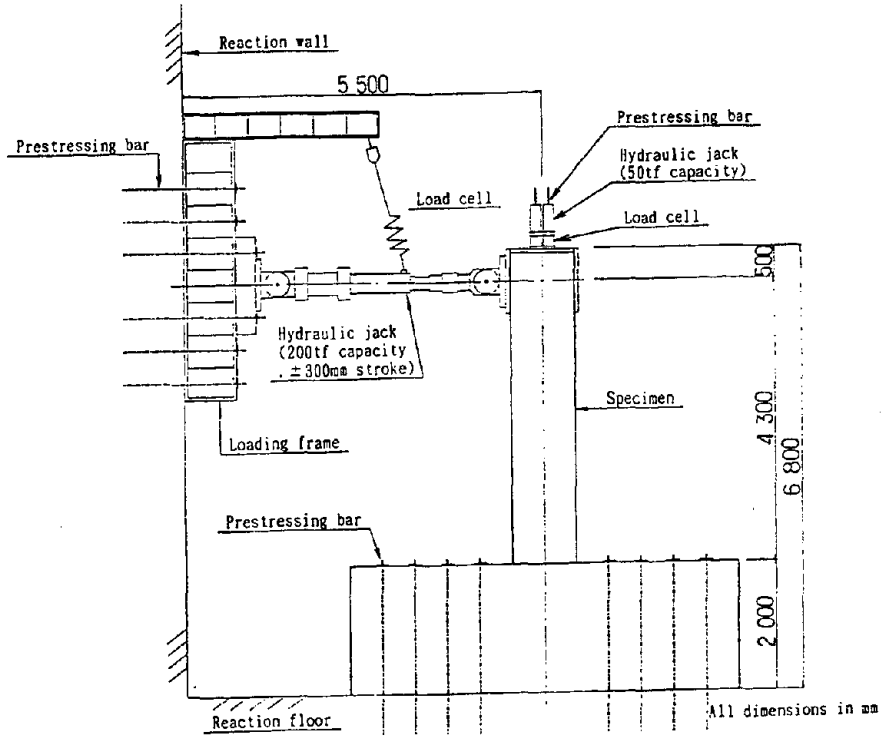
Fig. 2 Loading arrangements and dimensions
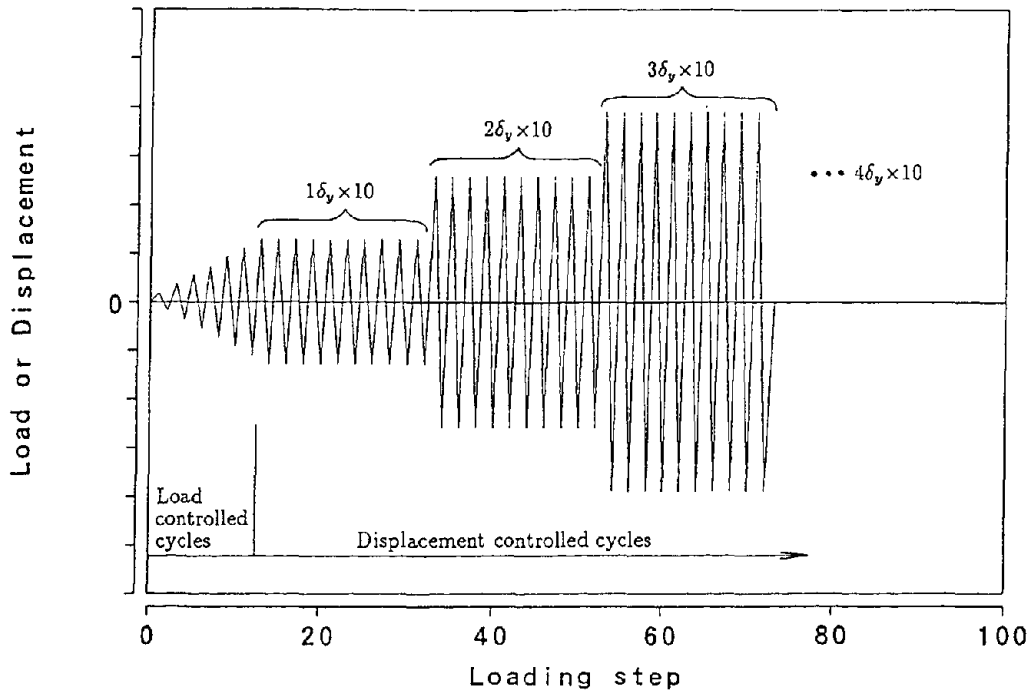
Fig. 3 Step-wise increasing symmetric loading displacement

163

All dimensinons in *mm*
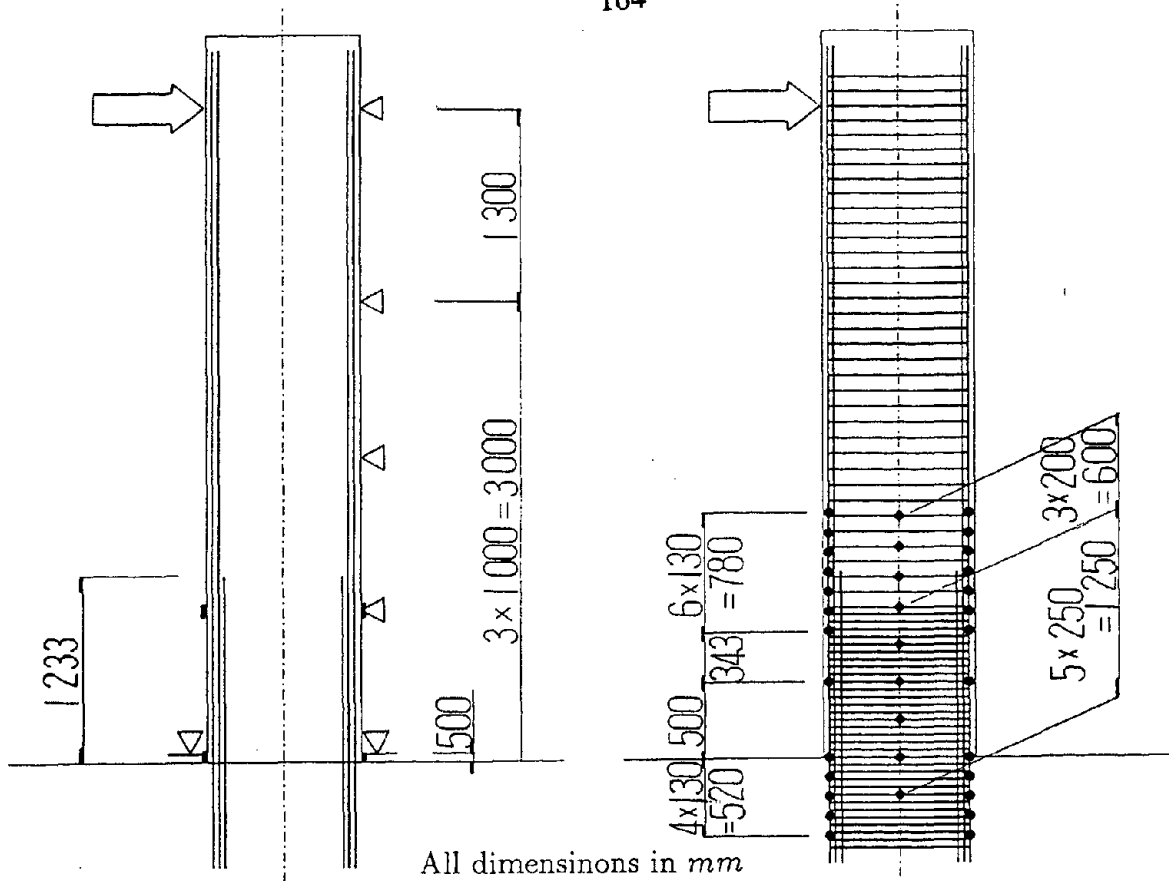
△ : Measurement of displacement   ● : Strain gauge in steel reinforcement

▮ : Concrete gauge   ◆ : Strain gauge in hoop reinforcement
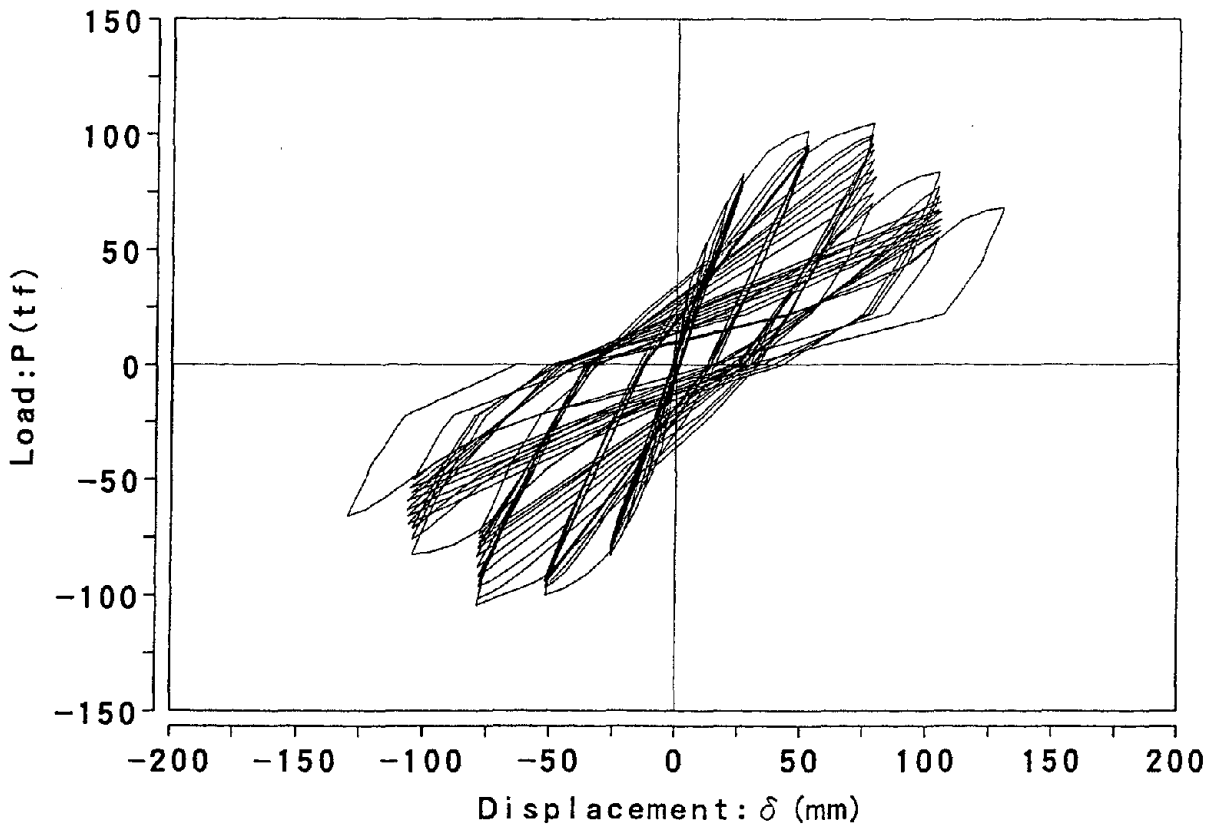
Fig. 4 Measurement locations

Fig. 5 Load-Displacement curves for the normal specimen

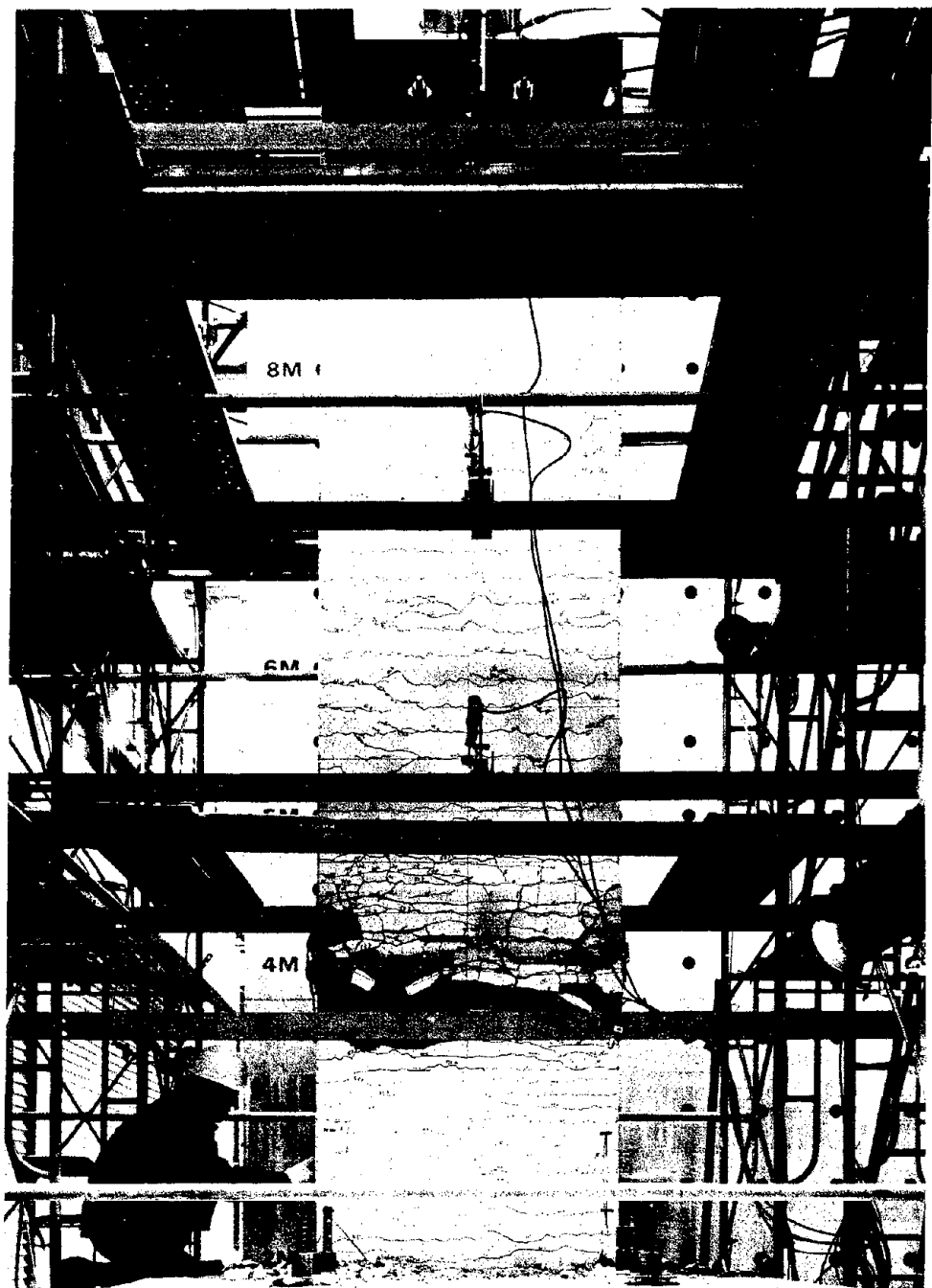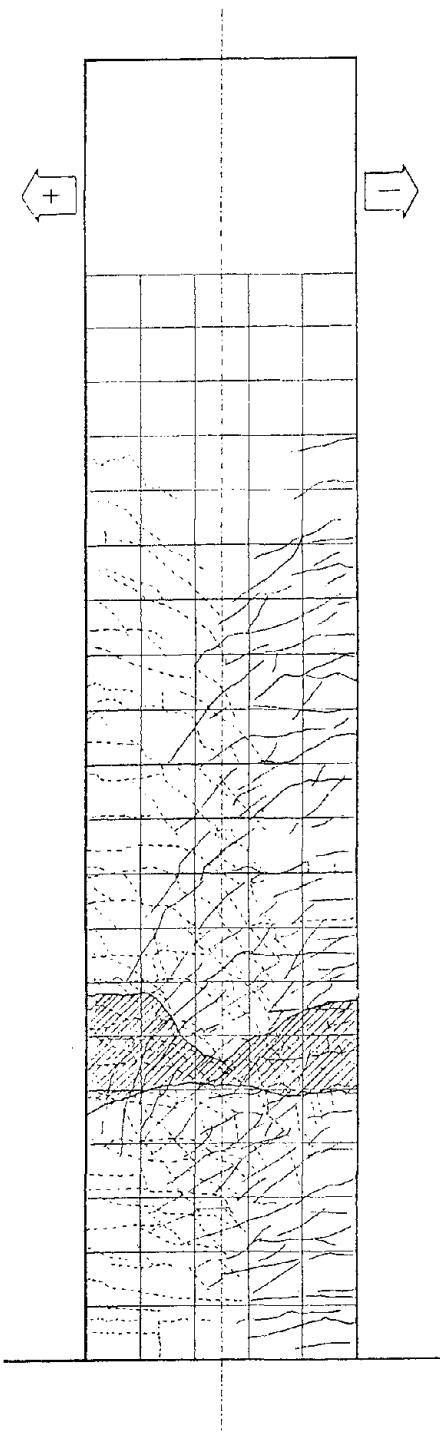Fig. 7 Cracking pattern for the normal specimen

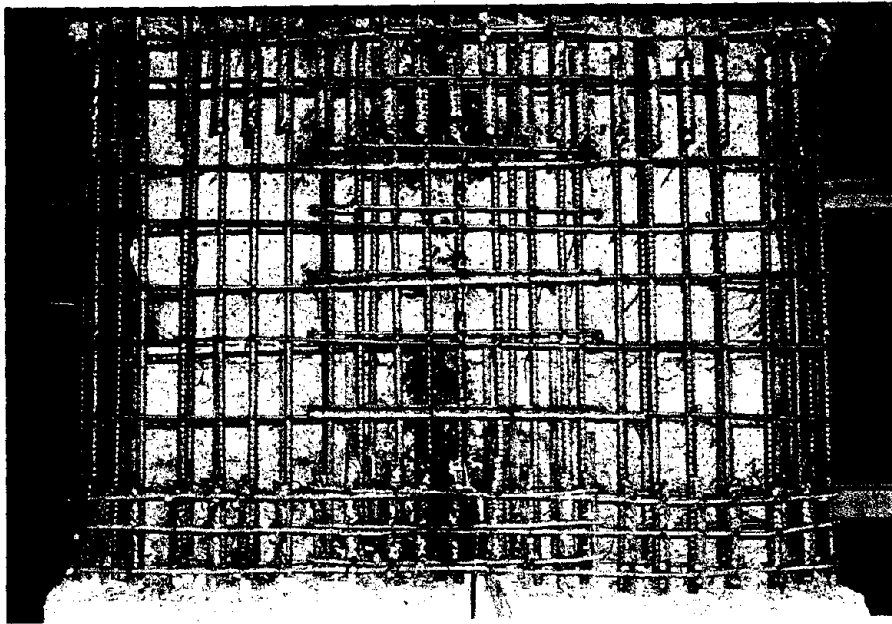Fig. 6 Cracking pattern for the normal specimen
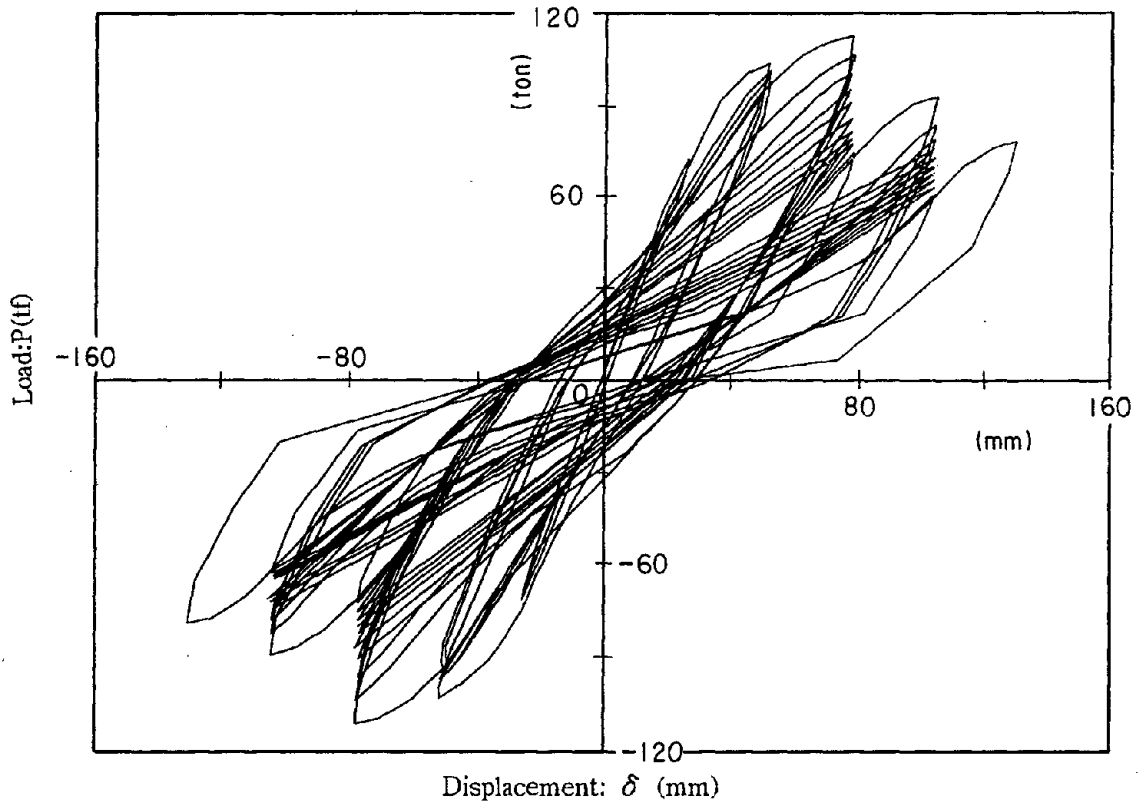
Fig. 8 Cutting and welding of the reinforcements

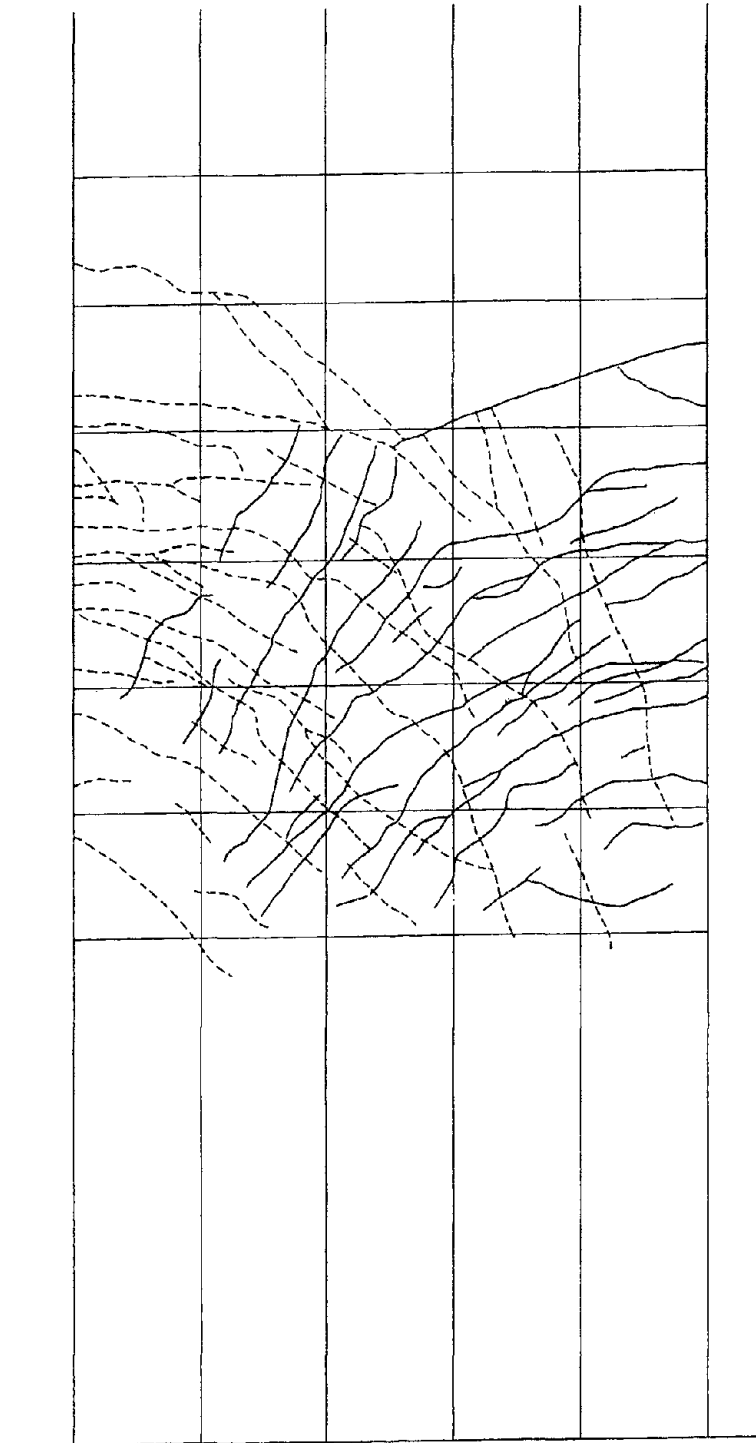Fig. 9 Load-Displacement curves for the repaired specimen

166

Fig. 10 Cracking pattern for the repaired specimen at 3 δ y
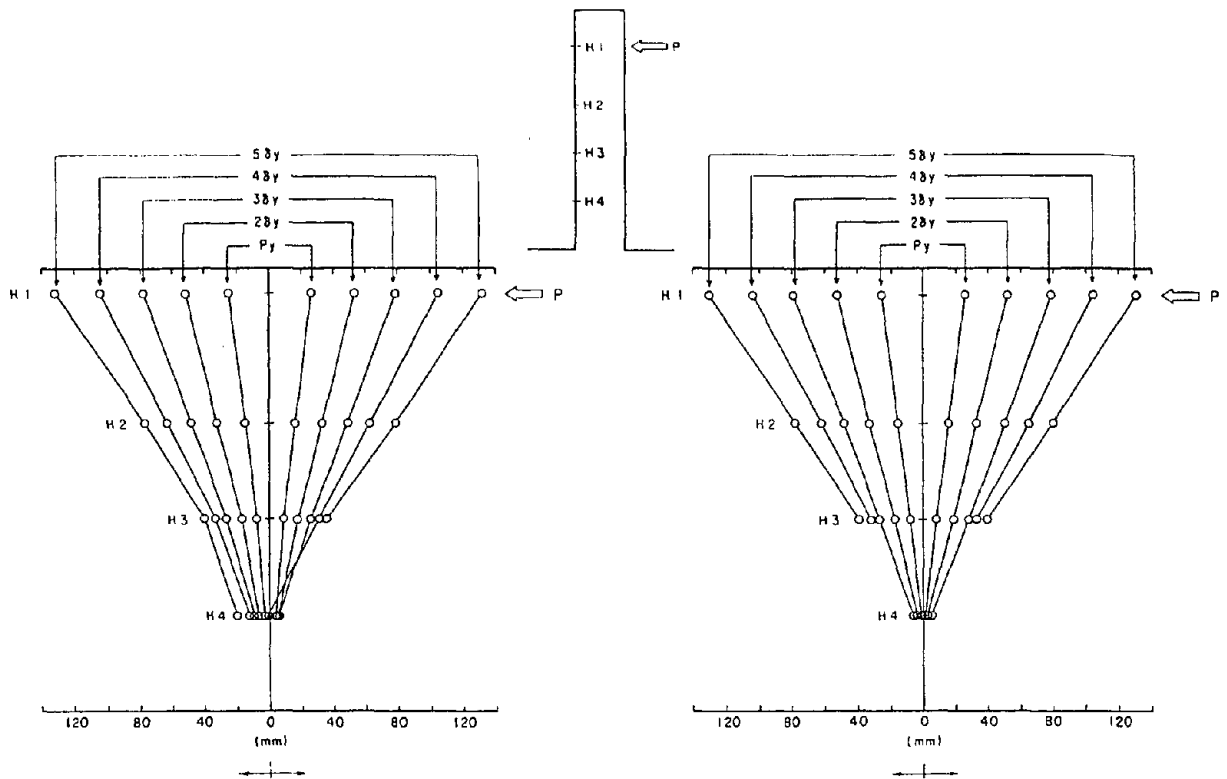
Fig. 11 The relationship between horizental displacement and height of the specimen
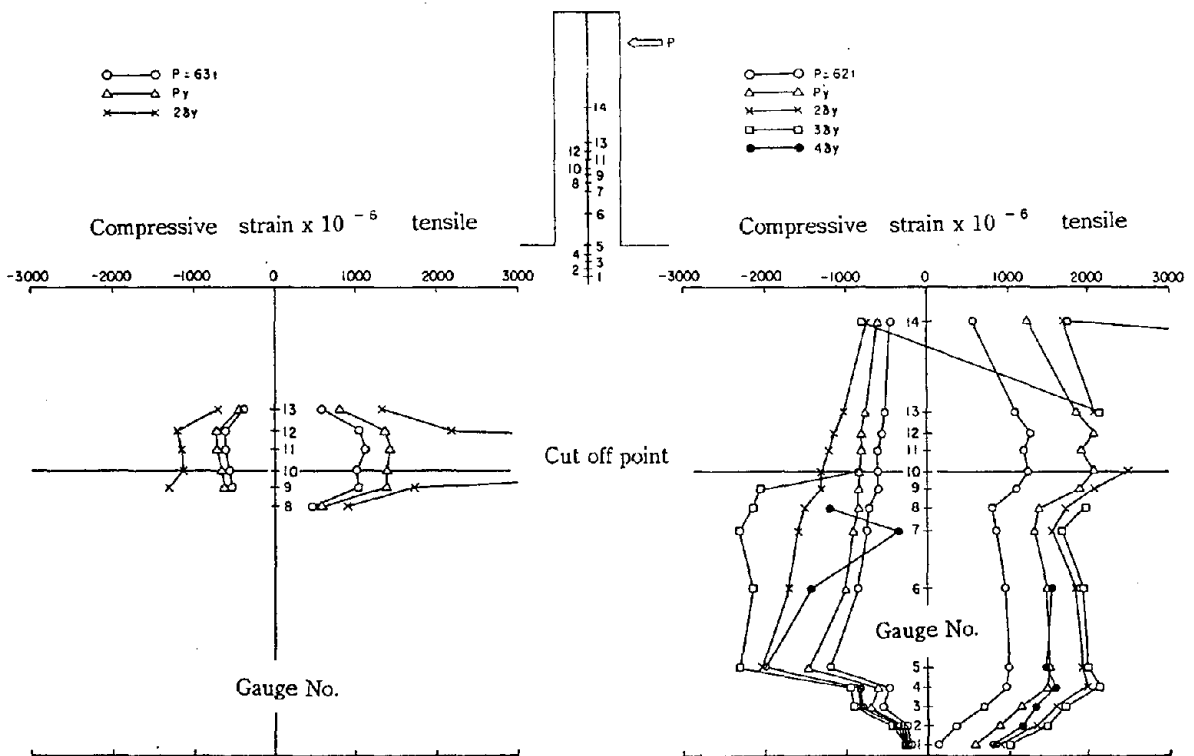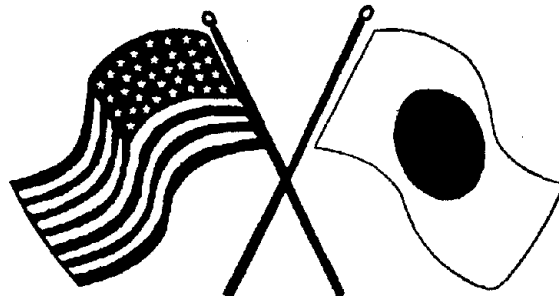(left: repaired specimen, right: normal specimen)

Fig. 12 The relationship between strain distribution and the load levels

168

SECOND U.S.-JAPAN WORKSHOP
ON SEISMIC RETROFIT OF BRIDGES

Santa Monica Column Splice and
Cap-Beam Proof Tests

G.A. MacRae, M.J.N. Priestley and F. Seible

January 20 and 21, 1994
Berkeley Marina Marriott Hotel
Berkeley, California

SANTA MONICA COLUMN SPLICE AND CAP-BEAM PROOF TESTS

Gregory A. MACRAE, M. J. Nigel PRIESTLEY and Frieder SEIBLE

Department of Applied Mechanics and Engineering Sciences
University of California, San Diego, La Jolla, California, USA

ABSTRACT

A series of 5 large scale tests are being carried out to assess the earthquake resistance of the Santa Monica Viaduct at the University of California, San Diego. This paper summarises the results of 2 lap-splice tests (SM1 and SM2) and one test of a column cap-beam joint subassemblage (SM3). The two tests on lap splices showed that the strength of the splices in many of the columns in the Santa Monica Viaduct is likely to be high enough that retrofit is not required. This is consistent with an analysis method for assessing the strength of lap-splices in columns. The failure of the cap-beam column subassemblage tested in the direction parallel to the cap-beam was initiated by joint shear failure. Strength degraded slowly with an increasing number of applied displacement cycles and the final behaviour was close to that of a pinned connection.

INTRODUCTION

As a consequence of a reassessment of the expected seismic performance of the Santa Monica Viaduct carried out by The Seismic Safety Review Panel (SSRP) [1], recommendations were made that a significant reduction in the scope and extent of planned retrofit measures could be made. If the SSRP recommendations are implemented, the result would be a saving of many millions of dollars. An analytical assessment procedure [2] that relies on new concepts of member and section performance was used for the recommended reduction in retrofit. It was further decided that full-scale testing of typical details should be carried out to validate the predicted response. As a consequence, a proof-test program was initiated at the University of California, San Diego to test five large-scale typical bridge elements.

The Santa Monica Viaduct consists of multi-column bents with a total of more than 2300 circular columns extending below the ground level as pile shafts of the same diameter. Columns are either 3ft (914mm) diameter or 4ft (1219mm) diameter and reinforcement varies from 12#11 (35mm) bars to 16#18 (57mm) bars. Lap-splices are provided for the main longitudinal reinforcement immediately above the ground surface. Cap-beams and beam-column joints were designed without considering the possibility of strong earthquake-induced ground motions. Critical reinforcement is grade 40 (nominal f_y = 276MPa). The maximum bending moment was expected to occur several diameters below the ground as shown in Figure 1. Hence the moment at the lap splice was expected to be significantly less than the maximum moment below the ground surface. Analyses by SSRP [1] estimate that the moments at the base may be up to 68% of the theoretical maximum moment developed at depth. Thus the value for α in Figure 1 is 68%.
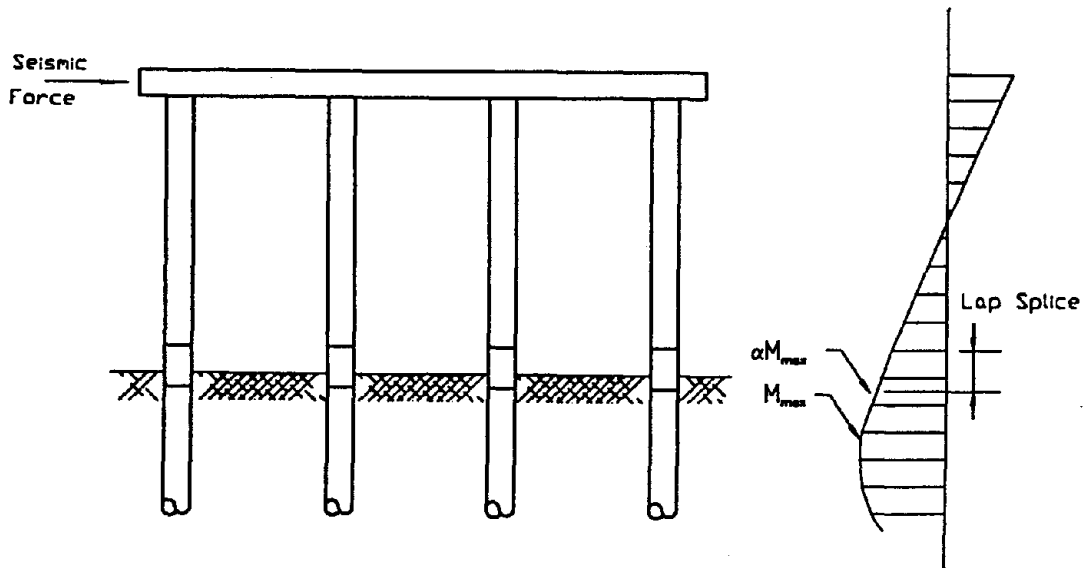
(a) Structural Configuration   (b) Moments

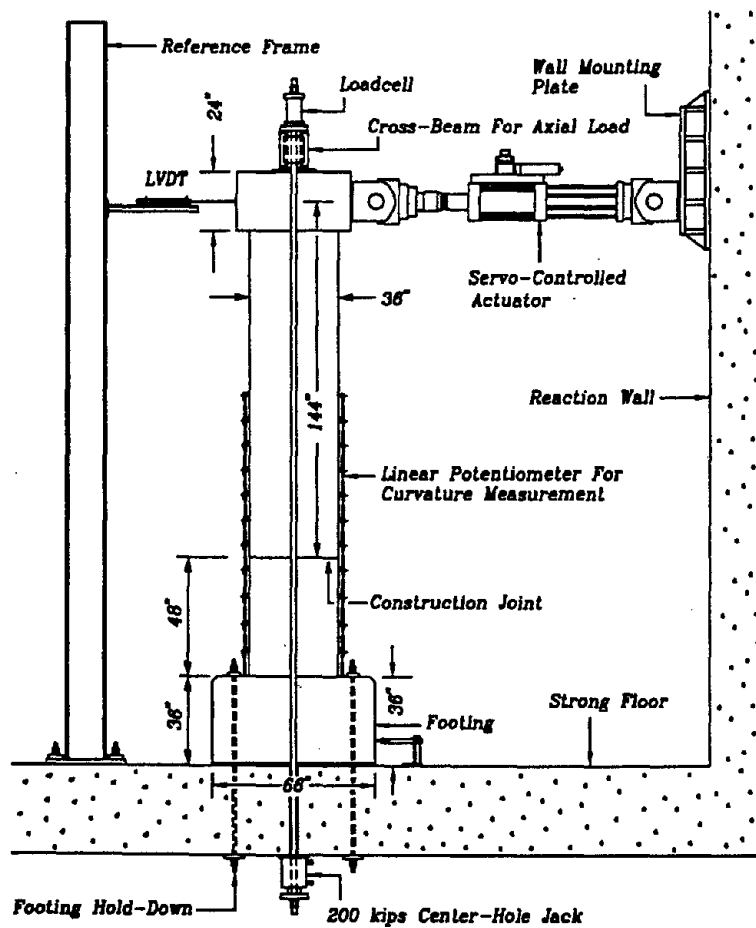Figure 1. Moments in Pile/Columns Under Transverse Response

Figure 2. Column Test Set-Up for Units SM1 and SM2
(1in = 25.4mm, 1kip = 4.45kN)

172

The first two units tested modelled the lap-splice details. The models consisted of a 3ft (914mm) diameter column with 16 #11 (35.8mm dia.) and 12 #18 (57mm dia.) Grade 40 (nom. 276MPa) longitudinal column reinforcing bars for SM1 and SM2 respectively. The third test unit in the sequence, SM3, is representative of a typical Santa Monica Viaduct cap-beam column joint. The connection between the column and cap-beam consists of the main longitudinal reinforcing steel extending a distance of 16 times the bar diameter into the cap-beam. No joint shear reinforcement is generally provided. Testing was carried out on an upside-down 3/4 scale model considering earthquake loading acting transverse to the bridge longitudinal axis and in-plane with the bent. A further cap-beam column joint test is to be carried out parallel to the bridge longitudinal axis and in-plane with the bent.

TEST INFORMATION

Material Characteristics: The target strength of the concrete was 5000psi (34.5kPa). Measured material tests were used for strength calculations. The steel grade used in the critical bars was Grade 40 (nom. 276MPa) however in non-critical components, Grade 60 (nom. 414MPa) steel was used and the spacing and bar size was scaled accordingly.

Column Theoretical Flexural Strength: Moment-curvature analysis [3, 4] was used to calculate the ideal moment of the section $(M_i)_p$ for the particular axial load used. The ideal lateral shear $(V_i)_p$ was able to be calculated from $(M_i)_p$.

Instrumentation: All units were heavily instrumented.

Testing Regime: The testing regimes for all tests were similar and consisted of 3 cycles to each displacement in the damage or post-yield range. The yield displacement, Δ_y, was calculated as $(V_i)_p/K$, where K is the stiffness of the unit obtained from the load cycles to approximately $\pm 0.75(V_i)_p$. After the initial load-controlled cycles testing was carried out to displacements corresponding to displacement ductilities, μ, of 1.0, 1.5, 2.0, 3.0, 4.0, 6.0 etc. until failure.

SANTA MONICA VIADUCT TEST #1 (16 #11 Bars (35mm dia) Lapped Splice)

The background to tests SM1 and SM2 are published elsewhere [5, 6, 7, 8] so only the conclusions of the research are published here. The test set-up, point of load application, and sizes of units SM1 and SM2 are shown in Figure 2. A construction joint was provided 48in (1219mm) above the footing to represent the column-pile interface. The longitudinal reinforcement for the column consisted of 16 #11 (35mm dia) bars lap-spliced over a distance of 30in (762mm) above the construction joint as shown in Figure 3. The transverse reinforcement consisted of #4 (12.7mm dia.) spiral with a pitch of 3.5in (89mm) and is detailed with the lap splice in the cover concrete with a lap length of 40in (1016mm), corresponding to $80d_b$. The 48in (1219mm) of column below the splice was strengthened by an inner ring of reinforcing steel which enabled the actual strength of the lap-splice to be investigated. The height of steel in the inner ring varied to minimize the effect of crack concentration at the splice base. The axial force was 400kips (1780kN).

173
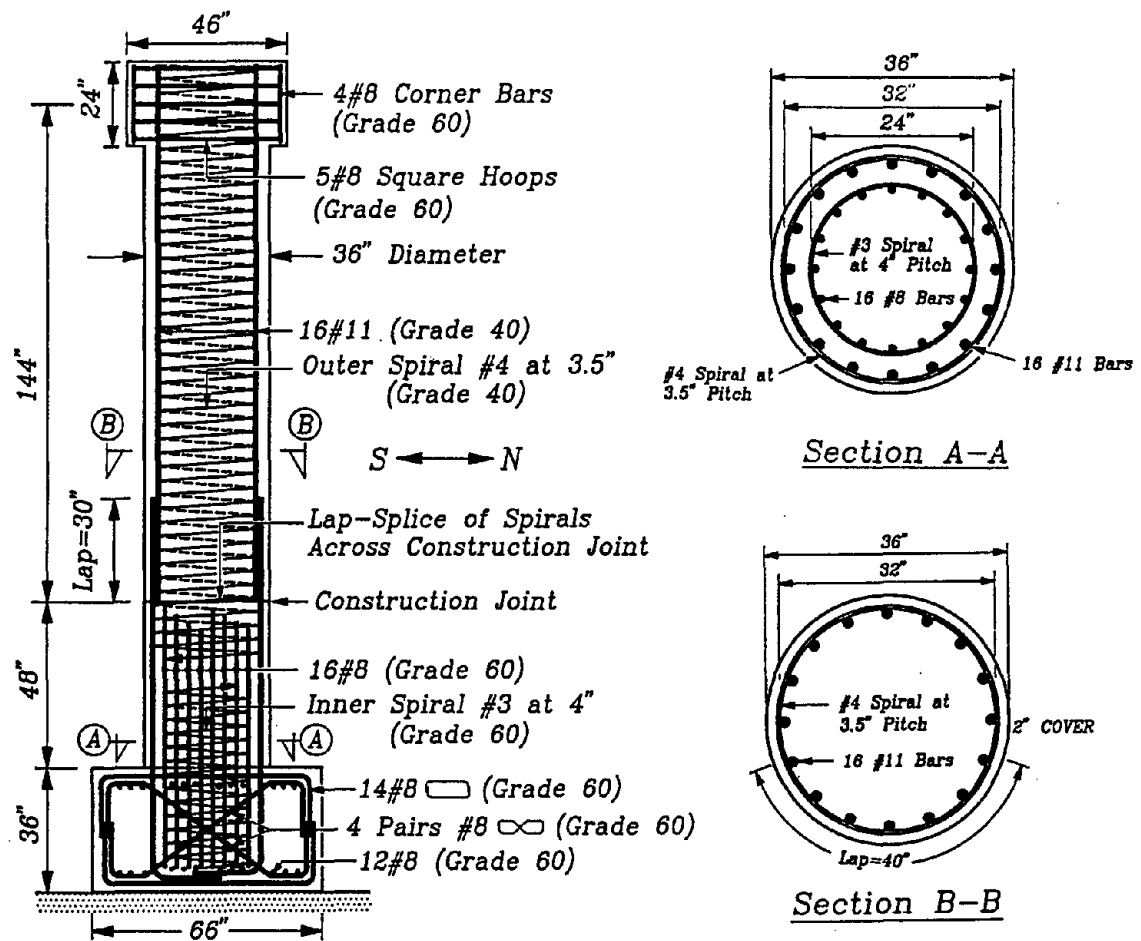
Figure 3. Reinforcement Details for Unit SM1

The lateral force displacement curve and curvature distributions for SM1 are shown in Figures 4 and 5 respectively. Concrete spalling initially occurred 10in (254mm) below the base of the splice. $(V_i)_p$ represents the lateral force corresponding to the ideal flexural capacity at the base of the lapped splice assuming plane sections remain plane. $(V_i)_p$ is 132kips (578kN). $(V_i)_{TS}$ represents the lateral force corresponding to the ideal flexural capacity with a 10in (254mm) tension shift in the critical region below below the base of the lapped splice due to inclined cracks (also known as the T-jd effect). $(V_i)_{TS}$ is 123.4kips (549kN). Figure 4 shows that unit SM1 was able to reach $(V_i)_{TS}$. Lap splice failure occurred during the cycles to a ductility of 3. The curvature distributions of Figure 5 showed the curvatures to be maximum at the base of the column during the initial cycles and at the base of the splice during the final cycles.

SANTA MONICA VIADUCT TEST #2 (12 #18 Bars (57mm dia) Lapped Splice)

The longitudinal reinforcement for the column consisted of 12 #18 (57mm dia) bars lap-spliced for a distance of 45in (1.14m) above the construction joint. The axial force was 400kips (1780kN). The transverse reinforcement was similar to SM1. The lateral force-displacement curve for SM2 is shown in Figure 6. The ideal flexural capacity at the base of the lapped splice, $(V_i)_p$, was 202kips (898kN) and $(V_i)_{TS}$, based on a 10in (254mm) tension shift, was 188.3kips (838kN).

After the first cycle to each displacement up to a displacement ductility of 1.0, the loading curve followed the same path showing a very stable hysteresis. Peak strengths occurred on the first cycle to μ=1.5. Maximum lateral force resistances were 202kips (898kN) in one direction and 182kips (810kN) in the other direction. These exceeded the likely maximum strength demand of $\alpha(V_i)_p$ (= 137kips (610kN)) under seismic response. With further cycles to the same displacement and with larger displacements the degradation increased significantly. The final degraded strength on the third cycle to μ=-3 was 41kips (181kN) or about 20% of the peak lateral strength. The hysteresis loop of this test, SM2 shows a much more pinched behaviour than that of SM1 possibly because bond failure occurred earlier in SM2.

THEORETICAL LAP SPLICE STRENGTH

A procedure for assessment of the lap splice strength has been proposed by Priestley [2]. The splice strength is the maximum value from the methods given below.

    a) Method 1. Highly Confined Section
Tests at UCSD have shown that there is a limit to the dilation of the concrete, ε_d, of about 0.001 before bond-slip occurs. Using this value of ε_d and Youngs modulus for steel, E_s = 29000ksi (200GPa), the effective confining stress, f_l, is given by Equation 1.

$$f_l = \frac{58A_b}{D's} \text{ (ksi)} = \frac{400A_b}{D's} \text{ (MPa)} \tag{1}$$

Here D' is the diameter of hoop or spiral, s is the spacing and A_b is the area of hoop or spiral. Allowing the standard coefficient of friction, μ, of 1.40 on the crack surface as
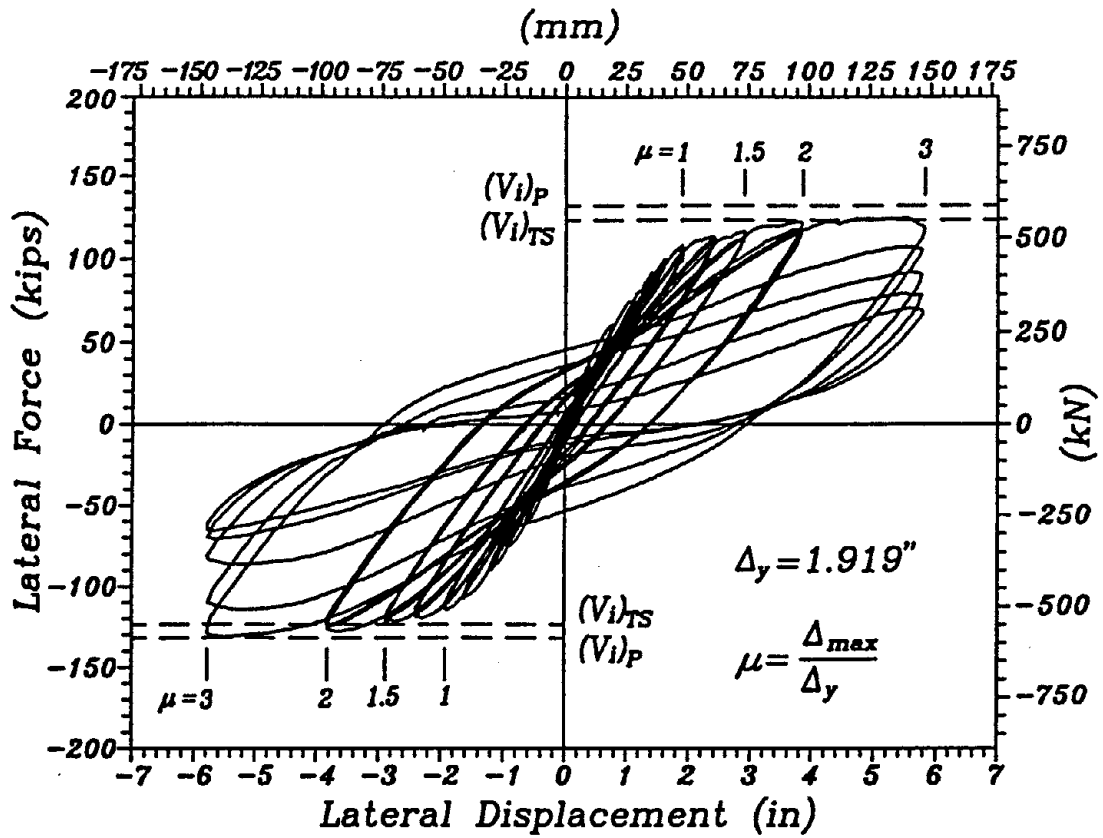
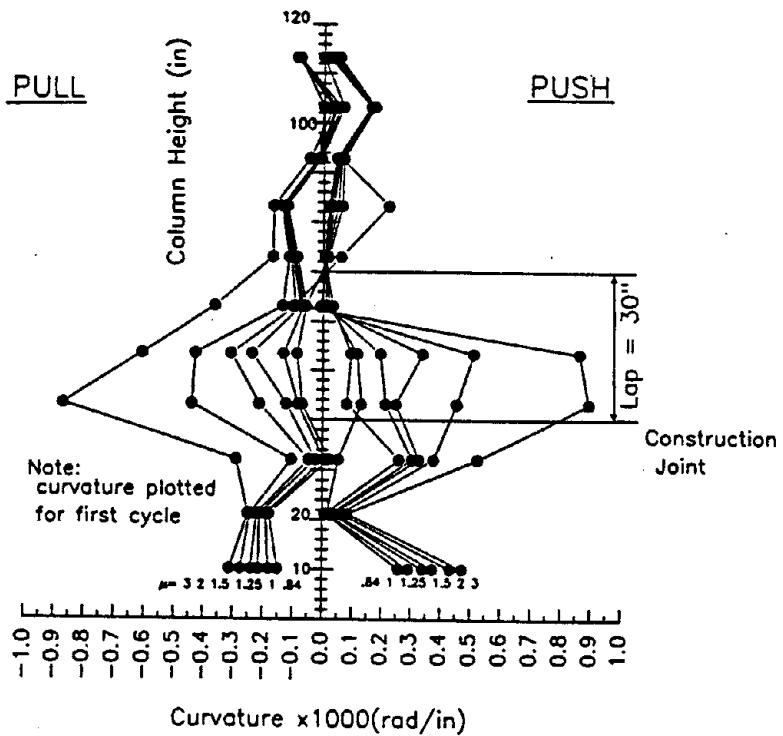Figure 4. Lateral Force-Displacement Response for SM1

Figure 5. Curvature Distributions Up the Column at
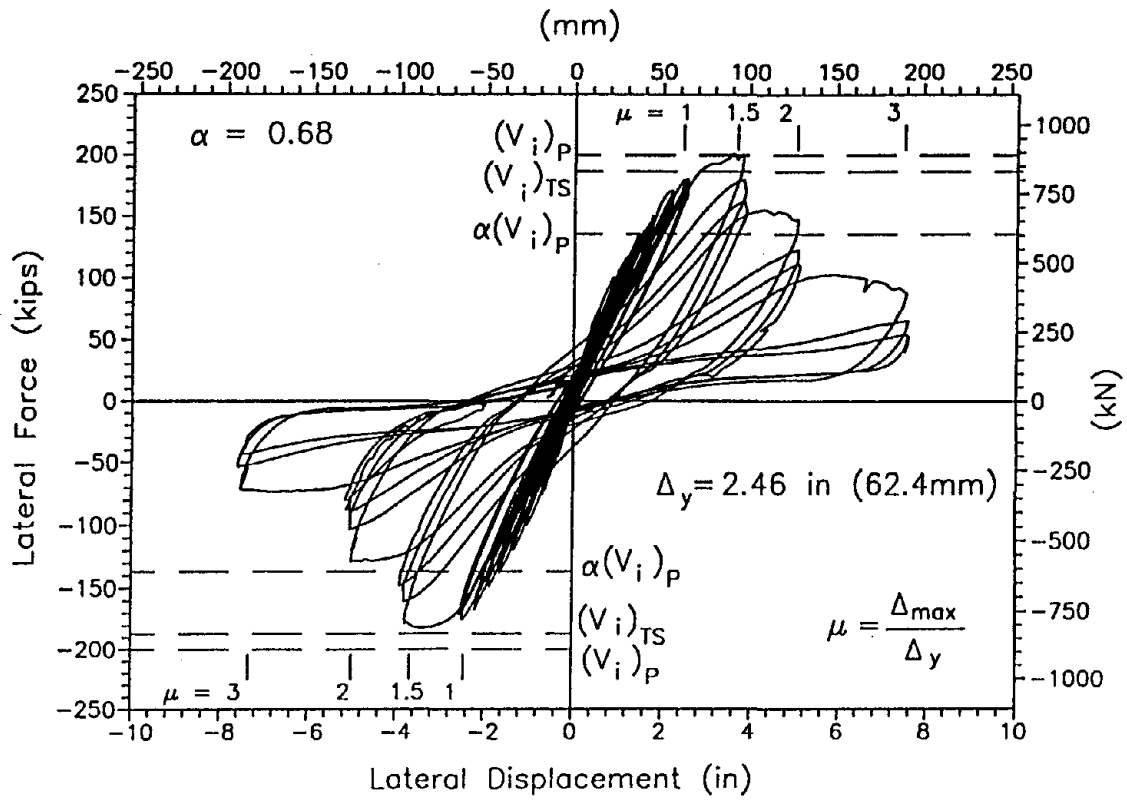First Excursion to Each Ductility Level (1in.=25.4mm)

176
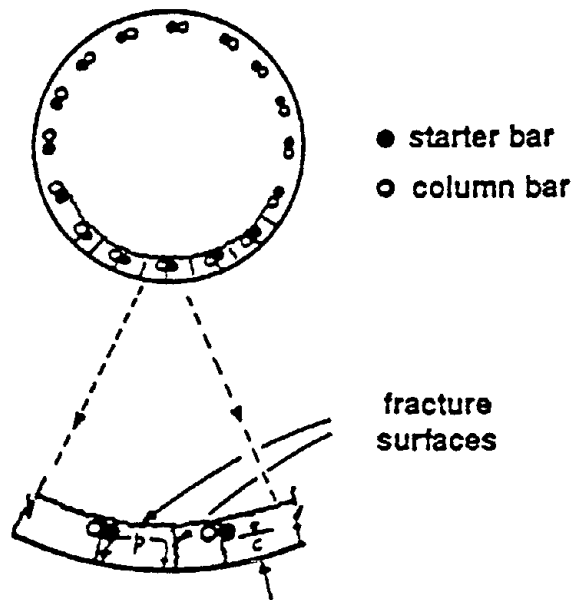
Figure 6. Lateral Force-Displacement Response for SM2

Figure 7. Fracture Surface for Lap-Splices in Circular Columns

177

shown in Figure 7, the tension force, T_b, able to be carried by any longitudinal bar is given by Equation 2.

$$T_b = 1.4 f_t \left[\frac{\pi D'}{2n} + 2(d_b + c) \right] l_s \qquad (2)$$

Here c is the cover, d_b is the diameter of main longitudinal bars, n is the number of main longitudinal bars and l_s is the splice length.

  b) Method 2. Lightly Confined Section

Equation 3 ignores the contribution of confining steel and considers only the tensile stress necessary to fracture the concrete failure surface of Figure 7.

$$T_b = f_t \left[\frac{\pi D'}{2n} + 2(d_b + c) \right] l_s \qquad (3)$$

Here f_t is the direct tension strength of concrete as given in Equation 4.

$$f_t = 4\sqrt{f'_c} \text{ (ksi)} = 0.33\sqrt{f'_c} \text{ (MPa)} \qquad (4)$$

The second method controls the estimate of design strength for both units SM1 and SM2.

Three existing code methods [9, 10, 11] as well as Priestley's method [2] were used to compare the development lengths of a bar as shown in Table 1. It was assumed that the splice strength was inversely proportional to the length provided. The code equations have been explained in references [5] and [6]. Here the required development lengths are based on the measured material properties. Some of the codes described below state that their equations should not be used for lap-splices with #18 bars due to lack of test information from such splices. The code equations were used anyway for comparison. Priestley's method [2] predicts that bars will carry significantly more stress than do the code methods.

Table 1. Predicted Development Lengths and Maximum Stresses

	Unit	ACI 318-83 [9]	ACI 318-89 [10]	ACI 408 [11]	Priestley [2]
Development Length	SM1	54.7in (1389mm)	41.8in (1062mm)	36.8in (36.0mm)	26.7in (679mm)
	SM2	72.7in (1847mm)	79.0in (2010mm)	91in (2308mm)	50.7in (1288mm)
Maximum Stress, f_s	SM1	24.2ksi (169MPa)	31.7ksi (218MPa)	36.0ksi (248MPa)	f_y
	SM2	25.8ksi (178MPa)	23.8ksi (164MPa)	20.7ksi (142.7MPa)	37.1ksi (255.6MPa)

As the full yield strength of the #11 bar, f_y (= 44.2ksi or 306.8MPa), was expected to able to be developed in unit SM1 according to Priestley's method, the full flexural strength of the unit of $(M_i)_p$ = 18,990in-kip (2144kNm) was predicted to be able to be attained. The lateral shear force was therefore $(V_i)_{TS}$.

178

The stress able to be achieved in unit SM2 was less than the yield stress of 41.8ksi (288MPa) indicating that the ideal moment from moment-curvature analysis would not be able to be attained. The maximum moment capacity of this unit was likely to be significantly more than the moment corresponding to the extreme tension bar reaching the stress calculated in Table 1 because other bars would still be able to carry increased force and the moment-curvature curve would still be expected to have a positive slope. A more realistic, but empirical estimation of the maximum strength is given in Equation 5.

$$V_{max} = \frac{f_s}{f_y}(V_i)_{TS}$$ (5)

$$= \frac{37.1ksi}{41.8ksi} 188.3kip = 167kip \ (744kN)$$

This value too was considered to be conservative as it is based on a constant moment over the splice which was not present in the test units. This theoretical strength is $(f/f_y) = 0.89$ times the ultimate flexural strength. As this is greater than the expected demand of 68% of the ideal flexural strength, the unit was expected to behave satisfactorily. The actual strength of SM2 was 182kips (810kN) showing that the theory was conservative and therefore appropriate for the strength assessment of real structures.

SANTA MONICA VIADUCT TEST #3 (Column Cap-Beam Subassemblage)

The third test unit in the sequence, SM3 was an upside-down 3/4 scale model representative of a typical Santa Monica Viaduct cap-beam column joint [12]. Loading was applied transverse to the bridge longitudinal axis and in-plane with the bent. The connection between the column and cap-beam consists of the main longitudinal reinforcing steel extending a distance of 16 times the bar diameter into the cap-beam. No joint shear reinforcement was provided. Existing code equations predict that both the column longitudinal reinforcing steel development length and the joint shear strength are inadequate and the column is likely to fail at a strength much lower than its flexural strength. However, as geometrical considerations restrict the development of a full mechanism, a higher strength than that obtained directly from code equations was expected.

The test configuration shown in Figure 8 was chosen to represent the prototype behaviour as closely as possible. The test regime is given in Figure 9. Lateral force and vertical force were applied to the top of the unit. Horizontal supports were provided at the height of the beam centre-line. A gap of 1/4in (6mm) was initially provided between the unit and reaction block on the south side to allow for the increase in length of the beam due to cracking. Cap-beam tie-down points were 96in (2438mm) from the column centreline as shown in Figure 10. Vertical supports at 62in (1575mm) and 98in (2489mm) each side of the column centreline ensured that a complete mechanism did not occur as soon as the beam hogging plastic hinge formed. A lap splice of the cap beam bars on one side of the column was provided in the soffit slab.
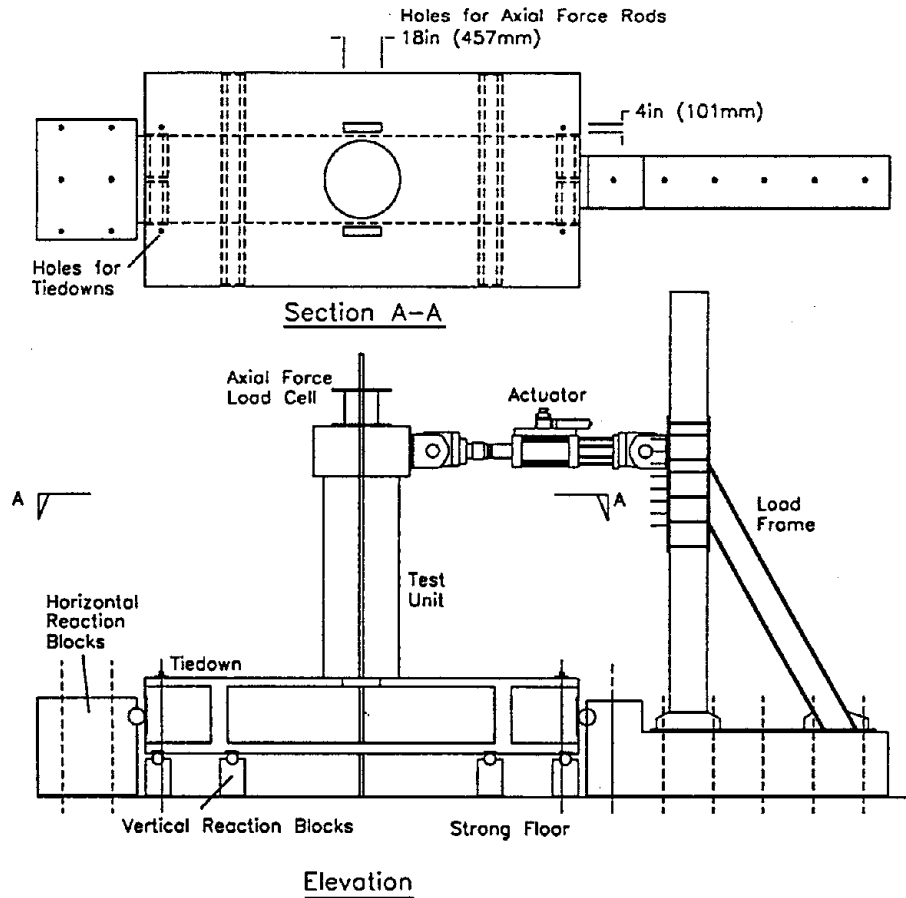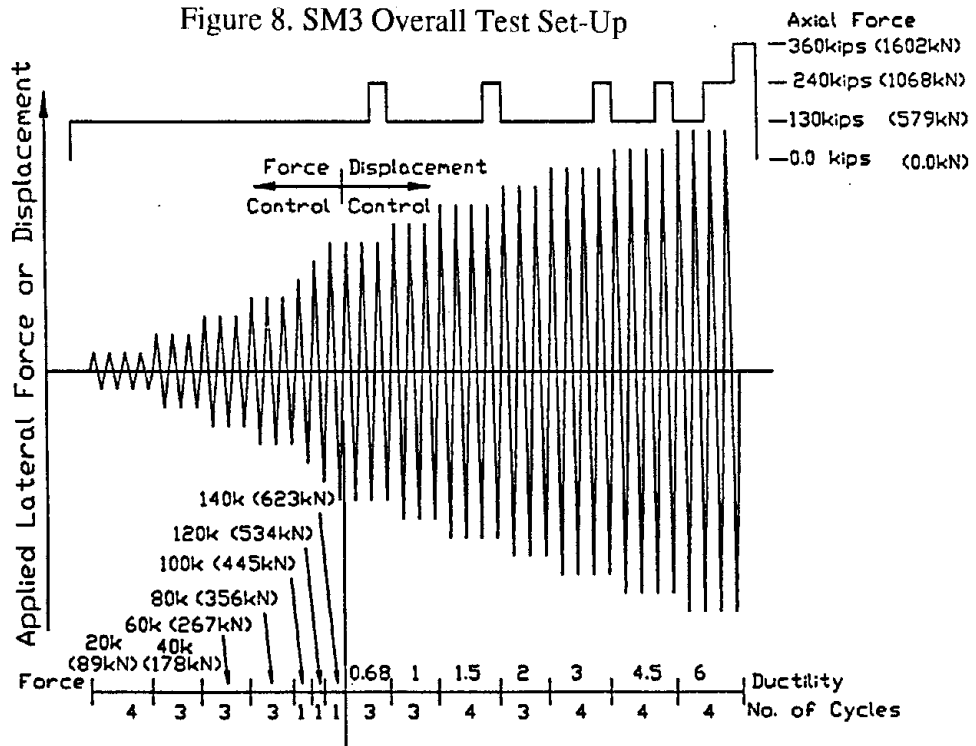
179

Figure 8. SM3 Overall Test Set-Up

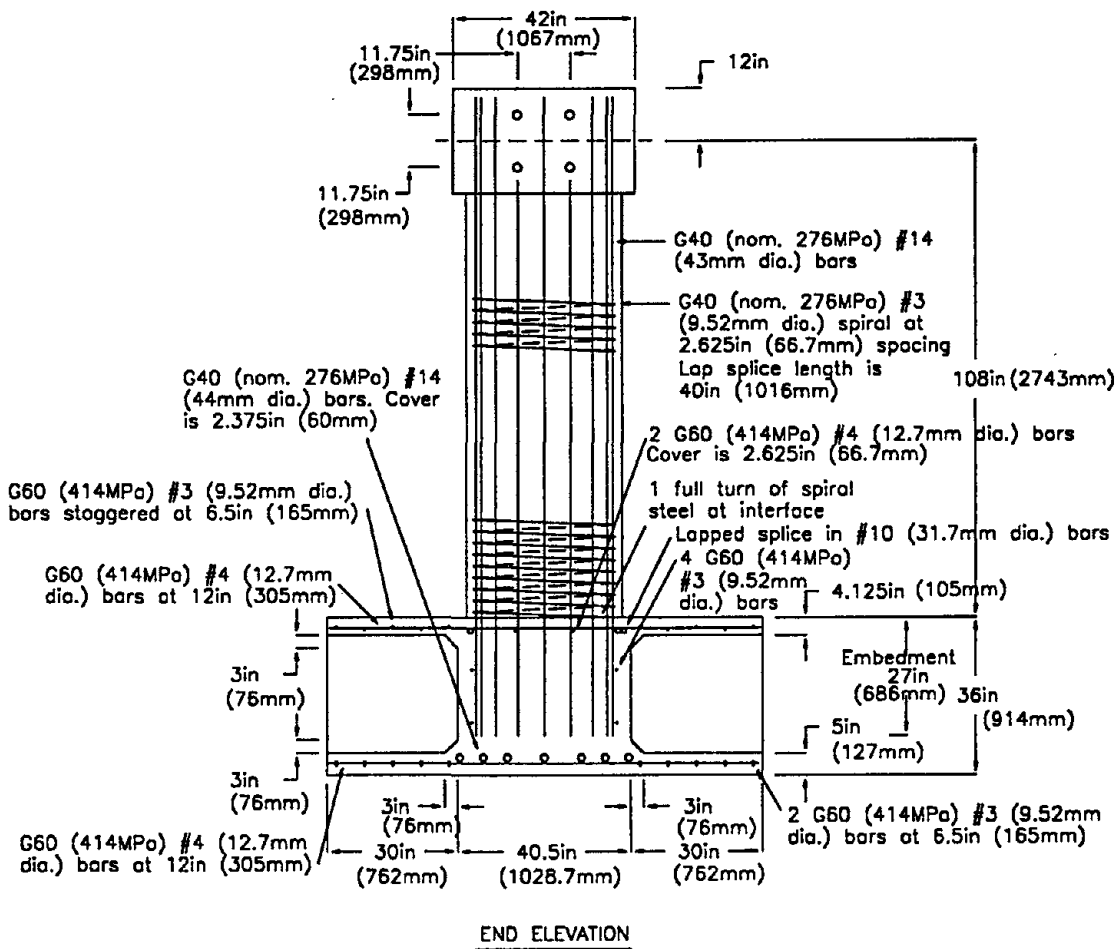Figure 9. Applied Lateral Force or Displacement Test Sequence

Section A-A

36in

1.5in (38mm) cover
to main bars

G40 (nom. 276MPa) #14
(43mm dia.) bars

G40 (nom. 276MPa) #3
(9.52mm dia.) spiral at
2.625in (66.7mm) spacing

Beam Stirrups

Beam Section B-B

42in
(1067mm)

11.75in
(298mm)

12in

11.75in
(298mm)

G40 (nom. 276MPa) #14
(43mm dia.) bars

G40 (nom. 276MPa) #3
(9.52mm dia.) spiral at
2.625in (66.7mm) spacing
Lap splice length is
40in (1016mm)

108in (2743mm)

G40 (nom. 276MPa) #14
(44mm dia.) bars. Cover
is 2.375in (60mm)

2 G60 (414MPa) #4 (12.7mm dia.) bars
Cover is 2.625in (66.7mm)

1 full turn of spiral
steel at interface

G60 (414MPa) #3 (9.52mm dia.)
bars staggered at 6.5in (165mm)

Lapped splice in #10 (31.7mm dia.) bars
4 G60 (414MPa)

G60 (414MPa) #4 (12.7mm
dia.) bars at 12in (305mm)

#3 (9.52mm
dia.) bars

4.125in (105mm)

3in
(76mm)

Embedment
27in
(686mm) 36in

5in
(127mm)

(914mm)

3in
(76mm)

3in
(76mm)

3in
(76mm)

2 G60 (414MPa) #3 (9.52mm
dia.) bars at 6.5in (165mm)

G60 (414MPa) #4 (12.7mm
dia.) bars at 12in (305mm)

30in
(762mm)

40.5in
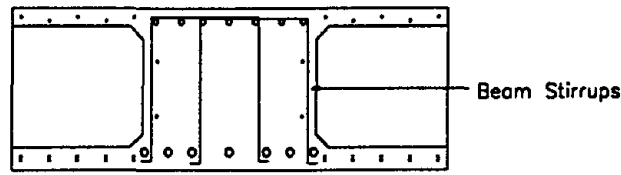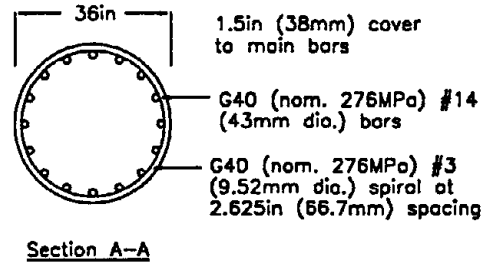(1028.7mm)

30in
(762mm)

END ELEVATION

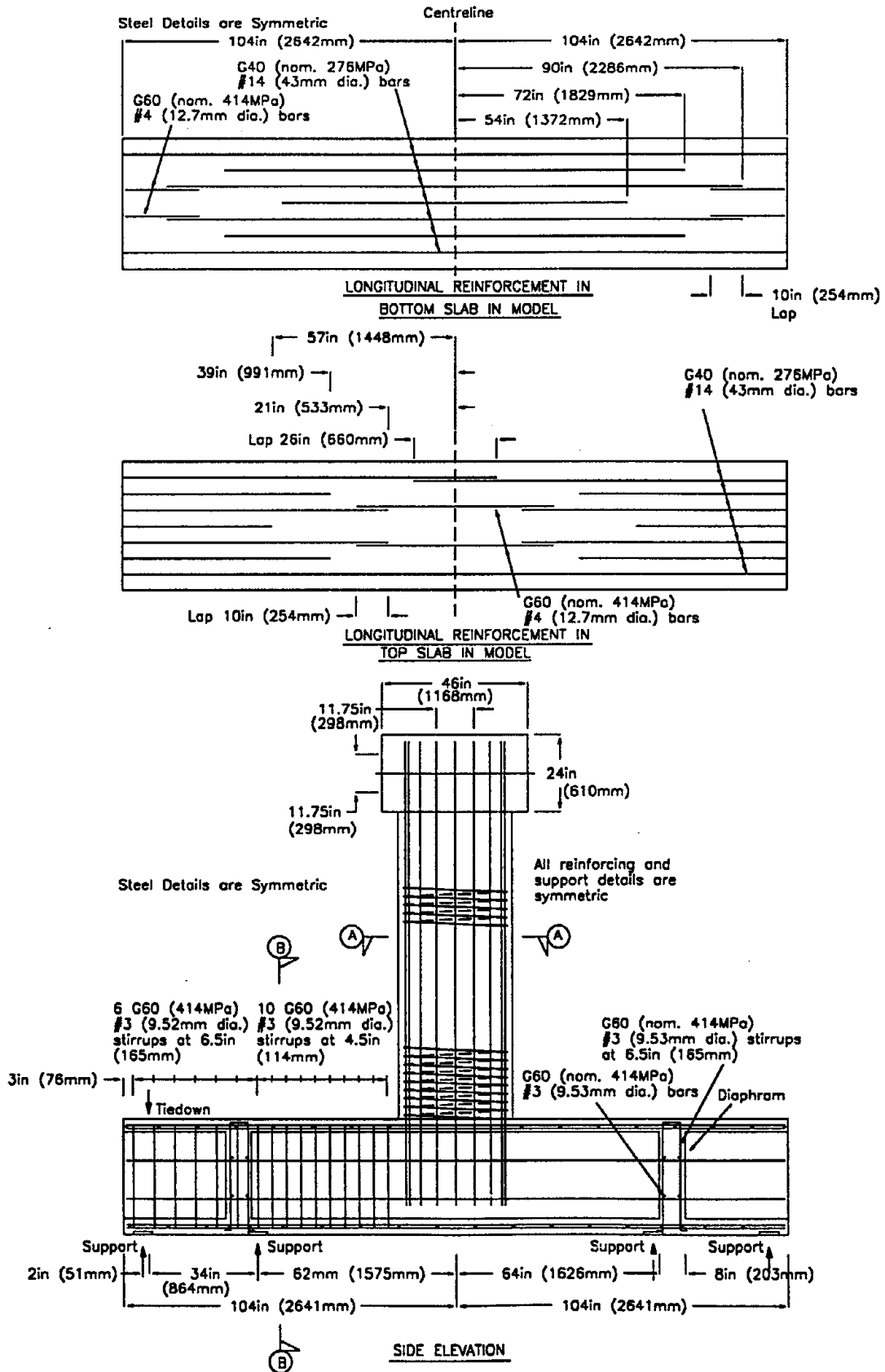Figure 10a. SM3 Reinforcement Details

181

Figure 10b. SM3 Reinforcement Details

The expected maximum axial load for the model was 240kips (1068kN) at the maximum displacement. However, in order to model the expected shear forces and moments of the prototype structure reasonably well, a lower axial load of 130kips (579kN) was applied in the test. This was equivalent to a nominal compressive stress of 127psi (0.88MPa) or $0.027f'_c$. The use of the lower axial load was not considered to significantly affect the behaviour of the beam-column joint. After cycles had been carried out under an axial load of 130kips (579kN), further cycles were sometimes carried out under an axial load of 240kips (1068kN) to see if this would cause further deterioration of the joint. At the end of the test, the axial load was increased to 360kips (1602kN) to see whether or not a punching shear failure of the column through the cap-beam and slab would occur. The ideal flexural strength of the column, $(M_i)_p$, was 21662in-kips (2448kNm) with an axial load of 130kips (579kN). This corresponded to an equivalent lateral shear force of $(V_i)_p$ = 201kips (894kNm).

Column cracking was observed during the cycles to 20kips (89kN) and the first joint shear crack as well as cracking of the top and bottom slabs were observed during the cycles to 80kips (356kN). During the cycles to increasing displacements, the joint shear cracks became more numerous and opened wider. The top slab was also seen to move relative to the column on the tension side of the column. Spalling of the cover concrete beside the joint was first seen during the cycles to a displacement ductility, μ, of 2. Cracks in the cap beam beside the road slab also became large. These joined up with the joint shear cracks. As the joint cover concrete spalled it could be seen that the column bars had bent toward the centre of the section during the cycling. The lap-splice of the beam bars in the soffit slab did not seem to have moved.

The subassemblage eventually suffered by a joint shear failure after cycles of repeated loading. Major strength degradation did not occur until after the first cycle to a drift ratio of about 2% or μ = 2.0 as shown in the hysteresis loop of Figure 11. The loop shapes
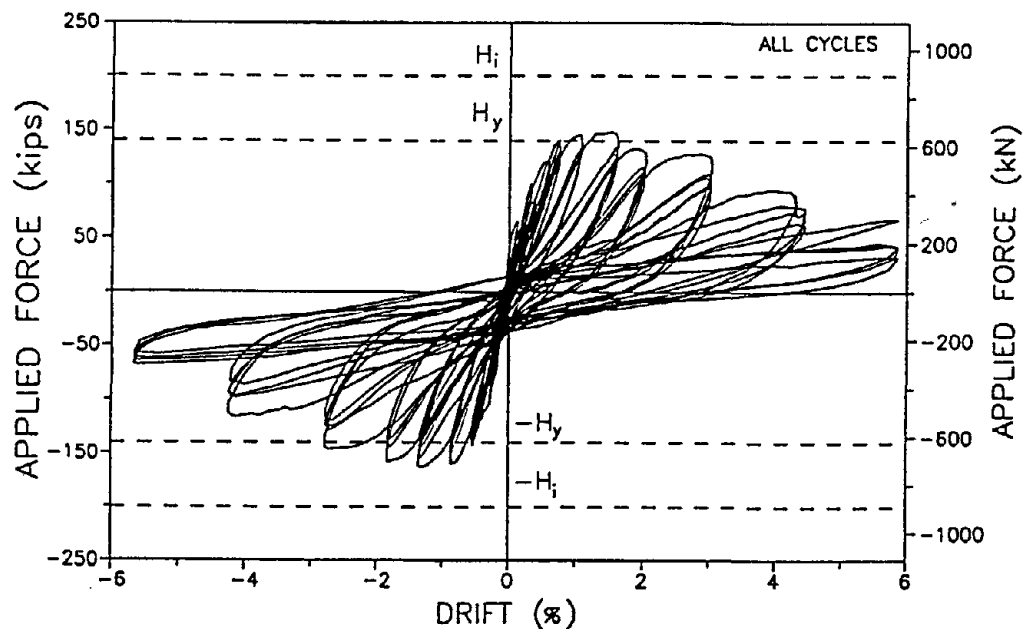

Figure 11. SM3 Hysteresis Curve Considering all Cycles of Loading

were severely pinched at moderate ductility levels as a result of cracking of the column and of the joint. The expected maximum strength of the column alone was 201kips (894kN), and the subassemblage maximum lateral force resistance was 163kips (725kN) in one direction and 148kips (659kN) in the other direction. Even when the axial load level was increased to 360kips (1602kN) no punch through of the column occurred. While the final strength was much less than the initial strength, the situation was significantly better than a pinned end.

The maximum joint shear strength was $3.05\sqrt{f'_c}$ (ksi) ($0.366\sqrt{f'_c}$ (MPa)). Further data analysis for this unit is being carried out and planning of the construction of a further unit to be loaded in the direction parallel to the cap-beam is underway.

CONCLUSIONS

Three test units representative of portions of the Santa Monica Viaduct have been tested at the University of California, San Diego. The major results are:

1) Both columns with lapped splices possessed at least 33% more strength in both directions than the expected demand of 68% of the ideal flexural strength. Retrofit of the splices tested here would therefore not be deemed unnecessary.

2) The method of Priestley [2] was shown to be suitably conservative in predicting the maximum strength of columns with lapped splices. A reason for this conservatism is that while no moment gradient was allowed for in the analytical approach, it was present in the experiment. Existing code equations were unrealistically conservative.

3) In the reversed cyclic loading test of the unreinforced cap-beam column connection, the subassemblage maximum lateral force resistance was 163kips (725kN) in one direction and 148kips (659kN) in the other direction. The theoretical maximum strength due to failure of the column alone was 201kips (894kN).

4) The cap-beam column connection suffered a joint shear failure. However the strength degradation was gradual with the cycles of repeated loading. The joint shear stress was = $3.05\sqrt{f'_c}$ (psi) = $0.254\sqrt{f'_c}$ (MPa).

5) Even under an axial load of 1.5 times the expected maximum column axial load a punching shear failure of the column through the deck did not occur.

6) If the full flexural strength at the base of a prototype column may be achieved the subassemblage may be expected to respond well. In the worst case, after a large amount of deformation is sustained the top connection would be effectively pinned.

ACKNOWLEDGMENTS

REFERENCES

1. Priestley M. J. Nigel, Allen Ely, Ronald F. Scott and Frieder Seible, "Seismic Safety Review of Santa Monica Viaduct Retrofit", *Report by the Seismic Safety Review Panel to the Caltrans Office of Structures Design*, Sacramento, California, January 1992.

2. Priestley M. J. Nigel, Seible Frieder and Chai Y. H., "Design Guidelines for Assessment, Retrofit and Repair of Bridges for Seismic Response", University of California, San Diego, *Structural Systems Research Report No. SSRP-92/01*, August 1992, pp120-129.

3. King D. J., Priestley M. J. N. and Park R., "Computer Program for Concrete Column Design", *Research Report No. 86/12*, Department of Civil Engineering, University of Canterbury, Christchurch, New Zealand, May 1986.

4. Mander J. B., Priestley M. J. N, and Park R., "Theoretical Stress-Strain Model for Confined Concrete", *Journal of the Structural Division*, ASCE, 114(8):1804-1826.

5. Priestley M. J. N., Seible F., Chai Y. H., Wong R., "Santa Monica Viaduct Retrofit - Full-Scale Test on Column Lap Splice with #11 [35mm] Reinforcement", University of California, San Diego, *Structural Systems Research Report No. SSRP - 92/08*, September 1992.

6. Priestley M. J. N., Seible F., MacRae G. A., Chai Y. H. and Wong R., "Santa Monica Viaduct Retrofit Full-Scale Test on Column Lap Splices with #18 [57mm] Reinforcement", *Report No. TR - 93/02*, Department of Applied Mechanics and Engineering Sciences, University of California, San Diego, January 1993.

7. Priestley M. J. N., Seible F., Chai Y. H. and MacRae G. A., "Santa Monica Viaduct Proof Tests", *Second Annual Caltrans Seismic Research Workshop*, Sacramento, 16-18 March 1993.

8. Priestley M. J. N., Seible F., MacRae G. A., Chai Y. H. and Wong R., "Santa Monica Viaduct Retrofit - Full-Scale Test on Column Lap-Splices with #11 [35mm] Reinforcement", *Third NSF Workshop on Bridge Engineering Research in Progress*, La Jolla, California, 16-17 November 1992.

9. ACI Committee 318, "Building Code Requirements for Reinforced Concrete (ACI 318-83)", *American Concrete Institute*, Detroit, Michigan, 1983.

10. ACI Committee 318, "Building Code Requirements for Reinforced Concrete (ACI 318-89)", *American Concrete Institute*, Detroit, Michigan, 1989.

11. ACI Committee 408, "Suggested Development, Splice and Standard Hook Provisions for Deformed Bars in Tension", *Concrete International*, Vol. 1, No. 7, July 1979, pp 45-56.

12. *MacRae G. A., Priestley M. J. N. and Seible F.*, "Santa Monica Viaduct Retrofit - Large Scale Column-Cap Beam Joint Transverse Test", Department of AMES, UCSD, Report No. TR-93/01, February 1994.

Seismic Reinforcement of Existing Reinforced Concrete Piers

K. Amari, H. Hanno, K. Ohtsuka and Y. Fujimoto
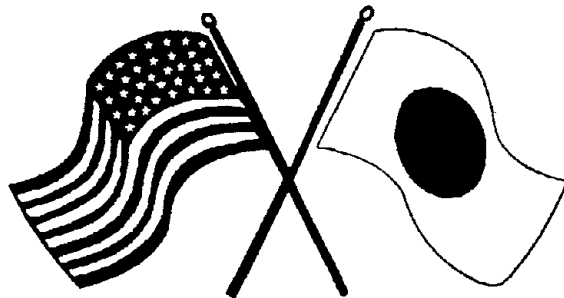
January 20 and 21, 1994
Berkeley Marina Marriott Hotel
Berkeley, California

SEISMIC REINFORCEMENT OF EXISTING REINFORCED CONCRETE PIERS

Kenichi Amari[*1],Hisamitsu Hanno [*2] , Keizo Otsuka[*3] and Yoshiichi Fujimoto[*4]

[*1] Manager, Maintenance Engineering Division, Maintenance and Facilities Department,
Metropolitan Expressway Public Corporation (MEPC)
1-4-1 Kasumigaseki Chiyoda-ku Tokyo Japan

[*2] Technical Chief, Maintenance Engineering Division, Maintenance and Facilities
Department,MEPC

[*3]Engineer,Engineering Management Division, Engineering Department, MEPC

[*4]Engineer,Road Structure Department, Paciffic Consultants Co.Ltd.
2-40-1 Kameido Koutou-ku Tokyo Japan

Abstract

This paper presents the results of various experiments made to study designs of reinforcement of existing reinforced concrete (RC) bridge piers for earthquake resistance, and describes methods of reinforcement.

The earthquake-resisting capacity of RC bridge piers has been discussed on various occasions and earthquake resistant requirements have been standardized by Specifications for Highway Bridges and other codes. However, some structures built in the past do not meet the current seismic design standards, and these structures have sometimes been damaged during earthquakes. For these reasons, experiments have been made to study on seismic designs, in particular to the region of main reinforcement cut-off and the bases of columns of existing RC bridge piers paying attention. As a result of these experiments, it has been decided to adopt steel plate jackets with epoxy resin, and the RC envelope method.

Introduction

Seismic design of structures is an important design check item in Japan where earthquakes occur frequently. Substructures, on which seismic loads act dominantly, are more important than superstructures. Therefore, seismic design methods are constantly being reconsidered. A new method of checking the ultimate load bearing capacity of RC structures during strong earthquakes was added to Specifications for Highway Bridges in 1990. However, existing RC bridge piers were designed based on the allowable stress design method and their safety with respect to their ultimate strength has not been checked. The region of main reinforcement cut-off of bridge piers were actually damaged during recent earthquakes. They provide evidence that many RC bridge piers have insufficient ultimate
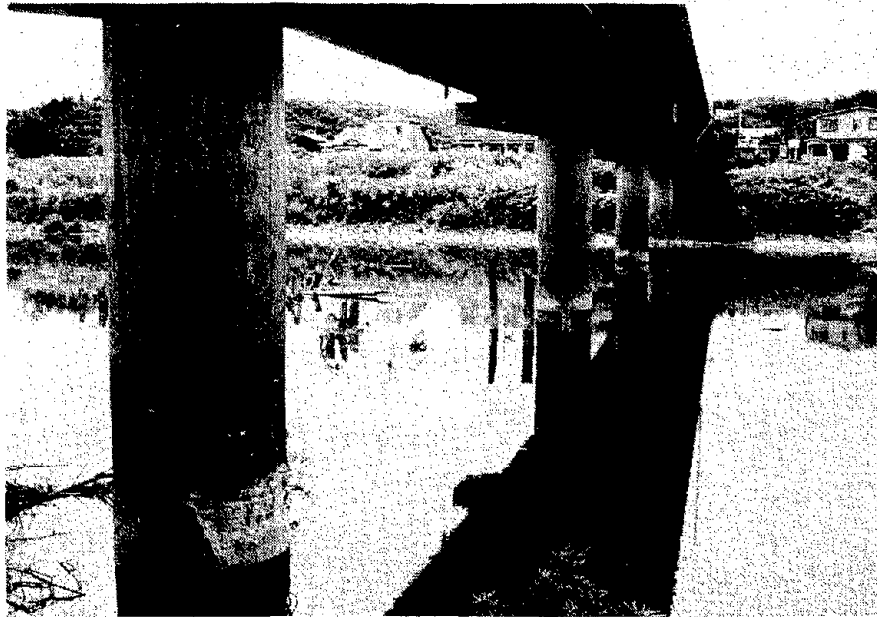
Photo-1 Damage of the Region of Reinforcement Cut-off

Check Earthquake Resistance

strength for earthquake resistance (Photo - 1). For these reasons, it is necessary to reinforce existing RC bridge piers to assure their safety during earthquakes.

For RC bridge piers, it is important to prevent brittle failures, such as the failure of concrete and the rupture of rebars, during earthquakes, although cracking of concrete and the yielding of steel members are allowable.

Earthquake-resisting capacity is checked here mainly to ensure the safety for their ultimate strength of the region of main reinforcement cut-off and the column base. Checking procedures are shown in Figure 1. Some bridge piers may be found to be defective in required earthquake-resisting capacity during the checking process. It was decided that they will be retrofitted as necessary.

Check of Anchorage Zone

During earthquakes in the past, main rebars of insufficient anchorage length and the lack of shear resisting force at the region of main reinforcement cut-off of columns were often noted in bridge piers designed based on the 1980 or earlier versions of Specifications for Highway Bridges (see Table 1). Shear failure can occur at the region of main reinforcement cut-off and this is one of the important items to check when reviewing the earthquake-resisting capacity.

Check of anchorage zones was mainly conducted for single piers or rigid-frame piers of rectangular or circular sections), having shear span ratios (h/D) more than 2 and side ratios (b/a) less than 1.4, located on comparatively poor foundation soils. The scope of work included checking of ultimate strength (safety factor of 1.2 or more) of rebars at the region of main reinforcement cut-off during earthquakes and the average shearing stress of concrete. [1]

190
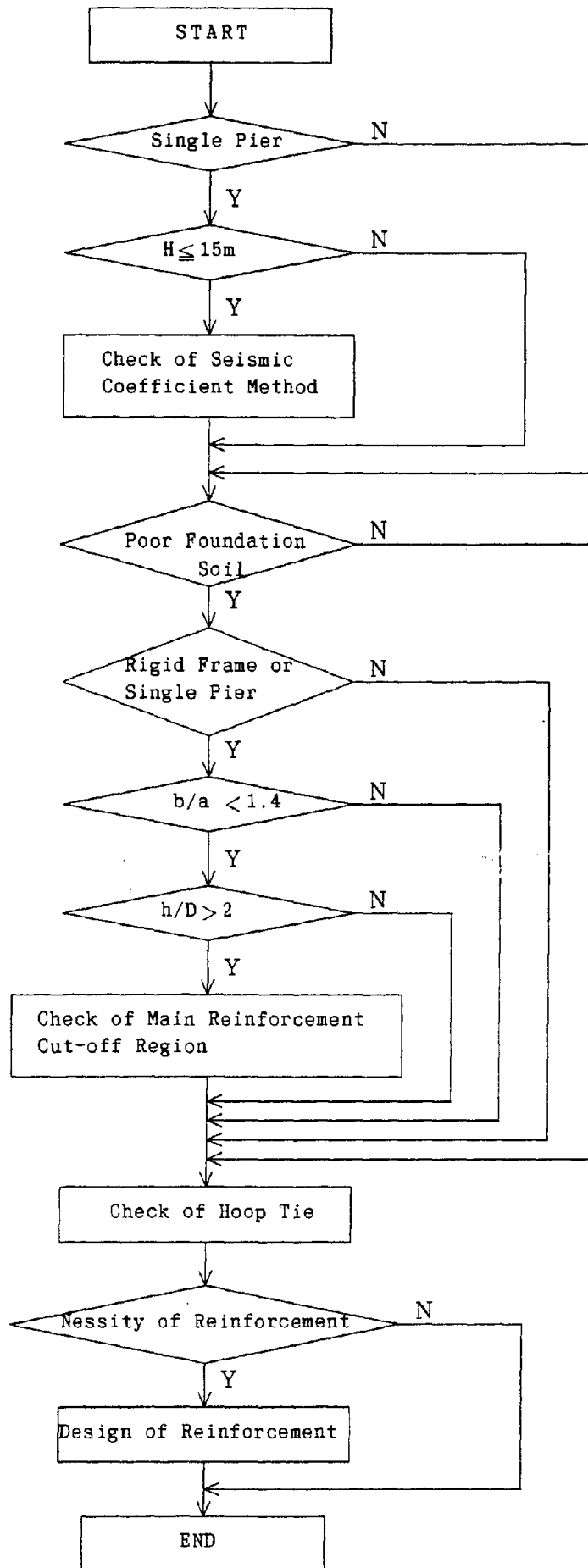
Fig.1 Flow Chart of the Check

START

Single Pier — N

H ≤ 15m — N

Check of Seismic
Coefficient Method

Poor Foundation
Soil — N

Rigid Frame or
Single Pier — N

b/a < 1.4 — N

h/D > 2 — N

Check of Main Reinforcement
Cut-off Region

Check of Hoop Tie

Nessity of Reinforcement — N

Design of Reinforcement

END

Table 1 Change of Design Method at the Region of Reinforcemnt Cut-off

	Prior to 1980	1980 and After
Anchorage length	·Provide either the length calculated by the following equation or at least 20ϕ from the point where reinforcing bar is not required by analysis : $$1 = \frac{\sigma sa}{4\tau cb}\,\phi$$ Where, σsa : Allowable tensile stress of reinforcing bar τcb : Allowable bond stress of concrete ϕ : diameter of reinforcing bar	·Length obtained by the left colum method ·Length where the tensile stress of the reinforcing bar becomes less than one-half of the allowable stress ·Length where share stress τ satisties the following equation : $$\tau < 2/3\tau a$$ Use the greatest length of the above for anchorage length

Allowable Share Stress of Concrete	Compressive Strength of Concrete σck(kgf/cm2)	$180<$ $\sigma ck<200$	$200<$ $\sigma ck<240$	$\sigma ck>240$	Compressive Strength of Concrete σck	210	240	270
	τa (kgf/cm2)	6	6.5	7	τa	3.6	3.9	4.2

Check of Column Base

In the 1990 Specifications for Highway Bridges, ultimate lateral strength method[2] was added. That method checks horizontal load bearing resistance to earthquake forces to determine the ultimate strength, taking into account the deformation capacity of RC bridge piers. This checking is applied here to existing RC bridge piers designed by the allowable stress design method to study the ultimate strength of the entire bridge pier. The procedure for checking ultimate lateral strength method is shown in Figure 2.
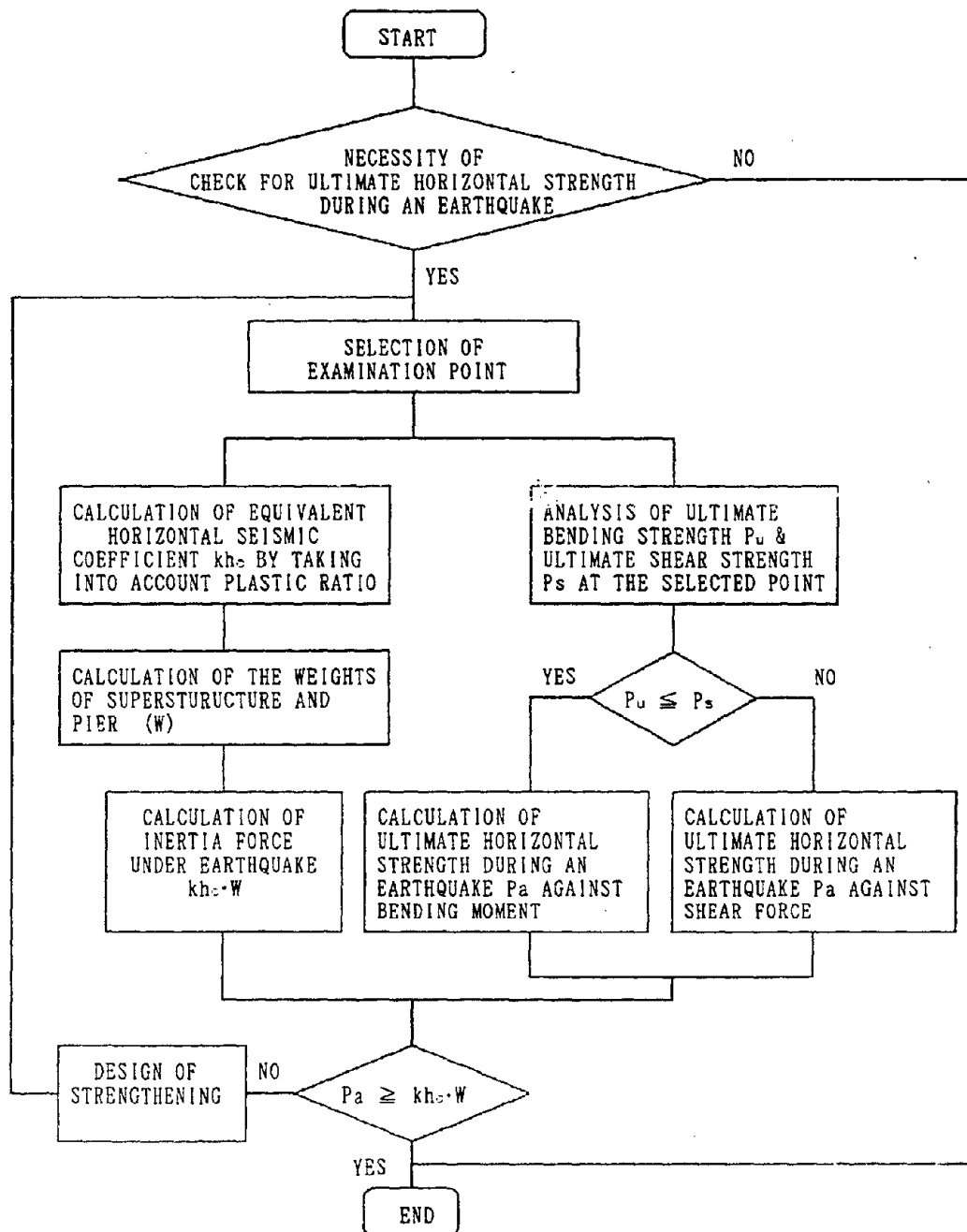

Fig.2 Check Flow of Ultimate lateral strength Method

Check of Volume of Hoop Ties

Some existing bridge piers have column base reinforcement with a small hoop tie ratio, 0.15% or less. These bridge piers are estimated to have basically small resistance against shear force and poor earthquake-resisting capacity, based on experience from past earthquakes. Therefore, it was decided to check the volume of hoop ties for all bridge piers, as one factor to determine the need for seismic retrofit.

Experiments Related to Seismic Retrofit

Objectives of Experiments

Experimental studies have previously been made on the region of main reinforcement cut-off.[3] Therefore, experiments were conducted on the seismic retrofit of column bases. Items of experiment are as described below.

Experiments on Flexural Retrofit   For flexural retrofit of RC members, both the RC envelope and the steel plate jacket/epoxy resin methods have been used. Experiments have already verified the static strength provided by these methods. However, the dynamic strength and resistance to deformation of these methods when they are applied to column bases have not been verified by experiments. Therefore, these experiments were made to verify the dynamic strength and deformation characteristics of two methods for the purpose of applying the methods to the design of retrofit.

Experiments on Shear Retrofit   Bridge piers that are judged to be in danger of shear failure while ultimate horizontal strength is being checked are generally deficient in hoop ties. But ultimate strength is checked only for the cross sections where flexural strength is minimum, but the sections with high flexural resistance but with little shearing strength, as seen in existing bridge piers, cannot be checked.

For these reasons, an experiment was made to determine the extent of shear retrofit for such cases.

Experiments on Joints between Two Methods   In areas where aboveground and underground portions are retrofitted continuously, the steel plate jacket method and the RC envelope method are used in combination, taking into consideration the appearance. In particular, when two methods are used for flexural retrofit it is necessary to assure the continuity of both methods. Therefore, it was decided to use stud bolts for steel plates as the

joint between two methods. The experiment was made to assure continuity, and to verify their effectiveness.

Experiment Methods

Experiments were all made by the displacement control method, repeatedly applying one static load and 10 dynamic loads. Methods of applying loads are shown in Table 2.

Table 2 Methods of applying loads

Load Level	Concrete Crack	Reinforcing Bar Yield	II	III	IV	V
Displacement	δc	δy	$2 \delta y$	$3 \delta y$	$4 \delta y$	$5 \delta y$
Static Load	○	○	○	○	○	○
Dynamic Load	—	○	○	○	○	○

Loads were statically applied at the loading level I, until it was estimated that the rebars yielded. Measured displacement and loads were defined to be elastic limit displacement δ_y and yield load P_y. At further loading levels, alternate loads were dynamically applied 10 times each by deformation control to achieve a deformation of integral times in reference to δ_y. The point where the resistance fell significantly below P_y during load application was defined to be failure. Loading equipment is shown in Figure 3.
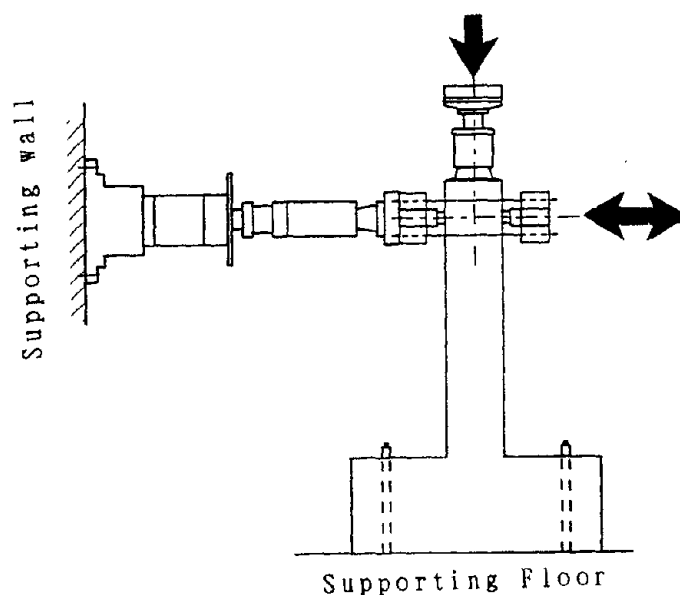

Fig.3 Loading equipment

Experiment Details of experiment and description of specimens are shown in Table 3 and Figure 4. Specimens No. 2 and No. 3 were mainly used for cases when retrofit steel was anchored in footings, and one specimen was used for the RC envelope method and one for the steel plate jacket method. Specimens No. 4 and No. 5 were mainly used for cases when the retrofit steel was not anchored. For specimen No. 5 is expected to improve deformation because of the confining effects of the steel plate.

Specimens were made as large as practicably possible, taking into account the shape effects and the capacity of the loading equipment. Actual structures have rectangular, circular and hollow sections, but a rectangular section was used in this experiment because this shape had been used quite often for repeated loading tests in the past. Lateral confining effect of the retrofit materials is smaller than for circular sections. This was another reason for using the rectangular sections.

Retrofit cross section is larger than actual, compared with the section of reference specimen, but a 6 cm thickness is considered to be the minimum for the RC envelope method if the possibility of construction is considered. For the steel plate method, 6 mm plate is considered to be minimum thickness for the same reason.

A working axial force of 20 kgf/cm^2 was used, taking into account the previous experiments and the dead loads acting on the rectangular column bases of existing bridge piers .

Table 3 Model Test Cases

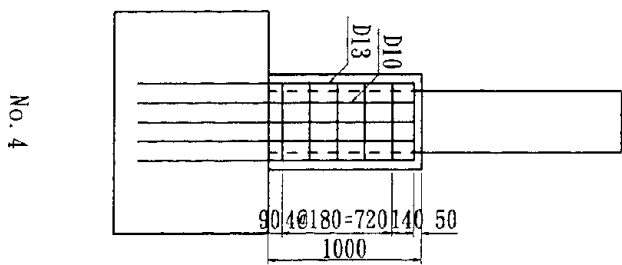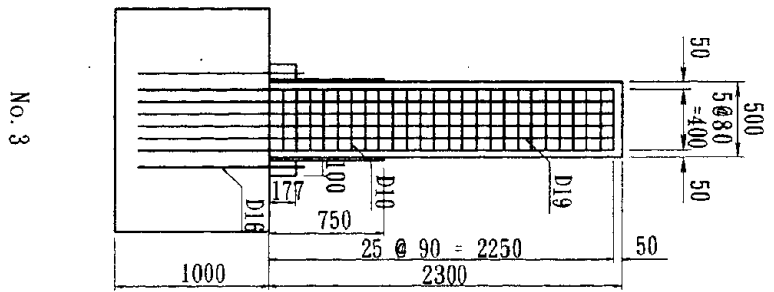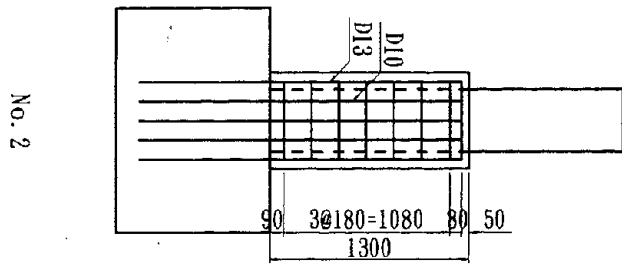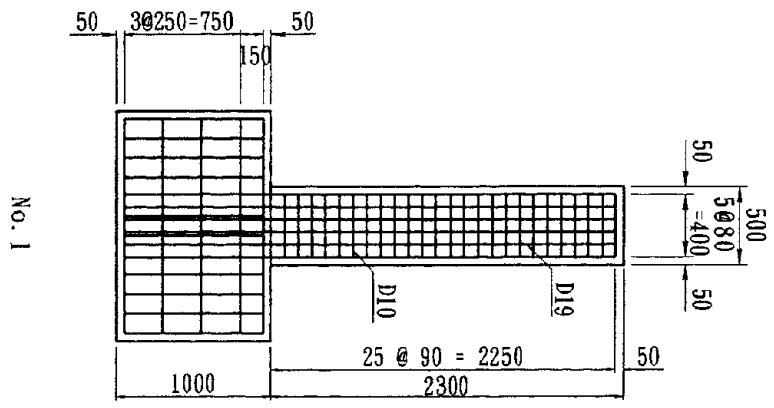| No.	Dimension of Test Model (cm)		Ratio of Span Length to Cross Section	Axial Force (kgf/cm2)	Remark
	Original	After Reinforcing			
1	50 x 50	——	4	20.0	Standard case for reiforcing
2	"	62 x 62	"	"	RC lining reinforcing (with anchorage)
3	"	t = 6 mm	"	"	Steel plate reinforcing (with anchorage)
4	"	62 x 62	"	"	RC lining reinforcing (without anchorage)
5	"	t = 6 mm	"	"	Steel plate reinforcing (without anchorage
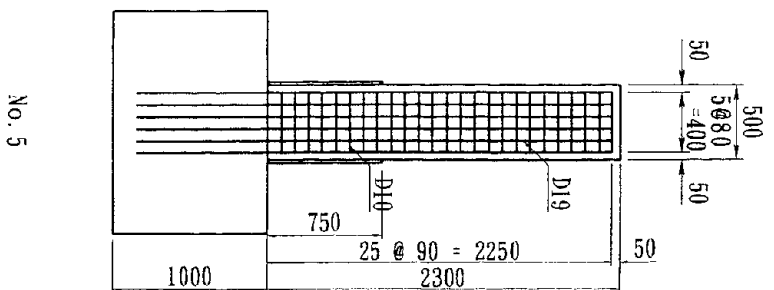
Fig.4 The Shape of Specimens

197

Results of Experiments The results of experiments are shown in Table 4. Load-displacement envelope curves of all specimens are shown in Figure 5.

Failure Modes Cracks occurring at times of failure are shown in Figure 6. Cracks occurred in all specimens first in the form of flexural cracks in a horizontal direction and later in the form of shear cracks in diagonal directions. However, the shear cracks did not continue to develop as the flexural cracks developed further.

For the reference specimen, concrete cover started to fall off and hoop ties were loosened when failure occurred, and bars were compressed and buckled, loosing their compressive strength. Conversely for specimens No. 2 and No. 4, retrofitted by RC envelope method, hoop ties were proper even after concrete cover fell off, but bearing strength decreased as main rebars fractured.

On specimen No. 4, at the time of failure cracks were found along cold joints of concrete placed over existing concrete in longitudinal directions. It can be assumed that these cracks occurred because the additional concrete cover was not anchored to the footing by rebars and the bonding of the concrete layers was not able to resist.

Table 4 The Results of Experiments

| Model No.	Yield Load (tf)	Maximum Load (tf)		Yield Displacement δy (mm)		Displacement Under Maximum Load (mm)		Maximum Displacement δu (mm)	Toughness Index $\delta u/\delta y$
		Measured Value	Calculated Value	Measured Value	Calculated Value	Measured Value	Calculated Value		
1	20.1	25.9	27.4	11.9	9.38	35.7	16.41	47.6	4
2	32.1	40.5	42.0	9.7	6.54	17.5	13.24	56.0	5.8
3	36.0	50.4	48.6	10.6	7.15	35.5	15.63	73.8	7
4	31.8	35.1	33.4	15.2	7.66	30.4	13.53	75.3	5
5	25.6	31.6	27.9	13.2	9.17	28.4	16.25	78.9	6
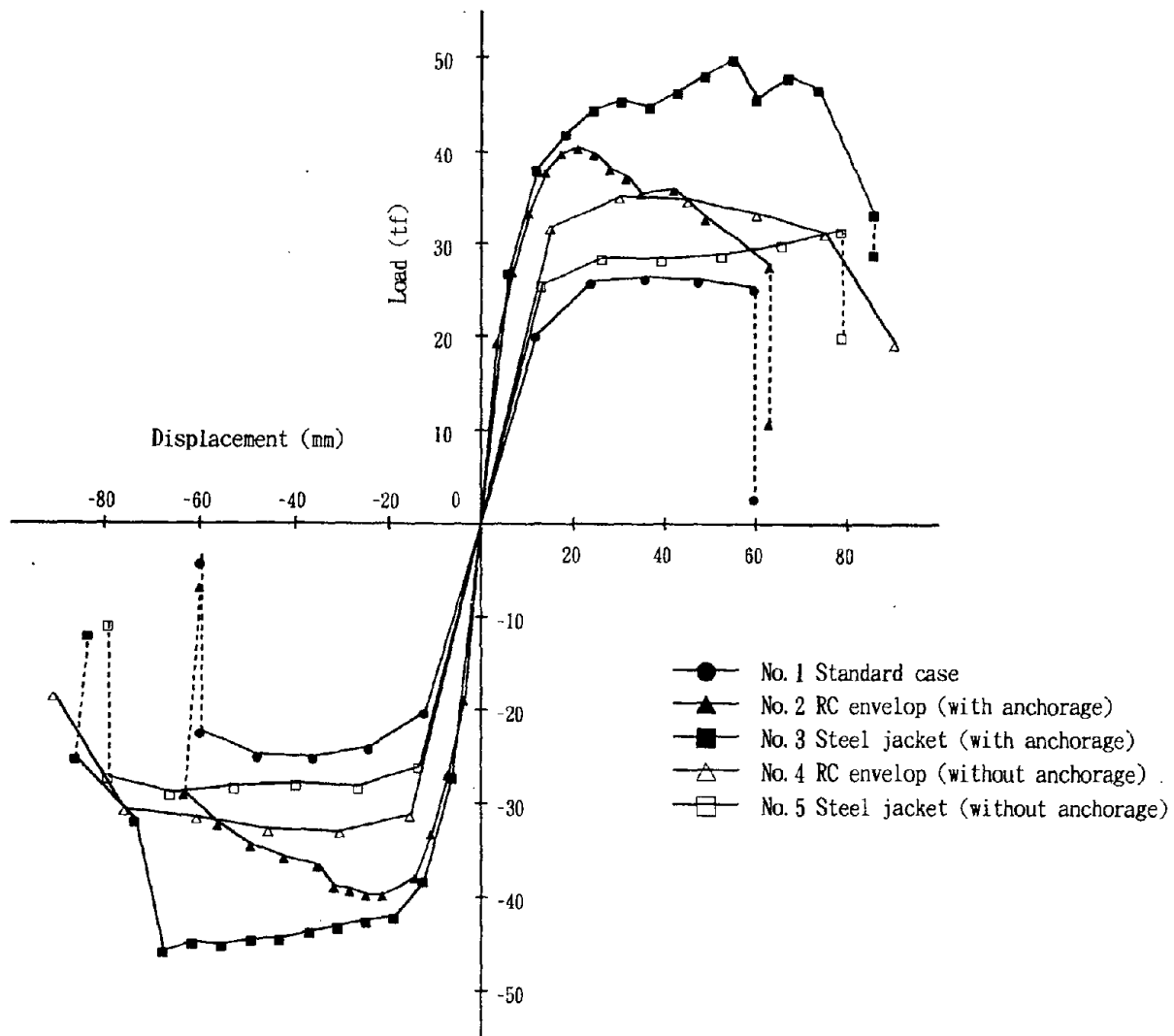
Fig.5 Load-Displacement Envelope Curves
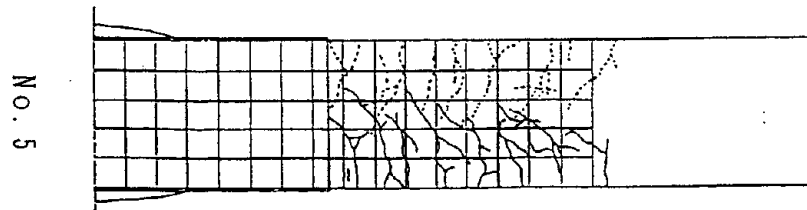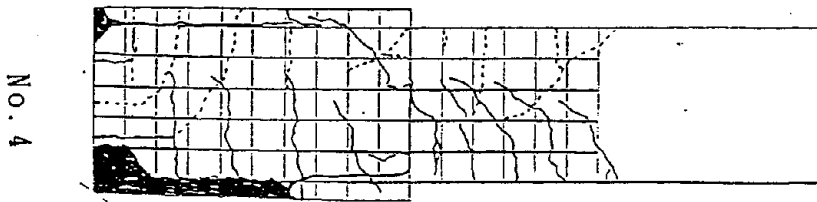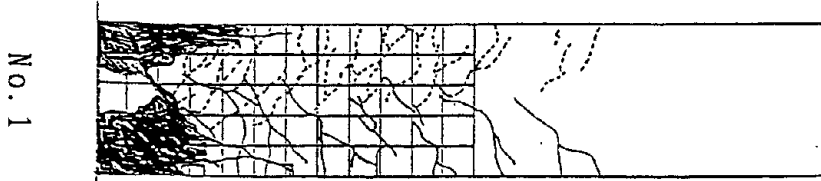
Figure 6. Cracks in the Failure

No. 1 No. 2 No. 3 No. 4 No. 5
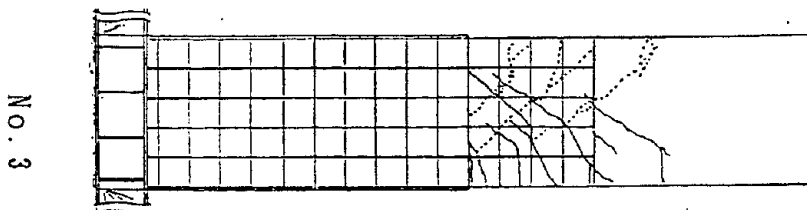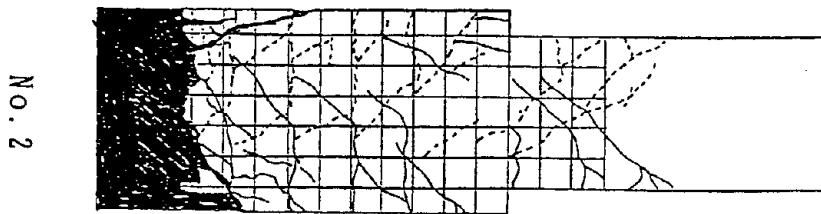
200

Ultimate Strength Values obtained by experiments closely match the calculated values of elastic properties, as shown in Table 4. It can be seen from this table that the dynamic strength of the retrofitted specimens can also be estimated, as well as the static strength. For specimens No. 3, 4, 5, the values obtained by the experiments were larger than values obtained by calculations when compared with specimens No. 1 and No. 2. It can be presumed that this was effected by the increased confining force in horizontal directions.

Energy Absorption Capacity Energy absorption capacity is larger for retrofitted specimens than for reference specimens. However, for specimen No. 3, the equivalent damping factor was smaller than others, as shown in Figure 7. This can be because the horizontal movement of column base under load was larger for specimen No. 3.

Fig.7 Equivalent Damping Factor

Extracted Length of Rebar   Measurements were made for stresses in rebars in the footing of specimen No. 1 to identify the length of rebars extracted. The results are tabulated in Figure 8 and Table 5.
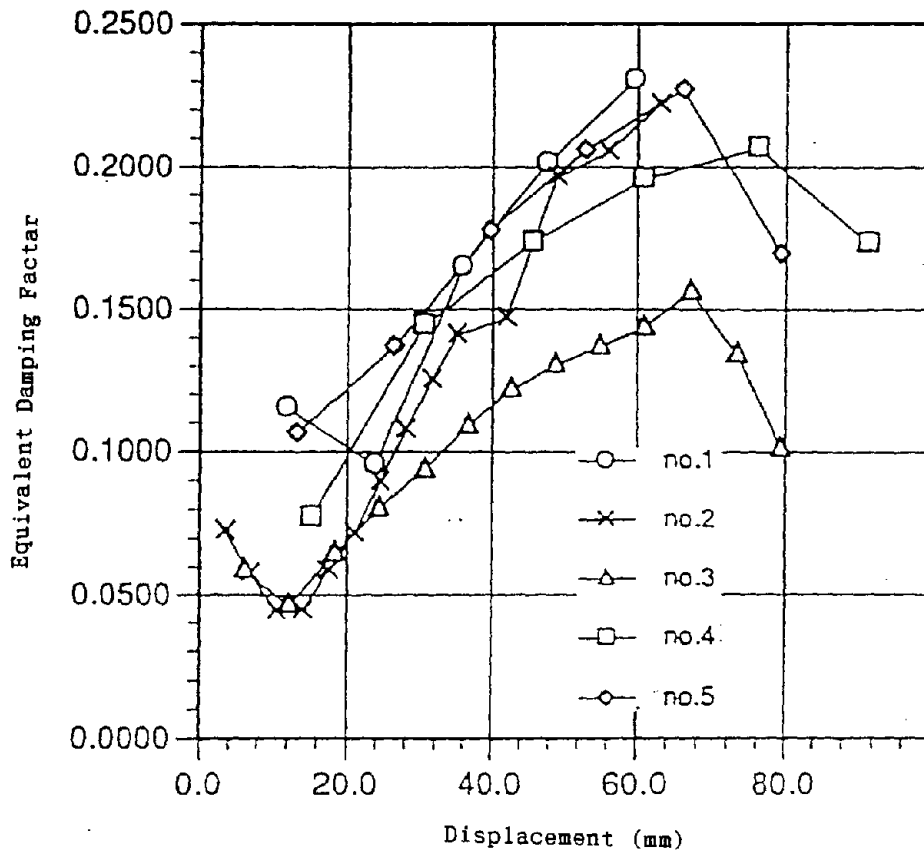
It can be seen that stresses in rebars are distributed nearly in a straight line until rebars yielded. It can be seen, conversely, that the ultimate stress in rebars in concrete did not change very much after they yielded, but strains measured at the interface between the column and footing exceeded 18,000 μ.

Reasons for differences in ultimate extracted length of rebars obtained from experiment and that obtained by simple formula, shown in Table 5, possibly because strains distributed from the interface to the measuring point 15 cm below the interface were assumed as a straight line slope to obtain the extracted length of rebars.

Table 5 Extracted Length of Rebar

Measured Value (cm)		Calculated Value* (cm)	
Yield	Failure	Yield	Failure
0.055	0.128	0.050	0.063

* Yield $\quad \triangle ly = 0.070 - 0.0054 \ (D \diagup \phi) + 0.00017 \ (D \diagup \phi)^2$

  Failure $\quad \triangle lu = 0.083 - 0.0054 \ (D \diagup \phi) + 0.00015 \ (D \diagup \phi)^2$

D :Distance between Reinforcing Bars

ϕ :Diameter of Reinforcing Bars
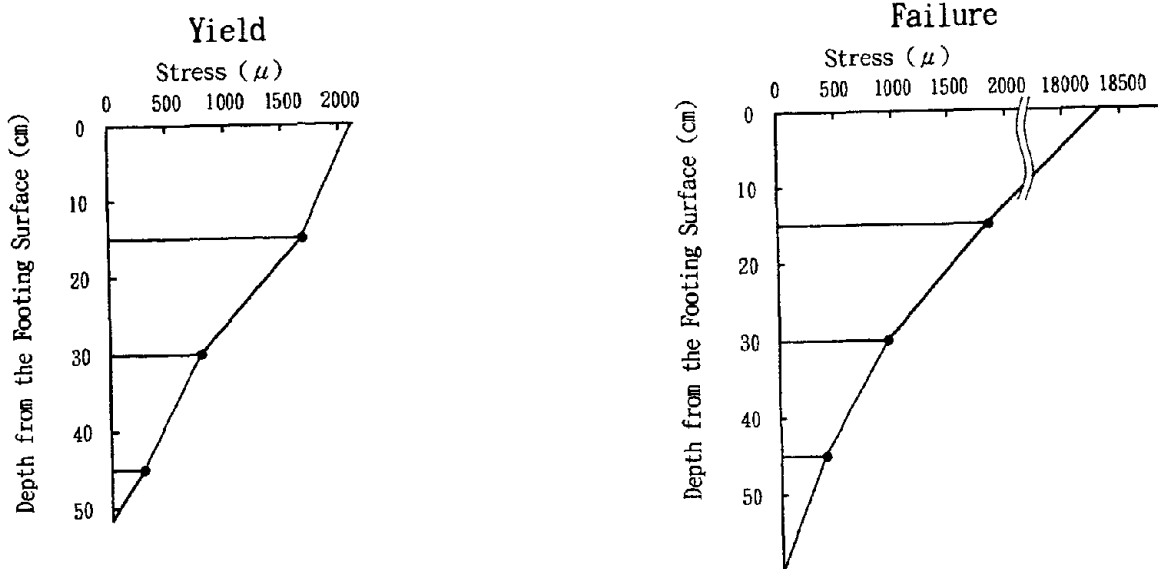
Fig.8 Rebar Stress in the Footing

Experiments on Shear Retrofit

Description of Experiments Experiments are tabulated in Table 6 and details of specimens are shown in Figure 9.

Shear span ratio of specimens was determined to be 3.0, so that specimens would easily fail by shearing. The volume of hoop ties for reference specimens was set to be 0.13%, since the volume of hoop ties for existing concrete bridge piers presumed to have failed by shearing was 0.15%.

Specimens No. 2 and No. 3 were made from reference specimens retrofitted within the range of 1D and 1.5D (D = column width of specimen).

Table 6 Model Test Cases

No	Cross Section	Share Span Ratio	Axial Force (kgf/cm^2)	Remark
1	50×50	3	20.0	
2	62×62	3	20.0	Retrofitted Length;1D
3	62×62	3	20.0	Retrofitted Length;1.5D

No.1   No.2   No.3
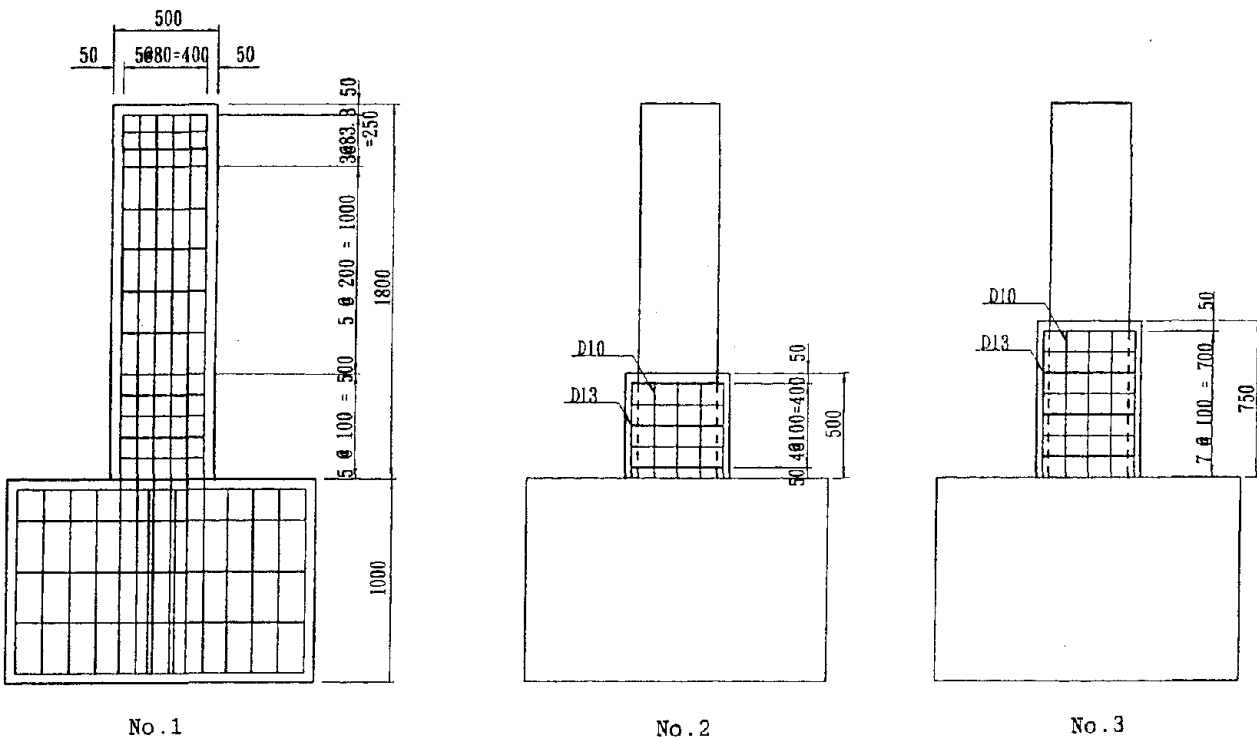
Fig 9 The Shape of Specimens

Results of Experiments

Failure Mode The failure modes for all specimens are shown in Figure 10. It can be seen from this figure that diagonal cracks occurred extensively in the center areas of columns for all specimens, and that bearing strength decreased by shear failure.

The failure zone moved upward as the area of retrofit increased. The figure shows that shear retrofit was effective, but the strength was insufficient for the shear forces acting on unreinforcing areas.

No.1   No.2   No.3
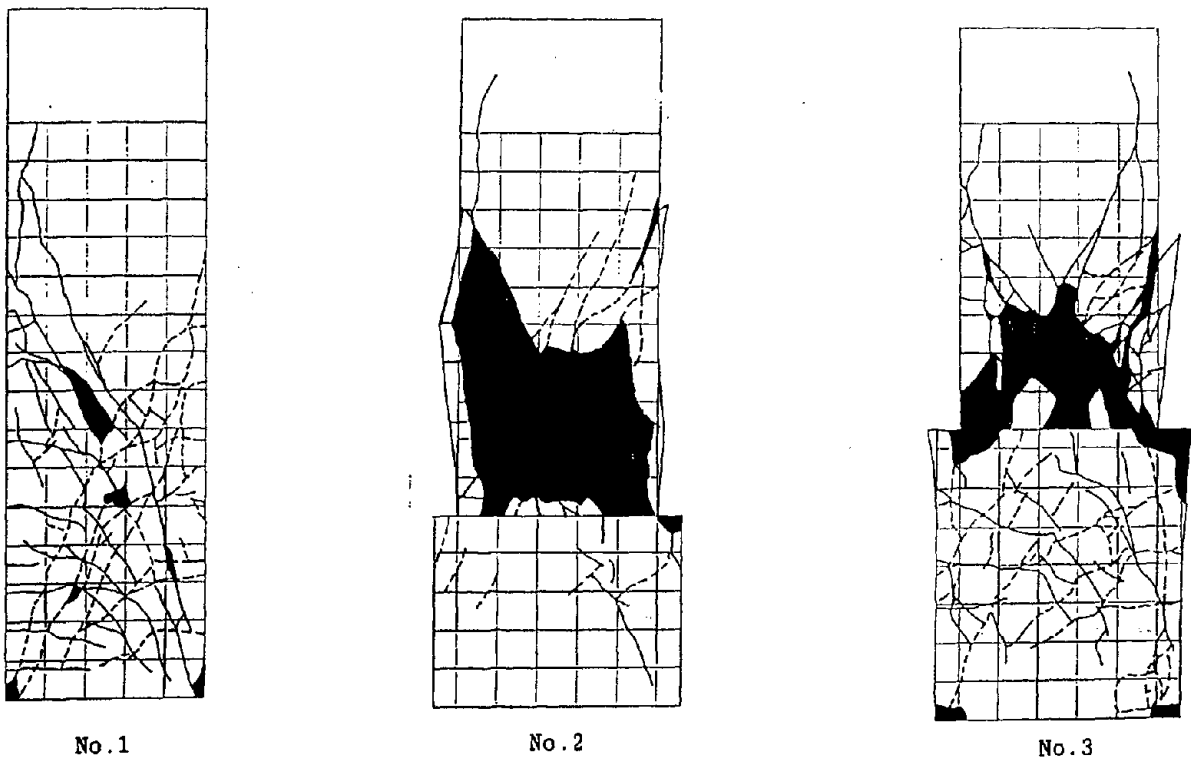
Fig.10 The Failure Modes

204

Ultimate Strength Load–displacement envelope curves are shown in Figure 11. It can be seen from the figure that heavily retrofitted specimen No. 3 failed at $6\delta_y$ and that a toughness nearly equal to bending failure has been secured. However, failure occurred in the form of shear failure, as described in subparagraph a. above.

Specimens No. 1 and No. 2 failed at 2δ and 3δ. It can be seen that these failed without toughness in the form of shear failure.

The ultimate strength nearly agreed with that obtained if the unreinforced areas are assumed to act as a corbel. It is presumed that this means that the ultimate strength after retrofit is obtained from the strength for shear of unreinforced area or flexural strength of the column base, whichever is smaller, because specimens retrofitted for shearing force have a sufficient strength.
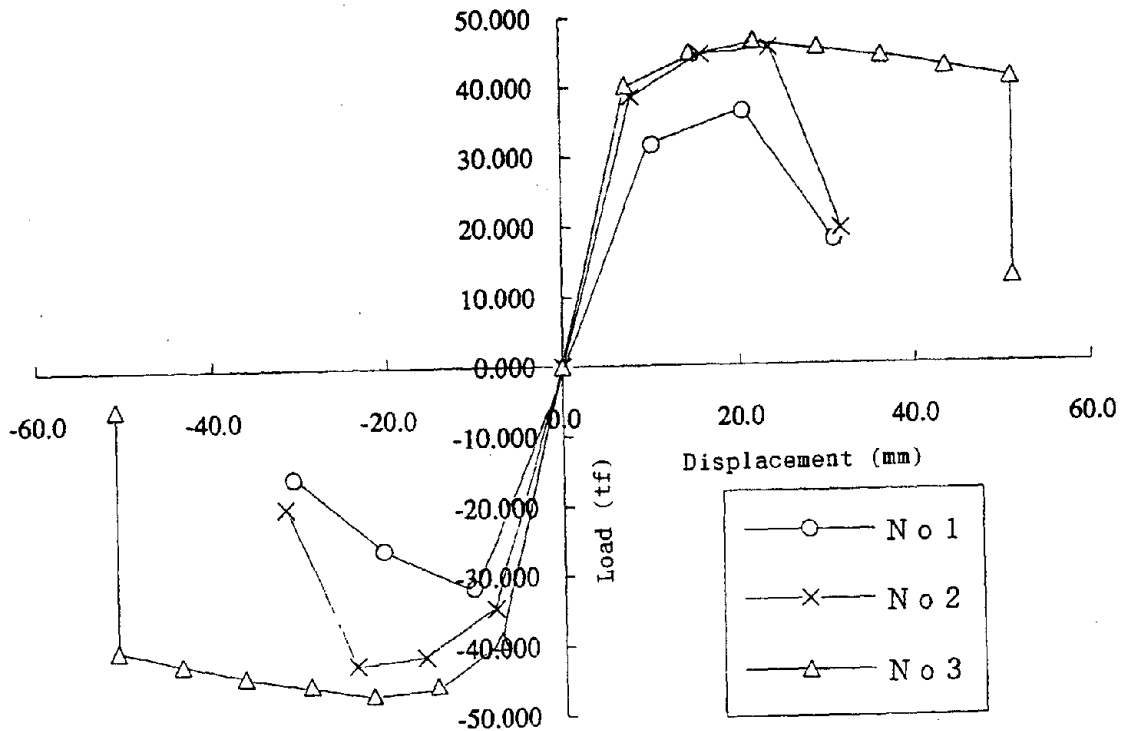
Fig. 11 Load–Displacement Envelope Curves

Description of Experiments   Experiments are tabulated in Table 7. The details of specimens are shown in Figure 12. Specimen No. 1 was made with a combination of a concrete envelope and a steel envelope, and joint materials such as stud bolts were not used. For specimen No. 2, stud bolts in the minimum number required by the yield strength of stud bolts were used. Conversely, for specimen No. 3 stud bolts were used at a rate 1.5 times that used for specimen No. 2.

Table 7 Model Test Cases

No	Cross Section	Share Span Ratio	Axial Force (kgf/cm²)	Remark
1	50 × 50	4	20.0	
2	62 × 62	4	20.0	Stud Bolts 2Lines
3	62 × 62	4	20.0	Stud Bolts 3Lines

No.1   No.2   No.3

Fig.12 The Shape of Specimens

Results of Experiments

Failure Mode   Cracks occurring at the time of failure are shown in Figure 13.Regarding specimen No. 1, cracks started to occur at the top corners of the RC envelope immediately after loads were applied, and spaces opened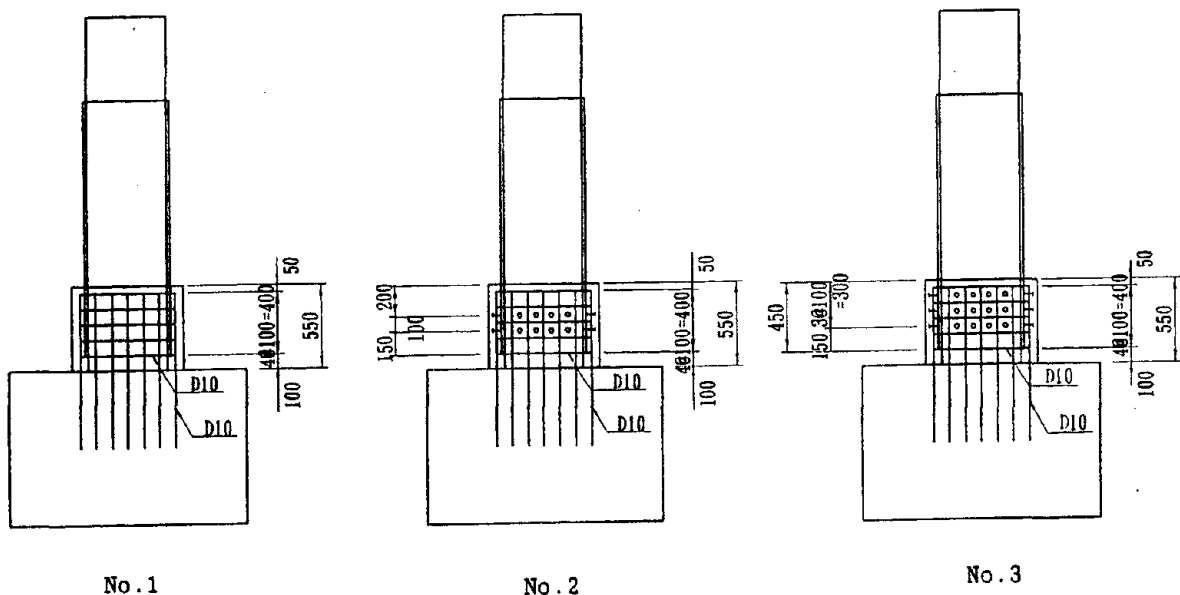 up between RC envelope and steel plate inside. Cracks became widespread according to the deflection increased. Failure occurred at the bottom of the inside steel plate.

For specimens No. 2 and No. 3, cracks first occurred in the RC envelope areas where stud bolts were installed and they developed over the entire area of the RC envelope. Progressive failure occurred with the concrete cover first falling off, then the rebars failed .

All the specimens failed by flexure.

Ultimate Strength   Load–displacement envelope curves are shown in Figure 14.
Specimen No. 1 failed at $7\delta_y$ but its maximum load did not reach the required level. This is because the resistance became smallest at the bottom of steel plate as the RC envelope and the steel envelope were not firmly integrated.

Significant differences were not noted for specimens No. 2 and No. 3 and they showed nearly equal toughness and load capacity.

Fig.14 Load–Displacement Envelope Curves

207
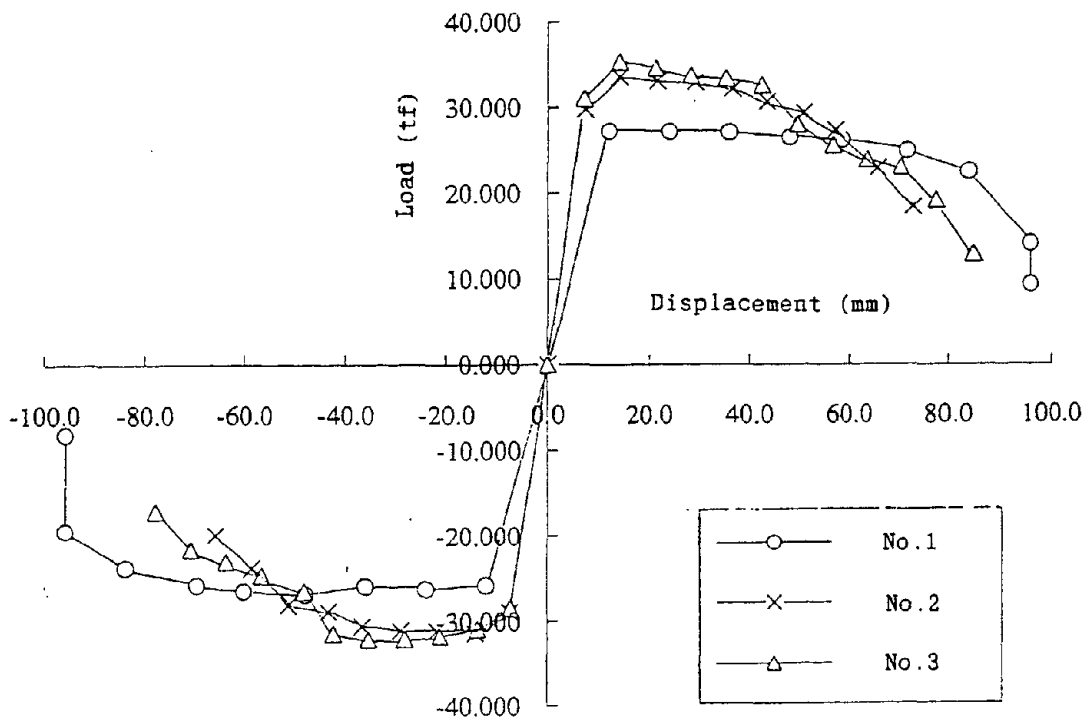
Table 8 The Results of Tests

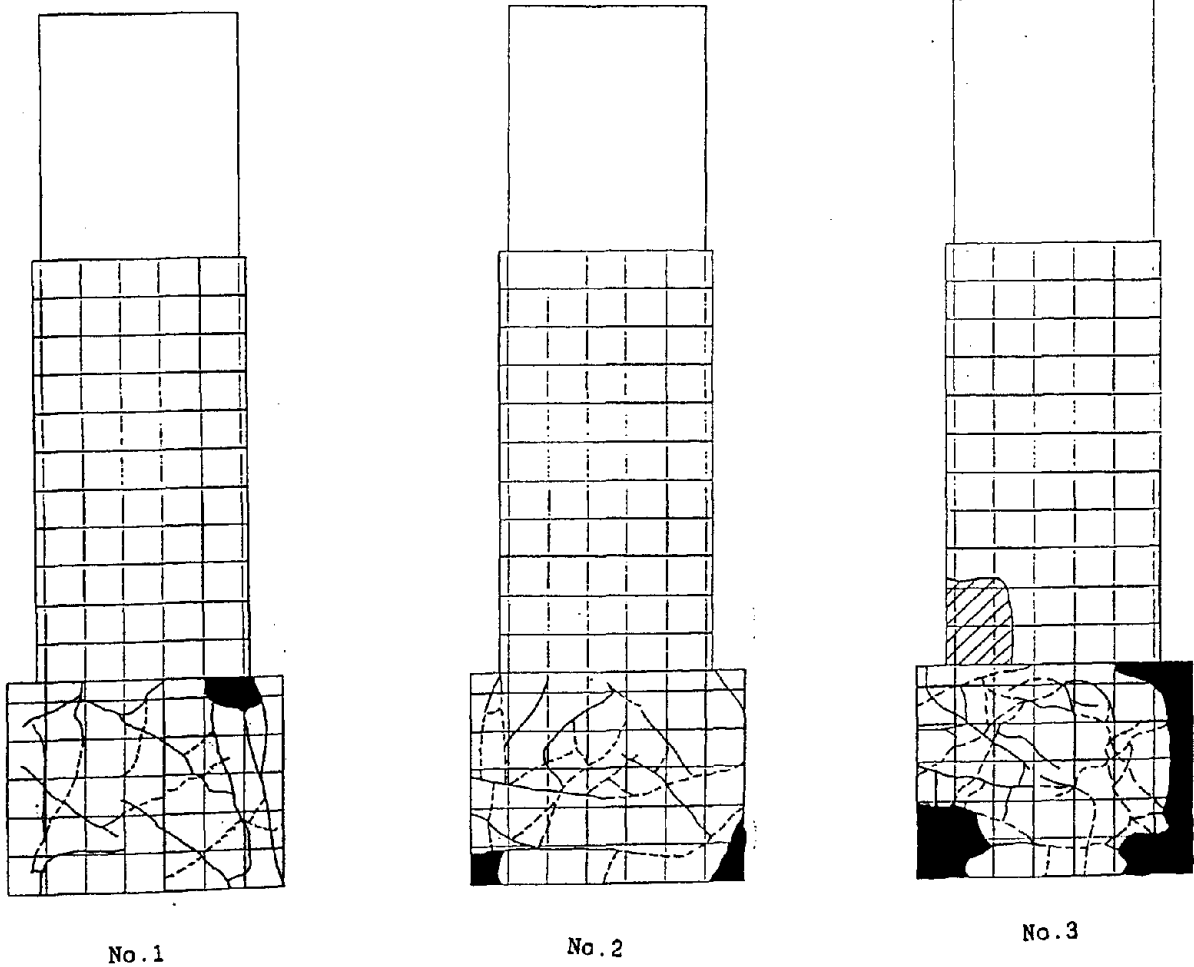| No.	Yield Load(tf)		Failure Load(tf)	
	Measured	Calculated	Measured	Calculated
1	27.2	29.3	27.2	31.4
2	29.7	29.3	33.1	31.4
3	31.1	29.3	35.4	31.4

No.1   No.2   No.3

Fig.13 The Failure Modes

Conclusions

From the results of experiments on column bases of RC bridge piers, it has been decided to adopt the steel jacket method using epoxy resin and the RC envelope method as methods of retrofit. The steel jacket method can be used effectively in urban areas where space is very limited. On the other hand, the RC envelope method can be easily constructed and is effective for underground column bases. It has also been verified that flexural retrofit for column bases is effective if retrofit members are anchored in footings.

For these reasons, it has been decided that the RC envelope method with anchoring to footings will be used for retrofit of underground portions of structures, and that the steel jacket method for aboveground portions of structures. In addition, it has been decided that combined method is used when bending retrofit covers both the underground and aboveground structures. It has been verified that the tensile strength of rebars in the RC envelope can be transferred to the reinforcing steel plates via the shear capacity of stud bolts if stud bolts are used for joining steel plates.

Methods of retrofit for shear retrofit is the same as for flexural retrofit. The extent of retrofit is normally limited to 1.0 D, but it has been decided that entire columns should be retrofitted when the ratio of hoop ties is small.

Discussion has been limited to the bridge piers as a subject of seismic retrofit, but studies should be continued including superstructures, to improve the earthquake-resisting capacity of entire bridges, by Mensin or other methods.

References

1) Ministry of Construction: "Earthquake Inspection Manual for Bridges (Draft)," October 1990

2) Japan Road Association: "Specifications for Highway Bridges V: Seismic Design," February 1990

3) Metropolitan Expressway Public Corporation: "Study on Methods of Retrofit for Anchor Zone of Concrete Bridge Piers," March 1988

Seismic Strengthening of Reinforced Concrete Bridge Pier Walls Designed to Old Standards

M.A. Haroun, G.C. Pardoen and R. Shepard
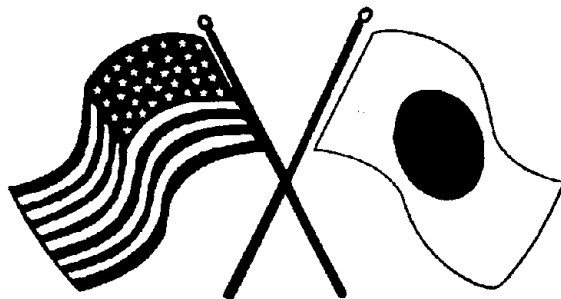
January 20 and 21, 1994
Berkeley Marina Marriott Hotel
Berkeley, California

SEISMIC STRENGTHENING OF REINFORCED CONCRETE BRIDGE PIER WALLS DESIGNED TO OLD STANDARDS

by
Medhat A. Haroun, Professor and Chairman
Gerard C. Pardoen, Professor
and Robin Shepherd, Professor
Department of Civil and Environmental Engineering
University of California, Irvine

ABSTRACT

A comprehensive experimental and theoretical study was conducted to provide an assessment of the seismic behavior of existing bridge pier walls built to old standards, and to provide a basis for the retrofit of these walls to improve their seismic resistance. This paper presents a comparison between the calculated ductility and strength of the tested half-scale specimens and those observed experimentally. It was found that the lap length splice of the vertical steel reinforcement had a significant effect on the ductility of the walls. In general, a good correlation was noted between the computed and observed response parameters. Furthermore, the observed displacement ductility factor was much higher than the design ductility factor. An efficient strengthening scheme was developed and its effectiveness was confirmed. Based on the outcome of the study, the acceptable limit on the displacement ductility factor for seismic qualification of bridge pier walls was raised from two to four.

INTRODUCTION

Possible deficiencies in existing bridge pier wall structures prompted a program for testing reduced-scale models of such walls under cyclic loading, complemented by analytical evaluation of their behavior. The principal concerns related to the seismic strength of existing pier walls centered on three issues:

- Many pier walls have less than 0.25% horizontal reinforcement which is required to control premature diagonal tension cracks.

- Lap lengths with footing dowels are typically a class "A" splice (16 times the bar diameter) rather than a class "C" splice (28 times the bar diameter). The shorter lap length may result in a brittle bond failure of reinforcement under cyclic loading.

- Lack of confinement ties in the plastic hinge zones may cause the vertical reinforcing bars to buckle under combined axial and lateral loads.

213

Experimental and theoretical investigations were conducted to evaluate strength, ductility, and failure mechanism of existing pier walls. They also involved a critical evaluation of potential corrective measures that could be taken to increase the strength of existing pier walls and their ability to undergo large deformations.

EXPERIMENTAL PROGRAM

An experimental investigation was conducted in two phases. In the first phase, half-scale models of existing pier walls were tested to evaluate their strength, ductility, and failure mechanism. It involved the testing of nine specimens with two different lap splices. Seven of the specimens were tested in their weak direction. The specimens were loaded vertically to simulate in situ dead loads and cycled with pseudo dynamic lateral loads to predetermined displacement levels. In the second phase, similar but wider specimens rehabilitated to increase strength and ductility, were tested to evaluate the effectiveness of these corrective measures. This phase involved testing of five specimens, four of which had different retrofit schemes.

Test Specimens

All specimens were half-scale models, 127 inch tall and 10 inch thick. Phase I walls were 38 inch wide and phase II walls were 98 inch wide. Vertical reinforcement was Grade 40 at a ratio of 0.56% whereas the horizontal reinforcement ratio was 0.15 %. Seven specimens incorporated class "A" lap splice (16 d_b) whereas the other five used class "C" splice (28 d_b). Four types of retrofit, as shown in Fig. 1, were employed. The sample for a retrofit type R1 is encased in 3/16 inch thick, 60 inch high steel plates with 0.75 inch nominal gaps between the wall and the plates filled with grout. Pass-through bolts, 5/8 inch in diameter patterned 2 feet on center, provided for the attachment between the plates and the wall. Retrofit R2 is similar to R1 except for the bottom row of bolts, for which spacing was reduced by 50% and additional 1/2 inch thick washers were added for each bolt. The third retrofit scheme consisted of only an 8 inch high, 1/2 inch thick plate placed at the bottom of the wall with bolts and 1/2 inch washers at 7.25 inch on center. The fourth retrofit is similar to the R3 retrofit scheme but the plate is 16 inch high which represents double the length of the lap splice type "A". Bolts in the retrofitted walls R3 and R4 were spaced to fit in between the vertical bars.

Test Procedure

A vertical load was applied on each specimen via two high strength steel bars and a double-channel steel beam placed atop the wall. For phase I walls, the applied vertical load was 62 kips whereas for the wide walls the load was 162 kips; this is approximately 5% of the axial compressive strength of each specimen. Horizontal loads were applied via a long stroke, 55-kip jack through three full cycles of a specified displacement. Figure 2 shows the test set-up including the locations of measurements. The initial cyclic displacement was set to a level less than the calculated yield displacement to ensure

214
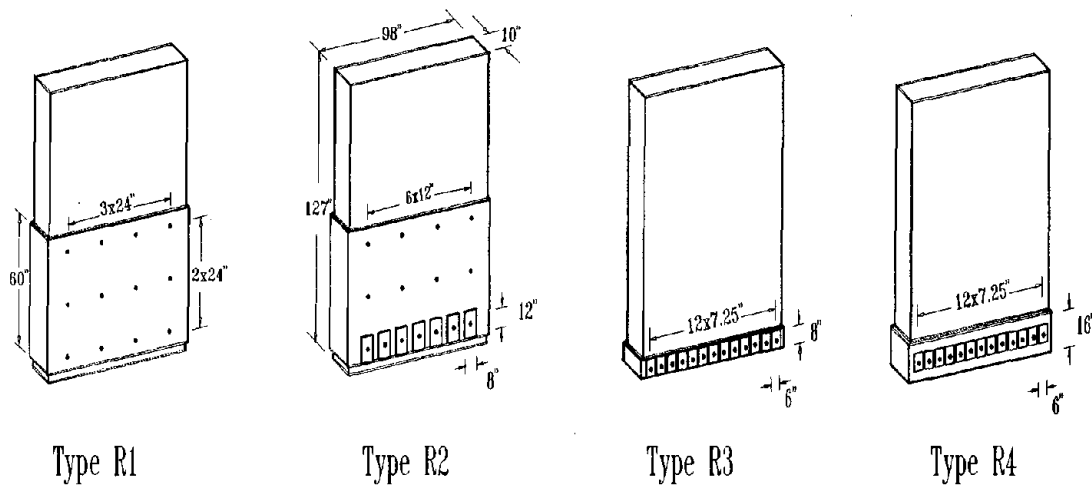
Figure 1: Retrofit Schemes of Pier Walls.
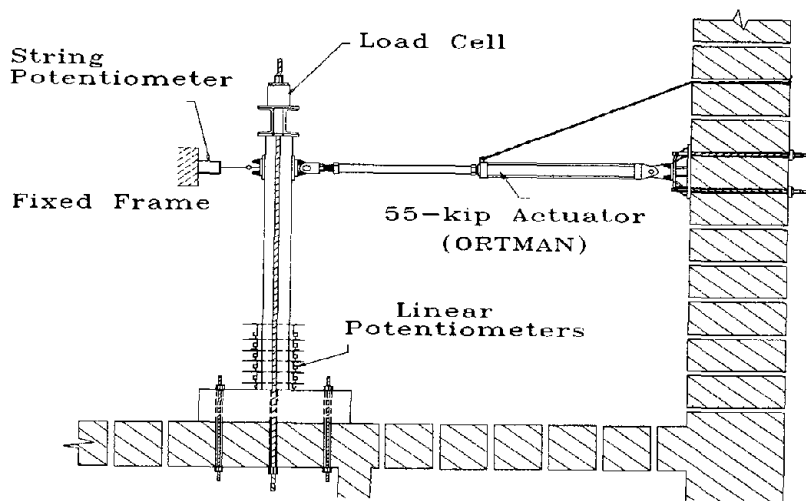
Figure 2: Test Set-up.

that the specimen was first cycled in its elastic range. Then, by observing the non-linear behavior of the specimen as displayed on the analog plotter, each specimen was cyclically loaded to its estimated yield point. Thereafter, the specimen was loaded to increasing displacement levels and the process was continued until the specimen was brought to failure. Displacements at the actuator's elevation were measured using a string potentiometer and were recorded on a data logger system. Consequently, the load-deflection hysteresis loops were constructed for each sample.

Test Observations

The samples were examined after failure and the major relevant observations are summarized below:

- The first crack was usually observed as a horizontal line near the end of the splice

215

Figure 3: Hysteresis Loops for R3 Retrofitted Wall.

length. Other cracks were also formed horizontally and distributed along the lower half of the wall. The largest cracks occurred near the wall base but no cracks were noted in the upper half of the wall.

- A substantial spalling of the concrete cover was observed for specimens with class "A" splice at the late stage of the experiment whereas the loss of cover for specimens with splice "C" took place at a higher ductility factor.
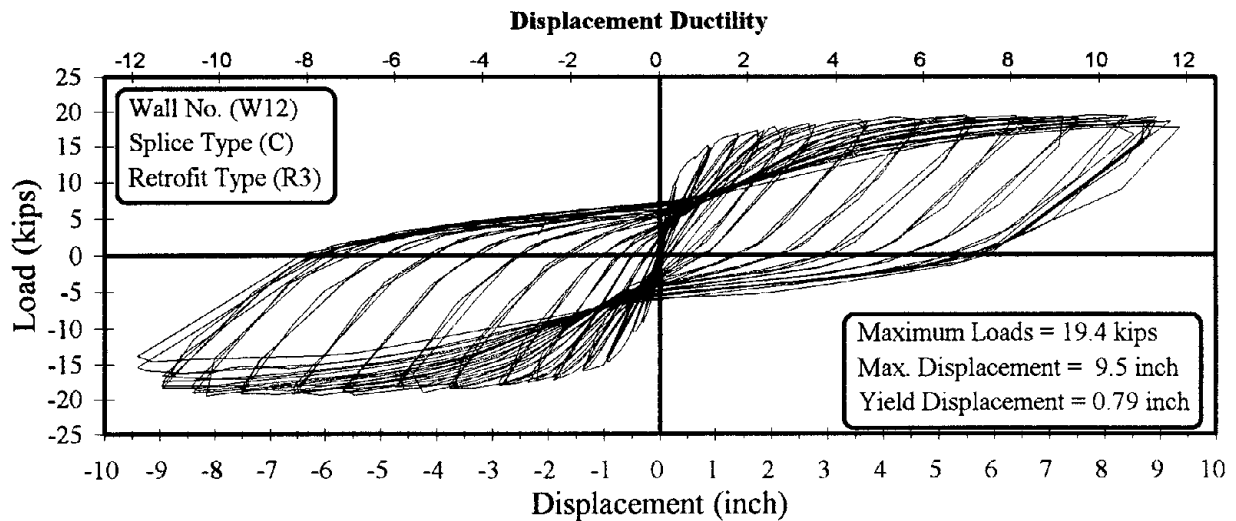
- A few of the reinforcement rebars in specimens with class "C" splice buckled whereas no buckling was observed for specimens with splice "A" indicating a major loss of the bond between the steel and the concrete.

- In the retrofitted walls, no loss of cover was detected, but buckling of the reinforcement was noted at the base of retrofit R1 and R2. These observations were recorded after removing the retrofitting steel plates. In retrofit type R3 and R4, large horizontal cracks were formed near the end of the splice length.

Analysis of Test Results

Figure 3 shows the hysteresis loops for a R3 retrofitted wall having a class "C" splice; a slight unsymmetry was noted in the load-deflection relation prior to averaging the data. To compare the behavior of the wall specimens, the envelope of the hysteresis loops for each wall was plotted in Fig. 4; the first number designates the specimen and the second letter designates the splice class. It was noted that

- In general, specimens with class "C" splice exhibited more ductility and strength than those with class "A" splice. A substantial reduction in stiffness was observed at the intermediate stage of testing for specimens with splice "A" as compared with splice "C" specimens due to bond loss. In addition, the observed average value of Δ_{u_c} (the displacement just prior to a significant reduction in the horizontal
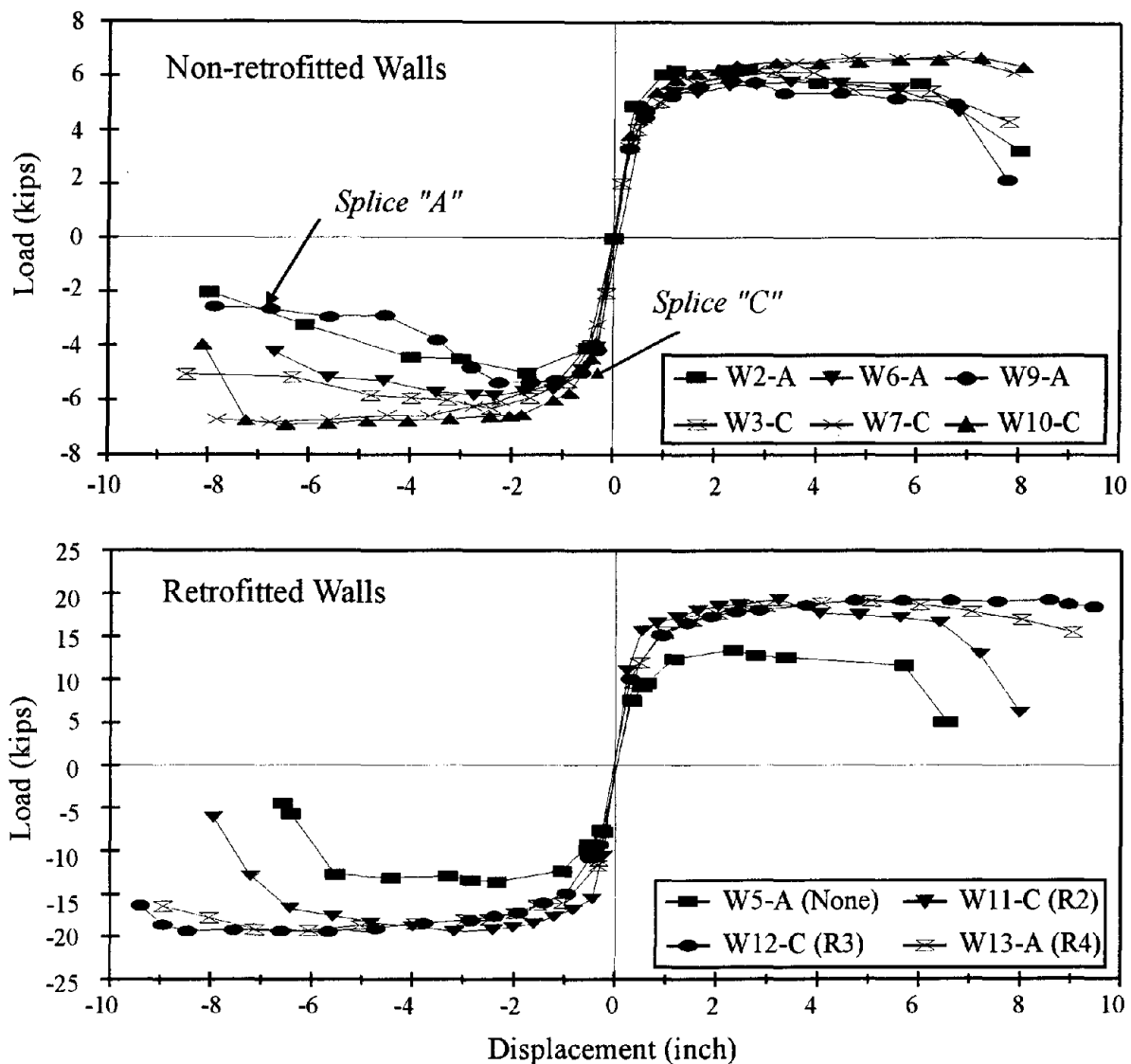
Figure 4: Envelopes of Hysteresis Loops.

load-carrying capacity) for walls with splice "C" is higher than those observed for walls with class "A" splice.

- The initial stiffness (the slope of the envelope in the elastic stage) is almost identical for all phase I specimens. For retrofitted walls, the specimen with R2 type retrofit showed the largest initial stiffness.

- During construction of wall sample W9-A, the form was shifted a little to cause smaller concrete cover in one side of the wall than the other.

- Phase I walls with no retrofit achieved no less than a ductility factor of six with no significant loss of the horizontal load capacity.

217

- Comparing wall specimens with R2 and R3 retrofit (both have class "C" splice), a moderate loss of stiffness in R2 was observed in the intermediate stage of testing. Near ultimate capacity, the specimens with R3 and R4 retrofit had the largest Δ_{u_e}.

- The ductility of walls with class "C" splice is substantially enhanced by using retrofit plates of height equals to the length of the lap splice. This retrofit scheme reduces the potential for buckling of the vertical reinforcement bars.

- The ductility of walls with class "A" splice is substantially enhanced by using retrofit plates of height equals to twice the length of the lap splice. This retrofit scheme reduces the potential for the slippage of the vertical reinforcement bars from the foundation dowels.

COMPUTATION OF DUCTILITY

The ductility of a structural element is generally defined as the member's ability to undergo deformations without a substantial reduction in its capacity. The ductility can be defined either by the curvature ductility factor which is the ratio of the curvature of the section at ultimate strength to the curvature when the tension reinforcement first reaches the yield state, or by the displacement ductility factor which is the ratio between the maximum horizontal displacements of the wall at ultimate and at first yield.

Curvature Ductility

The curvature ductility is calculated according to the definition (Park, 1988)

$$\mu_c = \frac{\phi_u}{\phi_y'} \qquad (1)$$

The curvature at first yield, ϕ_y, is the curvature when the longitudinal tension reinforcement first reaches the yield state. Since the value of ϕ_y is difficult to determine from experimental results, an elasto-plastic behavior was assumed (Mander, 1983) to approximate the moment-curvature relation, and accordingly,

$$\phi_y' = \phi_y \frac{M_i}{M_y} \qquad (2)$$

where M_i is the moment capacity of the wall section using the ACI-89 code approach in which ϵ_{cu}, the maximum concrete strain, is equal to 0.003 and M_y is the moment calculated at first yield of the longitudinal steel.

The section curvature at ultimate strength is calculated when the strain at the extreme fiber of the concrete compression block reaches the value of ϵ_{cu} based on the unconfined stress-strain relation for the concrete (= 0.004).

218

Displacement Ductility

The displacement ductility is calculated from the following definition

$$\mu_d = \frac{\Delta_u}{\Delta_y'}$$ (3)

The maximum horizontal displacement of the wall at yield (Δ_y) is calculated when the critical section reaches its yield capacity (M_y)

$$\Delta_y = \int_0^L \phi(x)x\,dx$$ (4)

where $\phi(x)$ is the curvature distribution along the wall height and x is the coordinate measured from the top of the wall. Again, the theoretical yield displacement will be modified by the ratio of (M_i/M_y) as indicated in Eq. 2. To calculate the ultimate displacement, an approximate method (Mander, 1983) is used. The total displacement of the wall is the sum of three displacement components

$$\Delta_u = \Delta_{y'} + \Delta_p + \Delta_s$$ (5)

where $\Delta_{y'}$ is the yield displacement, Δ_p is the plastic deformation due to the nonlinearity of the moment-curvature response which occurs when the steel has yielded and/or the concrete enters the inelastic zone, and Δ_s is the deformation due to shear which was ignored in this analysis as it is very small. The plastic deformation can be calculated from (Paulay and Priestley, 1992)

$$\Delta_p = \theta_p(L - 0.5L_p)$$ (6)

where the plastic hinge rotation θ_p is evaluated from

$$\theta_p = \phi_p L_p = (\phi_u - \phi_{y'})L_p$$ (7)

in which ϕ_u is the maximum curvature at the base and L_p is the length of the plastic hinge which was empirically assumed. It should be noted that bond slip between the reinforcement and the concrete is not considered in the calculations. As such, the results for splices "A" and "C" are the same throughout the analysis.

CALCULATED AND OBSERVED BEHAVIOR

Figure 5 presents a comparison between computed and measured response parameters: the maximum horizontal load, the displacement at yield, the displacement at ultimate and the displacement ductility factor. The calculated horizontal loads at ultimate and the corresponding experimental values are generally in good agreement. To determine the horizontal displacement at yield experimentally, it was suggested in the literature that Δ_{y_e} be evaluated at 75% of M_i, and consequently, $\Delta_{y_e'}$ is 1.33 Δ_{y_e}. However, it was found that this procedure provides relatively smaller values than anticipated
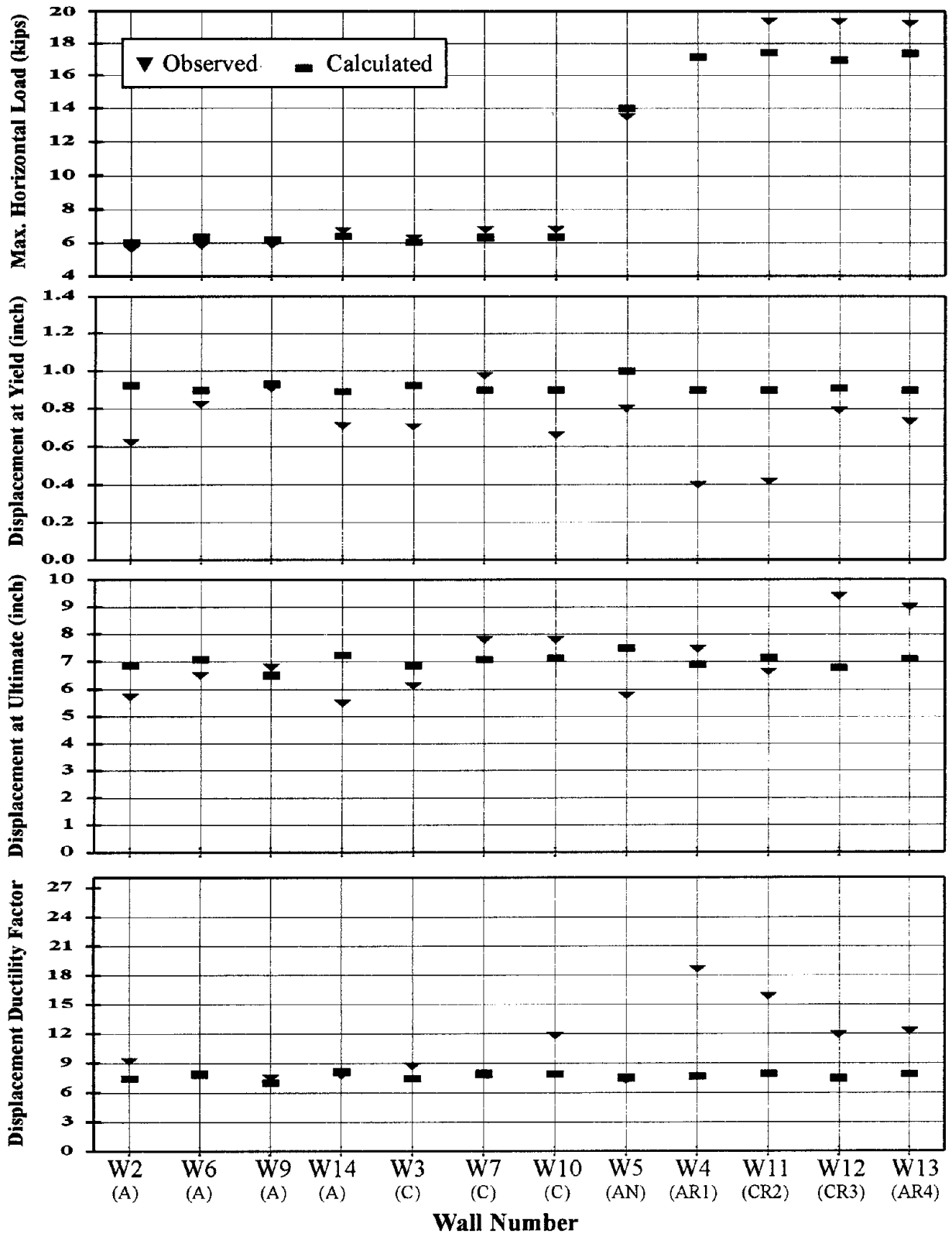
Figure 5: Observed and Calculated Response Parameters.

for $\Delta_{y_e'}$. A more realistic and "conservative" approach is used herein to evaluate Δ_{y_e} corresponding to 90% of M_i; a detailed discussion of the methods of evaluation of the displacement at yield both experimentally and theoretically is presented by Haroun and Haggag (1994). The most important finding from Figure 5 is that the minimum observed displacement ductility factor of all walls, even with the conservative estimate of $\Delta_{y_e'}$, is larger than six which is substantially higher than the customary design ductility factor of two.

CONCLUSIONS

Pier walls with class "A" splice are likely to suffer bond failure at less than their nominal flexural strength. A better performance was noted for walls with class "C" splice. The calculated displacement ductility factor and maximum horizontal load have generally good correlation with the observed parameters, although the analysis still needs modifications to handle the variation in lap splice class and the different retrofit schemes. All proposed retrofit schemes increased the wall stiffness; however, retrofit type R3 and R4 are the most efficient in enhancing the ultimate wall displacement. The observed lowest displacement ductility factor of all walls substantially exceeded the ductility factor recommended in design standards. Accordingly, the California Department of Transportation has recently increased the acceptable limit of the displacement ductility factor for seismic qualifications from two to four.

ACKNOWLEDGEMENTS

REFERENCES

American Concrete Institute, Building Code Requirements for Reinforced Concrete, ACI 318-89, Detroit, Michigan, 1989.

California Department of Transportation, Bridge Design Specifications, June 1990.

Haroun, M.A., Pardoen, G.C., Shepherd, R. and Haggag, H.A., "Retrofit Strategies for Bridge Pier Walls," Proceedings of the Fifth U.S. National Conference on Earthquake Engineering, EERI, Chicago, July, 1994.

Haroun, M.A., and Haggag, H.A., "Correlation of Observed and Calculated Displacement Ductility Factors for Reinforced Concrete Bridge Pier Walls," to be submitted to

the ACI Structural Journal, 1994.

Mander, J.B., "Seismic Design of Bridge Piers," Thesis, Civil Engineering Department, University of Canterbury, New Zealand, 1983.

Park, R., and Ruitong, D., "Ductility of Doubly Reinforced Concrete Beam Sections," ACI Structural Journal, Vol. 85, March-April 1988, pp. 217-225.

Paulay, T., and Priestley, M.J.N., Seismic Design of Reinforced Concrete and Masonry Buildings, John Wiley & Sons, 1992.

Priestley, M.J.N., and Park, R., "Strength and Ductility of Concrete Bridge Columns under Seismic Loading," ACI Structural Journal, Vol. 84, January-February 1987, pp. 61-76.

SECOND U.S.-JAPAN WORKSHOP ON SEISMIC RETROFIT OF BRIDGES

Seismic Response of Reinforced Concrete Bridge Piers Subjected to Eccentric Loading

K. Kawashima, S. Unjoh and H. Mukai
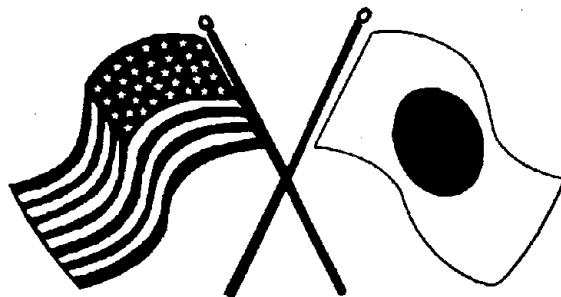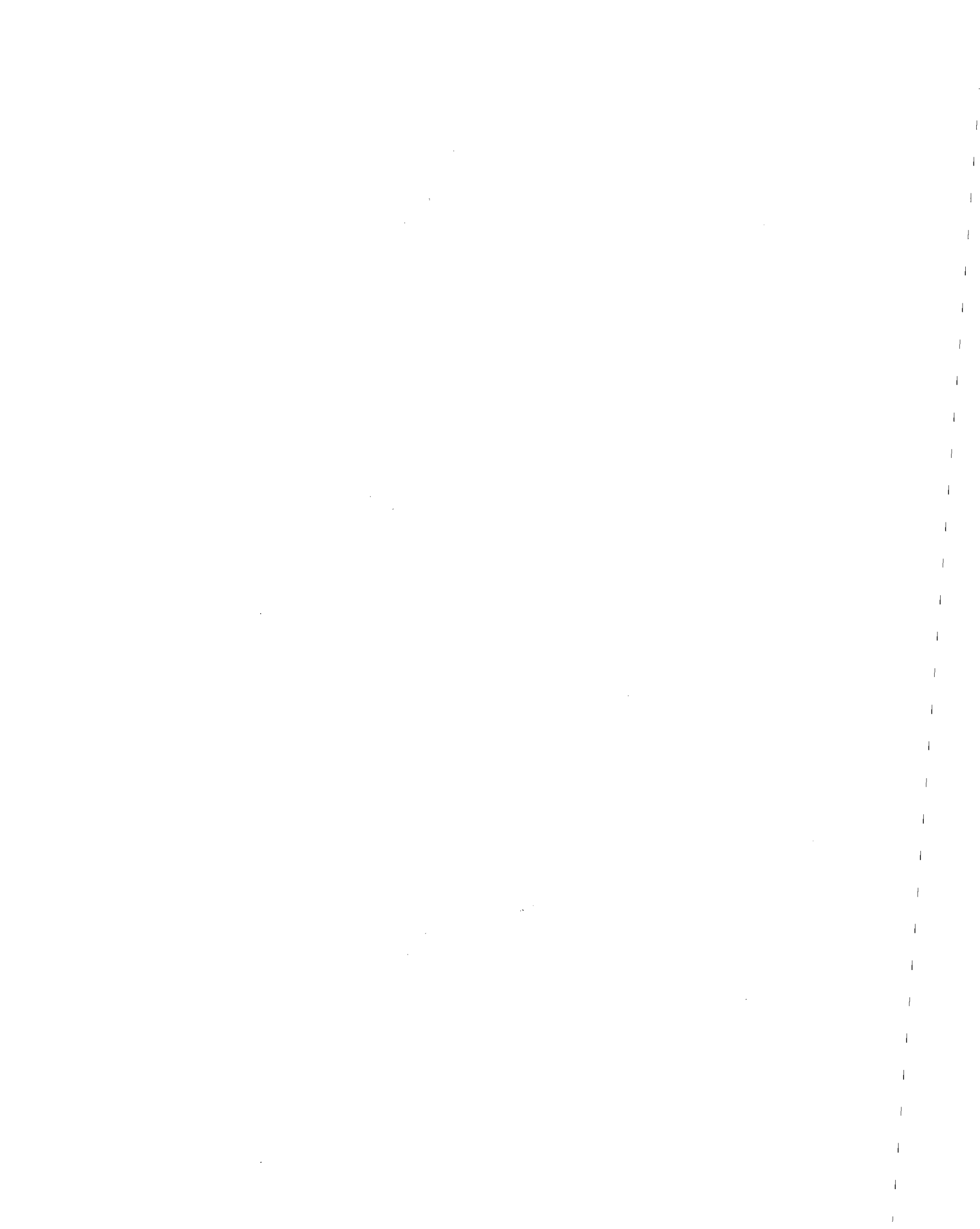
SEISMIC RESPONSE OF REINFORCED CONCRETE BRIDGE PIERS SUBJECTED TO ECCENTRIC LOADING

Kazuhiko KAWASHIMA[1], Shigeki UNJOH[2] and Hidetoshi MUKAI[3]

1) Head, Earthquake Engineering Division, Public Works Research Institute, Ministry of Construction, Tsukuba Science City, Japan
2) Senior Research Engineer, ditto
3) Assistant Research Engineer, ditto

ABSTRACT

Presented are the seismic response characteristics of C−shaped reinforced concrete bridge piers which is subjected to eccentric loading by the dead weights of superstructure and cantilevered beam. The shaking table test and dynamic loading tests of model piers were made to investigate the seismic response characteristics. It is found that the response of pier increased only in one direction in which the bending moment increased and that the excessive residual displacement was developed. It is also found that the ductility significantly decreased with increase of bending moment by the eccentric loading.

INTRODUCTION

Recently, new types of structures have been constructed in urban areas by land use restriction and other construction conditions. C−shaped reinforced concrete (RC) bridge pier as shown in **Fig. 1** are one of the typical examples. However, the seismic response characteristics of this type of RC piers have not yet been studied. Because the C−Shaped RC piers are subjected to eccentric loading by the dead weights of superstructure and cantilevered beam, it is anticipated that the seismic response of the piers is developed only in one direction during an earthquake. Therefore is an important subject to investigate the strength and ductility characteristics and to develop the seismic design method against large−scale earthquakes.

This paper presents the seismic response characteristics of C−shaped reinforced concrete bridge piers through the shake table test and dynamic loading tests of model piers.

DEFINITION OF ECCENTRIC LOADING

In order to define the amount of the eccentric loading, bending moment ratio is

assumed as

$$r_M = \frac{M_E}{M_0 + M_E} \tag{1}$$

where

r_M : bending moment ratio

M_E : bending moment by design seismic load, and

M_0 : bending moment by eccentric loading of superstructure and cantilevered beam

Eq.(1) shows that when the eccentric loading increases r_M deceases, on the other hand, when the eccentric loading decreases r_M increases. $r_M = 1$ means concentric loading.

Fig. 2 shows distribution of the bending moment ratio r_M based on the survey of 45 existing C–shaped RC bridge piers in the Metropolitan area, bending moment ratio r_M is in the range of 0.4 − 0.9. Averaged bending moment ratio r_M is 0.55.

SEISMIC RESPONSE CHARACTERISTICS OF C–SHAPED RC PIER BASED ON SHAKING TABLE TESTS

Bridge Pier Model Studied

In order to investigate the seismic response characteristics of a C–shaped RC pier, shaking table test was made at the Public Works Research Institute. Objective of the shaking table test is to investigate how the C–shaped pier responds and behaves in the transverse direction to a bridge axis during an actual earthquake.

Fig. 3 shows a C–shaped bridge pier model used for the shaking table test. Details of the pier model was determined based on the actual bridge pier. The actual pier with average bending moment ratio, r_M , of 0.55 was selected as a prototype. The height of pier is 10.2m and the height of girder is 1.5m. The similarity ratio of the pier model with the prototype pier was assumed as 1/4.6.

The specimen has an effective height, h, of 2.55m and cross section of 52cm × 42cm (width along bridge axis : 52cm). The shear span ratio h/d, which is defined as the effective height divided by the effective depth, d, of the cross section of 37cm, is 6.9. Longitudinal reinforcing bars are arranged by 5 reinforcing bars with diameter of 16mm (D16) in the initial compression side by the eccentric loading, 5 reinforcing bars with that of 22mm (D22) in the tension side, and 3 reinforcing bars with that of 16mm (D16) in the other sides. The reinforcement ratio is 0.45, 1.06 and 0.27, respectively. Tie reinforcement was arranged by 17.3cm pitch by reinforcing bars with diameter of 10mm (D10). Tie reinforcement ratio is 0.16. Averaged yielding stress of the longitudinal and tie reinforcement was 35.38KN for D16, 34.32KN for D22 and 34.83KN for D10. Averaged compression strength of the concrete was 3.29KN. It should be noted here that since weight of the superstructure supported by the pier model is 393.2KN, seismic coefficient of

the pier model can be regarded as 0.27. Axial stress by the dead weight of superstructure was 90N. Computed yield displacement, δ_y, corresponding to one displacement ductility factor and yield strength of the pier in the direction in which the bending moment increases are 75.5KN and 20.5mm computed from the shifted origin. On the other hand, in the direction in which the bending moment decreases they are 115.7KN and 91.3mm, respectively.

Shaking Table Test

A pier model is fixed at the center of the shaking table and two spans of simply supported girders with total weights of 393.2KN and length of 15m were placed on the pier model. Because two ends of the girder could not be supported by the shaking table, they are supported by the two steel frames placed outside of the table. The pier model and girders were connected by fixed bearings. The steel frames and girder were connected by movable roller bearings so that inertia force developed at the girder during excitation be directly applied to the pier model. It should be noted here that although the direction of the eccentric loading is assumed to be transverse direction, the girder axis was set up in parallel direction with transverse direction of the pier model. However, since the two girders was to load the weight of superstructure and to simulate the inertia force, the direction of the girders is not important.

The shaking table was excited along transverse direction to bridge axis (direction to the girder axis of model bridge). An acceleration record triggered at the Hachirogata during the Nihon−kai−chubu, Japan, Earthquake of 1983 was used as an input motion by reducing the time axis one half so that the predominant frequency of the record matches with the fundamental natural frequency of the pier model. Intensity of the record was assumed as 3.5 times the original.

Extensive instrumentations were made to measure basic parameters including accelerations at the foot of pier and at the girder as well as relative displacement of the girder with reference to shaking table. Inertia force of the superstructure was computed by multiplying the acceleration developed at the girder by the mass of girder.

Seismic Response Characteristics

Fig. 4 shows acceleration of shaking table, response acceleration and displacement of girder. Although measured peak acceleration of shaking table is 812cm/s^2, this is spike−like response and effective seismic intensity to excite the pier model is about 0.35G as assumed. The pier model developed residual lateral displacement with an amount of 16cm at the pier crest in the direction in which eccentric weight is loaded. However, the stopper for preventing falling−off of girders worked at this moment. If the stopper was not installed the larger residual displacement would be developed. Such a permanent displacement is clearly observed in **Fig. 5** from biased inelastic response displacement. The drift of response displacement was developed at time 12sec when the first large excitation,

which exceeded the yielding displacement, loaded. However, after the excitation with larger displacement at time 17sec, the residual displacement reached to about 16cm. Therefore, accumulation of drifting of response displacement after the first large excitation seems to be less significant. It should be noted here that although the residual displacement was developed in the shaking table test of RC pier model subjected to concentric loading, the amount was much smaller than that mentioned above.

Fig. 5 shows the failure mode of the pier model after the excitation by shaking table. Compression failure was found in the compression side by the eccentric loading. Only horizontal tension crack was found in the tension side.

Fig. 6 shows the hysteresis loop of the load–displacement relation obtained through the shaking table test. The biased displacement response was clearly developed after the first significant excitation with larger displacement exceeding the yield displacement. The degradation of the stiffness in accordance with nonlinear response can be clearly observed.

DYNAMIC LOADING TEST OF RC PIER MODELS

Bridge Pier Models Studied

In order to investigate the strength and ductility characteristics of C–shaped RC pier, dynamic loading tests were made. Fig. 7 shows a C–shaped bridge pier model used for the dynamic loading test. The pier models are basically the same as the shaking table test as mentioned in the above. Three pier models in total were tested, in which bending moment ratio, r_M , and loading direction was varied as a parameters to be investigated.

All pier models have a loading effective height, h, of 2.55m and cross section of 52cm ×42cm (width along in bridge axis : 52cm). The shear span ratio, h/d, is 6.9. The bending moment ratio, r_M , was assumed as 0.69 (P–60; small eccentric loading), 0.55 (P–62; medium eccentric loading) and 0.51 (P–64; large eccentric loading), in which the specimen number is the serial number of pier models tested at the Public Works Research Institute. P–62 has the same condition as one used for the shaking table test. The detail of the piers is the same as P–62. Eccentric weight in transverse direction was not loaded for P–65. Axial loading was assumed as 196.1KN which is the same as the shaking table test. Therefore, axial stress by the axial loading is 90.2N. It should be noted here that the axial force to P–60 was assumed as 127.5KN (axial stress is 58.8N) because of limitation of loading apparatus.

Dynamic Loading Test

The pier model was anchored to the reaction wall with bolts. The large–stroke dynamic actuator, which was installed to the reaction wall in such a manner, was fixed to the head of the pier model. Also, axial loading apparatus was fixed to the head of the pier models so that the necessary eccentric loading be applied. At the pier crest the steel–made apparatus was set for the purpose to eccentrically impose the axial force.

228

Fig. 8 shows the pattern of loading displacement for dynamic loading tests. The yield displacement corresponding to one ductility factor was assumed as an unit loading displacement. However, the pier models subjected to eccentric loading is initially displaced by displacement of δ_0. Therefore, unit loading displacement, δ_1, was assumed with the assumption of that the origin is shifted to the initial point as

$$\delta_1 = \delta_y - \delta_0 \tag{2}$$

where

δ_1 : unit loading displacement

δ_y : yielding displacement

δ_0 : initial displacement by eccentric loading

The pier models were subjected to a series of step-wise increasing symmetric displacement cycles as shown in **Fig. 8**. At each step, 10 cycles of loading with the same displacement amplitude was carried out. It should be noted here that the yield displacement was determined by computation with the strain of main reinforcement at the base. The loading velocity was assumed as 1cm/s. The loading direction was assumed as transverse and longitudinal directions depending on the test objectives.

Failure Mode of Pier Models

Fig. 9 shows the failure mode of P—62 ($r_M = 0.55$; medium eccentric loading). Damage of a side parallel to the loading direction is shown. During δ_1 to δ_2 loading cycles, only small horizontal cracks were found on the concrete surface. This is by the loading in the plus side (the loading in which bending moment increases, this side is referred to A—side), no cracks was found at the minus side (the loading in which bending moment decreases, this side is referred to B—side). After δ_3 loading cycles the cracks was initiated to be developed in B—side. During δ_4 loading cycles, diagonal cracks were developed from the bottom of A—side to B—side. With increase of loading cycles, the significant cracks were developed at the bottom of B—side and cover concrete was spalled—off. During δ_6 loading cycles, concrete of the bottom of pier was failed with a triangular wedge shape and 2 reinforcing bars were fractured in the B—side. During δ_7 loading cycles, deformation of pier was significantly extended at the base and the pier was inclined. It should be noted here that comparing of the failure mode with the shaking table test result, the failure mode was significantly different between two tests. Although the diagonal crack was developed in the dynamic loading test, such diagonal crack was not developed during the shaking table test. This is because that although displacement in the minus side was forced to be loaded to the pier in the dynamic
loading test, displacement during shaking table test was developed in one direction in which the bending moment increases.

Figs. 10 and **11** show the failure modes of P—60 ($r_M = 0.69$; small eccentric loading) and P—64 (r_M ; large eccentric loading). In case of P—60, from δ_1 loading cycles, crack was developed also in the B—side. Then the crack increased in both A—side

and B−side. During δ_6 loading cycles, cover concrete was spalled−off in the both sides of the bottom. During δ_7 loading cycles, 3 longitudinal reinforcing bars were fractured. The difference in the failure mode between P−62 and P−60 is that the damage was developed in both sides and the progress of the damage of P−60 with loading cycles became slower than that of P−62.

On the other hand, in case of P−64 (r_M=0.51; large eccentric loading), during δ_3 loading cycles the diagonal crack was developed. The cover concrete in the B−side of the bottom was spalled−off during δ_4 loading cycles. During δ_5 , concrete at the bottom of B−side was failed by compression and one longitudinal reinforcing bar was fractured. Comparing with the failure mode of P−62, the progress of damage of P−64 became faster than P−62.

Strength and Ductility Characteristics

Fig. 12 shows the effect of bending moment ratio, r_M , on load−displacement relation. In the plus side in which the bending moment increases, the displacement range in which load reaches to peak and the displacement increase stably was shorter as the bending moment ratio is smaller. Therefore, the bending moment ratio is smaller, the ductility becomes smaller.

Table 1 shows the strength and ductility of the tested pier models. The ductility was almost same when r_M is 0.69 and 0.55, but when the r_M is 0.51 the ductility decreases to one of half of those. The ratio of peak strength by yield strength of the P−64 decreases by 10% than P−60 and P−62.

CONCLUDING REMARKS

In order to investigate the seismic response characteristics of C−shaped reinforced concrete bridge piers which is subjected to eccentric loading in the transverse direction to bridge axis by the dead weights of superstructure and lateral beam, the shaking table test and dynamic loading tests of model piers were made to investigate the seismic response characteristics.

According to the above results the following conclusions may be deduced:

1) When the pier model subjected to eccentric loading, the displacement was developed only in one direction in which the bending moment increases. The large amount of residual displacement was finally developed.

2) When the bending moment ratio is 0.51, the ductility decreases to one half that greater than 0.55. Therefore, the bending moment ratio is smaller, ductility becomes smaller.

REFERENCES

1) Kawashima, K., Hasegawa, K., Koyama, T. and Yoshida, T.(1988) "Hysteretic Behavior

of Reinforced Concrete Bridge Piers by Dynamic Loading Tests and Shaking Table Tests," Ninth World Conference on Earthquake Engineering, Tokyo—Kyoto, Japan

2) Kawashima, K., Hasegawa, K., Koyama, K. and Yoshida, T.(1985) "Experimental Investigation on Dynamic Strength and Ductility of Reinforced Concrete Bridge Piers, (Part.1)," Technical Memorandum of PWRI, No.2232

4) Iwasaki, T., Kawashima, K., Hasegawa, K., Koyama, T. and Yoshida, T.(1987) "Effect of Number of Loading Cycles and Loading Velocity of Reinforced Concrete Bridge Piers," 19th Joint Meeting, Wind and Seismic Effects, UJNR, Tsukuba, Japan

5) Iwasaki, T., Kawashima, K., Hasegawa, K. and Yoshida, T.(1988) "Dynamic Strength and Ductility of Reinforced Concrete Bridge Piers," 20th Joint Meeting, Wind and Seismic Effects, UJNR, Gaithersburg, Maryland

6) Iwasaki, T., Ueda, O., Kawashima, K., Hasegawa, K. and Yoshida, T(1989). "Inelastic Behavior of Reinforced Concrete Bridge Pier, —Effect of Bilateral Loading and Circular Hollow Section—," 21st Joint Meeting, Wind and Seismic Effects, UJNR, Tsukuba, Japan

7) Kawashima, K., and Koyama, T.(1988) "Effect of Number of Loading Cycles on Dynamic Characteristics of Reinforced Concrete Bridge Pier Columns," Structural Eng./Earthquake Eng., Proc. JSCE, Vol.5, No.1, pp.183—191

8) Kawashima, K., and Koyama, T.(1988) "Effect of Cyclic Loading Hysteresis on Dynamic Behavior of Reinforced Concrete Bridge Pier," Structural Eng./Earthquake Eng., Proc. JSCE, Vol.5, No.2, pp.343—350

231

Table 1 Strength and Ductility of Pier Models

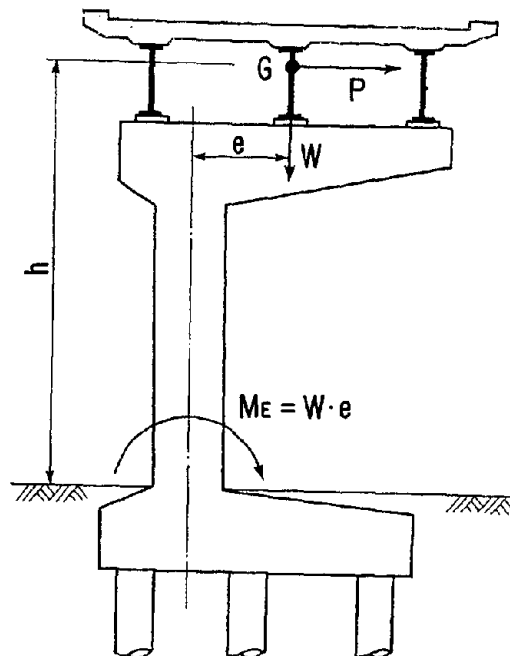|	P–60	P–62	P–64
Loading Direction	Trans.	Trans.	Trans.
Bending Moment Ratio r_M (Eccentric Loading)	0.69 Small	0.55 Medium	0.51 Large
Yield Strength P_y (KN)	124.5	147.1	223.6
Peak Strength P_{max} (KN)	145.1	179.5	238.3
P_{max}/P_y	1.17	1.22	1.07
Yield Displacement δ_y (cm)	1.6	1.3	2.0
Ultimate Displacement δ_u (cm)	8.8	7.3	5.4
Ductility Factor δ_y/δ_u	5.5	5.6	2.7

Fig. 1 C–Shaped Reinforced Concrete Bridge Pier Subjected to Eccentric Loading
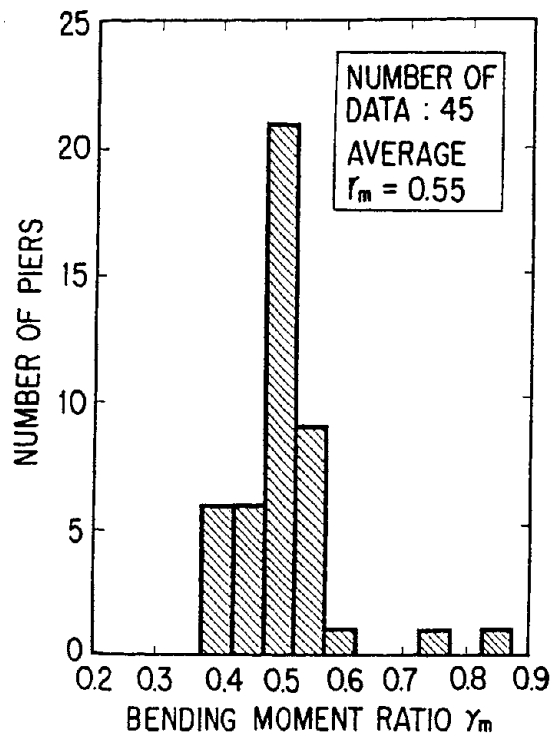
232

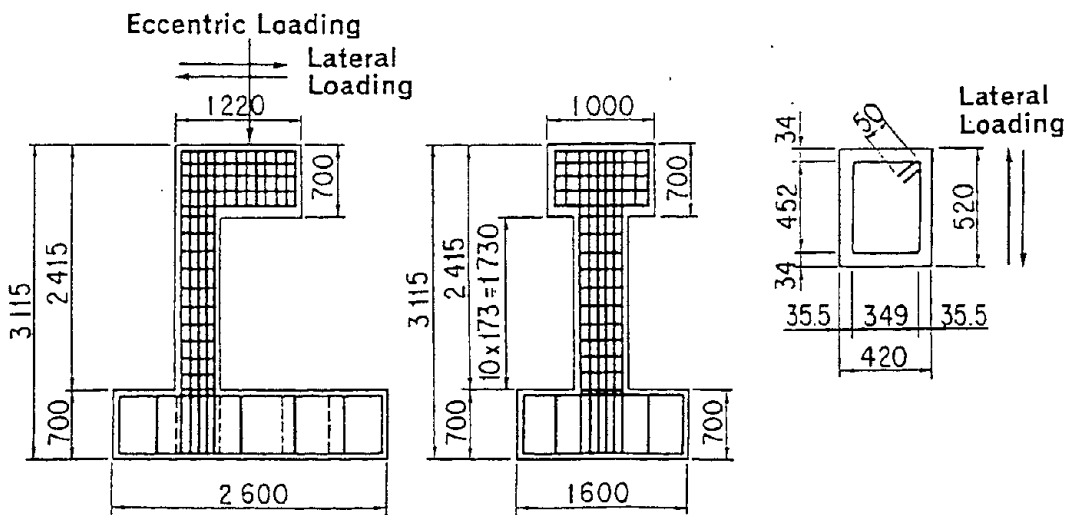**Fig. 2** Distribution of Bending Moment Ratio of Actual Bridge Piers Surveyed

Fig. 3 C—Shaped Bridge Pier Model for Shaking Table Test
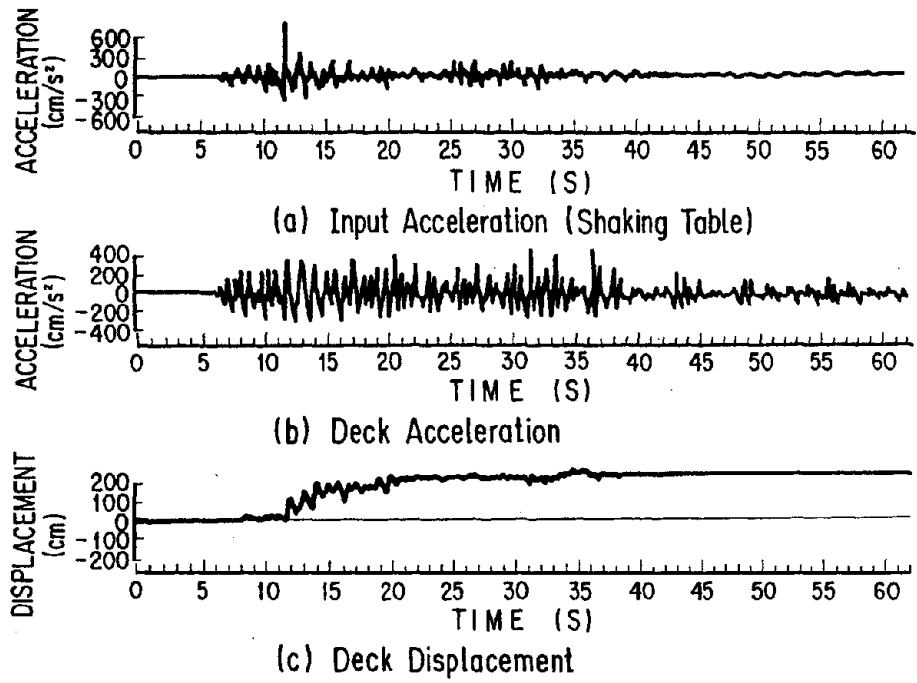
Fig. 4 Response Accelerations and Displacement
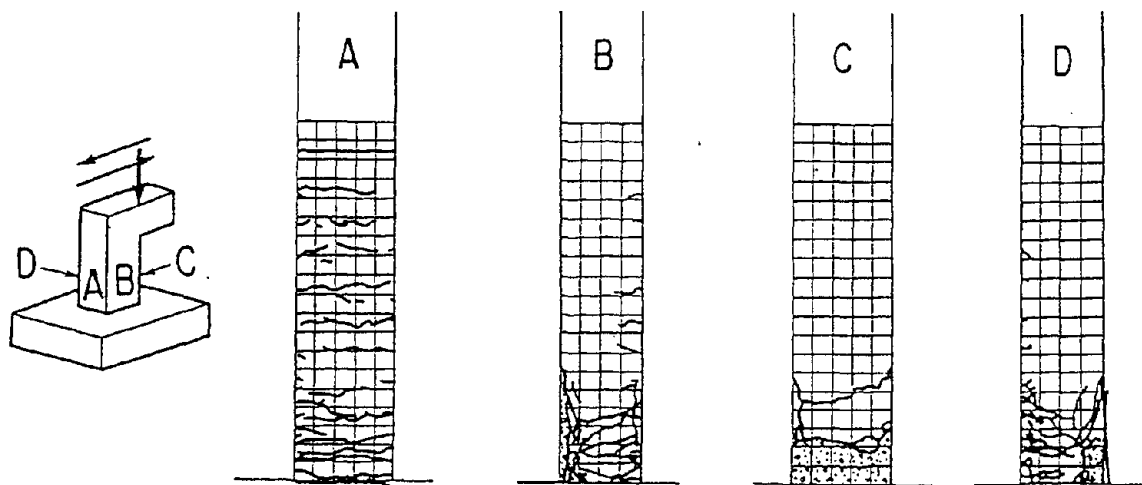
Fig. 5 Failure Mode of the Pier Model after Excitaion by Shaking Table

234
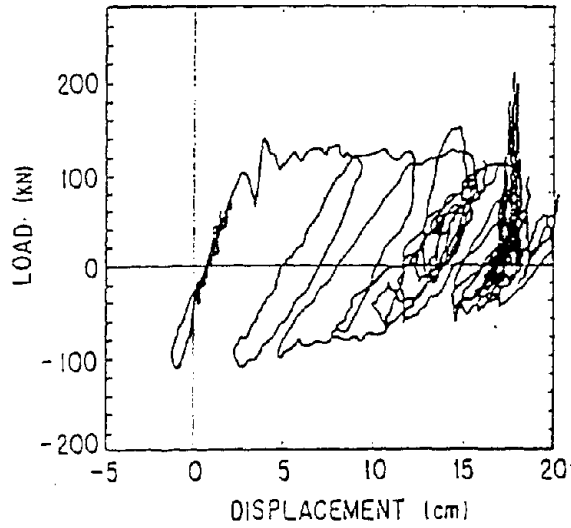
Fig. 6 Hysteresis Loop of load–displacement relation obtained through Shaking Table Test
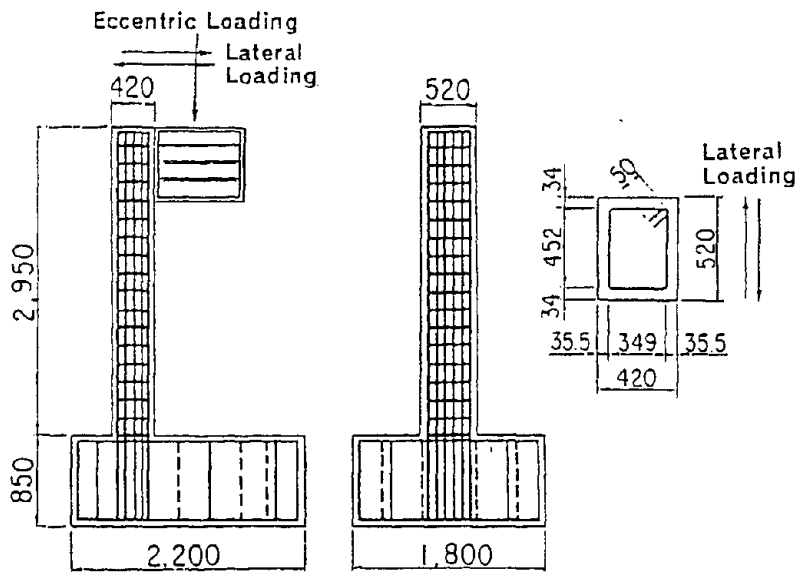
Fig. 7 C–Shaped Bridge Pier Model for Dynamic Loading Tests

235

δ_y : Yield Displacement
δ_E : Displacement by Eccentric Loading
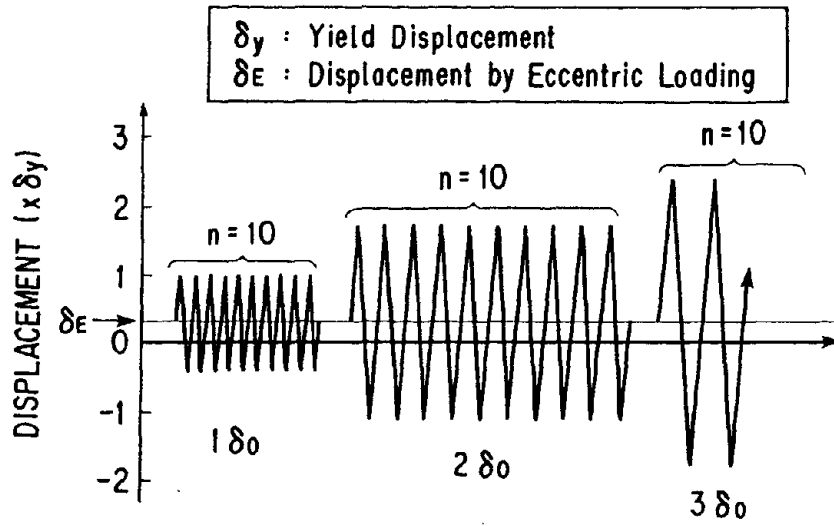
Fig. 8 Loading Pattern of Displacement for Dynamic Loading Tests
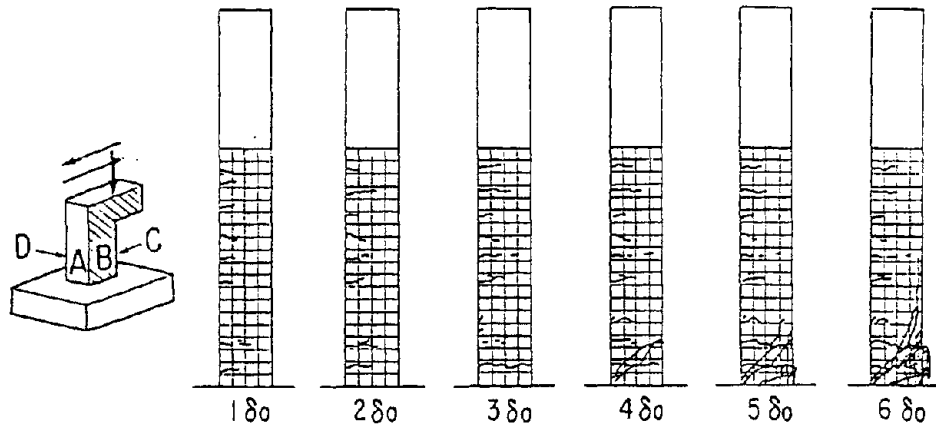
Fig. 9 Failure Mode of P−62 (r_M=0.55)
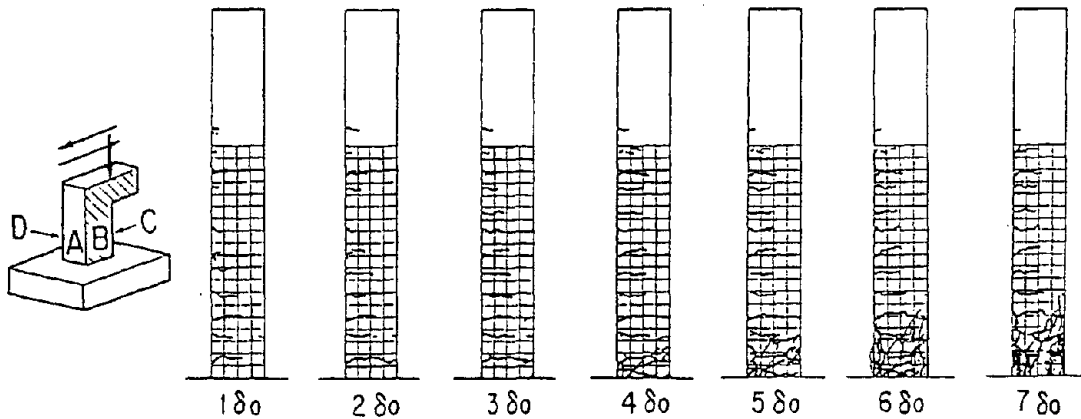
Fig. 10 Failure Mode of P−60 (r_M=0.69)
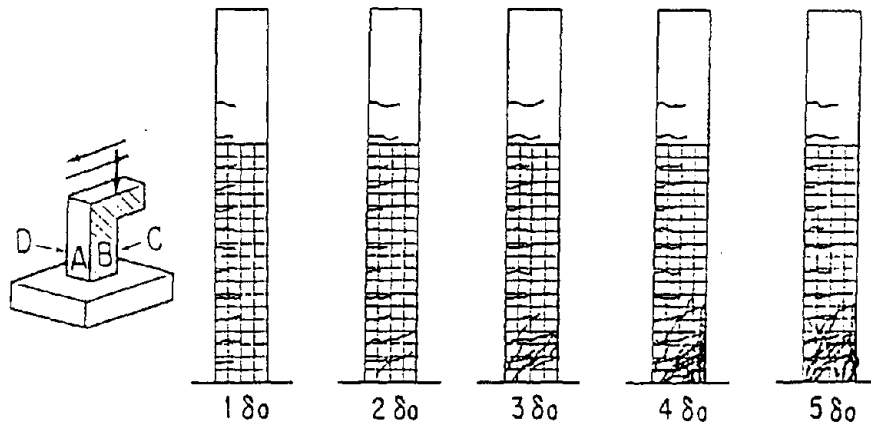
Fig. 11 Failure Mode of P-64 (r_M=0.59)
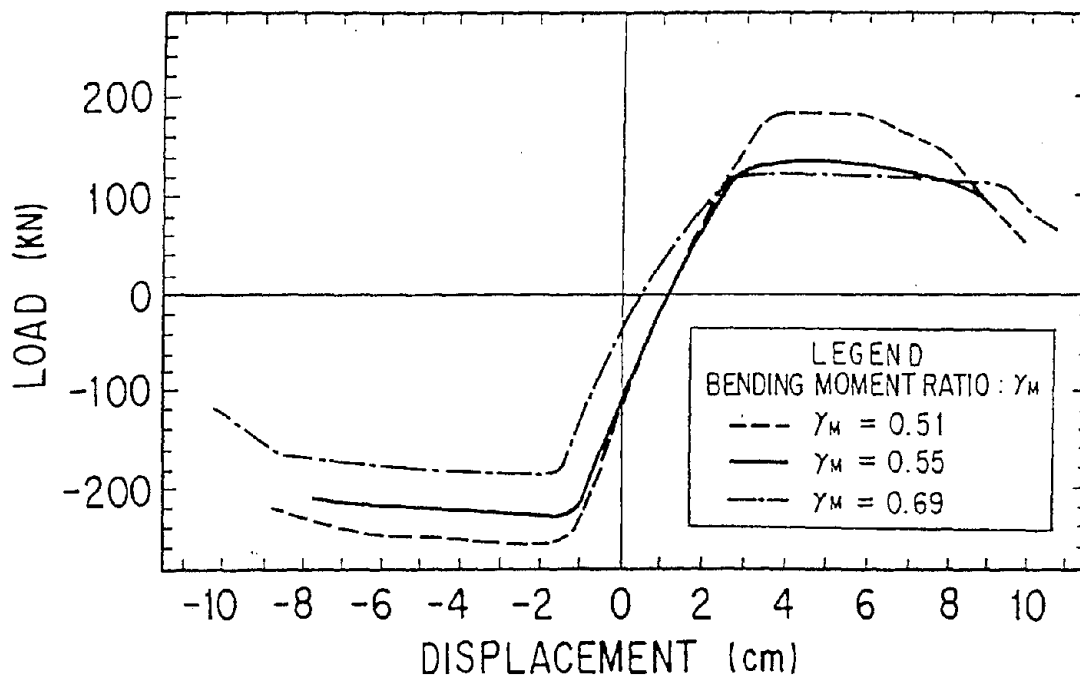
Fig. 12 Effect of Bending Moment Ratio r_M on Load-Displacement Relation

SECOND U.S.-JAPAN WORKSHOP ON SEISMIC RETROFIT OF BRIDGES

Seismic Retrofit Procedures for Reinforced Concrete Bridge Piers in the Eastern United States
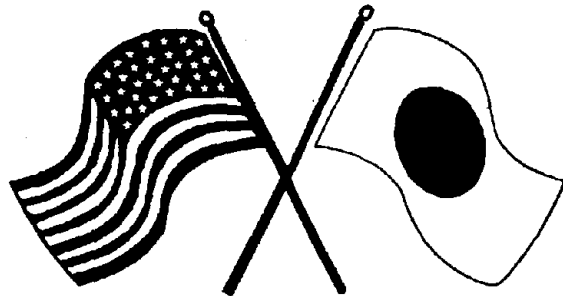
J. Mander and S. Chen

SEISMIC RETROFIT PROCEDURES FOR REINFORCED CONCRETE BRIDGE PIERS IN THE EASTERN UNITED STATES

by
J.B. Mander and S.S. Chen
Department of Civil Engineering
State University of New York at Buffalo, USA.

ABSTRACT

Existing highway bridges constructed in the eastern and central United States typically possess multiple-column pier bents. This paper is concerned with the seismic retrofitting of such bridge piers based on experimental studies of a 1950-60's era design both at one-third scale and full size. Pre-retrofit experimental results show that this class of pier may possess a moderate degree of ductility but damage is mostly located in the connection zones. As the columns exhibited a reasonable measure of ductility, these were left untouched and the pier was retrofitted by jacketing the capping beam and providing longitudinal unbounded post-tensioning to enhance column rebar anchorage and improve the joint core shear capacity. Post-retrofit performance demonstrated that the post-tensioned jacketing solution is effective in moving the damaged region from the joint core to plastic hinges in the column end zones.

INTRODUCTION

Most existing bridges constructed in the eastern and central United States have been primarily designed for carrying gravity loads. Design lateral loads arising from wind forces, traffic induced centrifugal forces on curved bridges, and hydrodynamic forces on bridge piers in river crossings are generally quite small when compared to earthquake lateral loads. Bridge collapses in the 1971 San Fernando earthquake and the more recent collapse of the Cypress double-deck I-880 interstate system in the 1989 Loma Prieta earthquake, which resulted in a significant number of fatalities, have led to upgrading of the AASHTO bridge design code[1]. The seismic provisions of this code now require design and construction of bridge structures that are capable of resisting small to medium ground motions in the elastic range with little or no structural damage. Bridge structures must possess a large deformation capability that permits dissipation of seismic energy in large earthquakes. The primary design objectives are two: to provide serviceability, and to prevent collapse of the structure and thereby minimize loss of life. Seismic resistance may be provided through: (a) ductile detailing of the bridge piers, which leads to energy dissipation in column hinges under lateral loading; (b) seismic isolation which may include some additional energy dissipation capability independent of the pier systems; or (c) a combination of (a) and (b).

Because the majority of existing bridges were constructed in the eastern and central United States prior to the time when seismic design was mandated by the AASHTO code, they do not have these ideal seismic resistant features. Nowadays, during routine rehabilitation there is a need to assess the seismic vulnerability of such bridges. If the strength and ductility capability is deemed inadequate it is necessary to develop appropriate and economical seismic retrofit measures.

241

Some 80% of the existing bridges constructed in the eastern and central United States consist of slab-on-girder spans supported by multiple-column pier bents. The columns of these piers generally possess only nominal transverse reinforcement: #3 or #4 hoops at 12″ centers (10 *mm* or 12 *mm* hoops at 300 *mm* centers). Due to the minimal amount of transverse column steel, the current ATC 6-2[2] based seismic evaluation techniques generally predict shear-brittle column behavior with no ductility capacity. The current vogue in the eastern United States is to remedy this perceived weakness by providing a Californian-style steel jacket retrofit to the columns[3], with the remainder of the pier bent being left untouched. More recent seismic evaluation recommendations would indicate vulnerable joint zones, but recommend few options for improving seismic resistance.

The seismic retrofit study presented in this paper is based on a typical eastern US style pier bent. The pre- and post-retrofit behavior of a one-third scale model pier and a companion full-scale prototype cap-beam-to-column subassemblage is experimentally investigated. The prototype specimen had been removed during the decommissioning of a 30 year old two span slab-on-girder bridge located at Niagara Falls, New York. The subassemblage specimen was tested to failure under quasi-static loading in the seismic lab at the State University of New York at Buffalo. Much of the damage in that full-sized specimen was located in the joint core itself; the column remaining mostly undamaged. The present research study deals with the capacity redesign and retrofit of the damaged connection regions to ensure improved seismic performance. This has been achieved by jacketing the existing cap beam with high strength concrete and providing longitudinal prestress to ensure that the cap beam remains elastic at all times, thus enforcing plastic hinging to occur in the column adjacent to the cap beam.

Pier-Bent Model Study

The one-third scale model pier bent was constructed and tested under quasi-static reverse cyclic loading. Dimensions of the pier are shown in Fig. 1. Note that load cells were placed at mid-height of the columns to measure the proportion of resistance in each column. The model was tested under quasi-static reverse cyclic loads with drift angles up to 5%.

Test results show that this pier behaved quite well with a moderate degree of ductility. In spite of inadequate transverse reinforcement the columns were capable of sustaining the 5% drift amplitude with little sign of distress. The failure mode was due to inadequate anchorage of the longitudinal column steel in the cap-beam-to-column connections. Due to inadequate joint core shear reinforcement as shown in Fig. 2(a), these joints also exhibited shear failures as seen by the extent of cracking in Fig. 2(a). This actual failure mode was not predicted by the current ATC 6-2[2]-based evaluation techniques. That evaluation method predicted a shear brittle column with no ductility capacity due to the inadequate transverse reinforcement.

The maximum observed cap beam-to-column joint shear stress demands arising from column flexure were $5.3 \sqrt{f'_c}\,(psi) = 0.44 \sqrt{f'_c}\,(MPa)$ and $4.5 \sqrt{f'_c}\,(psi) = 0.38 \sqrt{f'_c}\,(MPa)$ for the exterior and interior joints, respectively. From the experimental results it was evident that this level of joint shear stress, although only modest, cannot be sustained for a significant number of load cycles.
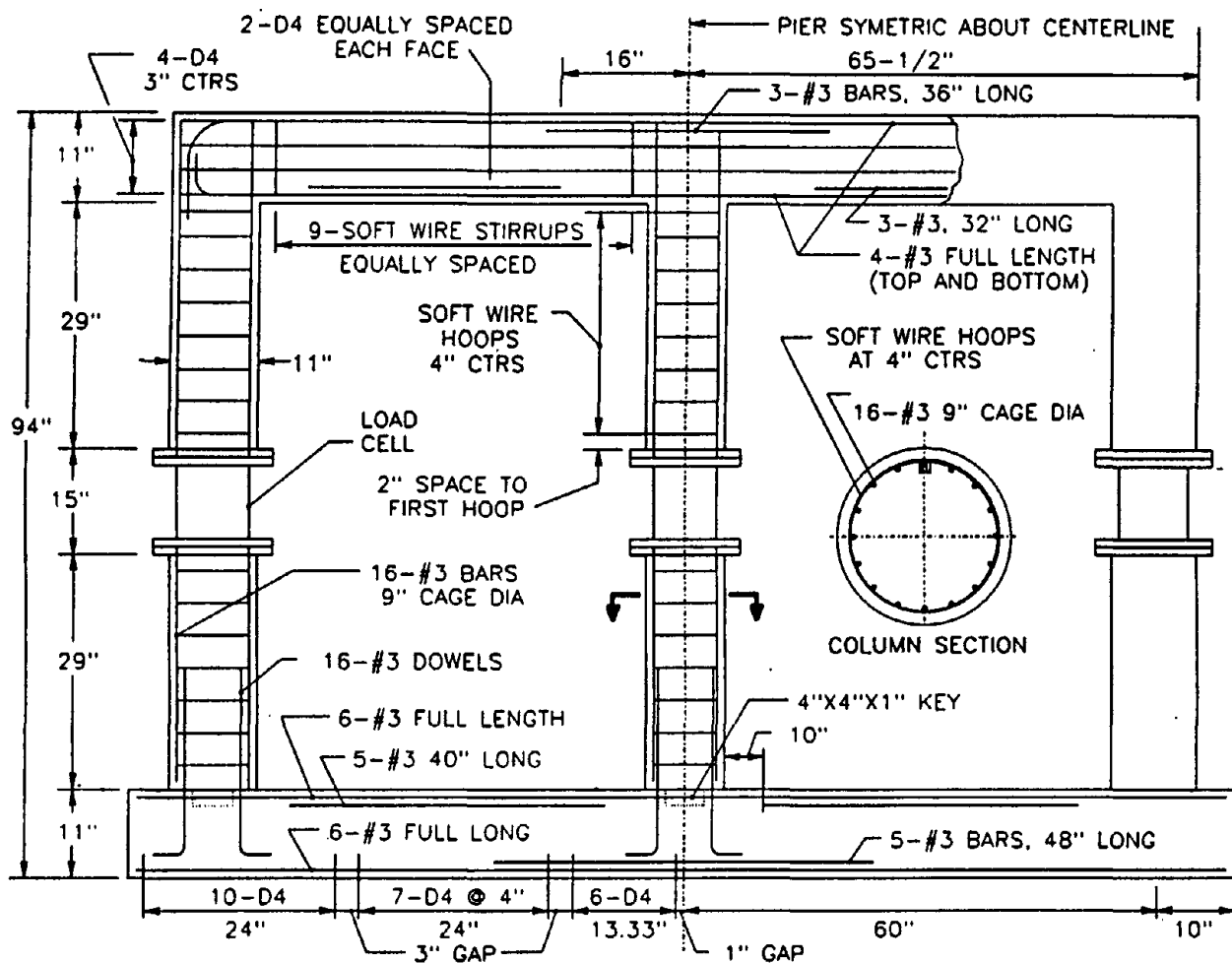
Fig. 1: Dimensions of the One-Third Scale Model Pier Bent

Failure of the spread footing was similar to the cap beam with little distress being evident in the column lap-splice as might be expected.

RETROFIT OF THE PIER-BENT MODEL

It was evident that due to the failure of the connection zones, traditional California-type steel jacketing retrofits would be detrimental to the performance rather than providing any improvement in seismic resistance. Such a retrofit would only place a higher shear demand on the joint zones. As the columns exhibited a reasonable measure of ductility, these were left untouched and the pier was retrofitted by jacketing the capping beam and providing longitudinal prestress to enhance column rebar anchorage and improve the joint core shear capacity. From that figure it will also be noted that the spread footing was strengthened as shown in Fig. 2(b) by casting a new beam around the column lap splice zone. This effectively overcame any potential column anchorage problems and moved the plastic hinge into the column above the lap splice.

120″

60″   60″

11′

29′   11′

15′

LOAD CELL

29′

11′

* HATCHED PART DENOTES SPALLED CONCRETE
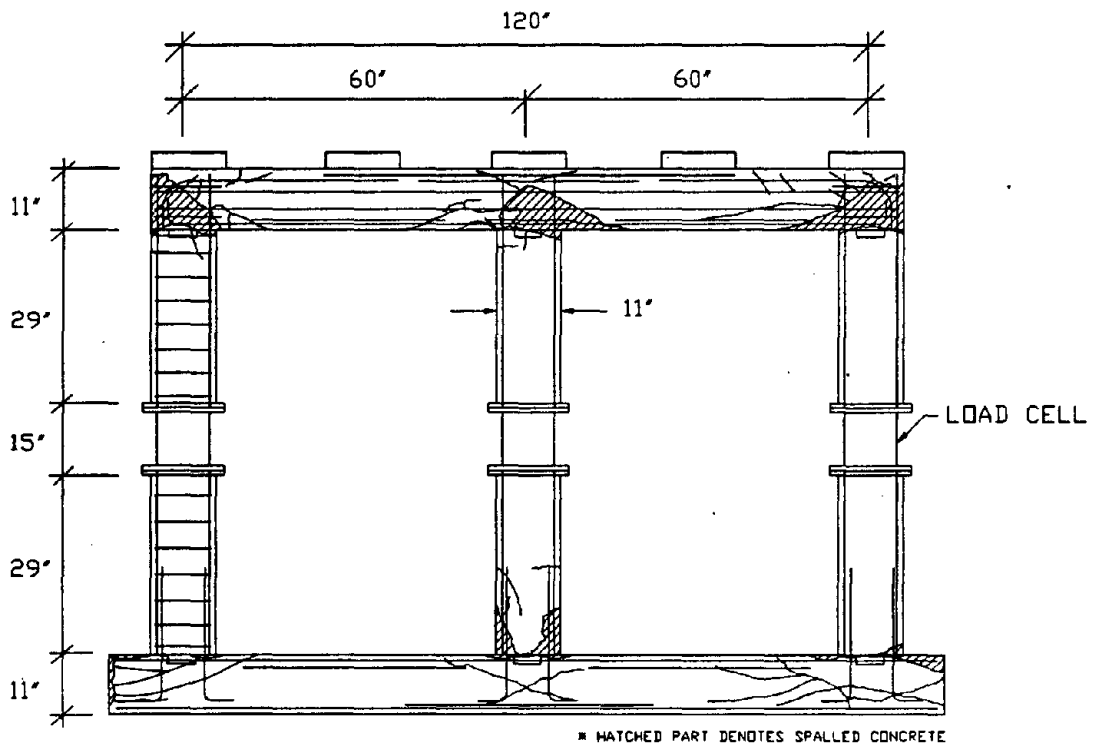
(a) DAMAGED BRIDGE PIER BY CYCLIC LOADING

LONGITUDINAL PRESTRESSING

2′
11′
2′
4′

P.S.C. JACKET

NEW FOUNDATION BEAM

15′

11′
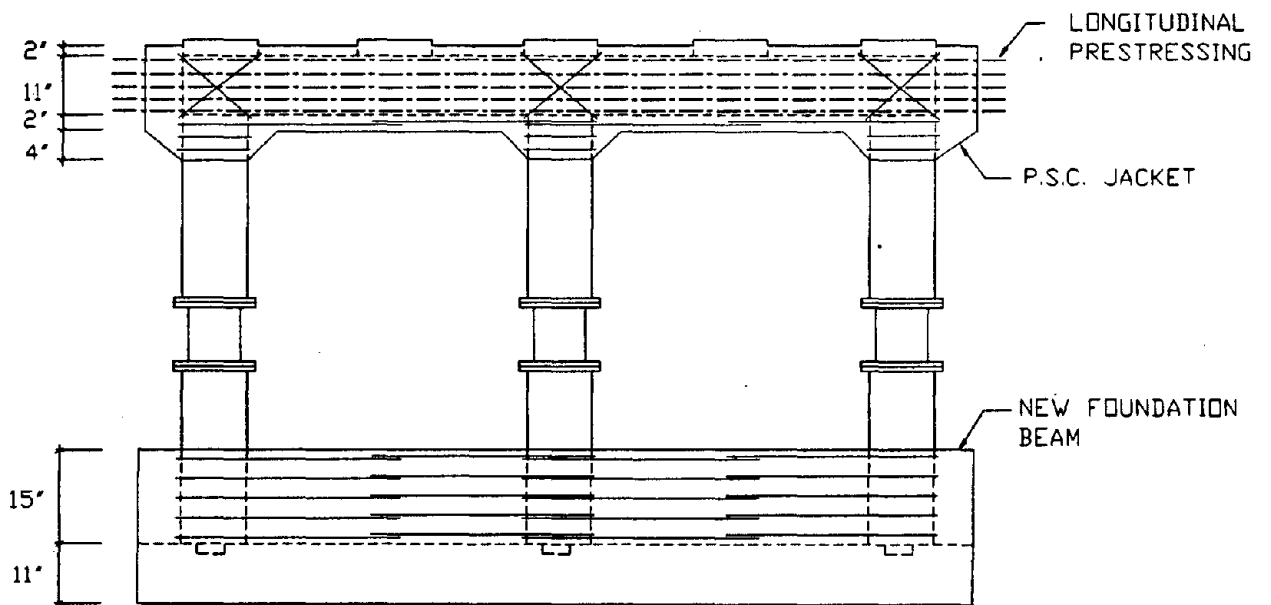
(b) RETROFITTED BRIDGE PIER

Fig. 2: Retrofit of the One-Third Scale Model Pier Bent

244

The specimen was retested following the same displacement path as before that is two cycles at nominal column drift angle of 0.5% , 1% , 2% , 3% , 4% and 5%. The retrofit demonstrated that it is possible to relocate the damaged regions from the joint core to plastic hinges in the column end zones. The columns finally failed prematurely in shear due to the presence of the load cells. Had these not been present, then failure would have been somewhat delayed.

The hysteretic performance before and after retrofit is presented in Fig. 3. It is evident that the retrofit is capable of changing the failure mode. The increase in strength is due to the shorter clear length of the columns. This also places a higher shear demand on the columns. With hindsight this was a poor feature of the retrofit. Instead of using a continuous beam cast around the column, it is considered desirable to retrofit the column lap splice zone as described in what follows.

RETROFIT OF COLUMN LAP-SPLICE ZONES

The retrofit of the splice zone in existing reinforced concrete columns can be achieved by reducing the shear demand, rather than increasing it as a by-product of retrofitting other regions, as mentioned above. One way of doing this is to cut the existing longitudinal steel within the lap splice zone, and then casting a reinforced concrete collar around the base of the column. This provides a rocking bridge column that should theoretically behave in a bilinear-elastic fashion. The size of the collar is proportioned such that the column is designed to remain elastic beneath the cap beam hinge. The "rocking" moment capacity of the column is given by

$$M_{rocking} = FH = PB \tag{1}$$

where F = lateral load or shear on the column, H = height from the rocking toe to the point of inflection, P = axial load and B = semi-base width which is the distance from the centroid of the column to the pivot point at the toe of the collar.

To investigate this approach one column was constructed and tested under cyclic lateral loading at increasing amplitudes up to column drift angles of 10% . The specimen is shown in Fig. 4(a) with the hysteretic response plotted in Fig. 4(b). Although this specimen is theoretically bilinear elastic as superimposed in Fig. 4(b), it is evident that significant energy was dissipated. The energy dissipation is ascribed to Coulomb friction between the lower column segment and the adjacent collar. The magnitude of friction between the silicone coated old concrete and the newly poured collar can be determined by considering the rigid body kinematics as follows.

Horizontal equilibrium requires that

$$F = \alpha F + R_h \tag{2}$$

where F = applied lateral load (column shear), R_h = horizontal component of the reaction at the toe, and α = proportion of the lateral load (shear) resisted in bearing at the interface of the old column base and the new collar. If the concrete collar is seated on a soft material with a low shear stiffness such as rubber or lead, then displacement compatibility at the base requires that most of the horizontal shear be resisted by bearing, thus $\alpha \rightarrow 1$.
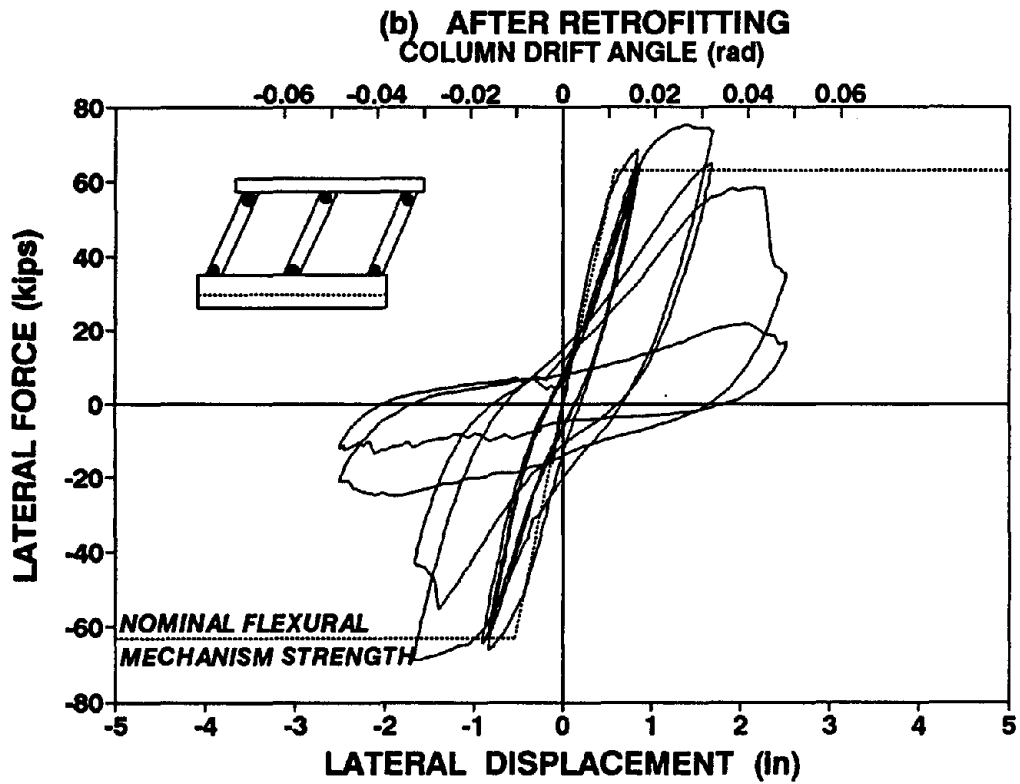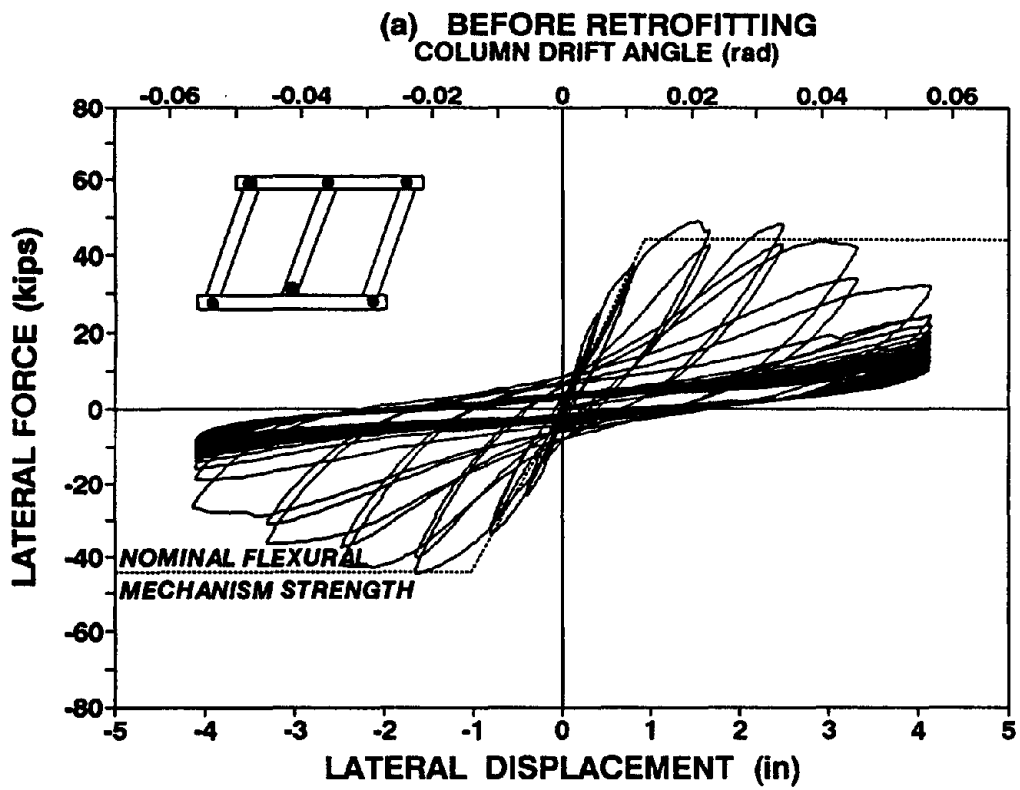
Fig. 3: Lateral Force - Displacement Hysteretic Performance of the
One-Third Scale Model Pier Bent

P = 45 Kips

F

Detail A

H = 49"

42"

12"

20"

18"

72"

D = 11"

Reinforced
Concrete
Collar

Saw Cut
Through
Longitudinal
Steel

$\mu\alpha F$

αF

B

R_h

R_v

Detail A
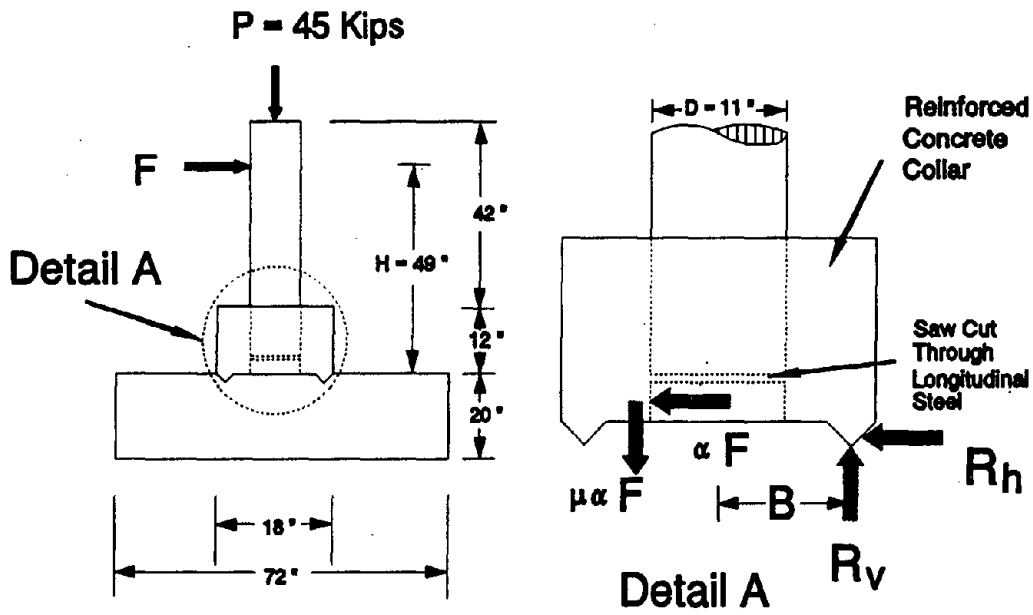
(a) "ROCKING" RETROFIT OF LAP SPLICE ZONE

(b) FORCE DRIFT RELATIONSHIP

THEORETICAL FORCE

PUSH

PULL

LATERAL FORCE F (KIPS)

COLUMN DRIFT ANGLE (%)

Fig. 4: A "Rocking" Retrofit of a Lap Splice Zone at the Base of a Column.

247

Moment equilibrium on uplift about the toe requires

$$F H = P B + \mu \alpha F (B + 0.5 D)$$ (3)

where D = column diameter, and μ = coefficient of friction. Thus from Eq. (3)

$$F = \frac{P B}{H - \mu \alpha (B + 0.5 D)}$$ (4)

By back calculation from the test results, it was found that $\mu \alpha$ = 0.56. This value of friction for the concrete-silicone interface is a relatively low value for friction associated with concrete, but if desired could be enhanced or reduced with careful detailing.

The resulting quasi-dynamic response, part of which is shown in Fig. 4(b), was very stable for a large number of cycles up to 10% drift amplitudes. Some minor deterioration in strength was evident due to cover spalling at the toe of the collar, but this could be remedied with improved detailing.

PRE-RETROFIT SEISMIC PERFORMANCE OF THE PROTOTYPE CAP BEAM TO COLUMN KNEE JOINT

The cap beam and exterior column of a full scale pier bent was retrieved from a 30 year old bridge located in Niagara Falls, New York. A self-equilibrating reaction frame was constructed and attached to the subassemblage specimen as shown in Fig. 5. Quasi-static reverse cyclic load testing (similar to the one-third scale model test) was applied to the prototype subassemblage. The resulting behavior was quite similar to the one-third scale model with the damage predominantly located in the joint zone. This damage was due to pull-out (bond slip) of the longitudinal joint steel. Due to the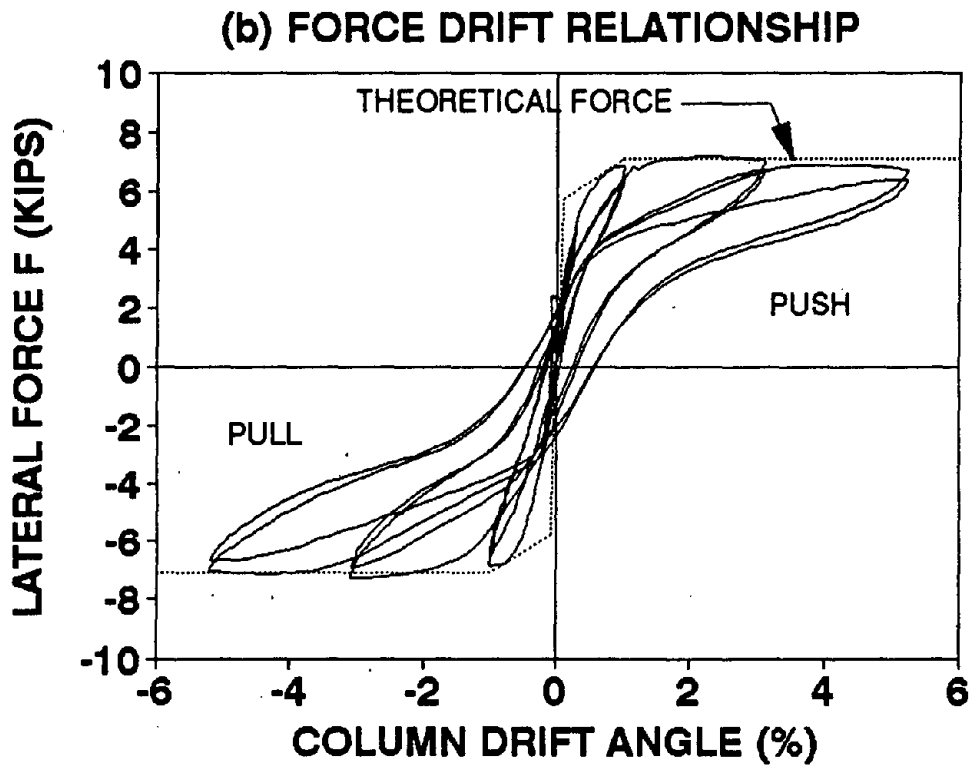 inadequate amount of transverse reinforcement within the joint, there was also considerable joint shear strength deterioration as evidenced by the badly cracked concrete joint core.

In spite of the absence of ductile steel detailing and the lack of a capacity design approach used for this class of bridge pier, it is evident that a moderate degree of ductile behavior can be obtained. However for tall pier bents that support important bridge structures, the displacement demands in severe earthquakes may be quite large. Under these special circumstances, retrofitting may be desirable. As mentioned previously, a steel jacket retrofit would not improve the present situation for strengthening of the capping beam to ensure a strong beam/weak column behavior. A dependable elastic joint has been chosen as the desired retrofitting solution and this is described in what follows.

SEISMIC PERFORMANCE OF PROTOTYPE RETROFIT

The full-scale subassemblage was retrofitted by using a high strength concrete jacket around the existing cap beam. Post-tensioning was applied to ensure the joint core remained elastic at all times. The advantage of using this retrofit technique is that the anchorage resistance of the longitudinal column steel can be improved by the slight increase in anchorage length and also the clamping effect arising from the applied prestress. Details of the retrofitted specimen are shown in Fig. 5. The longitudinal prestress was provided by ten 1″ diameter high strength (Dywidag™) threadbars. The post-tensioned force was 1000 kips giving a prestress of 494 psi (3.4 MPa).

248

The retrofitted prototype specimen was retested by following the same displacement path used previously (for both the prototype and the one-third scale model). The performance of the prototype specimen before and after retrofitting is shown in Fig. 6. It is evident from the two graphs that the strength in the "pull" direction increased somewhat due to the shorter clear column length in the retrofitted specimen. In the "push" direction, however, the strength did not increase significantly as a result of the retrofit/repair. This is attributed to the previous loss of bond to the anchorage of the longitudinal steel on the inside of the knee joint. It is evident that this was not repaired as effectively as the reinforcement on the outside of face of the joint. The modified flexural strength reflects the reduced tension capacity of the longitudinal steel on the concealed inner side of the joint.
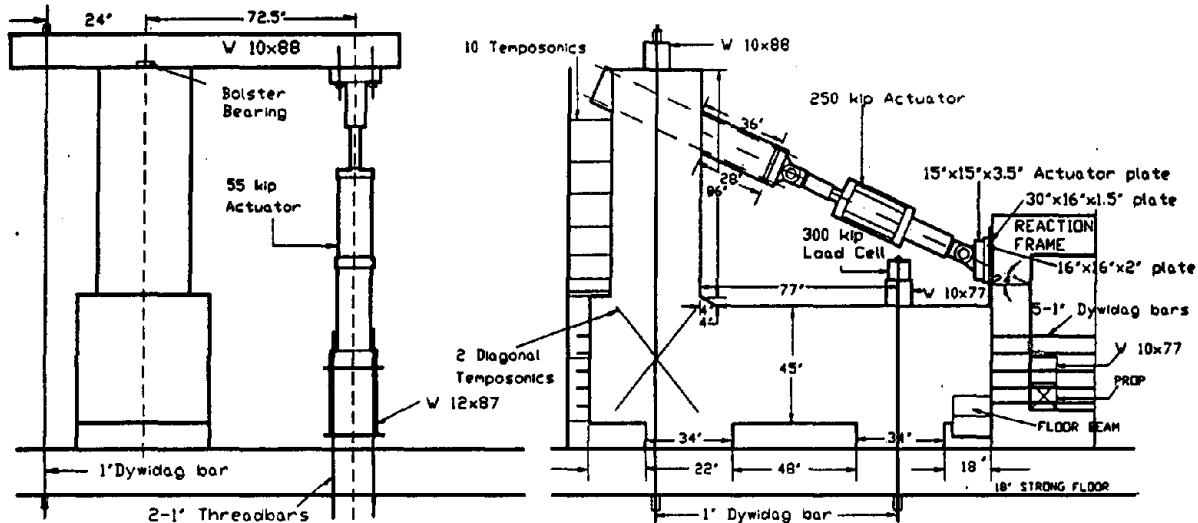
(a) TEST SETUP FOR VIRGIN AND RETROFITTED SPECIMEN
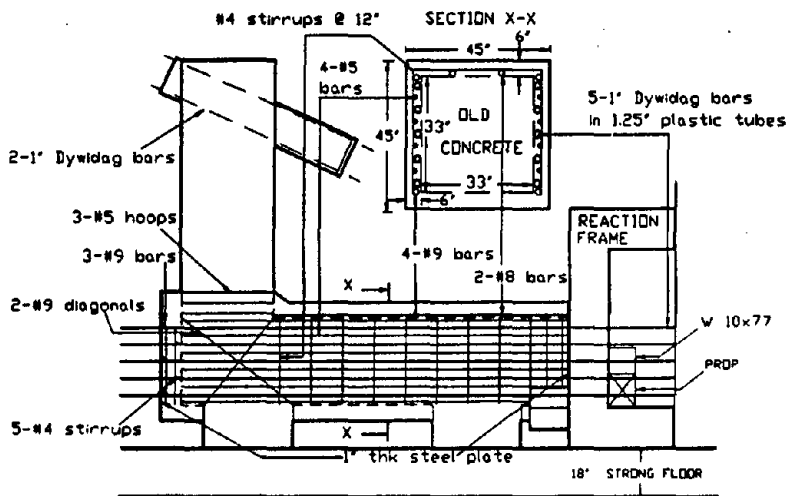
(b) REINFORCEMENT DETAIL FOR CAP BEAM RETROFIT

Fig. 5: Testing of the Prototype Specimen Before and After Retrofit, Showing (a) the Test Set-Up, and (b) the Retrofit Details.

249

Fig. 6: Hysteretic Behavior of the Prototype Specimen Before and After Retrofit

250

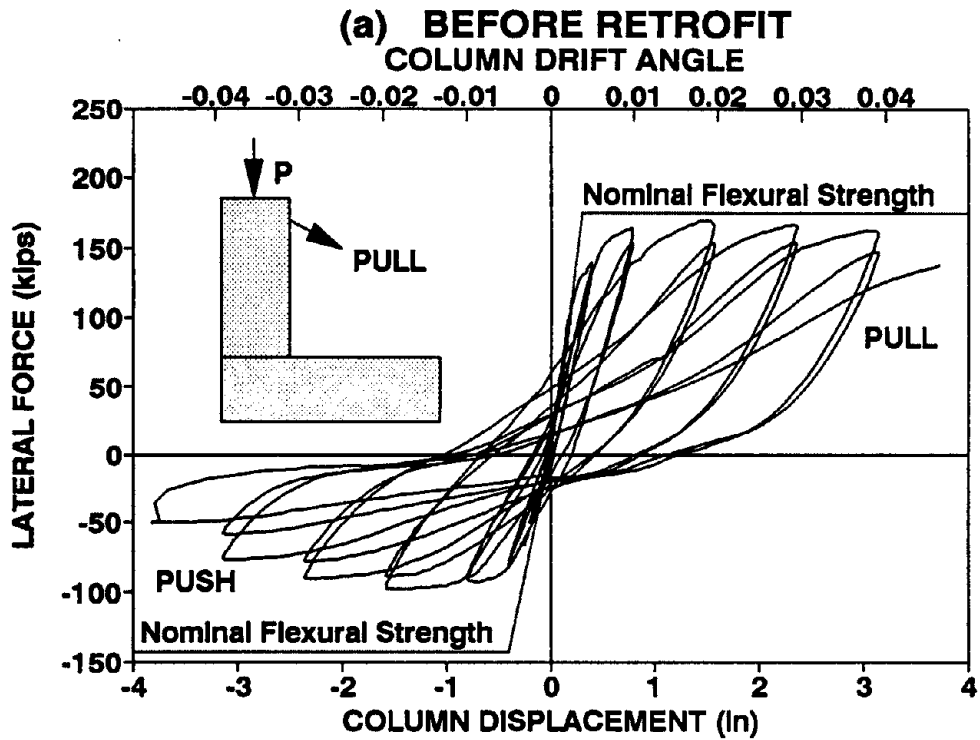Incipient failure for the retrofitted specimen was at a drift amplitude of +5% when large diagonal shear cracks developed in the pull direction. Following the formation of these cracks, a large demand was placed on the circular hoops which progressively fractured after the third loading cycle at the +5% drift amplitude.

The results of this full-scale test confirmed that the retrofit method was particularly effective in moving the failure zone out of the knee joint and into the column. Apart from some superficial cracking of the cap beam outside the joint zone, the cap beam and joint zone remained elastic throughout the test. It should be noted that the bond problems mentioned above would not normally be an issue for a retrofitted underlined specimen.

SEISMIC RETROFITTING RECOMMENDATIONS FOR PIER-BENTS WITH CRITICAL JOINTS

The capacity design philosophy for new structures enables the designer to select a desirable hierarchy of failure mechanisms for framed structures. Regions not participating in the primary energy dissipating mechanism have a measure of capacity protection by providing overstrength to those regions. In principle, a plastic mechanism is chosen such that the necessary overall displacement ductility can be developed that leads to the smallest inelastic rotational demands in the plastic hinges. For building frames this generally leads to a beam sidesway mechanism with strong columns and weak beams. Thus, soft story mechanisms are avoided as the rotational demands on the columns are excessive. For bridges, however, it is generally not possible to avoid a column sidesway mechanism. Therefore, the plastic hinge regions within columns need to be carefully detailed to ensure ductile behavior.

The capacity design philosophy can be adapted and applied to the seismic retrofit and/or repair of existing gravity load designed bridge piers. The procedure will be referred to herein as *capacity analysis and redesign*. The average gravity load inducing axial stress in non-seismically designed bridge piers existing in eastern United States is often low ($P_e < 0.1 f'_c A_g$). Moreover, ductility demands on columns arising from a column sidesway mechanism may not be excessive, particularly in zones of low to medium seismicity such as the central and eastern United States. Plastic hinge zones in such columns may have sufficient inherent ductility capacity to withstand the ductility demand. This means that in accordance with capacity design principles, those areas not participating in the primary energy dissipating mechanism should have a measure of capacity protection to ensure elastic behavior. This may require some retrofitting of those areas. Thus the primary objectives in *capacity analysis and redesign* for existing gravity load designed bridge piers are three: (i) To enhance the shear strength capacity and bond strength of the longitudinal column bars at the cap beam-column joint; (ii) To upgrade the ductility capacity of the column hinges at ground level, particularly if a lap-splice is present and improve the column-foundation joint; (iii) To ensure that columns possess sufficient ductility capacity to withstand expected rotational demands. The foregoing order in principle reflects the order of importance. If all upgrading features cannot be implemented in the redesign stage, then it is suggested that the most important aspects be tackled first.

Capacity Analysis of Columns
The first step in the procedure is to determine the flexural overstrength capacity of the columns in the bridge pier. This is then used as a basis of evaluating the weak links within the designed hierarchy of failure mechanisms. The column overstrength moment capacity may be

assumed to be[5]: $M_p = (6/5) \times 1.25 M_n^{col} = 1.5 M_n^{col}$, where M_n^{col} = nominal flexural strength of the column.

The retrofit schemes presented herein assume that the existing columns, by virtue of their low axial load levels, possess sufficient ductility capacity to withstand the modest seismic demands imposed on them in low to moderate seismic risk zones such as the eastern and central United States. Furthermore, it is assumed that the columns are sufficiently slender ($M/Vd > 2.5$) so that the shear strength demand is smaller than the capacity. In any case the strength and ductility capacity should be assessed.

Redesign of Cap Beam

Since the existing pier cap beam has sufficient strength to sustain gravity load, the capacity redesign process need only consider additional seismic force due to column overstrength. Two solutions are possible for cap beam redesign; either an ordinary reinforced concrete jacket, or a prestressed concrete jacket. The prestressed concrete solution is preferred as it provides superior shear resistance and bar anchorage, but most importantly is more easily constructed. The magnitude of the required cap beam prestress force (P_p) can be determined from an elastic stress analysis using a maximum allowable[5] tension stress of f_t, as follows:

$$M_p < f_t \frac{bh_b}{6} + P_p \frac{h_b}{6}$$ (5)

where $f_t = 12\sqrt{f'_c}(psi) = \sqrt{f'_c}(MPa)$, b = width of cap beam and h_b = the cap beam depth.

The shear force applied to the cap beam can be determined from the overstrength plastic column-elastic beam mechanism. If sufficient prestress is applied to the cap beam, then additional transverse reinforcement may not be needed. The uncracked shear capacity of a prestressed concrete beam may be assessed from the code[5] equation $v_{cw} = 3.5\sqrt{f'_c}(psi) + 0.3 P_p / (bh_b)$. If this stress is exceeded then the cap beam should be detailed in accordance with the principles of reinforced concrete design.

Shear Strength of Cap Beam-Column Joint

From the plastic column-elastic beam mechanism it can be shown from geometry and force equilibrium the vertical shear force demand can be computed for vertical force interior and exterior, respectively:

$$V_{jv(i)} = \frac{M_p}{jd}\left[1 - 1.5jd\frac{l_c + h_b}{l_b l_c}\right]$$ (6)

$$V_{jv(e)} = \frac{M_p}{jd} - \frac{P_e}{2}$$ (7)

where $jd = z_c = d - d' \approx 0.8 D_c$ = internal moment arm in column section, D_c = diameter for a circular column, P_e = column axial load, and subscripts (i) and (e) denotes interior and exterior, respectively. Again, V_{jv} may be resisted by the prestressed concrete if the cap beam is post-tensioned where the capacity can be assessed from the equation[5]

252

$$V_{ju} = 3.5\sqrt{f'_c}\,b_w d + 0.3P \qquad\qquad (8)$$

where V_{ju}= elastic shear strength of a prestressed concrete beam. If $V_{jv} > V_{ju}$ then the joint is liable to crack. The joint should then be redesigned and detailed as a conventional reinforced concrete system, with the joint shear being resisted by concrete strut and reinforcing steel truss mechanisms. respectively. Capacity design procedures of such reinforced concrete joints may be found in Paulay and Priestley[6].

Anchorage of Flexural Reinforcement: Cap Beam Anchorage

In most of the gravity load designed columns of existing highway bridge construction the longitudinal column bars are anchored into the cap beam with a relatively short straight anchorage. Under reverse cyclic loading during earthquake ground motions yielding of those bars in the column penetrates into the anchorage zone. Pullout may result after a number of cycles of loading. It is, therefore, generally necessary to enhance the anchorage of these bars. The development length may be enhanced by providing a fillet between the column and cap beam as shown in Fig. 5(b). Longitudinal prestress may also be used to enhance the pullout resistance of the bars. Theoretical conditions pertaining to the amount of prestress and fillet size is presented in what follows.

It is well known that the bond phenomena is provided by a combination of chemical adhesion of the concrete to the steel reinforcement bars, mechanical resistance from the deformation lugs, and frictional resistance. The frictional resistance which becomes effective at the final stage can be idealized as a Mohr-Coulomb failure criteria. Initially resistance is mobilized by chemical adhesion. This is soon destroyed when the bond stress increases resulting in bond slip particularly under cyclic loading. Mechanical bearing of the lugs then plays a major role in resisting the applied bar forces until the concrete between successive lugs begins to fail in sliding shear. Following this stage, bond resistance is provided by friction between the ribs and the surrounding concrete. The frictional resistance is due to the existence of either passive or active confinement.

Previous researchers have performed extensive experimental work on bond resistance under laterally confining pressure. However, much of the data is scattered through a wide range and a careful interpretation for seismic design purposes is required. According to the report of ACI Committee 408[7], the straight anchorage terminating in external beam-column joints subjected to large load reversals is given by

$$l_d = (f_y d_b) / \left(25\sqrt{f'_c\,(psi)} \right) \qquad\qquad (9)$$

where l_d = development length of the bar and d_b= bar diameter. Therefore, the residual (passive) bond stress implied by Eq. (9) is $u_o = 6.25\sqrt{f'_c}\,(psi)$. Where a reasonable confinement can be expected, the bond strength can be represented by assuming a Mohr-Coulomb failure criteria:

$$u_b = u_o + \mu f_{ps} \qquad\qquad (10)$$

where μ = frictional coefficient, and f_{ps}= externally applied normal pressure/prestress. Based on the previous research work described in Refs 8 to 10, a residual coefficient of friction of $\mu = 0.25$ can be assumed. The dependable pull-out stress (f_b) of a deformed reinforcing bar is

therefore computed from

$$f_b = (4\,u_o + 2.55\,\mu\,f_{ps})\,l_{em}\,/\,d_b \qquad (11)$$

where l_{em} = the provided embedment length of the bar. Using the aforementioned parameters for u_o and μ in this equation gives a design relationship:

$$f_b = \left(25\sqrt{f'_c\,(psi)} + 0.64\,f_{ps}\right) l_{em}\,/\,d_b \;\; > \;\; 1.25 f_y \qquad (12)$$

The dependable pullout capacity is thus provided by choosing appropriate values of f_{ps} and l_{em}.

Anchorage of Flexural Reinforcement: Lap Splice Zone at Base of Columns

Experimental work by Paulay[11] has shown that lap splices can sustain large plastic hinge rotations if sufficient transverse reinforcement is provided to properly clamp the splice bars together. A retrofit may use this technique, however, removal of existing concrete cover to enable the new hoops to be placed tightly around the longitudinal steel is a difficult task. Alternatively, steel jacketing may be used in the lap splice alone. This method has been used extensively in California and is described in Ref. 3. However, the use of steel casings in the northeastern and midwestern states should be applied with caution owing to the severe corrosion problems associated with deicing salts. It is therefore advocated that the lap splice zone be eliminated (also strengthening a weak spread footing) by casting a new reinforced concrete foundation beam around the existing column-splice/starter bars. This retrofit option should only be used if the columns have a dependable shear capacity at flexural overstrength, otherwise the following option is recommended.

A rocking base connection can be formed as a retrofit alternative by cutting the existing longitudinal reinforcement above the footing/pile cap level and casting a reinforced concrete collar around the lap splice zone. This reduces the shear demand and makes a very ductile bilinear elastic mechanism with the ability to dissipate some energy through Coulomb friction and radiation damping as given by Eq. (4).

CONCLUSIONS

The following conclusions are drawn from this study:

1.   Existing non-seismically designed bridge piers that have columns with low levels of axial load ($P_e < 0.1 f'_c A_g$) generally possess sufficient ductility capacity to withstand moderate earthquakes, in spite of the absence of transverse confining reinforcement.

2.   The joint connections of existing pier bents tend to be the weak zones due to the absence of a capacity design and detailing philosophy. Thus the currently fashionable steel jacketing column retrofits help little, if at all, in such situations.

3.   The cap beam to column joint zones of existing pier bents may be effectively retrofitted by casting a high strength concrete jacket around the existing cap beam. Longitudinal prestress is provided to: (i) enhance the cap beam flexural strength (enforcing a strong beam-weak column ductile mechanism); and (ii) improve the joint shear strength and anchorage of the longitudinal column reinforcement.

254

4.   Lap splice zones at the base of the columns may be eliminated by either: casting a new strong beam over the existing spread footing/pile cap thus moving the column's plastic hinge zones above the splice; or forming a "rocking" column by making a circumferential cut through the existing lap splice zone and casting a reinforced concrete collar around the column, the collar being sized to provide an appropriate moment capacity.

Acknowledgements

REFERENCES

1.   AASHTO, "Standard Specifications for Highway Bridges", Fifteenth Edition, American Association of State Highway and Transportation Officials, Washington, D.C., 1992.

2.   ATC 6-2, "Seismic Retrofitting Guidelines for Highway Bridges", Applied Technology Council, 1983.

3.   Chai, Y.H.; Priestley, M.J.N; and Seible, F., "Seismic Retrofit of Circular Bridge Columns for Enhanced Flexural Performance", ACI Structural Journal, V. 88, No. 5, pp.572-584, Sept.-Oct. 1991.

4.   NCEER Report to FHWA and US Congress, "Seismic Retrofitting Manual for Highway Bridges," prepared by the National Center for Earthquake Engineering Research, State University of New York at Buffalo, NY, November 1993.

5.   ACI Committee 318, "Building Code Requirements for Reinforced Concrete and Commentary (ACI 318-83)", American Concrete Institute, Detroit, 1983.

6.   Paulay, T. and Priestley, M.J.N., Seismic Design of Reinforced Concrete and Masonry Structures, John Wiley and Sons, Inc., New York, 1992.

7.   ACI Committee 408, "Abstract of: State-of-the-Art-Report: Bond under Cyclic Loads", ACI Materials Journal, V. 88, No. 6, pp. 669-673, Nov.-Dec. 1991.

8.   Hungspreug, S., "Local Bond Between a Steel Bar and Concrete Under High Intensity Cyclic Load", Ph.D. Dissertation, Cornell University, Ithaca, New York, 1981.

9.   Eligehausen, R.; Popov, E.P.; and Bertero, V.V., "Local Bond Stress-Slip Relationships of Deformed Bars Under Generalized Excitations", Report No. UCB/EERC 83-23, Earthquake Engineering Research Center, University of California, Berkeley, California, 1983.

10.   Malvar, L.J., "Bond of Reinforcement Under Controlled Confinement", ACI Materials Journal, V. 89, No. 6, pp. 593-601, Nov.-Dec. 1992.

11.   Paulay, T., "Lapped Splices in Earthquake-Resisting Columns" ACI Journal, Title No. 79-44, pp.458-469, 1983.

SECOND U.S.-JAPAN WORKSHOP ON SEISMIC RETROFIT OF BRIDGES

A Stress-Strain Model for
Reinforced Concrete Bridge Piers
Confined by Hoop Reinforcement
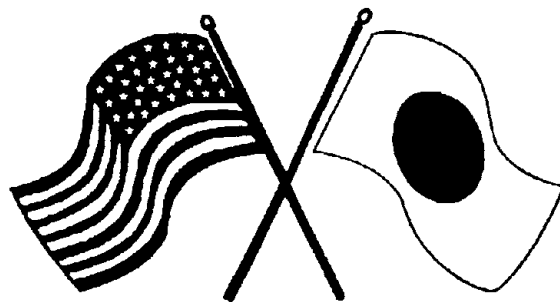
J. Hoshikuma, K. Kawashima and K. Nagaya

A STRESS-STRAIN MODEL FOR REINFORCED CONCRETE BRIDGE PIERS CONFINED BY HOOP REINFORCEMENT

J. Hoshikuma[1], K. Kawashima[2] and K. Nagaya[3]

1) Research Engineer, Earthquake Engineering Division, Public Works Research Institute, Ministry of Construction, Tsukuba Science City, Japan
2) Head, ditto
3) Assistant Research Engineer, ditto

ABSTRACT

In this paper, a stress-strain model of concrete which takes account of confinement effect is proposed based on a series of loading tests for reinforced concrete column specimens, with circular and square cross section, containing various hoop reinforcement. Predominant factors for controlling the stress-strain relation of the concrete columns were examined, and the stress-strain model consisting of an exponential function and a straight line was proposed. The predicted relation provides better agreement with test results than the previous models.

INTRODUCTION

A large seismic lateral force causes reinforced concrete bridge piers to be in inelastic range. However, the confinement associated with hoop reinforcement increases the ductility and the energy absorption of reinforced concrete bridge piers. It is, therefore, significant to incorporate the effect of hoop reinforcement into seismic design to evaluate the ductility of reinforced concrete bridge piers.

This paper proposes a stress-strain model of confined concrete which can be used in seismic design of reinforced concrete bridge piers. To examine the effect of confinement on ductility of concrete, a series of loading tests of confined concrete columns were conducted and modeling of the stress-strain curve is clarified.

BACKGROUND OF THE RESEARCH

Previous Researches

Prof. Park and other researchers have already made significant researches on the confinement effect on ductility of concrete. **Table 1** compares typical previous

Table 1 Review of Stress−Strain Model for Confined Concrete

Proposer	Stress−Strain Model for Confined Concrete			Applicable Cross Sectional Shape
	Ascending Part	Descending Part	Residual Stress	
Park	$f_c = K f_{co} \left\{ \dfrac{2\varepsilon_c}{0.002K} - \left(\dfrac{\varepsilon_c}{0.002K} \right)^2 \right\}$	$f_c = K f_{co} \{ 1 - Z_m (\varepsilon_c - 0.002K) \}$	20% of maximum stress	Rectangle
Sheikh	$f_c = K f_{co} \left\{ \dfrac{2\varepsilon_c}{\varepsilon_{s1}} - \left(\dfrac{\varepsilon_c}{\varepsilon_{s1}} \right)^2 \right\}$	$f_c = f_{cc} \{ 1 - Z (\varepsilon_c - \varepsilon_{cc}) \}$	30% of maximum stress	Rectangle
Mander	$f_c = \dfrac{f_{cc} x r}{r - 1 + x^r}$ where $x = \dfrac{\varepsilon_c}{\varepsilon_{cc}}$, $r = \dfrac{E_c}{E_c - E_{sec}}$			Circle Rectangle Wall
Muguruma	$f_c = E_i \varepsilon_c + \dfrac{f_{co} - E_i \varepsilon_m}{\varepsilon_m^2} \varepsilon_c^2$ and $f_c = \dfrac{f_{co} - f_{cc}}{(\varepsilon_{co} - \varepsilon_{cc})^2} (\varepsilon_c - \varepsilon_{cc})^2 + f_{cc}$	$f_c = \dfrac{f_{cu} - f_{cc}}{\varepsilon_{cu} - \varepsilon_{cc}} (\varepsilon_c - \varepsilon_{cc}) + f_{cc}$	———	Circle Rectangle
Fujii	$f_c = E_i \varepsilon_c + \dfrac{f_{co} - E_i \varepsilon_{co}}{\varepsilon_{co}^2} \varepsilon_c^2$ and $f_c = \dfrac{f_{co} - f_{cc}}{(\varepsilon_{co} - \varepsilon_{cc})^3} (\varepsilon_c - \varepsilon_{cc})^3 + f_{cc}$	$f_c = f_{cc} - E_{des} (\varepsilon_c - \varepsilon_{cc})$	20% of maximum stress	Circle Rectangle

stress—strain models proposed for confined concrete.

In 1971, Park proposed a stress—strain model consisting of a second order parabola and a straight line. In this model, confinement effect was incorporated into the gradient at the stress descending part and the parameters were determined based on the experimental tests by Soliman, Roy and Bertero[1]. In 1982, Park revised the original model by introducing an allowance for the enhancement in the concrete strength due to confinement effect, which was assumed to be proportional to volumetric ratio and yield strength of hoop reinforcement, and inversely proportional to strength of unconfined concrete[2].

Sheikh proposed a stress—strain model idealizing the confinement effect in terms of the peak stress and a confinement effectiveness coefficient[3,4]. The confinement effectiveness coefficient depends on the layout of hoop reinforcement. The gradient at the stress descending part is similarly evaluated with Park's.

Mander proposed a fractional expression which was applicable to both the stress ascending and descending parts[5]. To evaluate the peak stress, confinement effectiveness coefficients for circular, square and wall sections were proposed based on the similar method to Sheikh's. Furthermore, a constitutive model involving a specified ultimate strength surface for multiaxial compressive stresses was used in this model, which enabled to develop a theoretical model without depending on a statistical analysis of test results. This model was found to provide good prediction for the test results[6].

In Japan, Muguruma proposed two second order parabolas for the stress ascending part[7]. A confinement effectiveness coefficient which took account of ineffectively confined core was included to evaluate the confinement effect. An evaluation method for the peak stress and the ultimate strain in terms of the confinement effectiveness coefficient was proposed based on the test results[8].

Fujii proposed a model consisting of a second order curve and a third order curve for the stress ascending part[9]. A confinement effectiveness coefficient which referred to Park was proposed, and the peak stress and the gradient at the stress descending part were formulated by a linear function of the confinement effectiveness coefficient based on a regression analysis of the test results.

Objectives of This Research

It is pointed out that reinforced concrete bridge piers constructed in Japan have largely concrete section and lower hoop reinforcement ratio in comparison with ones constructed in U.S.A. and New Zealand. **Table 2** shows a summary of the previous compressive loading tests for the confined concrete columns to study the effect of confinement. **Table 3** shows a requirement of hoop reinforcement as provided in the Specifications[10]. Although reinforced concrete bridge piers generally have the volumetric ratio of hoop reinforcement of 0.3% to 0.5%, there are few researches in which test specimens with the volumetric ratio of hoop reinforcement of 0.3% to 0.5% were used. A few specimens containing the volumetric ratio of hoop reinforcement of less than 0.5%

Table 2 Test Specimens in Previous Researches

Researcher	Cross Sectional Shape	Size of Specimen (cm)	Volumetric Ratio of Hoop Reinforcement(%)	Remarks
Park[1]	Rectangle	10×15	0.35~1.87	by Soliman, eccentric loaded
		12.8×12.8	2.07~2.39	by Roy
		10×10	1.09~1.81	by Bertero, High strength Concrete
Sheikh[3]	Rectangle	30×30	0.76~2.40	
Mander[6]	Circle	ϕ 50	0.60~2.50	Spiral Reinforcement
	Rectangle	45×45	1.86~1.97	
	Wall	15×70	1.62~7.87	
Muguruma[8]	Circle	ϕ 15	0.76~2.79	Spiral Reinforcement Some Specimens Containing High Tensile Steel
	Rectangle	19.4×19.4	0.40~3.13	
Fujii[9]	Circle	ϕ 15	0.62~4.02	
	Rectangle	15×15	0.62~2.50	

were tested by Park and Muguruma, however, these are special cases because some were subjected to eccentric loading and the others used high tensile steel for hoop reinforcement. Therefore, the previous models are not enough to study the effect of confinement in the range of low hoop reinforcement ratio.

Table 3 Requirement of Hoop Reinforcement

Ratio of Longitudinal Reinforcement p_t(%)	$0 < p_t \leq 0.5$	$0.5 < p_t \leq 1.0$	$1.0 < p_t$
Volumetric Ratio of Hoop Reinforcement ρ_s(%)	0.3	0.4	0.5

In this research, a series of compressive loading tests on hoop reinforcement considering volumetric ratio, spacing and hook configuration of hoop reinforcement as parameters are conducted taking account of Japanese design practice. It is the main purpose of this research to propose a stress—strain model for reinforced concrete bridge piers.

LOADING TEST OF CONFINED CONCRETE COLUMNS

Specimens and Experimental Procedure

The details of the specimens are given in **Table 4**. Both small and large specimens which are designated herein as S Series and L Series were constructed to evaluate the confinement effect in terms of volumetric ratio, spacing and hook configuration of hoop reinforcement. The specimens with square cross section were tested in the S Series (S6 to S10). Specimens L6, L7 and L8 used hoop reinforcement with semicircular, rectangular and sharp—angled hook as shown in **Fig. 1**, respectively. The hook was fabricated in accordance with the Specifications[10].

Photo 1 shows an experimental set—up with 30MN universal testing machine. All specimens were subjected to uniaxial compressive loading under displacement control, and loading rate was set as 1mm/min. The deformation of specimen between top and bottom was measured by linear potentiometers and the longitudinal strain was obtained by dividing the deformation by the height of specimen. To accurately record the stress—strain curve including the stress descending part, dynamic electric instrumentation was used.

Effect of Hoop Reinforcement Ratio

Fig. 2 shows stress—strain curves taking the hoop reinforcement ratio as parameter. In **Fig. 2**, a predicted relation which will be described later is also shown for comparison. Although the initial stiffness of each specimen is approximately equal, the peak stress and the strain corresponding to the peak stress increase as the hoop reinforcement ratio increases. Substantial deterioration of the compressive capacity after the peak stress is also

Table 4 Test Specimens

| Series		Dimension of Specimens (mm)	Strength of Unconfined Concrete (MPa)	Hoop Reinforcement		Volumetric Ratio of Hoop Reinforcement (%)	Hoop Reinforcement Joint
				Material Diameter	Spacing (cm)		
S	S1	$\phi\,200$ h=600	18.5	SR235 $\phi\,6$	15	0.39	Weld
	S2				10	0.58	
	S3				5	1.17	
	S4				2.5	2.33	
	S5				1.25	4.66	
	S6	200 × 200 h=600	23.2	SR235 $\phi\,6$	15	0.39	Weld
	S7				10	0.58	
	S8				5	1.17	
	S9				2.5	2.33	
	S10				1.25	4.66	
L	L1	$\phi\,500$ h=1500	28.8	SD295 D10	15	0.39	Weld
	L2				10	0.58	
	L3				5	1.16	
	L4			SD295 D13	30	0.34	
	L5			SD295 D16	30	0.54	
	L6			SD295 D10	10	0.58	Rectangular Hook
	L7						Sharp−angled Hook
	L8						Semicircular Hook

(a)Semicircular Hook   (b)Rectangular Hook   (c)Sharp−angled Hook
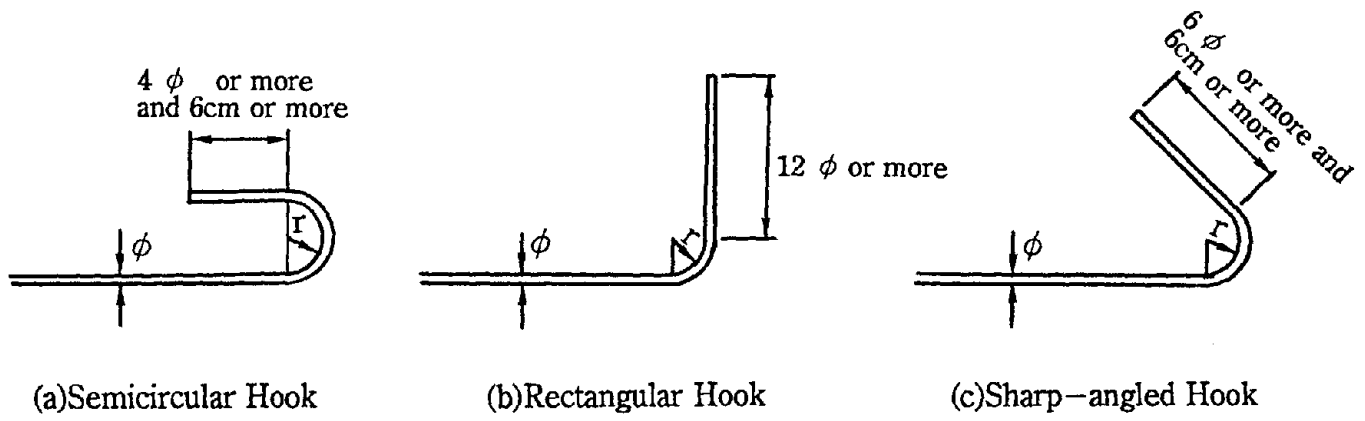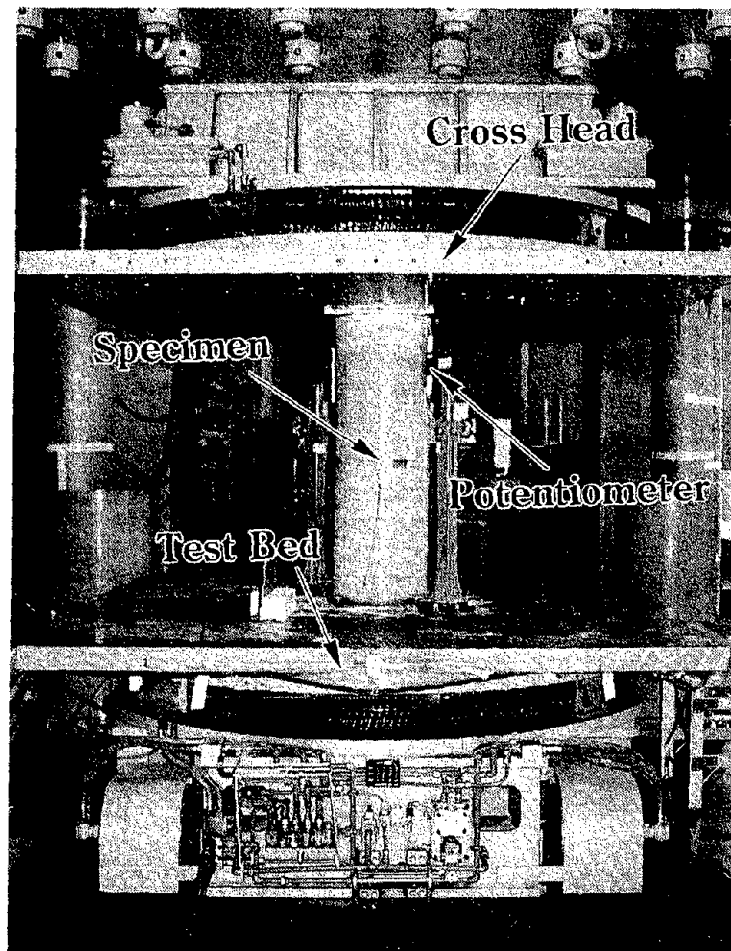
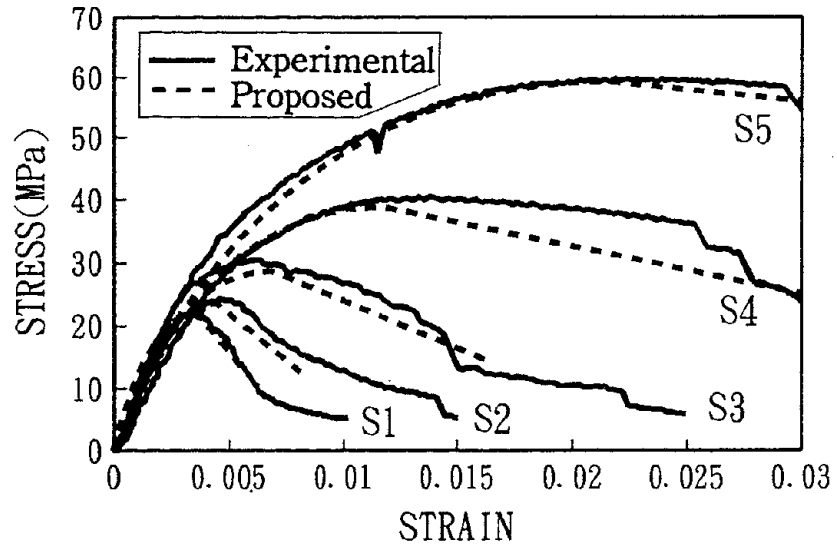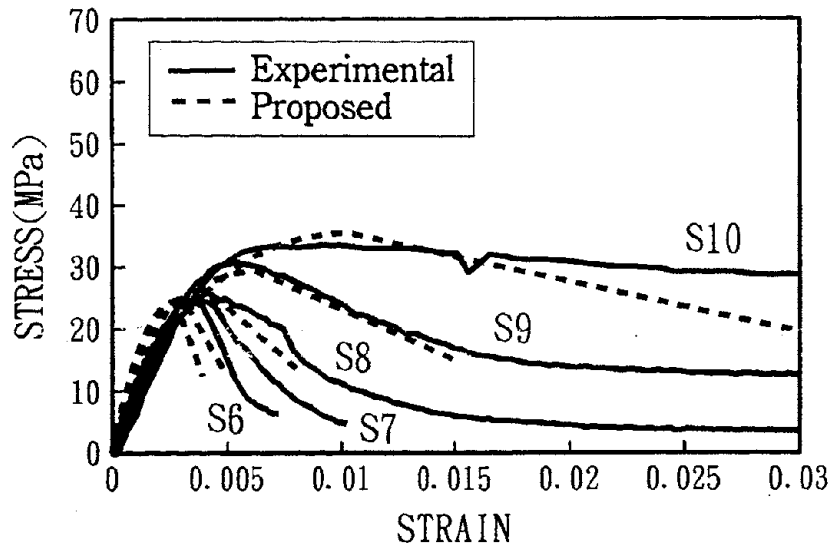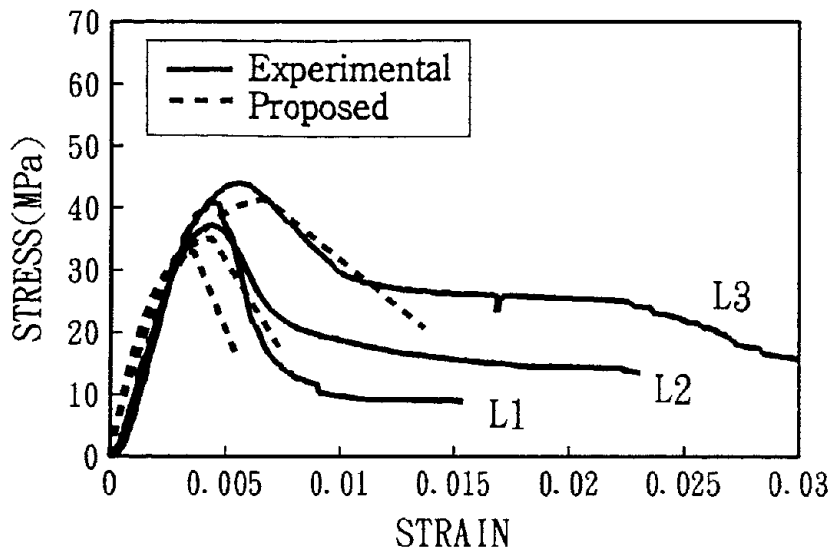**Fig. 1** Hook Configuration of Hoop Reinforcement

Photo 1 Experimental Set−up with 30MN Universal Testing Machine

(a)S Series (Circular Section)

(b)S Series (Square Section)

(c)L Series (Circular Section)

Fig. 2 Comparison of Stress—Strain Relation between Test Results and Predicted Model by Eq.(7)

prevented as the hoop reinforcement ratio increases. It is noted that the square confinement effectiveness is quite different from the circular. Therefore, the effect of cross sectional shape is significant to evaluate the confinement effect.

The stress—strain curve consists of three parts, i.e., stress ascending part, stress descending part and stress converging part. Severe damage such as spalling—off of core concrete, buckling of longitudinal reinforcement and rupture of hoop reinforcement were developed and progressed at the stress converging part. **Photo 2** shows the failure mode of the test specimens L1 to L5. It is observed that the damage of core concrete becomes less as the hoop reinforcement ratio increases.

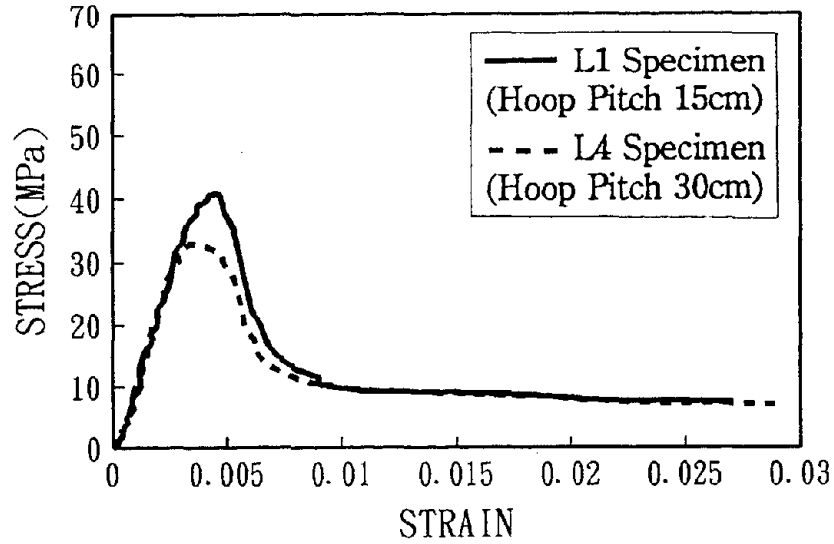*Effect of Spacing of Hoop Reinforcement*

Fig. 3 shows the effect of spacing of hoop reinforcement for the same hoop reinforcement ratio. It is noticed even if the same amount of hoop is provided, deterioration after the peak stress is considerably significant when the spacing of hoop reinforcement increases. According to **Photo 2**, serious outward buckling of longitudinal reinforcement with spalling—off of core concrete was developed in L4 and L5 specimens, which had the spacing of hoop reinforcement of 30cm. Therefore, if the same amount of hoop reinforcement is provided, it is effective in seismic design to place the hoop reinforcement with smaller interval.

Effect of Hook Configuration of Hoop Reinforcement

Fig. 4 shows the effect of hook configuration of hoop reinforcement on the stress—strain curve. Although the peak stress is approximately equal, the gradient at the stress descending part for L7 specimen, which used the sharp—angled hook, is slight smaller than the others. A certain reason for this is not sure, however, L6 and L8 specimens, which used smaller and larger angled hook, respectively, show similar stress—strain relation with L2 specimen, which used the welded hoop. It may be, therefore, said that the scatter of the test results is not significant. In all specimens, rupture of hoop reinforcement was developed not at the hook. This mean that the confinement is enough and the effect of hook configuration is not significant, if the hook is designed in accordance with the Specifications.

MODELING OF THE STRESS–STRAIN RELATION

According to the previous stress—strain models, the stress ascending part has been mostly formulated by a second order parabola as shown in **Table 1**. This is because a second order parabola is simple and well represents the stress—strain relation. However, it should be noted that the second order parabola expression can consider three boundary conditions, though the stress—strain model of concrete need to consider the following four boundary conditions.

(a)Hoop Reinforcement Ratio Approximately 0.35%
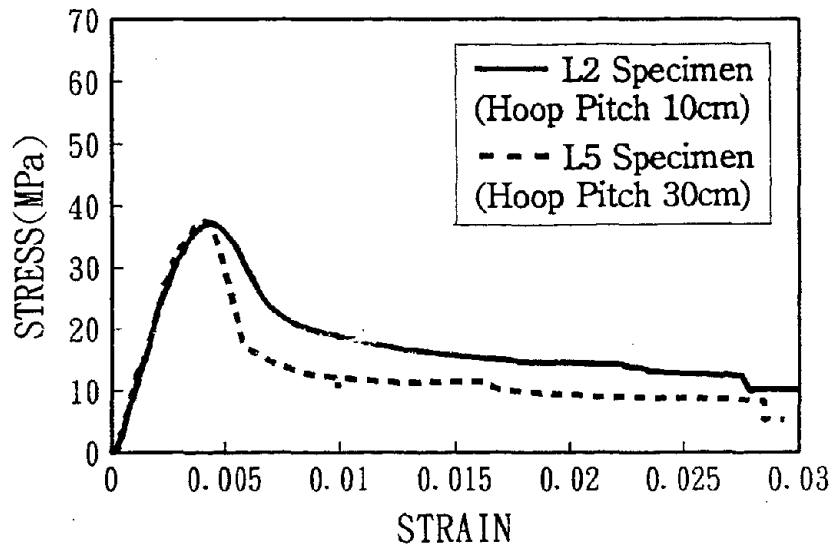
(b)Hoop Reinforcement Ratio Approximately 0.55%

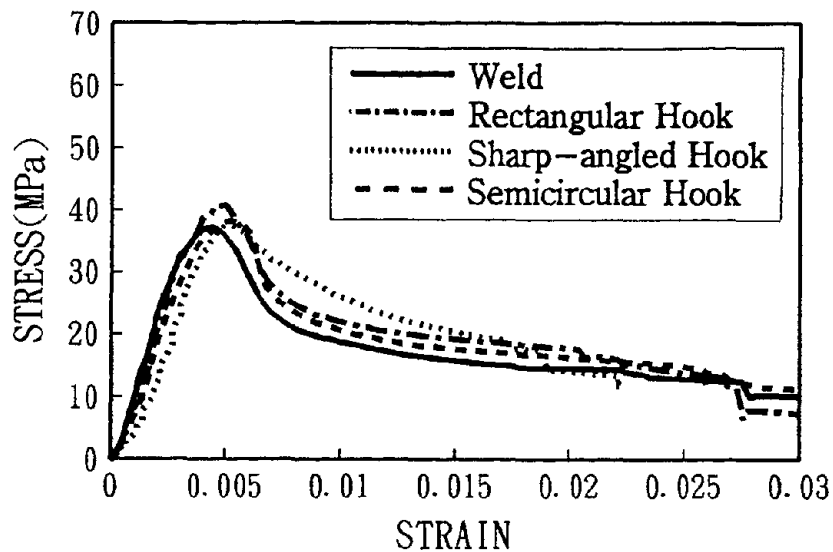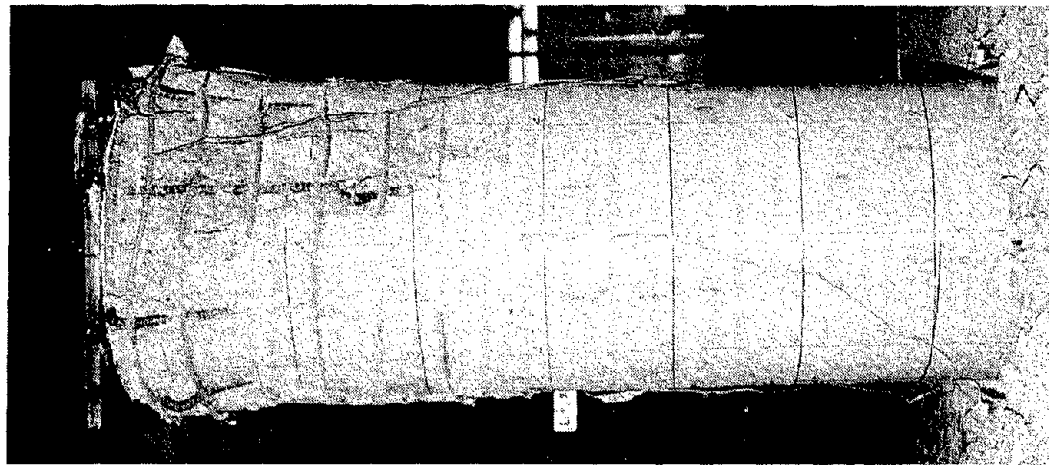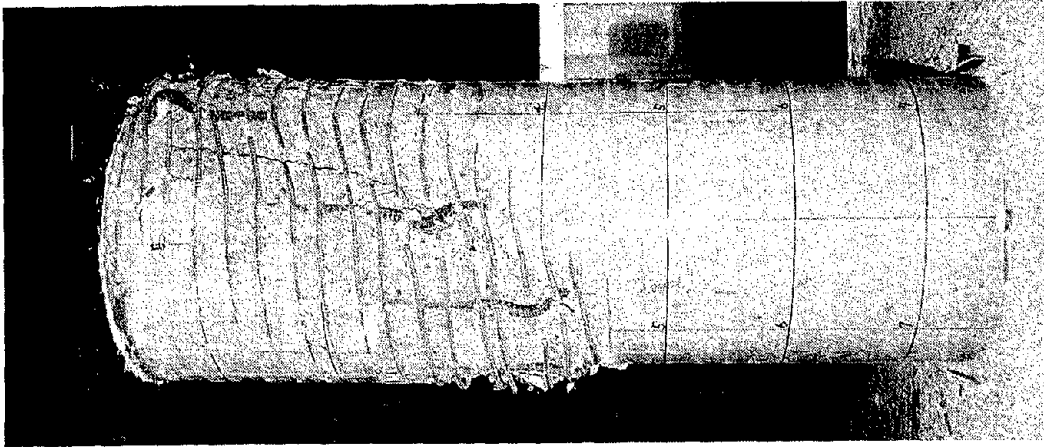**Fig. 3** Effect of Spacing of Hoop Reinforcement

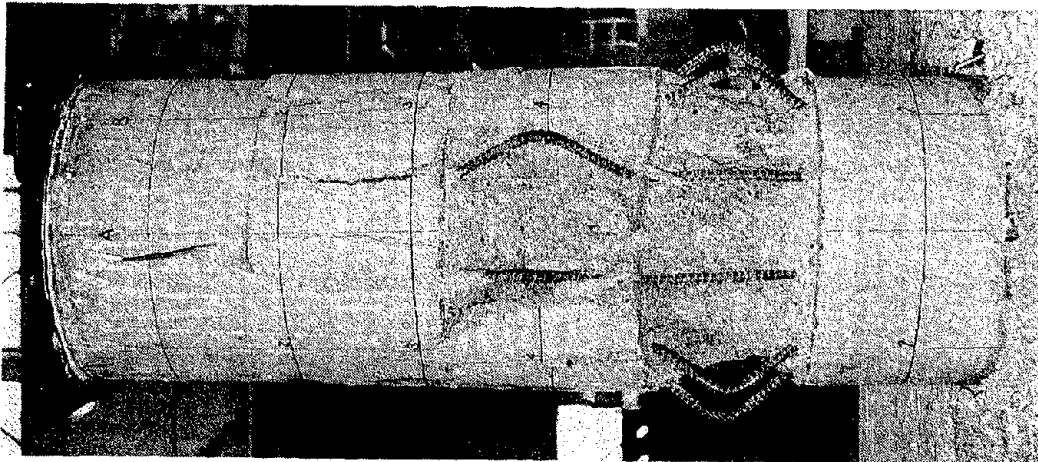**Fig. 4** Effect of Hoop Reinforcement Joint

(a)L1 Specimen

(b)L2 Specimen

(c)L3 Specimen

Photo 2 Failure Mode of Specimens

269

(d)L4 Specimen   (e)L5 Specimen

Photo 2 Failure Mode of Specimens

a) Initial Condition : $f_c = 0$　at $\varepsilon_c = 0$　　　　　　　(1)

b) Initial Stiffness Condition : $d\,f_c/d\,\varepsilon_c = E_c$　at $\varepsilon_c = 0$　　(2)

c) Final Condition : $f_c = f_{cc}$　at $\varepsilon_c = \varepsilon_{cc}$　　　　　(3)

d) Peaked Condition : $d\,f_c/d\,\varepsilon_c = 0$　at $\varepsilon_c = \varepsilon_{cc}$　　(4)

By disregarding Eq.(2), most of the previous models adopted the expression as

$$f_c = f_{cc}\left[\frac{2\varepsilon_c}{\varepsilon_{cc}} - \left(\frac{\varepsilon_c}{\varepsilon_{cc}}\right)^2\right] \tag{5}$$

However, the initial stiffness $2f_{cc}/\varepsilon_{cc}$ in Eq.(5) depends on the hoop reinforcement ratio, while, as shown in **Fig. 2**, the test results show that the initial stiffness is independent of the hoop reinforcement ratio. For avoiding such unconsistency, Mander adopted a fractional function including the initial stiffness as one of the four boundary conditions. And Muguruma and Fujii proposed to consider Eq.(2) as well as Eqs.(1) and (3) in formulating the second order parabola expression. But Muguruma and Fujii used two equations to represent the stress−strain relation at the ascending part.

To include Eq.(2), and for avoiding to adopt two equations at the ascending part, it is proposed here to assume the stress of concrete as

$$f_c = C_1\,\varepsilon_c{}^n + C_2\,\varepsilon_c + C_3 \tag{6}$$

in which C_1, C_2, C_3 and n are constants to be determined from Eqs.(1) to (4). The exponential function enables to simplify the expression and to satisfy the four boundary conditions. By substituting Eqs.(1) to (4) into Eq.(6), one obtains

$$f_c = E_c\,\varepsilon_c\left\{1 - \frac{1}{n}\left(\frac{\varepsilon_c}{\varepsilon_{cc}}\right)^{n-1}\right\} \tag{7}$$

where

E_c : initial stiffness(MPa) and is defined by the Specifications[10] as shown in **Table 5**

n : a coefficient and is given as

$$n = \frac{E_c\,\varepsilon_{cc}}{E_c\,\varepsilon_{cc} - f_{cc}} \tag{8}$$

Table 5 Initial Stiffness of Concrete (MPa)

Strength of Unconfined Concrete	20.6	23.5	26.5	29.4	39.2	49.0
Initial Stiffness	2.30×10^4	2.45×10^4	2.60×10^4	2.75×10^4	3.04×10^4	3.24×10^4

Because the effect of confinement on the initial stiffness is not significant, the initial stiffness is assumed here by the Specifications.

On the other hand, as shown in **Fig. 5**, the stress descending part is modeled from

271

the test results by a straight line as

$$f_c = f_{cc} - E_{des}(\varepsilon_c - \varepsilon_{cc})$$ (9)

where

E_{des} : gradient at the descending part(MPa)

It is important in **Fig. 5** to define the ultimate strain ε_{cu} so that the gradient E_{des} at the descending part be determined. It is assumed here that the ultimate strain ε_{cu} be taken as the strain corresponding to 50% of the peak stress f_{cc}. When the strain exceeds ε_{cu}, the damage of concrete is substantial and unrepairable. By substituting $f_c = 0.5 f_{cc}$ into Eq.(9), the ultimate strain ε_{cu} is obtained as

$$\varepsilon_{cu} = \varepsilon_{cc} + \frac{f_{cc}}{2E_{des}}$$ (10)

Park, Sheikh and Fujii considered the residual stress of 20% or 30% of the peak stress at the stress converging part. In the proposed model, however, special efforts to idealize the stress converging part was not made, because the idealization at such region is not important in seismic design due to excessive and unrepairable damage.
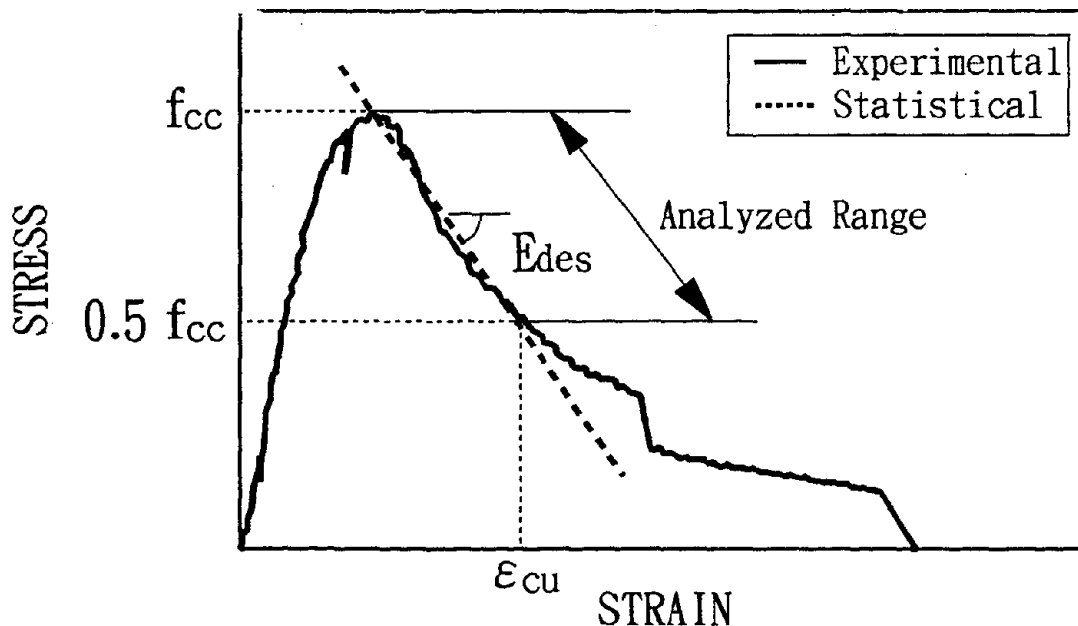

Fig. 5 Definition of Ultimate Strain and Gradient at Stress Descending part

EVALUATION OF CONFINEMENT EFFECTIVENESS

In the proposed model by Eq.(7), factors for controlling the stress—strain relation of confined concrete are the peak stress, the strain corresponding to the peak stress and the gradient at the stress descending part. The effect of confinement on the three parameters was examined based on the test results.

Parameters of confinement effectiveness may be represented as volumetric ratio, confining dimension, confining configuration, yield strength of hoop reinforcement, and strength of unconfined concrete. Because, it makes the expression complicate to incorporate all parameters into the model, volumetric ratio, confining configuration, yield strength of hoop reinforcement and strength of unconfined concrete are considered as the minimum parameters required to formulate a simple model. Other parameters may mostly be regulated by the Specifications.

Fig. 6 shows the confinement effectiveness $\rho_s f_{yh}/f_{co}$ vs. the peak stress f_{cc} thus idealized. The peak stress f_{cc} is proportional to volumetric ratio ρ_s and yield strength f_{yh} of hoop reinforcement, and is inversely proportional to strength of unconfined concrete f_{co}. It is observed that the relation may be approximated by a linear function with different gradient depending on the confining configuration. From a regression analysis for each confining configuration, the relation is written as

$$\frac{f_{cc}}{f_{co}} = 1.07 + 3.70 \frac{\rho_s f_{yh}}{f_{co}} \quad : \text{for circular confinement} \tag{11}$$

$$\frac{f_{cc}}{f_{co}} = 1.02 + 1.01 \frac{\rho_s f_{yh}}{f_{co}} \quad : \text{for square confinement} \tag{12}$$

By comparing Eq.(11) and Eq.(12), it is noted that the gradient of the linear approximation for the square confinement is approximately 30% of the gradient for the circular confinement. This clearly shows that the confining configuration has a significant influence on the confinement effect.

Fig. 7 shows the confinement effectiveness $\rho_s f_{yh}/f_{co}$ vs. the strain ε_{cc} corresponding to the peak stress relation. Although some specimens with low hoop reinforcement ratio provide the larger ε_{cc} vs. $\rho_s f_{yh}/f_{co}$ relation may be lineally approximated. From a regression analysis for each confining configuration, the following relation is obtained as

$$\varepsilon_{cc} = 0.00216 + 0.0335 \frac{\rho_s f_{yh}}{f_{co}} \quad : \text{for circular confinement} \tag{13}$$

$$\varepsilon_{cc} = 0.00277 + 0.0126 \frac{\rho_s f_{yh}}{f_{co}} \quad : \text{for square confinement} \tag{14}$$

It is noted that confinement effectiveness to ε_{cc} for the square confinement is approximately 55% of that for the circular confinement.

273

(a)Circular Confinement

$$\frac{f_{cc}}{f_{co}} = 1.07 + 3.70\frac{\rho_s f_{yh}}{f_{co}}$$

$$\frac{f_{cc}}{f_{co}} = 1.02 + 1.01\frac{\rho_s f_{yh}}{f_{co}}$$
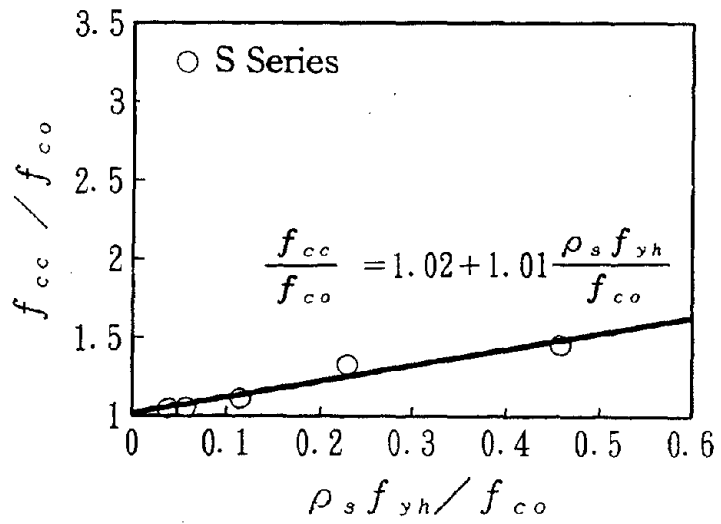
(b)Square Confinement

Fig. 6 Relation between Confinement Effectiveness and Peak Stress

274

(a)Circular Confinement

(b)Square Confinement

Fig. 7 Relation between Confinement Effectiveness and Strain at Peak Stress

275

Fig. 8 shows the confinement effectiveness $\rho_s f_{yh}/f_{co}^2$ vs. the gradient at the descending part. It is observed that the gradient E_{des} at the descending part is inversely proportional to $\rho_s f_{yh}/f_{co}^2$. By regressing the test data, it is written as

$$E_{des} = \frac{12.07}{\rho_s f_{yh}/f_{co}^2} \quad : \text{for circular confinement} \tag{15}$$

$$E_{des} = \frac{16.04}{\rho_s f_{yh}/f_{co}^2} \quad : \text{for square confinement} \tag{16}$$

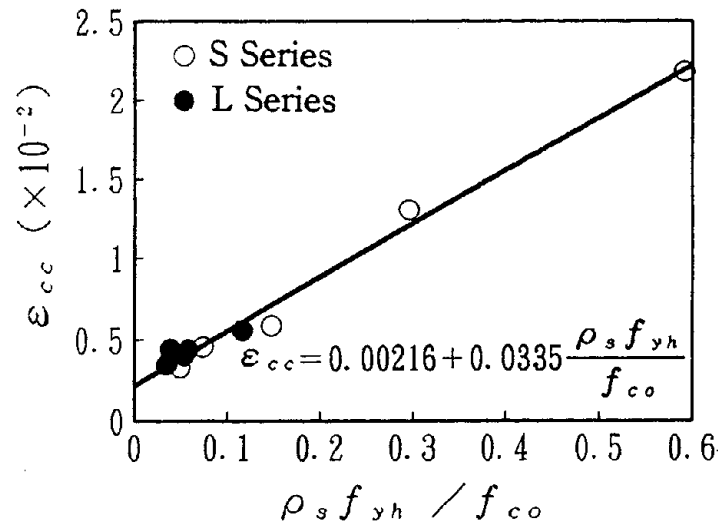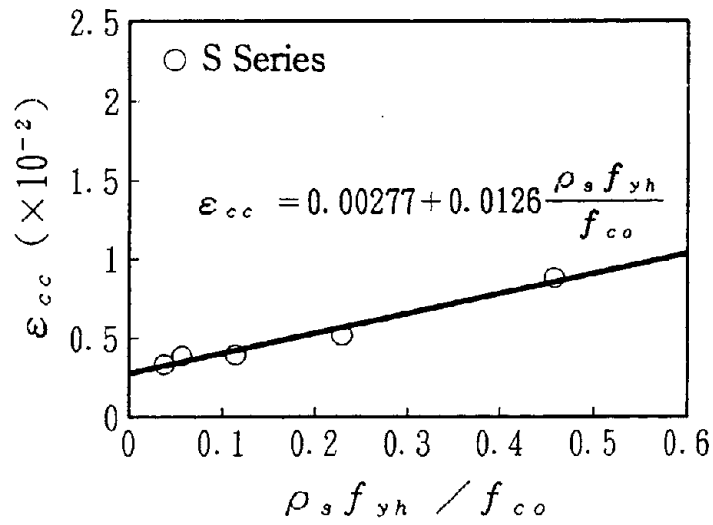It is noted that E_{des} of square confinement is about 1.33 times larger than E_{des} of circular confinement.

From Eqs.(11) to (16), the effect of confinement may be written as

$$\frac{f_{cc}}{f_{co}} = 1 + 3.70\alpha \frac{\rho_s f_{yh}}{f_{co}} \tag{17}$$

$$\varepsilon_{cc} = 0.002 + 0.033\beta \frac{\rho_s f_{yh}}{f_{co}} \tag{18}$$

$$E_{des} = 12\gamma \frac{f_{co}^2}{\rho_s f_{yh}} \tag{19}$$

in which α, β, γ are modification factors depending on cross sectional shape and are given in **Table 6**.

Based on Eqs.(17) to (19), the stress—strain relation was computed for the thirteen specimens in **Table 4**. This is plotted in **Fig. 2** in comparison with the test data. The predicted relations are in very good agreement with the test results. It should be noted that because the initial stiffness condition is included in the model, the gradient at the stress ascending part predicted is independent of the hoop reinforcement ratio.

For the reference, if Eq.(5) is adopted, the stress—strain relation becomes as shown in **Fig. 9**. In Eq.(5), f_{cc} and ε_{cc} were provided by Eqs.(17) and (18). The gradient predicted at the stress ascending part is appreciably smaller than the test result. And also, as expected, it decreases as the hoop reinforcement ratio increases.

Table 6 Modification Factors

Confinement	α	β	γ
Circular	1	1	1
Square	0.3	0.55	4/3

(a) Circular Confinement

$$E_{des} = \frac{12.07}{\rho_s f_{yh}/f_{co}{}^2}$$

(b) Square Confinement

$$E_{des} = \frac{16.04}{\rho_s f_{yh}/f_{co}{}^2}$$
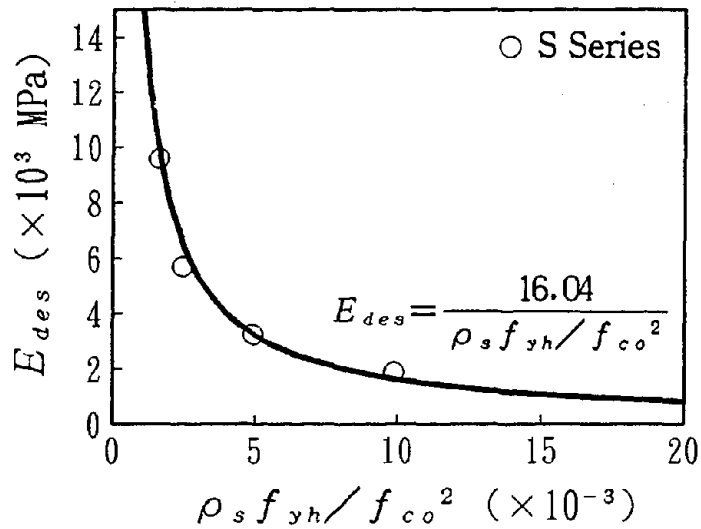
Fig. 8 Relation between Confinement Effectiveness and Gradient at Stress Descending Part

277
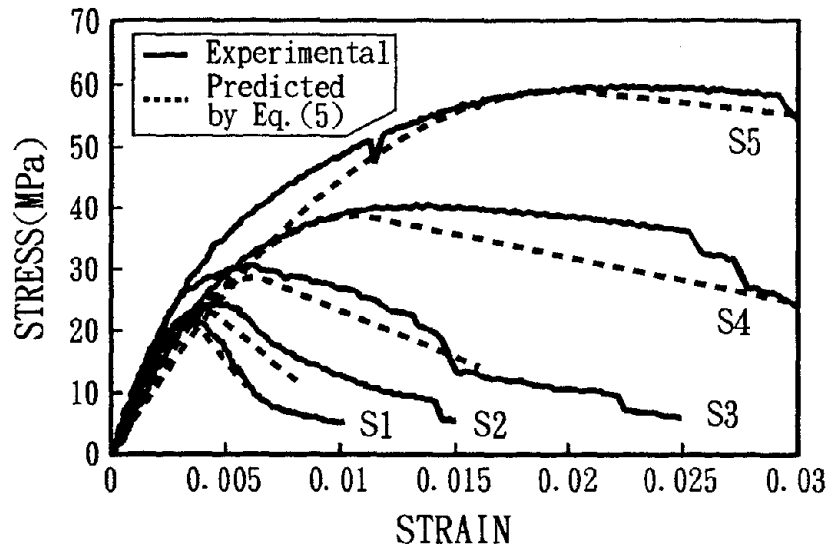
Fig. 9 Stress−Strain Relation by Eq.(5)

COMPARISON WITH PREVIOUS MODELS

To show the effectiveness of the proposed model, the stress−strain relation predicted by the previous models was computed for the test specimens, and compared with the test results.

Figs. 10 to **14** compare the predicted relation by previous models with the test results. It is observed that the previous models mostly evaluate the gradient at the stress ascending part larger than the test results. By comparing **Fig. 2** with **Figs. 10** to **14**, it is obvious that the proposed model predicts the peak stress, the strain at the peak stress and the gradient at the descending part more accurately than the previous models. The gradient at the descending part predicted by the proposed model approximates to test results much better than the previous models, because the effect of low hoop reinforcement ratio is incorporated into the proposed model.

From this comparison, the proposed model provides better agreement than the previous models to the stress−strain relation of confined concrete with low hoop reinforcement ratio.

278

Fig. 10 Stress—Strain Relation by Park
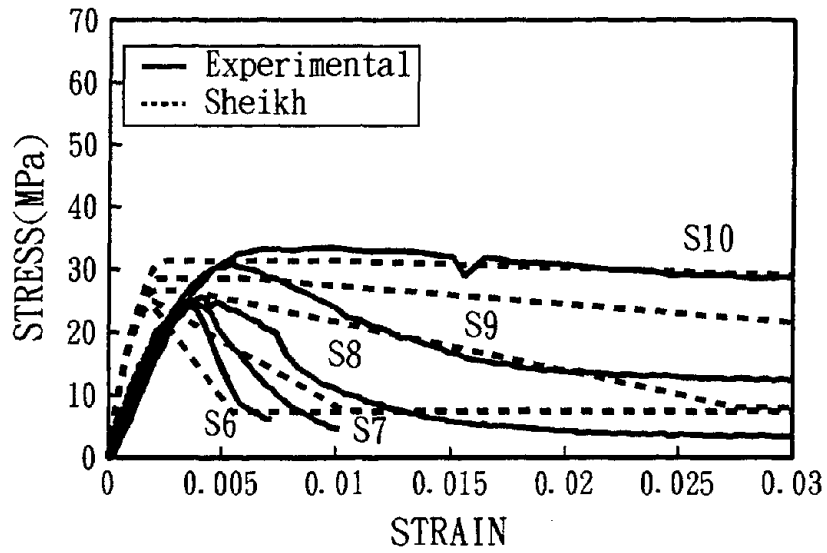
Fig. 11 Stress—Strain Relation by Sheikh

279
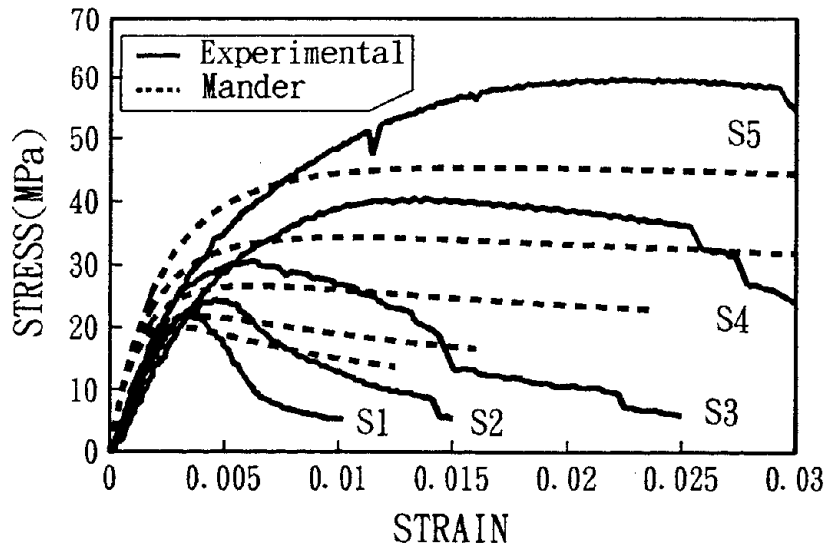
(a) S Series (Circular Section)

(b) S Series (Square Section)

(c) L Series (Circular Section)

Fig. 12 Stress—Strain Relation by Mander

(a) S Series (Circular Section)

(b) S Series (Square Section)

(c) L Series (Circular Section)

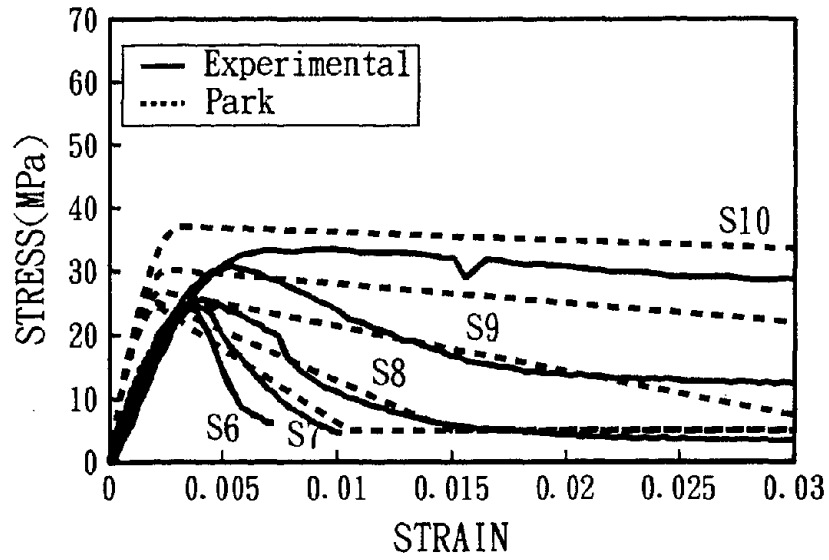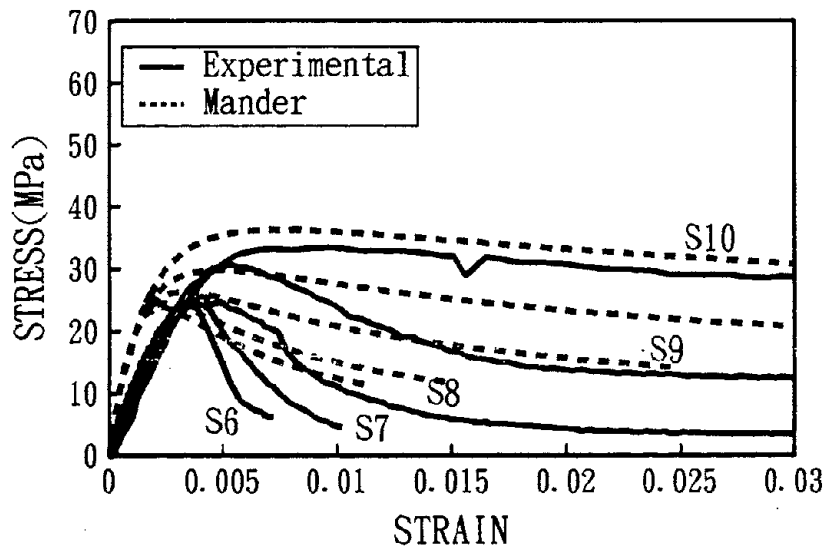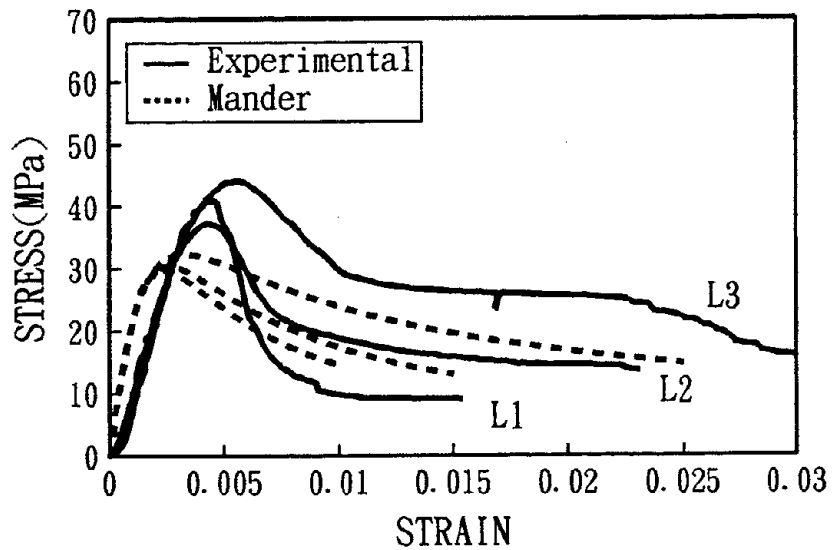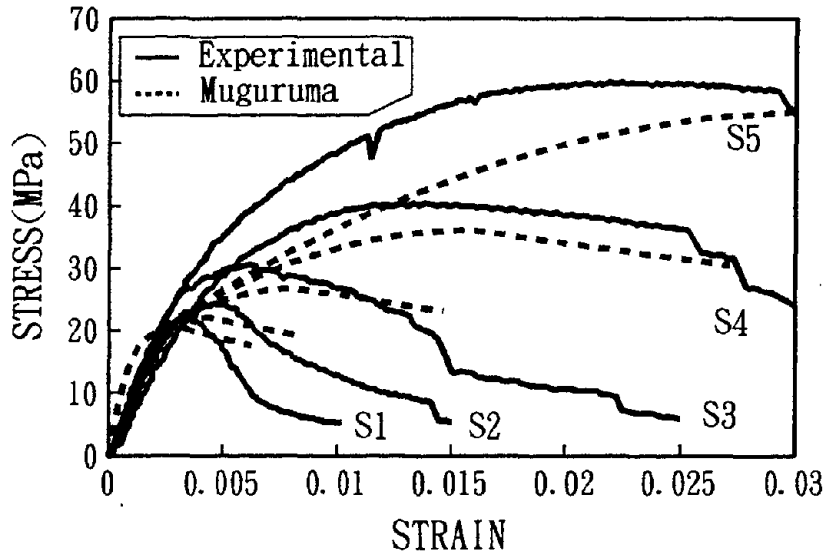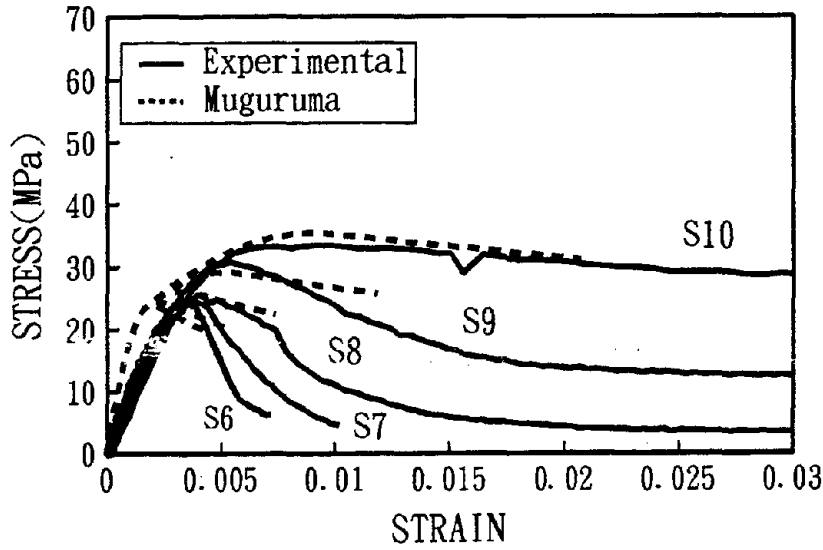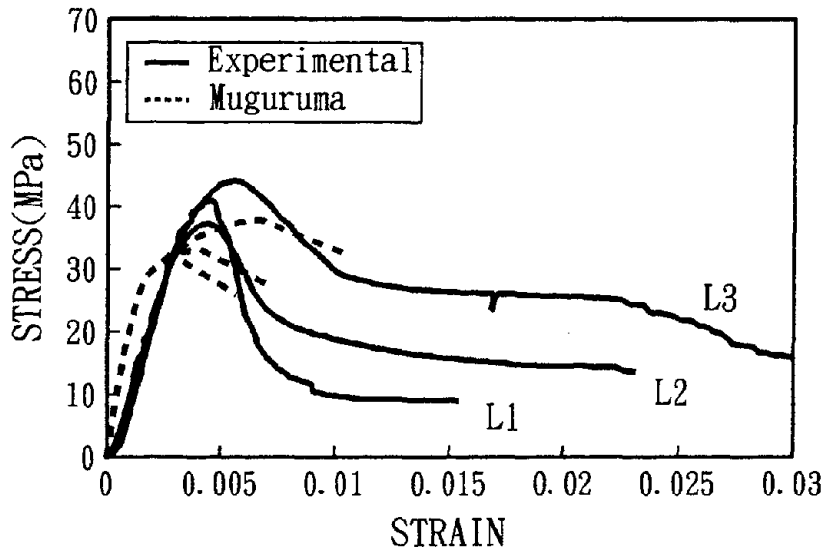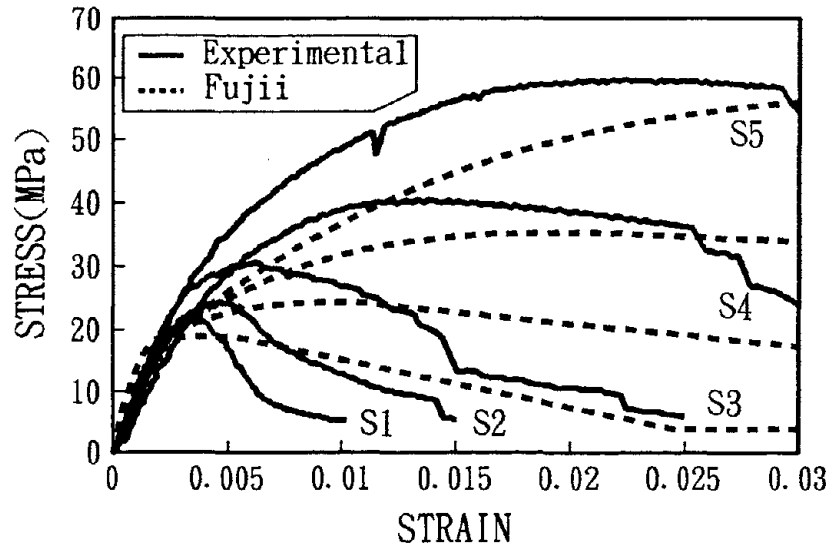**Fig. 13** Stress—Strain Relation by Muguruma

(a) S Series (Circular Section)
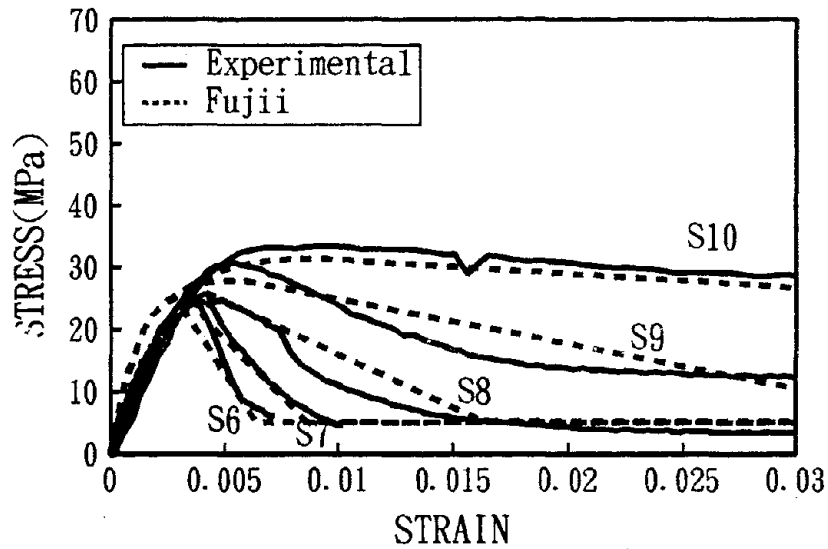
(b) S Series (Square Section)
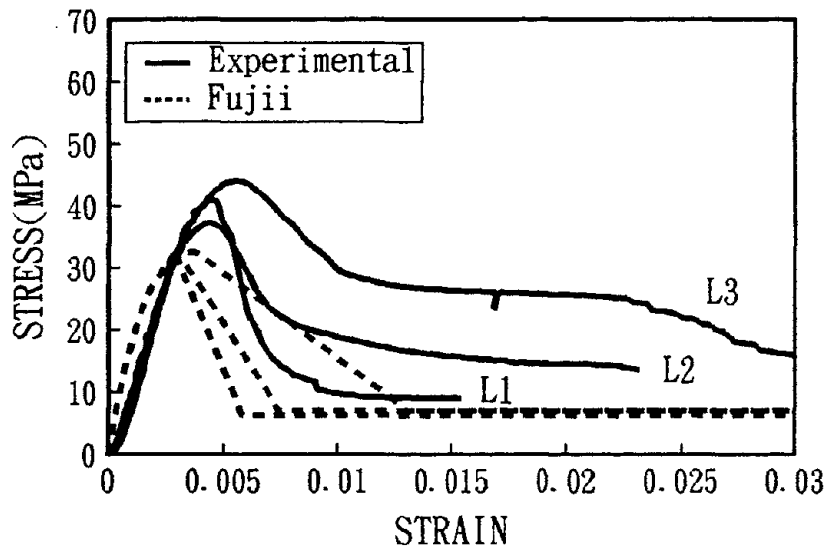
(c) L Series (Circular Section)

Fig. 14 Stress—Strain Relation by Fujii

CONCLUDING REMARKS

To propose an accurate stress−strain model of confined concrete with low hoop reinforcement ratio, a series of loading tests were made for fifteen confined concrete columns. The conclusions from the study presented herein may be deduced as;
1) To consider four boundary conditions by Eqs.(1) to (4) into the stress−strain relation of concrete, the exponential function given by Eq.(7) is proposed.
2) The ultimate strain ε_{cu} is defined as the strain corresponding to 50% of the peak stress, because th idealization of stress−strain relation over the strain ε_{cu} is not important in seismic design due to substantial and unrepairable damage of concrete.
3) The peak stress, the strain at the peak stress and the gradient at the descending part are proposed to be evaluated by Eqs.(17) to (19) based on the loading test results for specimens with a cross sectional dimension of 20 to 50cm and the volumetric ratio of hoop reinforcement of 0.3 to 4.7%.
4) In comparison with the previous models, the proposed model seems to provide better agreement with the test results for the confined concrete with low hoop reinforcement ratio.

REFERENCES

1) Kent, D. C. and Park, R. : Flexural members with confined concrete, Journal of the Structural Division, ASCE, Vol.97, No.ST7, pp.1969−1990, Jul. 1971
2) Park, R. et al : Ductility of square−confined concrete columns, Journal of the Structural Division, ASCE, Vol.108, No.ST4, pp.929−950, Apr. 1982
3) Sheikh, S. A. and Uzumeri, S. M. : Strength and ductility of tied concrete columns, Journal of the Structural Division, ASCE, Vol.106, No.ST5, pp.1079−1102, May 1980
4) Sheikh, S. A. and Uzumeri, S. M. : Analytical model for concrete confinement in tied columns, Journal of the Structural Division, ASCE, Vol.108, No.ST12, pp.2703−2722, Dec. 1982
5) Mander, J. B., Priestley, M. J. N and Park, R. : Theoretical stress−strain model for confined concrete, Journal of the Structural Division, ASCE, Vol.114, No.ST8, pp.1804−1826, Aug. 1988
6) Mander, J. B., Priestley, M. J. N and Park, R. : Observed stress−strain behavior of confined concrete, Journal of the Structural Division, ASCE, Vol.114, No.ST8, pp.1827−1849, Aug. 1988
7) Muguruma, H. et al : A stress−strain model of confined concrete, Annual Report on Cement Engineering, Vol.34, pp.429−432, 1980
8) Muguruma, H. et al : A study on the improvement of bending ultimate strain of concrete, 24th Structural Engineering Symposium, pp.109−116, 1978
9) Fujii, M. et al : A study on the application of a stress−strain relation of confined

concrete, Annual Report on Cement Engineering, Vol.42, pp.311−314, 1988

10) Japan Road Association : Part Ⅳ Design of Foundations, Design Specifications of Road Bridges, Feb. 1991

SECOND U.S.-JAPAN WORKSHOP ON SEISMIC RETROFIT OF BRIDGES

Evaluation and Retrofitting of Existing Bridge Footings
Y. Xiao, N. Priestley and F. Seible
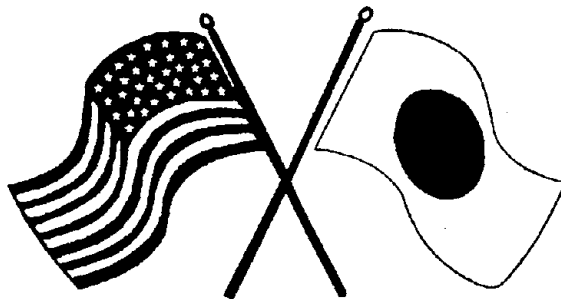
January 20 and 21, 1994
Berkeley Marina Marriott Hotel
Berkeley, California

EVALUATION AND RETROFITTING OF EXISTING BRIDGE FOOTINGS

by

Yan Xiao; M.J. Nigel Priestley; Frieder Seible

Structural Systems, Department of Applied Mechanics and Engineering Sciences
University of California at San Diego, La Jolla, CA92093-0085, USA.

SUMMARY

One "as built" and three retrofitted model column footings have been tested under simulated seismic actions. The test results of "as built" footing indicated that column/footing joint shear failure is a potential danger to most existing bridge structures. The test results also indicated that if there is no dependable tensile capacity in the pile/footing connections a rocking behavior may dominate pier response, which may result in minimizing damage to the footing and column. Model column footings retrofitted using current retrofit standards developed relatively stable hysteretic responses up to moderate ductility levels. However, experimental observations, and theoretical analyses based on the strut-tie model and yield line theory indicated that with current footing retrofit design, which lacks the consideration for joint shear, the reinforced concrete overlay may not develop a fully effective post-cracking mechanism. Improved retrofit details including deep dowels, to insure development of an effective joint shear resisting mechanism, are proposed and verified by the experimental results.

INTRODUCTION

Steel jacketing of existing bridge columns to enhance their flexural and shear strengths and to improve their ductility has been recognized as the most efficient method for column retrofit and has been implemented into retrofit practices in California[1,2]. While methods for retrofitting columns are now well developed, there are still many other problems in existing bridge structures which must be addressed. One of such problems is related to bridge footings. The design for bridge footings in 1950's to early 1970's typically was based on elastic analysis under relatively low lateral seismic input compared to current design provisions. Consequently, the following potential problems are likely inherent in many older bridge footings.

Inadequate pile capacities: The piles of existing bridges are often not able to resist tension and may separate from the footing. This may in fact be beneficial as rocking can occur and the forces entering the structure may be significantly lower than if the columns yield in flexure. Thus, significant economic benefits can be expected as it is possible that by utilizing the rocking a lesser amount of retrofit or even no retrofit may be required.

Inadequate footing strength: Since only a bottom reinforcement mat designed for a low level of earthquake input is common in most existing older footings, flexural failure may be expected due to excessive positive and negative moment induced by an actual seismic attack. Also, because there is no shear reinforcement in most existing footings, the shear strength of the footing is solely provided by the plain concrete. Typically this is insufficient to resist the shear force induced by ultimate column input. In addition, column/footing joint shear failure is also expected in many existing bridge structures due to the lack of joint shear reinforcement and poor details for column longitudinal bars. The deficiency in column/footing joint is the most difficult to retrofit and repair.

"AS BUILT" AND RETROFITTED FOOTING TEST PROGRAM

In order to investigate the seismic performance of existing bridge footings and to develop efficient retrofit measures, a comprehensive bridge footing research program has been carried out at the University of California at San Diego. Four large-scale column footing models have been tested. One of the footings was tested under the condition of "as built", and others were tested after retrofit. Table-1 summarizes column footing test details. The models were approximately 1/3 scale of typical prototypes.

The reinforcement details for the "as built" column footing F1RA are shown in Fig.1. The column had a longitudinal reinforcement ratio of 2.5%. As shown in Fig.1(b), the "as built" footing was reinforced only with a two dimensional #6@3.25in.(@83mm) bottom steel mat. Fig.2(a) and (b) show column details of the retrofitted circular column footing and retrofitted rectangular column footings, respectively. The column longitudinal steel ratios were 5%. The potential plastic hinge region with a length of 48in.(1219mm) of the columns were retrofitted by site-welded steel jackets for improved flexural ductility. For circular column footing F2CR, a 3/16in.(4.76mm) thick circular steel jacket was used. The circular jacket was slightly oversized than the existing column, and the gap between the jacket and the existing column was filled by cement grout. For retrofitted rectangular

Table-1 Column Footing Test Details

Test Unit	Footing Retrofit	Column			Test	Axial Load (kips)
		Section	Steel	Retrofit		
F1RA	"As Built"	Rectangular 19.25in. Wide 28.75in. Deep	32#6 G40 Steel Ratio= 2.5%	"As Built"	Rocking-1	150
					Rocking-2	250
					Capacity	400
F2CR	Caltrans Typical	Circular 24in. Diameter	52#6 G40 Steel Ratio= 5.1%	3/16in. Thick Cylindrical Steel Jacket	Capacity	400
F3RR	Caltrans Typical	Rectangular 19.25in. Wide 28.75in. Deep	14#8 G40 & 28#7 G40 Steel Ratio= 5.0%	3/16in. Thick Elliptical Steel Jacket	Capacity	400
F4RR	Deep Dowel	Rectangular 19.25in. Wide 28.75in. Deep	14#8 G40 & 28#7 G40 Steel Ratio= 5.0%	3/16in. Thick Elliptical Steel Jacket	Capacity	400

Note: 1in.=25.4mm; 1kip=4.45kN.

288
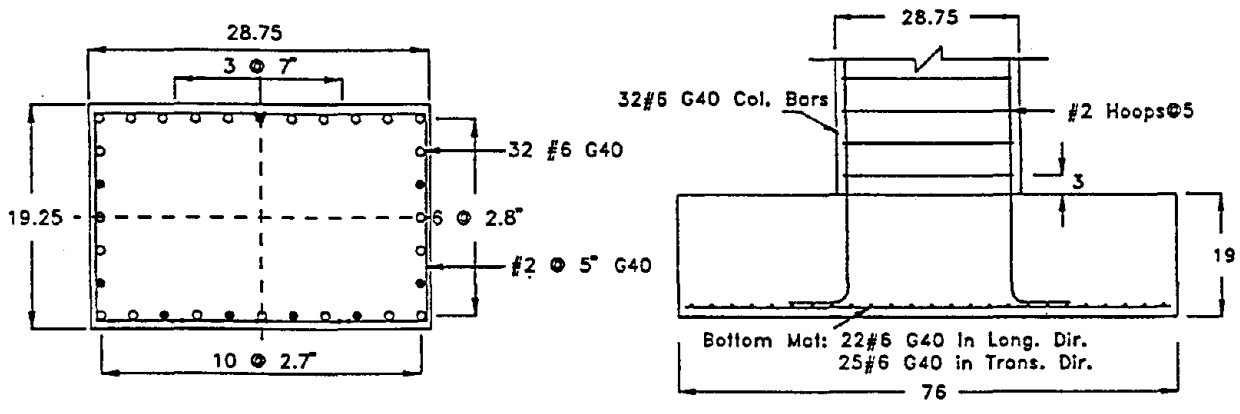
(a) "As Built" Column Details   (b)"As Built" Footing Details
Fig.1 Reinforcement Details of "As Built" Column Footing F1RA (1in.=25.4mm)
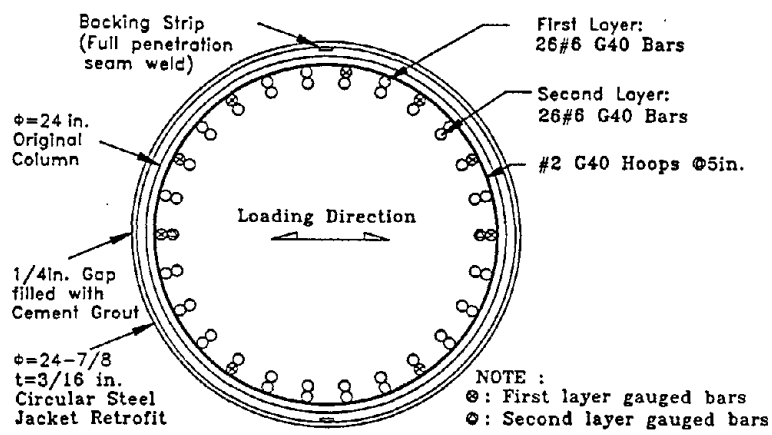
(a) Circular Column Section of F2CR
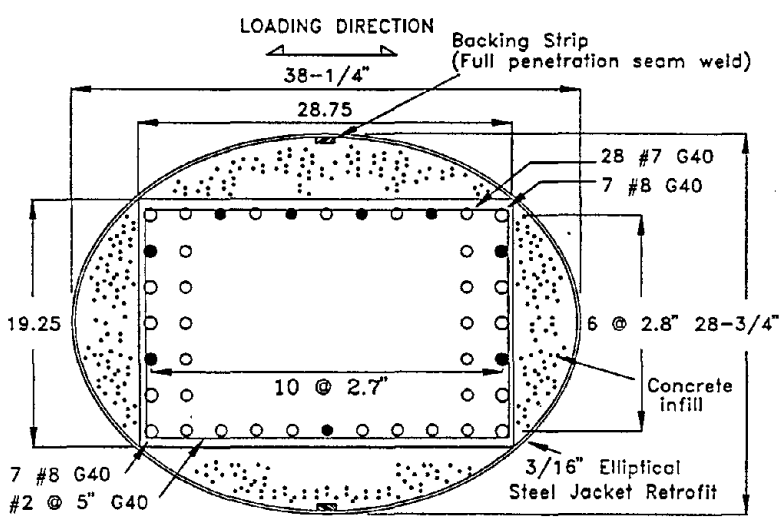
(b) Rectangular Column Section of F3RR, F4RR
Fig.2 Retrofitted Column Details (1in.=25.4mm)

289

column footings F3RR and F4RR, 3/16in.(4.76mm) thick elliptical steel jackets were used, with the gap between the jackets and the columns filled by concrete. For all cases, a vertical gap of 1in.(25.4mm) was provided between the jacket and the retrofitted footing to ensure that the jacket did not bear against the footing.

Based on current footing design, the existing 76in.×76in.×19in. (1930mm×1930mm ×483mm) footings of F2CR and F3RR were enlarged to 108in.×108in.×23.5in. (2743mm× 2743mm×597mm), and retrofitted with additional top and bottom flexural steel and vertical stirrups, connected with original footings by deformed #2 (noted as D6, nominal diameter = 6mm) dowels, as illustrated in Fig.3(a). F4RR was the counterpart specimen of F3RR, and was designed by improved retrofit design procedure with considering
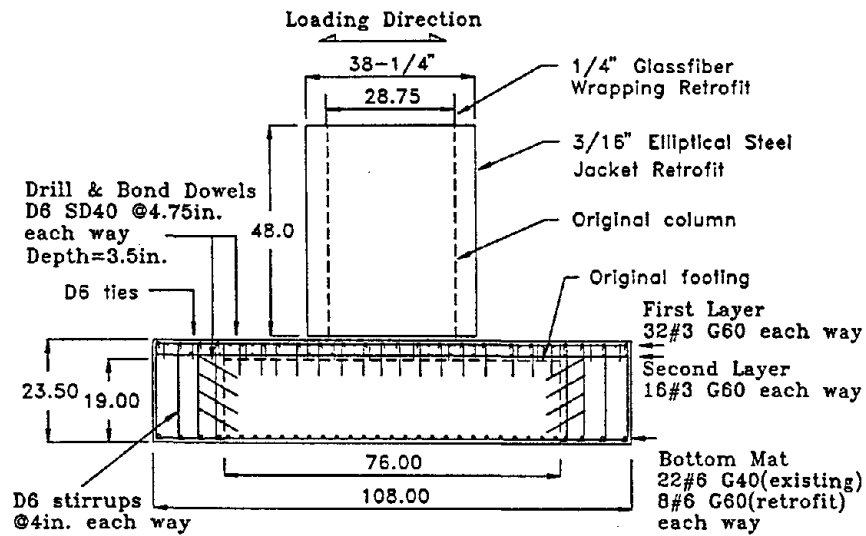
(a) Rectangular Column Footing F3RR
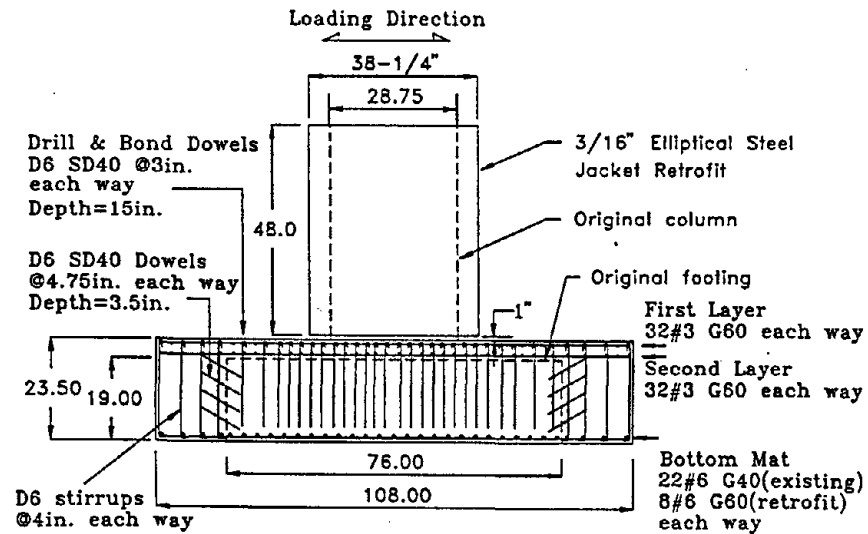
(b) Rectangular Column Footing F4RR
Fig.3 Retrofitted Footing Reinforcement Details (1in.=25.4mm)

290

column/footing joint shear. The footing of F4RR had the same dimensions as F3RR, however included deep dowels and slightly heavier overlay reinforcement, as shown in Fig.3(b), to ensure sufficient overlay capacity against the pull-out force resulted from the tensile steel in column critical section.

Ready mixed concrete with a design strength of 5ksi(34.5MPa) was used throughout. Grade 40 steel (nominal strength=40ksi=276MPa) was used in the "as built" column footing F1RA and the existing portions of the retrofitted column footings. Grade 60 steel (nominal strength =60ksi=414MPa) was used for retrofit reinforcement.

The test setup is shown in Fig.4. The footing was supported on 2.2in.(56mm) thick fiberglass-reinforced elastomeric pads, which were chosen to represent the flexibility of the pile foundation. In the rocking tests of F1RA, the footing was sat on the pad and was free of uplifting. However, in the capacity tests of "as built" column footing F1RA and retrofitted column footings, the rocking of the footing was restrained by 5/8in.(15.9mm) diameter high strength rods attached to the test floor. The rods were first snug tightened over a piece of 1/8in.(3.2mm) steel packing material. The packing material was then removed in order to allow the footing to have some uplift before the rods started to stretch and apply forces. The resulting 1/8in.(3.2mm) gap was provided to allow elastic unloading of the compressed elastomeric pads simulating the pile compression stiffness.
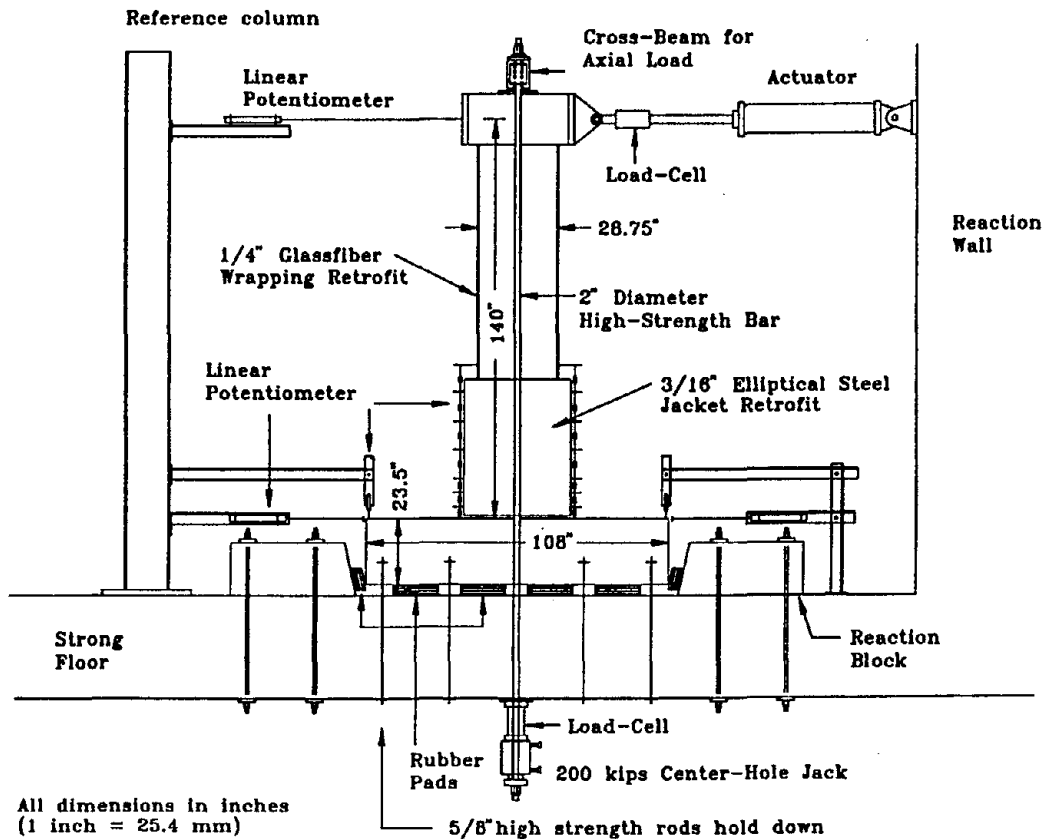
Fig.4 Test Setup (1in.=25.4mm, 1kip=4.45kN)

TEST RESULTS OF "AS BUILT" COLUMN FOOTING

Rocking Responses: Two rocking tests under different axial loads were conducted for "as built" footing F1RA. Fig.5 shows the experimental hysteretic response under the axial load of 150kips(667kN) and the corresponding predicted monotonic rocking behavior. The pier developed "S" shaped hysteresis loops under the rocking condition, as shown in Fig.5. After developing the uplift, the hysteretic response showed a gradually reduced stiffness and the peak horizontal forces were limited at a level of 30kips(134kN). In other words, the horizontal force input to the pier was limited after developing rocking. The hysteretic curves for both loading and unloading showed a negative gradient due to the effect of P-delta. For an elastic rocking system, the unloading response should follow the same track as loading. The difference between the loading branch and unloading branch shown in Fig.5 was due to a small drop of the axial load. Fig.5 also showed that relatively good agreement was obtained between the test results and theoretical prediction.

Capacity Test: After the rocking tests, the F1RA footing was attached to test floor and a final capacity test was conducted. Fig.6 shows the final hysteretic response. The dashed lines in Fig.6 show the predicted capacity corresponding to the first yield of column steel, H_y, and the ideal flexural strength, H_{if}, corresponding to an concrete ultimate compressive strain of 0.005. The calculation was carried out using Mander et.al's stress-strain model for confined concrete[3]. As shown in Fig.6, the hysteresis loops were stable until a peak displacement of 3.2in.(81mm) was achieved. The pier developed a maximum force of 68kips(303kN) in both push and pull directions, which was slightly lower than the predicted theoretical ideal flexural strength. A sudden drop in the force carrying capacity of the pier occurred due to the shear failure of column/footing joint, during the push cycle to achieve a displacement of 4.0in.(102mm). After this stage, the strength degradation of the pier became significant due to losing column/footing joint shear resistance, as evidenced by the excessively opened joint shear cracks as shown in Fig.7.
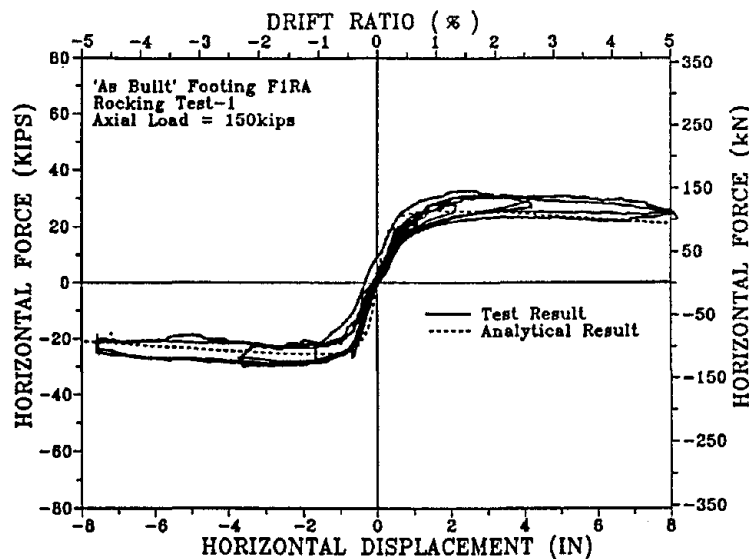
Fig.5 Rocking Response of F1RA
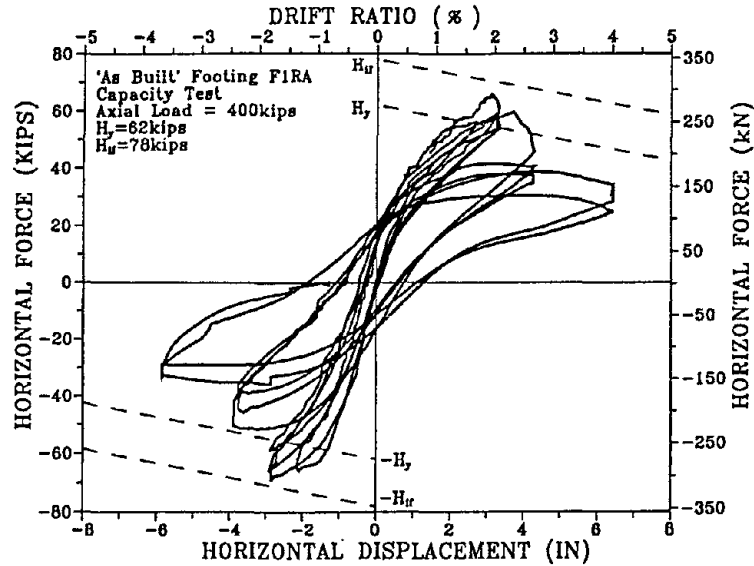
Fig.6 Final Hysteretic Response of F1RA
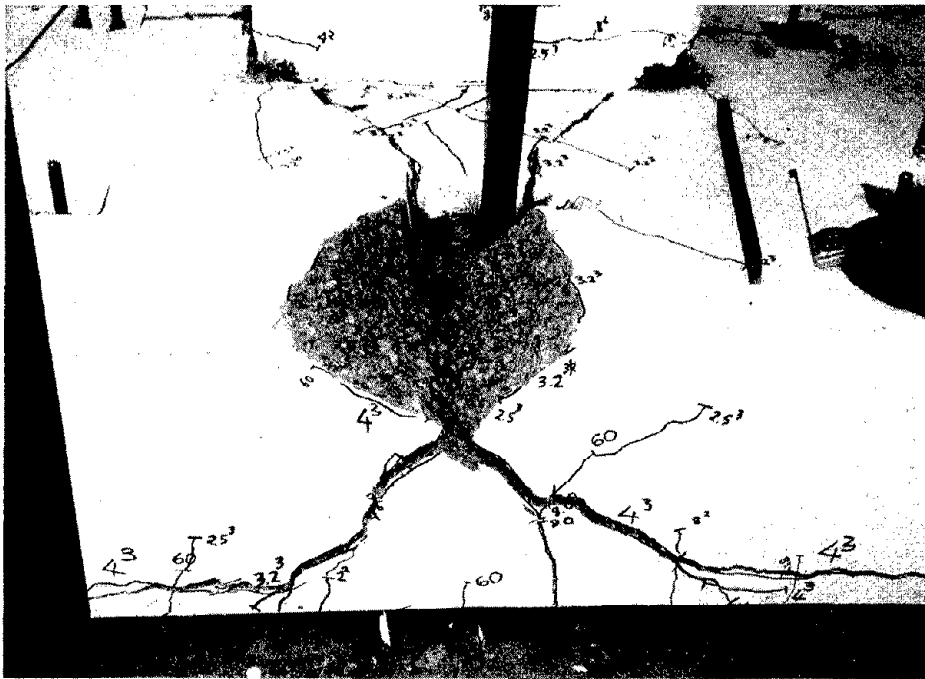
Fig.7 Column/Footing Joint Shear Failure

TEST RESULTS OF RETROFITTED COLUMN FOOTINGS

The horizontal force - displacement hysteretic response histories for retrofitted footings are shown in Fig.8(a) to (c), respectively. The dashed lines in Fig.8 show the theoretical predictions for the capacities of the pier corresponding to the first yield of column longitudinal reinforcement, H_y, and the ideal flexural strength, H_{if}.

293

(a) Circular Column Footing F2CR

DRIFT RATIO (%)

-7 -6 -5 -4 -3 -2 -1 0 1 2 3 4 5 6 7

HORIZONTAL FORCE (KIPS)

HORIZONTAL FORCE (kN)

100 75 25 0 -25 -50 -75 -100

400 300 100 0 -100 -200 -300 -400

Retrofitted Footing F2CR
Axial Load = 400kips
H_y=63kip
H_u=81kip

H_u
H_y
$-H_y$
$-H_u$

μ=1 1.5 2 3 4

μ=4 3 2 1.5 1

-12 -10 -8 -6 -4 -2 0 2 4 6 8 10 12

HORIZONTAL DISPLACEMENT (IN)

(b) Rectangular Column Footing F3RR

DRIFT RATIO (%)

-7 -6 -5 -4 -3 -2 -1 0 1 2 3 4 5 6 7

HORIZONTAL FORCE (KIPS)

HORIZONTAL FORCE (kN)

150 100 50 0 -50 -100 -150

600 400 200 0 -200 -400 -600

Retrofitted Footing F3RR
Axial Load = 400kips
H_y=115kip
H_u=136kip

H_u
H_y
$-H_y$
$-H_u$

μ=1 1.5 2 3 4

μ=4 3 2 1.5 1

-12 -10 -8 -6 -4 -2 0 2 4 6 8 10 12

HORIZONTAL DISPLACEMENT (IN)

(c) Rectangular Column Footing F4RR

DRIFT RATIO (%)

-7 -6 -5 -4 -3 -2 -1 0 1 2 3 4 5 6 7

HORIZONTAL FORCE (KIPS)

HORIZONTAL FORCE (kN)

150 100 50 0 -50 -100 -150

600 400 200 0 -200 -400 -600

Retrofitted Footing F4RR
Axial Load = 400kips
H_y=115kip
H_u=136kip

H_u
H_y
$-H_y$
$-H_u$

μ=1 1.5 2 3 4 5

μ=5 4 3 2 1.5

-12 -10 -8 -6 -4 -2 0 2 4 6 8 10 12

HORIZONTAL DISPLACEMENT (IN)

Fig.8 Hysteretic Responses of Retrofitted Column Footings

294

Circular Column Footing F2CR: As shown in Fig.8(a), the retrofitted circular column footing F2CR developed a ductile hysteretic response up to a total displacement ductility factor of $\mu=4.0$, or a total drift ratio of 5.8%, where the loading was terminated due to the limitation in axial loading system. The hysteresis loops were stable and showed little degradation upon recycling at the given ductility level. The predicted ultimate flexural strength was first reached during the loading to $\mu=1.5$. The further increase in the peak horizontal forces was due to the strain hardening in column longitudinal reinforcement. Although the pier developed an excellent hysteretic response, excessive cracks and concrete crushing of the overlay were observed at the column toe.

Rectangular Column Footing F3RR: The retrofitted rectangular column footing F3RR developed its theoretical flexural strength at a total displacement ductility level of $\mu=1.5$, however, there was not much further increase in the force carrying capacity. As shown in Fig.8(b), the hysteresis loops of the pier were stable until $\mu=3.0$, or a total drift ratio of 4.8%. However, the degradation of the horizontal force became significant during loading cycles with a peak ductility factor of $\mu=4.0$. The overall shape of the hysteresis loops indicates relatively small energy absorption capacity. The significant degradation in the force carrying capacity of the pier was caused by the deterioration of the footing overlay resistance to the pull-out force induced by the tensile steel in column critical section, as evidenced by the extensive cracking of the top overlay, shown in Fig.9. At the peak displacement ductility factor $\mu=4.0$, the top overlay was lifted up about 3/4in. (19mm) at the tension toe of the column, also indicating the severe damage to the top overlay.

Fig.9 Crack Patterns of Retrofitted Footing F3RR

295

Rectangular Column Footing F4RR: As shown in Fig.8(c), compared to its counterpart specimen F3RR, retrofitted column footing F4RR developed more stable hysteretic behavior with improved energy absorption capacity until a total displacement ductility factor of $\mu=5$, where the loading was terminated due to the limitation in axial loading system. Since the footing of F4RR was stronger with the use of deep dowels than that of F3RR, the pier was able to develop a larger horizontal force carrying capacity resulted from the strain hardening of column longitudinal reinforcement. Although well distributed cracks were observed on the top overlay, their widths were smaller than those observed for F3RR. The footing appeared to be solid and monolithic, and the deformation of the pier seemed to be mainly contributed by the plastic rotation of the column plastic hinge, as evidenced by the wide opening of the gap between the jacket and the footing.

STRUT-TIE MODEL AND YIELD LINE THEORY

Strut and tie models and yield line theory have been developed to investigate the complicated column/footing joint shear resisting mechanisms of retrofitted footings and to establish rational retrofit design methods[4].

Pre-Cracking Mechanisms in Retrofitted Footings: The moment curvature analysis for the critical column section of F3RR indicated that the footing was subjected to a resultant tensile force, $T_c=708$kips (3149kN), a resultant compressive force, $C_c=1108$kips (4928kN) and a shear force, $V_c=136$kips (605kN). These input forces are balanced by two tie-down forces, R_{t1} and R_{t2}, and reaction forces, R_v and R_h.
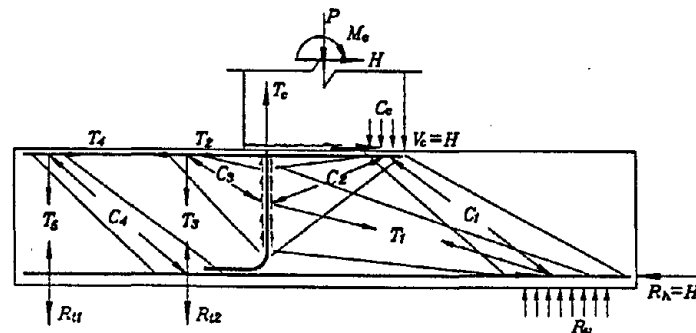
(a) Strut and Tie Model for Retrofitted Footing
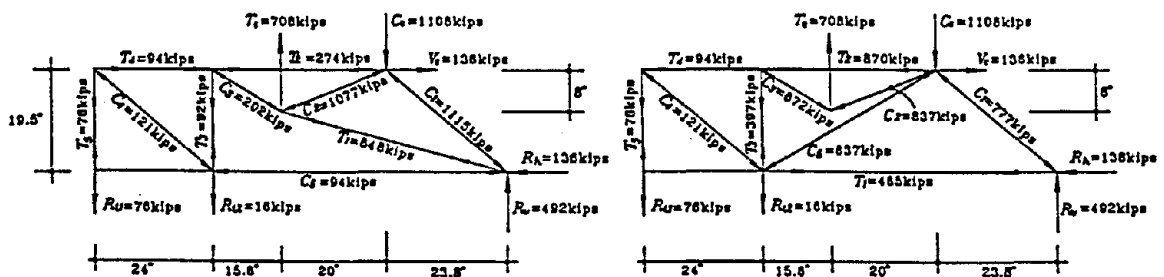
(b) Forces in Pre-Cracking Footing   (c) Forces in Post-Cracking Footing
Fig.10 Resisting Mechanisms in Retrofitted Footing (1in.=25.4mm, 1kip=4.45kN)

A pre-cracking strut and tie model considered for F3RR is shown in Fig.10(a). Resultant compressive force, C_c, and shear force, V_c, are mainly resisted by a diagonal strut, C_1, transferred to the compression zone of rubber pads and reaction block. The resultant tensile force, T_c is transferred to the footing and resisted by a concrete tension tie, T_1, and two compression struts, C_2, C_3. The compression strut C_2 radiates from the compression zone of the critical column section. While compression strut, C_3, is equilibrated by tension ties, T_2, T_3, and T_4, which are provided by reinforcement in the retrofit extension portion and the top overlay. The forces in the vertical stirrups are combined into the vertical ties, T_3 and T_5.

Fig.10(b) shows the calculated equivalent truss forces induced in the members of the pre-cracking strut and tie model. It is assumed that the resultant tensile force T_c is decreased to zero by bond at a depth of 18in. (457mm), and the application point of, T_c, is taken as 9in. (229mm), i.e., half the bond length, below critical column section. As is shown in Fig.10(b), a large tensile force of 848kips (3772kN) is required for concrete tension tie, T_1. Using the effective joint width of 48in.(1219mm), and footing effective depth of 21.5in.(546mm), this force yields an excessive tensile stress of 848kips/(48in.×

21.5in.)=822psi(5.64MPa)=11.8$\sqrt{f_c{}'}$psi(0.7$\sqrt{f_c{}'}$MPa), indicating the high probability of joint cracking.

Post-Cracking Mechanisms in Retrofitted Footings: The post-cracking strut and tie model is shown in Fig.10(c). The major change due to joint shear cracking is that the compression strut, C_2, is split into two compression struts, C_2 and C_5. In the post-cracking system, the resultant tensile force, T_c, is only resisted by the internal strut C_2 and the external strut C_3. The internal strut force, C_2, radiates into the compression zone of the column critical section and can be balanced by other compression struts. The horizontal component of the external strut force, C_3, is balanced by a horizontal tie T_2, which is provided directly by the top overlay reinforcement. Additional resistance of T_2 is from the diaphragm resisting mechanism of the top overlay, similar to the mechanism discovered by Paulay and Priestley for slab and column joints[5]. On the other hand, since the stirrups are provided only in the extension portion of the retrofitted footing, which are far away from the column, the vertical component of strut force, C_3, has to be transferred to the tension tie, T_3, through the slab function of the top overlay. Such an out-of-plane resisting mechanism is expected to be weaker than other resistance, thus, the capacity of the retrofitted footing is depended on the overlay capacity against the pull-out force, i.e., the vertical component of the external strut force, C_3.

Yield line theory can be used to determine the top overlay capacity. A yield line pattern as shown in Fig.11(a) is assumed for the top overlay slab, *ABCD*, in which part of the slab, *BCGH* is assumed to have no displacement since no upward force is active in this region, and the rest of the overlay is lifted up under the action of P_v, as shown in Fig.11(b). Using virtual work method the ultimate upward force, P_{vu}, can be calculated as follows.

297

$$P_{vu} = \Sigma m_i L_i \theta_i \qquad\qquad (1)$$

where, m_i is the ultimate moment per unit length of a yield line with the length of L_i, and θ_i the rotation angle corresponding to a unit displacement at the application point of P_v. A computer program "FOOTYIEL" is developed for the calculation. The moment capacities of the yield lines are calculated based on the equivalent concrete stress block recommended by ACI318-89. The depth of the top overlay slab is taken to be the sum of the overlay depth and the depth of the dowels. Fig.12 shows the input data and output data of "FOOTYIEL" for retrofitted footing F3RR.

For retrofitted footing F3RR, the overlay capacity was calculated to be equal to 380kips (1690kN), which is smaller than the vertical component of the strut force, C_3, or 397kips (1766kN). This indicates that the top overlay of F3RR was marginally not able to support the vertical component of strut force, C_3, and its capacity would degrade under the action of cyclic loading, eventually leading to the footing failure, as described previously.
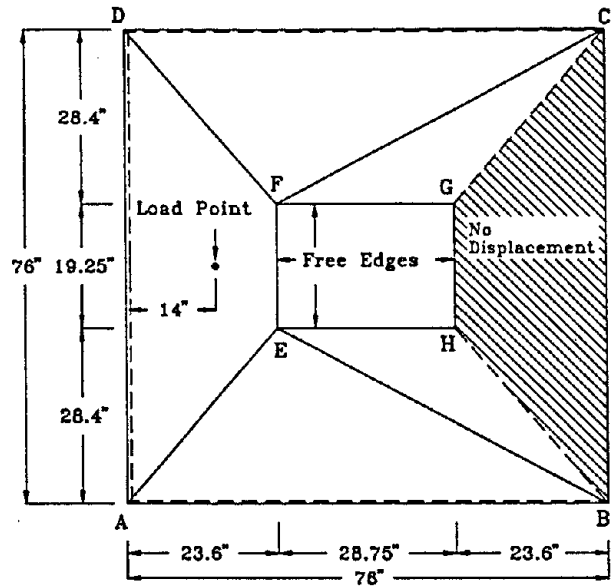
(a) Yield Line Pattern
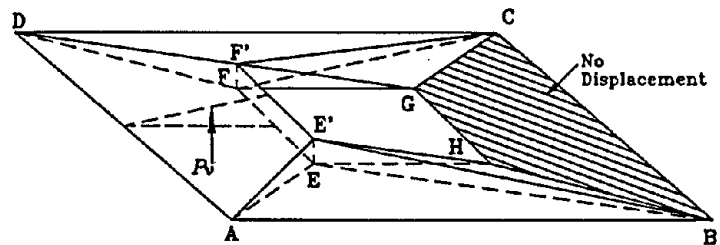
(b) Displacement
Fig.11 Yield Line Pattern and Displacement of Top Overlay (1in.=25.4mm)

298

```
----- Input Data for FOOTYIEL.FOR -----------------    -----
----------------------------------------------------    -----
                      Column Section Shape:rectangular
               Column Overall Depth (in):    28.75
                     Column Width (in.):    19.25
               Overlay Slab Length (in):    76.00
                Overlay Slab Width (in):    76.00
                      Overlay Depth (in):     4.50
                       Dowel Depth (in):     3.50
             Cover to Top Layer Steel (in):     1.00
  Vertical Force Application Point from Edge (in):    14.00
     Longitudinal Steel Area of Top Layer(in^2/in):    .0300
     Transverse Steel Area of Top Layer (in^2/in):    .0340
     Longitudinal Steel Area of 2nd Layer(in^2/in):    .0160
     Transverse Steel Area of 2nd Layer (in^2/in):    .0170
                 Retrofit Steel Strength(ksi):    68.00
         Existing Footing Concrete Strength(ksi):     4.98
                Retrofit Concrete Strength(ksi):     4.90
------------------------------------------------    -----
--- Is the above data correct (y or n)?
y
----- Output Data for FOOTYIEL.FOR -----------------    -----
Ultimate Vertical Component Pv (kips):      380.457100
----------------------------------------------------    -----
Stop - Program terminated.
```

Fig.12 Input and Output Data of Program "FOOTYIEL"

For retrofitted circular column footing F2CR, the analyses indicated that the overlay of F2CR had larger margin against the pull-out force induced by the tensile steel in critical column section, which was reflected in the excellent hysteretic response, as shown in Fig.8(a). Similar analyses also indicated that in the case of retrofitted column footing F4RR, the use of deep dowels significantly increased the effective depth of the overlay and thus its capacity against the pull-out force, consequently, resulting in the significantly improved hysteretic response compared to F3RR, as shown in Fig.8(c).

CONCLUSIONS

The rocking tests of an "as built" column footing indicated that if there is no dependable tension capacity in the piles, a rocking behavior is likely to dominate the response of the pier, consequently, the damage is minimal. In the capacity test with restraining the rocking, the "as built" footing suffered a brittle column/footing joint shear failure, resulting significant loss in load carrying capacity. On the other hand, the tests of retrofitted footings indicated that the lack of column footing joint shear design is a potential problem in current retrofit design procedure. Although retrofitted column footing F2CR developed an excellent hysteretic response, retrofitted column footing F3RR suffered severe footing damage caused by column/footing joint shear distress and the potential deformation ability of the retrofitted column could not be fully utilized. The complicated resisting mechanism in the retrofitted footing can be analyzed by strut and tie models and yield line theory. As an improvement to the current footing retrofit design methodology, it is recommended that the analytical model proposed in this paper be used to determine the capacity of the footing overlay, and to design the appropriate overlay

depth, dowel length and reinforcement. The retrofitted footing using the improved design with deep dowels has been verified by the test results.

ACKNOWLEDGMENTS

REFERENCES

1. Chai, Y.H.; Priestley, M.J.N. and Seible, F., "Seismic Retrofit of Circular Bridge Columns for Enhancing Flexural Performance," ACI Structural Journal, Vol.88, No.5, Sep.-Oct. 1991, pp.572-584.
2. Priestley, M.J.N.; Seible, F.; Xiao, Y.; and Verma, R., "Steel Jacket Retrofitting of Reinforced Concrete Bridge Columns for Enhanced Shear Strength, Part 1 and Part 2," Accepted for Publication, ACI Structural Journal, May, 1993.
3. Mander, J.B.; Priestley, M.J.N. and Park, R., "Theoretical Stress-Strain Model for Confined Concrete," Journal of Structural Division, ASCE, Vol.114, No.8, Aug. 1988, pp.1804-1826.
4. Xiao, Y.; Priestley, M.J.N.; and Seible, F., "Seismic Assessment and Retrofit of Bridge Footings," Structural Systems Research Project, Report SSRP92/10, November, 1992.
5. Paulay, T. and Priestley, M.J.N., "Seismic Design of Reinforced Concrete and Masonry Building," John Wiley & Sons, Inc., 1992, 744p.

SECOND U.S.-JAPAN WORKSHOP ON SEISMIC RETROFIT OF BRIDGES

Seismic Evaluation and Retrofit of Major Steel Bridges

A. Astaneh-Asl, R. Donikian, R. Imbsen and C. Seim
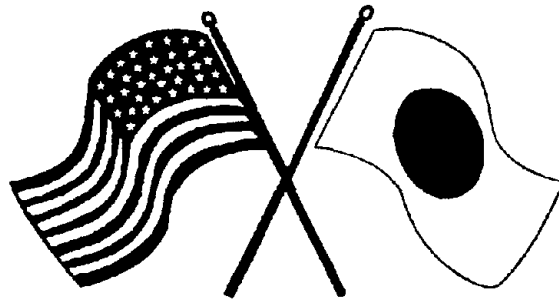
SEISMIC EVALUATION AND RETROFIT OF MAJOR STEEL BRIDGES

Abolhassan Astaneh-Asl, Professor, Department of Civil Engineering, Berkeley, USA

Roupen R. Donikian, Project Manager, Cygna Consulting Engineers, Oakland, USA

Roy A. Imbsen, President, Imbsen & Associates, Inc., Sacramento, CA, USA

Charles Seim, Senior Principal, T.Y. Lin International, San Francisco, CA, USA

SUMMARY

Since the October 17, 1989, Loma Prieta earthquake in northern California, seismic studies of a number of major steel bridges in the San Francisco Bay area have been conducted. Studies included: (1) establishing appropriate ground motions to be used in seismic evaluation, (2) developing realistic models of the bridge structures, (3) conducting elastic and inelastic time history and response spectra dynamic analyses, (4) identifying seismic vulnerabilities; and, (5) developing seismic retrofit strategies and concepts to remove the seismic vulnerabilities. This paper summarizes studies completed to date on seismic evaluation and retrofit of the East Bay Crossing of the San Francisco-Oakland Bay bridge, San Mateo-Hayward bridge, Benicia-Martinez bridge and Golden Gate bridge. A summary of seismic vulnerabilities and retrofit strategies for these bridges is provided.

INTRODUCTION

The magnitude 7.1 Loma Prieta earthquake of October 1989 caused some minor damage to major steel bridges in the San Francisco Bay area. The only significant damage was the collapse of a 50-foot (15.3m) segment of the upper and lower decks of the San Francisco-Oakland Bay Bridge which resulted in closure of the bridge for one month while the repairs were being done. Since 1990, the California Department of Transportation (Caltrans) and the Golden Gate Bridge and Transportation District have commissioned a number of research and development projects on seismic evaluation and retrofit of major steel bridges in the San Francisco Bay. Four of the studies summarized in this paper include a suspension bridge (Golden Gate), a riveted Warren and cantilever truss bridge (East Bay Crossing of the Bay Bridge), a modern welded cantilever truss bridge (Benicia-Martinez), and a modern welded steel box girder bridge (San Mateo-Hayward).

PERFORMANCE CRITERIA FOR SEISMIC RETROFIT

Performance criteria established by the California Department of Transportation and currently used in seismic evaluation and retrofit of major steel bridges are as follows:

1. The bridge should be able to behave *almost elasticity* during a small or moderate earthquake.
2. The bridge should be able to survive major earthquakes without collapse or serious damage that would impair the *full functionality* of the bridge after a major earthquake. Damage that is not easily detectable and repairable, particularly underwater damage, should be prevented.

The first criterion is intended to prevent significant and costly damage during more frequent small and moderate earthquakes. The second criterion is intended to ensure that major bridges will remain functional after major earthquakes. This is due to the important role that major bridges play in the post-earthquake economical life as well as emergency response of affected communities. Using the above criteria, four of the San Francisco Bay area's major bridges, shown in Figure 1, have been evaluated. The bridges are: San Mateo-Hayward, Benicia Martinez, Golden Gate and East Bay Crossing of the Bay Bridge. A summary of seismic studies of each bridge follows.

A. SEISMIC VULNERABILITY ASSESSMENT OF SAN MATEO-HAYWARD BRIDGE

(Donikian, 1993)

The San Mateo-Hayward Bridge has a length of approximately seven miles (11.3 km), and consists of a 1.85-mile(3 km)-long steel bridge at the west end connected to a 4.9-mile (7.9 km)-long concrete trestle on the east side, Figure 1.

The steel bridge is composed of 18 single-span anchor units connected by suspended spans in an alternating sequence. The connections of anchor units and suspended spans constitute the hinges in the system with an alternating sequence of tied hinges at one end, and expansion hinges with rod restrainers at the other end of the suspended units. The anchor unit spans are 208 feet (63 m), and 292 feet (89 m). Vertical clearance of the main span is 138 feet (42 m) above the waterline.

The deck structure consists of a dual steel box girder orthotropic deck superstructure supported by pin bearings on dual steel and concrete towers. The channel spans consist of a 750-foot (229 m) main span and two 375-foot (114 m) side spans. The substructure consists of 38 bell-shaped concrete piers supported on steel H-pile foundations. The substructure piers consist of dual reinforced concrete rectangular columns, typically 11 feet x 4 feet (3.4 m x 1.2 m) and hollow shafts.

The subsurface soil conditions at the site consist of soft-to-medium stiff clays (Bay mud) that extend to depths of approximately 50 feet (15 m) below the mudline. Depth to bedrock is estimated at 700 feet (210 m) below sea level.

A.1. Structural Component Performance Criteria

Inelastic response of steel components is assessed in terms of available load ductility levels as measured by interaction relations. For axial load and bending, the interaction relation is established (Astaneh-Asl 1993b) as a parabolic function of axial load and biaxial moment

$\left(p + m_x^2 + m_y^2 \le R^2\right)$, and for shear, the interaction ratio is a function shear and moment $\left(v^2 + m^2 \le R^2\right)$, (Astaneh-Asl, 1993b). Where, p, m and v are normalized axial force, bending moment and shear forces respectively. The term R is Response Modification Factor for the component under investigation (Astaneh-Asl, 1993b).

The performance criteria for the evaluation of the reinforced concrete flexural members are in terms of *displacement ductilities* (Donikian 1993). Deformation-based performance criteria and shear capacities of the concrete components are computed using M.J.N. Priestley's recommended method. Foundation performance was evaluated on the basis of load-displacement curves developed by Geomatrix (Donikian 1993) for the foundation soil-pile groups.

A.2. Finite Element Models

The finite element discretization of the steel structural model is shown in Figure 2. This model consists of almost 6000 degrees of freedom, and is assembled using the deck super-elements to account for dual box girder behavior Various models were generated to simulate: (a) dynamic response due to multiple support excitation; (b) variability of the ground motions along the bridge alignment; (c) soil-structure interaction; and (d) expansion hinge nonlinearities and variations in gap stiffness.

A.3. Response Analyses

The following three types of models were used in the analyses: (a) Type 1; linear elastic "tension" models with expansion hinges modeled as two-way tension-compression elements; (b) Type 2; models incorporating the limited nonlinearities associated with expansion hinges. The hinges were modeled using tension-only restrainer elements and compression-only gap elements. These were used for multiple support excitation time history analyses; and (c) Type 3; general nonlinear models incorporating both expansion hinge nonlinearities and material nonlinearities associated with plastic hinges.

The types of analyses conducted consist of: (a) Uniform Response Spectrum (URS) Analyses with the objective of obtaining preliminary seismic demand estimates and performing parametric studies; (b) Multiple Support Time History (MSTH) Analyses consisting of a series of multiple support time history analyses with the objective of obtaining realistic estimates of displacements and deformations in the structure; and (c) Uniform Base Time History (UTH) Analyses, mainly performed for calibration purposes to serve as a tool for comparing results obtained by the URS and MSTH analyses.

Some of the significant results obtained from the dynamic analyses of the steel structure are highlighted here. Figure 3 shows steel tower R-factors (Response Modification Factor) for steel piers compared to allowable value of 5. The allowable values of R-factors were established by A. Astaneh-Asl (1993b) for various components of the San Mateo-Hayward bridge and were confirmed by inelastic analyses (Donikian, 1993). These results indicate that the variability of ground motions along the bridge alignment has a significant effect on structural response, and that

response due to multiple support excitation seems to be closely related to response due to time delay effects of propagating ground motions.

A.4. Conclusions on Seismic Studies of the San Mateo-Hayward Bridge

For vulnerability assessment of large structures such as the San Mateo-Hayward Bridge, with strong nonlinearities due to expansion hinges, multiple support time history analysis is the rational alternative to the much too conservative uniform response spectrum method. The following conclusions were drawn from the study: (1) load based criteria (Z-factors) are unreliable for concrete components; (2) deck restrainers and expansion hinge behavior play a major role in the performance of the superstructure; (3) effects due to multiple support excitation are significant. Specifically, there is significant reduction in demand compared to estimates obtained by conventional uniform response spectrum analyses. However, in some cases, the demand on some components may be higher compared to uniform time history excitation cases; and (4) uncertainties such as foundation stiffness and ground motion variabilities must be carefully assessed for structural response analyses of large structures.

B. SEISMIC EVALUATION OF THE BENICIA-MARTINEZ BRIDGE

(Imbsen, 1993)

The Benicia-Martinez Bridge (George Miller, Jr. Bridge) is a high-level, deck-type, welded truss bridge with welded girder approach spans. This 6215-foot (1894 m) long structure carries I-680 over the easterly end of Carquinez Strait. The general view of the bridge is shown in Figure 1. The navigation channel vertical clearance is 138 feet (42 m). The truss section consists of seven 528-foot (161 m) spans, two 429-foot (131 m) spans and one 330-foot (100 m) span. All trusses are 33 feet (10 m) in depth (center-to-center of chords). The 330-foot (100 m) span is simply supported. Two trusses at a spacing of 42 feet (12.8 m) center-to-center are braced with top and bottom lateral bracings, end sway frames at piers, and intermediate sway frames.

The truss spans are supported by reinforced concrete cellular pier shafts on cellular reinforced concrete footings resting on groups of eight or ten six-foot (1.8 m) diameter, concrete-filled steel caissons.

Contract work for the initial four-lane, 67-foot (20.4 m) wide structure began in 1959 and was completed in 1962. Earthquake restrainers and reinforced concrete support and shear blocks were added in 1980. In 1991, the structure was widened equally on each side to its present width of 77 feet, 6 inches (23.6 m).

B.1. Multiple-Support-Excitation Seismic Response Analysis

For long extended structures subjected to out-of-phase input motions at multiple supports, there are two response aspects which induced vibrational and quasi-static effects. In the

306

conventional dynamic analysis, only the vibrational component of the response is considered. To account for both the vibrational effect and the quasi-static effect, the total displacement formulation was implemented in the IAI-NEABS program (an enhanced version of NEABS program) using the direct-integration time history analysis method (Imbsen, 1993).

B.2. Seismic Vulnerabilities

The seismic vulnerabilities of the structure are:

Truss Structure System

a. Floor beam Connection to the Main Truss
b. Main Truss Members
c. Lateral Bracings and Transverse Sway Frames
d. Expansion Hinge Hangers of the Drop-in Spans
e. Bearings

Pier-Caisson Structure

Critical sections of the concrete pier shaft and caisson foundations are shown in Figure 4. The critical areas are:

a. Concrete Pier Columns
b. Concrete Footings
c. Steel Caissons

B.3. Seismic Retrofit Study

Seismic resistance of the structure can be improved by providing strength, ductility and energy dissipation, and seismic isolation.

Two retrofit alternatives were developed. In the first strategy, the substructure and bearings are strengthened significantly to increase the capacities of the substructure. Supplemental damping is provided to the structure system by using friction dampers in the transverse sway frames to reduce the seismic demand. In a second retrofit alternative, *hybrid sliding-restraining bearings* are used. These are conventional low-profile bearings designed to slide at a certain horizontal force level, and, at a predetermined level, additional restraint will be provided to limit the relative movement.

B.4. Conclusions on Seismic Studies of the Benicia-Martinez Bridge

A detailed seismic investigation of the Benicia-Martinez Bridge has been carried out with the primary objective to establish the construction cost estimate for required retrofit work. The seismic evaluation was conducted for the Safety Evaluation earthquake (1000-year return period) and two Function Evaluation earthquakes (300-year and 100-year return period). The most critical components are truss bearings and non-ductile hollow concrete shaft piers.

307

Under the safety evaluation earthquake, concrete piers are highly deficient in both flexural and shear. At the lower level events, the flexural seismic demands were reduced; however, the seismic demands for shear were still high. This shifting of governing failure mode (from flexure for the safety evaluation earthquake to shear for the function evaluation earthquake) dictates the priority and urgency of seismic retrofit.

Two retrofit strategies for main truss spans were proposed. Strategy No. 1 requires strengthening of the substructure to a higher capacity level. Supplemental damping introduced selectively. However, the overall scheme is still essentially a strength approach. Strategy No. 2 utilizes conventional components, but allows the relative movement at bearings. However, energy dissipating seismic links and seismic stoppers are provided at each bearing to improve the seismic performance. Both strategies provide satisfactory seismic performance. However, Strategy No. 2 relies less on the strengthening of existing components, always a difficult and expensive task, Strategy No. 2 is the preferred approach.

C. SEISMIC PERFORMANCE AND RETROFIT OF THE GOLDEN GATE BRIDGE

(Seim, 1993)

The Golden Gate Bridge, one of the most renowned bridges in the world, opened to traffic on May 28, 1937. The bridge is operated by the Golden Gate Bridge, Highway and Transportation District. The 9154-foot (2790 m) overall length of the bridge consists of the steel truss approach viaducts, the Fort Point steel arch, the 3940-foot (1200 m) steel suspension bridge, concrete anchorages and anchorage housings, and the art deco concrete pylons.

Immediately following the Loma Prieta earthquake, the District engaged T.Y. Lin International (TYLI) to perform a seismic evaluation, and later, to develop concept retrofit studies. The 1990 seismic evaluation revealed that a major earthquake would cause severe damage to the bridge. The *Seismic Retrofit Studies* in 1991 included development and evaluation of concept retrofit measures as well as estimation of their construction costs and schedules.

C.1. Site Specific Seismic Risk, Response Spectrum and Ground Motions

The determination of site specific seismic risk, response spectrum and ground motions were based on the relative location of nearby faults and the reoccurrence interval of the seismic event, and computer emulations of ruptures on nearby faults. Three different seismic events (San Andreas fault rupture scenario) were developed to define three independent ground motions. One set of ground motions was developed for the Hayward fault, but it did not control.

C.2. Seismic Performance Criteria

The District's performance criteria required the retrofit measures to preserve life and allow the bridge to be used immediately after the largest expected event, first for emergency vehicles and then for the toll paying general public. To guide the designers, design criteria for the retrofit project were developed based on the Design Criteria from the new AASHTO Load and Resistance Factor Design.

C.3. Seismic Analysis

Global models were created for the major structures. Local models were developed for specific areas such as the base of the main towers and the stiffening trusses.

C.4. The Suspension Bridge

The characteristics of the suspension bridge that most significantly influence its seismic analysis are summarized below.

Large Displacement Effects and Multiple Support Excitation

Ground motion will be different at each of the widely spaced supports. The multiple support excitation analysis imposes relative displacements between the towers and the anchorage blocks that induce both static and dynamic stresses. These analyses found only a minor increase, or in some cases, a decrease, in the stresses in the structure, but the displacement of the expansion joints is generally larger.

Dynamic Characteristics

The suspension bridge has a long fundamental period of vibration that yields large displacements and lower seismic forces than for shorter period structures, but higher vibration modes with a shorter period can make an important contribution. The 67th mode was close to the first longitudinal mode of the towers and contributed greatly to the towers' seismic forces and pounding on the stiffening trusses.

The analysis showed that the main cable and suspenders remain elastic. Yielding of structural elements is confined to local areas such as parts of the towers, pylons and lateral bracing. Seismic displacements of the suspension bridge are on the order of several feet across the expansion joints. When the expansion joint closes, large impact forces are transmitted and change the dynamic properties and the response of the bridge.

The towers are not anchored to the reinforced concrete piers with anchor bolts. For service loads, the towers were considered to be fixed. However, uplift of the towers occurs with strong motions that significantly change the towers' response characteristics. The rocking motion of the tower bases reduces the seismic stresses at the towers but increases the deflections.

Structural Modeling

Two-dimensional models of the entire bridge were used for preliminary studies. Three-dimensional models of the entire bridge were used for final studies. A detailed three-dimensional finite element model of the tower base region was used to study the stress distributions and moment-rotation relationships of this critical part of the bridge. While most structural members are modeled explicitly, the main span stiffening truss system is modeled using linear super-elements to reduce the size of the numerical problem since inelastic response of the stiffening truss is confined to the side span only.

309

Modal and Response Spectrum Analysis

The modal analysis was performed to compute the vibrational properties. The natural frequencies and mode shapes computed from the analysis were compared with the one obtained from ambient vibration tests. This comparison provided a way to verify the computer models.
Nonlinear Time History Analysis

The analyses of the global response of the bridge to multiple-support ground motion excitations are performed using a dynamic nonlinear finite element program using "gap" elements.

The nonlinear dynamic analyses are performed by integrating the coupled equations of motion in the time domain. The ground motion excitation was applied as a time-varying displacement boundary condition at each of the six supports.

C.5. Vulnerabilities and Retrofit of the Suspension Spans

The proposed retrofit measures are summarized in Figure 5 and include both tuning the structures by allowing uplift or addition of damper devices, and strengthening the structures to minimize the damage. The vulnerable areas for the suspension bridge and the proposed retrofit are:

a. Connection between Stiffening Trusses and Towers: Impact between the main span stiffening trusses and the towers as displacements exceed the existing displacement capacity. The proposed retrofit includes the installation of large capacity dampers at this location.

b. Side Span Stiffening Trusses: High tension and compression stresses are developed in the chords. A detailed local nonlinear model of a chord member shows that the required ductility is attainable.

c. Main Towers: Uplift due to rocking motion of the tower causes high contact stresses at the toe of the uplifting base, requiring strengthening of the steel plates.

d. Concrete Piers: The piers supporting the main towers are subjected to high bearing stresses under uplift conditions. The installation of reinforcing at the top of the piers will provide confinement.

e. Reinforced Concrete Pylons: New ductile concrete walls inside the pylons are proposed to increase strength and ductility.

f. Cable Saddles: The connection of the cable saddles to the tower tops need to be strengthened for shear stresses due to differential cable tension.

g. Deck Panels: The connections of the orthotropic steel plate panels to the floor beams need upgrading due to high horizontal shear forces.

C.6. Conclusions on Seismic Studies of the Golden Gate Bridge

The seismic retrofit studies have shown that retrofit measures can be developed, designed and constructed to provide adequate capacity to resist the demands from a major earthquake occurring on the San Andreas fault. Contract plans and retrofit designs are expected to be completed in late 1994. The three-year construction period is scheduled to start in early 1995.

D. SEISMIC EVALUATION AND RETROFIT OF THE EAST BAY CROSSING OF THE BAY BRIDGE (Astaneh-Asl, 1993a)

The San Francisco-Oakland Bay Bridge is an 8.3-mile (13.4 km) long steel structure designed and constructed in the 1930's. The bridge consists of two separate structures. The West Bay Crossing, spanning the Bay between San Francisco and Yerba Buena Island, consists of two suspension bridges placed in tandem and has a length of about 2.5 miles (4 km). The East Bay Crossing, which also has a length of about 2.5 miles (4 km) over the water, consists of a number of 288-foot (88 m) and 504-foot (154 m) span trusses and a 2420-foot (738 m) long cantilever truss, as shown in Figure 1. The Bay Bridge has two, 65-foot (20 m) concrete decks, each deck carrying five lanes of traffic. The reinforced concrete decks are supported on steel transverse stringers, which in turn are connected to floor transverse plate girders. The floor plate girders are connected to two main longitudinal trusses at their panel points (Astaneh-Asl 1993a). The majority of connections are riveted angles or gusset plates. Laced riveted built-up members are used throughout the bridge.

To assess the seismic condition of the East Bay Crossing of the Bay Bridge, a research project was initiated at the University of California at Berkeley in 1990 (Astaneh-Asl 1993a). The research project had several major inter-related areas of emphasis and activity. These were:

- To establish performance criteria for components of the bridge to achieve the global performance criteria discussed in the previous section,
- To establish seismic Safety Evaluation Earthquake (SEE) ground motions for the site,
- To conduct geotechnical studies and develop ground motions that will reach sub-structure of the bridge,
- To develop realistic 2-dimensional and 3-dimensional elastic as well as non-linear models of the superstructure,
- To conduct time-history and response spectra dynamic analyses of the existing structure as well as of the structure after implementing a number of promising retrofit strategies.
- To establish seismic vulnerabilities and to develop efficient retrofit concepts and strategies to achieve the performance criteria stated in previous section.

D.1. Seismic Vulnerabilities of the East Bay Crossing of the Bay Bridge

A summary of seismic vulnerabilities of the East Bay Crossing is shown in Figure 6. The vulnerable areas are: the substructure east of Pier E5, reinforced concrete piers E1 and E17 through E23, steel towers particularly Pier E9, bottom chord eye-bars of 504-foot span trusses and floor plate girders in the areas between the deck and trusses.

D.2. Seismic Retrofit Concepts

In developing retrofit recommendation to mitigate the vulnerabilities, the main criteria were to ensure that underwater damage is prevented and the gravity load carrying components of the bridge remain essentially elastic. Yielding of existing components of the bridge that do not participate in carrying gravity were used to control and reduce global seismic response.

311

Retrofit Concepts for the Super-Structure

Several retrofit strategies to mitigate seismic vulnerabilities of the superstructure have been developed and proposed (Astaneh-Asl 1993a). Figure 7 shows the most promising retrofit strategy for the superstructure. The strategy consists of using "semi-rigid" devices at strategically placed locations. The steel based devices have a force displacement response of elastic, plastic yield plateau and then kinematic hardening regimes. The proposed devices are expected to remain within the elastic range during small and moderate earthquakes and become a passive energy dissipater during the major earthquakes as the device enters plastic yield plateau regime of behavior. The third phase of behavior, the kinematic hardening, is used to control and prevent large displacements that can occur in an elastic-perfectly plastic system.

Retrofit Concepts for the Sub-Structure

The strategy proposed for retrofit of the sub-structure consists mainly of adding new ductile steel or steel/concrete composite piles outside the existing foundations and constructing new ductile reinforced-concrete jackets around the existing foundations and pedestals.

D.3.   Conclusions on Seismic Studies of the East Bay Crossing of Bay Bridge

The seismic studies of East Bay Crossing indicated that the reinforced concrete piers and foundations are non-ductile and need major strengthening. The substructure supported on timber piles need strengthening. Bottom chord eye-bars of trusses and some steel towers need strengthening.

The vulnerabilities can be removed by either adding to the strength and stiffness or by utilizing semi-rigid devices at strategic locations. Use of semi-rigid devices results in significant reduction of seismic forces without noticeable increase in displacements. Therefore, the use of semi-rigidity in developing efficient and economical retrofit strategies is recommended.

CONCLUSIONS

The seismic studies of four major steel bridges in the San Francisco Bay indicated that: for San Mateo-Hayward bridge, Benicia Martinez bridge and the East Bay Crossing of the Bay bridge, all supported on soil, the reinforced concrete substructure was the most vulnerable area. For the Golden Gate bridge, supported on rock, some components of the steel super-structure were vulnerable.

Feasibility of two retrofit strategies has been studies. In the first strategy, in a traditional way, the strength and stiffness of the structure are increased to match the demand. In the second strategy, by introducing passive energy dissipation and isolation mechanisms, such as friction or semi-rigid systems, the seismic demand on the structure is decreased while the capacities are increased as needed. The second strategy appears to be more economical and efficient.

ACKNOWLEDGMENTS

REFERENCES

Astaneh-Asl, A. (1993a). "Seismic Retrofit Concepts for the East Bay Crossing of the San Francisco-Oakland Bay Bridge." *Proceedings*, First US. Seminar on Seismic Evaluation and Retrofit of Steel Bridges, Department of Civil Engineering, University of California at Berkeley, San Francisco, California, October 18.

Astaneh-Asl, A. and Shen, J.H. (1993b). "Seismic Performance and Design Considerations in Steel Bridges," *Proceedings*, First US. Seminar on Seismic Evaluation and Retrofit of Steel Bridges, Department of Civil Engineering, University of California at Berkeley, San Francisco, California, Oct. 18.

Donikian, R. (1993). "Seismic Vulnerability Assessment of the San Mateo-Hayward Bridge." *Proceedings*, First US. Seminar on Seismic Evaluation and Retrofit of Steel Bridges, Department of Civil Engineering, University of California at Berkeley, San Francisco, California, Oct. 18.

IAI (1991). NEABS Nonlinear Earthquake Response Analysis of Bridge Structures and Post-Processing Programs, Imbsen & Associates, Inc., Sacramento California.

Imbsen, R.A. and Wen, D.L. (1993). "Seismic Evaluation of Benicia-Martinez Bridge." *Proceedings*, First US. Seminar on Seismic Evaluation and Retrofit of Steel Bridges, Department of Civil Engineering, University of California at Berkeley, San Francisco, California, October 18.

Seim, C., Ingham, T. and Rodriguez, S. (1993). "Seismic Performance and Retrofit of the Golden Gate Bridge." *Proceedings*, First US. Seminar on Seismic Evaluation and Retrofit of Steel Bridges, Department of Civil Engineering, University of California at Berkeley, San Francisco, California, October 18.
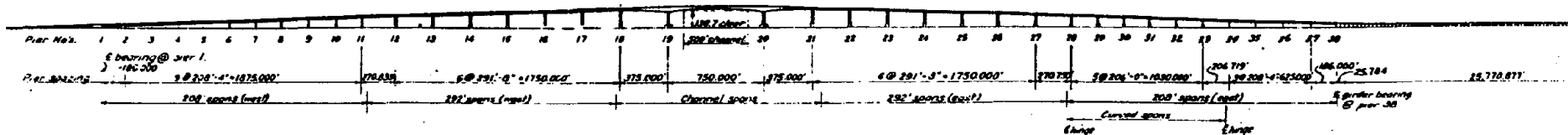
San Mateo-Hayward Bridge
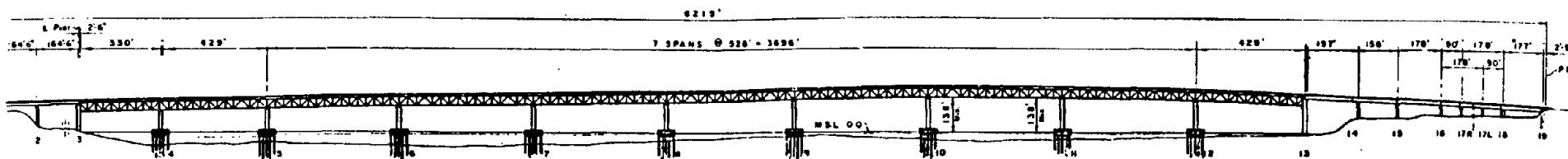
Benicia-Martinez Bridge
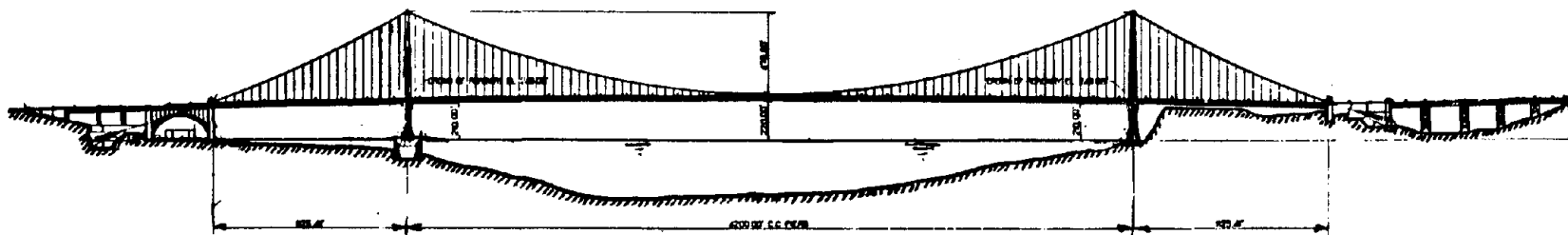
Golden Gate Bridge
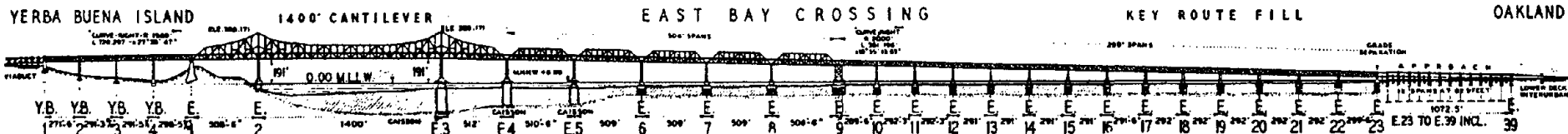
East Bay Crossing of San Francisco-Oakland Bay Bridge

Note: Views do not have the same scale.

Figure 1.   Views of Four Steel Bridges Discussed in the Paper
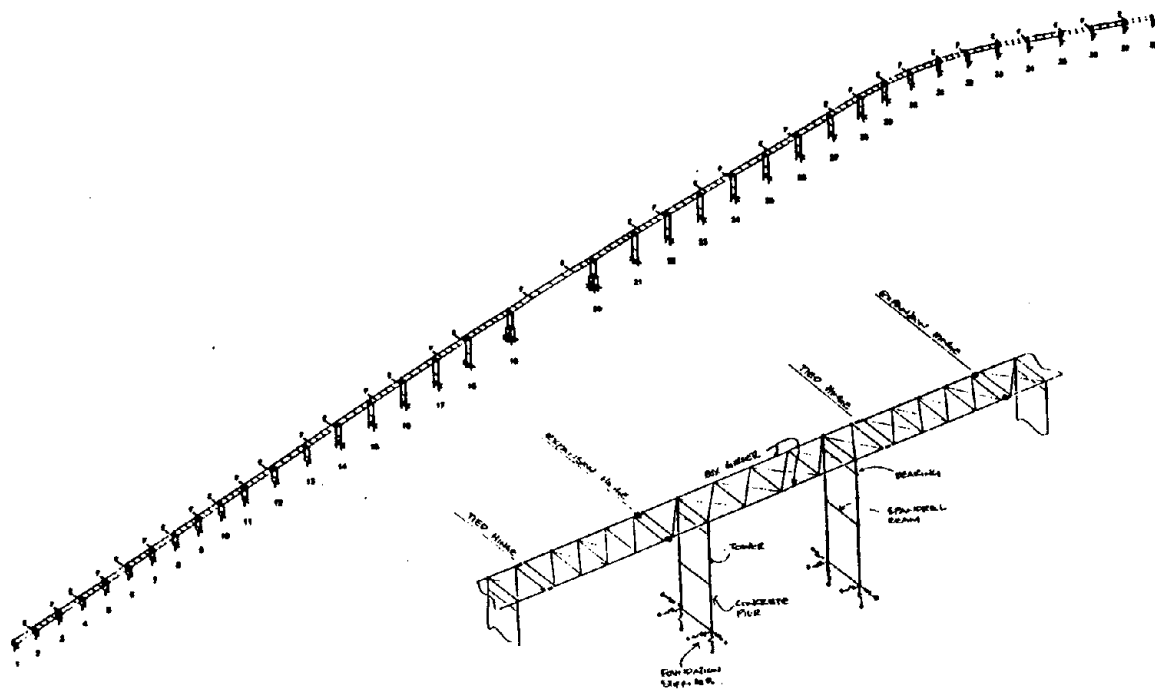
Figure 2.   Finite Element Model of the San Mateo-Hayward Bridge (Donikian, 1993)
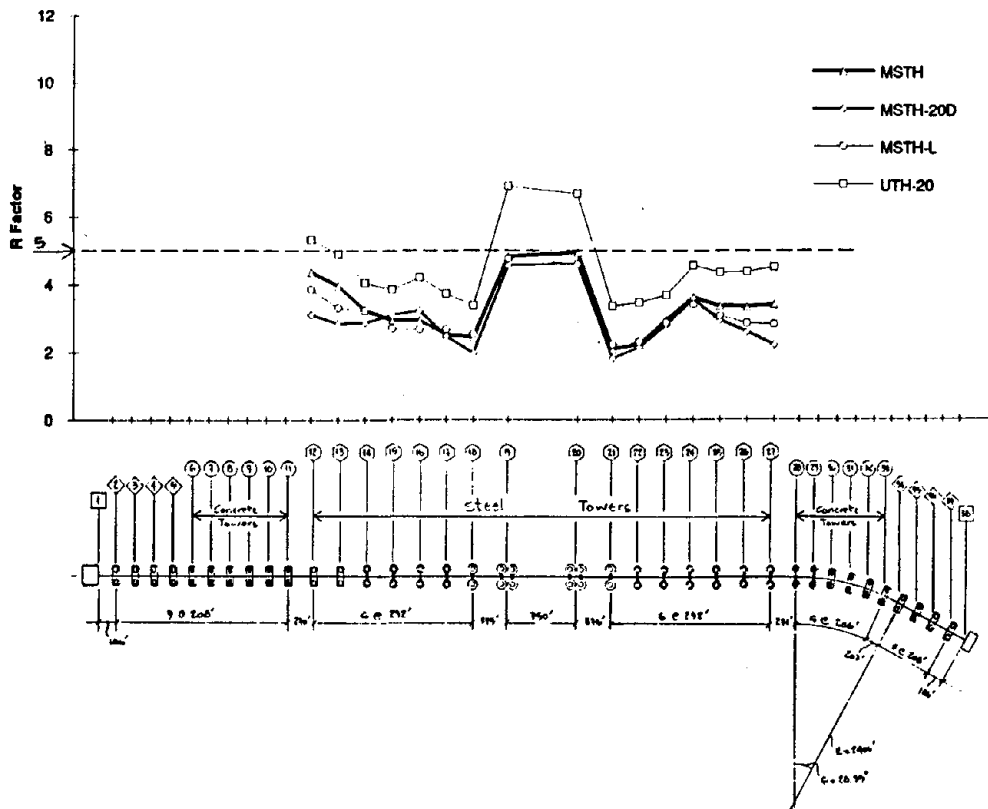
Figure 3.   R-Factors for Steel Towers of San Mateo-Hayward Bridge (Donikian, 1993)

Figure 4. Critical Sections of the Substructure of the Benicia-Martinez Bridge

316

Figure 5. Golden Gate Bridge Retrofit Measures (Seim, 1993)

317

Saddle:
◇ *Strengthen saddle/cable connection by adding steel dowels*

Tower Shaft

Tower Strut

◇ *Install dampers*

South Viaduct:
◇ *Install isolators,*
❖ *Replace some members,*
❖ *Add cover plates,*
◇ *Strengthen foundation*

Fort Point Arch:
❖ *Install dampers,*
❖ *Add cover plates.*
❖ *Replace some members*

Cable

Suspender

❖ *Wind Cross Bracing*

North Viaduct:
◇ *Install isolators,*
❖ *Replace and add some members.*
❖ *Add cover plates,*
◇ *Strengthen foundation*

◇ *Install dampers*

◇ *Install dampers*

Stiffening Trusses

❖ *Wind Stabilizers*

◇ *Install dampers*

South Anchorage Housing:
◇ *Strengthen by reinforcing internally*

Pylon S2:
◇ *Strengthen by reinforcing internally*

Pylon S1:
◇ *Strengthen by reinforcing internally*

South Tower

Tower Base:
◇ *Strengthen with additional steel plates and angles*

Pier Top:
◇ *Confine concrete with prestressed steel tendons*

North Tower

Pylon N1:
◇ *Strengthen by reinforcing internally*

North Anchorage Housing:
◇ *Strengthen by reinforcing internally*

Legend
◇ *No change in visual appearance*
❖ *Change in visual appearance*

Golden Gate Bridge Retrofit Measures

① R/C Pier E1 needs strengthening.
② R/C footing uplifts.
③ Steel towers need some strengthening.
④ Expansion joint should be opened.
⑤ Bottom chord eye-bars need modification.
⑥ Steel towers need some strengthening.

⑦ R/C foundations and timber piles need strengthening.
⑧ Steel tower E9 needs major strengthening.
⑨ Steel towers and trusses need some strengthening.
⑩ R/C Pier E17 needs strengthening.
⑪ Truss-to-pier connections need strengthening.

Figure 6. Seismic Vulnerabilities of the East Bay Crossing of Bay Bridge (Astaneh-Asl, 1993a)

Steel "Semi-rigid" devices are added to top of Pier E1 and pin hole slotted to enable the structure to become semi-rigid during maximum credible earthquakes.
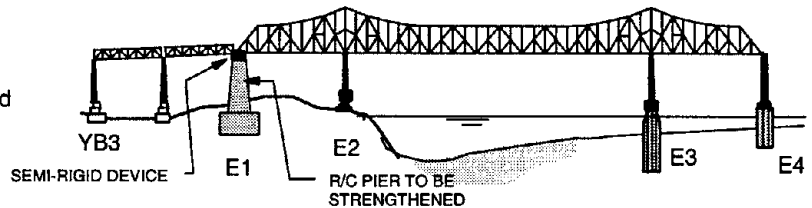
Add semi-rigid devices to the base or better to top of Pier E9 to permit the pier to become semi-rigid during maximum credible earthquakes. Bottom chord eye-bars of 504-foot trusses strengthened.
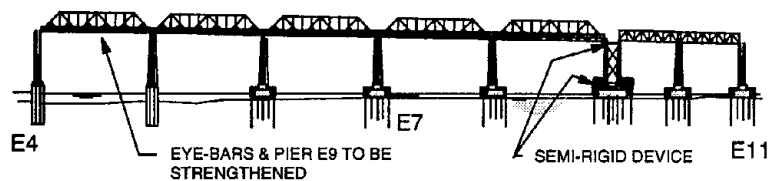
Add semi-rigid devices to top of Pier E17 to permit the structure to become semi-rigid during maximum credible earthquakes. Bottom chords of some of the trusses may need strengthening.
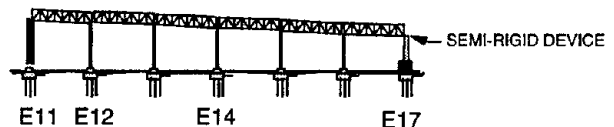
Add semi-rigid devices to the truss shoes of each span.
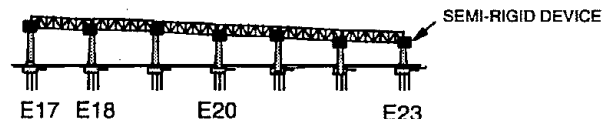
Adding "Semi-rigidity" but Maintaining Original Articulation

Figure 7. One of the Efficient Retrofit Strategies for the Bay Bridge (Astaneh-Asl, 1993a)

318

Tests and Research on Carbon Fiber Strengthening of Existing Bridges

N. Ogata, Y. Maeda and H. Ando
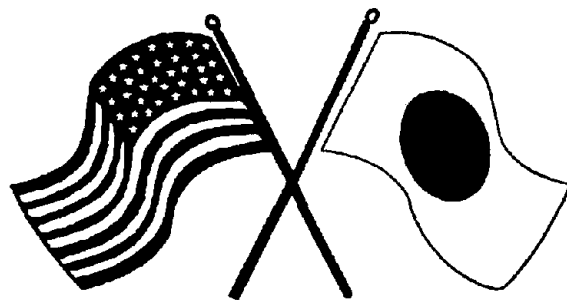
TESTS AND RESEARCH ON CARBON FIBER STRENGTHENING OF EXISTING BRIDGES

Norio Ogata [1]   Yoshifumi Maeda [2]   Hirofumi Ando [3]

[1]Head, Bridge Section, Research Institute, JHPC, 1-4-1 Tadao, Machida City, Tokyo, 194 Japan
[2]Deputy Head, Bridge Section, Research Institute, JHPC, 1-4-1 Tadao, Machida City, Tokyo, 194 Japan
[3]Engineer, Bridge Section, Research Institute, JHPC, 1-4-1 Tadao, Machida City, Tokyo, 194 Japan

ABSTRACT

At present, highway bridge substructures must be strengthened against major earthquake. The Conventional strengthening methods include lining with reinforced concrete and steel plate bonding. We have reviewed a new method of bonding newly developed carbon fiber sheets, which may replace the existing methods. Bridge pier model testing indicated that ductility of specimens reinforced with the carbon fiber was improved, and that this method of reinforcement is suitable for practical use.

The need to strengthen superstructures has also become necessary as a result of increased motor vehicle weight and traffic volume. We reviewed the carbon fiber strengthening method to the superstructure and verified its potential through beam model testing.
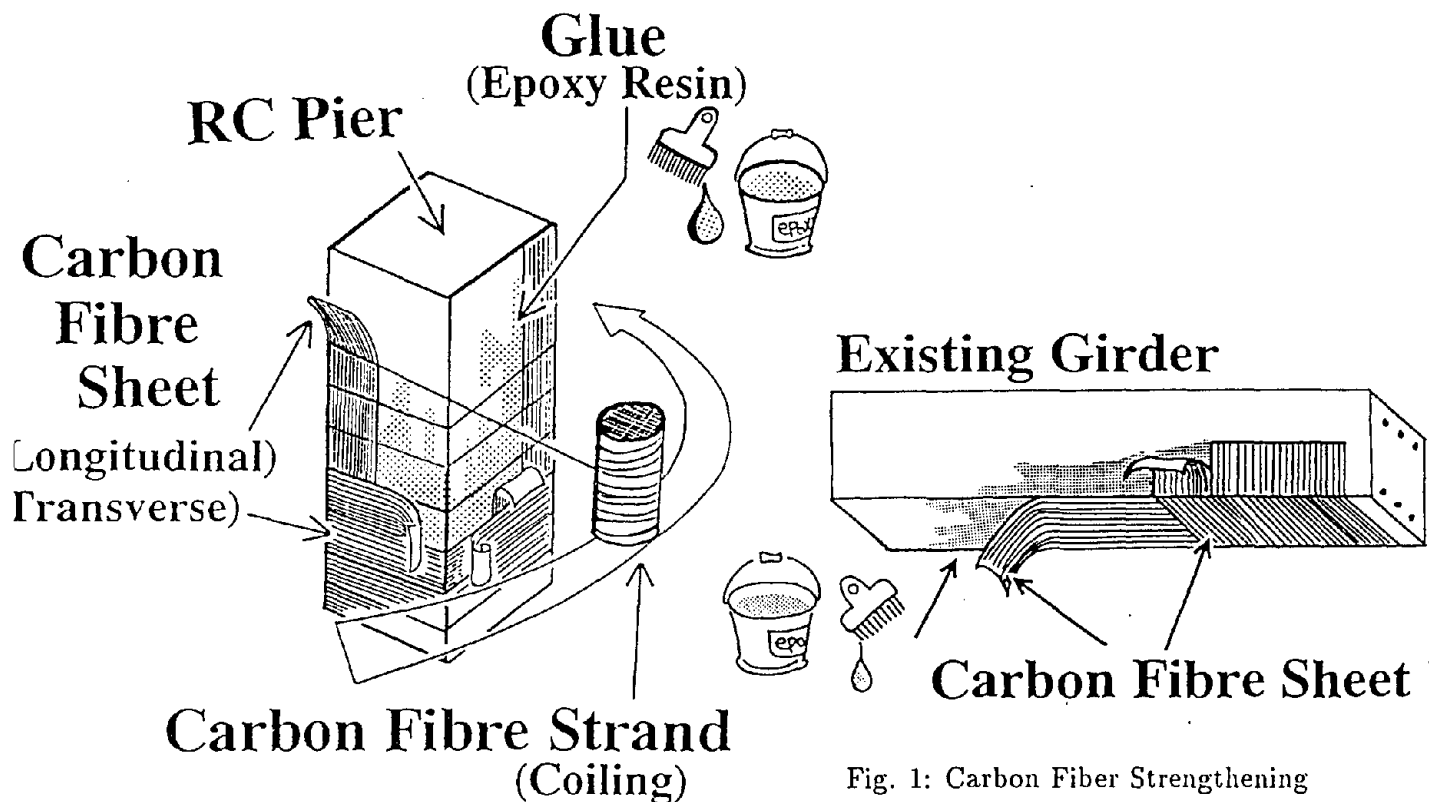
Fig. 1: Carbon Fiber Strengthening

INTRODUCTION

Although ordinary reinforced concrete bridge piers have a cut-off (transitional position) for longitudinal reinforcing bar to achieve an economic design of steel bars, some piers do not have sufficient anchorage length for the longitudinal reinforcing bar or enough stirrups, so that damage may occur at the cut-off part during major earthquake. Traditional countermeasures include the reinforced concrete lining method and the steel plate bonding method. Reinforced concrete lining is inexpensive but has problems such as increased sections and weight, chipping work, and noise problem.

Steel plate bonding does not create any more section and weight but is expensive to carry out and requires anchor driving work and rustproof treatment. Moreover, on present highway bridges, load often exceeds the design value because of the increasing weight of motor vehicles and growing traffic volume, so that the strengthening of the superstructure has become necessary. (Another strengthening method, the steel plate bonding method, is considered complicated due to the anchor driving and resin filling.) Therefore, we reviewed strengthening with carbon fiber, which has high strength and elasticity. Tensile strength is $25,000 kgf/cm^2$, Young's modulus is $2.5 \times 10^6 kgf/cm^2$, weight only $175g/m^2$ and thickness $0.1mm$. Increases in section and weight can thus be kept very low. Carbon Fiber is produced in sheets and strands for easy processing and working. Only bonding work is needed; anchoring is not necessary. Thus strengthening work will not damage the existing structure.

USE OF CARBON FIBER STRENGTHENING ON THE SUPERSTRUCTURE

In order to investigate the performance of carbon fiber strengthening of bridge piers and to establish design and work methods, we conducted loading tests on bridge pier models.

No.1, No.2, No.5 Specimens

Cross Section

(unit : mm)

No.3, No.4 Specimens
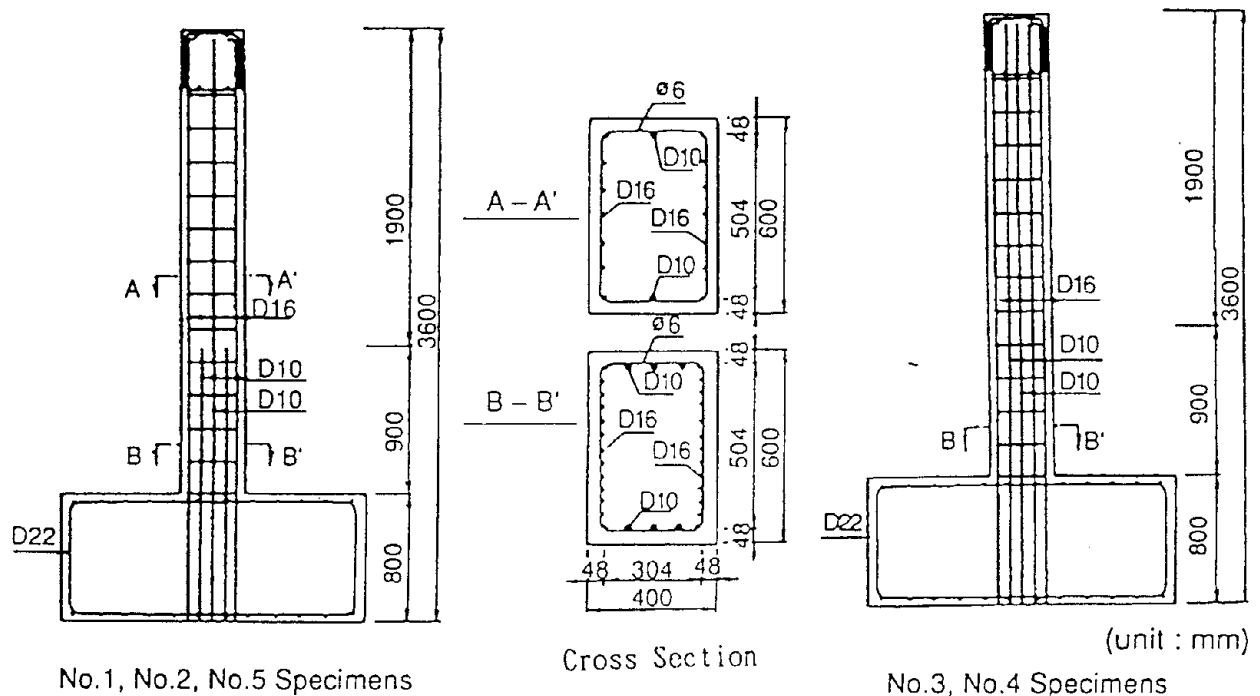
Fig. 2: Specimens of Pier Model Test

322

Table. 1: Specimens of Pier Model Test

| No. | Height of Cut-off | Length of CF Strengthening | | | | Sheets of CF | | |
| | | Length of Upper CF from Cut-off (mm) | Length of Lower CF from Cut-off (mm) | Total (mm) | Base of Column (mm) | Cut-off | | Base of Column |
						Longitudinal	Lateral	Lateral
1	900	-	-	-	-	-	-	-
2	900	450	450	900	-	2	2	-
3	-	-	-	-	600	-	-	1
4	-	-	-	-	600	-	-	2
5	900	530	400	930	500	2	2	2
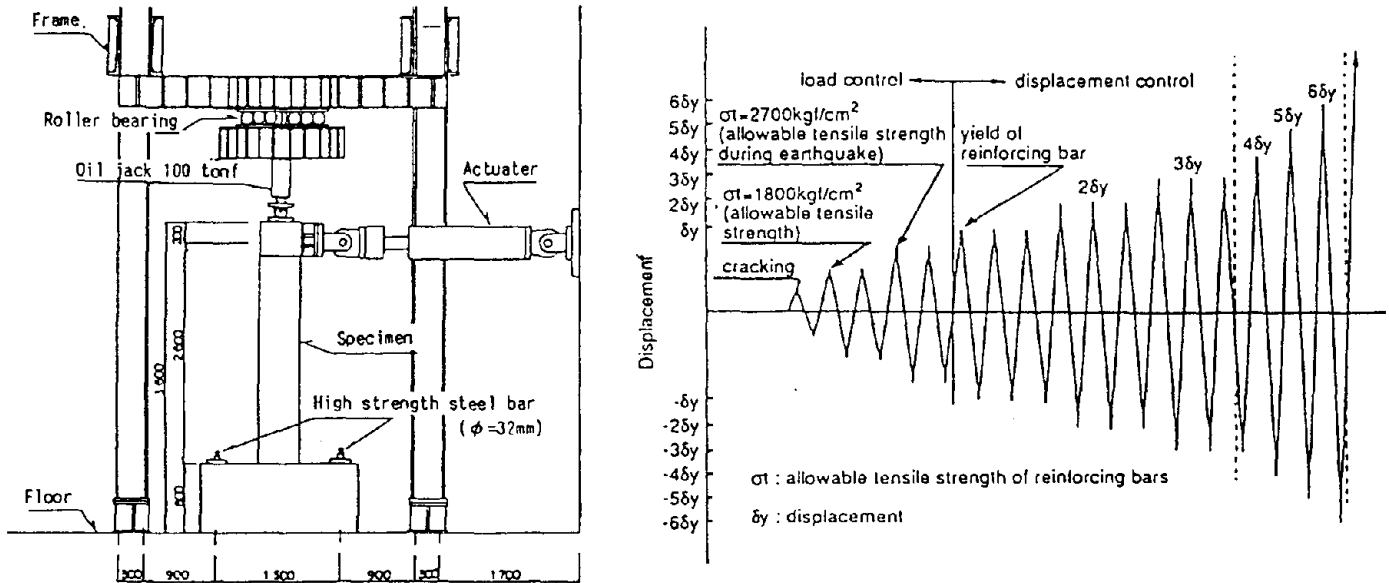
Fig. 3: Loading Apparatus and Pattern

Shape and Sizes of Specimens

Dimensions of specimens are shown in Fig. 2 and Table 1. For the $No.5$ specimen only, we damaged the cut-off and base of column; the damaged portions were then repaired with mortar and the cracked portions filled with epoxy resin and bonded carbon fiber, to assess performance after an earthquake.

Test Method

In the loading method, horizontal cyclic loading was given at the top of column while applying an vertical loading ($6kgf/cm^2$) corresponding to the reaction to the dead load of superstructure. The loading pattern is shown in Fig. 3. δ_y in the Figure represents the horizontal displacement of the top of the pier column due to the yielding of the reinforcing bars at the base of column.

Test Results

Test results are shown in Fig. 4 and Table 2. Here, we defined cracking as when visually noticeable appear cracks, yielding as when the reinforcing bars in the longitudinal direction on the tensile side have yielded, and the ultimate state as when concrete fails or carbon fiber is ruptured.

Table. 2: Results

Spec. No.	Cracking		Yield		Ultimate		Max Load		Ductility Rate μ	Failure Type
	Load P_c (tonf)	Displ. δ_c (mm)	Load P_y (tonf)	Displ. δ_y (mm)	Load P_u (tonf)	Displ. δ_u (mm)	Load P_{max} (tonf)	Displ. δ_{max} (mm)		
1	2.8	2.6	10.4	20.6	11.5	61.7	11.5	61.7	3.0	Bending
2	2.9	2.8	12.6	27.6	13.4	113.0	13.9	55.3	4.1	Shear
3	2.5	1.9	13.0	26.2	14.5	131.0	13.9	52.1	5.0	Bending
4	3.0	2.2	11.9	22.0	15.5	244.2	15.5	244.2	11.1	-
5	3.5	2.2	10.0	22.3	10.7	111.7	14.5	63.8	5.0	Bending

Fig. 4: Results

324
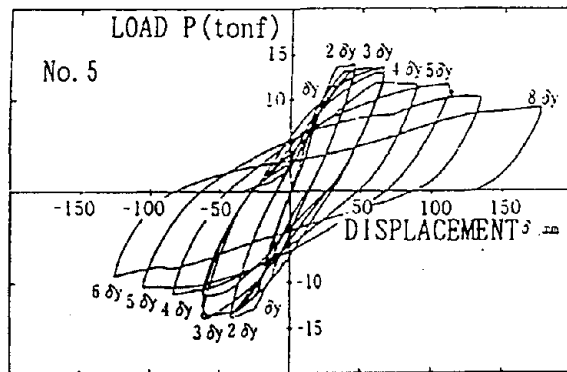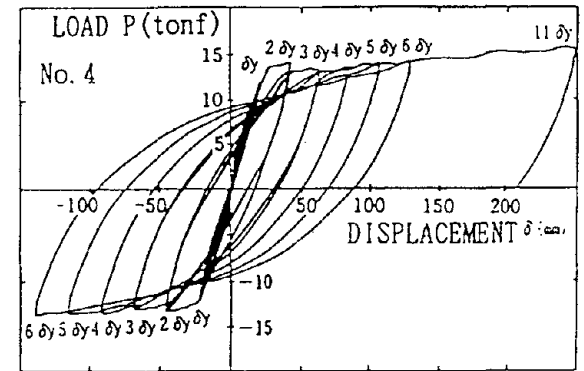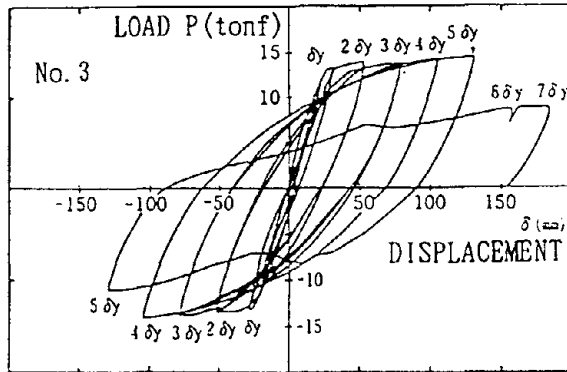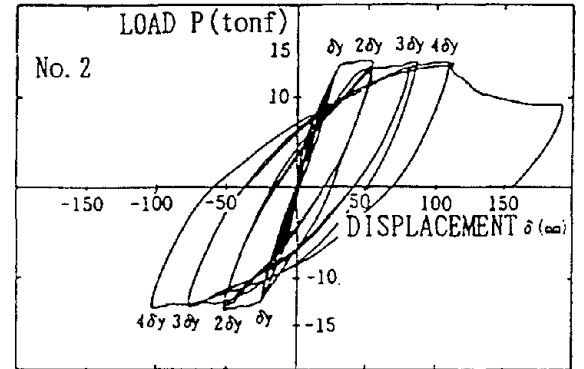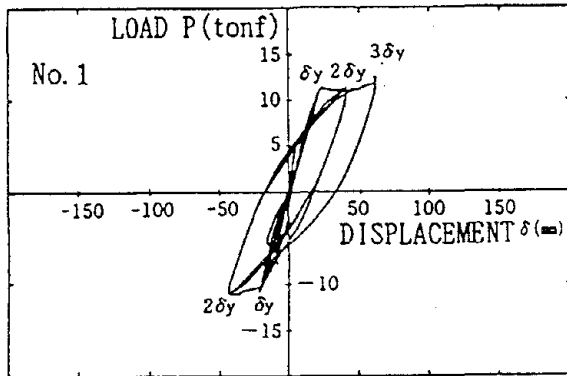
Fig. 4(a): Results

Specimen No.1
Bending failure at the cut-off
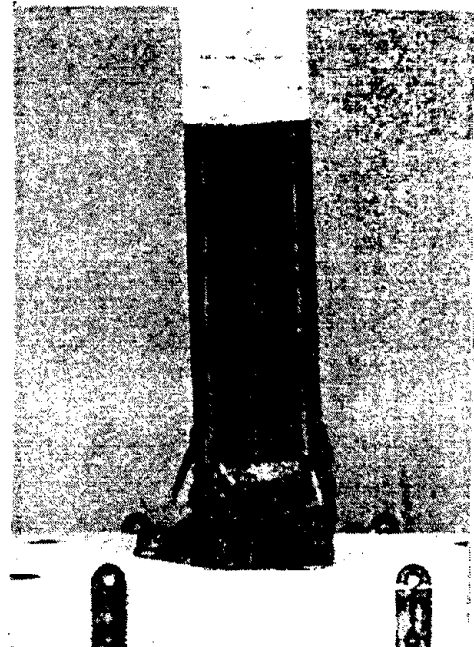
Fig. 4(b): Results

Specimen No.5
Bending failure at the base of column

The failure position of the No.1 specimen was at the cut-off portion of the reinforcing bars, while the failure position of the No.2 specimen shifted to the base of column. Thus it would appear that bending yield strength can be enhanced by bonding carbon fiber in the longitudinal direction.

The No.2 specimen suffered bending shear failure, but this changed to bending failure for the No.3 specimen, where the carbon fiber was wound in the direction of stirrups.

For the No.3 specimen, which had a amount of strand equivalent to one sheet wound around the base of column, failure was due to bending, and ultimate displacement was longer than the non-reinforced No.1 specimen. The No.4 specimen, which had two strengthning sheets in the lateral direction of the base of footing, did not fail under loading up to the maximum capacity of the loading device. Thus it was proven that deformation is improved by carbon fiber strengthening in the lateral direction.

The No.5 specimen was repaired after deliberately damaging it as stated above. The failure position shifted from the cut-off section to the base of column, failure itself was due to bending, and ductility was improved.

Discussion
Effect of Reinforcement

The experiment showed that the failure position shifted from the cut-off part to the base of column after bonding carbon fiber in the longitudinal direction, and that failure was due to bending when carbon fiber was bonded in the rateral direction, establishing its shear strengthening performance. Also, winding carbon fiber confines, the inner concrete and enhances the ductility of the bridge pier.

Energy Absorption

Generally, energy absorption improves as the area surrounded by the displacement of bridge pier and acting force increases, and the pier becomes more resistant to earthquake. Fig. 5 shows
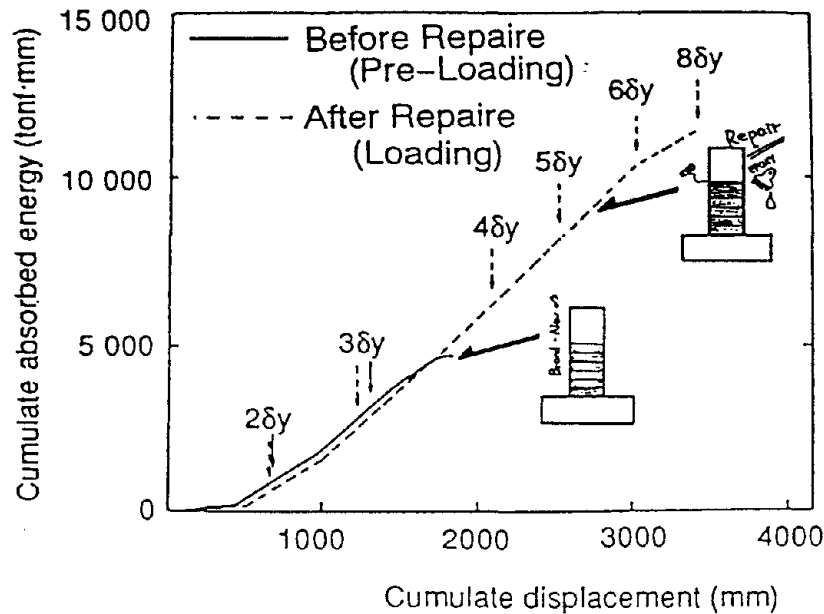
Fig. 5: Energy absorption

energy absorption before and after repair. With respect to the same cumulative deformation, energy absorption is slightly greater before repair compared to after repair. However the tilts are almost parallel, and tilts do not change until $6\delta_y$ after repair, from which it can be said that energy absorption did not fall until the ultimate state. From this, the present method was confirmed to be an effective for strengthening against earthquake. Also, if parts damaged by earthquake are properly repaired, energy absorption recovers to the same level as before and yield strength also recovers. This method is therefore considered to be excellent for strengthening following earthquakes.

USE OF CARBON FIBER STRENGTHENING ON THE SUPERSTRUCTURE

The superstructure of highway bridges are subject to repeated and continuously loading over long periods, lowering their durability against fatigue. We subjected a beam strengthened bonding with carbon fiber to 2 million cyclic loadings, and then performed static loading tests and reviewed the applicability of carbon fiber to beam members.

Shape and Dimensions of Specimens

Specimens were set up as shown in Table 3 for actual reinforced concrete and prestressed concrete bridges. Shapes and dimensions are shown in Fig. 6. Cracks were created in advance by applying a bending load, and strengthening carried out by bonding two layers of $20cm$-wide, $0.1mm$-thick carbon fiber. The design load was set such that the reinforcing bars would reach the allowable tensile stress $(= 1,800 kgf/cm^2)$. Strengthening was originally to be applied to the whole area of the bottom surface $10cm$ inwards from both supports. However carbon fiber began to peel off at the interface with the concrete of $No.2$ specimen during static loading; therefore for $Nos.3$ to 5 an overlapped carbon fiber portion was made at each end of bonding portion and the reinforcement area extended up to the end of the beam member.
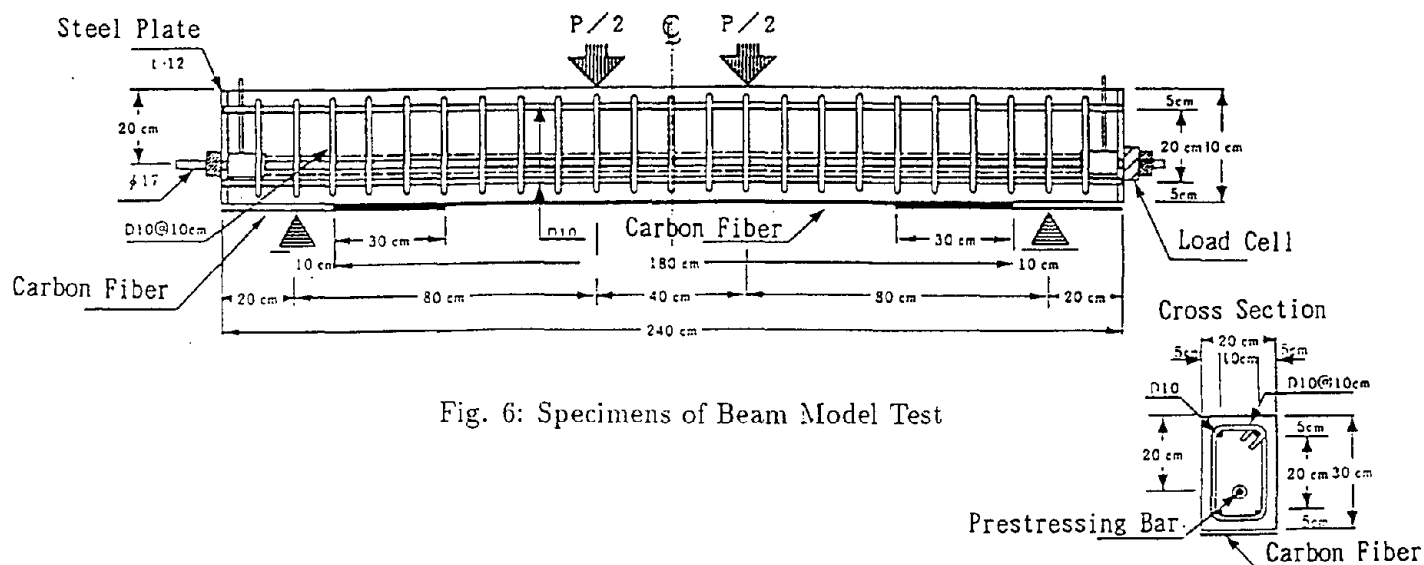
Fig. 6: Specimens of Beam Model Test

Table. 3: Specimen of Beam Model

Spec.No.	Strengthen with CF	Pre-Loading	Structural Type	Loading Type
1			PC	Static
2	○	○	PC	Static
3	○	○	PC	Cyclic (Allowable stress)
4	○	○	PC	Cyclic (Yield stress)
5	○	○	RC	Cyclic (Yield stress ×90%)

Test Method

Fatigue loading: *Nos.3* to 5 specimens in Fig. 7 were subjected to 2 million cyclic loadings at 3 to 4 *Hz*. Particular attention was given to the stress of reinforcing bars at the tensile side of the section of specimen. Upper and lower limit loads for load management were controlled as shown in Table 4.

Static test: Upon completion of fatigue loading test. we carried out static loading tests. Load, displacement and strain were measured

Test Results

The test results are listed in Table 5. Values were calculated from the results of material tests.

Situation of Failure

Fatigue tests: No anomaly such as peeling-off and rupture was found in *No.3*, for which the upper limit load was set to design load (load-creating tensile stress in reinforcing bars $= 1,800 kgf/cm^2$), or *No.5*, for which 90% of yield for reinforcing bars was used. In *No.4*, where the upper limit load was set to yield load (load-creating tensile stress of reinforcing bars $= 3,900 kgf/cm^2$), the carbon fiber peeled off and the load dropped after about 28,000 cycles. At this point repeated loading of *No.4* was terminated. For non-strengthened specimens. the open cracks were widest on the bottom surface, while cracks on the bottom surface of specimens were mostly closed. It appears that the occurrence of

327
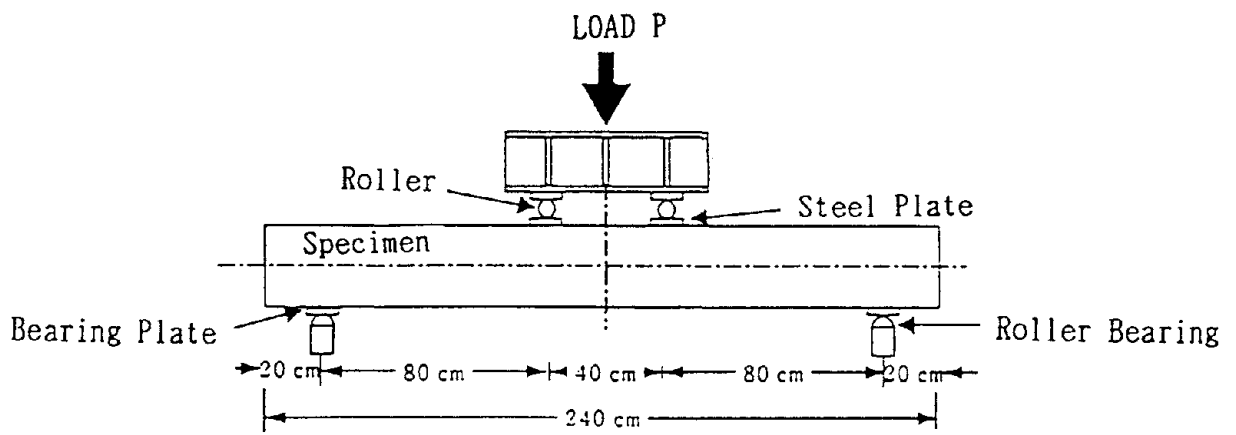
Fig. 7: Loading Apparatus

Table. 4: Conditions of Cyclic Load

Spec. No.	Upper level		Lower level	
	Load (tf)	Stress of tensile-steel bar (kgf/cm²)	Load (tf)	Stress of tensile-steel bar (kgf/cm²)
3	11.0	about 1800	3.0	about 0*
4	13.5	about 3900	3.0	about 0*
5	7.3	about 3400	3.0	about 600

* : Stress by prestressing was also taken into account.

cracks on the bottom surface was restricted by the carbon fiber bonded to the entire bottom surface area.

Static tests: In the *No.2* specimen, the bonded carbon fiber peeled off from the central part to the left side of the specimen during loading up to 18.7*t*, and the load decreased considerably. An examination of the peeled carbon fiber revealed chips of bottom concrete stuck on. We considered that deterioration, tensile strength and shear strength of concrete at the sticking interface are closely linked with the peeling off process. In *Nos.3* to 5, the carbon fiber peeled off in the middle but remained fixed by supports at both the ends of member, so that the specimens resisted against load in an unbonded state until finally, the carbon fiber at the center ruptured and failure occurred. Fig. 8 shows the cracks after static loading in *Nos.1* and 3. It can be seen that the cracks in *No.3* are more scattered than in *No.1*(non-strengthening).

Displacement

Fatigue tests: Fig. 9 shows the displacement at the central part of the beam, periodically measured at each repeating cycle for the *No.3* specimen. The displacement become larger as the repeating cycles increased in all state of upper limit loading, lower limit loading and non-loading(residual value). However, displacement tended to stabilize after about 10,000 cycles. This suggests a sufficient fatigue durability for 2 million repeats.

Static tests: Fig. 10 shows the relationship between the load of each specimen and the displacement at the center in static tests. In *No.3* both strength and displacement are much larger than *No.1*(non-strengthening) even after fatigue loading. Compared to *No.2* (without fatigue loading), dis-

Table. 5: Results

Spec. No.	Fatigue Loading			Static Loading				Condition
	Upper Level (tf)		Condition	Yield stress		Max stress		
				$\frac{expe.(tf)}{calc.(tf)}$	Ratio	$\frac{expe.(tf)}{calc.(tf)}$	Ratio	
1	-	-	-	$\frac{12.9}{13.1}$	0.98	$\frac{14.5}{15.0}$	0.97	Bnding failuer
2	-	-	-	$\frac{14.5}{15.1}$	0.96	$\frac{18.7}{20.5}$	0.91	Peeling of CF (18.7tf)
3	11.0	Allowable	No problem	$\frac{14.1}{15.1}$	0.94	$\frac{20.9}{20.5}$	1.02	Peeling of CF (18.7tf) Braking of CF (17.9tf)
4	13.5	Yield	Peeling of CF (28.000 cycle)	$\frac{-}{15.1}$	-	$\frac{14.9}{20.5}$	0.77	Braking of CF (14.9tf)
5	7.3	Yield ×90%	No problem	$\frac{8.0}{8.0}$	1.00	$\frac{15.5}{16.4}$	0.95	Peeling of CF (15.5tf) Braking of CF (15.4tf)
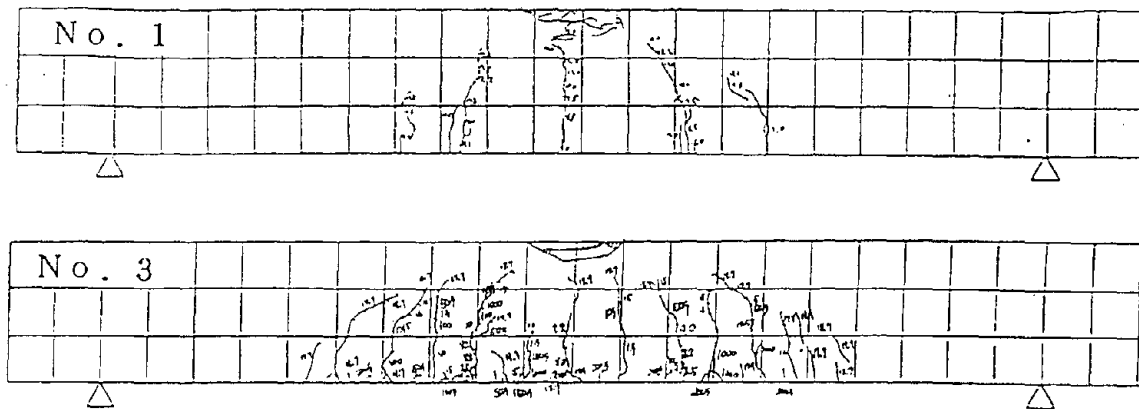
Fig. 8: Cracks after Static Loading

placement increased slightly from crack occurrence load ($7tf$) to near the design load ($11tf$) indicating the influence of fatigue. However, peeling-off of carbon fiber occurred at almost the same displacement and maximum load values are almost the same, so there will be no problems even against cyclic loading. In the case of $No.5$(reinforced concrete), the peeling-off of carbon fiber began just before reaching maximum load; however a sudden drop in load was not seen, the maximum load was almost the same as the analysis values, and the ultimate displacement was elongated.

Strain

Fig. 11 shows the strain distribution (during upper limit load) in the central section of the beam during repeated loading of the $No.3$ specimen. Even though the repeated loading cycles increased, the strain distribution on the section almost perfectly held a plane, thereby indicating that carbon fiber bears the load without being deteriorated by fatigue.

329
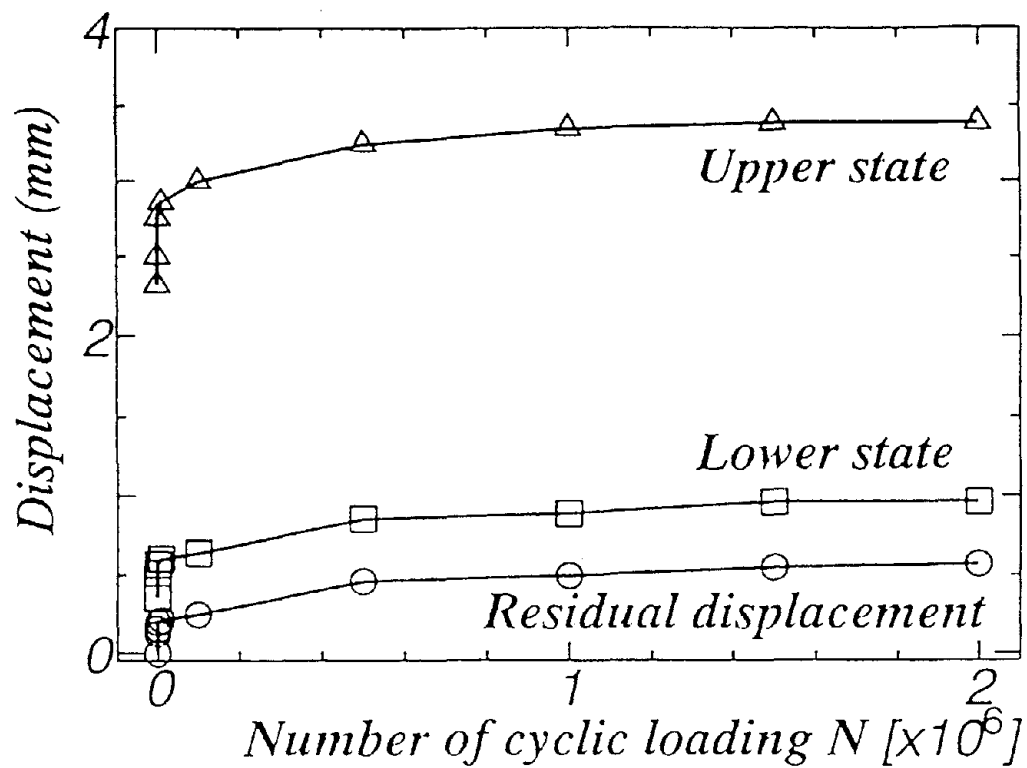
Fig. 9: Displacement during Fatigue Tests
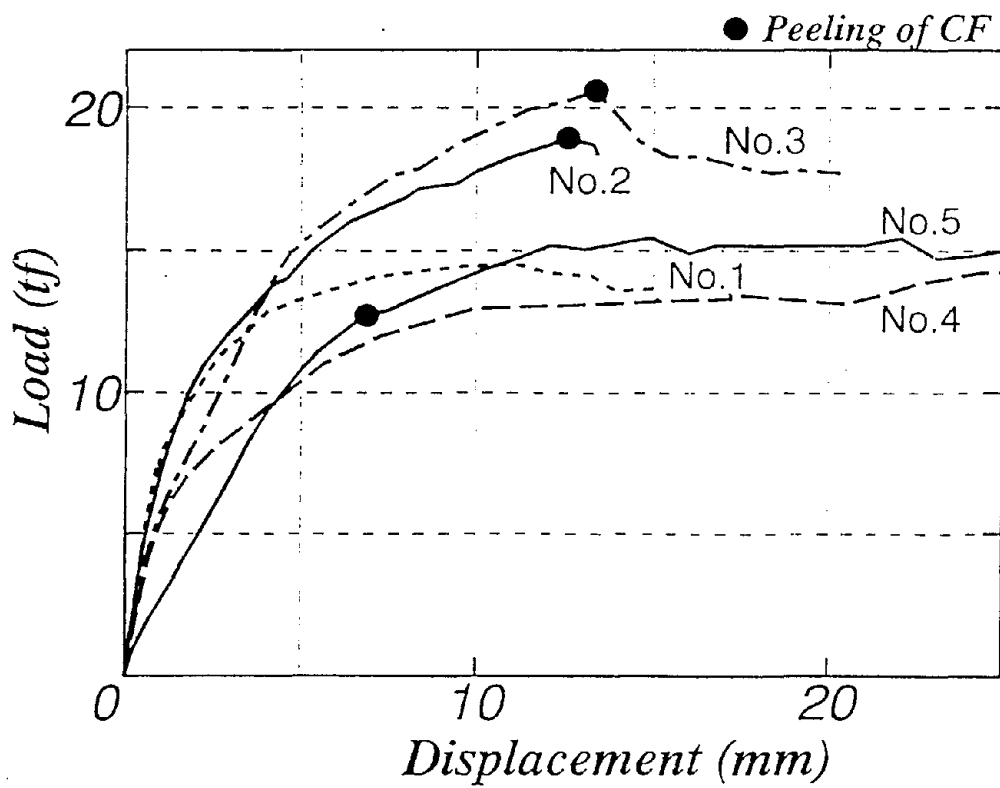
Fig. 10: Relationship between Load and Displacement
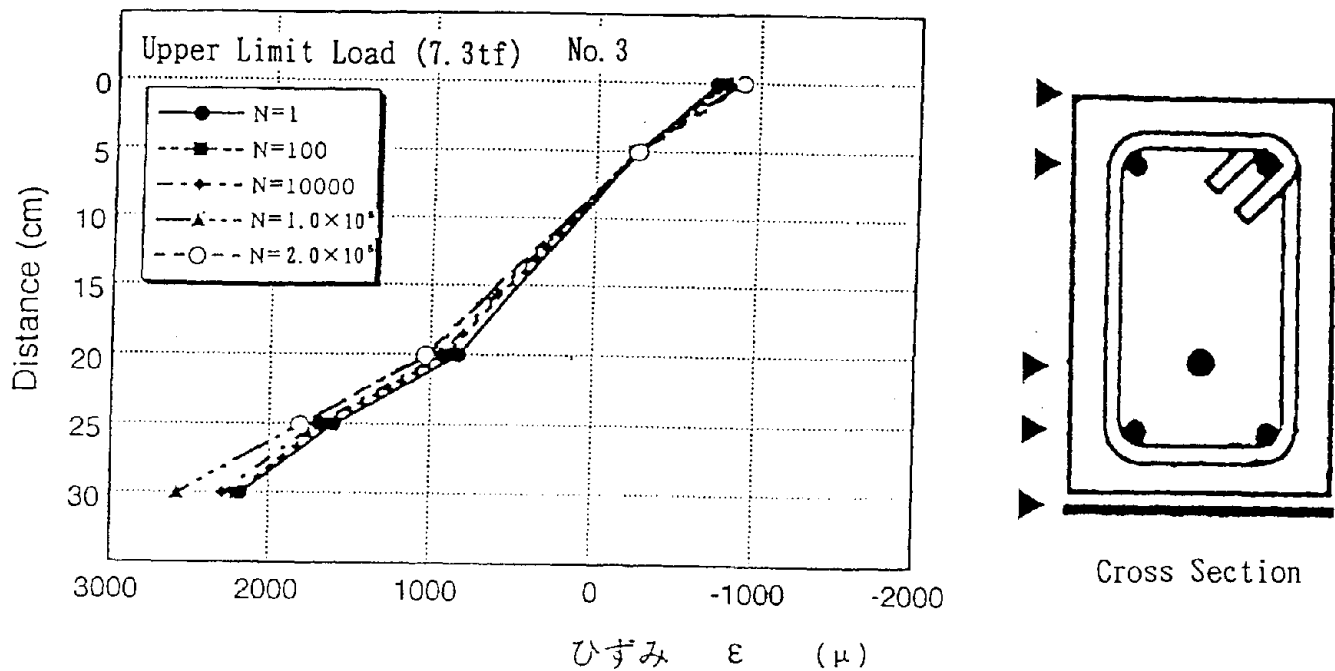
Fig. 11: Strain Distribution

CONCLUSIONS

Use of Carbon Fiber Strengthening on the Substructures

We found that if carbon fiber is bonded in the longitudinal direction of a reinforced concrete bridge pier, then the bending strength can be improved, the failure position can be shifted from the cut-off position to base of column, and if bonded in the direction of the stirrups, the ductility can also be improved. In this report we calculated the number of sheets used for reinforcement such that all of the acting shearing forces would be borne by the carbon fiber. We are currently considering the resistance to shearing forces by a conbination of concrete, stirrups and carbon fiber for greater economy. We are planning to carry out verification tests for this economic approach.

Use of Carbon Fiber Strengthening on the Superstructures

Carbon fiber is not damaged at the design load level, is a strong strengthening material, and provides strengthening even after repeated loading. The strength of members can be calculated using conventional methods (converted to reinforced concrete). In the future, additional studies will be required into the peeling observed during tests, as well as on effective fixing methods for end portions.

EXCEPTION PLAN OF CARBON FIBER STRENGTHENING ON EXISTING PIER

The Keiyo-Highway is a part of the metropolitan area expressway network, and linkes Metropolice Tokyo and Chiba Prefecture.(Fig. 12) It didn't only help take care of the radial traffic disposal of Metropolice Tokyo, but also contributed to the development of the Keiyo-industrial area.

331

Currently, the Keiyo-Highway'sdaily traffic volume(avarage) amounted to 100,000 vehicles, and widening of road has become necessary because of countermeasure to traffic congeston. Bridges need widening of substructures as superstructures widened, but there are occasions when it is impossible to widen substructures because of adjustment load, adjustment area, and buried structures. In that cases, strengthening of substructures is necessary to resist a dead load attended widening superstructures, and live load. Moreover, construction noise must be kept low as adjustment houses stand roof by roof by the road.

For the above-mentioned, we adopted Carbon Fiber Strengthening Method instead of RC lining method.

Table. 6 showes parametrics of the bridge which is the object of strengthening this time, and Fig. 13 showes widening pier general view. Fig. 13(a) is Typical widening with RC. It needs reinforcing pile and footing widening construction. (Existing foundation has piles about 33.5m length, we want the construction cost to keep low, and it is impossible to widen foundation becouse of adjustment load.) On the other hand, Widening with Carbon Fiber Strengthening does't need any more reinforcing piles. Figs. 14 and 15 showes Carbon Fiber construction detailes.

This construction will be started on July in this year.
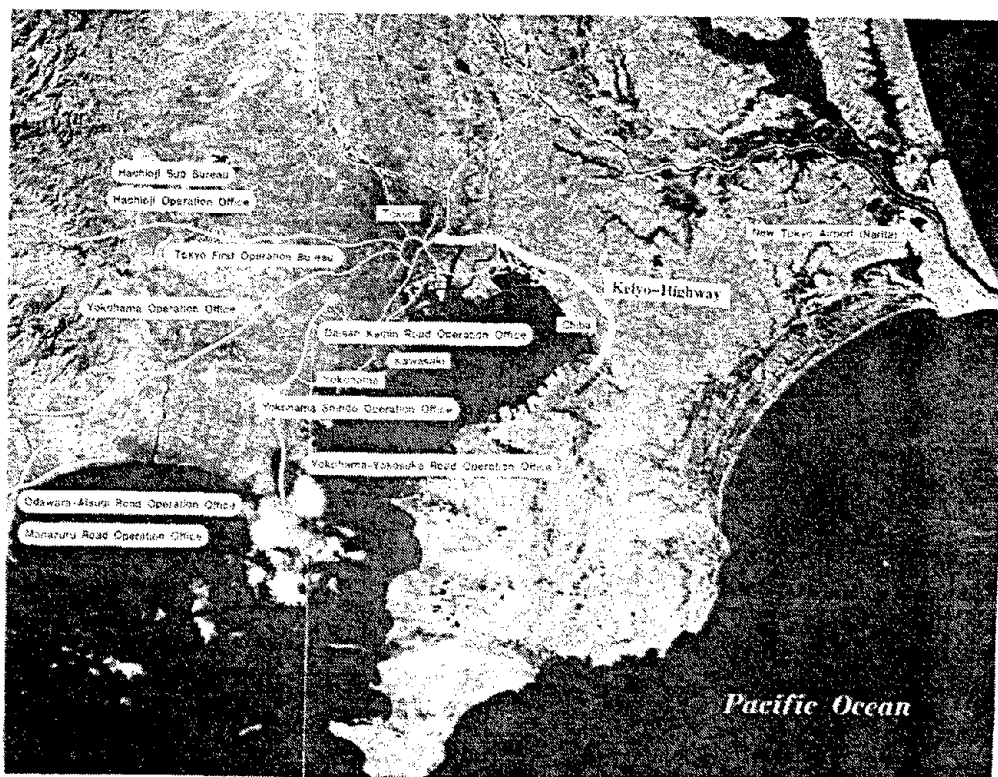
Fig. 12: Keiyo-Highway

Table. 6: Parametrics

Bridge Name	Keiyo-Highway Honmachi-Viaduct
Length	L=166.2 m
Span	4@20.6, 4@20.6
Superstructures	4-span coutinuous PC Box-girder bridges
Substructures	Counterforted buttressed abutment ×1 Wall type pier ×7
Foundations	Cast in place concrete pile (ϕ1000, Length=33.5m) ×8
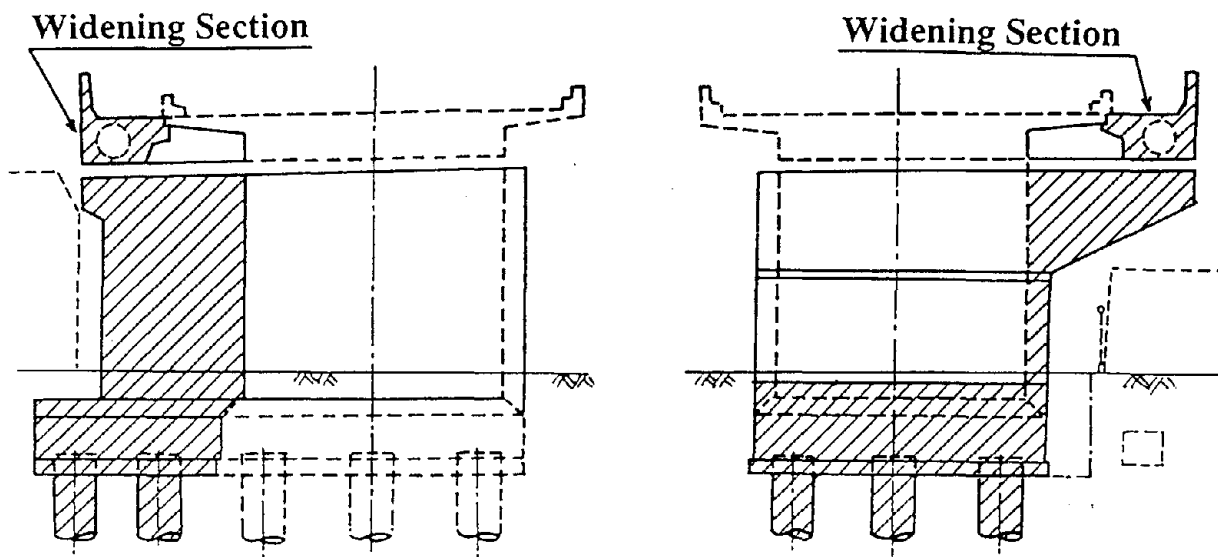
(a)Typical Widening with Reinforced Concrete   (b)Widening with Carbon Fiber Strengthening

Fig. 13: General View

Longitudinal CF (1 Ply)

Transverse CF (1 Ply)

Transverse CF (1 Ply)

Transverse CF (2 Ply)

Longitudinal CF (2 Ply)

Transverse CF (2 Ply)

Fig. 14: Pier detail

Deformed Bar ϕ 22

New Footing

Steel Plate

Existing Footing

Resin Cement Mortar

Drilling ϕ 30
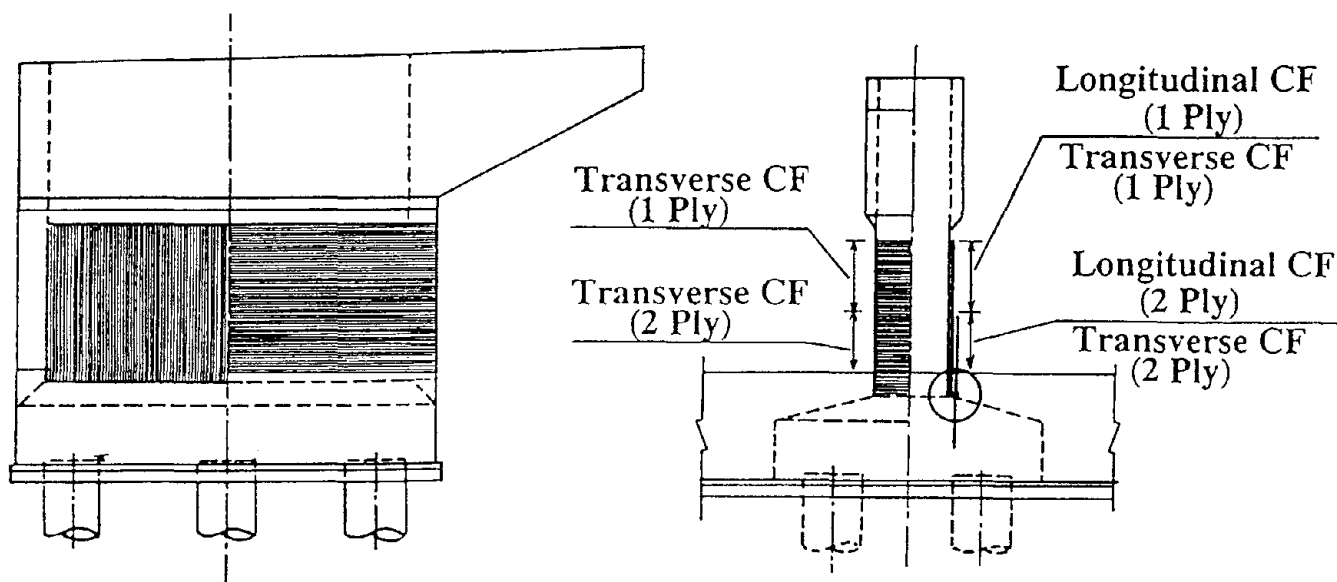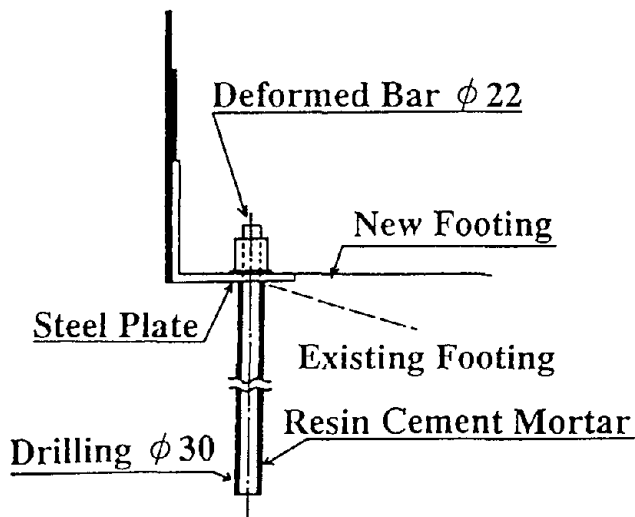
Fig. 15: Anchorage detail

Shear Strengthening of Existing Reinforced Concrete Column by Winding with Ararnid Fiber

T. Okamoto, M. Tanigaki,
M. Oda and A. Asakura
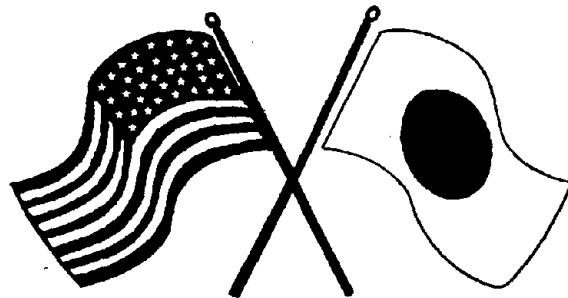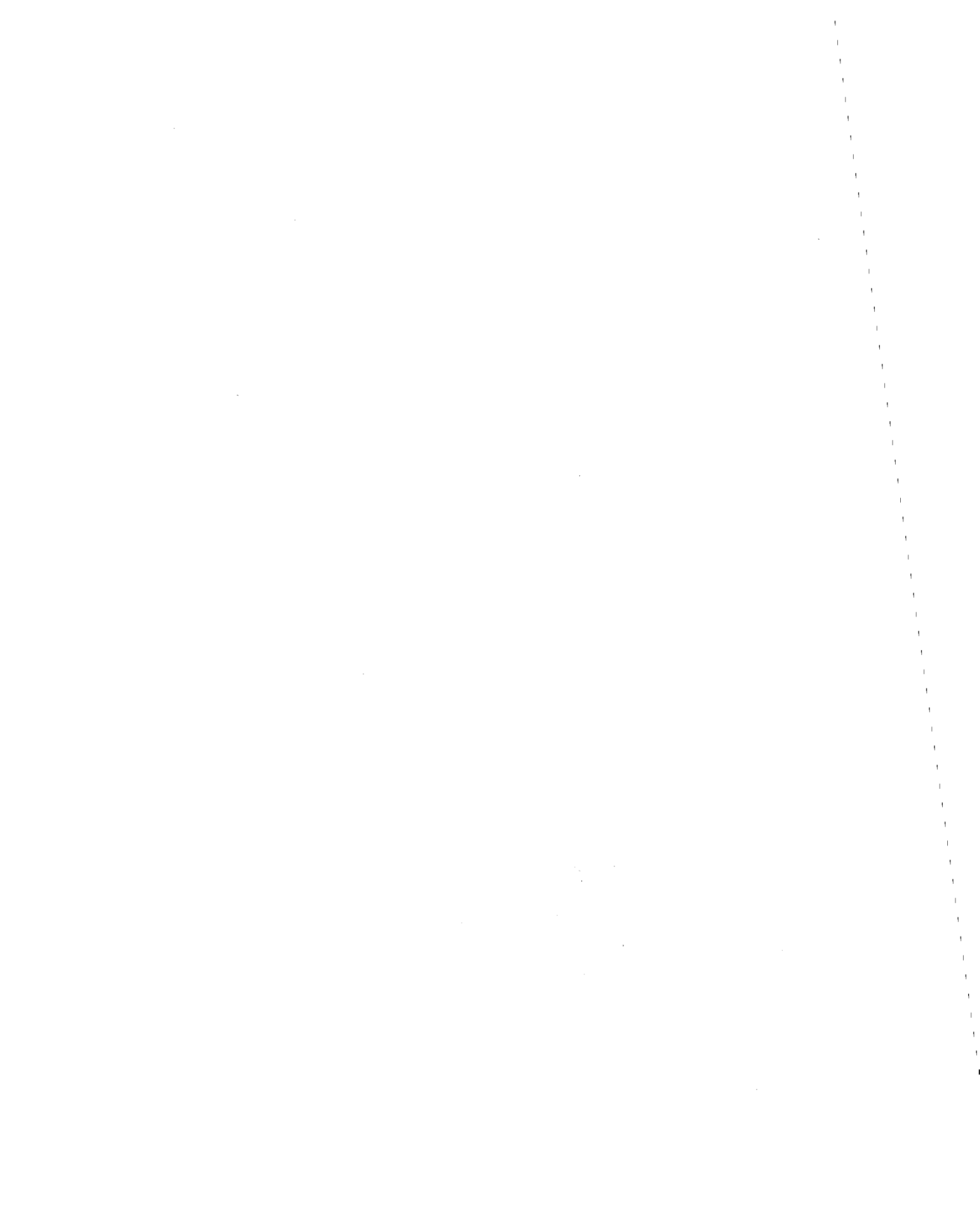
Shear Strengthening of Existing Reinforced Concrete Column by Winding with Aramid Fiber

Tadashi Okamoto (I)
Masaharu Tanigaki (II)
Minoru Oda (II)
Akira Asakura (III)

SUMMARY

The authors have proposed a method to strengthen existing concrete structures by winding the columns helically with aramid FRP(fiber reinforced plastic) tape considering the workability at the site.
To investigate the efficiency of FRP winding, loading tests of cantilever concrete columns were conducted. Total of 8 specimens were made by winding with aramid FRP tapes around reinforced concrete columns. The test results demonstrated that the proposed winding methods were effective to increase shear capacities and flexural ductilities of the concrete columns. The evaluation of participation of winding FRP for shear capacity of concrete column was also discussed.

1. INTRODUCTION

In Japan as well as in other countries, there are many infrastructures that need to be repaired or strengthened. Most of these infrastructures are buildings and bridges etc. which were damaged by earthquakes. Also infrastructures designed according to the previous code should be strengthened to conform with the revised guidelines against earthquake loading.
Methods for shear reinforcement of existing reinforced concrete columns include those using welded wire fabric and mortar, or steel plates, or tie plates [1]. A method in which high strength fiber is wound around columns has also been proposed, and the effectiveness of a winding method using carbon fiber has been reported[2]. This winding method makes use of the material characteristics of aramid fibers that are high strength, light weight and high durability and is expected the advantages of high strengthening effect and good workabilities etc. This paper describes the results of basic experiments conducted to ascertain the effectiveness of winding with aramid fiber for shear strengthening of concrete columns.

2. TESTING PROGRAM

2.1 Fiber Materials for Winding

The fiber materials for winding used in experiments were the three varieties of "Braided tape", "UD(Uni-Directional) tape"(Photo. 1), and "Sheet". Braided tape is aramid fiber woven in braid form and is approximately 2 cm in width. UD tape is a fabric woven in tape form using aramid fiber in the axial direction and glass fiber in the transverse direction having a width of approximately 7.5 cm. The quantities of fiber per cross section of Braided tape and UD tape were the same at
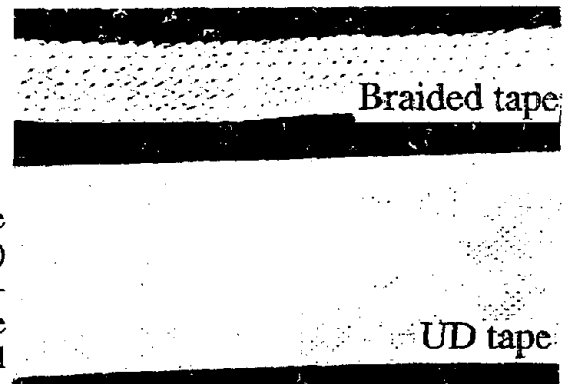
Photo.1 Reinforcing materials

(I) Senior Research Engineer, R&D Division, Mitsui Construction Co.
(II) Research Engineer, Technical Research Lab., Mitsui Construction Co.
(III) Architectural Division, Sho-Bond Corporation

307,200 deniers(1 denier=1 g/9,000 m), while Sheet was 7,630 deniers per 1 cm width.

The material characteristics of the winding fibers are given in Table 1. The tensile strengthes are the results of tensile tests on Braided tape and UD tape impregnated with epoxy resin. UD tape being thin and wide in shape showed local rupturing at tensile test and test values were low, but UD tape can be considered to have higher strength in actual winding condition than in material tensile test. Therefore, in calculating the shear capacity of strengthened specimens, the material strength of Braided tape was applied both to UD tape and to Sheet of the same fiber quantity as Braided tape.

Unit

1 tonf	= 9.81KN
1 kgf/cm^2	= 0.0981 MPa

Table 1 Characteristics of winding materials

	Braided tape	UD tape
Tensile strength	5.58tonf	3.67tonf
Cross-sectional area	0.345cm^2	

2.2 Specimens

A list of specimens is given in Table 2. A total of eight specimens was fabricated and the test parameters were shear reinforcement quantity of existing reinforced concrete portion, quantity of winding fibers, and type of winding fibers.

The existing reinforced concrete column was a cantilevered member having square cross section as shown in

Table 2 List of specimen

Specimen	Existing reinforced concrete		Winding material	Winding pitch (mm)
	Flexural reinforcement	Shear reinforcement		
A-0	4-D16 Pt=1.27%	D6@100 pw'=0.256%	None	——
ABS-15			Braided tape	@150
B-0		ϕ3@100 pw'=0.056%	None	——
BBS-15			Braided tape	@150
BBS-10				@100
BBS-5				@50
BF-10			UD tape	@100*1
BS-10			Sheet	@0*2

*1:same fiber quantity as BBS-10
*2:total fiber quantity is equal to BBS-10

Specimen cross section
bxD=250x250
Shear span
a=625

Flexural reinforcement
4-D16
Shear reinforcement@100
A Type D6
pw'=0.26%
B Type ϕ3
pw'=0.06%
unit:mm

Fig.1 Existing reinforced concrete

Winding pitch x=15,10,5cm
Braided tape,UD tape

Superposing 4 to 5 layers
Sheet

Fig.2 Wound condition

Table 3 Reinforcing steel materials test results

Part used	Kind	Yield strength kgf/cm^2	Tensile strength kgf/cm^2
Flexural reinforcement	D16	4535	6350
Shear reinforcement	D6	3575	5157
	ϕ3	6040	6523

Table 4 Concrete materials test results

Age (day)	Compressive strength kgf/cm^2	Young's modulus ×10^{5}kgf/cm^2	Splitting strength kgf/cm^2
14	303	2.83	19.9
21	317	2.89	27.1
32	330	2.88	31.1

Fig. 1, and there were the two varieties of different shear reinforcement quantities, e.g, Type A (pw=0.26%) and Type B (pw=0.06%). The material characteristics of the concrete and reinforcing steel are given in Tables 3 and 4.

Type A consisted of two specimens which have no reinforcement and Braided tape wound around at a pitch of 15 cm, while Type B consisted of six specimens which have no reinforcement, Braided tape at 15-, 10-, and 5-cm pitches, UD tape at 10-cm pitch, and Sheet having the same fiber quantity as BBS-10.

Winding around a column was done coating column surfaces with epoxy resin, winding on fiber material, and impregnating with resin. Smoothing of concrete column corners before winding was not provided. As shown in Fig. 2, Braided tape and UD tape were wound on helically, and Sheets cut into widths of 16 cm bonded on one layer at a time superposing 4 to 5 layers so as to have necessary fiber quantity.

2.3 Evaluation of Capacities of Specimens

The calculated values of capacities of the specimens are shown in Table 5.
The ratios of shear capacity(cQs) to flexural capacity(cQm) of specimen A-0 and specimen B-0 are 0.93, 0.79, respectively.

The ultimate shear strength after winding was calculated evaluating shear reinforcement quantity by Eq. (1) and using Arakawa's equation [4] conventionally used in Japan. Here, evaluation of reinforcement ratio fpw was made by Eq. (2) taking into consideration the difference in Young's modulus of reinforcing steel and winding fiber, and that all the winding fibers at various heights did not necessarily carry identical tensile forces. Tensile strength fσwy was evaluated by Eq.(3) giving consideration to tensile strength reduction at corners [5].

Table 5 Calculated capacities of specimens

Type	Specimen designation	Existing reinforced concrete			Wound column			
		cQm (tonf)	cQs (tonf)	cQs/cQm	fpw (%)	fpw×fσwy	cQsf (tonf)	cQsf/cQm
A	A-0		10.1	0.93	0.00	0.00	10.1	0.93
	ABS-15				0.10	9.92	11.8	1.09
B	B-0	10.9	8.6	0.79	0.00	0.00	8.6	0.79
	BBS-15				0.10	9.92	10.9	1.00
	BBS-10				0.14	14.88	11.7	1.08
	BBS-5				0.28	29.76	13.6	1.25
	BF-10				0.15	14.88	11.7	1.08
	BS-10				0.15	14.88	11.7	1.08

<Explanations of notations>
cQm:Flexural capacity of existing reinforced concrete
cQs:Shear capacity of existing reinforced concrete
cQsf:Shear capacity after winding fibers
Note)Specified design strength of concrete   Fc=300kgf/cm²

Flexural capacity: cQm=0.9at σy d/a
Shear capacity (Arakawa's equation [4]):

$$cQ_s = \left\{ \frac{0.068p_t^{0.23}(180+F_c)}{\frac{M}{Qd}+0.12} +2.7\sqrt{p_w \sigma_{wy}} \right\} bj$$

at   : Sectional-area of tensile reinforcement
σy   : Yield stress of reinforcement
d   : Effective depth of beam
a   : Shear span
pt   : Ratio of sectional-area of tensile reinforcement
σB   : Concrete compressive strength
M/Q d : Ratio of shear span
b   : Beam width
j   : Distance between compressive and tensile reinforcement
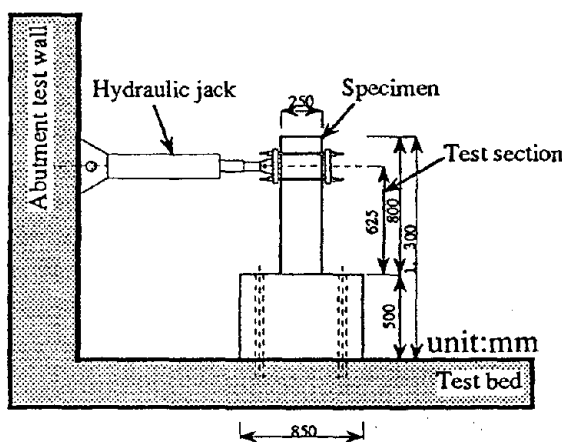
Fig.3 Loading apparatus

Table 6 Loading rules

	1	2	3	4	5	6	7
Deformation angle (rad)	1/400	1/200	1/150	1/100	1/75	1/50	1/25
Deformation (mm)	1.56	3.13	4.17	6.25	8.33	12.5	25.0

339

$$p_w\sigma_{wy} = p_w'\sigma_{wy}' + f_{pw}f\sigma_{wy} \quad (1)$$

$$f_{pw} = 1/2\, f_{pw}' \quad (2)$$

$$f\sigma_{wy} = 2/3\, f\sigma_{wy}' \quad (3)$$

where

f_{pw} : Equivalent shear reinforcement ratio of winding fiber
$f\sigma_{wy}$: Tensile strength of winding fiber
f_{pw}' : Shear reinforcement ratio of winding fiber
$f\sigma_{wy}'$: Tensile strength of fiber material
p_w' : Shear reinforcement ratio of existing reinforced concrete
σ_{wy}' : Yield stress of shear reinforcement in existing reinforced concrete

2.4 Testing Method

The loading apparatus is shown in Fig. 3. A Hydraulic jack was used for cyclic loadings applied at the top of the column. No axial load was applied. The rules for loading used are given in Table 6.

3. TEST RESULTS

Load-deformation relationships are shown in Fig. 4. With Type A, A-0 having no reinforcement failed in shear after flexural yielding, while ABS-15 which had been strengthened showed no reduction in maximum load even at deformation of 1/25 rad.
Looking at Type B, B-0 having no reinforcement failed in shear before flexural yielding, while in the case of BBS-15 wound with Braided tape at a pitch of 15 cm shear failure with rupturing of fiber occurred after flexural yielding and load was reduced. The specimen BBS-10 wound at a pitch of 10 cm showed flexural yielding failure, and although reduction in maximum load did not occur up to deformation of 1/25 rad under positive loading, there was slight reduction at the final cycle in negative loading. The specimen BBS-5 wound at a pitch of 5 cm showed no reduction in maximum load up to the final cycle, and flexural yielding failure occurred.
The specimen BF-10 wound with UD tape showed no reduction in maximum load up to the final cycle and flexural yielding failure occurred. The specimen BS-10 strengthened with Sheet indicated properties similar to BBS-10 and BF-10 under positive loading, but fibers broke at corners at deformation of 1/33 rad under negative loading and maximum load was reduced.

Envelopes of Types A and B wound with Braided tape, and of different varieties of winding material types are shown in Fig. 5. The envelopes of Type A and B wound with Braided tape show maximum load strength to be raised with increase in winding fiber quantity, and it can be seen that deformation capability is increased. The envelopes by varieties of winding material types are for comparisons of specimens containing equal amounts of fiber, and although there are hardly any differences under positive loading, there are reductions in maximum load with Braided tape (BBS-10) and Sheet (BS-10) under negative loading.

The final failure condition is shown in Photo. 2. Specimens which showed shear failure were the three of A-0, B-0, and BBS-15. Although in the case of BBS-15 fiber broke at corners, breaking of fiber did not occur in other specimens reinforced with Braided tape. With BBS-10, depressing concrete at corners by fiber material was observed. In contrast, this was not seen with BF-10 using UD tape and BS-10 using Sheet and it is considered the restraining effects on concrete were greater than for the case of Braided tape (BBS-10). However, with BS-10, the sheet material ruptured from near column base corners to upward direction at the ultimate stage.
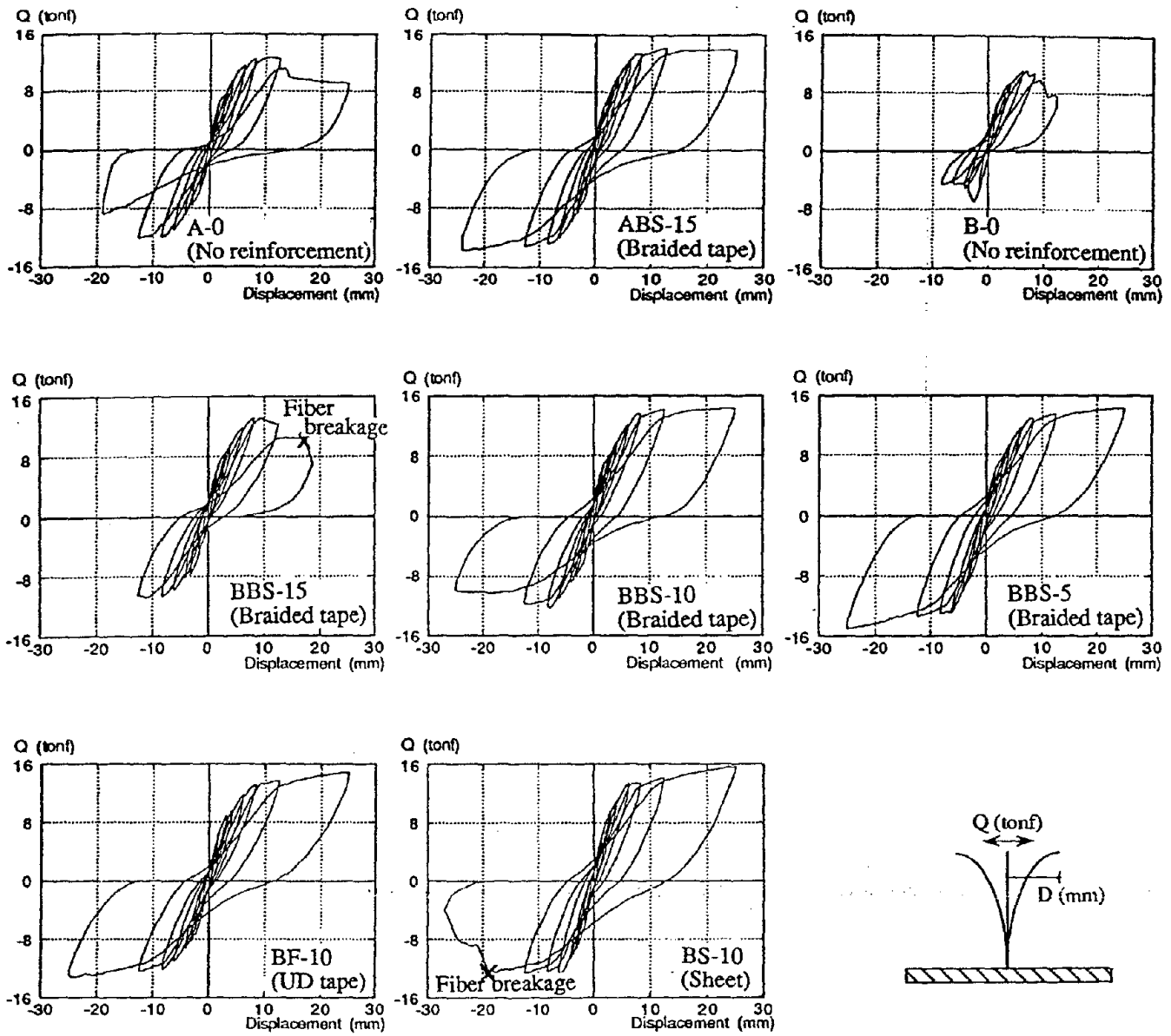
Fig.4 Load-deformation relationship
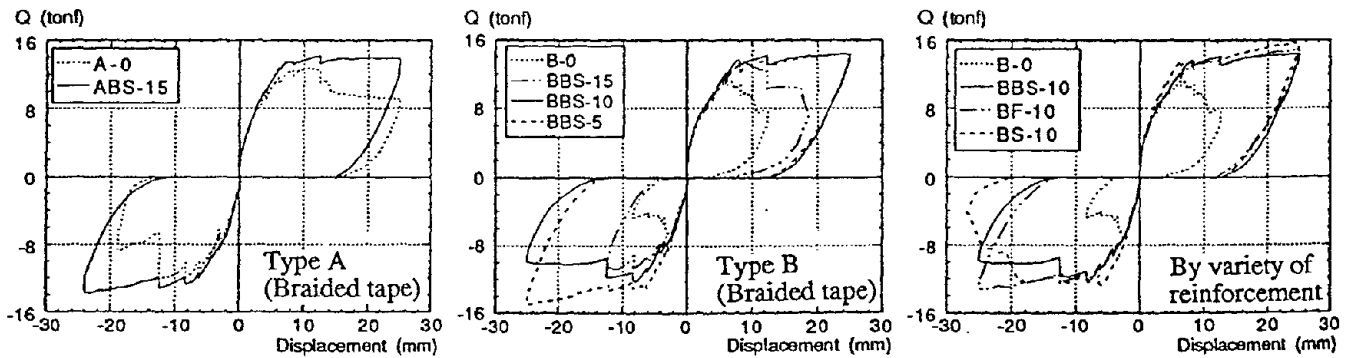
Fig.5 Load-deformation envelopes

341

Photo.2 Failed conditions

The test results are given in Table 7. All specimens showed hardly any difference in the loads when first cracks in bending and shear were initiated. Flexural yielding loads were approximately 13 tonf for all specimens, while a tendency was seen for maximum loads to be increased as the amount of winding material increased. The specimens of which the ratios of shear capacity after winding fibers to flexural capacity are greater than 1.00 showed flexural failure with ductile deformation.

4. DISCUSSION

4.1 Maximum Load

The relationship between shear reinforcement quantity($pw\sigma wy$) and maximum load(cQu) is shown Fig. 6. Shear reinforcement quantities were calculated based on Eq.(1).

Specimens with $pw\sigma wy$ less than 18.3 failed

Table 7 Test results

Specimen	First crack load		Flexural yielding load cQy (tonf)	Maximum load cQu (tonf)	Failure mode
	Flexural (tonf)	Shear (tonf)			
A-0	4.7	6.8	12.6	12.7	BD→SD
	-3.3	-7.1	-11.8	-12.1	
ABS-15	3.5	8.9	13.4	14.2	BD
	-2.8	-7.7	-12.3	-13.8	
B-0	4.0	7.1	—	11.2	SD
	-3.1	-6.7	—	-7.1	
BBS-15	5.1	7.8	—	13.2	BD→SD(CD)
	-2.9	-5.9	-10.0	-10.8	
BBS-10	4.2	7.2	13.4	14.4	BD
	-2.7	-6.5	-12.1	-12.3	
BBS-5	3.9	6.5	12.9	14.4	BD
	-3.6	-6.8	-13.0	-15.0	
BF-10	7.3	7.3	13.0	14.9	BD
	-3.1	-5.4	-12.0	-13.2	
BS-10	—	—	13.4	15.7	BD→CD
	—	—	-12.4	-12.8	

Upper:positive loading   Lower:negative loading

<Failure mode>

BD:bending failure SD:shear failure CD:fiber breakage

342

n shear and maximum load increased with increase in quantity of winding fiber. Specimens of)wσwy 18.3 or over showed flexural yielding failure, and maximum loads were more or less constant. Calculated values by AIJ Guideline equation [6] and Arakawa's equation [4] were also indicated in Fig. 6 for comparison, but effectiveness of fiber winding could not be discussed quantitatively, because the number of specimens showing shear failures were few. On the other hand, the maximum load of specimens failed in flexural yielding was approximately 14.7 tonf which were approximately 1.35 times the calculated value of flexural capacity. This is considered to have been because concrete at the compression side was restrained by the winding fibers, but further studies are still needed regarding details.

4.2 Deformation Capacity

The relationship between shear strengthening quantity (pwσwy) and ultimate deformation angle of specimen (Ru) is shown in Fig. 7. Ru increased according as pwσwy increases. Specimens of pwσwy 12.1 or higher did not show any reduction in maximum load even at deformation of 1/25 rad when testing ended, and it can be considered that deformation capacity will be even greater. There was a tendency for compressive strain of concrete at the ultimate state to become greater as the amount of winding fiber increased. Consequently, it may be considered that the improvement in deformation capacity due to winding is not only because of an increase in shear capacity, but also because of the contribution of the effect of compressive ductility of concrete due to the restraining action of winding fiber.

5. CONCLUSION

The results obtained through the loading test on reinforced concrete beams strengthened by winding with aramid fiber may be summarized as follows:

(1) Shear capacities increased as the amount of aramid fiber wound around columns increased.

(2) Strengthening by fiber winding was also effective in increasing compressive ductility of concrete and improved deformation capacities of members.

Fig.6 Shear reinforcement quantity(pwσwy) -ultimate load (eQu) relationship

AIJ Guideline equation [6]:

$$Vu = b\, jt\, pw\, \sigma wy \cot\phi + \tan\theta\, (1-\beta)\, b\, D\, v\, \sigma B/2$$

ϕ : Angle of inclination of shear crack to the axial direction of member in truss mechanism

jt : Distance of between tensile reinforcement and compressive reinforcement

θ : Angle of arch to the axial direction of member in arch mechanism

$\beta = \{(1+\cot^2\phi)\, pw\, \sigma wy\} / (v\, \sigma B)$

v : Effective coefficient of concrete compressive strength
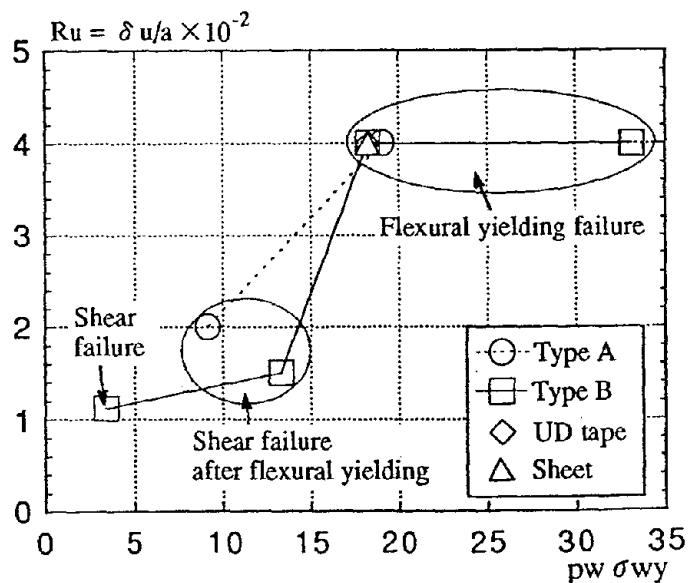
Fig.7 Shear reinforcement quantity(pwσwy) -ultimate deformation angle of member (Ru) relationship

343

In closing, the conclusions drawn here are based on the results of basic experiments for using aramid fiber as shear strengthening of columns. It is further planned to conduct various experiments with quantity of winding fibers and axial forces as parameters to more quantitatively evaluate strengthening effect.

REFERENCES

1. Japan Building Disaster Prevention Association: Guideline for Evaluation of Earthquake-resistant Capacity of Existing Reinforced Concrete Buildings, 1990
2. Kobatake, Y. et al.: Retrofit Method of Existing Reinforced Concrete Members by Carbon Fiber Spiral Hoops, Proceedings of the Japan Concrete Institute, Vol. 11, No. 1, 1989, pp.861-866.
3. Hasuo, K. et al.: Study on braided aramid fiber rod (Part 14. Tensile properties and their distributions), Summaries of Technical Papers of Annual Meeting of AIJ, A, 1991, pp.687-688.
4. The Building Center of Japan: Guidelines to Structural Calculation under the Building Standard Law, 1991.
5. Fukuyama, H. et al: Experimental Study on Tensile Strength at the Bending Part of Fiber Reinforced Composite Materials: Summaries of Technical Papers of Annual Meeting of AIJ, C, 1991, pp.801-802.
6. Architectural Institute of Japan: Design Guidelines for Earthquake Resistant Reinforced Concrete Buildings Based on Ultimate Strength Concept, 1990
7. Endo, K. et al.: Shear Behavior of Concrete Beams Reinforced with Braided High-Strength Fiber Rods in Spiral Shape, Transactions of The Japan Concrete Institute, Vol. 11, 1989.

SECOND U.S.-JAPAN WORKSHOP
ON SEISMIC RETROFIT OF BRIDGES

Increasing the Seismic Failure
Resistance of Highway Structures
A. M. Shirole and A.H. Malik
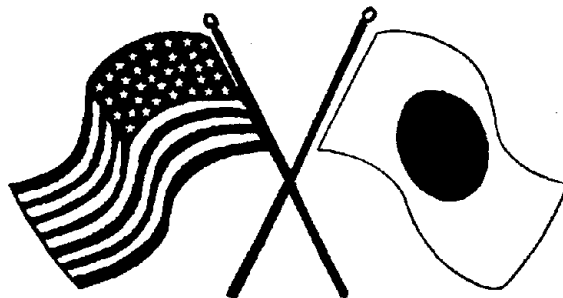
January 20 and 21, 1994
Berkeley Marina Marriott Hotel
Berkeley, California

INCREASING THE SEISMIC FAILURE RESISTANCE
OF HIGHWAY STRUCTURES

ARUN M. SHIROLÉ, P.E. and AYAZ H. MALIK, P.E.
NEW YORK STATE DEPARTMENT OF TRANSPORTATION
ALBANY, NEW YORK

ABSTRACT

This paper presents case studies of the seismic retrofitting of highway structures as part of their rehabilitation. These retrofit activities were generally aimed at improving the seismic force resistance of steel rocker bearings, bearing support, pin and hanger systems, and pier columns with insufficient confinement. The projects involved replacing the rocker bearings with energy absorbing elastomeric bearing pads, linking the simply supported spans (or suspended spans) to act as a continuous redundant superstructure, and strengthening piers by jacketing.

The paper highlights the typical vulnerable details associated with the majority of existing bridges, and current methods of retrofitting each element in order to minimize damage and reduce the potential of collapse during an earthquake.

INTRODUCTION

There are currently 19,560 bridges in New York state under the jurisdiction of state and local bridge agencies. These bridges vary in type, age, material and structural details. The original design of the majority of these structures did not include the potential for seismic loads. As a result, a major seismic event can cause these structures to be seriously damaged, endangering public safety, and interrupting vital life lines, especially when the damage to the structure is catastrophic. It has been the principal objective of the retrofit measures to minimize the potential for damage so that the structure remains functional even after the seismic event, or requires only a temporary repair in order to maintain functional life lines.

RETROFITTING POLICY

Economic constraints preclude immediately retrofitting the entire population of existing bridges. Therefore, a retrofit program based on "priority" is necessary. The NYSDOT Interim Seismic Policy outlines the prioritization guidelines for selecting candidate structures for seismic retrofit. This retrofit work is incorporated into the regularly scheduled rehabilitation of the candidate structure. Pursuant to this policy, many rehabilitation projects let during the past two years have included seismic retrofit actions along with the regular rehabilitation work.

RETROFIT CASE STUDIES

The following three case studies discuss recent highway structure seismic retrofit projects and show how the seismic failure resistance of the substructures has increased:

CASE STUDY 1: North Bound I-87 Bridge over East River Road

This project included three bridges built in 1965, each consisting of three simply supported spans similar in design and detail. The project is located near Exit 24 of Route I-87, 130 miles south of the Canadian border and 200 miles north of New York City. A typical bridge is shown in Figure 1. The bridge has a skew of 35 degrees, a normal width of 33'-2" (fascia to fascia), and carries two one-way travel lanes. The total length of the bridge is 152 feet, which includes three simply supported spans of 44, 54, and 54 feet. Each span includes five 33WF 118 rolled beams with partial cover plates at the bottom flanges, spaced 7'-6" on center. The beams support an 8 1/2" thick concrete composite deck as shown in Figure 1. All beams were supported on low, sliding-type steel bearings. Substructures include two reinforced concrete piers (three columns per pier), and two seat-type abutments. The substructures are supported on spread footings on rock.

The following retrofitting measures were implemented to enhance the redundancy of the structure by providing continuity:

1) Three spans were made continuous by splicing both top and bottom flanges and the web. The flange splice plates were extended as far out as necessary to accommodate the additional stress in the vicinity of the proposed continuous supports. Bolted connections were used for field splicing, (Figure 2).

2) Partial cover plates at the bottom flanges were bolted to enhance the fatigue life of the welded ends of the plates as per AASHTO specifications. These ends will experience stress reversal due to continuity, (Figure 3).

3) Bottom flange splice plates were used as sole plates for the proposed bearings because of the limited height available.

4) At the piers, the two lines of existing steel sliding bearings were replaced with a single line of elastomeric bearings placed at the centerline of each pier.

347

STRUCTURE TYPE	PIER COLUMN CAPACITY (C)			SEISMIC GROUP LOADS DEMAND (D)			C/D
	P_{axial} (K)	M_{trans} (K ft.)	M_{long} (K ft.)	P_{axial} (K)	M_{trans} (K ft.)	M_{long} (K ft.)	
Existing	193	154	238	135	108	167	1.426
Simply Supported	376	122	246	128	41	84	2.934
Retrofitted	611	86	135	140	20	31	4.355
Continuous	620	104	112	138	23	25	4.487

CASE STUDY 2: County Road 61 over the Barge Canal

This project involves a 593 foot long continuous bridge located near Utica N.Y., in the central region of New York State. The bridge, which was built in 1954 has a skew of 21 degrees and is 31 feet wide (fascia to fascia). The bridge is composed of four spans. The spans are 120, 233, 120, and 120 feet long. Each span consists of four built-up riveted steel girders spaced 8'-8" on center (Figure 4). Pin-hanger details were used in the design of the girders in the second and fourth spans to suspend part of the length of the structure as shown in Figure 5. All girders were supported on rocker bearings. The girders carry an 8 1/2" thick concrete composite deck. The substructures included solid piers on spread footings with no piles.

The following seismic retrofitting measures were implemented for this structure:

1) Pins and hangers at the suspended portions of spans two and four were replaced by bolted splice plates. (Figure 6)

2) Rocker bearings were replaced by multi-rotational (pot) bearings.

3) Existing concrete deck was replaced by a lightweight exodermic deck (60 pounds per sq. foot) to control the overstress in the steel girders in the vicinity of the piers. (Figure 7)

COUNTY ROAD 61 OVER BARGE CANAL

STRUCTURE TYPE	PIER COLUMN CAPACITY (C)			SEISMIC GROUP LOADS DEMAND (D)			C/D
	P_{axial} (K)	M_{trans} (K ft.)	M_{long} (K ft.)	P_{axial} (K)	M_{trans} (K ft.)	M_{long} (K ft.)	
Conc Deck w/hinges	1331	5650	5987	1775	7529	7978	0.750
	3532	19518	12077	1761	9729	6020	2.006
Lgt.Wgt. Deck no hinges	1553	5983	6697	1615	6215	6957	0.998
	4340	21687	13751	1615	8083	5125	2.683

CASE STUDY 3: Route 29 over East Branch of Hudson River

The existing structure at this site is a 5-span, 5-girder bridge with a 5-girder simple approach span, carrying Rte. 29 over the East Branch of the Hudson River (the Champlain Canal) in northeastern New York State. Built in 1959, the bridge is 536'-6" long and 36'-11" wide, with a 160' pin and hanger suspended center span and 3 pile-supported piers 35' high. The east end approach span uses low sliding bearings; all the other bearings are of the high rocker type.

Because of numerous fatigue-prone details, it was decided to do a complete superstructure replacement using 3 spans of 5 continuous girders on multi-rotational (pot) bearings and a single 5-girder approach span, supported on the west end on elastomeric bearings and on the east end on a new integral abutment. The 3 existing piers were retained to support the new structure (Figures 8 & 9).

The 3 piers to be retained were retrofitted to meet seismic criteria by the addition of a one foot jacket of reinforced concrete, secured to the sound concrete of the existing piers by drilled and grouted ties (Figure 10).

RTE 29 OVER EAST BRANCH HUDSON RIVER

STRUCTURE TYPE		PIER COLUMN CAPACITY (C)			SEISMIC GROUP LOADS DEMAND (D)			C/D
		P_{axial} (K)	M_{trans} (K ft.)	M_{long} (K ft.)	P_{axial} (K)	M_{trans} (K ft.)	M_{long} (K ft.)	
Existing Pier	Deck-Conc.	7931	34749	11665	2631	11520	3867	3.016
		493	644	2403	2645	3456	12890	0.186
Retrofitted Pier	Deck-Conc.	14123	48940	24067	3102	10745	5284	4.555
		3084	3130	17101	3192	3224	17613	0.971
	Deck-LWT Conc.	14631	56938	22519	2853	11095	4388	5.132
		3524	4112	18075	2853	3328	14628	1.236

COST DATA

The data collected, as an average of the bids for various elements, indicate an increase in the rehabilitation cost of the structures of 15% to 20% due to seismic retrofitting.

COST OF RETROFITTING

CONTINUITY:
    COST PER SPLICE $1900.00

PLATES & BOLTS:
    PLATES, BOLTS,
    REM EXIST. DIAPH,
    PLATE AND REINSTALLING
    EXIST. DIAPH. $6300.00

RESTRAINERS:
    COST/PER SET OF
    RESTRAINERS $3750.00

CONCLUSION

Seismic retrofitting, as part of the regular rehabilitation program, is designed to provide increased assurance against catastrophic failure due to earthquakes. The wide variety of bridges built over a period of years requires development of a variety of details, on a project to project basis. It is important to examine each structure individually for a cost effective approach. For example, New York State Department of Transportation is currently planning work on projects which will need retrofitting to relieve overstressed conditions for existing pile foundations and to retrofit masonry piers for uplift due to moderate earthquakes.

I-87 N.B. OVER EAST RIVER

TRANSVERSE SECTION

EXISTING

RETROFIT

FIG. 1   352

3 Spc. @ 3" = 9" (Typ.)

3'-4"

1½"

1½"

A

B

A325-⅞"ØBolts

7 Spc. @ 3" = 1'-9"

Upstation

3"

2"

2"

Diaphragm bracket clip for flange splice plate

Bearing Assembly Item 565.1901

Masonry Plate

Load Plate

Steel Laminated Elastomeric Bearing

Bevelled Splice Plate

⅜"

A **B**

Grade on Structure

A

B

12¼"

15½"

12¼"

SPLICE PLATE AT PIER

No Scale

TYPICAL ELEVATION AT PIERS

No Scale

353

FIG. 2

SECTION A-A
SCALE : NONE

EXISTING
WF SECTION

7/8" ∅ A325 BOLTS

1 15/16 "

2 1/16 "

3" 3"

4" × 7/8" × 1'-2" ℞

8 1/2" × 13/16 " × 1'-2" ℞

6"

FILLER ℞ - SAME
THICKNESS AS
COVER ℞

EXISTING WF SECTION
1'-2"

1 1/2"   3"   5"   3"   1 1/2"

7/8" ∅ A325 BOLTS

4" × 7/8" × 1'-2" ℞

BOTTOM
FLANGE

FILLER ℞ - SAME
THICKNESS AS
COVER ℞
1/2" × 13/16 " × 1'-2" ℞

EXISTING
FILLET WELD

EXISTING
COVER ℞

BOTTOM FLANGE COVER PLATE RETROFIT
SCALE : NONE

FIG. 3
354

COUNTY ROAD 61 OVER BARGE CANAL

31'-0" (Out to Out)

TGL

2'-6"   8'-8"   8'-8"   8'-8"   2'-6"
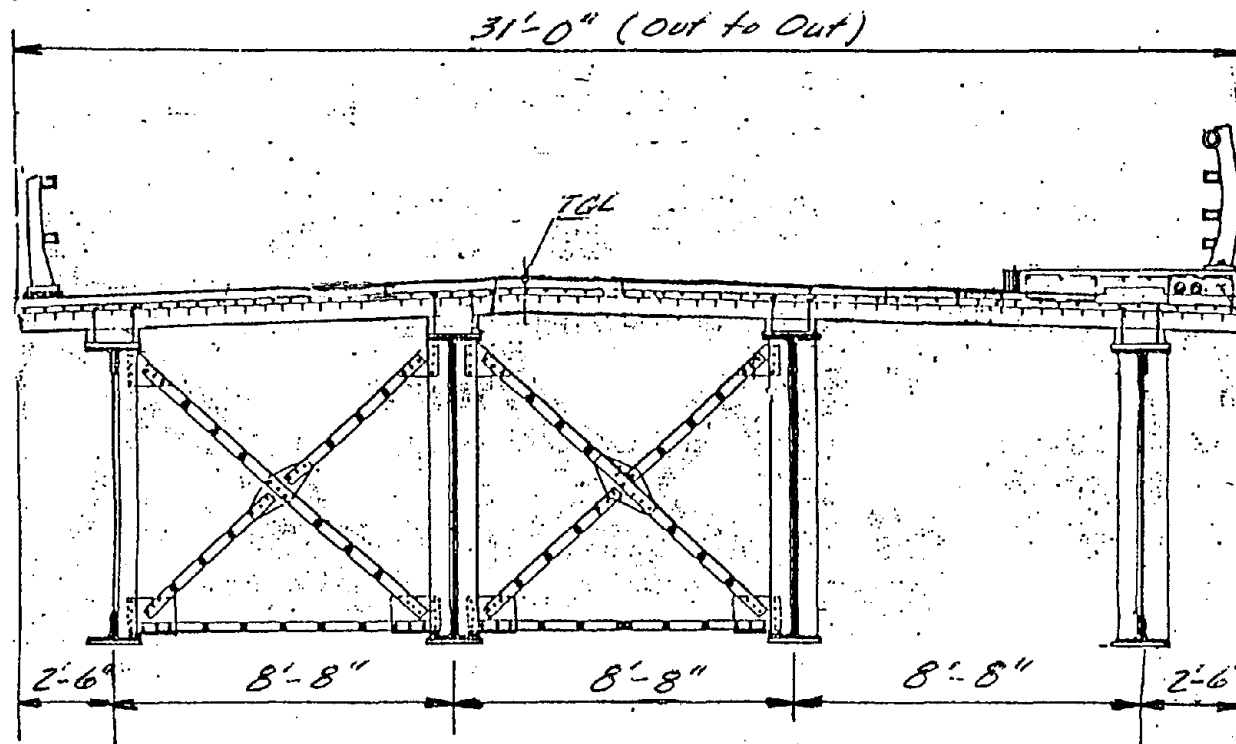
PROPOSED TRANSVERSE SECTION   (LOOKING SOUTH).

COUNTY ROAD 61 OVER BARGE CANAL

ELEVATION

120'-0" 36'-6" 160'-0" 36'-6" 120'-0" 24'-0" 96'-0"

356

FIG. 5

PL 16"x ¾"

2-PL's 6"x ¾"

2-PL's 75½"x52"

Existing 2~L's 8x6x1"

2-PL's 6"x ¾"

PL 16"x ⅝"

90½" Back to Back L's

¾"

18-1"ø Bolts @ 4"

Existing 2~Web PL 90"x ½"

4-Bolts @4"

2"

5"

Existing 2~L's 8x6x1"

2-PL's 75½"x½"x52"

Existing 2~Web PL 90"x ⅜"

Existing 2~L's 8x6x¾"

2-PL's 6"x ¾"

Existing 2~L's 8x6x¾"

2-PL's 6"x ¾"-5"

PL 16"x ¾"
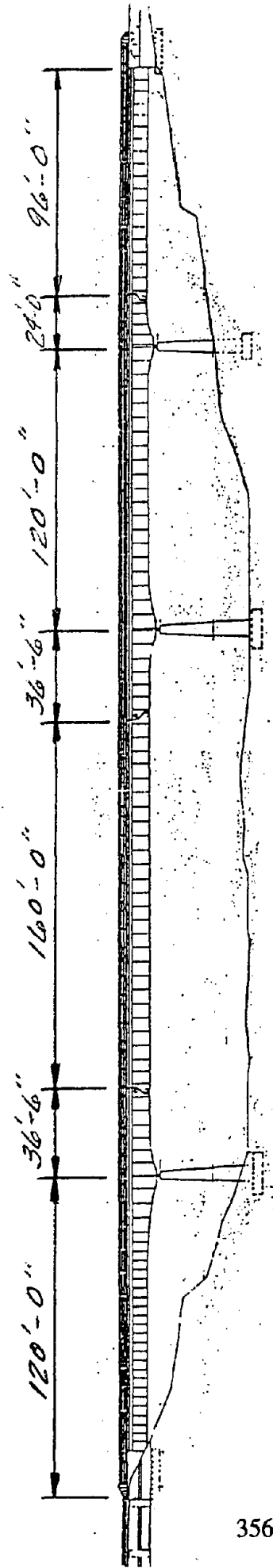
PL 16"x ¾"x13'-0" @ Location 4 & 7 Top
PL 16"x ¾"x11'-0" @ Location 4 & 7 Bottom
PL 16"x ¾"x5'-0" @ Location 5 & 8
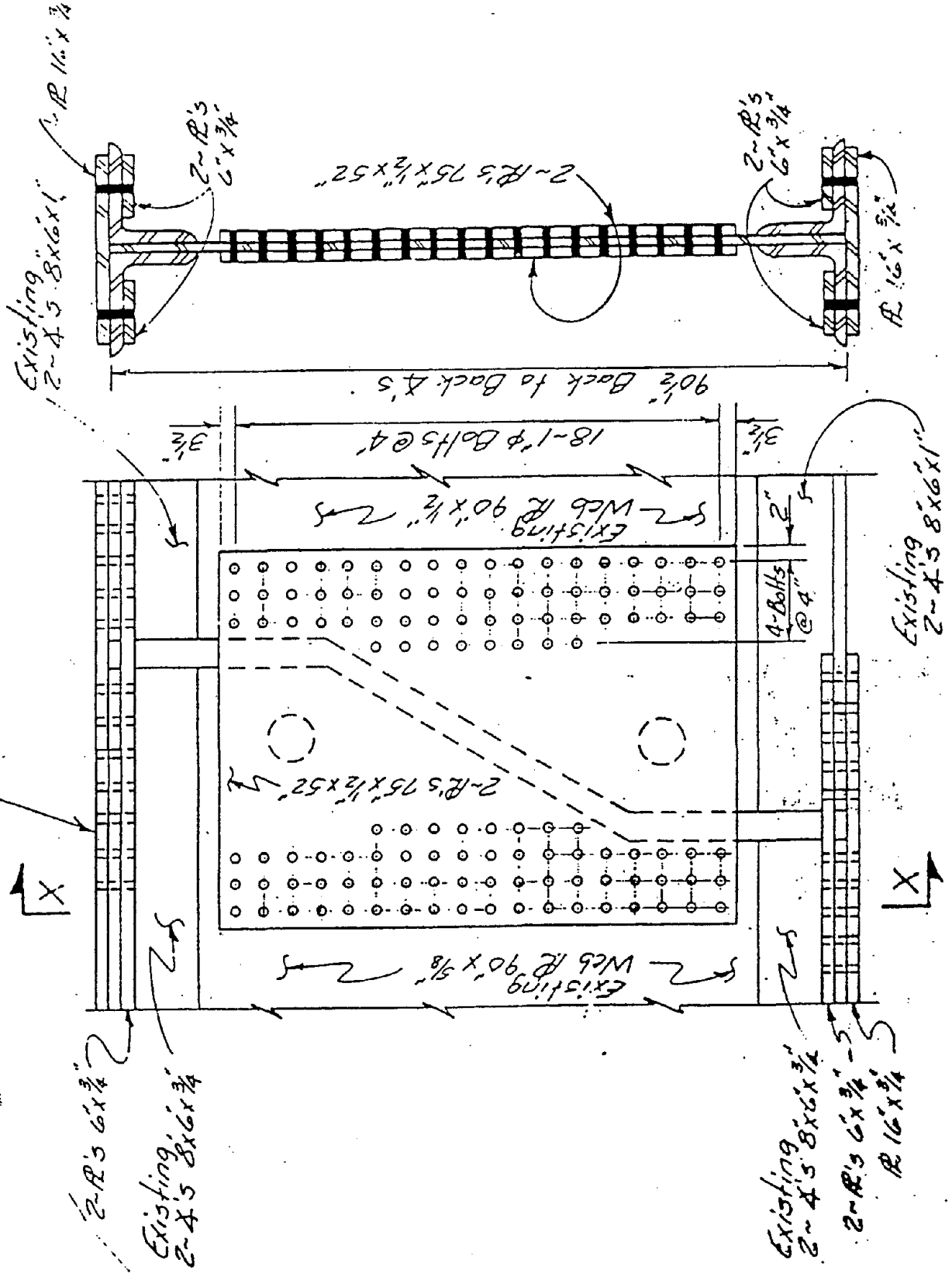
X

EXODERMIC BRIDGE DECK

Min. 3" Structural Concrete Overlay

Epoxy coated
Reinforcing Bars

Vertical Studs

Distribution Bars

Tertiary Bars

Main Bearing Bars

FIG.7

358

ROUTE 29 OVER
EAST BRANCH OF HUDSON RIVER

40'-0"

8'-0"   8'-0"   8'-0"   8'-0"   8'-0"

TRANSVERSE SECTION

FIG. 8

114'-0"   244'-0"   114'-0"

New Superstructure

ELEVATION

FIG. 9

360
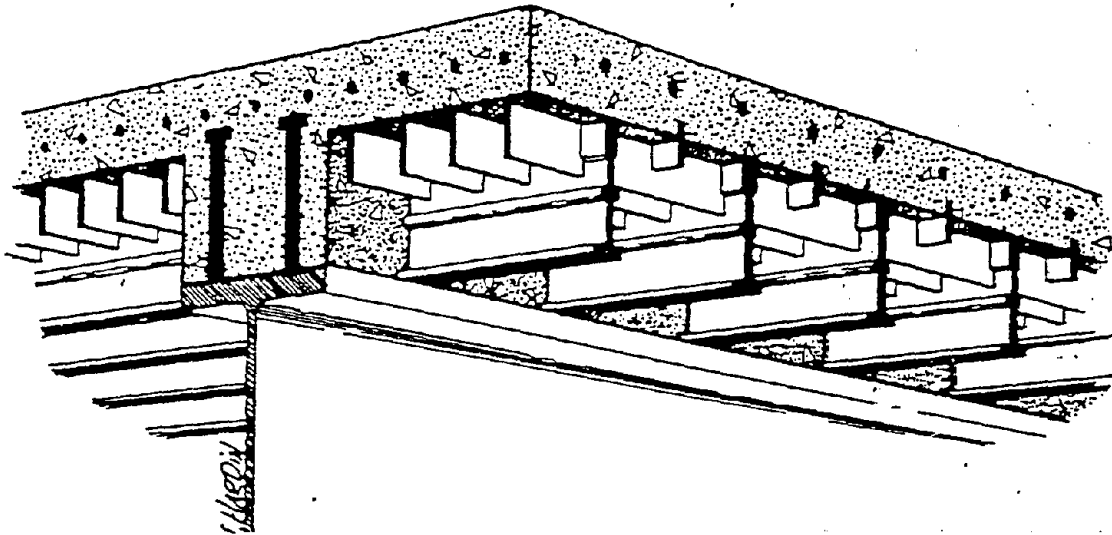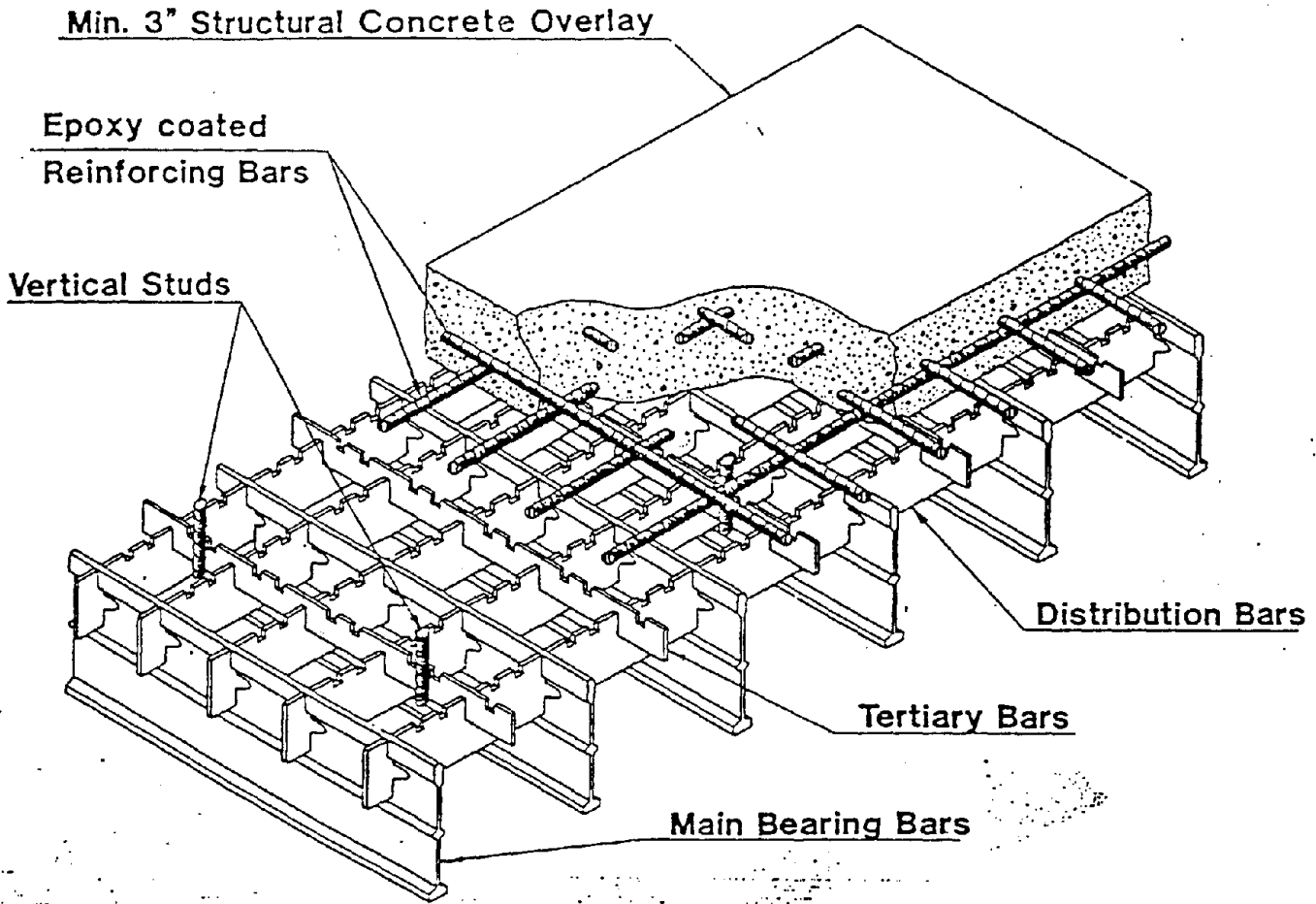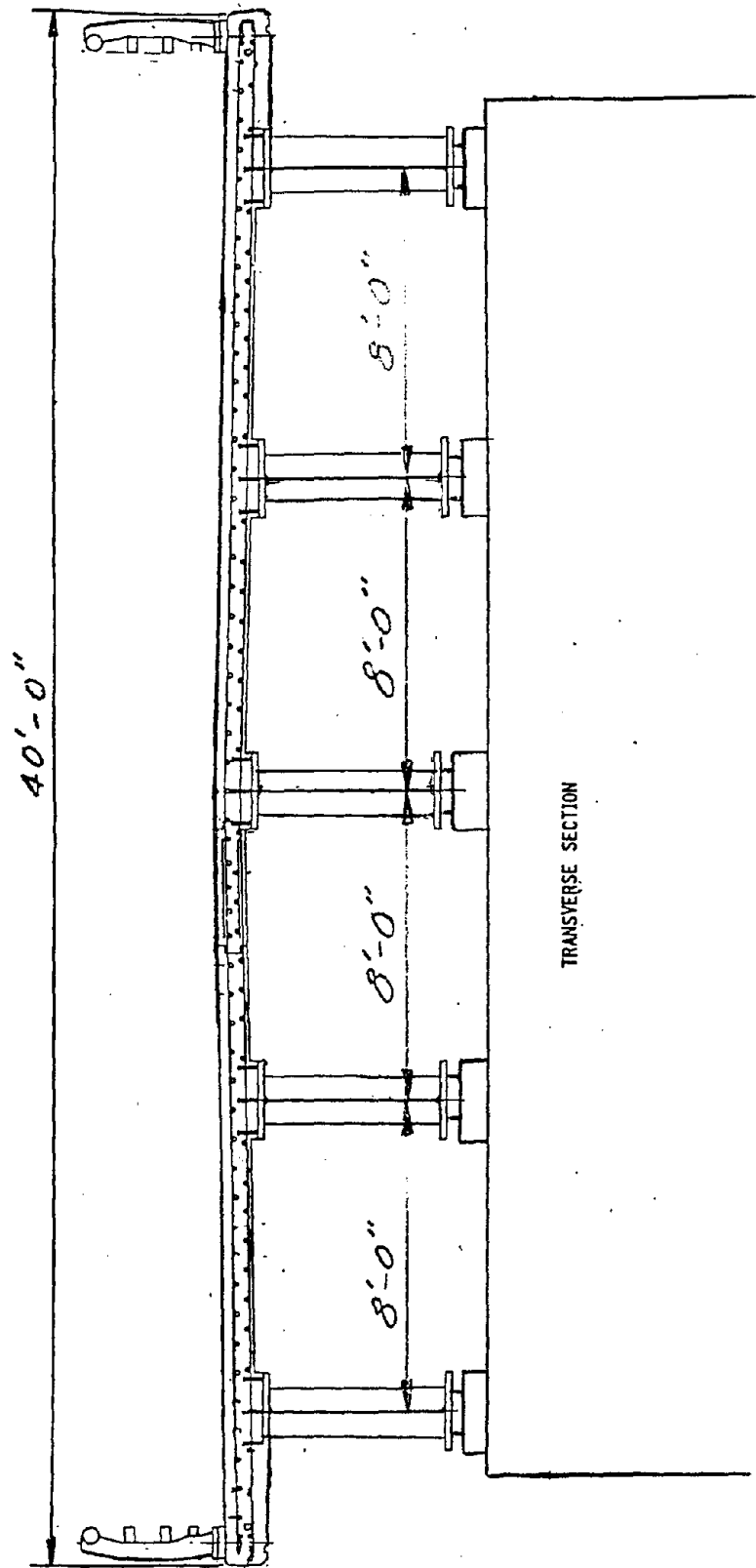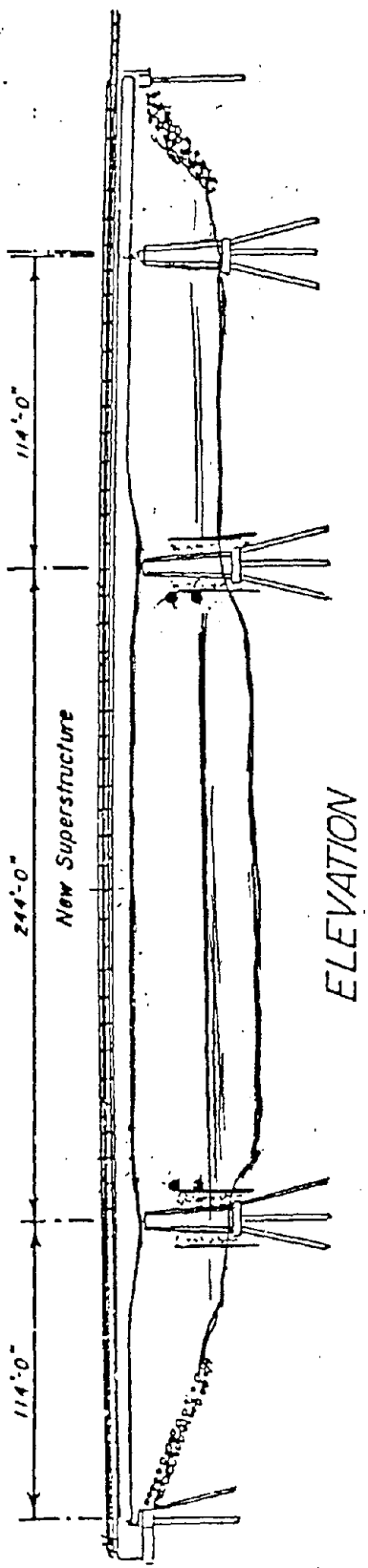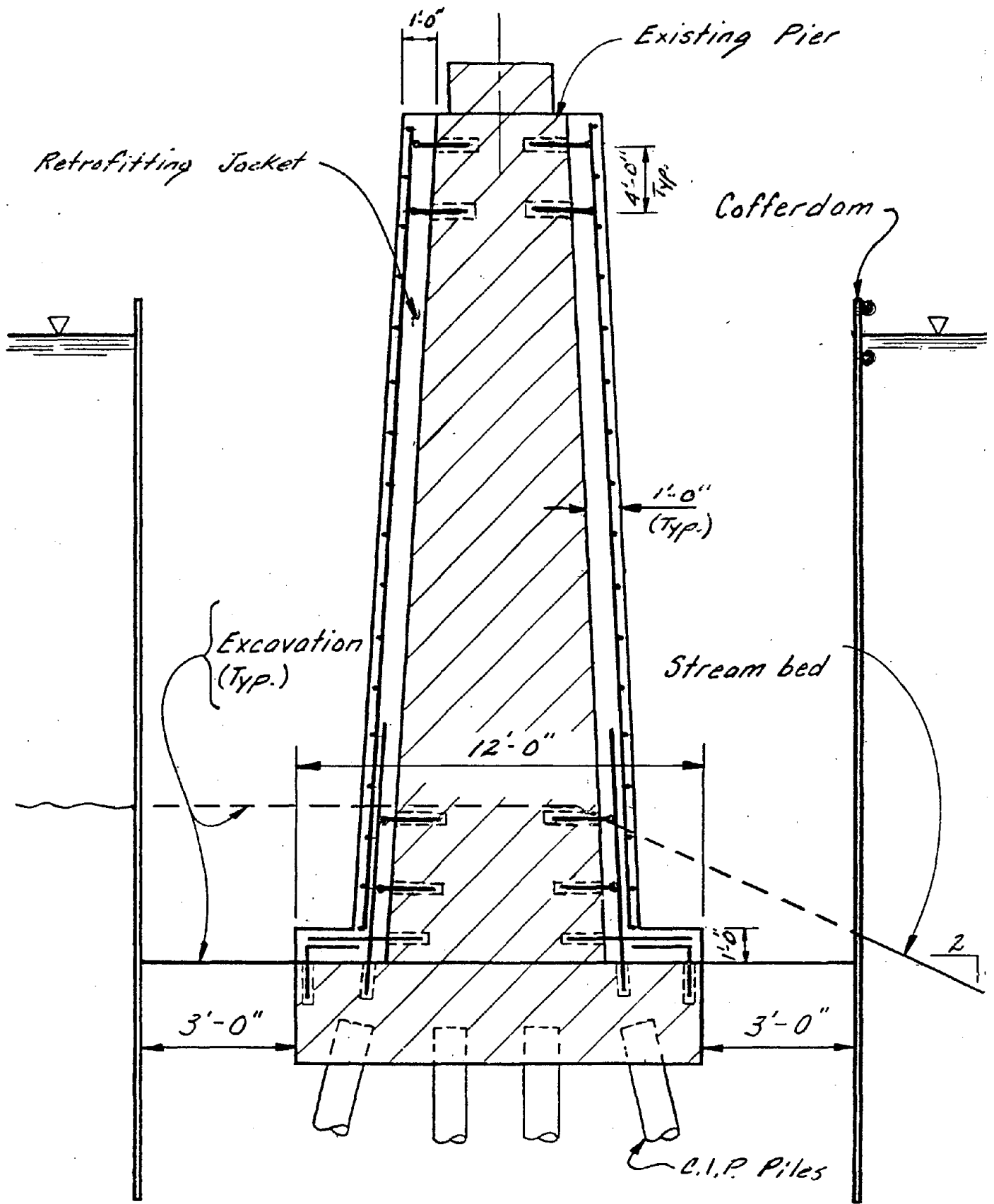
TYPICAL PIER SEISMIC RETROFIT

FIG. 10

SECOND U.S.-JAPAN WORKSHOP ON SEISMIC RETROFIT OF BRIDGES

Seismic Analysis and Retrofit Concepts for the Ballard Bridge North Approach

U.C. Vasishth and J.S. Jacobson
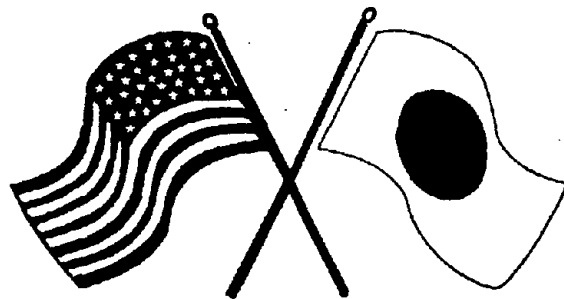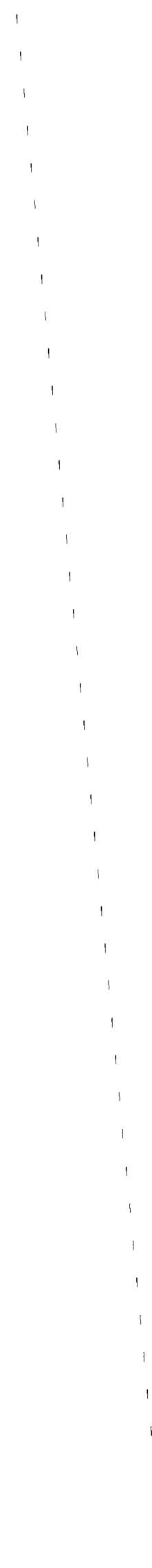
SEISMIC ANALYSIS AND RETROFIT CONCEPTS FOR THE BALLARD BRIDGE NORTH APPROACH

Umesh C. Vasishth[1] and Jay S. Jacobson[2]

ABSTRACT

Three different types of seismic analysis were performed and resulting retrofit schemes developed for the Ballard Bridge in Seattle, Washington. The bridge spans over the Lake Washington Ship Canal which connects Puget Sound to Lake Washington.

This paper presents the various analysis techniques performed and methods proposed for the retrofit of the substructure elements of the north approach. These consisted of attaching shear walls and grade beams to the bents, pier cap strengthening and base isolation.

An analysis was first performed using an elastic seismic evaluation of the structures dealing with capacity and demand ratios. Because of the resulting high cost of retrofitting the bridge, a cost savings was realized by performing both a nonlinear "Push" analysis used by Caltrans and developed by University of California at San Diego, and a base isolation analysis.

Cost estimates for different types of retrofit schemes and their relative merits are presented. The resulting cost savings and risks associated with the use of a nonlinear "Push" analysis and base isolation are discussed.

INTRODUCTION

As part of a growing concern for the safety of the bridges in Western Washington following two seismic events, the City of Seattle Engineering Department (SED) has launched a seismic analysis and retrofit program. Their main objective is to have the major lifeline structures functional following an earthquake, and prevent catastrophic failure of as many bridges as possible, given a fixed budget. SED decided to make the best use of the available funds by using state of the art technology.

The Ballard Bridge built in 1939 is one of the major structures spanning over the Lake Washington Ship Canal in Seattle, Washington. As a result of in-depth discussions with the several engineering firms and seismic researchers involved with the program, it was decided that the Ballard Bridge would be retrofitted and considered the main lifeline structure spanning the Ship Canal. Condition surveys of all the candidate structures also

1. President, Exeltech Engineering, 2627 A Parkmont Lane S.W., Olympia, WA 98502
2. Project Engineer, Exeltech Engineering, 2627 A Parkmont Lane S.W., Olympia, WA 98502

played an important role in deciding which structure to retrofit and what retrofits to perform. The work was then divided into three distinct segments: the north approach, the south approach and the main bascule span.

Structure Description

The north approach of the Ballard Bridge consists of two different sections (Fig. 1). The first section is a 5 span variable depth reinforced concrete T-beam superstructure supported on multi-column bents (Fig. 2). The structure was widened in 1953 by adding variable width concrete box girders on each side of the existing superstructure, supported on single columns. Both the original columns and the columns for the widening are founded on individual spread footings, with the exception of Pier 4, which is a wall type pier on a pile footing.

The second section of the north approach is a 4 span steel plate girder superstructure with a reinforced concrete deck supported by steel transverse floorbeams (Fig. 3). The superstructure is supported on double column bents connected together at their tops with an arched concrete cross-beam. Their foundations consist of individual pile footings at both columns.

The north approach is bracketed by the north abutment which is of wall and pilaster construction on a spread footing, and the north bascule pier which is a massive concrete anchor pier for the main bascule span.

The deck for the concrete section of the north approach is discontinuous at several locations for expansion joints, in-span hinges and interfaces with the abutment and north approach steel section. A drop-in suspended span exists in span 3, with in-span hinges contained in spans 1 and 5. The deck for the steel section of the north approach is discontinuous only at the north bascule pier and the interface with the concrete section.

Site Geology

The subsurface conditions at the bridge site were derived from previous soil borings performed for the original construction of the bridge in 1939 and from local geologic maps. It was found that the north approach to the bridge lies on alluvial deposits basically consisting of sandy, clayey silt with scattered organic matter which overlie glacial deposits of gravelly sand with varying amounts of silt and clay. The glacial soils are found approximately 5 to 10 feet below the existing ground line.

Danger of landslides resulting from seismic activity is low due to the relative flat topography of the bridge site. In the opinion of the geotechnical consultants, the alluvial soils are relatively cohesive and the glacial deposits are dense, therefore, the liquefaction potential in the area of the north approach is low.

Seismic Analysis Parameters

Based on the relatively recent history of seismic events (the 1949 and 1965 earthquakes) and in accordance with AASHTO design specifications, all seismic analyses were performed using a peak acceleration of 0.30g. This acceleration represents a 10% probability of being exceeded in a 50 year interval. AASHTO soil profile type II was used to characterize the soil based on the recommendations of the geotechnical engineers.

The Importance Classification of the bridge is I, which represents a "lifeline" structure carrying an emergency route whose use is deemed critical following a seismic event.

Seismic Performance Objectives

The main objective of retrofitting the north approach was to prevent catastrophic failure and keep the bridge functional following a seismic event. While a certain amount of damage to the structure is acceptable, it should not threaten it's integrity or stability, and should be readily repairable to keep it functional.

Architectural considerations, cost feasibility and construction practicality also played a substantial role in determining which seismic retrofits to perform. The retrofits not only have to be buildable, but should use the construction budget wisely. By keeping an open dialogue with city officials, the desired seismic performance objectives were met and the best interest of the community will be served.

SEISMIC ANALYSIS PROCEDURES AND RESULTS

The seismic analysis of the Ballard Bridge North Approach consisted of two separate phases and three analysis techniques: elastic analysis, inelastic analysis and base isolation. All three of these techniques are distinctly different in their methodology, and each results in different retrofit schemes. It should be noted that although the outcome of the analyses differ, all three have both merits and risks involved. The merits and risks of a variety of schemes are being carefully considered by those involved before a decision is made regarding which retrofits to perform.

Elastic Analysis

A multi-mode elastic seismic analysis of the "as-is" structure was performed by Sverdrup Corporation as part of the original phase of work. This analysis involved modeling the bridge three dimensionally using the MSTRUDL computer program and the accepted conventional techniques of AASHTO and ATC 6-2. Several significant problem areas in both the superstructure and the substructure were identified by the analysis and

367

also by field observations made of the as-built structure. The capacity/demand ratios of the critical structure elements were calculated in conformance with Ref. 2.

COMPONENT	C/D RATIO
EXPANSION JOINTS & BEARINGS	
Displacement - r_{bd}	0.4
Force - r_{bf}	0.4
REINFORCED CONCRETE, PIERS, & FOOTINGS	
Anchorage of Longitudinal	
Reinforcement - r_{ca}	0.3
Splices in Longitudinal	
Reinforcement - r_{cs}	0.1
Confinement Reinforcement - r_{cc}	0.4
Column Shear - r_{cv}	0.1
Footings - r_{fr}	0.3
ABUTMENTS - r_{ad}	N/A
LIQUEFACTION - r_{sl}	N/A

Insufficient bearing seat widths exist at Pier 5 and at the north bascule pier where rocker type assemblies are used. This type of bearing assembly can be unstable for longitudinal displacements, and if the seat width is too narrow, the girders could possibly jump off of the pier cap if the bearings overturn.

A similar type of problem exists at the concrete drop-in sections within spans 1 and 3. One end of these drop-in sections contain expansion rocker type bearings, which pose the same problems as mentioned above. Combined with the insufficient seat widths at Pier 5 and the north bascule pier, there are four areas where excessive longitudinal displacements may cause superstructure instability problems.

The steel superstructure section of the north approach is comprised of two main longitudinal plate girders. The deck is supported on transverse floorbeams, which bear on the two main girders. These transverse floorbeams have no positive longitudinal support, and pose a stability problem should the deck experience large longitudinal displacements. While this alone may not cause a catastrophic failure to occur, severe damage to the concrete deck may occur.

The transverse bracing of the two main steel girders consist of 4 and 5 inch angle members that brace the bottoms of the girders to the floorbeams, which are spaced every 10 feet. The bottom flange lateral bracing consists of 3 inch angle members forming brace points at 30 foot intervals. These members do not have adequate capacity to transmit seismic loads through the superstructure.

The substructure columns were found to be deficient in several areas using current seismic design standards. Bending and shear forces resulting from elastic seismic loads are far greater than the column capacity. Inadequate detailing of the confinement reinforcement, lap splice lengths and development lengths of the main column reinforcing steel eliminate the possibility of plastic hinges forming.

Based on the criteria used in Ref. 2, fourteen retrofit concepts were developed to improve the structure's elastic seismic capacity:

1. **As-is Condition** - This option considers leaving the bridge in it's "as-is" condition and doing no retrofits. No cost is associated with this option, but none of the problem areas are addressed. This option was quickly eliminated from consideration.

2. **Remove and Replace Transition Slab** - The transition slab between the original and widening portion of the concrete section would be removed and cast back into place with proper dowel anchorage to each side. This retrofit option creates a more positive connection between the original and widening concrete sections so that they will act as a single unit. (Fig. 2)

3. **Restrainers in the Concrete Section** - Restrainer cables would be added at the expansion end of the drop-in span 18 feet to the left of Pier 3. These restrainers address the insufficient bearing seat width and instability of the existing rocker bearing. (Fig. 4)

4. **Longitudinal and Transverse Shear Walls** - Transverse shear walls would be added between the 3 original concrete section columns of Piers 1, 2 and 3. In addition, a longitudinal shear wall would be placed between the center columns of Piers 1 and 2, and another encompassing the center column of Pier 3 with it's own independent footings. Their purpose is to increase the shear capacity of the columns and essentially attract the seismic loads to a portion of the bridge that will be designed for the necessary forces.

5. **Transverse Shear Wall at Pier 5** - This transverse shear wall would be added between the two columns of Pier 5 to increase it's lateral seismic capacity.

6. **Transverse Shear Keys and Catchers** - This involves adding transverse shear keys and a catcher system to Pier 5 where the original concrete section T-beams are supported. The expansion bearings at Pier 5 are the vulnerable rocker type previously mentioned. The catcher system would prevent the superstructure from becoming unseated should the rocker bearings topple during a seismic event. (Fig. 5)

7. **Catcher for Concrete Box** - A catcher system would be added to the widened section of Pier 5 to serve the same purpose as for retrofit option no. 6. (Fig. 6)

8. **Longitudinal Girder Shear Connectors** - This concept constitutes adding a shear connector system to the tops of both main girders of the steel section of

the north approach. The main goal is to add stability to the floorbeam system preventing them from toppling over under seismic loads.

9. **Superbent at Pier 7** - A massive superbent system would be added at Pier 7 to considerably stiffen the bent. It would act as the main transverse and longitudinal resistance to the seismic loads for the steel section of the approach. (Fig. 7)

10. **Transverse Diaphragms** - This involves adding stronger transverse cross-bracing between the two main steel girders at Pier 5 and the north bascule pier, and girder stop shear keys to positively tie the cross-bracing to the pier cap. The transverse stiffness of the superstructure would be improved significantly.

11. **Longitudinal Girder Stops** - At the proposed superbent at Pier 7, longitudinal girder stops would be added to limit the amount of longitudinal differential displacement between the superstructure and substructure.

12. **Restraint System at Pier 5** - Much like retrofit option no. 7, a catcher system would be added to increase the amount of longitudinal displacement the steel girders can withstand without causing the span to fall off of it's support.

13. **Expansion Joint Closure and Sidewalk Chord Strengthening** - Basically this option closes the north approach expansion joints and strengthens the sidewalk section so that the bridge deck will act as a diaphragm for the bridge.

14. **Restrainers and Catchers at Bascule Pier** - A cable restrainer and catcher system would be added to the north bascule pier to address the insufficient bearing seat width and instability of the existing rocker bearing. (Fig. 8)

The construction costs associated with the above retrofit options were calculated and tabulated for comparison. They include mobilization, 25% markup, 25% for contingency, 20% for pre-construction engineering costs and 15% for construction engineering costs. It should be noted that Option 1 has been omitted for the purpose of this discussion since it has subsequently been decided to have the Ballard Bridge be a main lifeline structure.

Option 2	$ 263,000
Option 3	$ 76,600
Option 4	$ 464,300
Option 5	$ 74,700
Option 6	$ 65,200
Option 7	$ 12,200
Option 8	$ 125,000
Option 9	$ 688,800

Option 10	$	66,700
Option 11	$	22,500
Option 12	$	11,800
Option 13	$	132,400
Option 14	$	28,900
Total	$ 2,032,100	

The benefit of this method of analysis is that if the structure is retrofitted to withstand the seismic loads elastically, it's condition following the design level event will likely be relatively undamaged and functional for vehicular traffic. The structure's behavior will be in the elastic range, much like it is for other standard bridge loadings. This results in larger factors of safety and less risk for those involved.

The disadvantage of this approach is that the ductility of the structure is not taken into account. The retrofitted structure is stiffer than the original structure, attracting a larger portion of the earthquake forces, and increasing the cost of retrofit.

Inelastic "Push" Analysis

After reviewing the results of the elastic analysis, the Peer Review Committee headed by Parsons Brinckerhoff Quade & Douglas recommended that the Ballard Bridge Approaches be re-analyzed using the "Push" analysis. This analysis was performed on Pier 2 by Exeltech Engineering using the computer programs in Ref. 4. Dr. Nigel Priestley performed a "Push" analysis on Pier 10 of the south approach representing a typical bent supporting the steel superstructure. These two bents are representative of the bents contained in the north approach, considering tributary length, height and type of construction. The California State Department of Transportation (CALTRANS) currently uses the "Push" method of analysis for seismic evaluation of existing concrete bridges. It is a limit-state analysis method that uses the benefits of a member's available ductility.

The "Push" analysis consists of placing a lateral load at the top of the pier and pushing it until all possible plastic hinges form, and the resulting forces, curvatures, concrete strains, reinforcing steel strains, displacements at each plastic hinge location and the lateral displacement capacity calculated. The displacement demand is taken from a refined multi-mode elastic response spectrum analysis of the bent. The displacement capacity is then compared against the displacement demand to evaluate the ultimate ability of the bent to survive the design seismic event.

CALTRANS Special Analysis Section has developed several computer programs to assist the engineer in assessing these values and tabulating them. Other structural computer programs to perform these tasks do exist and are currently being developed and tested. For the purpose of analyzing the Ballard Bridge approaches, the programs developed by CALTRANS were used (Ref. 4).

371

Most of the analysis criteria regarding concrete and reinforcing steel strain capacities was based on Ref. 3. The final compressive strain in the concrete and reinforcing steel, and the final tensile strain in the reinforcing steel were established. Due to the light amount of confinement reinforcing in the columns, the final compressive strain in the concrete was limited to 0.005. The final compressive strain in the column reinforcement was confined to 0.002 since high compressive strains when the lap splice is located in plastic hinge regions can cause the splice to degrade under cyclical loading. The tensile strain of the reinforcing steel was limited to 0.05. If the tensile elongation of a reinforcing bar is too great, buckling can occur in compression when the applied load is reversed.

Other factors considered during the "Push" analysis include confinement reinforcement, lap splice lengths, embedment lengths, lateral displacements, shear capacity and footing capacity. The areas found to be deficient were then incorporated into the model and the bent re-analyzed with these deficiencies in place to account for the expected behavior. The results of the "Push" analysis performed on Pier 2 & 10 is summarized as follows:

1. **Confinement Reinforcement** - The amount of reinforcing steel provided in the column for confinement is taken into account when setting the limiting value of compressive strain in the concrete. The confinement reinforcement provided in the concrete section columns was considered light, #4 single hoops @ 12" spacing. The steel section column confinement reinforcement was somewhat better, but also considered to be light, #6 single hoops @ 18" spacing. In both cases, the confinement steel spacing is constant over the entire height of the columns. No confinement zones in the end regions were detailed or accounted for. As a result, the limiting value of compressive stress in the concrete was taken to be 0.005.

2. **Lap Splice Lengths** - The lap splices in all columns considered were found to be acceptable according to the criteria presented in Ref. 3. Although the confinement reinforcement was considered to be inadequate, the compressive strain in the concrete at the lap splice regions all were at or below 0.002. Therefore, the danger of excessive longitudinal microcracking in the lap splice region is minimal, and bond failure is not a concern.

3. **Column Rebar Embedment Lengths** - Using the larger of AASHTO 8.25.1 or 30 d_b as the criteria, the embedment lengths in the columns were checked. The original columns in the concrete section of the north approach were all found to be adequate. However, the embedment length of the columns in the widening area were found to be deficient. To account for this, these columns were considered to be pin connected at their base in the "Push" analysis model. The steel section columns were well within acceptable parameters.

4. **Footing Capacities** - The footings were checked for shear, moment and bearing capacities. It was necessary to verify whether the plastic moment capacity of the column could be developed. The existing footings were checked to ascertain whether they can develop the column plastic moments. The only problem area encountered was the lack of moment capacity of the footings supporting the columns of the widened concrete section. The footings contain bottom mat reinforcement only, and as a result the plastic moment of the column cannot be developed. Since the columns were considered pin connected at these locations, it was not necessary to make any further adjustments to the "Push" model. However, this situation was given due consideration during the retrofit development process.

5. **Column Shear Capacity.-** The column ultimate shear capacity was checked against the plastic shear demand at the critical locations in each column. No deficient areas were found. The tops of the columns were detailed as longitudinal hinges where they connect into the superstructure. This was achieved in the original design by stopping the column main steel at the bottom of the superstructure, and providing short vertical dowels spaced transversely to attach the column to the superstructure. The dowels provide no longitudinal moment capacity. To be conservative, a check was made of their adequacy to transfer the plastic shear force in a shear-friction situation. All connections provided sufficient capacity.

6. **Pier Displacement Capacity** - After performing the final "Push" analyses on Piers 2 and 10, the displacement capacities and demands were considered. To introduce slightly more conservatism into the analysis, the displacement demand was taken as the larger of that calculated by standard ARS methods or that determined in the refined multi-mode elastic response spectrum analysis. Both values were relatively close (less than 1/2" difference). The displacement capacities and demands were considered in terms of ductility by dividing the displacements by the idealized yield displacement of the pier. The capacities of the two typical piers analyzed were found to be within a comfortable range.

Pier 2 :   Displacement Capacity = 7.1"
           Displacement Demand = 4.7"
           Idealized Yield Displacement = 3.6"
           Displacement Ductility Capacity = 2.0
           Displacement Ductility Demand = 1.3

Pier 10 : Displacement Capacity = 5.8"
           Displacement Demand = 4.4"
           Idealized Yield Displacement = 3.4"
           Displacement Ductility Capacity = 1.7
           Displacement Ductility Demand = 1.3

7. **Post-earthquake Vehicle Capacity** - The north approach piers were analyzed for their ability to support HS-20 vehicle loading using their anticipated post-earthquake condition. The HS-20 vehicle was considered in order to simulate an emergency vehicle. The displacement calculated by equating the column P-Δ capacity to the column plastic moment capacity was compared against the "Push" analysis displacement demand. The P-Δ capacity was much greater than the displacement capacity determined from the "Push" analysis. Ultimately the piers contained sufficient post-earthquake vehicle capacity.

Several seismic retrofit schemes were developed in order to address insufficient details, scarcity of soils testing data and to improve the longitudinal response of the system:

1. **Transverse Grade Beam at Piers 1, 2 & 3** - The five columns in Piers 1, 2 & 3 will be connected at the groundline with a grade beam. In the event that the soil does not have the assumed lateral capacity at every pier, the grade beam will help develop the resistance required. In addition, the grade beam will greatly assist in inducing the plastic hinges to form in the columns. (Fig. 9)

2. **Pier 4 Shear Stop and Footing Reinforcement** - The top of Pier 4 is detailed as a hinge. However, no transverse restraint is provided. Shear keys should be added to provide the necessary lateral restraint. In addition, it would be beneficial to add a top mat of reinforcing in the footing to strengthen it to carry the larger loads that could result from the shear blocks becoming engaged. (Fig. 10 & 11)

3. **Pier 5 Post Tensioned Cap Beam** - This option consists of core drilling through the existing pier cap and post-tensioning it to increase the shear capacity. Plastic hinging will effectively be forced into the tops of the columns. The details of this pier are similar in nature those of the south approach, therefore it is necessary to retrofit them similarly. (Fig. 12)

4. **Longitudinal Shear Walls at Pier 3** - This involves adding longitudinal shear walls at Pier 3 to strengthen the concrete section of the approach for longitudinal response.

5. **Cap Beam Reinforcing at Piers 6, 7 & 8** - This option basically contains the same retrofit as option 3. It consists of drilling through the existing pier cap and post-tensioning it to increase the shear capacity.

6. **Longitudinal I-Beam Bracing** - The main goal of this option is to add stability to the floorbeam system preventing them from toppling over under seismic loads.

The construction costs associated with the above retrofit options are given in the following table:

Option 1	$ 81,000
Option 2	$ 23,000
Option 3	$ 13,000
Option 4	$ 90,000
Option 5	$ 39,000
Option 6	$ 76,000
Total	$ 322,000

These costs include the same mobilization, markup, contingency, pre-construction engineering costs and construction engineering costs as for the elastic analysis retrofits.

The benefit of this method of analysis is that the estimation of the structure's seismic capacity includes the contribution from inelastic action, taking advantage of the member's ductility. The important factors are accounted for in the capacity calculations resulting in a more economical and streamlined analysis. As a result, the retrofits tend be less extensive and more cost effective.

It should be noted that this is not a 3 dimensional analysis. The relative stiffnesses of the different piers and rotation of the unit as a whole are not taken into account, nor is the combination of transverse and longitudinal forces. It is not considered to be a conservative analysis.

Base Isolation Analysis

A separate analysis was performed by Sverdrup Corporation on the Ballard Bridge Approaches investigating the effect of isolation bearings on the seismic response of the bridge. In general, isolation bearings rely on energy dissipation through yielding of a lead core to dampen the superstructure forces that are transmitted to the substructure. The seismic loads can effectively be redistributed for greater control of where the critical points will occur. The analysis of the north approach was made with the assistance of a computer program developed by the isolation bearing manufacturer (Ref. 7).

The isolation bearings significantly changed the response of the structure by reducing the forces transmitted to the piers from a plastic level to an elastic level. The seismic displacements increased as a result of the isolated structure having more flexibility, but it should be noted that a large portion of the displacements occur through

the bearing and not from deformation of the pier. The seismic demand was reduced to a satisfactory level. Other than replacing the existing bearings with the base isolation bearings and related modifications, no other seismic retrofits were necessary. The construction costs for retrofitting the north approach with the new bearing system varies from pier to pier because of modifications needed to the piers in order to fit the isolation bearings.

Piers 1, 2 & 3	$ 278,000
Pier 4	$ 117,000
Piers 5, 6, 7 ,8 & No. Bascule Pier	$ 294,000
North Abutment	$ 274,000
Total	$ 963,000

The main advantage of using the base isolation bearings is the significant reduction in force transmitted to the substructure (in order of magnitude of 3-5 times less), thereby minimizing the demand on the members and allowing for greater displacements. The damage resulting from a seismic event will effectively be limited.

The costs related to replacing the existing bearings can be quite substantial.

COST COMPARISON

In comparing the costs of retrofitting the north approach to the Ballard Bridge using the three distinctly different methodologies, a sizable savings was realized by exploring alternative methodologies to using an elastic analysis. For the "Push" analysis and base isolation retrofits, $480,200 worth of superstructure and standard substructure retrofits consisting of ties and seat extensions are added. These retrofits are listed among the elastic analysis retrofits (options 2,3,6,7,11,12&14). They represent the minimum amount of upgrades needed to avoid a catastrophic failure of the superstructure.

	Construction Cost	Savings over Elastic Retrofits
Retrofits Resulting from Elastic Analysis	$ 2,032,100	
Retrofits Resulting from "Push" Analysis and required superstructure modifications	$ 802,200	$ 1,229,900
Retrofits Resulting from Base Isolation Analysis and required superstructure modifications	$ 1,443,200	$ 588,900

By using the "Push" analysis, the cost of the required retrofits was reduced by more than half from those determined from the conventional elastic analysis. The base isolation type of analysis also performed resulted in nearly a 30% savings over the original elastic analysis retrofits. While these two alternate methods did not eliminate the need for seismic retrofits, they substantially reduced the amount of retrofitting required, resulting in the significant savings.

CONCLUSIONS

This paper summarizes and compares the results of three methods of seismically analyzing and retrofitting the north approach structure to the Ballard Bridge. The importance of this bridge as a main lifeline structure prompted those involved with the project to carefully consider all options available with regard to which analysis and retrofit methods to use.

It is important, however, to realize that more risk is involved using the newly developed "Push" analysis or the base isolation system. The advantages and disadvantages have to be carefully weighed against the amount of risk that the engineer or owner is willing or able to take.

Some members of the Peer Review Committee are recommending using the "Push" analysis for the retrofit of Piers 1 through 5, and base isolation for Piers 5 through 9. The results of the "Push" analysis show that the structure can withstand the seismic demands, but there is no significant factor of safety. The possibility of substantial cracking and damage exists. The concrete approaches are over land, and if considerable cracking does occur, they can be quickly shored and made functional. Conversely, the steel spans are over water, making quick repairs and strengthening difficult should major cracking and damage occur. The cost will be not be significantly higher than that from the retrofits for an entire "Push" analysis.

It was mentioned in several meetings that ATC 6-2 (Ref. 2) should be revised. It tends to be conservative and results in costly retrofits.

ACKNOWLEDGMENTS

The authors would like to thank the City of Seattle Engineering Department and Sverdrup Corporation for the opportunity to work on the Ballard Bridge seismic retrofit project with them. Many individuals from these two organizations together with personnel from Parsons Brinckerhoff Quade and Douglas participated in numerous "brainstorming" and organizational meetings.

We are grateful to James Gates, Ray Zelinski and Mark Seyed from Caltrans, who together with Nigel Priestley from University of California at San Diego reviewed calculations and procedures, sharing their knowledge and experience with all those involved.

Shannon & Wilson, Inc. provided the geotechnical expertise by preparing the geological assessments of the soils present at the site, and research of the seismological history.

REFERENCES

1.   American Association of State Highway and Transportation Officials, AASHTO, Standard Specifications for Highway Bridges, Fifteenth Edition, 1992, including latest addenda and revisions.

2.   Applied Technology Council, "Seismic Retrofitting Guidelines For Highway Bridges", Report No. ATC 6-2, Aug. 1983.

3.   Priestley, M.J.N., Seible, Frieder, and Chai, Y.H., "Design Guidelines For Assessment Retrofit And Repair Of Bridges For Seismic Performance", SSRP 92-01, Aug. 1992.

4.   California Department of Transportation (CALTRANS), "Seismic Bridge Analysis Package", by Mark Seyed, Apr. 1993.

5.   Sverdrup Corporation, "Ballard Bridge - North Approach", Final Report, Feb. 1993.

6.   Sverdrup Corporation, "Ballard Bridge Approaches, "Push" Analyses and Isolation Bearing Analyses", Report, Nov. 1993.

7.   Dynamic Isolation Systems, Inc. (DIS), "Design of DIS Force Control Bearings", Copyright 1990.

Figure 1

379

TRANSITION SLAB (TYP.)

APPROX. EXIST. GROUND

20'-3⅝"

29'-9⅝" (9.1 m)

27'-0⅝" (8.2 m)

9'-6"

3'-0"

4'-6" ∅
(1.4 m ∅)

4'-0" SQ.
(1.2 m SQ.)

8'-6"

2'

2'

15'-6" (4.7 m)

11'-0" (3.4 m)

11'-0" (3.4 m)

11'-0" (3.4 m)

15'-6" (4.7 m)

16'-6" (5.0 m)

15'-6" (4.7 m)

15'-6" (4.7 m)

16'-6" (5.0 m)

TYPICAL BENT
NORTH APPROACH - CONCRETE SECTION
(PIER 2 SHOWN, PIERS 1 & 3 SIMILAR)

380

Figure 2

5'-4"
(1.6 m)

42'-0"
(12.8 m)

5'-4"
(1.6 m)

10'-6"±
(3.2 m ±)

28'-0"
(8.5 m)

VARIES FROM 27'-7" TO 35'-9¼"
(VARIES FROM 8.4 m TO 10.9 m)

APPROX. WATER LINE

APPROX. MUD LINE

TYPICAL BENT
NORTH APPROACH - STEEL SECTION

Figure 3

EARTHQUAKE RESTRAINER LAYOUT
At Sta. 28+50.04 & Sta. 28+86.04
Scale: 1/4" = 1'-0"

Notes:
1. Top slab and reinforcing steel omitted for clarity.
2. Install longitudinal and transverse restrainers normal to the joint.
3. Restrainers at Sta. 28+50.04 as shown, at Sta. 28+86.04 similar.
4. The contractor shall verify all dimensions shown before any material is ordered and fabricated.

Box Girder Dimensions									
Station	A	B	C	D	E	F	G	H	J
28+50.04	5'-6½"	5'-5½"	3'-0"	6'-1"	5'-9"	1'-9"	1'-9"	2'-11"	2'-11½"
28+86.04	4'-8½"	4'-7½"	1'-9"	6'-7"	6'-7"	2'-4"	2'-4"	3'-2"	2'-7½"

EARTHQUAKE RESTRAINER LAYOUT
At Sta. 27+44.04
Scale: 1/4" = 1'-0"

Notes:
1. Top slab and reinforcing steel omitted for clarity.
2. Install longitudinal and transverse restrainers normal to expansion joint.
3. The contractor shall verify all dimensions shown before any material is ordered and fabricated.
4. Box girder west as shown. Box girder East Similar.

BALLARD BRIDGE NORTH APPROACH
RESTRAINER LAYOUT

Figure 4

382

Figure 5

GIRDER STOPS & CATCHERS AT PIER NO. 5
Scale: 1/4" = 1'-0"
9302BA5

SECTION A-A
Scale: 1/4" = 1'-0"

SECTION E-E
Scale: 1/2" = 1'-0"
9302BE5

DETAIL B
Scale: 1/2" = 1'-0"
9302BB5

Elevation

383

THE CITY OF SEATTLE
DEPARTMENT OF ENGINEERING
GARY ZARKER DIRECTOR OF ENGINEERING

BALLARD BRIDGE NORTH APPROACH
TRANSVERSE SHEAR KEYS AND CATCHERS

DETAIL C (S2-8)
Scale: 3/4" = 1'-0"
9302BD5

SECTION G-G
Scale: 3/4" = 1'-0"
9302BD5

DETAIL H (-)
Scale: 1" = 1'-0"
9302BA10

DETAIL D (S2-8)
Scale: 1/2" = 1'-0"
9302BC5

SECTION J-J

Figure 6

384

RETROFIT OPTION 9
SUPERBENT AT PIER 7

NEW 4'-0" Ø DRILLED SHAFT (TYP.)

APPROX
WATER
LINE

APPROX
MUD
LINE

NEW CONC.
SUPERBENT

EXIST. CONC. PIER

EXIST. STEEL
SUPERSTR.
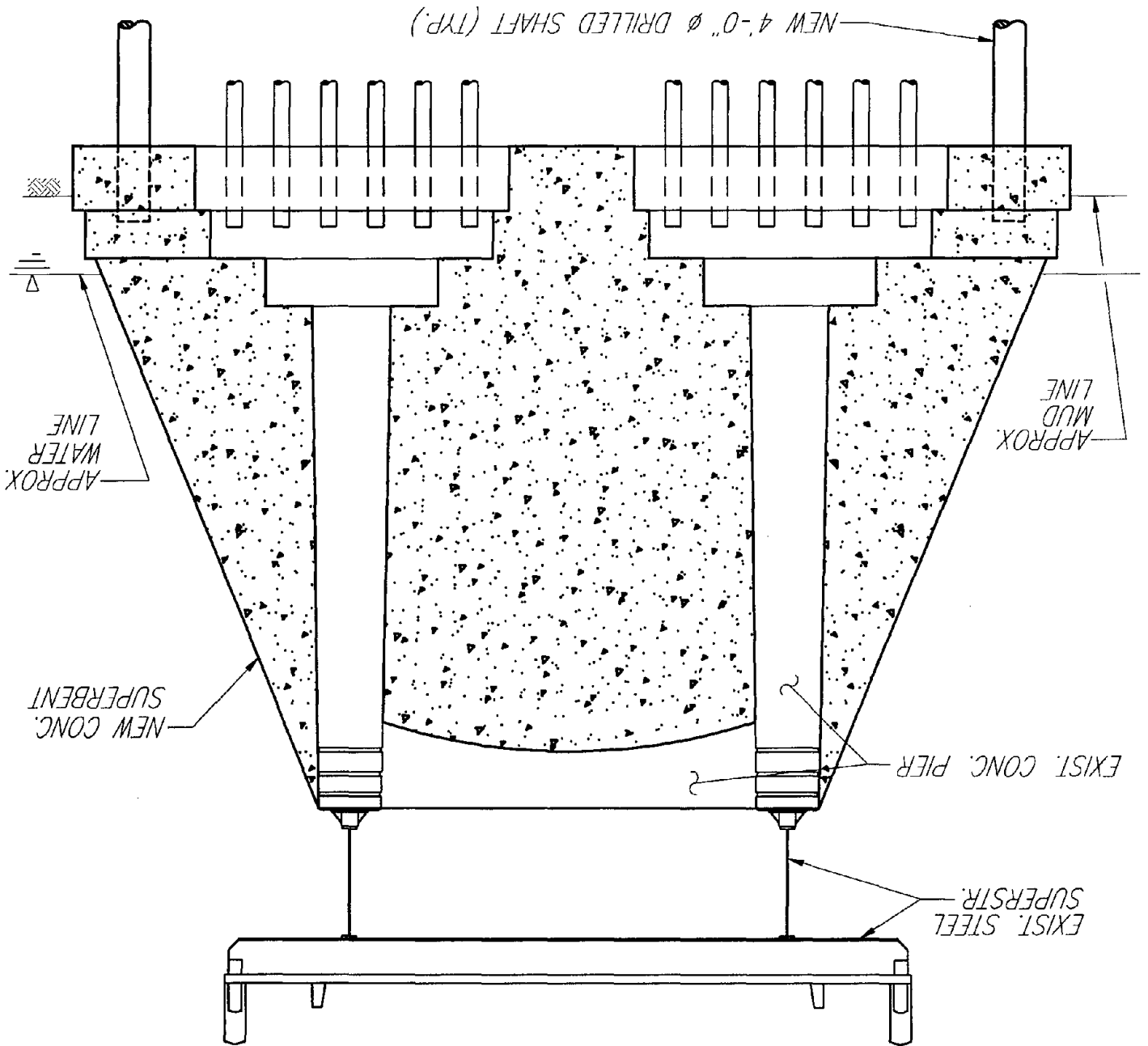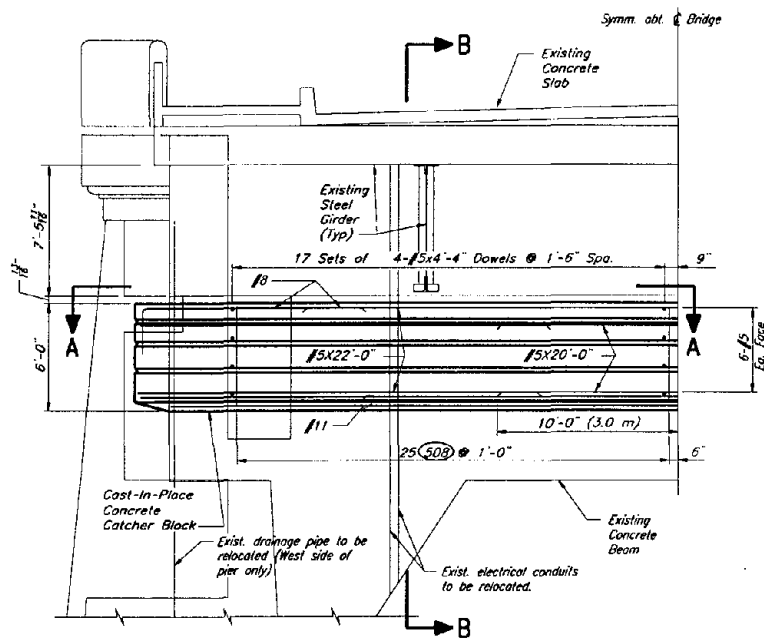
Figure 7

ELEVATION
Scale: 1/4"=1'-0"
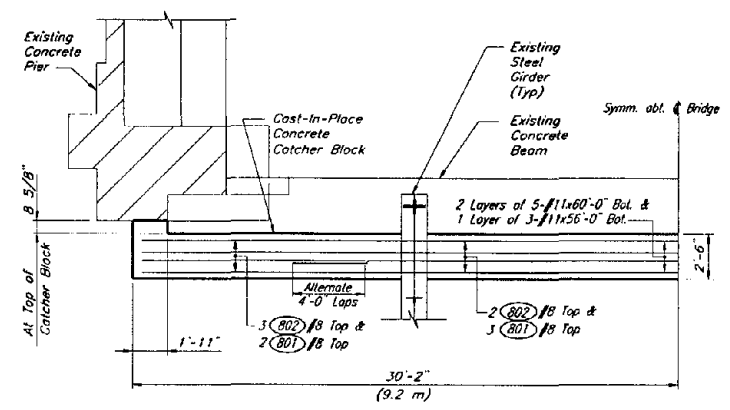
SECTION A-A
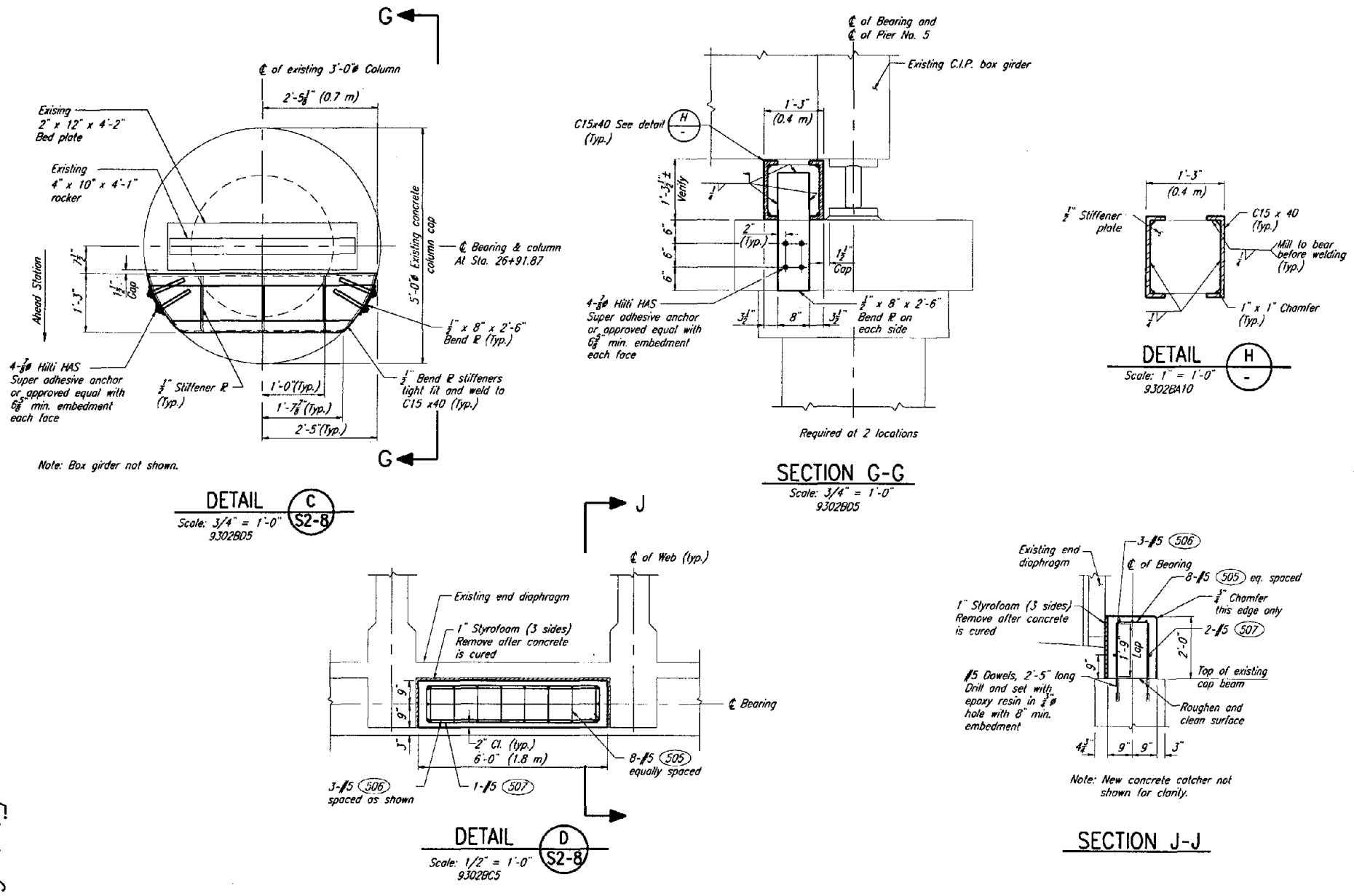Scale: 1/4"=1'-0"
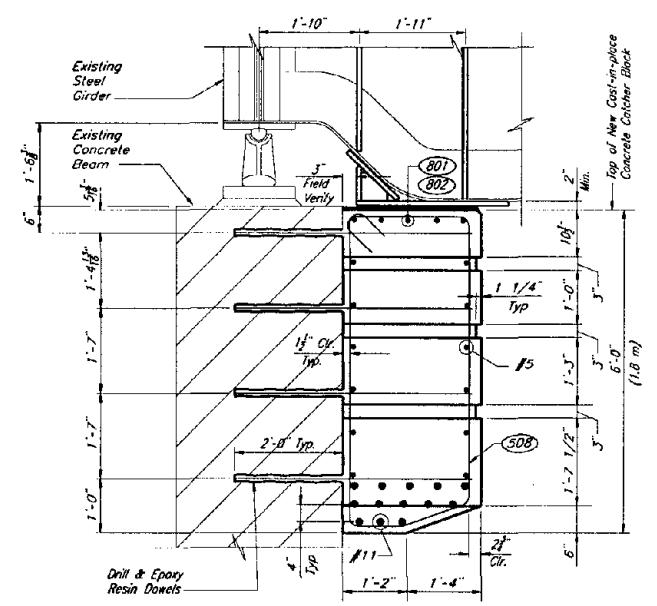
SECTION B-B
Scale: 3/4"=1'-0"

Figure 8

EXELTECH
CONSULTING ENGINEERS
OLYMPIA, WASHINGTON

APPROVED FOR ADVERTISING
KENNETH J. NAKATSU
DIRECTOR OF ADMINISTRATIVE SERVICES
SEATTLE, WASHINGTON   19

NAME OR INITIALS AND DATE	INITIALS AND DATE
DESIGNED	REVIEWED:
CHECKED	DES CONST.
DRAWN	TRANS. SVC. PROJ. MGR.
CHECKED	RECEIVED
DESIGN REVIEW	REVISED AS BUILT

THE CITY OF SEATTLE
DEPARTMENT OF ENGINEERING
GARY ZARKER DIRECTOR OF ENGINEERING

ORDINANCE NO.   APPROVED

FUNC.

RESTRAINERS AND CATCHERS
AT BASCULE PIER

PC
R/W
CO
VAULT PLAN NO.

PROP. SUPERSTRUCTURE
DIAPHRAGM RETROFIT (TYP.)

¢ BENT

NOTE: REINFORCING NOT SHOWN IN
THIS VIEW FOR CLARITY.

PROPOSED
GRADE BEAM
(TYP.)

APPROX. EXIST. GRADE

9'-0"±

4'-0"

9" (TYP.)

A

A

4'-6"±
(TYP.)

4'-0"
(TYP.)

5'-0" (PIER 1), 4'-6" (PIER 2),
3'-3" (PIER 3)

15'-6" (TYP.)

SYMM. ABOUT ¢

34'-6" (PIER 1),32'-0" (PIER 2),29'-6" (PIER 3)
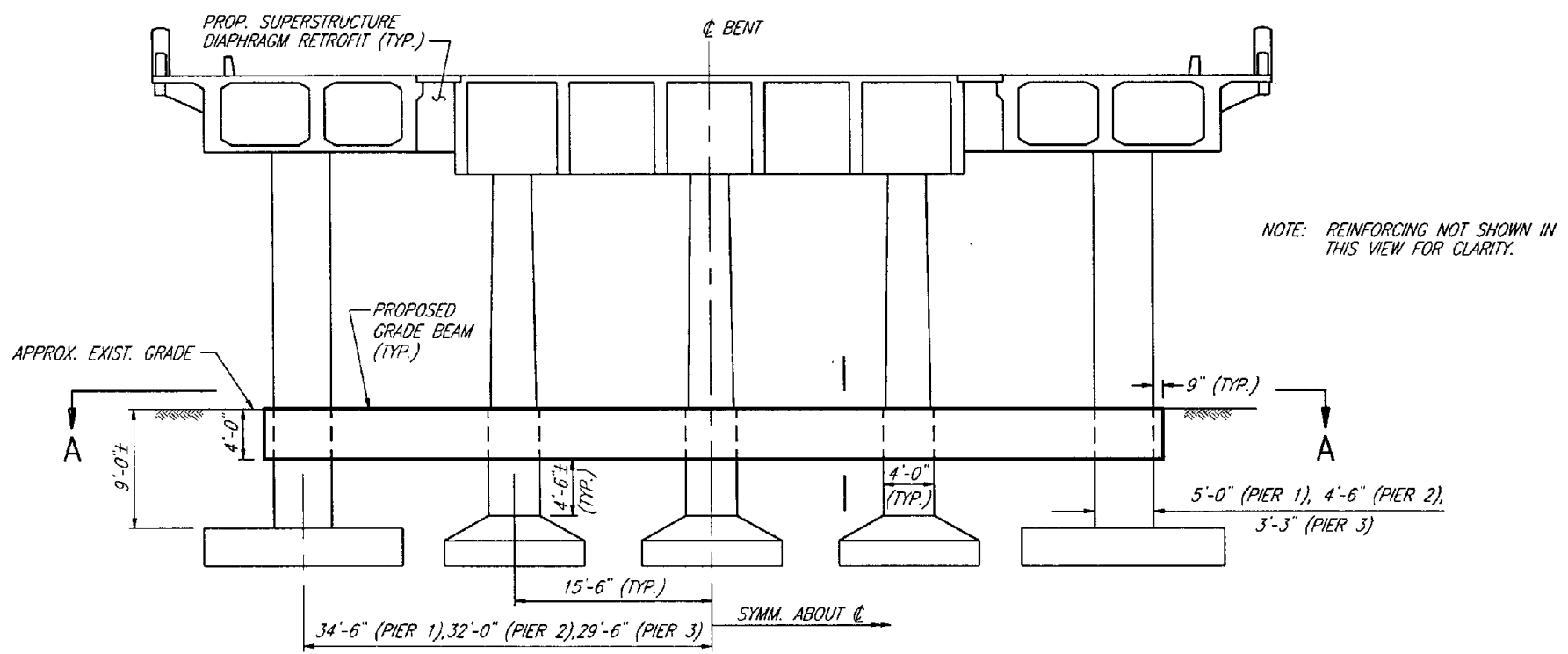
TYPICAL BENT ELEVATION (BENT 2 SHOWN, BENTS 1 & 3 SIMILAR)

SCALE: $\frac{1}{8}$" = 1'-0"

#7 BAR (TYP.)

3-#4 TOP & BOT.,
TYP. BET. COLUMNS

#7 BAR (TYP.)

1-#4 ☐

6'-6" (PIER 1), 6'-0" (PIER 2),
5'-6" (PIER 3)

1 - #4 ☐

8 - #4 ☐
@ 18"±

8 - #4 ☐
@ 18"±

8 - #4 ☐
@ 18"±

8 - #4 ☐
@ 18"±

75'-6" (PIER 1), 70'-0" (PIER 2), 63'-9" (PIER 3)
(23.0 m PIER 1, 21.3 m PIER 2, 19.4 m PIER 3)
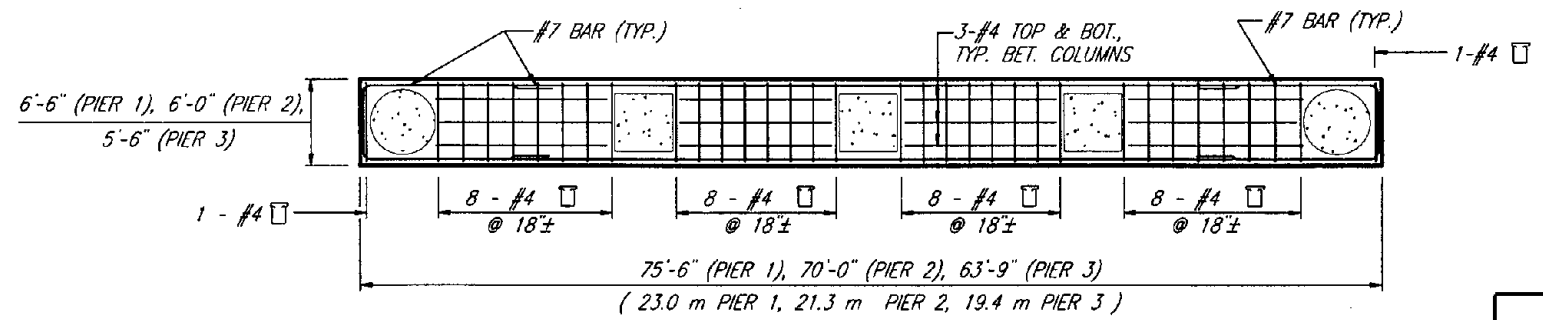
SECTION A-A

SCALE: $\frac{1}{8}$" = 1'-0"

EXELTECH
CONSULTING ENGINEERS
OLYMPIA, WASHINGTON

BALLARD BRIDGE
NORTH APPROACH
RETROFIT OPTION 1
TRANSVERSE GRADE BEAMS

387
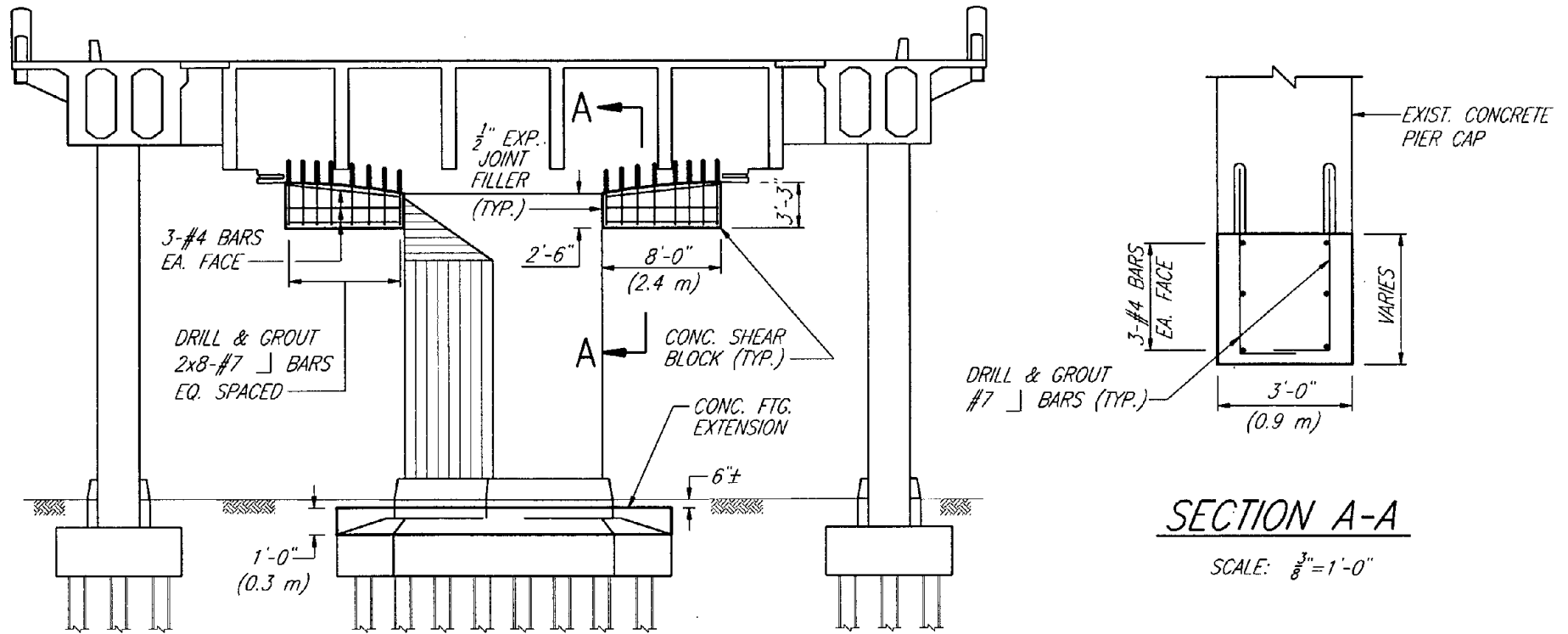
Figure 9

PIER NO. 4 ELEVATION

SCALE: $\frac{1}{8}"=1'-0"$

½" EXP.
JOINT
FILLER
(TYP.)

3-#4 BARS
EA. FACE

DRILL & GROUT
2x8-#7 ⌐ BARS
EQ. SPACED

CONC. SHEAR
BLOCK (TYP.)

CONC. FTG.
EXTENSION

2'-6"

8'-0"
(2.4 m)

3'-3"

6"±

1'-0"
(0.3 m)

A

A

SECTION A-A

SCALE: $\frac{3}{8}"=1'-0"$

EXIST. CONCRETE
PIER CAP

3-#4 BARS
EA. FACE

VARIES

DRILL & GROUT
#7 ⌐ BARS (TYP.)

3'-0"
(0.9 m)

NOTE: FOOTING RETROFIT REINF. NOT SHOWN FOR CLARITY.
FOR FOOTING RETROFIT DETAILS, SEE SHT. 2 OF 2.

388

Figure 10

EXELTECH
CONSULTING ENGINEERS
OLYMPIA, WASHINGTON

BALLARD BRIDGE-NORTH APPROACH
RETROFIT OPTION 2
SHEAR BLOCKS & FTG. STRENGTHENING
SHT. 1 OF 2
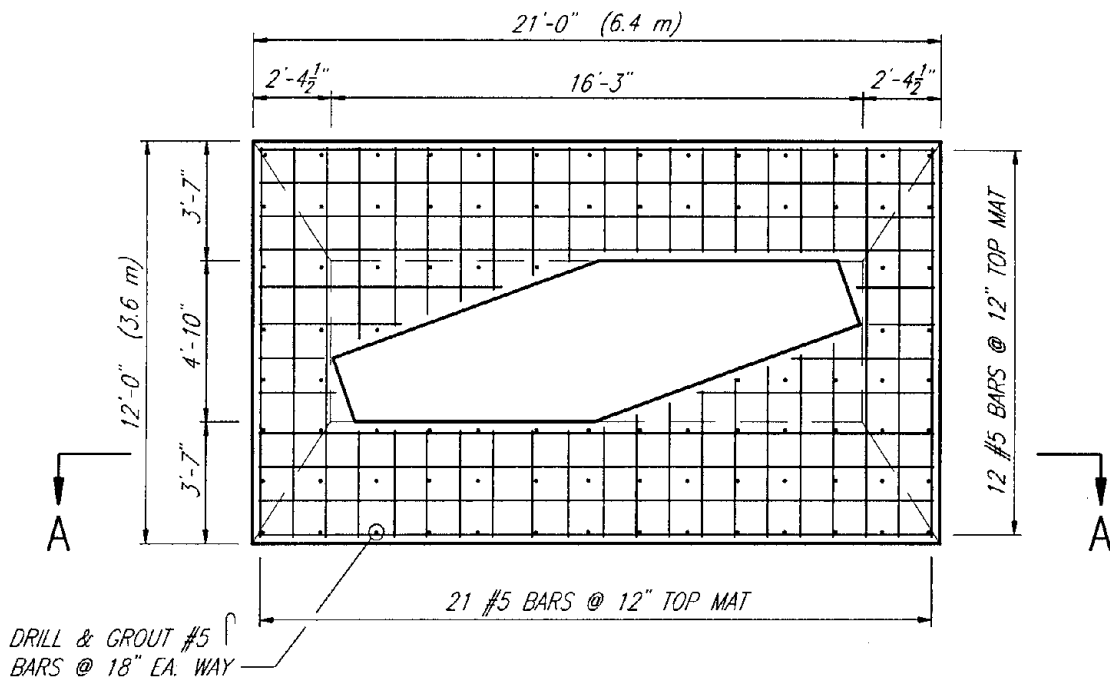
PIER 4 MAIN FOOTING PLAN

SCALE: $\frac{1}{4}$"=1'-0"
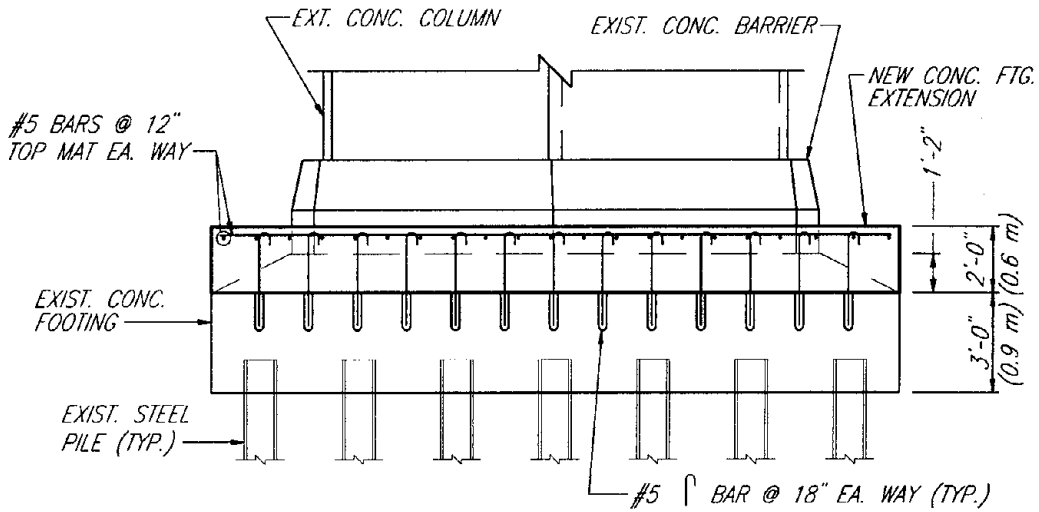
21'-0" (6.4 m)

2'-4$\frac{1}{2}$"   16'-3"   2'-4$\frac{1}{2}$"

3'-7"

12'-0" (3.6 m)   4'-10"

3'-7"

12 #5 BARS @ 12" TOP MAT

A   A

21 #5 BARS @ 12" TOP MAT

DRILL & GROUT #5 BARS @ 18" EA. WAY

SECTION A-A

SCALE: $\frac{1}{4}$"=1'-0"

EXT. CONC. COLUMN   EXIST. CONC. BARRIER

NEW CONC. FTG. EXTENSION

#5 BARS @ 12" TOP MAT EA. WAY

EXIST. CONC. FOOTING

EXIST. STEEL PILE (TYP.)

#5 BAR @ 18" EA. WAY (TYP.)

1'-2"

2'-0" (0.6 m)

3'-0" (0.9 m)

BALLARD BRIDGE-NORTH APPROACH
RETROFIT OPTION 2
SHEAR BLOCKS & FTG. STRENGTHENING
SHT. 2 OF 2

EXELTECH
CONSULTING ENGINEERS
OLYMPIA, WASHINGTON

Figure 11

CORE DRILL FOR 2-2"∅ POST-TENSIONING DUCTS

A

EXIST. CONC. PIER CAP

₵ COL. (TYP.)

2'-0"

28'-0" (8.5 m)

2'-0"

5'-0"

4-0.6"∅ POST-TENSIONING STRANDS (TYP.)

R ½" STEEL ANCHOR PLATE (TYP.)

EXIST. CONC. COL.

1'-6"

A

2"∅ DUCT FOR POST-TENSIONING TENDON

NOTE: SUPERSTRUCTURE NOT SHOWN FOR CLARITY

APPROX. WATER LINE

APPROX. MUD LINE
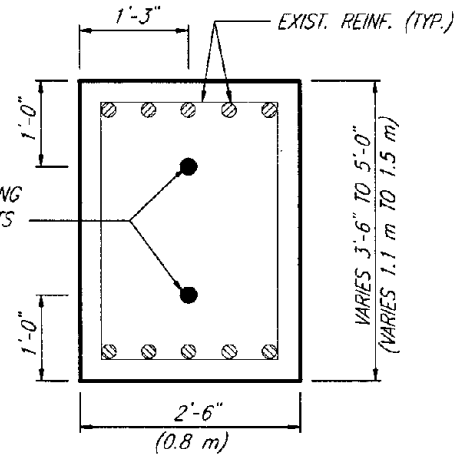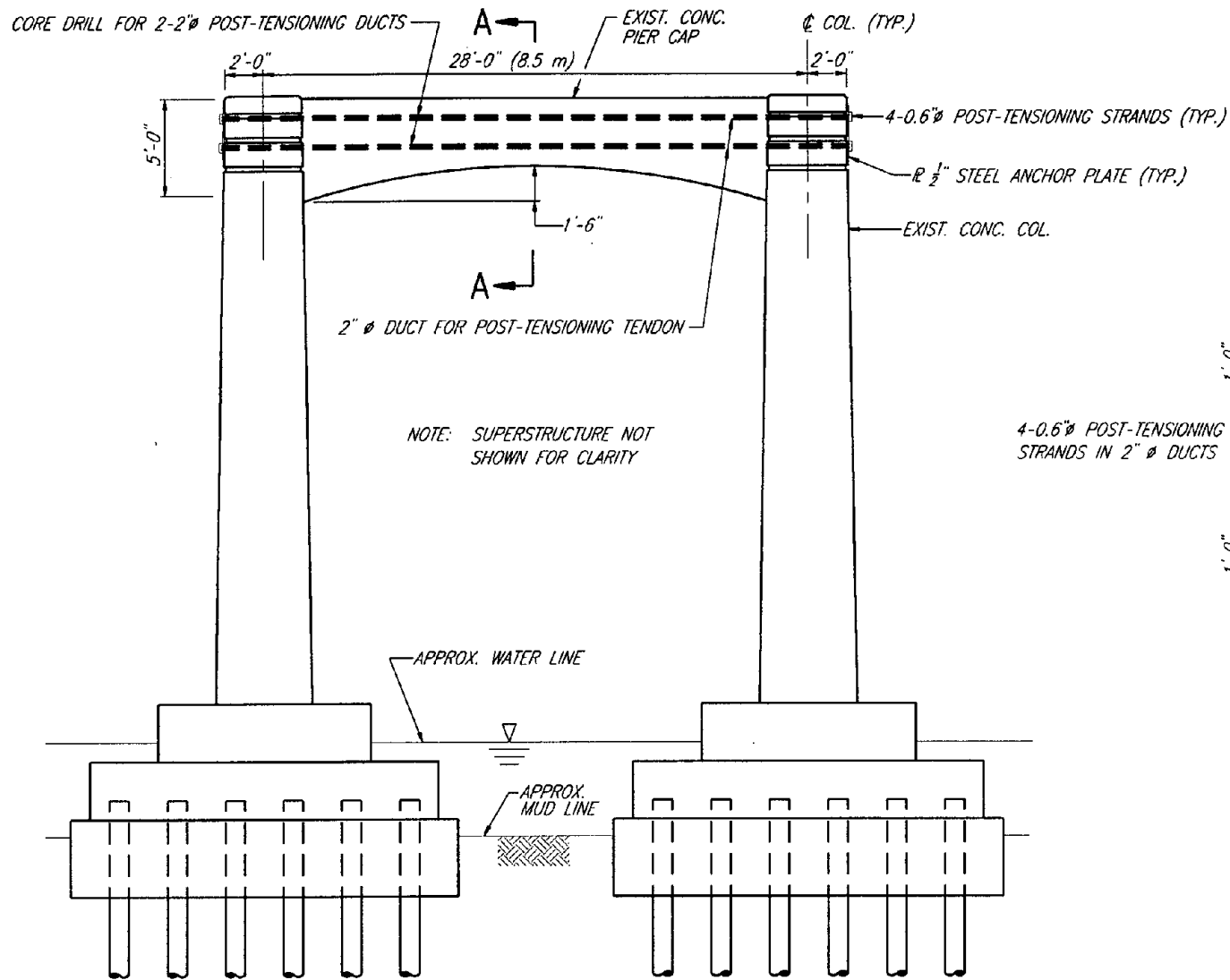
PIER 5 ELEVATION

SCALE: 3/16"=1'-0"

1'-3"

EXIST. REINF. (TYP.)

1'-0"

VARIES 3'-6" TO 5'-0" (VARIES 1.1 m TO 1.5 m)

4-0.6"∅ POST-TENSIONING STRANDS IN 2"∅ DUCTS

1'-0"

2'-6" (0.8 m)

SECTION A-A

SCALE: 3/4"=1'-0"

390

Figure 12

EXELTECH
CONSULTING ENGINEERS
OLYMPIA, WASHINGTON

BALLARD BRIDGE-NORTH APPROACH

RETROFIT OPTION 3

PIER 5 CAP BEAM STRENGTHENING

SECOND U.S.-JAPAN WORKSHOP ON SEISMIC RETROFIT OF BRIDGES

Bridge Retrofit Analysis and Earthquake Damage

L.H. Sheng, S. Mitchell and C.V. Ho
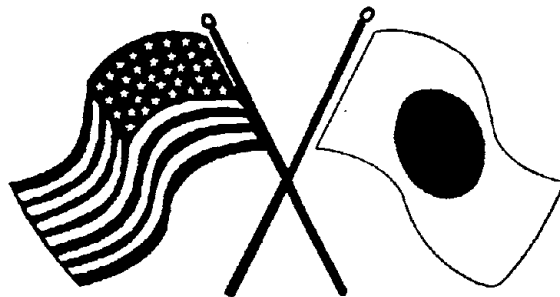
January 20 and 21, 1994
Berkeley Marina Marriott Hotel
Berkeley, California

Bridge Retrofit Analysis and Earthquake Damage

L.H. Sheng[1], S. Mitchell[2], and C.V. Ho[3]

Abstract

The California Department of Transportation (CALTRANS) initiated the single column retrofit program after the 1986 Whittier earthquake. After the 1989 Loma Prieta earthquake, a bridge retrofit program was established for all publicly owned bridges. Initially, all retrofit analyses were based on the traditional strength reduction approach in determining the demand/capacity ratio. In recent years, a static push-over method has been incorporated to investigate the structures' ductility capability. In this paper, three bridges are investigated for damage caused by various earthquakes. One bridge totally collapsed during the 1971 San Fernando earthquake, the second bridge suffered minor damage at the time, and the third bridge was damaged during the 1989 Loma Prieta earthquake. Nonlinear structural analyses are performed to identify the cause of the damage. Further studies with current structure retrofit analysis guidelines are performed. Results from the retrofit analyses are then compared with bridge damage to validate the current analytical methods.

Background

The California Department of Transportation began the structure retrofit project after the 1971 San Fernando Earthquake. The Phase 1 hinge retrofit was completed in 1986. At the same time, we were trying to develop a retrofit analysis strategy. After performing a number of nonlinear dynamic analyses, it was concluded nonlinear analysis is too time consuming for bridge retrofits. The nonlinear analyses required much more effort in the input of complicated parameters and sorting out the data from huge results files.

By comparing the results from nonlinear dynamic analysis to the regular response spectrum analysis, we find that the bridge dynamic response is bound by the tension and compression models. The bridge frame response to the dynamic load is either by itself (tension model) or is pushed by the adjacent frame (compression model). Consequently, this approach has become the basis of retrofit diagnostic analysis.

---

[1] Senior Bridge Engineer, Office of Earthquake Engineering, Division of Structures, California Department of Transportation, Sacramento, CA 95816.

[2] Senior Bridge Engineer, Office of Earthquake Engineering, Division of Structures, California Department of Transportation.

[3] Civil Engineer, Office of Earthquake Engineering, Division of Structures, California Department of Transportation.

Retrofit Analysis

The first step in the retrofit analysis is the diagnostic analysis. A Caltrans standard response spectrum analysis is performed to determine the dynamic strength demand from the design spectrum. If the ductility demand from this analysis is lower than the existing columns' ductility capacity then there is no need to retrofit the existing bridge. Otherwise, bridge computer model will then be modified for tension and compression models to determine the maximum strength demand.

There are two factors that make retrofit analyses more difficult than regular design analyses.

1. Existing structure layout and boundary conditions.
2. Unknown material strengths after aging.

These factors are typically encountered when attempting to reproduce as-built behavior in the lab. Engineers usually do not know the exact structure geometry layout and material strength. Items that must be considered include: actual column length after backfill, abutment stiffness, footing stiffness, and actual concrete and steel strength. The as-built contract plan is the only document an engineer can rely on.

After the column retrofit program began, we gradually noticed that the traditional strength demand approach had a tendency to be conservative. In some particular cases, there is so much retrofit work that needs to be performed that it is more economical to replace the whole structure. To reduce the required retrofit work, a more rational analysis approach was needed. In 1990, we began to review our analysis methods and to try to correlate the results with actual earthquake damage experienced by bridges. In this paper, we will review three bridges that had been more or less damaged by various earthquakes. Traditional response spectrum analysis, non-linear time history analysis, and the push-over method were used to correlate the damage seen after earthquakes. The influences of the cracked and gross section properties are also investigated.

Los Angeles Aqueduct (Foothill Blvd.)

Bridge description

The Los Angeles Aqueduct is a continuous, three span, reinforced concrete box girder bridge (figure 1,2), and is located to the North of the intersection of Balboa Boulevard and San Fernando Road. The Abutments and the 2 column bents are skewed about 52°. Abutment 1 was above and very close to the wall of a rigid frame underground structure. The structure is about 4 kilometers from the Sierra-Madre-San Fernando Fault.

Damage report

This bridge suffered little damage during the 1971 San Fernando earthquake. There was cracking and spalling at the west wingwalls and the fill and structure settled about 1 foot. This settlement did not appear to cause damage to the superstructure and columns.

Structure analysis

The BAG program was used to generate both the CALANSR and STRUDL input files. The superstructure is modeled with linear elements while columns are modeled using the inelastic beam column elements. The inelastic elements consider the bending moment to be uniform over the entire length. The abutments are modeled with gap friction elements. The gap friction element is oriented in such a way that its X axis coincides with the bearing plane. This computer model is shown as figure 3. The column's gross and cracked moment of inertia were calculated as 14 ft^4 and 4.24 ft^4.

The structure was loaded with strong motion data from Pacoima Dam recorded during the San Fernando earthquake. The spectrum is depicted in figure 4. The bridge and the Pacoima Dam strong motion instrument site are about 6 miles apart and both are located in the near field region of the San Fernando earthquake source.

Analysis results

The vibration modes from STRUDL and CALANSR models are compared as follows:

	STRUDL		CALANSR	
Mode	Uncracked	Cracked	Uncracked	Cracked
1	0.20	0.22	0.20	0.22
2	0.11	0.12	0.11	0:12
3	0.07	0.09	0.07	0.10

It is somewhat surprising to see the cracked and uncracked column moments of inertia did not affect the response of the first 2 modes. This is due to the stiff superstructures interaction with the abutment dominating the response. The linear time history analysis reaches the maximum response (force or displacement) at 6.22 seconds while the nonlinear time history analysis reaches the maximum response at 8.22 seconds. This difference is due to the inclusion of a gap at the abutment in the nonlinear model. The nonlinear analysis also shows a higher response when compared to linear analysis. The elastic response from all analyses seem to be consistent with the damage reported after the earthquake.

Rte 5/405 separation (Truck Lane)

Bridge description

The Route 5/405 Separation is located approximately 2 miles West of the City of San Fernando and 1.6 miles from the Sierra Madre-San Fernando Fault. This is a cast-in-place prestressed concrete box girder bridge with two 177 feet spans on a curved, skewed (38 to 45 degrees), alignment (figure 5). The bridge is supported by two rectangular columns that are 29 feet in height and on spread footings.

Damage report

This bridge collapsed during the 1971 San Fernando earthquake. The columns were completely shattered (figure 6) causing the superstructure to break into three pieces (figure 7) as it fell. The structure was a complete loss and was immediately demolished and removed.

Structure analysis

The BAG program was used to generate both the CALANSR and STRUDL input files. The modeling technique is the same as for the Los Angeles Aqueduct discussed above. This computer model is shown in figure 8. The column's gross and cracked moments of inertia were calculated as 34.5 ft^4 and 27.6 ft^4 in the longitudinal direction and 22.0 ft^4 and 19.4 ft^4 in the transverse direction.

The structure was loaded with strong motion data from the Pacoima Dam recorded during the San Fernando earthquake. The bridge and the Pacoima Dam strong motion instrument site are about 6 miles apart and both are located in the near field region of the San Fernando earthquake source. The strong motion data was rescaled following the peak horizontal acceleration attenuation equation with a factor of 1.25.

Analysis results

The vibration modes from STRUDL and CALANSR models are compared as follows:

	STRUDL		CALANSR	
Mode	Uncracked	Cracked	Uncracked	Cracked
1	0.50	0.50	0.49	0.49
2	0.41	0.43	0.41	0.43
3	0.38	0.39	0.38	0.38
4	0.19	0.19	0.19	0.19
5	0.17	0.17	0.17	0.17

Like the Los Angeles Aqueduct Bridge, different cracked and uncracked moments of inertia of columns did not greatly affect the response of the first 5 modes. The linear time history analysis reached the maximum response (displacement or force) at 6.22 seconds while the nonlinear time history analysis reached the maximum response at 8.36 seconds. This is similar to the Los Angeles Aquaduct bridge. The linear time history analysis also shows a moment demand larger than column capacity. This is consistent with the nonlinear analysis which shows columns yielding. Although there is only a minor difference in first 5 structural frequencies between gross and cracked sections, the maximum displacement from cracked section results is larger than from gross section results.

There are three possibilities failure scenarios for this structure:

1. Flexure failure: As indicated above, the structure demands more column strength than what it can carry. After reviewing the structures' damage report, it is unlikely that this is the cause.

2. Shear failure: After detailed evaluation of the shear capacity of the column, both linear and nonlinear analysis showed column shear demand exceeds the shear capacity based on the current shear capacity recommendation from University of California, Berkeley. A plane frame push-over analysis did not indicate a shear failure while a moment ductility analysis did indicate a shear failure. This is likely due to the plane frame analysis underestimating the cap stiffness or yielding prematurely. The moment ductility analysis considered the column to be fixed-fixed. This structure will fail in shear before a flexure failure occurs.

3. Axial failure: Based on the structures' damage report, it is likely that vertical failure played a role in this structures' failure. A totally shattered column can only be caused by a large vertical force. Because of the lack of vertical strong motion data, we did not evaluate the vertical response of this bridge. It is likely that it started with a shear failure and then collapsed due to vertical force.

Mococo Overhead Offramp

Bridge description

The Mococo Overhead Offramp is a continuous reinforced concrete slab bridge supported on reinforced concrete pile extensions (figure 9) and is located on I-680 near the East city limit of Martinez. The offramp is supported at one end with a pile cap abutment and a fixed support at bent 6L where it transitions into the Mococo Overhead structure. Bents 2 through 13 and 15 consist of 6 columns while Bents 14 and 15 are composed of 5 columns. There are thermal expansion joints located at spans 6 and 11. The structure straddles a drainage canal and is supported on a very soft peat with brown clay sitting on top of sandstone and fine sandy silt.

Damage report

This bridge suffered minor damage during 1989 Loma Prieta earthquake. The column pile extensions at Bents 4, 5, 6, and 8 have cracks at the top, extending 2 feet down from the deck soffit. Bents 2 and 3 have cracks from the ground up to deck soffit. The hinge in Span 6 has spalls on the rail and the edge of deck on the inside of the curve. The hinge at Span 11 has a crack in the deck on the outside of the curve.

Structure Analysis

The BAG program was used to generate both the NEABS and STRUDL input files. In the NEABS model (figure 10), the top and bottom column elements were modeled using the elasto-plastic flexural beam-column elements. Hinges were modeled using nonlinear expansion joint elements. The cap normal bending moment of inertia was calculated assuming an effective width of the column diameter plus 6 times the deck thickness on each side of the column. Cap stiffnesses were modeled as in typical Caltrans STRUDL models where Ix and Iz are taken as 1000 times the normal bending moment of inertia.

Column capacities were calculated based on nominal material properties of fc'=3250 psi, fy=40 ksi, and ecu=0.003 as well as estimated material properties of fc'=5000 psi, fy=50 ksi, and ecu=0.01. After applying the over-strength capacity factor of 1.3 to the nominal column strength, the column moment capacity is 62.4 kip-ft. The column moment capacity is 63.0 kip-ft for the maximum material property condition. An effective fixity was calculated base on BDA (Bridge Design Aids) 12-49.

The structure was loaded with strong motion data from the Richmond City Hall parking lot (CSMIP station 505, figure 11) which contains data from 3 channels.

Analysis results

The vibration modes from STRUDL and NEABS models are compared as follows:

| | STRUDL - Hinge Free | | NEABS | |
Mode	Uncracked	Cracked	Uncracked	Cracked
1	1.40	3.14	1.37	2.75
2	1.34	2.58	1.23	2.00
3	1.14	1.79	1.12	1.78
4	0.79	1.70	0.83	1.48
5	0.50	0.58	0.64	1.43

	STRUDL - Hinge Fixed		NEABS	
Mode	Uncracked	Cracked	Uncracked	Cracked
1	1.35	2.32	1.37	2.75
2	1.01	1.96	1.23	2.00
3	0.52	0.61	1.12	1.78
4	0.46	0.51	0.83	1.48
5	0.30	0.34	0.64	1.43

Hinges free   : Longitudinal force released at hinge
Hinges fixed : Longitudinal force not released at hinge

Both linear and nonlinear uncracked models showed that plastic hinges formed (figure 12). One unexpected difference is that the nonlinear analysis predicted larger moments in the frame between Bent 12 and abutment 6L. The cracked model remains elastic throughout the entire time history analysis. Both linear and nonlinear uncracked models and linear cracked model showed similar displacements pattern (figure 13).

The column section properties used in the analyses greatly influenced the solution. Using uncracked column bending moments of inertia produced extensive yielding in the columns throughout the bridge while using cracked column bending moments of inertia produced no yielding. This can be explained by comparing the eigenvalue data of the different structure models.

Conclusion

Three bridges have been reviewed for earthquake damage and results have been compared with damage reports. The traditional Caltrans dynamic analysis is adequate to determine the strength demand for retrofit purposes. Because none of these bridges has strong motion instrumentation installed, it is difficult to determine which model will be better to estimate the structures displacement.
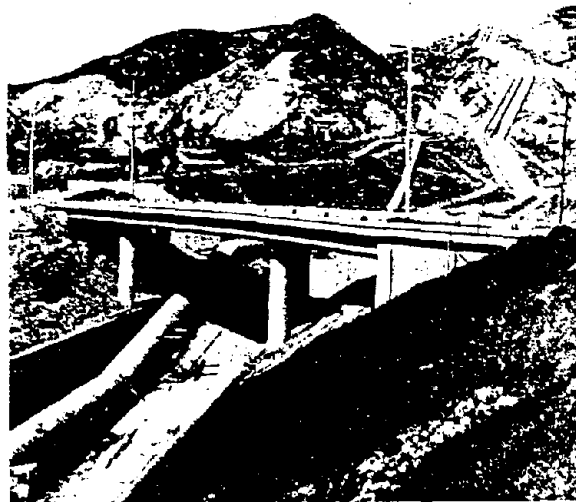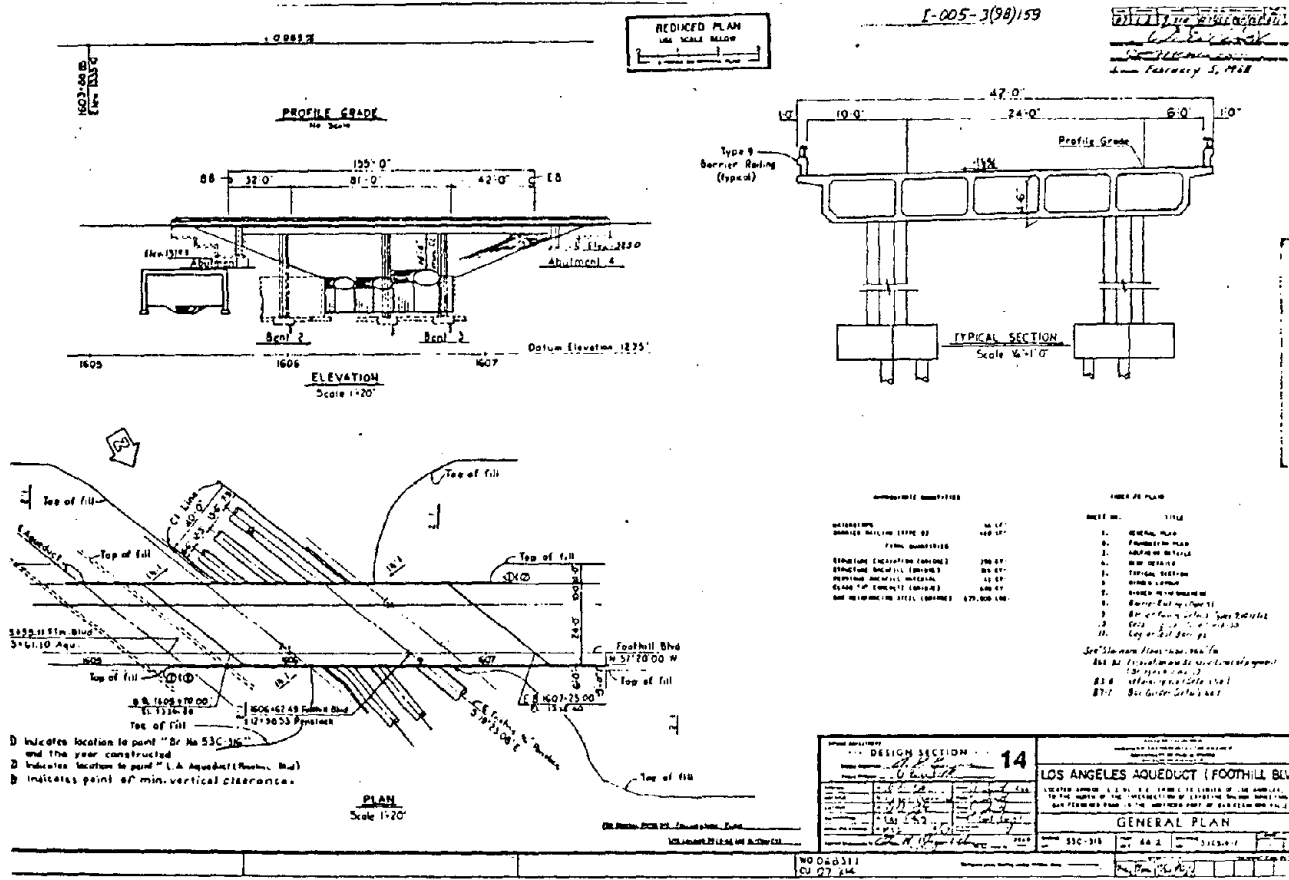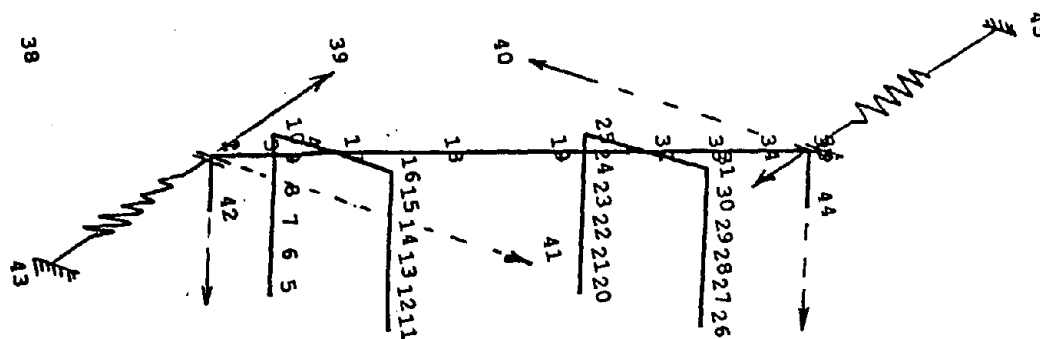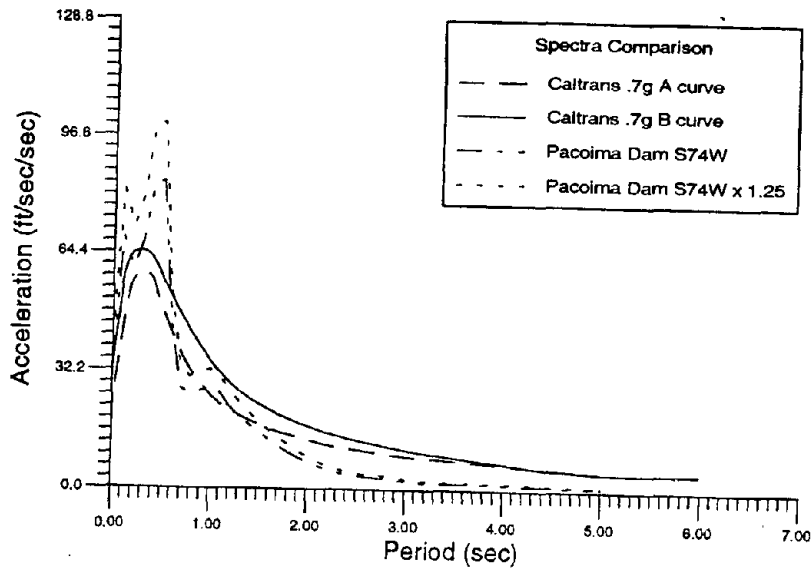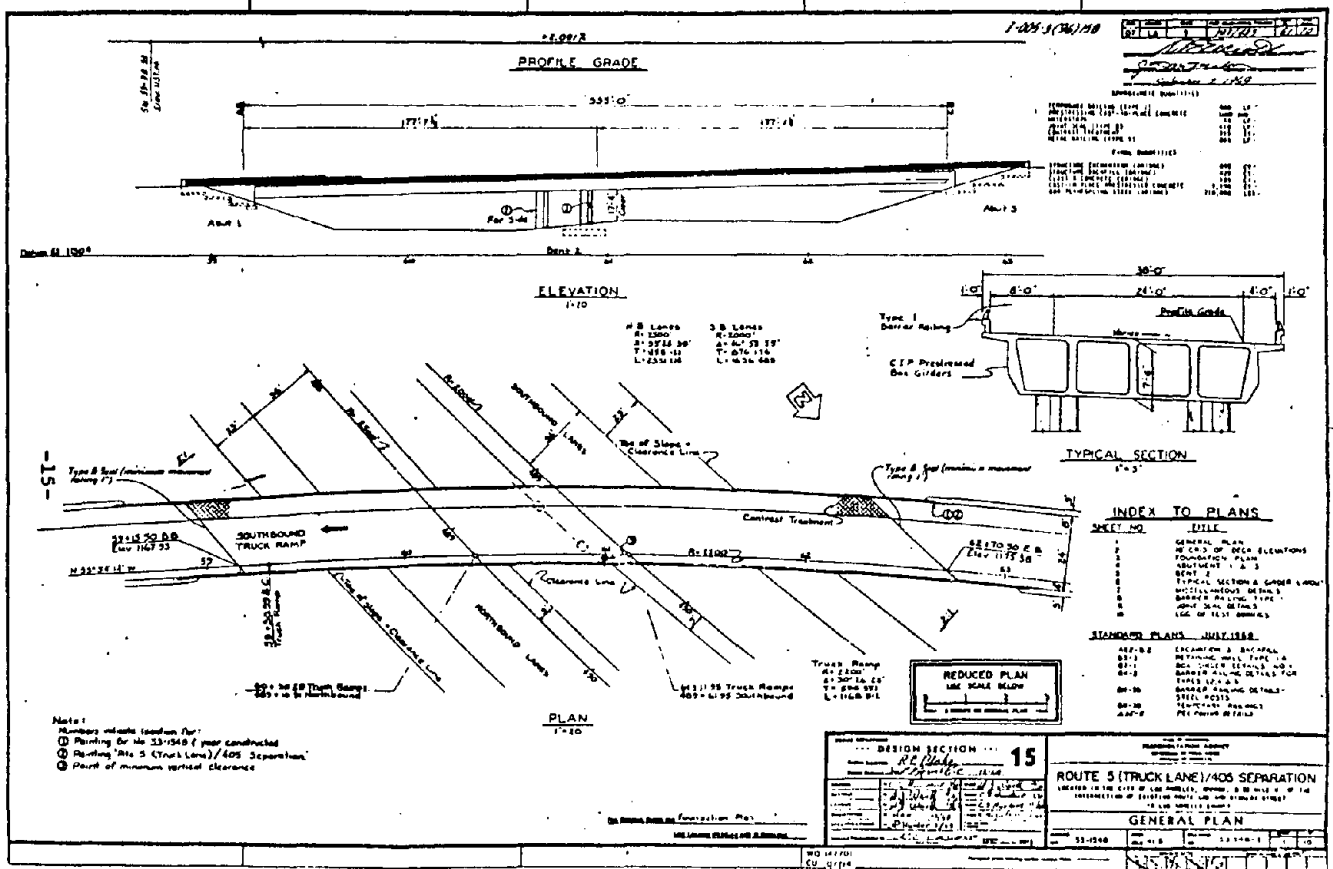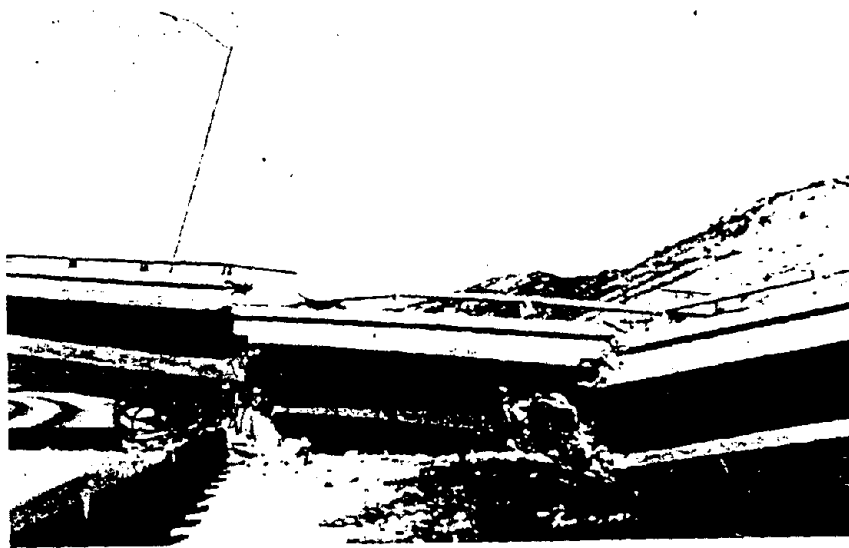

Figure 1

Figure 2
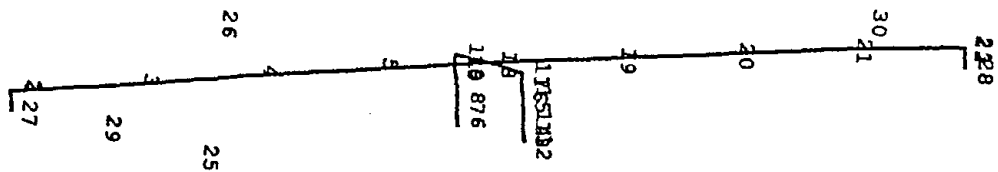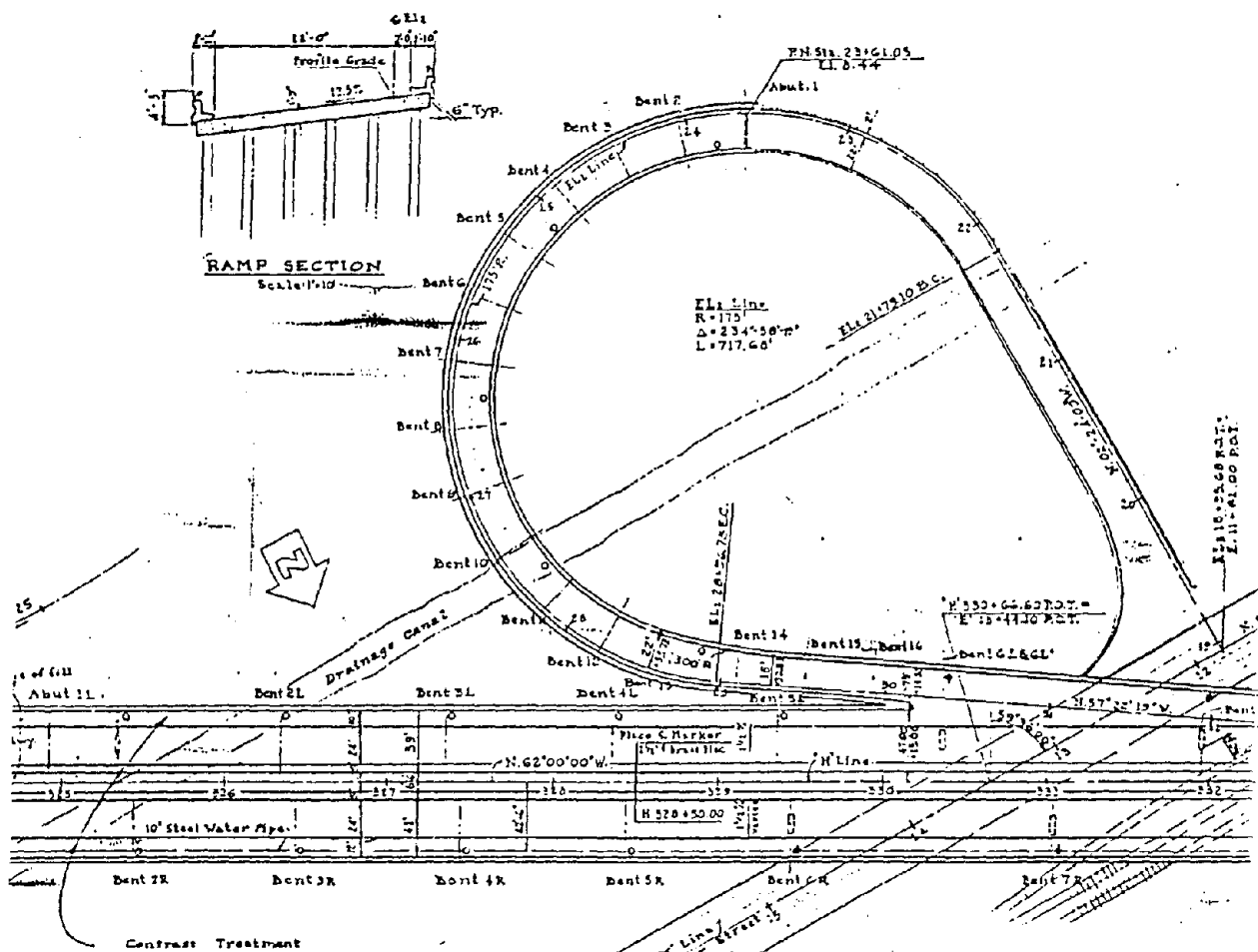

Figure 3

Figure 4

Figure 5

Figure 6

Figure 7

Figure 8

RAMP SECTION

MOCOCO OVERHEAD OFFRAMP GEOMETRY

Figure 9
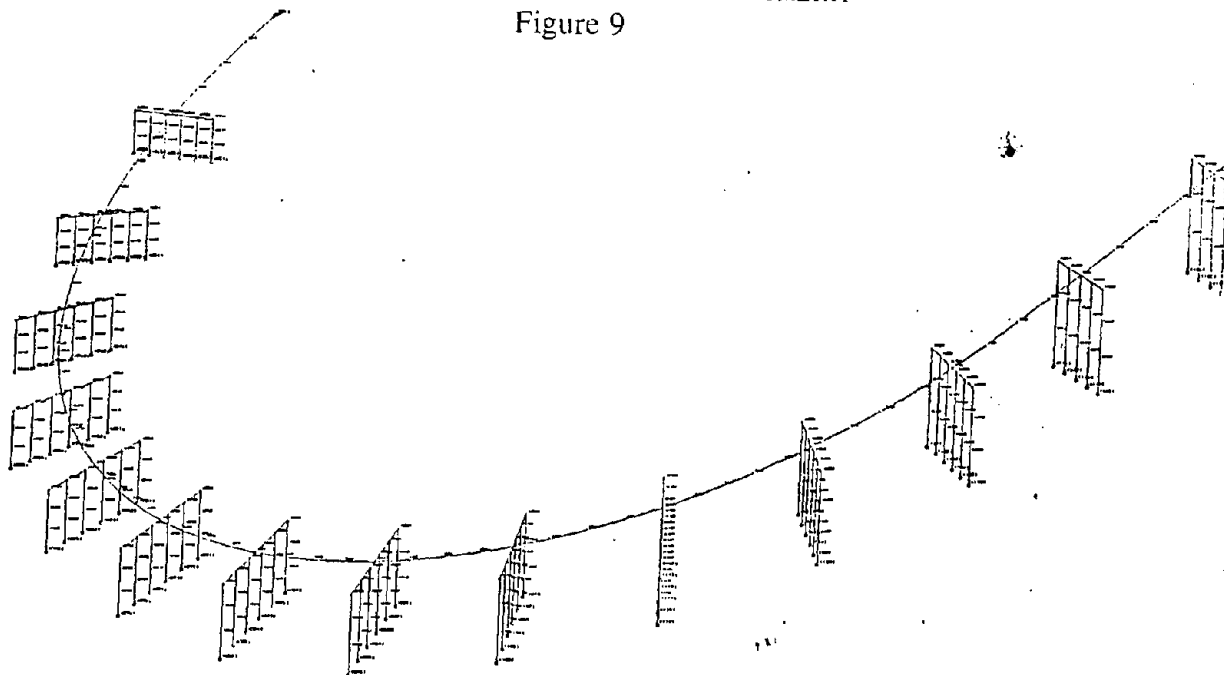
Figure 10

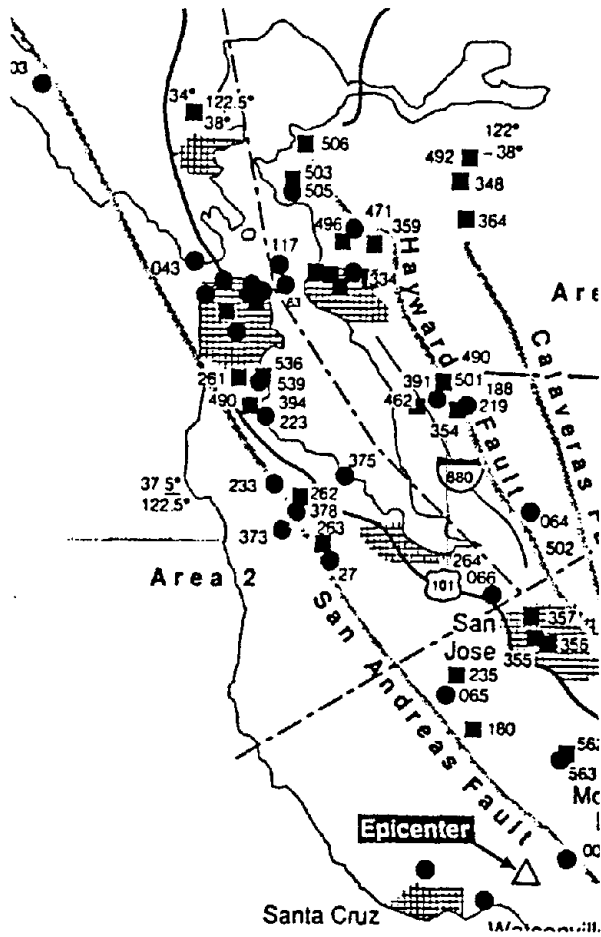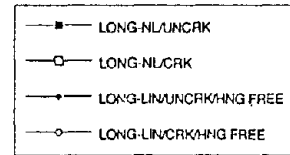Figure 11

Figure 12

Z-DISPLACEMENT -- NONLINEAR VS. LINEAR
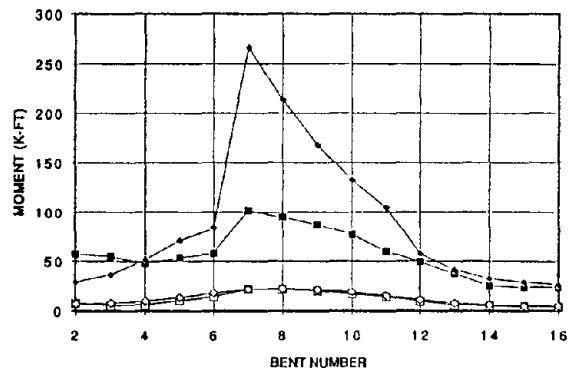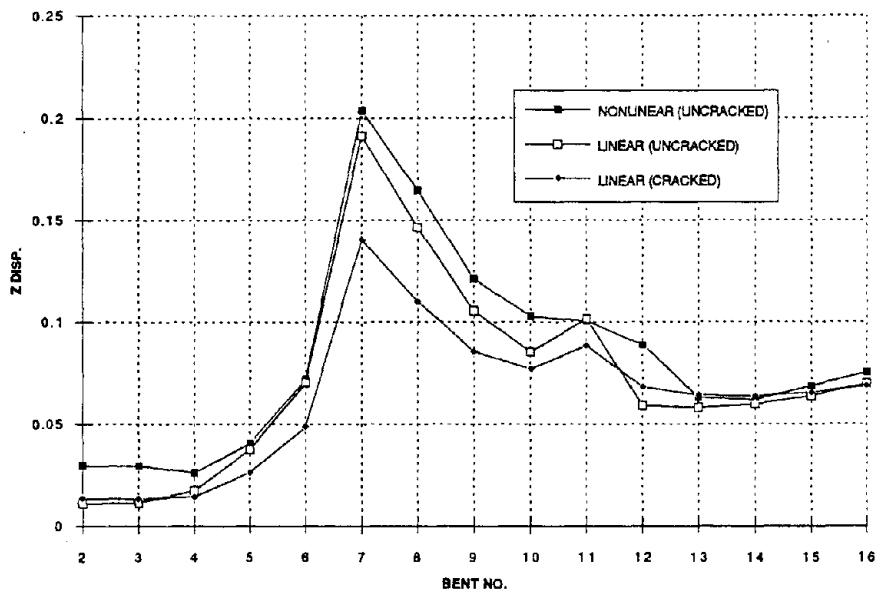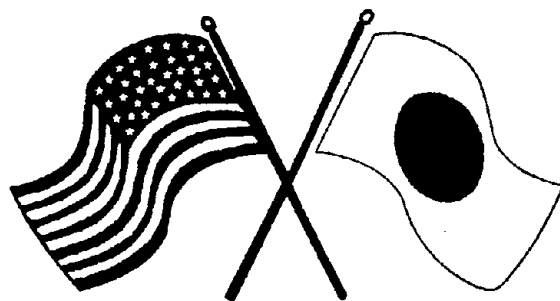

Figure 13

Second U.S.-Japan Workshop on Seismic Retrofit of Bridges

Seismic Vulnerability of the Alaskan Way Viaduct

*J. De La Colina, S. Ryter,
M.O. Eberhard, S.L. Wood,
S.L. Kramer and N. Sivaneswaran*

SEISMIC VULNERABILITY OF THE ALASKAN WAY VIADUCT

Jaime De la Colina[1], Stanley Ryter[2], Marc O. Eberhard[3],
Sharon L. Wood[4], Steven L. Kramer[5] and Nadarajah Sivaneswaran[6]
Department of Civil Engineering, University of Washington, Seattle

SUMMARY

This paper summarizes results of an ongoing investigation of the seismic vulnerability of the Alaskan Way Viaduct. The Alaskan Way Viaduct is a cast-in-place, reinforced concrete structure that runs for approximately 2.2 miles along Elliot Bay in downtown Seattle. Approximately 1.7 miles of the viaduct has two decks. The double-deck structure was selected for detailed evaluation because it is an important link in the region's transportation network, it is underlain by deep deposits of loose hydraulic fills, it lacks the reinforcement details that are specified in current codes and it superficially resembles double-deck viaducts that were damaged during the 1989 Loma Prieta Earthquake.

Two approaches were used to study the viaduct's vulnerability to earthquakes. A three-dimensional, linear model of the viaduct was developed and used to calculate capacity/demand ratios for structural members using the procedures described in the Applied Technology Council's "Seismic Retrofitting Guidelines for Highway Bridges" (ATC-6-2)[1]. In addition, monotonic pushover analyses were performed using two-dimensional, nonlinear models of the structure, following the recommendations of Priestley et al. at the University of California at San Diego (UCSD) [2]. Because the fill properties are highly variable, the investigators performed the linear and nonlinear analyses for both pinned and fixed-base conditions. This case study provides the opportunity to compare the results of the two assessment procedures.

INTRODUCTION

The Alaskan Way Viaduct is important to the economy of Seattle because it provides one of only two North-South corridors through the city. An average of 86,000 vehicles use the structure daily. The 2.2-mile long viaduct is located on land near the present shoreline of Elliot Bay, but most of the alignment is offshore of the historical shoreline. From a geotechnical point of view, the site selection was unfortunate because the structure is underlain by hydraulic fill that was placed at the turn of the century. The structure's vulnerability is compounded by its structural details, which are typical of construction in the 1950's and do not satisfy current code requirements.

---

[1]Research Associate and Assistant Professor, Univ. Aut. del Edo. de México, Toluca, México
[2]Graduate Research Assistant
[3]Assistant Professor
[4]Visiting Associate Professor and Associate Professor, University of Illinois, Urbana
[5]Associate Professor
[6]Research Associate

To help decide whether and how the Alaskan Way Viaduct's earthquake resistance should be improved, the Washington State Department of Transportation (WSDOT) asked the investigators to assess the viaduct's seismic vulnerability. Though the structure contains many atypical features, such as outriggers and offramps, only two typical structural units are being evaluated initially. One unit is representative of the double-deck portion's northern half, which was designed by the City of Seattle Engineering Department, and the second unit is typical of the southern half, which was designed by WSDOT. This paper discusses only the assessment of the WSDOT-designed typical unit.

The first two sections describe the typical WSDOT unit and its foundation conditions. The next section presents the results of an evaluation of the structure using dynamic, linear analysis, following the procedures recommended by ATC-6-2[1]. Then, the paper presents the results of the nonlinear, static analyses and of the evaluation procedures proposed by Priestley et al. [2]. The paper concludes with a discussion of the lessons learned from implementing the two procedures.

DESCRIPTION OF TYPICAL UNIT

Longitudinal and transverse elevations of a typical WSDOT-designed unit are shown in Fig. 1. The 184-ft unit has three bays (57, 70 and 57 ft) in the longitudinal direction and one 47-ft bay in the transverse direction. A two-in. gap separates adjacent units in the longitudinal direction. The road surfaces are 35.5 and 57.5 ft above the base of the columns.

Interior columns are 4 ft by 3.5 ft, and the exterior columns are 4 ft by 2 ft. In the longitudinal direction, 7 ft-4 in. deep girders span between the columns, and 5-ft deep beams span between the columns in the transverse direction. In addition, two interior beams per bay and four longitudinal stringers support the 6.5-in. thick reinforced concrete slabs.

Over most of the column's height, the longitudinal reinforcement ratio is 1.1% for the interior columns and 1.5% for the exterior columns. Counter to intuition, the column reinforcement ratio increases to 1.7% (interior columns) and 3.6% (exterior columns) at the top of the second story. Reinforcement details in the structure are typical of 1950's construction. A short splice (20 bar diameters) located immediately above the pile cap connects the column reinforcement to the starter bars anchored in the foundation. A second splice is located above the lower deck. Transverse reinforcement in the columns is minimal, consisting of #3 hoops, spaced at 12 in. on center. Longitudinal reinforcement in the beams and girders was selected to resist moments induced by gravity loads, and typically, the positive moment reinforcement is not adequately anchored in the supporting members. Open stirrups are used to resist shear forces in the beams. No transverse reinforcement was placed in the beam-column joints.

The columns are supported on 3.5-ft thick pile caps and 18-in. diameter concrete piles. The pilecaps have a mat of bottom reinforcement, consisting of #9 bars at 7.5 in. spacings in each direction, but they have no top reinforcement. The tops of the piles are embedded into the pile cap, but the depth of embedment is uncertain. No steel connects the piles to the cap.

Concrete with a compressive strength of 3000 psi was specified for all members except for the pile caps, where the specified compressive strength was 2200 psi. Reinforcing bars with a specified yield stress of 40 ksi were used throughout the WSDOT-designed structure.
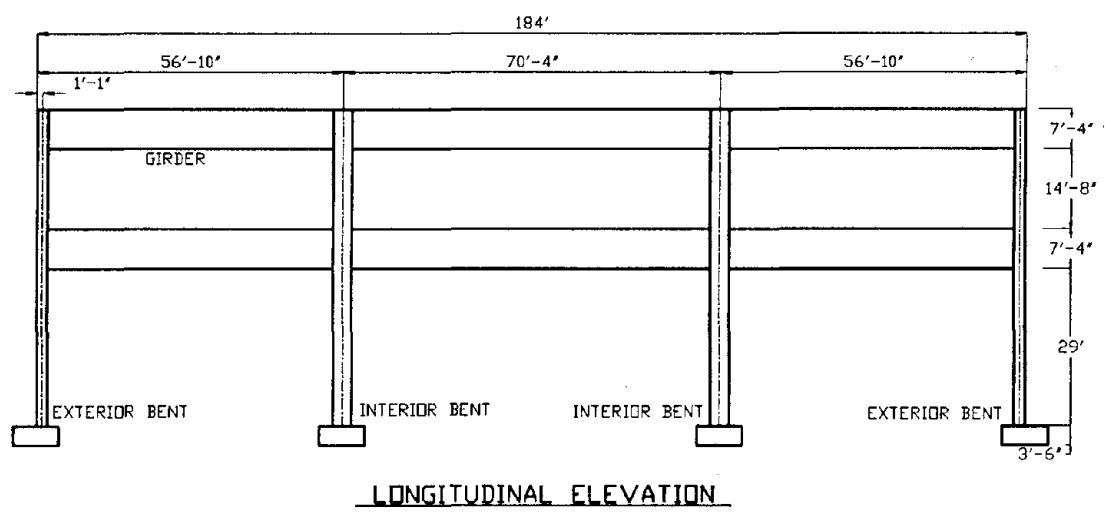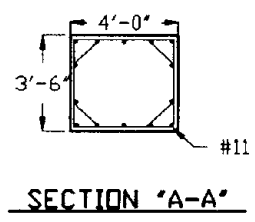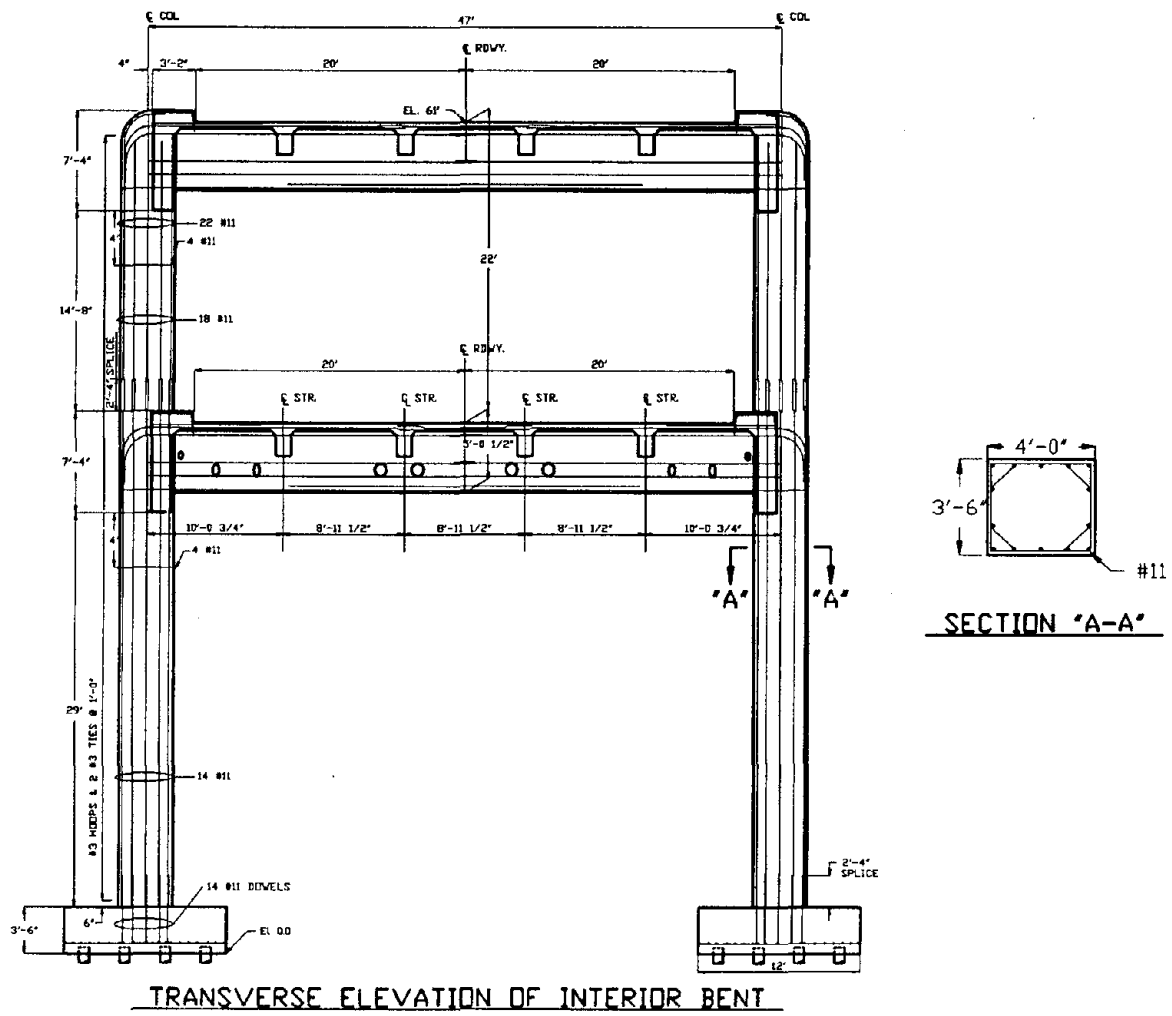
408

TRANSVERSE ELEVATION OF INTERIOR BENT

SECTION 'A-A'

LONGITUDINAL ELEVATION

Figure 1. Typical WSDOT-Designed Unit

409

SOIL CONDITIONS

The present alignment of the viaduct is largely located offshore of the original shoreline of Elliot Bay. Between 1903 and 1928, large portions of the Elliot Bay tidelands were hydraulically filled with soil by the regrading of Denny and Beacon Hills. These fills extend to depths of nearly 70 ft along the alignment of the viaduct. Along the northern portion of the viaduct, the fills are underlain by dense, glacial till. Along the southern portion, a soft, natural tideland deposit lies between the fill and the underlying till. A subsurface profile along the length of the viaduct is shown in Fig. 2.
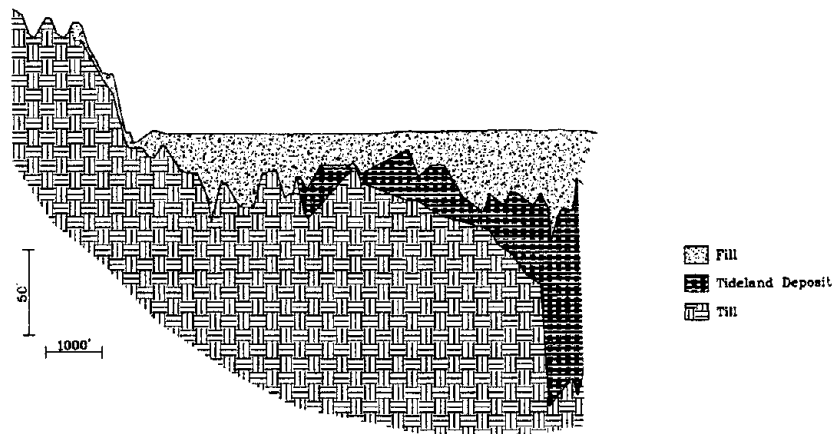
Figure 2. Subsurface Profile Along Viaduct

The fill soils play an important part in the seismic vulnerability of the viaduct. Because most of the fill was deposited by pluviation through water, the fill is loose and saturated (the groundwater level is at a depth of about 10 ft over most of the length of the structure). Standard penetration test (SPT) resistances are highly variable, reflecting the random nature of the material and its placement, but average about 10 blows/ft (Fig. 3). A statistical analysis of the SPT data showed no trends in variance with depth. Cone penetration test (CPT) results confirmed the loose and variable nature of the fills. The results of downhole, shear-wave velocity test, using both conventional and seismic cone techniques, were consistent with those of the penetration tests; shear-wave velocities in the fill average from 400 ft/sec to 500 ft/sec.

The natural tideland soils that underlie the fill along the southern portion of the viaduct are also loose and saturated. Though somewhat siltier than the fill soils, the penetration resistances and shear-wave velocities are similar to those of the fill. The underlying glacial till is considerably more dense. SPT and CPT resistances and shear-wave velocities increase markedly at the fill/till border; the shear-wave velocity of the till reaches a value of 2,500 ft/sec at depths of 225 - 250 ft. Tertiary bedrock depths vary from about 1,600 - 3,300 ft.

The soil conditions are likely to strongly affect the viaduct's seismic response. Therefore, additional field tests and analyses are being performed to estimate the ground-motion characteristics for the site, the potential for liquefaction and the foundation properties. Because

410

these estimates will be accompanied by great uncertainty, preliminary analyses have focused on standard response spectra and extremes of foundation rotational stiffness. The effect of foundation translational flexibility has not yet been considered, but this effect may be important as well. The piles were designed as end-bearing piles, and consequently, many extend only a few feet into the dense till.
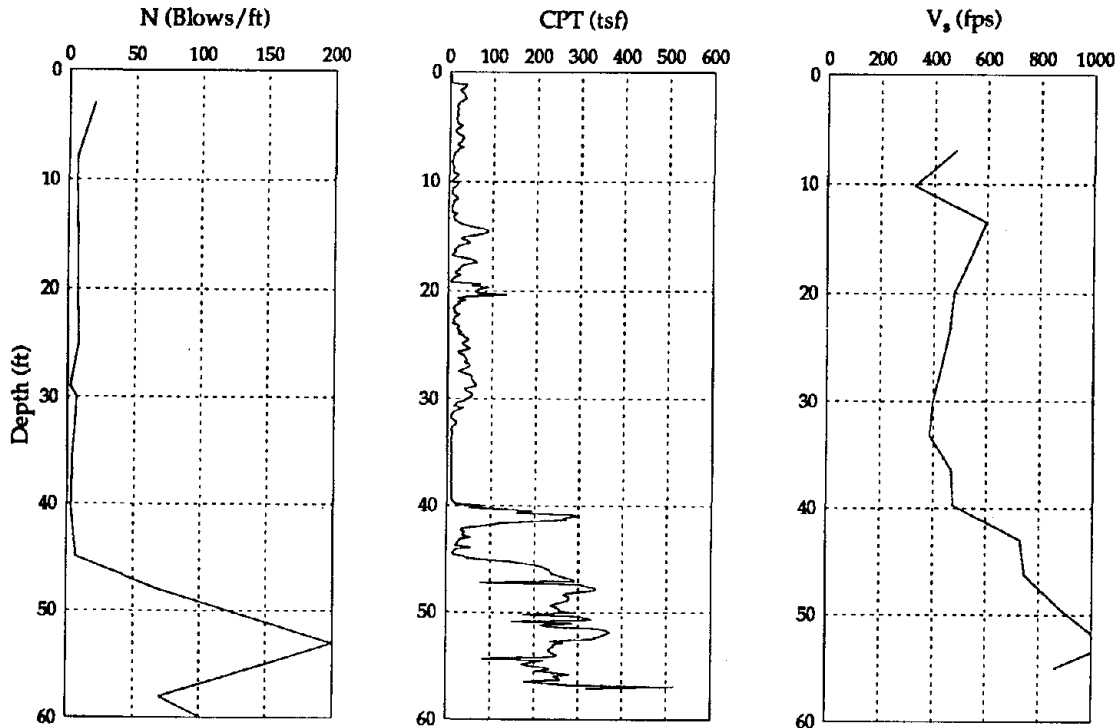
Figure 3. Measured Properties of Fill

LINEAR DYNAMIC ANALYSIS

The results of the ATC-6-2 evaluation are summarized in this section. The ATC guidelines rely heavily on ratios of member capacities to demands (C/D ratios). Member demands for each cross-section were computed with a linear, 3-dimensional, finite-element model of the typical unit shown in Fig. 1. The capacities of the structural members were calculated using material strengths equal to 1.5 times the specified the specified concrete compressive strength and 1.1 times the nominal steel yield stress, as suggested by Priestley et al [2].

The analyses were conducted for both pinned and fixed-base conditions. The longitudinal and transverse seismic responses of the structure were considered independently, and member forces induced by gravity loads were included in the analyses.

Description of the Structural Model

The finite-element model of a typical three-bay unit contains 956 spring, frame and shell elements (Fig. 4). To compensate for cracking that was observed in the structures and for

cracking that will occur early in the earthquake, all members were modeled using a moment of inertia equal to one-half the gross-section value. The column stiffness was increased in the joint regions by a factor of eight to simulate the increased stiffness of these regions. The commercial finite-element analysis program ANSYS 5.0 was used for all linear analyses.
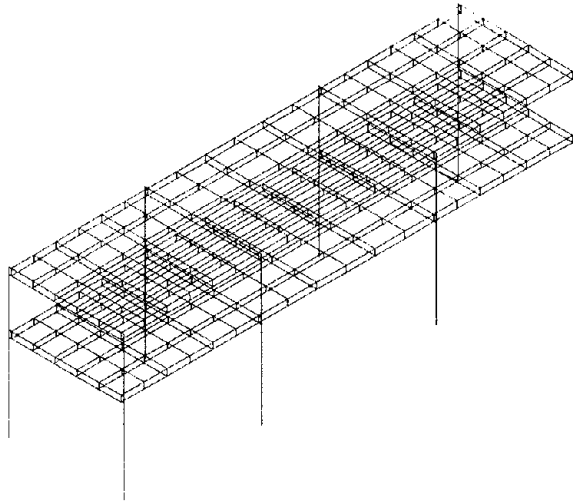

Figure 4. ANSYS Finite-Element Model
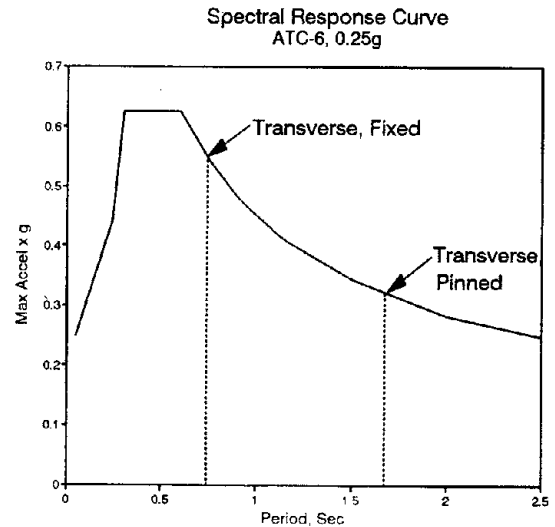
Figure 5. ATC-6 Response Spectrum

Results of the modal analyses are summarized in Table 1. The first-mode shape is dominated by translation in the longitudinal direction for both the fixed and pinned-base models. The second mode shape corresponds to translation in the transverse direction, and the third mode is primarily torsional response. The choice of foundation fixity has a large influence on the calculated periods of vibration. The periods of the first three modes for the model with a pinned base are approximately twice the corresponding periods of the fixed-base model.

Table 1. Computed Modal Properties

	Units	Mode 1	Mode 2	Mode 3	Mode 4
FIXED-BASE STRUCTURE					
Period	sec	0.91	0.76	0.66	0.19
Spectral Acceleration	g	0.46	0.54	0.59	0.39
Effective Mass (transverse)	% of weight	-	98.5	-	-
Effective Mass (longitudinal)	% of weight	99.1	-	0.7	-
PINNED-BASE STRUCTURE					
Period	sec	2.02	1.63	1.45	0.202
Spectral Acceleration	g	0.28	0.32	0.35	0.40
Effective Mass (transverse)	% of weight	-	99.0	0.1	-
Effective Mass (longitudinal)	% of weight	99.5	-	-	0.3

During the geotechnical phase of this investigation, site-specific response spectra will be developed. However, the initial analyses were conducted using the response spectrum specified in ATC-6 for soft soils (Soil Type III). Consistent with the seismicity in the Seattle region, a peak ground acceleration of 0.25g was adopted for the analyses. The response spectrum is shown in Fig. 5.

Capacity/Demand Ratios

The ATC-6-2 evaluation procedures quantify the seismic vulnerability of individual members with capacity/demand ratios. Figure 6 shows calculated flexural capacity/demand ratios for an interior transverse frame for both the fixed and pinned-base assumptions. For longitudinal response, only the fixed-base results are shown.

The capacity/demand ratios for flexural response (R_{ec}) were similar for the transverse and longitudinal directions. Flexural hinges are expected to develop at both ends of the lower columns when the base of the columns is fixed. If foundation rotation prevents yielding at the base of the columns, flexural hinges are expected to develop at the top of the lower columns. Calculated C/D ratios for flexure, R_{ec}, ranged from 0.3 to 0.7 in the lower columns. Flexural hinges could also occur at the ends of the first-level transverse beams and longitudinal girders. C/D ratios ranged from 0.4 to 0.8 at the ends of the lower-level beams and girders. Flexural yielding of the upper columns was not expected because, in the second story, the C/D ratios typically exceeded 1.2. The relatively low demands that were computed for the second-story are reasonable. Analysis of the structure under gravity loads revealed that the column moments are higher in the second story than in the first. (This explains why the longitudinal reinforcement ratio is higher for the second story.) In contrast, the seismic moments are larger in the first story.

Capacity/demand ratios were also used to evaluate the susceptibility of the structure to potentially brittle modes of failure. Figure 6 shows representative values for all of the ratios associated with the evaluation of the details. Anchorage failure at the base of the columns is reflected in R_{ca}. Anchorage failure of the beam reinforcement, a possibility not explicitly covered by ATC-6-2, is quantified by R_{an}. The failure of the splices is considered in computing R_{cs}, and shear failures are described by R_{cv}. Inadequate transverse confinement in the columns is quantified by R_{cc}; and failure of the footing is described by R_{fr}.

The anchorage length provided at the base of the columns is greater than the required length. Therefore, the computed C/D ratios for anchorage, R_{ca}, depended on the strength of the footing and the foundation conditions. Specifically, the value of R_{ca} was computed as 1.3 times the flexural capacity/demand ratio for the footing.. Consequently, R_{ca} was as low as 0.41 for the fixed case, but was much large for the pinned case (R_{ca} = 2.86 for transverse response). The limited development lengths for the beam reinforcement resulted in R_{an} being as low as 0.40.

On the basis of C/D ratios, catastrophic splice failure was predicted by ATC-6-2,. The splice length is too short, the amount of transverse confinement is insufficient, and the confinement reinforcement spacing is too large. These three factors combine to produce C/D ratios for the splices, R_{cs}, for the fixed case that are all less than 0.05 at the bottom column splice. In some cases, R_{cs} is as low as 0.02. The ratios are somewhat higher for the pinned conditions and for the top-story splice, but in general, R_{cs} is less than 0.15.

INTERIOR FRAME
FIXED BASE

INTERIOR FRAME
PINNED BASE

Rec=1.06 Rcc=2.74 Rcv=1.49	
Rec=2.06 Rcc=5.32	Rcs=0.03 Ran=0.48
Rec=0.48 Rcc=1.24 Rcv=1.33	
Rec=0.40 Rcc=1.03 Rcv=1.11	Rcs=0.02 Rca=0.41 Rfr=1.28

Rec=1.23 Rcc=3.18 Rcv=1.49	
Rec=3.87 Rcc=9.99	Rcs=0.19 Ran=0.40
Rec=0.30 Rcc=0.77 Rcv=1.18	
Rec=2.73 Rcc=7.05 Rcv=10.69	Rcs=0.15 Rca=2.86 Rfr=8.80

LONGITUDINAL FRAME
FIXED BASE

Rec=1.89 Rcc=4.73 Rcv=2.01	Rec=1.37 Rcc=3.55 Rcv=1.77		
Rec=1.88 Rcc=4.70	Rec=2.68 Rcc=6.95	Rcs=0.13	Rcs=0.11 Ran=0.74
Rec=0.54 Rcc=1.35 Rcv=2.08	Rec=0.47 Rcc=1.22 Rcv=1.27		
Rec=0.54 Rcc=1.35 Rcv=2.08	Rec=0.42 Rcc=1.09 Rcv=1.14	Rcs=0.03 Rca=0.59 Rfr=1.20	Rcs=0.02 Rca=0.74 Rfr=2.28

Figure 6. Capacity/Demand Ratios for Typical Unit

414

Brittle shear failure in the columns, another potential failure mechanism, was not found to be critical, based on the shear capacity/demand ratio, R_{cv}. The lowest value of R_{cv} was 1.14.

Failure precipitated by inadequate transverse confinement is not as much of a problem as one might suspect in a structure that has open ties fabricated from #3 bars, spaced at 12 in. The relatively high values of Rcc are a consequence of the structure's large strength and of the fact that ATC 6-2 permits the engineer to used a ductility factor of 2, even if ties are improperly anchored. The values for R_{cc} hover around 1.0 at the base in the fixed case but are well above 1.0 in all other locations.

On the basis of C/D ratios for shear and moment demands in the footing, the strength of the footing was found to be adequate. However, in this evaluation, joint shear failure was not considered at the base of the columns because ATC-6 does not include a check of joint shear. In addition, the evaluation did not consider failure of the piles.

NONLINEAR STATIC ANALYSIS

This section reports the results of a second evaluation of the WSDOT unit's vulnerability to earthquakes. Consistent with the recommendations of Priestley et al.[2] at the University of California at San Diego (UCSD), the researchers estimated the lateral force-displacement response of typical transverse and longitudinal frames. Although estimates of the actual foundation properties will be incorporated into the analyses in the future, the results presented here correspond to the fixed-base and pinned-base conditions only. In preliminary analyses, the influences of reinforcing splices, bar anchorage slip and joint failure were neglected. In subsequent analyses, the influence of splice deterioration was considered.

Structural Model and Analysis Procedure

The structure was idealized as a set of orthogonal planar frames whose columns and beams consisted of a series of prismatic segments. A typical transverse frame model is shown in Fig. 7. A similar model was constructed for the longitudinal direction. Within the joint regions, the linear segments were assumed to have a moment of inertia approximately 100 times larger than those of the rest of the elements. Outside the joints, the nonlinear moment-curvature (M-ϕ) relationships for the segments reflected the variation in longitudinal reinforcement along the length of the members. To obtain a good representation of the curvature distribution along frame members, short segments were used near member ends where large rotations were expected.

Moment-curvature relationships were computed for each beam and column segment on the basis of the reinforcement specified on the structural plans, a concrete compressive strength of 4500 psi and a steel yield stress of 44 ksi. The stress-strain relationship for concrete was based on the model suggested by Park et al. [3]. The stress-strain relationship for the reinforcing steel was modeled using three linear segments representing the initial stiffness, the yield plateau, and strain hardening. The capacity of each cross-section was defined by the point at which either the concrete reached a compressive strain of 0.005 or the longitudinal steel reached a tensile strain of 0.05.

The contribution of the slab reinforcement to the flexural capacity of the beams and girders was considered by assuming a portion of the slab to be effective in both tension and
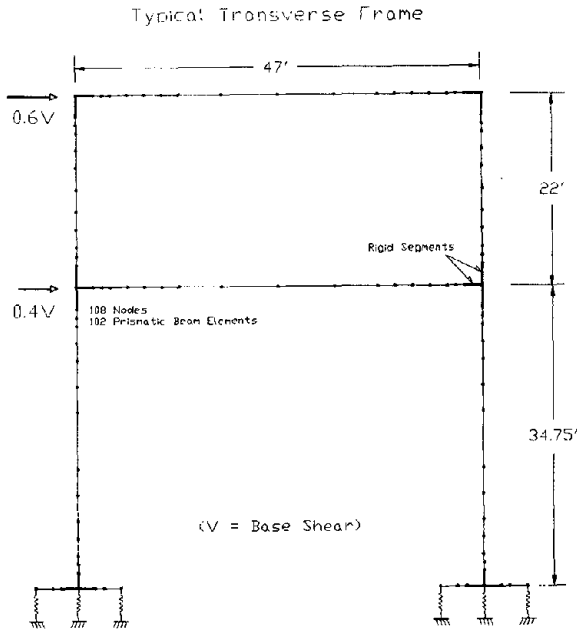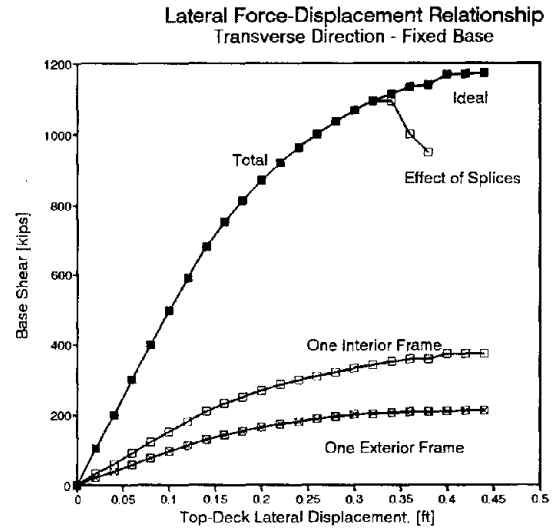
Figure 7. Model of Transverse Frame

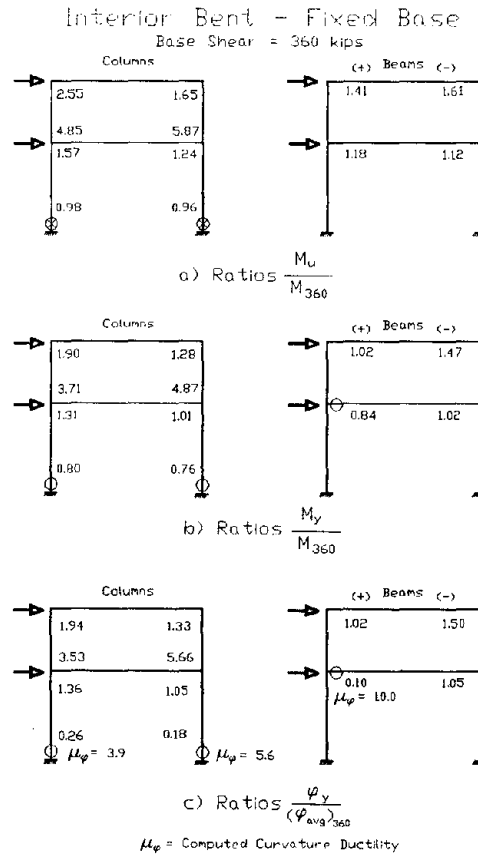Figure 8. Computed Force-Deflection Relationship

for Transverse Response

Figure 9. Extent of Yielding in Interior Bent, Fixed-Base Condition

416

compression. The width was selected according to the T-beam provisions of the ACI Building Code (ACI 318-89) [4].

The nonlinear force-displacement response of the frames was calculated using a secant-stiffness algorithm. The stiffness of each segment was updated during each force increment using the calculated moment-curvature relationship and the average curvature in the element. Flexural and axial deformations were considered, but shear deformations were neglected. Gravity loads were included in the calculations. The analysis stopped when a member reached its ultimate curvature or when the frame mobilized its maximum lateral-force resistance.

Computed Lateral-Force Response

Lateral force-displacement relationships for interior and exterior frames are shown in Fig. 8 for the fixed-base condition. The computed lateral-load capacity for the entire unit in the transverse direction, approximately 1200 kips, corresponds to 24% of the total weight. The displacement capacity of the top deck was computed to be approximately 0.4 feet, which corresponds to a drift ratio of 0.7 percent.

Figure 9 provides a summary of the calculated distribution of inelastic response in the interior transverse frame at the maximum computed base shear of 360 kips. For the columns and beams, Fig. 9(a) shows the ratios of the flexural strength to the moment demand at the maximum base shear (M_u/M_{360}). Figure 9(b) shows the ratio of the yield moment to the moment demand at the maximum base shear (M_y/M_{360}). Figure 9(c) shows the ratio of the yield curvature to the average curvature at the maximum base shear ($\phi_y/(\phi_{avg})_{360}$). These results correspond to ideal response, and therefore, they do not reflect the influence of anchorage slip, splice deterioration or joint failures. Yielding at the base of the first-story columns occurred first, and ductility demands were large at this location. Yielding in the beams was limited to one location, although yielding was imminent in two other locations. The analysis was stopped when the curvature demand at the column bases exceeded its capacity, precluding the formation of a mechanism for the entire structure.

Additional nonlinear analyses demonstrated that the strength and stiffness of the structure is approximately equal in the transverse and longitudinal for the fixed-base condition. For both directions, the lateral-load capacity of the typical unit in both is approximately 25% of the weight of the structure (Table 2). The corresponding displacement at the top deck is approximately 0.7% of the viaduct's height. The difference between the two directions is much larger for the pinned-base case; the lateral-load capacity is reduced to 14% for the transverse direction and 11% for the longitudinal direction. With the exception of the fixed-base, transverse frame discussed above, the frame analysis stopped when a story mechanism formed in the lower level.

To enable comparison of the linear-elastic demands with the computed capacities, the researchers computed an equivalent elastic base-shear strength for the structure. This strength was computed by multiplying the structure's stiffness by the maximum lateral displacement computed by nonlinear analysis. The spectral acceleration capacities, $S_a(c)$, correspond to the equivalent elastic base shears divided by the structure's weight. Finally, a measure of the structure's vulnerability is given by dividing $S_a(c)$ by the spectral acceleration demand, $S_a(d)$, determined from the ATC-6 spectrum. Note that this procedure is consistent with the concept of equal linear and nonlinear displacements proposed by Veletsos and Newmark[5] for long-period structures.

417

Table 2. Computed Lateral Capacities of the WSDOT Section

Support Condition	Direction	Maximum Base Shear		Max. Top-Deck Lateral Displacement	
		[kips]	[% of Weight]	[ft]	[% of Height]
Fixed	Transverse	1120	24	0.40	0.7
	Longitudinal	1080	23	0.33	0.6
Fixed (w/splices)	Transverse	1080	23	0.33	0.6
	Longitudinal	1030	22	0.23	0.4
Pinned	Transverse	676	14	0.70	1.2
	Longitudinal	520	11	0.50	0.9

Table 3. C/D Ratios for Equivalent Elastic Base Shear, Fixed-Base Case

Direction	Case	Displacement at Resultant of Seismic Forces	Equivalent Elastic Base Shear, V_e	$S_a(c) = V_e/Weight$	$S_a(c)/S_a(d)$
		[ft]	[kips]	[g]	[g]
Transverse $S_a(d)=0.45g$	No splices	0.38	2190	0.46	1.02
	w/splices	0.28	1630	0.35	0.78
Longitudinal $S_a(d)=0.46g$	No splices	0.31	1890	0.40	0.87
	w/splices	0.21	1280	0.27	0.59

The results shown in Table 3 indicate that, for the fixed-base case, the ratios of capacities to demands are 1.02 for the transverse direction and 0.87 for the longitudinal direction. The difference between the two results is almost entirely attributable to the difference in displacement capacities, rather than to differences in strengths. Even without considering the structural details, it appears that the adequacy of the structure's seismic resistance is questionable.

Evaluation of Details

As noted earlier, the results discussed in the previous sections did not consider the influence of anchorage pullout, splice deterioration, member shear failure and joint shear failure. These failure modes are considered in the following discussion.

To consider the influence of limited development lengths, the investigators compared the computed demands and capacities along the length of the structural members. Figure 10, for example, shows the bending moment demands and capacities for the bottom-deck, end beam of an interior bent. The demands are shown for dead load (DL) and for several combinations of dead load plus lateral load near the capacity of the frame. In these figures, the numbers that accompany the letters DL represent the base shear in the frame (in kips). The capacities, denoted by dotted lines, were computed assuming a development length of 30 bar diameters. For the beam that is shown, it appears that the critical region is the positive-moment zone near the member end, where the capacity is limited by the short anchorage length of the bottom layer of longitudinal bars into the columns.

Bending Moment Diagrams
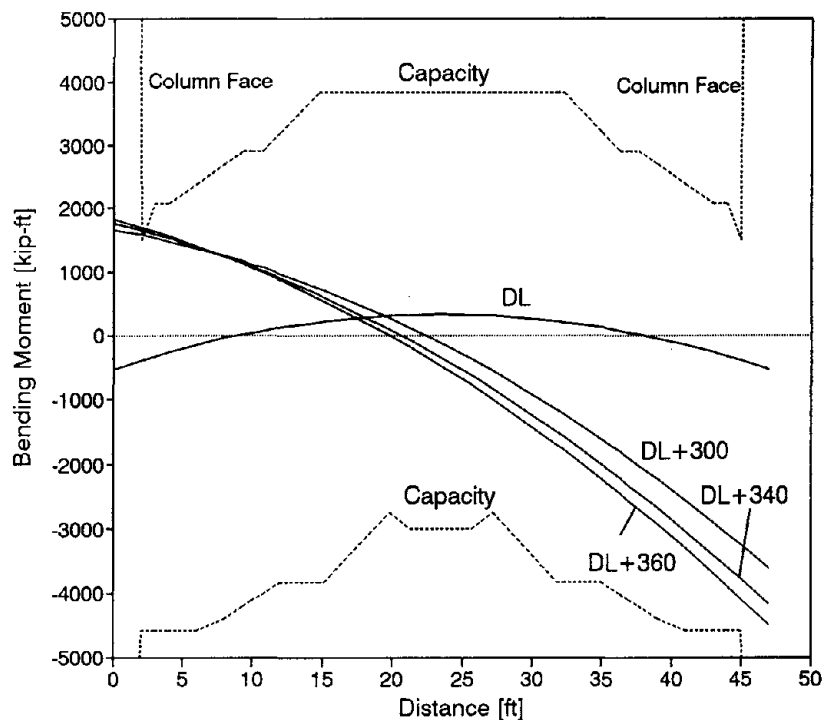### Interior Bent - Bottom End Beam

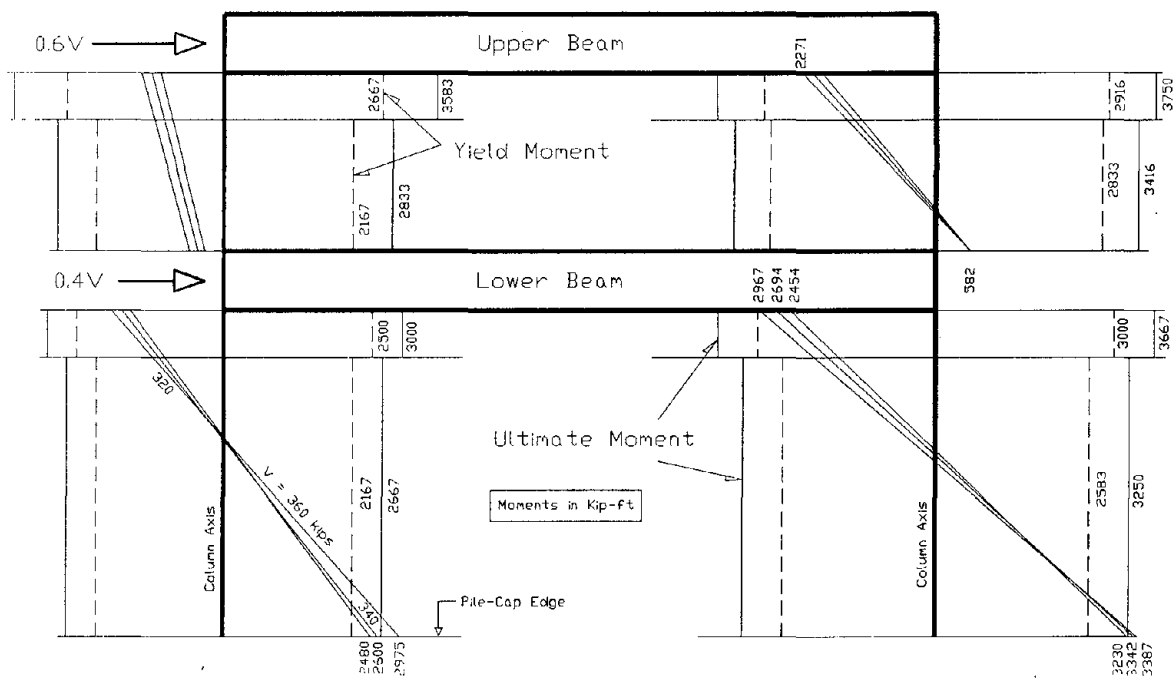Figure 10. Representative Bending Moment Diagrams For Transverse Beams

Figure 11. Representative Moment Diagrams for Columns

Figure 11 shows the moment demands and capacities for the columns of the interior transverse frame. Flexural capacities in columns were computed with the axial loads resulting from the combined action of gravity and seismic lateral forces. The critical sections are located at the base of the lower-level columns. Anchorage lengths are not critical for the columns because the anchorage at the base is adequate and because the demands are small for the top story.

Splices had been identified to be inadequate by the ATC-6 procedure. The splices were evaluated again following recommendations proposed in Priestley et al. [2]. On the basis of the specified splice detail, a modified moment-curvature relationship was computed for the splice region and the nonlinear analyses were repeated. The moment capacity of the splice region did not change, but the splice resistance decreased rapidly after the concrete compressive strain reached a value of 0.002. As shown in Table 3, the computed lateral-force capacity of the frames remained about the same, but the displacement capacity decreased by up to 30%. The computed C/D ratio of 0.59 is unacceptable.

Shear-force capacities, V_n, were computed using the following equation, which takes into account the contribution of concrete, transverse steel and axial load:

$$Vn = 2\sqrt{f'c} \cdot bw \cdot d + \frac{Av \cdot fyt \cdot d}{s} + 0.2P$$

where, f 'c = assumed strength of the concrete, b_w = width of beam or column, d = effective depth of beam or column, A_v = transverse area of stirrups, f_{yt} = yield stress of stirrups, s = stirrups spacing, and P = axial load. An analysis of the results indicates that shear failure in beams is unlikely.

Two procedures were followed to evaluate the joints, one based on the maximum tensile stress, f_{tmax}, and one based on the maximum shear stress, v_{max}. To compute the maximum tensile stress, bending moments and shear forces induced by gravity and seismic loads were considered. The axial load in the columns were considered but axial load in the beams caused by inertial forces were neglected. The value of f_{tmax} was computed for the extreme condition corresponding to 1.3 times the beam yield moment. To compute v_{max}, only the moment from the beams was considered. The computation of v_{max} was performed for two conditions. The first corresponds to 1.3 times the beam yield moment; and the second corresponds to the maximum beam moment resulting from the nonlinear analysis. These stresses are denoted as f_{tmax}, v_{max-1}, and v_{max-2}, respectively; and they are listed in Table 4 in terms of $\sqrt{f'c}$.

Table 4. Stresses in Joints of Interior Transverse Frames

Joint	$(f_t)_{max}/\sqrt{f'c}$	$(v)_{max-1}/\sqrt{f'c}$	$(v)_{max-2}/\sqrt{f'c}$
Top Opening (Left)	2.9	2.7	2.5
Top Closing (Right)	6.5	6.5	4.1
Bottom (Left)	1.8	2.7	2.9
Bottom (Right)	7.0	8.3	7.1

If the values of Table 4 are compared with the value of $3.5\sqrt{f'c}$ suggested by Priestley et al. [2] and by Moehle et al. [6] to predict the failure of unreinforced joints, it appears that the joints are vulnerable when the slab reinforcement is placed in tension.

SUMMARY

Constructed in the 1950's, the Alaskan Way Viaduct is critical to the transportation network for the City of Seattle. The structural details are inadequate in comparison with current requirements. Geotechnical considerations are dominated by the presence of loose, saturated fill and tideland soils. These soils will strongly influence the ground motion characteristics at the site. Liquefaction of these soils is likely, and the effects of liquefaction may overshadow the effects associated with ground shaking.

Both the ATC-6 evaluation and the nonlinear analyses found that, in most cases, the base-shear strength is limited by formation of a first-story, flexural mechanism. The splices were identified as vulnerable because they are too short and insufficiently confined. The response of the structure is strongly affected by its ability to develop flexural moments at the base of the columns, and consequently, splice or foundation failure would greatly increase the Alaskan Way Viaduct's vulnerability to earthquakes. The joints where also found to be vulnerable, but this finding depends on the amount of slab reinforcement that is assumed to contribute to joint shear.

Shear failure is unlikely. Reinforcement anchorage is inadequate in some cases, but this problem is unlikely to greatly reduce the structure's lateral-force resistance. Because the structure is strong, ductility demands are small and the poor confinement for the columns is not critical for locations where the reinforcement is continuous.

REFERENCES

1. "Seismic Retrofitting Guidelines for Highway Bridges (ATC-6-2)", Applied Technology Council, Redwood City, California, August, 1983.

2. Priestley, M.J.N., Seible, F., and Chai, Y.H., "Design Guidelines for Assessment Retrofit and Repair of Bridges for Seismic Performance." Report No. SSRP-92/01. Department of Applied Mechanics and Engineering Sciences. University of California, San Diego. August, 1992.

3. Park, R., Priestley, M.J.N., and Wayne, D.G., "Ductility of Square-Confined Concrete Columns," *Journal of the Structural Division*. ASCE. Vol. 108. No. ST4. April, 1982. pp. 929-950.

4. American Concrete Institute. "Building Code Requirements for Reinforced Concrete (ACI-319-89)". American Concrete Institute. Detroit. 1989.

5. Veletsos, A.S. and Newmark, N.M., "Effect of Inelastic Behavior on the Response of Simple Systems to Earthquake Motions," *Proceedings*, 2nd World Conference on Earthquake Engineering, Vol. 2, Japan, 1960, pp. 895-912.

6. Moehle J.P., Thewalt, C.R., and Mahin, S.A., "Evaluation and Upgrading of Multi-Column Bridges". Personal Communication.

SECOND U.S.-JAPAN WORKSHOP ON SEISMIC RETROFIT OF BRIDGES

Evaluation and Upgrading of Multi-Column Bridges

J.P. Moehle, C.R. Thewalt, S.A. Mahin and L.N. Lowes
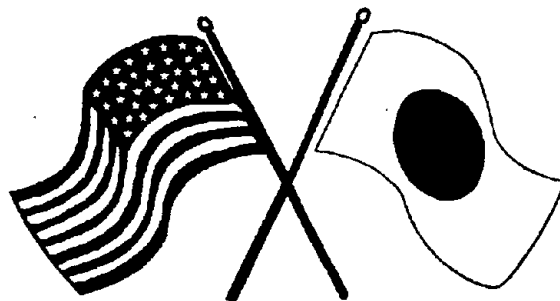
EVALUATION AND UPGRADING OF
MULTI-COLUMN BRIDGES

Jack P. Moehle[1], Chris R. Thewalt[2], Stephen A. Mahin[3], and Laura N. Lowes[4]
University of California at Berkeley

ABSTRACT: Recent research is examining the seismic behavior of reinforced concrete bridge structures constructed in California before the implementation of special requirements for ductility in the 1970s. Whereas earlier work focused on behavior of hinge restrainers and single-column structures, recent experience indicates existence of critical vulnerabilities in multi-column structures as well. We here describe the generic characteristics of multi-column bridges including columns, bent caps, outriggers and joints, and the methods for seismic upgrading of these elements. We include results of experimental and analytical research where available.

INTRODUCTION

The 1989 Loma Prieta earthquake exposed the vulnerability of many multi-column, multi-level reinforced concrete bridge structures, in particular, those constructed in the 1970s and earlier. These structures are prevalent in urban environments where scarcity of land requires the stacking of roadways; they become increasingly complex where multiple elevated roadways intersect. Deficiencies include inadequate three-dimensional frames and a variety of structural inadequacies in footings, columns, beam-column joints, bent caps, and outriggers. Many of these inadequacies were apparent in bridge damage and collapse observed following the Loma Prieta earthquake. Others have been identified through study of structural drawings of undamaged bridges.

Immediately following the 1989 earthquake, Caltrans initiated redesign efforts on several multi-column, multi-level concrete bridge structures in the San Francisco Bay Area. The effort assembled a team of design consultants and peer reviewers from California, technical advisors from the University of California, and Caltrans bridge designers. The effort created a unique opportunity for an in-depth, practical focus on the main issues involved in evaluation and redesign of these structures.

Also immediately following the 1989 earthquake, Caltrans redoubled its ongoing seismic research effort. Research before the Loma Prieta earthquake focused on evaluation and rehabilitation of restrainers and single-column reinforced concrete bridge structures. The current research effort continues studies on restrainers and single-column structures, and adds a major emphasis on elements and systems of multi-column, multi-level reinforced concrete bridges.

These efforts have provided insights into evaluation and rehabilitation needs for existing reinforced concrete multi-level and multi-column bridge structures. This manuscript summarizes some of the ideas and data resulting from the work.

---

[1]Professor of Civil Engineering, Director of Earthquake Engineering Research Center
[2]Assistant Professor of Civil Engineering
[3]Nishkian Professor of Structural Engineering
[4]Graduate Student of Structural Engineering

MULTI-COLUMN ELEVATED ROADWAYS

Elevated roadways typically contain a relatively sparse framing system in comparison with typical buildings. Thus, whereas in buildings an evaluation may take advantage of redundancy, in bridges the evaluation must be sensitive to the relatively low redundancy. The evaluation and redesign must establish the existence of a complete three-dimensional frame and the adequacy of its elements.

Typical Framing Systems

Figure 1 depicts a typical pattern of framing for a San Francisco double-deck viaduct. As is common in multi-column bridges, columns are pin-connected to pile-supported footings. Given the pinned connection, resistance to lateral loads must be provided by a three-dimensional frame above ground.
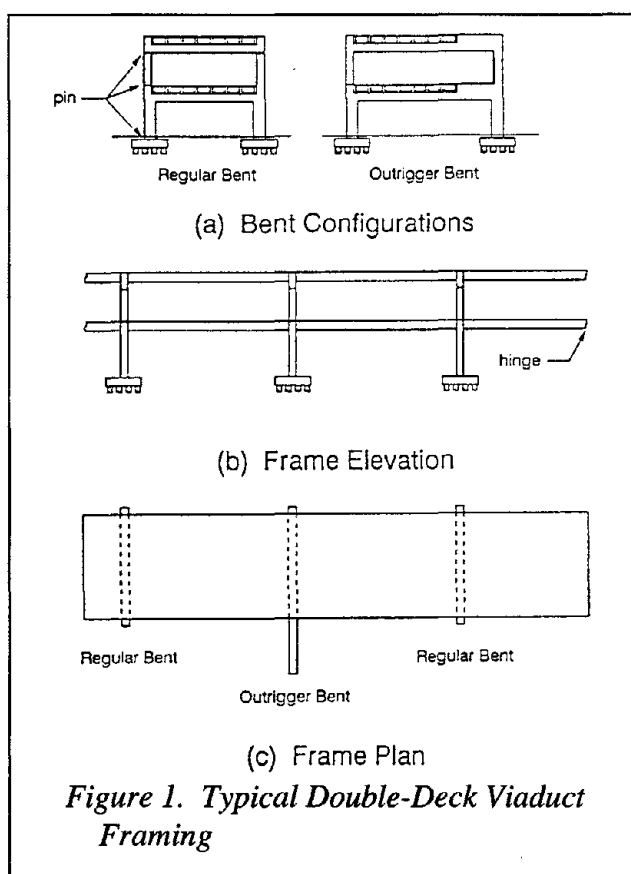

(a) Bent Configurations

(b) Frame Elevation

(c) Frame Plan

Figure 1. Typical Double-Deck Viaduct Framing

Resistance to lateral loads transverse to the roadway commonly occurs by framing among columns, bent caps, and cap-column joints. Resistance to longitudinal loads appears not to have been contemplated in the original design of many freeways, but usually occurs through rigid framing among the columns, bent caps, and longitudinal box girders (the roadway itself). Longitudinal action thus results in box girder flexure and bent cap torsion (and weak axis bending and shear in the case of outriggers), neither of which is likely to have been considered in proportioning or detailing of these members in the original design.

Locating Inelastic Action

For several reasons, it is generally preferred that all inelastic action in the frame be confined to the columns rather than the beams or the connections. The column has a simple, well-defined cross section, usually with low axial load stresses, so design for expected 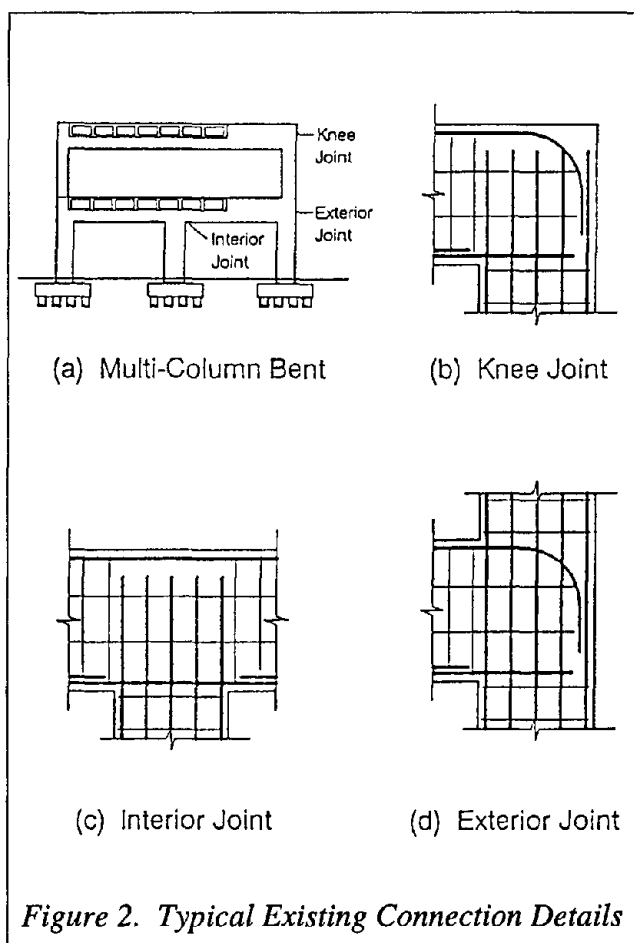inelastic actions is relatively straightforward. Furthermore, any column damage that occurs during an earthquake can be readily observed and repaired. Arguments against formation of soft stories in bridge structures are not compelling because axial load stresses are low, and the number of "story" levels is seldom greater than two.

Inelastic flexural action of cap beams may be acceptable where the superstructure is bearing-supported, because in this case the beam cross section is clearly defined and its behavior can be evaluated with some confidence. Where beams are monolithic with the superstructure, beam

426

plastic hinging should be avoided because (a) the cross section of the beam cannot be uniquely defined and (b) hinging may result in undesirable superstructure damage. Inelastic response of outriggers and of cap-column connections is best avoided because techniques for producing stable response have not been advanced.

Beam-Column Connections

The 1989 Loma Prieta earthquake exposed the vulnerability of concrete bridge structures to failures of inadequately reinforced beam-column connections. Research at UC Berkeley is particularly attentive to the design and redesign requirements for typical beam-column connections in bridge framing systems.

Figure 2. Typical Existing Connection Details

(a) Multi-Column Bent   (b) Knee Joint

(c) Interior Joint   (d) Exterior Joint

Connection geometries and details of primary interest include those depicted in Figure 2. Connections in typical pre-1970s bridge construction in California do not have joint transverse reinforcement, with the exception of nominal cap beam skin reinforcement that extends into or through the joint. Where column reinforcement terminates in the joint, hooks are usually not present. Bent cap bottom bars are likely to terminate within the joint without a hook.

EXPERIMENTAL RESEARCH

At UC Berkeley experimental research of concrete bridge structures has focused on several important elements of the typical multi-column, multi-level framing system: exterior beam-column connections, interior beam-column connections and outriggers. Research projects have investigated the behavior of existing typical designs as well as the behavior of upgraded elements.

Exterior Beam-Column Joints

Figures 2(a) and 2(d) show the configuration and reinforcing detail for a typical exterior beam-column joint. Contemplation of this joint provides several issues for investigation: response of cap-beam to cyclic shear stress, adequacy of beam reinforcement anchorage, and joint shear capacity.

427

Relatively little is known about the cyclic shear behavior of large cross sections with light reinforcement as is common in bent caps. Not having definitive laboratory data, we recommend Equation 1 for cap beam shear strength.
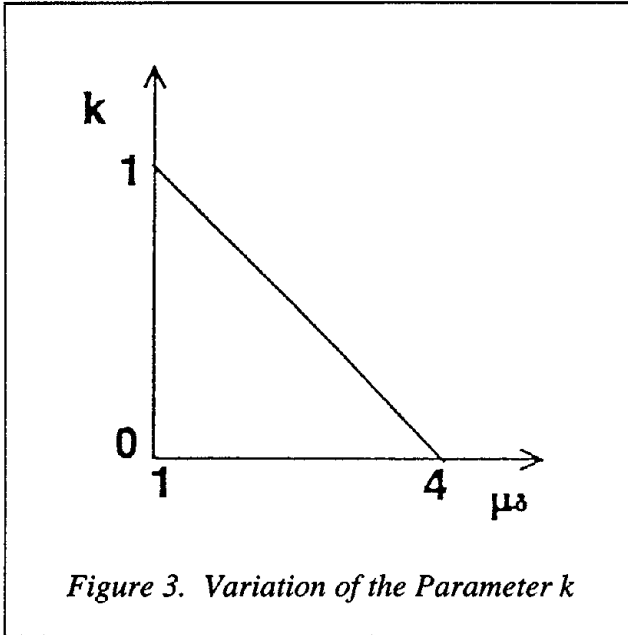

Figure 3. Variation of the Parameter k

$$V_n = V_c + V_s \quad\text{........................ (1a)}$$

$$V_c = k(0.85 + 120\rho_w)\sqrt{f'_c}b_w d$$
$$\leq 2.4k\sqrt{f'_c}b_w d \quad\text{..... (1b)}$$

$$V_s = \frac{A_v f_{yt} d}{s} \quad\text{................... (1c)}$$

Where V_c = nominal concrete strength in pounds, k varies with ductility demand according to Figure 3 [Moehle and Aschheim; 1993], ρ_w = ratio of longitudinal tension reinforcement, f'_c = concrete compressive strength in psi, b_w = web width in inches, and d = effective depth in inches. Where shear strength of the beam is not adequate, bolsters can be added to provide additional shear strength.
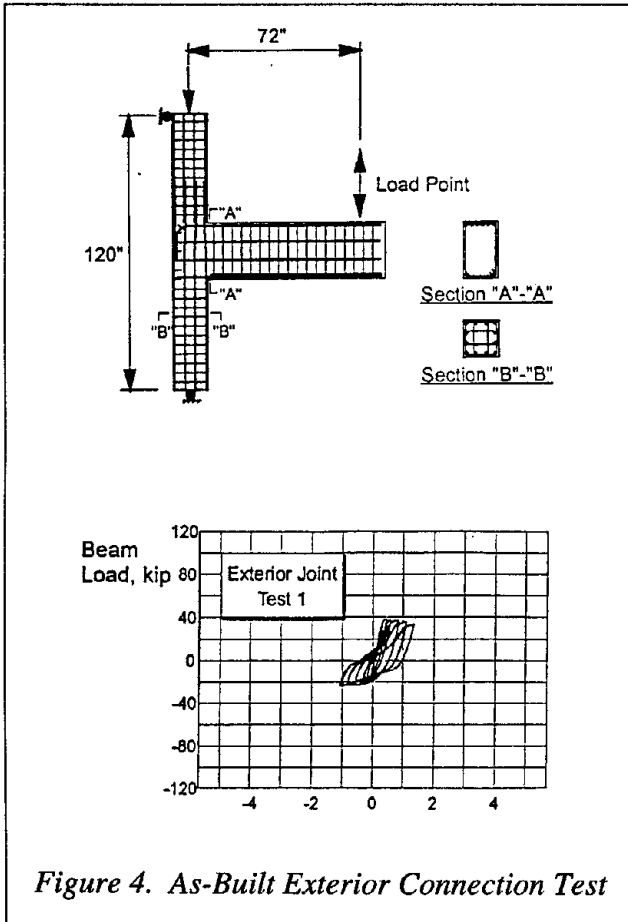
Figure 4 illustrates the measured beam load-displacement relation for a model of a typical exterior beam column connection [Moehle and Soyer; 1993]. For this model, the beam moment strength was less than the sum of the column moment strengths and the beam shear capacity was adequate. Failure of the beam was due to sliding along a single, wide crack in the beam adjacent to the joint face. Growth of the crack width is attributed to two phenomena: (1) Under upward beam load, the plastic hinge was restricted to a short length of beam adjacent to the joint because of the termination of the majority of beam bottom bars near the joint, and (2) Because top reinforcement area significantly exceeded bottom reinforcement area, the top reinforcement never yielded in compression, so yield strains in top steel grew progressively. As testing progressed, sliding along the interface ensued.

Figure 4. As-Built Exterior Connection Test

428

Strengths correspond to yield of top beam longitudinal reinforcement for downward beam load and yield of bottom beam longitudinal reinforcement for upward beam load. As is typical in existing construction (Figure 2(d)), most of the beam bottom bars terminate near the connection, with the remaining bars extending into the joint a distance of approximately 20 bar diameters without a hook.

In this test, as well as in field tests on the Cypress Street Viaduct [Bollo; 1990], the bottom bar embedment was adequate for development of the Grade 40 bars (specified $f_y = 275$ MPa) for numerous inelastic loading cycles. (Adequacy of the bottom bar anchorage is less certain for bents where the column undergoes inelastic rotations adjacent to the anchored beam bar.)

With the minimal joint reinforcing typical to pre-1970 construction, the joint had sufficient capacity to develop the yield strength of the beam. Moehle and Soyer [1993] report that under simulated gravity and seismic loading, nominal joint shear stress of $5.5\sqrt{f'_c}$ psi was sustained without appreciable joint cracking.

Strengthening techniques for bent caps loaded in flexure and shear include addition of bolsters and/or external prestressing (Figure 5). Prestressing may suffice in cases where shear strength of
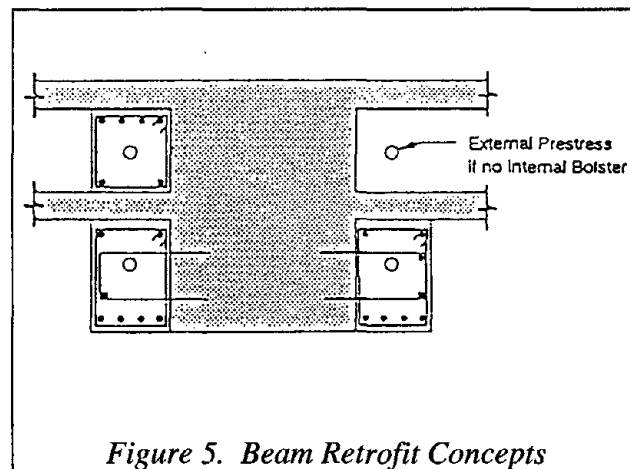

External Prestress
if no Internal Bolster

Figure 5. Beam Retrofit Concepts

the cap beam is adequate. (Note that prestressing is likely to enhance the shear strength of the cap beam [Collins and Mitchell; 1987].) As discussed previously, where shear strength of the beam is not adequate, bolsters provide additional shear strength. Mahin [1992] presents details of a bolster design for one of the San Francisco double-deck viaducts.

A second exterior connection test involved upgrading the connection shown in Figure 4. The beam was strengthened by addition of external post-tensioning. Figure 6 shows details and results of the test. Failure of the strengthened connection was by development of diagonal cracks and
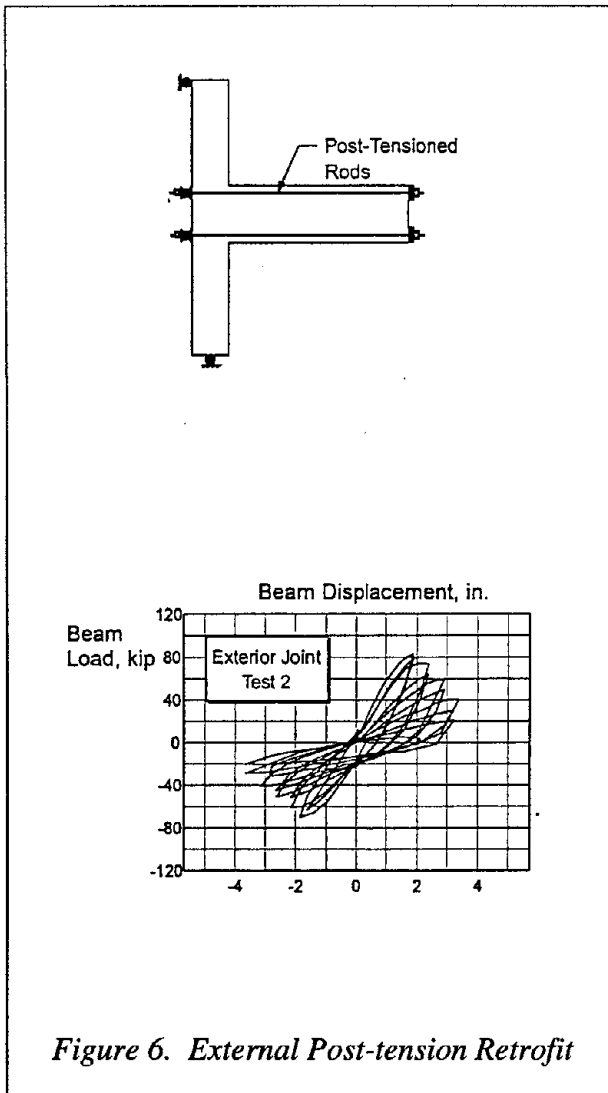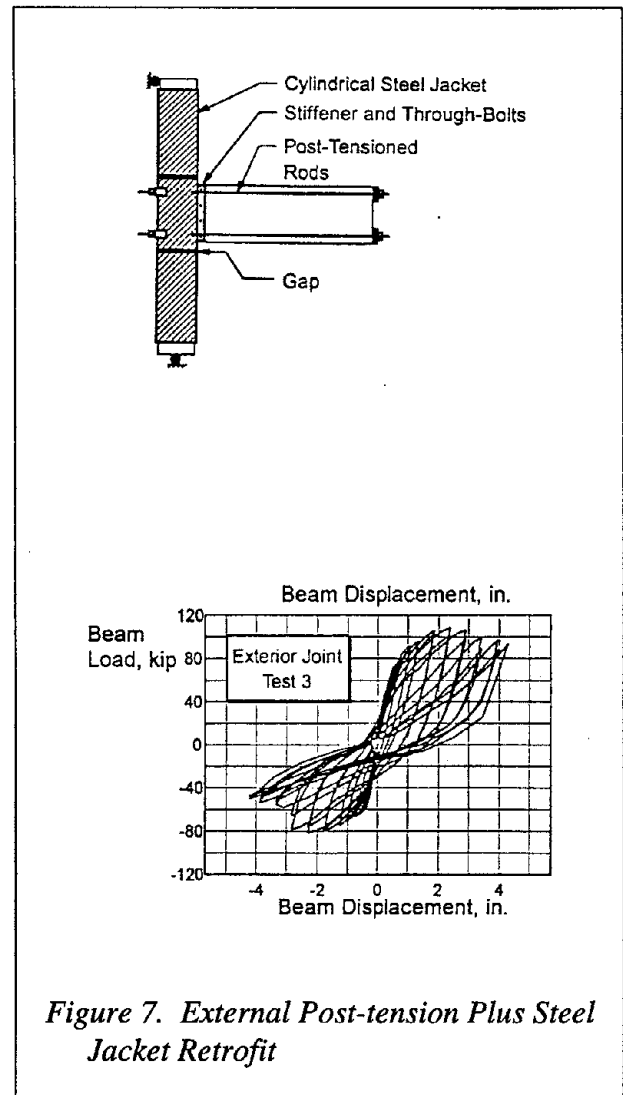
Figure 6. *External Post-tension Retrofit*

Figure 7. External Post-tension Plus Steel Jacket Retrofit

eventual disintegration of the concrete in the joint. By the end of the test, the stress in the post-tensioning rods had increased significantly, resulting in a total joint shear stress at failure equal to approximately $12\sqrt{f'_c}$ *psi*.

A final retrofit on an exterior connection involved post-tensioning, identical to that used in the preceding test, plus jacketing of the column and joint with a cylindrical steel jacket (Figure 7). The jacket was discontinuous just below and just above the joint, so that flexural strength of the column would not be increased excessively and so that deformations of the column would not be imposed on the jacket surrounding the joint. Also, the jacket around the joint had to be discontinued where it met the beam; at this location the jacket edge was stiffened and bars were passed through the beam to improve continuity. Under simulated gravity and seismic loading this specimen performed quite well. Final failure was due to exhaustion of beam rotation capacity.

430

Interior Beam-Column Connections

Interior beam-column connections provide a very similar joint configuration to that of the exterior beam-column connection. Figure 8 shows the reinforcing details for a model of a typical interior connection used in experimental testing conducted at UC Berkeley. As with the exterior connection, reinforcing details that could be expected to result in poor seismic performance include: column bars with straight development length into the joint of 20 bar diameters, minimal beam bottom steel continuous through the joint region, and minimal shear reinforcing in the joint region. Figure 8 shows the measured column load-displacement relation for the model [Moehle and Lowes; 1993]. A gravity load of $0.03Agf'c$ was maintained in the column during the entire test. Strengths correspond to approximately 60 percent of the flexural yield strength of the column section at the face of the joint. Failure of the as-built model was through slip of the column bars within the joint region. The nominal joint shear stress at the initiation of column bar slip was equal to approximately $4.5\sqrt{f'_c}\, psi$, a sufficiently small value for a T-joint to indicate that failure of joint concrete in shear did not contribute to the connection failure.

A concrete bolster for the cap-beam was investigate as a seismic upgrade for the connection . Figure 9 shows the reinforcing details and behavior of a strengthened connection. The bolster provided additional flexural strength for the cap beam, ensuring that inelastic flexural action of the
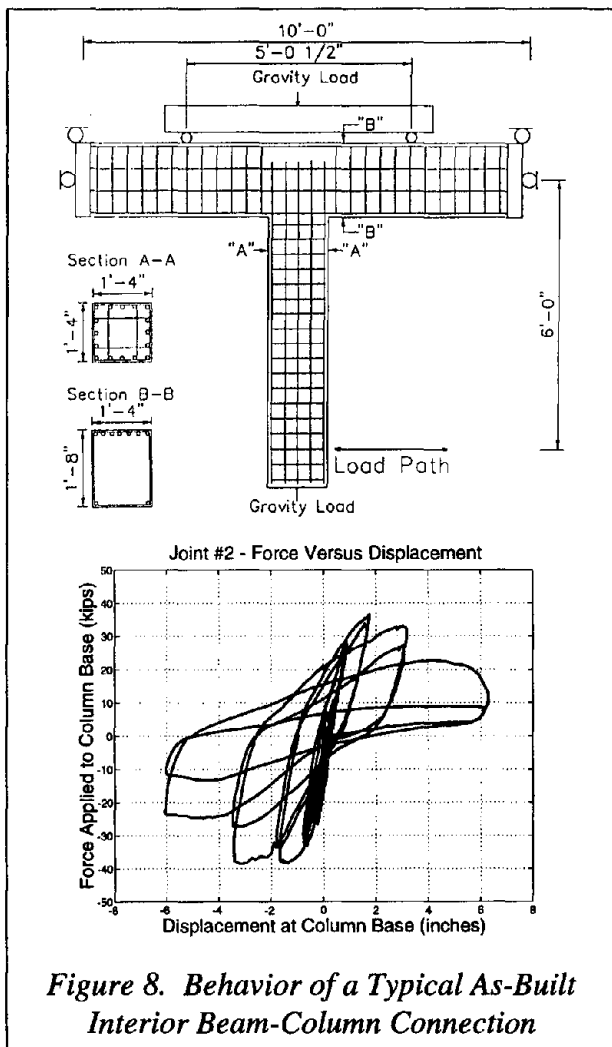

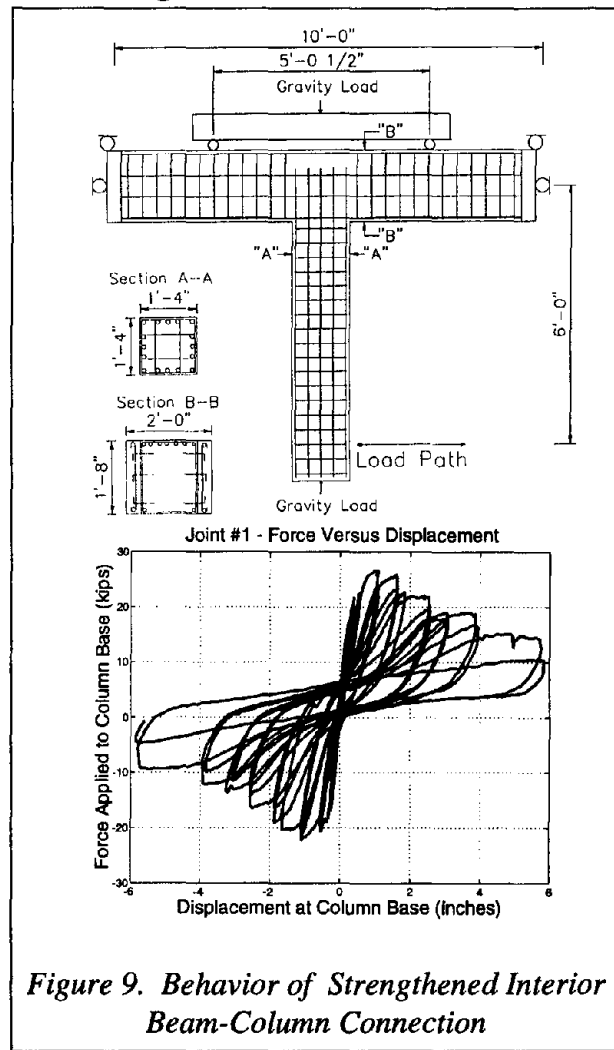Figure 8. Behavior of a Typical As-Built Interior Beam-Column Connection

Figure 9. Behavior of Strengthened Interior Beam-Column Connection

431

beam would not degrade anchorage of the column reinforcing steel. Additionally, bolster concrete in the joint region increased cover to the anchored column reinforcing steel and reduced joint concrete shear stress. As with the as-built connection, a gravity load of 0.03Agf'c was maintained in the column during the entire test. Strengths correspond approximately to the flexural yield strength of the column section at the face of the joint. Failure of the strengthened connection was again through slip of the column bars within the joint region. The joint shear at the initiation of column bar slip was approximately $4.0\sqrt{f'_c}$ psi.

Outriggers

Outriggers (Figure 1) are common in locations where obstructions do not permit the supporting columns to be located beneath the superstructure. Transverse and longitudinal bridge response results in combined biaxial flexure, biaxial shear, and torsion in the outrigger beam. Transverse reinforcement of existing outriggers commonly comprises U-shaped stirrups that do not provide adequate shear/torsion capacity.

Thewalt and Stojadinovic [1992] report tests on as-built and retrofitted outriggers (Figure 10). They identify a number of failure modes; however, two main failure modes predominated for the as-built they have considered. First, the essentially unreinforced joint was incapable of developing the strengths of the adjacent column and beam for in-plane loading. Second, when the joint was strengthened, the outrigger beam was incapable of ductile response to the resulting combined bending, shear, and torsion actions. Figure 10 plots transverse and longitudinal responses of the as-built outrigger and of the as-built outrigger with a strengthened joint. Standard procedures were capable of estimating as-built strengths for the outrigger beam and column segments. Deformation capacities of the as-built system were considered unacceptable for most applications.

Thewalt and Stojadinovic [1992] investigated two outrigger retrofits. A concrete retrofit added bolsters to the outrigger, providing closed hoops so that the torsional strength was approximately double the cracking capacity. The bolsters extended around the joint, strengthening it so that effectively elastic joint behavior resulted. Figure 11 shows the retrofit and its performance. At large deformations, the outrigger beam failed in torsion, with distributed but widening cracks, and extensive spalling of cover concrete. Although this retrofit maintained strength through large deformations, the extensive diagonal cracking to the outrigger may be considered acceptable.
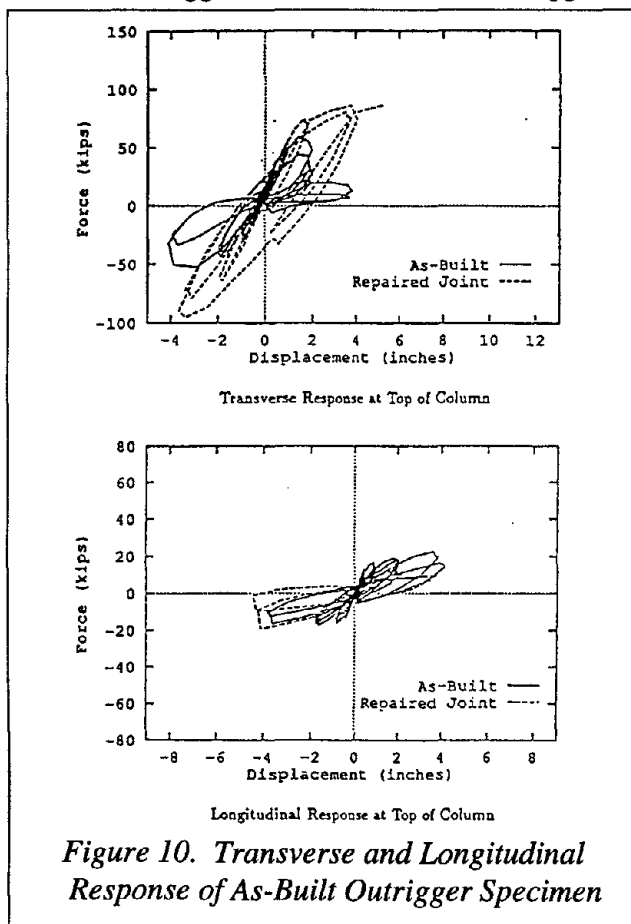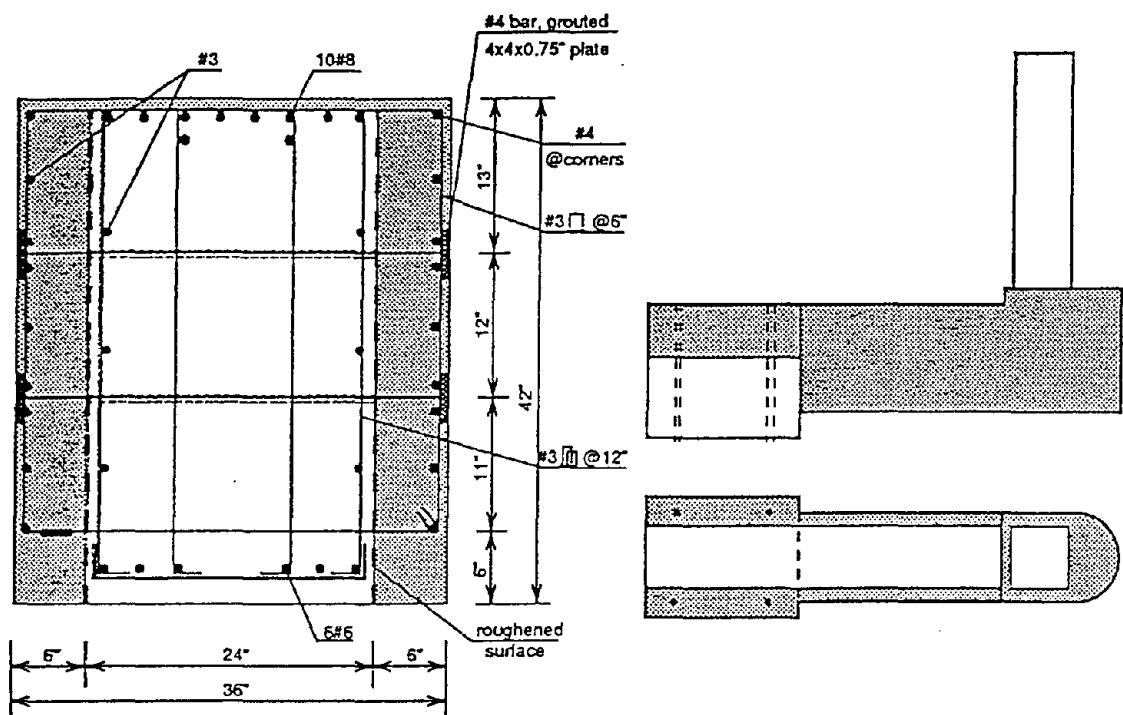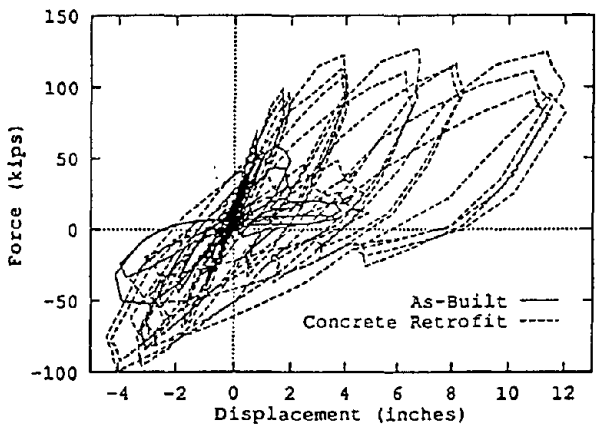

Figure 10. Transverse and Longitudinal Response of As-Built Outrigger Specimen

432

Figure 11. *Configuration and Behavior of Outrigger Concrete Retrofit*

A second retrofit strategy investigated by Thewalt and Stojadinovic [1992] involves strengthening the outrigger beam to avoid inelastic behavior in the outrigger beam. The engineer can select either steel or concrete jackets for this purpose. Key considerations for the retrofit design include (a) post-tensioning into the box girder to provide required weak-axis bending strength, (b) dowels between new and existing concrete to transfer interface shear primarily due to weak-axis bending, (c) closed perimeter ties in a concrete jacket, or sufficient steel thickness in

a steel jacket, to provide required torsion strength. Retrofit of the joint and column may also be required.

Figure 12 depicts details and behavior of an outrigger with a steel jacket designed so the outrigger would remain elastic. Stiffeners in the joint area were provided to resist expected compression struts. At large deformations, the column failed; the outrigger was nearly elastic.

Behavior of the knee joint segment of outriggers has been the subject of research efforts at both UC Berkeley and UC San Diego. Tests on the Cypress Street Viaduct [Bollo, et al.; 1990] and laboratory outrigger bents [Thewalt and Stojadinovic; 1992] indicate that joint failure of unreinforced joints can occur at nominal joint shear stresses as low as 3.5 $\sqrt{f'_c}$ psi. Joint shear
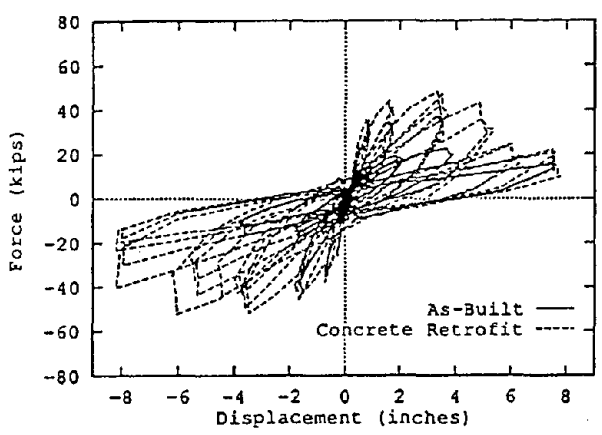

(a) Section   (b) Layout

Transverse Response at Top of Column   Longitudinal Response at Top of Column

Figure 12. Details and Behavior of Outrigger Steel Retrofit

434
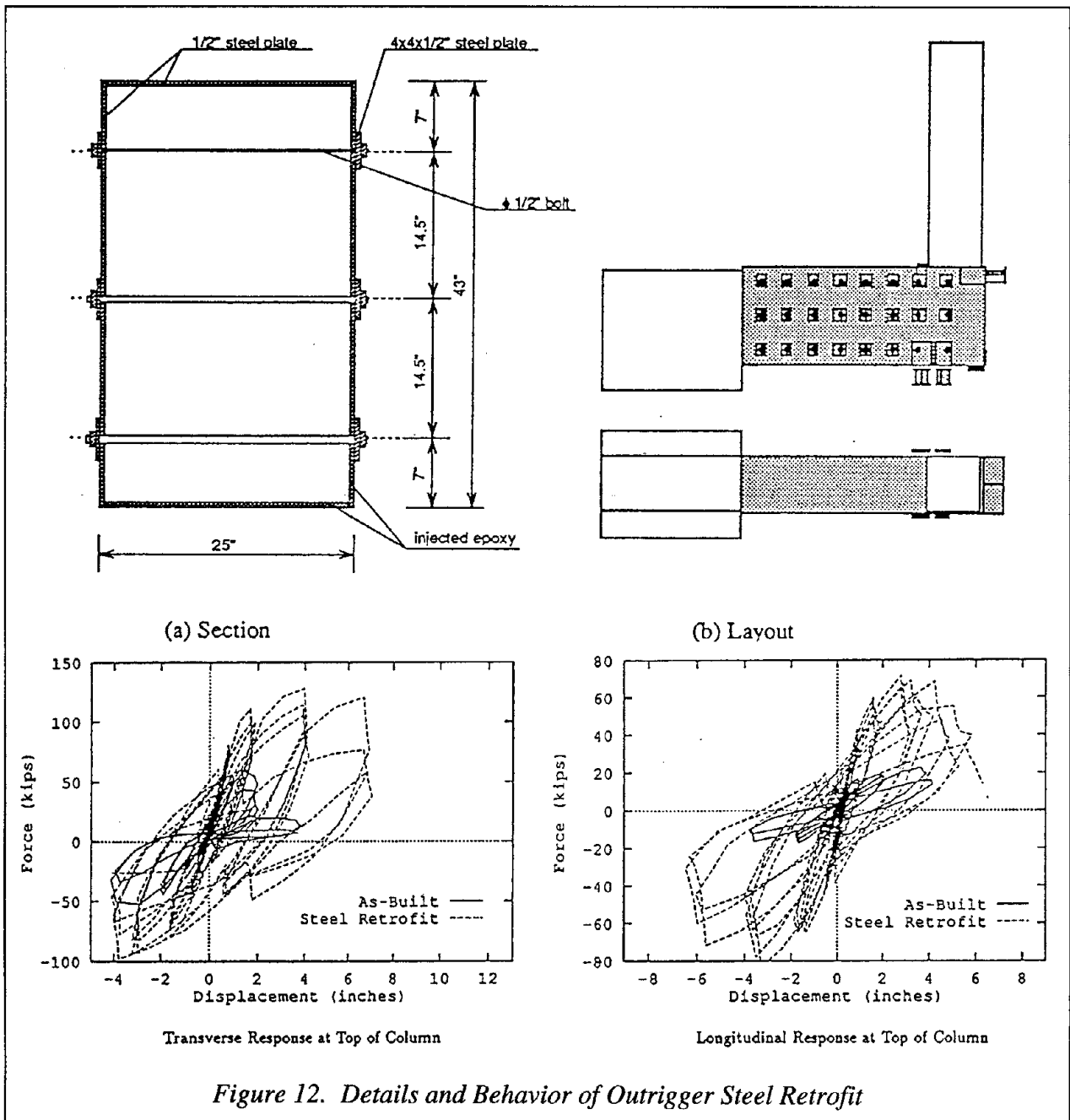
failure results in rapid degradation of load resisting properties (see Figure 11). The concrete bolster retrofit investigated by Thewalt and Stojadinovic [1992] resulted in a knee joint capable of remaining essentially elastic at an average nominal shear stress of 5.4 $\sqrt{f'_c}$ psi. The steel jacket outrigger retrofit investigated by the same provided a knee joint capable of maintaining an average nominal shear stress of 5.4 $\sqrt{f'_c}$ psi without damage.

Studies of outrigger retrofit are ongoing at UC Berkeley [Thewalt and Stojadinovic; 1992]. Goals for a second phase of study include: maintaining ductility and drift capacity of the outrigger while forcing failure into the column and simplifying construction of the retrofits.

CONCLUSIONS

Investigation of the seismic behavior of multi-column concrete bridges has identified frame elements and connections that are typically inadequate in pre-1970 systems. Experience and research have provided techniques for evaluating expected response and possible upgrading strategies. The methods described in this paper are under continuing development.

ACKNOWLEDGMENT

REFERENCES

[Bollo; 1990] - M. Bollo, S. A. Mahin, J. P. Moehle, R. M. Stephen, and X. Qi, "Observations and Implications of Tests on the Cypress Street Viaduct Test Structure," *Report No. UCB/EERC-90/21*, Earthquake Engineering Research Center, University of California at Berkeley, December 1990, 274 pp.

[Collins and Mitchell; 1987] - M. Collins and D. Mitchell, *Prestressed Concrete Basics*, Canadian Prestressed Concrete Institute, Ottawa, Ontario, Canada, 1987, 614 pp.

[Mahin; 1992] S. A. Mahin, F. Zayati, S. Mazzoni, and R. Boroschek, "Evaluation of the Seismic Performance of Retrofit Concepts for Double Deck Reinforced Concrete Viaducts," *Proceedings*, Seminar on Seismic Design and Retrofit of Bridges, University of California at Berkeley, June 1992.

[Moehle and Aschheim; 1993] - "Shear Strength and Deformability of RC Bridge columns

Subjected to Inelastic Cyclic Displacements," *Report No. UCB/EERC-92/04*, Earthquake
Engineering Research Center, University of California at Berkeley.

[Moehle and Lowes; 1994] - J. P. Moehle and L. Lowes, "Behavior and Retrofit of Concrete
Bridge Interior Beam-Column Connections," Technical Report, University of California,
Berkeley, January 1994. In preparation.

[Moehle and Soyer; 1993] - J. P. Moehle and C. Soyer, "Behavior and Retrofit of Exterior RC
Connections," *Proceedings*, Caltrans Research Workshop, March 1993.

[Thewalt and Stojadinovic; 1992] - "Behavior and Retrofit of Bridge outrigger Beams, "
Proceedings, Tenth World Conference on Earthquake Engineering, Madrid, Spain, July 1992.

SECOND U.S.-JAPAN WORKSHOP ON SEISMIC RETROFIT OF BRIDGES

A Seismic Retrofitting Manual for Highway Bridges
I. Buckle, I. Friedland and J. Cooper
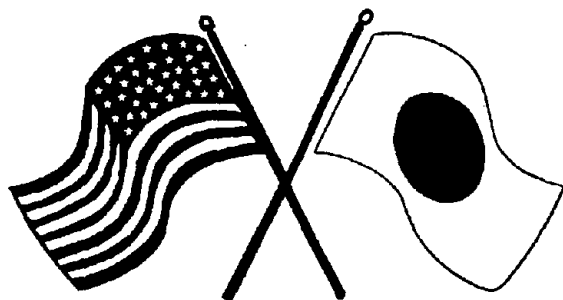
January 20 and 21, 1994
Berkeley Marina Marriott Hotel
Berkeley, California

A SEISMIC RETROFITTING MANUAL
FOR HIGHWAY BRIDGES

Ian G. Buckle and Ian M. Friedland
National Center for Earthquake Engineering Research
Buffalo, New York

James D. Cooper
Federal Highway Administration
Washington, D.C.

ABSTRACT

In 1983, the Federal Highway Administration (FHWA) published a set of guidelines for seismic retrofitting of highway bridges. These guidelines presented what was then considered to be the state-of-the-art for screening, evaluating, and retrofitting of seismically deficient bridges. In the 10 years since publication of the FHWA guidelines, there has been significant progress in understanding the response of bridges and in the development of new and improved retrofit technologies. As a consequence, the 1983 guidelines have recently been updated and reissued as a retrofit manual. This paper describes this revision, which was performed by the National Center for Earthquake Engineering Research under contract to the FHWA, and discusses a number of significant changes made in the new manual.

BACKGROUND

Of all the components of a typical highway system, the highway bridge has been the most closely studied for seismic vulnerability. As a consequence, standards have been developed and adopted nationwide for the seismic design of new bridges. By comparison, the seismic retrofitting of existing bridges is a relatively new endeavor. Only a few retrofitting schemes have been used in practice and, given the present state of knowledge, retrofitting is still somewhat of an art requiring considerable engineering judgement.

The San Fernando, California, earthquake of 1971 caused a significant amount of bridge damage and, as a result, initiated a large research effort into seismic bridge design and behavior in the mid- to late 1970s. The majority of this work was jointly sponsored by the California Department of Transportation (CALTRANS), the FHWA, and the National Science Foundation. The primary goal of this effort was to *minimize* the risk of unacceptable damage during a design earthquake. One result of this effort was the publication by the American Association of State Highway and Transportation Officials (AASHTO) of the first comprehensive national highway

bridge seismic design guide, the AASHTO "Guide Specification for Seismic Design of Highway Bridges," in 1983.

The San Fernando earthquake also provided the impetus for the FHWA and CALTRANS to address the seismic retrofitting of existing bridges to withstand earthquake forces and movements. The culmination of this effort was the publication of the 1983 FHWA report "Seismic Retrofitting Guidelines for Highway Bridges" (Report No. FHWA/RD-83/007) which was based primarily on research results and information available in the late 1970s. At the time the guidelines were issued, the existing technology for highway bridge retrofitting was limited and many of the proposed techniques had not been field demonstrated. In the 10 or so years since, new and improved technologies for retrofitting bridge columns and footings have been developed and implemented, together with methods to stabilize soils to prevent liquefaction, and to ensure adequate connections between the bridge superstructure and substructure. Many of these advances in the state-of-the-art are the result of an aggressive research program which was begun by CALTRANS following the Loma Prieta earthquake which occurred near San Francisco in October 1989.

THE SEISMIC RETROFITTING MANUAL FOR HIGHWAY BRIDGES

In order to capture these advances in seismic retrofitting and to make the current state-of-the-art available to bridge owners and engineers, the FHWA initiated a project to update the 1983 guidelines. This effort has resulted in a new document titled the "Seismic Retrofitting Manual for Highway Bridges" (hereafter referred to as the Retrofitting Manual) which was completed near the end of 1993 by the National Center for Earthquake Engineering Research (NCEER), under contract to the FHWA.

The new Retrofitting Manual offers procedures for evaluating and upgrading the seismic resistance of existing highway bridges. Specifically it contains:

☐ a preliminary screening process to identify and prioritize bridges that need to be evaluated for seismic retrofitting;

☐ a methodology for quantitatively evaluating the seismic capacity of an existing bridge and determining the overall effectiveness of alternative seismic retrofitting measures; and

☐ retrofit measures and design requirements for increasing the seismic resistance of existing bridges.

The Retrofitting Manual does not prescribe requirements dictating when and how bridges are to be retrofitted. The decision to retrofit a bridge depends on a number of factors, several of which are outside the scope of the Manual. These include, but are not limited to, the availability of funding, as well as political, social, and economic considerations. The primary focus of the Retrofitting Manual is directed towards the engineering factors.

440

MAJOR CHANGES

The Retrofitting Manual is based in large part on the 1983 guidelines. In some cases, existing material was updated as appropriate. In other cases, completely new material has been added. One notable editorial change is the format of the new document: the 1983 guidelines used a specification–language format followed by a commentary; the new Retrofitting Manual presents guidelines, recommendations, and commentary in one combined section. This shift in style, from a specification to a technical report, led to the change in title from "Guidelines" to "Manual," and it is believed that this improves overall readability. In addition, the Manual format reflects the fact that the state-of-practice in bridge seismic retrofitting is changing rapidly at this time, and that it is premature to prepare specifications at a time when new insight and experience is an almost daily occurrence.

Major technical changes in the Retrofitting Manual include the following:

☐ An increased emphasis is placed on bridge importance, and the minimum requirements for retrofitting "essential" bridges have been increased, even in low seismic zones. This has been achieved by redefining the Seismic Performance Categories (SPC) so that, for example, an essential bridge that was previously in SPC A is now classified as SPC B with more rigorous retrofitting requirements as a consequence.

☐ A new preliminary screening algorithm has been introduced which separates the quantitative evaluation of structure vulnerability and seismic hazard from the subjective assessment of importance and other societal issues. A two-part procedure is thus proposed which first involves the ordering of all bridges based on a numerical rating of structure vulnerability and seismic hazard. A prioritized list is then obtained by reordering this first list to include such judgmental issues as importance, non-seismic deficiencies, remaining useful life, network redundancy, and economic and political factors. A new Priority Index is then defined which is a mix of engineering and societal factors.

☐ In addition to the capacity/demand (C/D) ratio method for detailed bridge evaluation, a second method based on equivalent lateral strength is now included. This method avoids some of the conservatism in the C/D method which can lead to unnecessarily expensive retrofit schemes. The new equivalent lateral strength method does require more effort to understand and apply; however, it's use is expected to result in lower retrofit costs.

☐ Expanded sections on retrofit measures are included, reflecting recent progress in the development of practical field techniques. These sections cover column strengthening using jackets, footing upgrades using overlays, and seismic isolation using elastomeric bearings. An expanded section on cable restrainers is also included. It is interesting to note that at the time the 1983 guidelines were issued, most of the

retrofitting techniques described therein were identified as *potential* retrofit measures since few, if any, had actually been implemented in the field at that time. In the intervening ten years, this situation has changed and most of the measures described in the new Manual are based on field experience.

Some of these technical changes are discussed in more detail below.

RETROFITTING PHILOSOPHY

The underlying philosophy in the new Retrofitting Manual is that, whenever practical, deficient components be strengthened to new design standards. At first sight this may appear to be inconsistent with the overall goals of retrofitting, and not economically justifiable if the structure as a whole will perform below the standards for new construction. There are two reasons that the Retrofitting Manual makes this recommendation. One is that the cost to strengthen a component to new design standards is usually not that much greater than the cost of partial strengthening. The second reason is that it is possible that retrofitting will be a phased operation that takes place over the life of the structure. Changes in construction technologies and economic situations may make it feasible to strengthen some components in the future even though it is not economical to do so now. If component retrofitting were performed to standards below those for new construction, it could become necessary to restrengthen these components during a second phase of retrofitting, resulting in a higher total cost.

There may be cases, however, where it is not feasible to strengthen components to new standards. In these cases, the Retrofitting Manual recommends a preference to at least strengthen such components to lower standards rather than to reject retrofitting altogether. The Retrofitting Manual provides guidance on the selection of acceptable levels of strengthening, but notes that this still requires the judgement of the engineer, taking into consideration the performance of the remainder of the structure.

The Retrofitting Manual also discusses a number of secondary factors that must be considered when retrofitting. One of these is the repairability of the structure following an earthquake. If possible, component strengthening should not be done at the risk of forcing damage to other components that are more difficult to inspect and repair. For example, it is undesirable to strengthen a ductile component if load would then be transferred to a nonductile or brittle component. This may be the case even if calculations indicated an overall increase in seismic capacity.

Maintenance and inspection of retrofitted components are also discussed in the Retrofitting Manual, as they should also be considered during the retrofit design stage. Many years may pass before a structure is subjected to an earthquake. The retrofit measure must be designed so that it can be maintained to function as planned when and if an earthquake does occur.

BRIDGE CLASSIFICATION

Before seismic retrofitting can be undertaken for a group of bridges, they must first be classified according to their Seismic Performance Category (SPC). The SPC is determined by a combination of seismic hazard and structure importance.

Seismic hazard is reflected in the Acceleration Coefficient, A, which is assigned to all locations covered by Division I-A of the AASHTO *Standard Specifications for Highway Bridges*. When multiplied by the acceleration due to gravity, g, the product, $A \cdot g$, represents the likely peak horizontal ground acceleration that will occur due to an earthquake sometime within a 475 year period. More rigorously, this acceleration has a 10 percent probability of being exceeded within a 50 year time frame.

Bridge importance is not so readily quantified. Two Importance Classifications (I) are specified in the Retrofitting Manual: essential and standard. "Essential" bridges are those which must continue to function after an earthquake or which cross routes that must continue to operate immediately following an earthquake. All other bridges are classified as "standard." The determination of the Importance Classification of a bridge is necessarily subjective and consideration should be given to societal/survival and security/defense requirements.

The societal/survival evaluation addresses a number of socio-economic needs and includes, for example, the need for access for emergency relief and recovery operations immediately following an earthquake.

Security/defense requirements may be evaluated using the 1973 Federal-Aid Highway Act, which required that a plan for defense highways be developed by each state. The defense highway network provides connecting routes to military installations, industries, and resources not covered by the Federal-Aid primary routes.

An "essential" bridge is therefore one that satisfies one or more of the following conditions:

☐ a bridge that is required to provide secondary life safety; e.g., a bridge that provides access to local emergency services such as hospitals. This category also includes those bridges that cross routes which provide secondary life safety, and bridges that carry lifelines such as electric power and water supply pipelines;

☐ a bridge whose loss would create a major economic impact; e.g., a bridge that serves as a major link in a transportation system;

☐ a bridge that is formally defined by a local emergency plan as critical; e.g., a bridge that enables civil defense, fire departments, and public health agencies to respond immediately to disaster situations. This category also includes those bridges that

443

cross routes which are defined as critical in a local emergency response plan and those that are located on identified evacuation routes; or

☐ a bridge that serves as a critical link in the security/defense roadway network.

Based on the above considerations for seismic hazard and importance, four Seismic Performance Categories are defined in the Retrofitting Manual as shown in Table 1.

Table 1. Seismic Performance Category

Acceleration Coefficient	Importance Classification	
	Essential	Standard
A ≤ 0.09	B	A
0.09 < A ≤ 0.19	C	B
0.19 < A ≤ 0.29	C	C
0.29 < A	D	C

These SPC's are assigned differently from those in the AASHTO specifications for new design, where no allowance for structure importance is made in seismic zones with acceleration coefficients less than 0.29. In view of the high cost of retrofitting, it is important to be able to distinguish between "essential" and "standard" structures and especially so in low to moderate seismic zones. Such a distinction also enables a more rational allowance to be made for the nature of the seismic hazard in the central and eastern U.S. where the maximum credible earthquake is expected to be significantly larger than the "design" earthquake (475 year-event). This implies that if an essential bridge in the east is to remain fully operational following a large earthquake, it will need to be retrofitted to a standard higher than that required by the current specification for new construction. This observation is reflected in the assignment of SPC's for essential bridges in Table 1.

THE RETROFITTING PROCESS

Seismic retrofitting is one solution for minimizing the hazard of existing bridges that are vulnerable to serious damage during an earthquake. Because not all bridges in the highway system can be retrofitted simultaneously, the most critical bridges should be retrofitted first. The selection of bridges for retrofitting requires an appreciation for the economic, social, administrative, and practical aspects of the problem, as well as the engineering aspects. Seismic retrofitting is only one of several possible courses of action; others include bridge closure, bridge replacement, or acceptance of the risk of seismic damage. Bridge closure or replacement is usually not justified by seismic deficiency alone and will generally only be considered when other deficiencies exist. Therefore, for all practical purposes, a choice must be made between retrofitting or accepting the seismic risk. This choice will depend on the importance of the bridge and on the cost and effectiveness of retrofitting.

444

The process of retrofitting bridges involves an assessment of a multitude of variables and requires the use of considerable judgement. It is therefore helpful to divide the process into three major stages. These are:

- preliminary screening;

- detailed evaluation; and

- design of retrofit measures.

Each of these stages is outlined below and described in further detail in the Retrofitting Manual. Figure 1 is a flow chart which illustrates the retrofitting process for each SPC.

PRELIMINARY SCREENING

Preliminary screening of an inventory of bridges is recommended to identify those bridges which are seismically deficient and those in the greatest need of retrofitting. This is particularly useful when a comprehensive retrofitting program is to be implemented.

The Retrofitting Manual describes a method for developing a Seismic Rating System which may be used to prioritize bridges on a highway system according to their need for seismic hazard reduction. Factors considered in the seismic rating process include structural vulnerabilities, seismic and geotechnical hazards, and bridge importance or criticality. In this way, the most hazardous bridges are identified. Bridges high on the list should be investigated further to determine the benefits of retrofitting. Because the decision to retrofit depends on political, social, and economic factors as well as engineering issues, high priority bridges may not necessarily be retrofitted. On the other hand, bridges with a lower priority may need to be retrofitted immediately.

One very important consideration that is not adequately reflected in the Seismic Rating System is the relationship of the bridge to other bridges on the system that may also be damaged during an earthquake. These types of considerations should be made prior to making a detailed evaluation of the seismic capacity of the bridge.

A further consideration when deciding if retrofitting is warranted is the age and condition of the bridge. It would not be rational to spend a large amount to retrofit a bridge with only five years of service life remaining. An unusually high seismic vulnerability may, however, be a justification to accelerate closure or replacement of such a bridge.

A bridge in poor physical condition that is scheduled for nonseismic rehabilitation should be given a higher priority for seismic retrofitting, since construction savings can be realized by performing both the nonseismic and seismic work simultaneously.
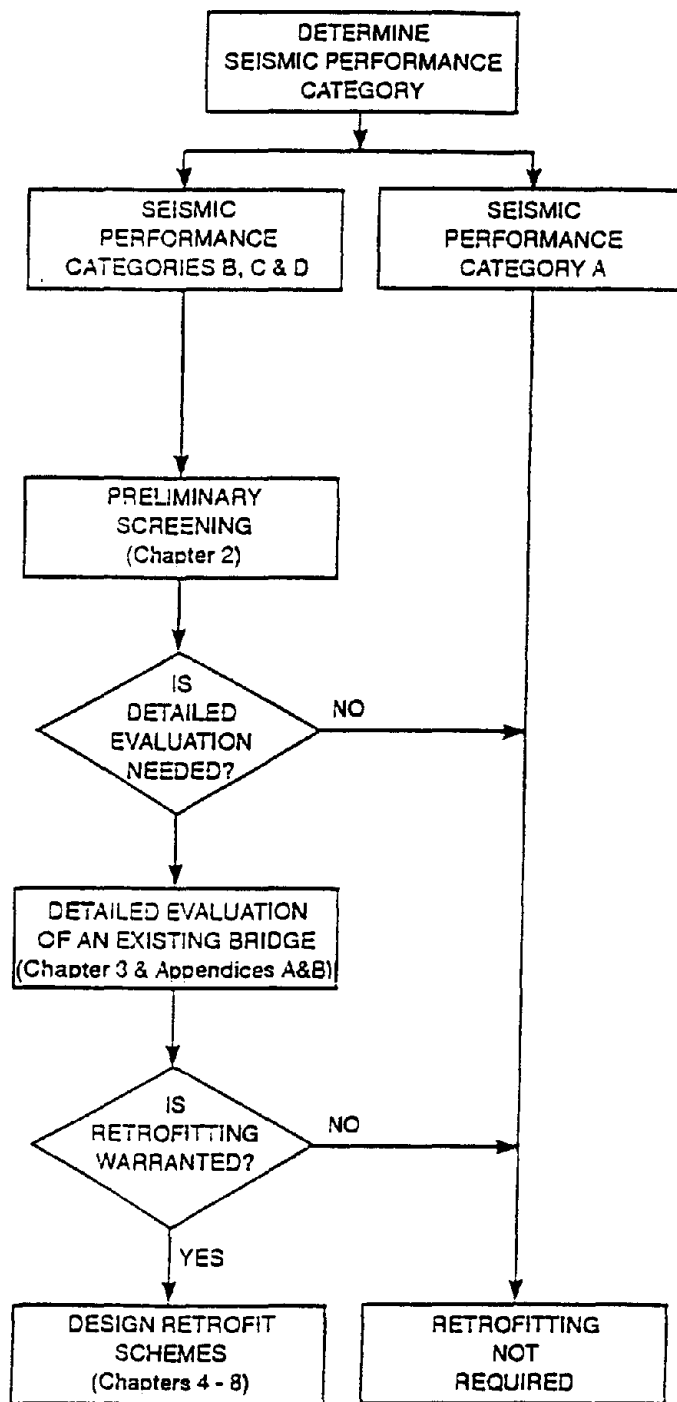
Figure 1. The Seismic Retrofitting Process

The above examples do not represent all possible cases, but they do illustrate some of the principles involved in a retrofitting decision. In most cases, the Seismic Rating System is used as a guide to making retrofitting decisions, but not as the final word. Common sense and engineering judgement will be necessary in weighing the actual costs and benefits of retrofitting, against the risks of doing nothing. Also, the effect on the entire highway system must be kept in mind.

The preliminary screening process recommended in the new Retrofitting Manual is demonstrated in Figure 2, where the terms are defined as follows: A is the acceleration coefficient for the bridge site; I is the bridge importance; V is the vulnerability rating of the bridge; S is the soil site coefficient; and E is the seismic hazard rating, which is based on the acceleration and site coefficients.

DETAILED EVALUATION

Two alternative methods for the detailed evaluation of existing bridges are currently available. One is based on a quantitative assessment of the "capacities" and "demands" of individual components of a bridge structure. The other evaluates the lateral strength of the bridge as a new structure.

Capacity/Demand Method — The first method was proposed in the 1983 FHWA Retrofit Guide and has been used in a modified form by CALTRANS since the early 1980's. In this method, the results from an elastic spectral analysis are used to calculate the force and displacement "demands" which are then compared with the "capacities" of each of the components to resist these forces and displacements. In the case of reinforced concrete columns, ultimate capacities are modified to reflect the ability of the column to resist post-elastic deformations. Capacity/Demand (C/D) ratios are intended to represent the decimal fraction of the design earthquake at which a local failure of the components is likely to occur. Therefore, a C/D ratio less than 1.0 indicates that component failure may occur during the design earthquake and retrofitting may be appropriate.

An overall assessment of the consequences of local component failure is necessary to determine the need for retrofitting. Retrofitting should be considered when an assessment indicates that local component failure will result in unacceptable overall performance. The effect of potential retrofitting may be assessed by performing a detailed re-evaluation of the retrofitted bridge.

The determination of what constitutes a serious consequence of component failure will depend on the importance of the bridge. Collapse of the structure is serious in almost all cases since there is always a potential for loss of life in such an occurrence. In other cases, severe distortions or critical loss of strength will impair the ability of the bridge to carry emergency traffic which is unacceptable for certain important bridges. Repairability of seismic damage is also a consideration. If repairs can be made quickly without serious delays to traffic, damage may be acceptable. This is another area in which engineering judgement is required.
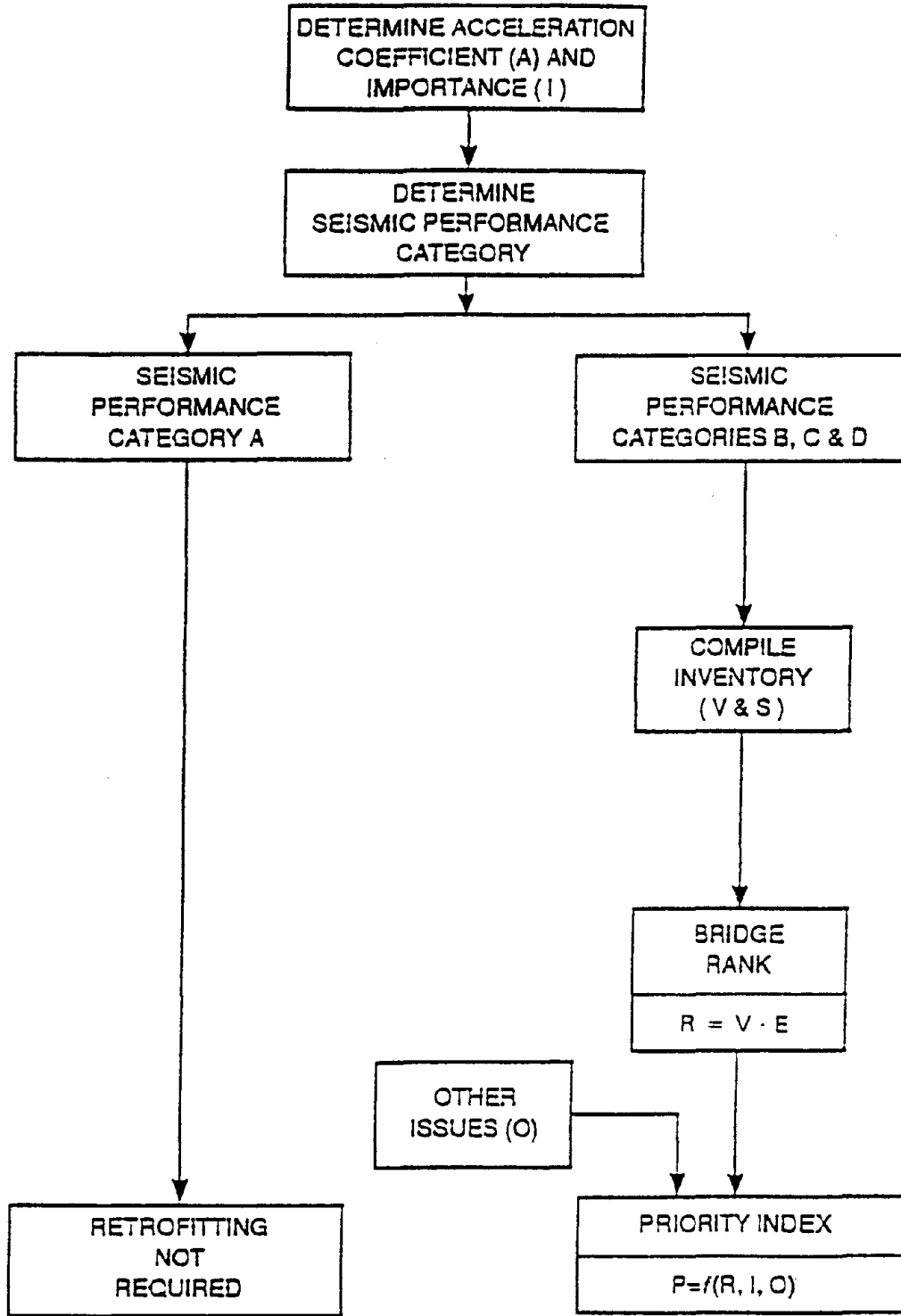
Figure 2. The Preliminary Screening Process

Once it has been determined to consider retrofitting, acceptable methods may be selected from among a number of those suggested in the Retrofitting Manual. If the seismic response of the structure is affected, then a reanalysis should be performed and new set of component C/D ratios calculated. The new C/D ratios will reflect a change in the size of the earthquake that will cause serious damage. A decision to use any retrofitting method will be based on a relative benefit-to-cost analysis. Hypothetically, this benefit-to-cost analysis may be objective and rigorous, but it is more likely that it will be subjective and based, in large part, on judgement.

Lateral Strength Method — The Retrofitting Manual also provides an alternative analysis approach which examines the lateral strength of the bridge as a system, or at least individual segments of the bridge as a system, and determines, through an incremental collapse analysis, the load-deformation characteristics of the bridge up to collapse. The fraction of the design earthquake that can be resisted without collapse is then an indicator of the need for retrofitting and the extent of strengthening required. This procedure therefore determines the strength and ductility of the critical collapse mechanism but it can also be used to identify the onset of damage when serviceability criteria may be important. The method emphasizes deformation capacity rather than strength since, although strength is important, it is less important than the ability to sustain substantial deformations without collapse. It is believed that fewer bridges assessed under this procedure will be found in need of retrofit than by the C/D ratio method. When retrofit is required, it should be less extensive. The increased level of effort required of the designer will then be offset by reduced retrofit costs in the field.

RETROFIT MEASURES

There are two alternative strategies that a designer may adopt when faced with retrofitting a bridge. One is based on conventional strengthening techniques which increase the capacity of the structure to meet the likely demand. This is the most common approach used in the United States at this time. The second strategy is based on reducing the demand on the structure such that its existing capacity is sufficient to withstand the given earthquake. This latter approach involved the use of an earthquake protective system, such as seismic isolation or the addition of a mechanical energy dissipation device. Both strategies are described and detailed in the Retrofitting Manual.

Conventional Retrofit Measures — The new Retrofit Manual describes conventional retrofit measures for bearings, seats, and expansion joints, including joint and bearing restrainers, bearing seat extensions, and overall bearing replacement. The Manual also discusses techniques for strengthening reinforced concrete substructures through column jacketing and wrapping, cap/column and column/footing joint strengthening, and cap beam retrofitting. Retrofit measures for foundations include strengthening footings for flexural and shear strength, ensuring adequate reinforcement anchorage, and sufficient strength in the pile/footing connection to resist overturning or uplift, along with problems related to abutments and approach slabs. Finally, the Manual also discusses problems associated with hazardous sites, including sites with liquefiable soils, bridges on or near unstable slopes, and bridges crossing or near active faults. These techniques represent the current state-of-the-art; however, the art is changing rapidly at this time.

Earthquake Protective Systems — The term "earthquake protective system" includes passive and active devices which can be installed in a bridge to minimize the seismic demand on the members of the structure. Active systems are considered outside the scope of the Manual but passive devices are being used in several states as a cost-effective retrofit measure for many bridge types. Passive systems discussed in the Manual include mechanical systems, which simply dissipate energy and thus reduce response, and seismic isolation systems, which change the natural period of a bridge so that earthquake loads are significantly reduced. The Manual provides a discussion on seismic isolation concepts and on some of the options available at this time for design and implementation.

SUMMARY

The new "Seismic Retrofitting Manual for Highway Bridges" contains detailed information about each of the major steps in the bridge seismic retrofit process, as shown in Figure 1. It describes procedures for preliminary screening of bridges along with two alternate procedures for the detailed evaluation of them. These evaluation methods include a quantitative evaluation of the C/D ratios for individual bridge components, and an alternative method based on assessment of a structure's lateral strength.

The procedures for evaluating bridges for retrofitting also include the identification and assessment of retrofit measures. A number of potential retrofitting measures and retrofit design requirements are discussed in the Manual. Specifically, retrofit measures for the types of bridge components which have performed poorly during past earthquakes are discussed in detail. Retrofitting by these or other equivalent methods should be considered when components are identified by a detailed evaluation as being deficient. The decision to use a retrofitting scheme will be based on an assessment of its effectiveness in preventing unacceptable overall performance, the cost of retrofitting, and the remaining service life of the bridge. The Retrofitting Manual also includes several worked example problems intended to help illustrate the process of planning the retrofitting of a typical highway bridge.

Detailed design of retrofit measures should be performed using the guidelines contained in the Retrofitting Manual in conjunction with the current AASHTO bridge design specifications. If possible, components which are selected for retrofitting should generally be strengthened to conform to the specifications for new construction, even though the structure may otherwise be seismically deficient.

ACKNOWLEDGEMENTS

Any opinions, findings, and conclusions or recommendations expressed in the Retrofitting Manual or this paper are those of the authors and do not necessarily reflect the view of NCEER, the FHWA, or the U.S. Department of Transportation.
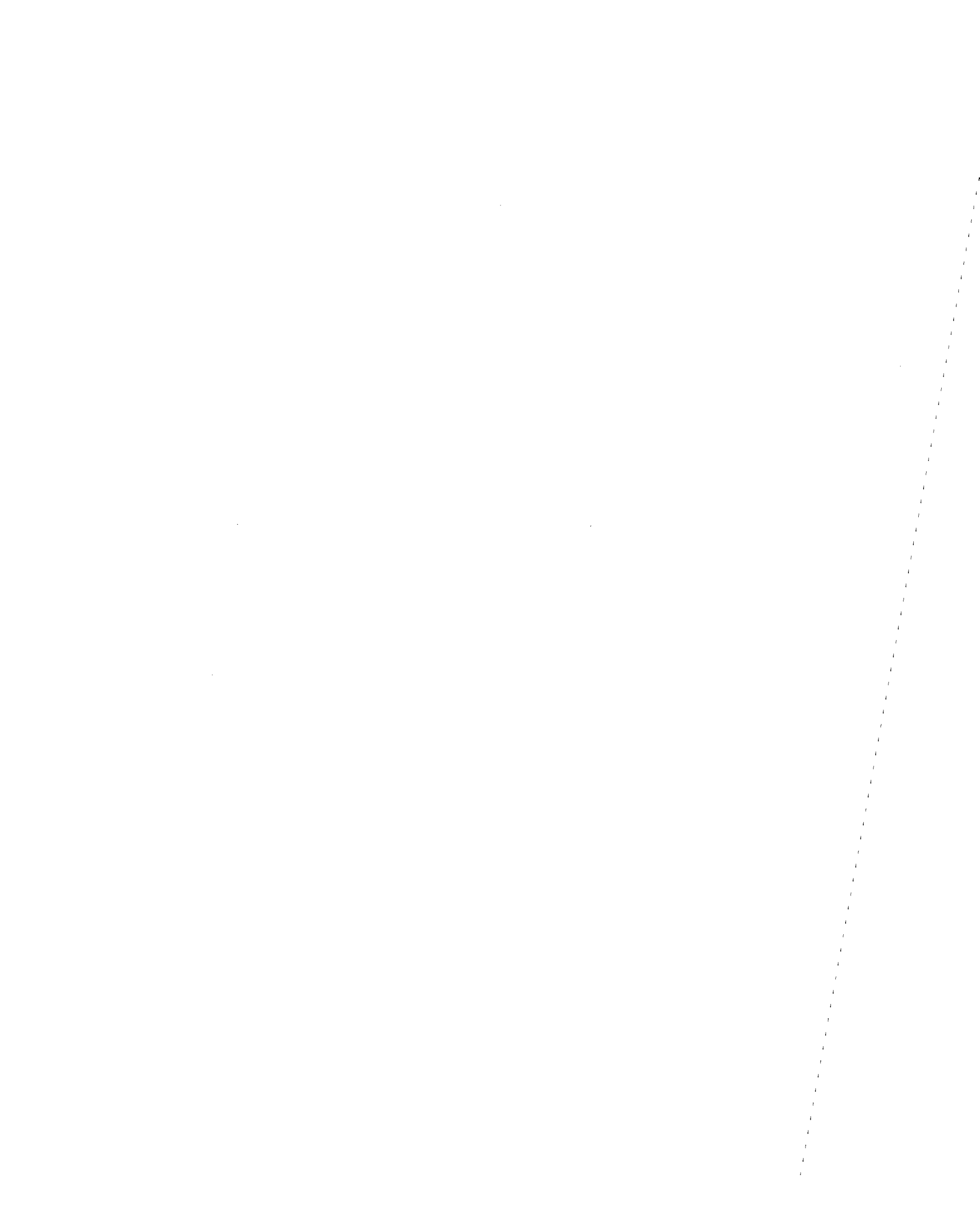
SECOND U.S.-JAPAN WORKSHOP ON SEISMIC RETROFIT OF BRIDGES

Collapse of the Cypress Viaduct and Seismic Performance of a Retrofitted Bent

H. Ohuchi, T. Matsuda and Y. Goto
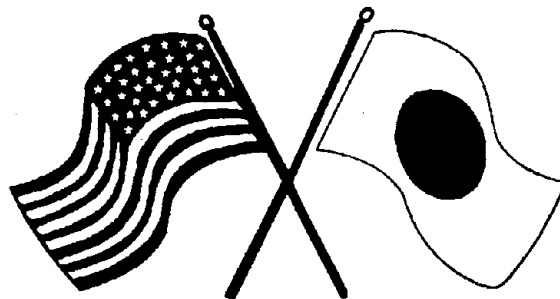
COLLAPSE OF THE CYPRESS VIADUCT AND
SEISMIC PERFORMANCE OF A RETROFITTED BENT

Hajime Ohuchi, Dr.Eng.
Structural Engineering Department
Technical Research Institute, Obayashi Co.

Takashi Matsuda, Ms.Eng.
Civil Engineering Department
Technical Research Institute, Obayashi Co.

Yozo Goto, Dr.Eng.
Civil Engineering Department
Technical Research Institute, Obayashi Co.
4-640 Shimokiyoto, Kiyose, Tokyo-204, Japan

ABSTRACT

This paper describes numerical simulation studies on the bent collapse of the Cypress Viaduct during the Loma Priata Earthquake and on the seismic performance of the same type bent retrofitted. The purpose of the 1st simulation is to identify bent damage due to ground condition and structural types and that of the 2nd simulation is to estimate seismic performance of the retrofitted bent. Systematized analyses provided following conclusions: 1)Amplified ground motion was appropriately predicted based on the multiple reflection theory. 2)Finite element nonlinear analyses provided good agreement with test results both of existed and retrofitted bents. 3)Nonlinear dynamic response analyses provided quantitative explanation on the relationship between ground condition, bent types and bent collapses and also ensured sufficient seismic safety of the retrofitted bent.

INTRODUCTION

Catastrophic collapse of the Cypress Viaduct at Loma Prieta Earthquake 1989, caused 41 fatalities and amount of economic losses in San Francisco Bay area. A great concern was concentrated even from overseas on the engineering issue to be resolved with 48 bents collapse in the 1.2 km long part of I-880 at the Cypress section. In the US., comprehensive seismic design specification was provided after the 1971 San Fernando Earthquake. However a great number of bridges including the Cypress Viaduct, were constructed in 1950's and 1960's. As the results, seismic vulnerability of existing bridges and seismic strengthening method were urged to investigate and a number of experimental and analytical studies have been conducted including field tests with survived bents. In these backgrounds, this paper presents numerical simulation studies on the collapse of the Cy-

press Viaduct and on the seismic performance of the retrofitted bent against several earthquakes consistent with the current US. seismic design guideline. A rational prediction of the Cypress Viaduct collapse is believed to contribute even in the Japanese future earthquake hazard mitigation practice. Also a prediction on the seismic performance of the retrofitted bent may provide effective information in promoting seismic strengthening program.

GENERAL

Damage Summary As shown in Fig.1[1], the cause of bent damages is considered to be deeply related with the underlying ground condition and the structure types. The Cypress north side section was on reclaimed soft soil, while the south side section on dense silty sand. In the north side, all the upper decks fell down onto lower decks except one span portion. On the other hand in the south side falling down of upper decks was prevented except about 150m portion adjacent to the north side.

The bent types are conceptually categorized into three structure types as shown in Fig.1 due to location of pinned joint and to bent-cap structural type, reinforced or prestressed concrete. B type bent was employed in many parts and all collapsed in the north side. Among five A type bents existed in the north side, two of them survived despite significant damages suffered. In the south end to north side, all the C type bents also collapsed.

Objectives and Procedures of Present Study Present numerical studies consist of two phases, i.e. collapse simulation of existed bents and seismic performance simulation of a retrofitted bent as illustrated in Fig.2.

The objective of 1st simulation is to provide rational answers to the following two questions:

1) Are bent collapse in the north side section and bent survival in the south side section predicted if considering different ground conditions?

2) Do B and C type bents collapse and an A Type bent not collapse in the north side section?.

As shown in Fig.2, analytical studies for this simulation consist of 4 parts:I) Dynamic response analysis of ground,II) Soil-foundation dynamic interaction analysis,III) Static nonlinear analysis of bent and IV) Nonlinear dynamic response analysis of bent.

The objective of 2nd simulation is to provide similar rational answer to the following question:

1)How much structural margin does retrofitted bent possess against earthquakes with acceleration amplitude consistent with the current seismic design standard ?

As shown in Fig.2, analytical studies for this simulation consist of two parts :V) Static nonlinear
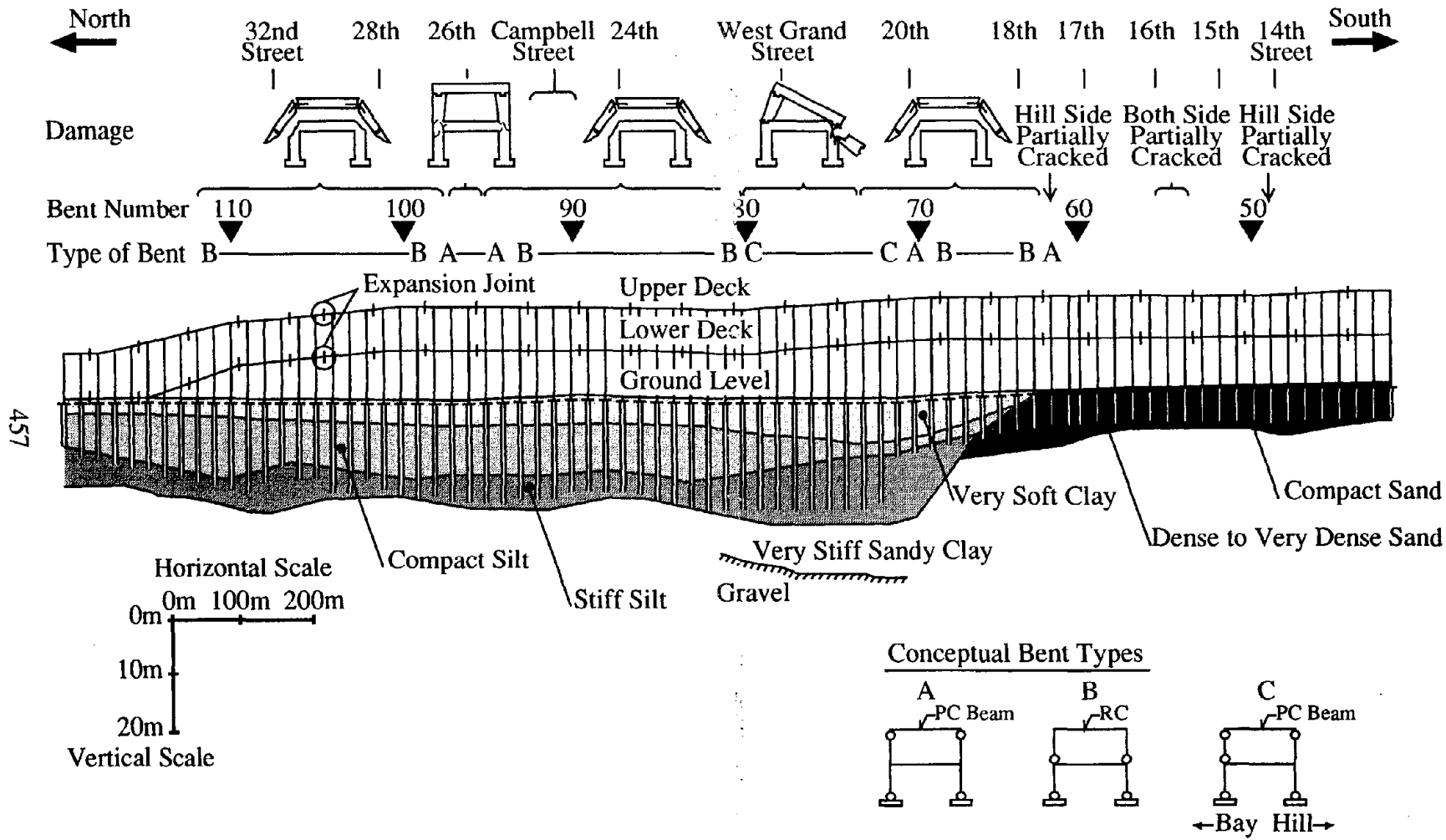
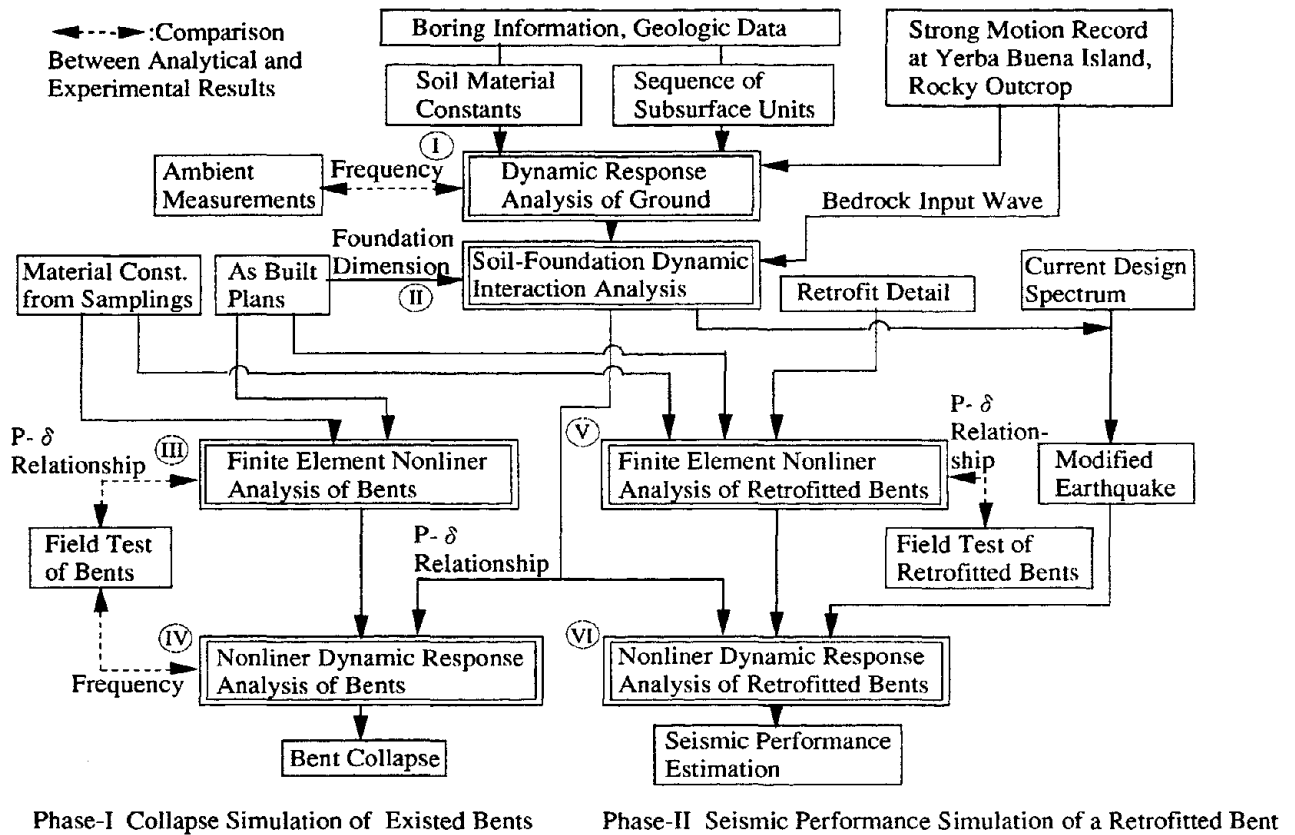Fig.1 I-880 Cypress Viaduct Damage Profile

◄---►:Comparison Between Analytical and Experimental Results

Boring Information, Geologic Data

Soil Material Constants | Sequence of Subsurface Units

Strong Motion Record at Yerba Buena Island, Rocky Outcrop

Ambient Measurements ◄--- Frequency ---► (I) Dynamic Response Analysis of Ground

Bedrock Input Wave

Foundation Dimension

Material Const. from Samplings | As Built Plans | (II) Soil-Foundation Dynamic Interaction Analysis

Retrofit Detail | Current Design Spectrum

P- δ Relationship (III) Finite Element Nonliner Analysis of Bents

(V) Finite Element Nonliner Analysis of Retrofitted Bents

P- δ Relationship | Modified Earthquake

Field Test of Bents

P- δ Relationship

(IV) Nonliner Dynamic Response Analysis of Bents

Field Test of Retrofitted Bents

Frequency

(VI) Nonliner Dynamic Response Analysis of Retrofitted Bents

Bent Collapse

Seismic Performance Estimation

Phase-I Collapse Simulation of Existed Bents   Phase-II Seismic Performance Simulation of a Retrofitted Bent

Fig.2 Analytical Study Procedure

analysis of retrofitted bent and VI) Nonlinear dynamic response analysis of retrofitted bent. Results from part I) and II) analyses are also utilized as an input motion and foundation characteristics for the part VI) dynamic response analyses.

From the damage observation of survived bent and from the available accelerogram observed in the nearby site, the transverse motion of bridge axis is considered as rather dominant. Accordingly, all the above analyses are carried out against transverse motion with neglecting structural contribution from the members parallel to the bridge longitudinal axis such as box girders except their gravity load.

COLLAPSE SIMULATIONS

Dynamic Response of Ground   A dynamic response of the multi-layered ground is predicted based on the multiple reflection theory.   An equivalent linearization method is utilized to consider nonlinear behavior of soils for material comparatively small input acceleration from bedrock.   Soil

458

layers in the north side and south side are appropriately modeled on the basis of boring log datas[2] and PS velocity logging datas[3]-[5]. As shown in Fig.1,a significant difference appears from the surface to 16.5m depth below ground line between both sides,i.e. soft bay mud from 2 to 6 m depth in the north side while dense silty sand from 4.5 to 16.5m depth in the south side. An accelerogram recorded at Yerba Buena Island(EW : 0.067G, NS : 0.029G), rocky outcrop about 7 km distant from the Cypress section is employed as an input wave from bedrock. This island consists of Franciscan formation identical to the bedrock of the Cypress section. The EW component is utilized as the incident wave from bedrock.

Fig.3 illustrates the calculated transfer function between bedrock and ground surface, in which first natural frequency predicted are respectively 0.61 and 0.68 Hz in both sides and their amplification factors are nearly equal to each other, however the amplification in the higher frequency region(1Hz ~4Hz) is larger in the north side than in the south side. The analytical period agrees fairly well with the measured value of 0.7Hz in the ambient vibration[6]. Fig.4 illustrates the calculated ground surface acceleration waves with maximum accelerations of 194 gal in the north side and of 135 gal in the south side. In these analyses, the attained maximum shear strain of each layer is in the range of $6.5 \times 10^{-5} \sim 9.4 \times 10^{-5}$.
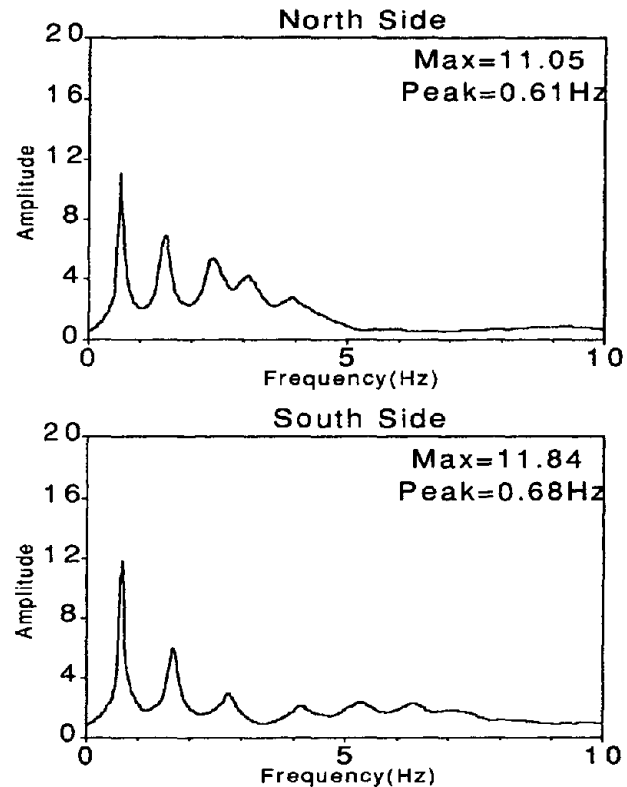

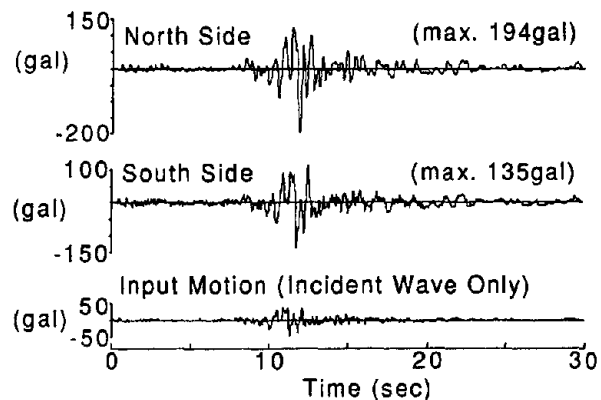Fig.3 Calculated Transfer Function Between Bedrock and Ground Surface

Fig.4 Ground Surface Acceleration on Multiple Reflection Theory

Soil-Foundation Dynamic Interaction   Representative analytical bents to be discussed in this paper are No.96, 88 and 71 for A,B and C type bents respectively. An asymmetric dynamic re-

sponse analysis is conducted with using axsymmetric finite elements as shown in Fig.5. As each column of a bent independently stands on the foundation with each other, a unit of pile cap-pile foundation system is idealized. The material characteristics of ground layers such as shear stiffness and damping are modeled based on the results obtained in the previous ground response analysis. The nonlinear behavior in the interface between soil and foundation is neglected because no ground surface cracks suggesting significant slip were observed in the post-earthquake field investigation.

A horizontal stiffness of the spring for pile foundation system and an effective input acceleration on the top of pile cap must be predicted for the three degrees of freedom system model later as shown in Fig.17. Fig.6 illustrates frequency dependent characteristics of the spring analytically obtained from load-displacement relationship under harmonic excitation at the pile top. The real part corresponds to stiffness while the imaginary part damping characteristics. The real part for the south side provides about 3.5 times that for the north side. The obtained effective input motion which is required to take the kinematic interaction into account, is shown in Fig.7. It is calculated by using axsymmetric finite element models shown in Fig.5 with input of the prescribed earthquake wave from the virtual bedrock.

Static Nonlinear Behavior of Existed Bents

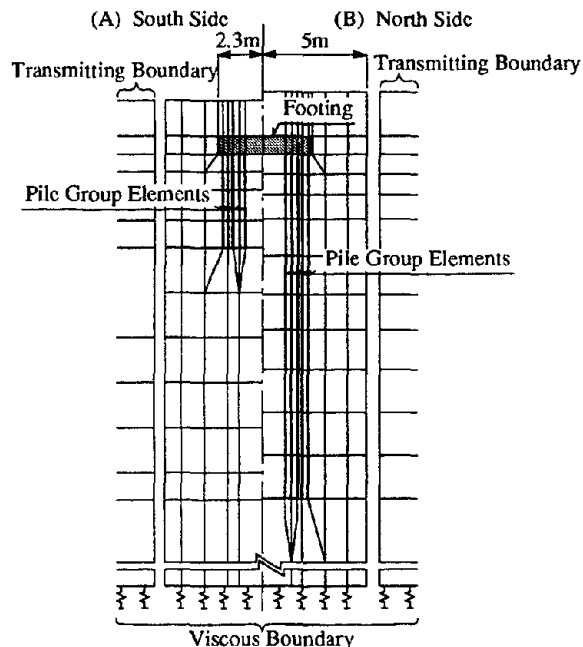A typical bent failure sequence[7] and an critical
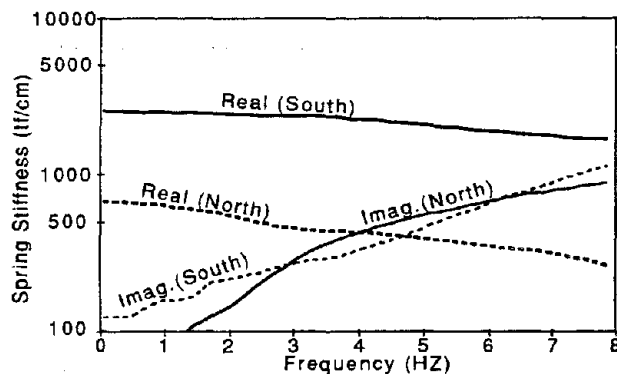

Fig.5 Axsymmetric FE Models for Interaction Analysis

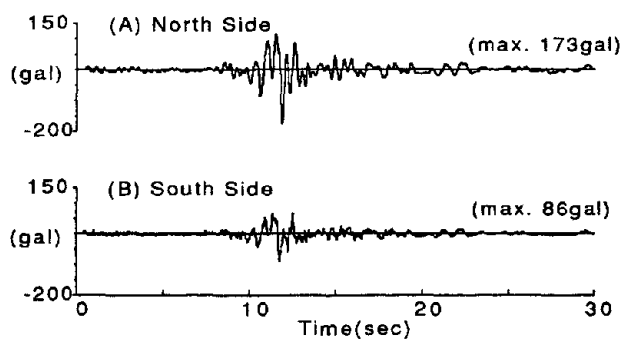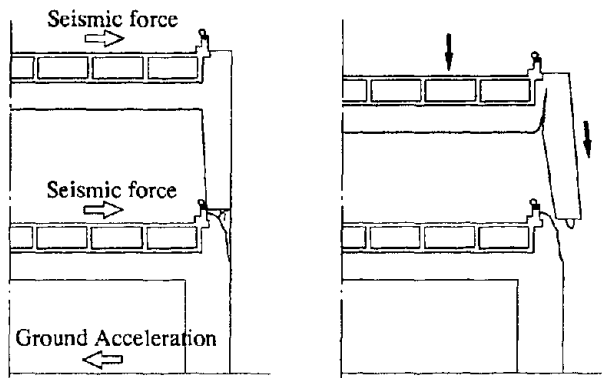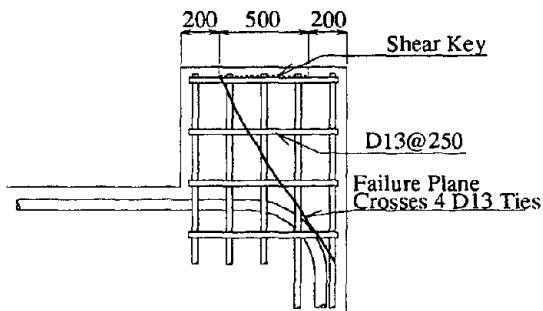**Fig.6 Frequency Dependent Characteristics of Spring**

Fig.7 Effective Ground Surface Acceleration

460

(A) Typical Failure Sequence of a B-type Bent (Ref.9)

(B) A Shear Crack Along Bent Down Rebar
in the Joint (Ref.9)

Fig.8 a Typical Bent Failure

Section A-A

**Fig.9 Dimension and Reinforcement Detail
of B Type Bent - No.88 (Ref.12)**

shear crack along bent down rebar in the joint are illustrated in Fig.8. The objectives in this section are to predict this critical shear failure and load-displacement relationships for the nonlinear dynamic response analysis in the following section. Caltrans conducted horizontal loading tests[8],[9] to estimate ultimate loading capacity of the existed bent (undestructive test) and to investigate seismic performance of the retrofitted bent (destructive test) with using the survived bents No.45-47 categorized as B type in the present study. The accuracy of present analyses will be verified through comparison with these test results.

Material constants are assumed on the basis of the sampling test results and design information[8]. Two dimensional finite element nonlinear analysis are conducted using 'ABAQUS' computer program[10] combined with the separate subroutine for concrete constitutive law[11]. The upper and the lower concrete through shear key are assumed as monolithically connected except those through fiber board. No damage suffered in the past is assumed with all bents. Fig.9 illustrates dimension and steel reinforcement arrangements of the representative bent(B type)[12].

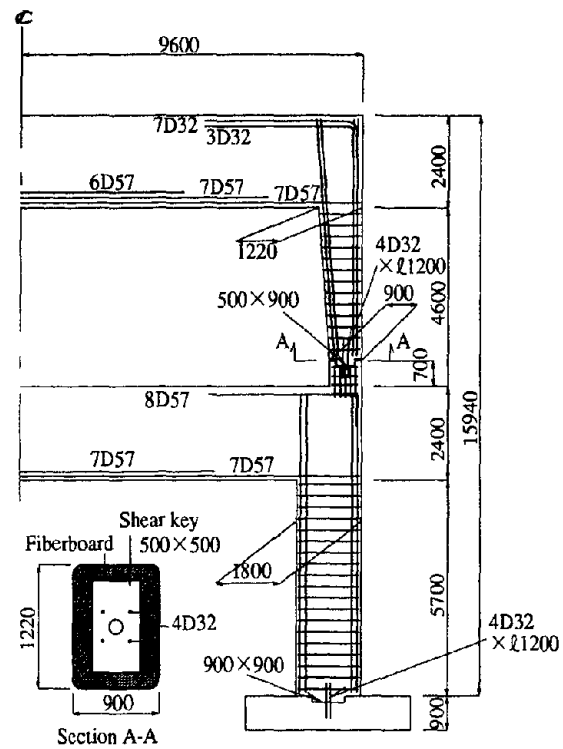As for the load application, after applying dead load,i.e. weights of bent caps and of one span

461

Fig.10 Crack Pattern at Final Stage(B Type)
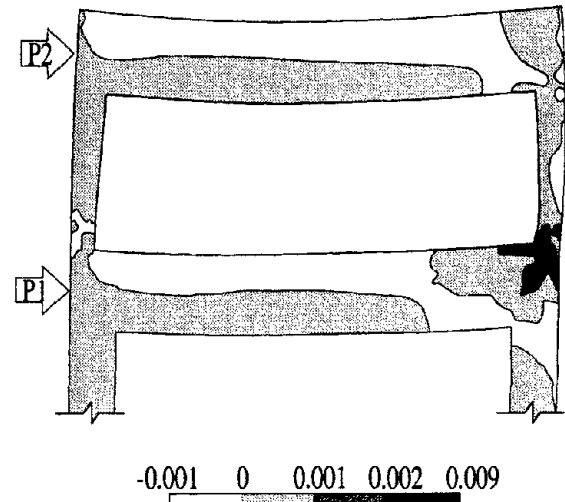

-0.001   0   0.001 0.002 0.009

Fig.11 ε_x Contour at Final Stage (B Type)

length box girder, static horizontal load uniformly distributed in each bent cap is proportionally increased. A horizontal load distribution along the height is determined by the 1st mode in the elastic modal analysis.

The predicted ultimate crack pattern of B type bent is illustrated in Fig.10. Even during dead load application, the shear crack initiates in the pedestal below the pinned joint of upper column due to shear force outward the joint. With horizontal load increased, this crack propagates diagonally along bent down rebar in the joint and then vertically into concrete outer coverage, which agrees with the failure mode illustrated in Fig.8. The left end of upper bent cap is critical in flexural crack shown as the broken line in Fig.10, which suggest that the flexural crack predominates at upper bent cap end as shown in Fig 8 when considering insufficient anchorage length of D57(No.18) for lower straight reinforcement (see Fig.9) and bond depression under cyclic horizontal load. Fig.11 illustrates horizontal strain contour of ε_x at an ultimate stage in which the strain concentration in the joint is comparable to the failure surface of Fig.8. When additionally considering less and insufficient shear reinforcement, i.e. tied hoop utilized, this type of shear failure must be likely encouraged.

Predicted load-displacement relationships for A, B and C type bents are respectively shown in Figs.12 to 14. As shown in Fig.12,
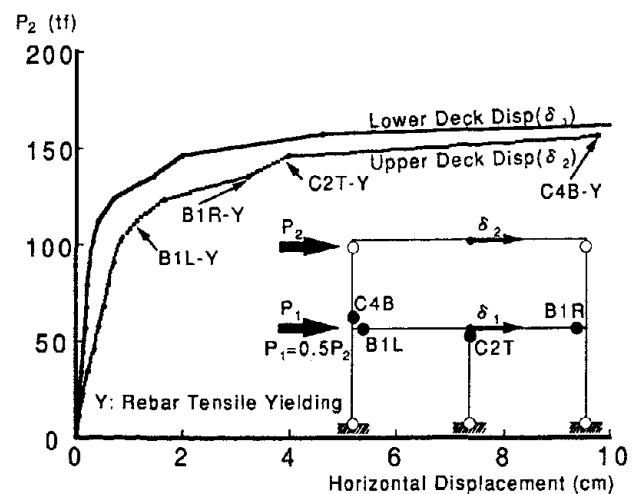

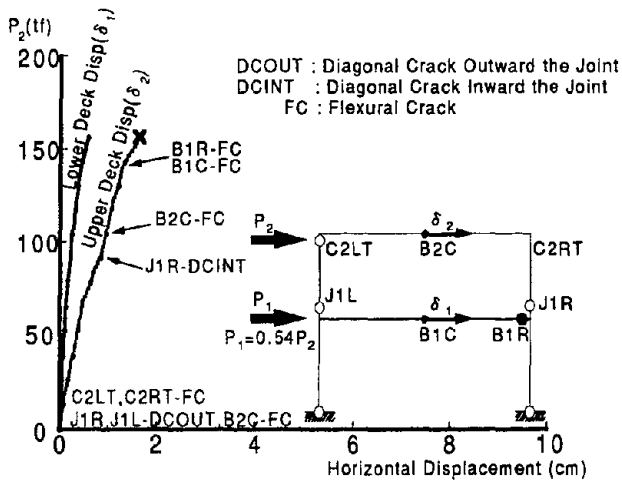Fig.12 Load-Displacement Relationship(A Type)
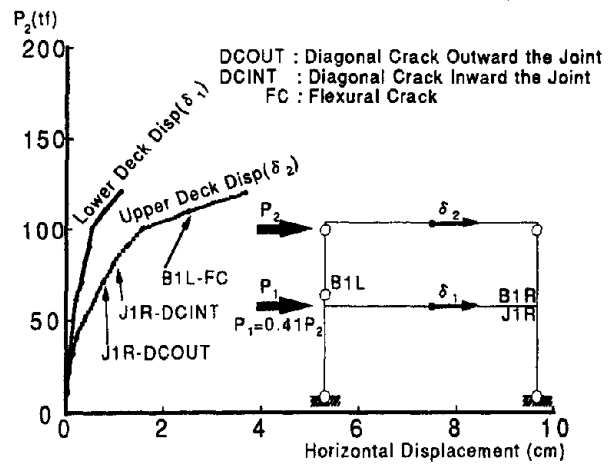
462

Fig.13 Load-Displacement Relationship(B Type)

Fig.14 Load-Displacement Relationship(C Type)

the analysis predicts ductile flexural-yielding-type failure for the A type bent. For the B type bent, after the joint shear cracks extend to the concrete coverage, most of shear reinforcement in the pedestal are predicted to yield. For the C type bent with pinned joints at both upper column tops, critical shear crack initiates from pedestal to joint at relatively higher horizontal load. However, because one of upper columns resists no horizontal load, the lateral shear force concentrates on the other column, resulting in

Fig.15 Load-Displacement Relationship(C Type)

lower ultimate loading capacity and lower lateral stiffness obtained rather than the B type bent.

The ultimate loading capacity of the B or C type bent is numerically defined as the load level when the internal lateral shear force in the critical column rapidly decreases unbalancing with the external horizontal load.
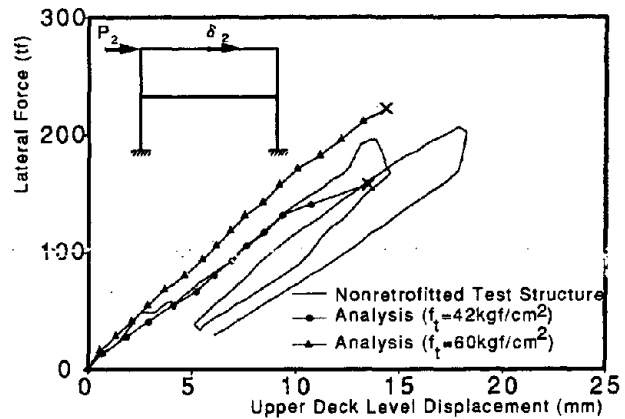
Comparison with Undestructive Test Results   In the field loading test, the horizontal load was applied only at the upper bent cap. Fig.15 illustrates load-displacement relationships where the analytical result ($f_t = 42 \, kgf/cm^2$) agrees fairly well with the experimental result. The predicted ultimate loading capacity is 156 tonf in comparison with 210 tonf in the experiment[8]. From taking account that the ultimate load is deeply dependent on shear crack initiation in the joint, the case with concrete tensile strength of $f_t = 60 \, kgf/cm^2$ is additionally analyzed to discuss its influ-

463

Fig.16 Three Degrees of Freedom
System Model for Nonlinear
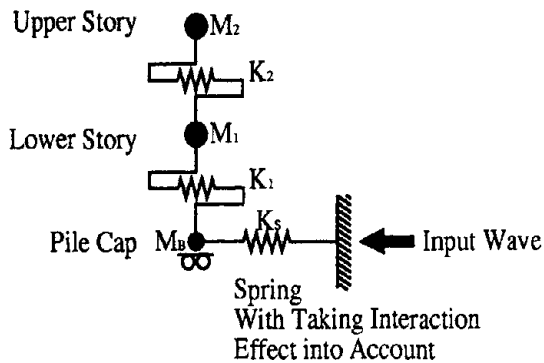Dynamic Response

Table 1 Natural Frequency of Bents

| Structure Type	Site	Frequency (Hz.)	
		1st	2nd
A Type (No.96)	North Side	2.07	4.99
	South Side	2.16	5.21
B Type (No.88)	North Side	2.40	5.60
	South Side	2.55 (2.50)*	6.25 (4.50)*
C Type (No.71)	North Side	2.17	5.54
	South Side	2.31	5.71

( )* : Forced Vibration Test Results

ence. The larger but more approximate ultimate loading capacity with 234 tonf is obtained for this case. The stiffness difference between $f_t = 42$ and $60 kgf/cm^2$ cases depends on the difference of crack growth especially during dead load application. When considering possible initial crack existence in the experimental bent, the intermediate value between these tensile strengths may be more reasonable to use. However,because of better prediction in stiffness, the case of $f_t = 42$ kgf/ cm^2 is employed in all the following analyses.

Nonlinear Dynamic Response of Existed Bents Nonlinear dynamic response analyses are conducted with using a three degrees of freedom system model including a spring taking soil-foundation interaction effect into account as shown in Fig.16. As for the enveloping curve of hysteresis models for each bent story, shear force-relative displacements obtained from the finite element nonlinear analyses are idealized into tri-linear type model. As for the hysteretic rule, the flexural-failure-type Takeda model[13] is utilized for both upper and lower stories of the A type bent. In the B and C type bents, the similar model is utilized for the lower story, while the origin-orient hysteresis model for the upper story failed in brittle shear. Based on the dynamic interaction analysis described in the former section, the spring characteristics at base(Fig.16) is idealized as a linear elastic model with damping calculated considering strain energy for radiation damping. Super-structure damping is uniformly assumed as of 3 %.

Table 1 shows elastic natural frequencies obtained from the three degrees of freedom system analyses. The analytical 1st natural frequency of 2.55 Hz agrees well with the forced vibration test result of 2.5 Hz.[7] for the B type bent.

The obtained response at the critical upper story are tabulated in Table.2 from which characteristic responses can be identified due to bent types and ground conditions. In the north side B and C

464

Table 2 Comparison of Bent Responses Between North Side and South Side

465
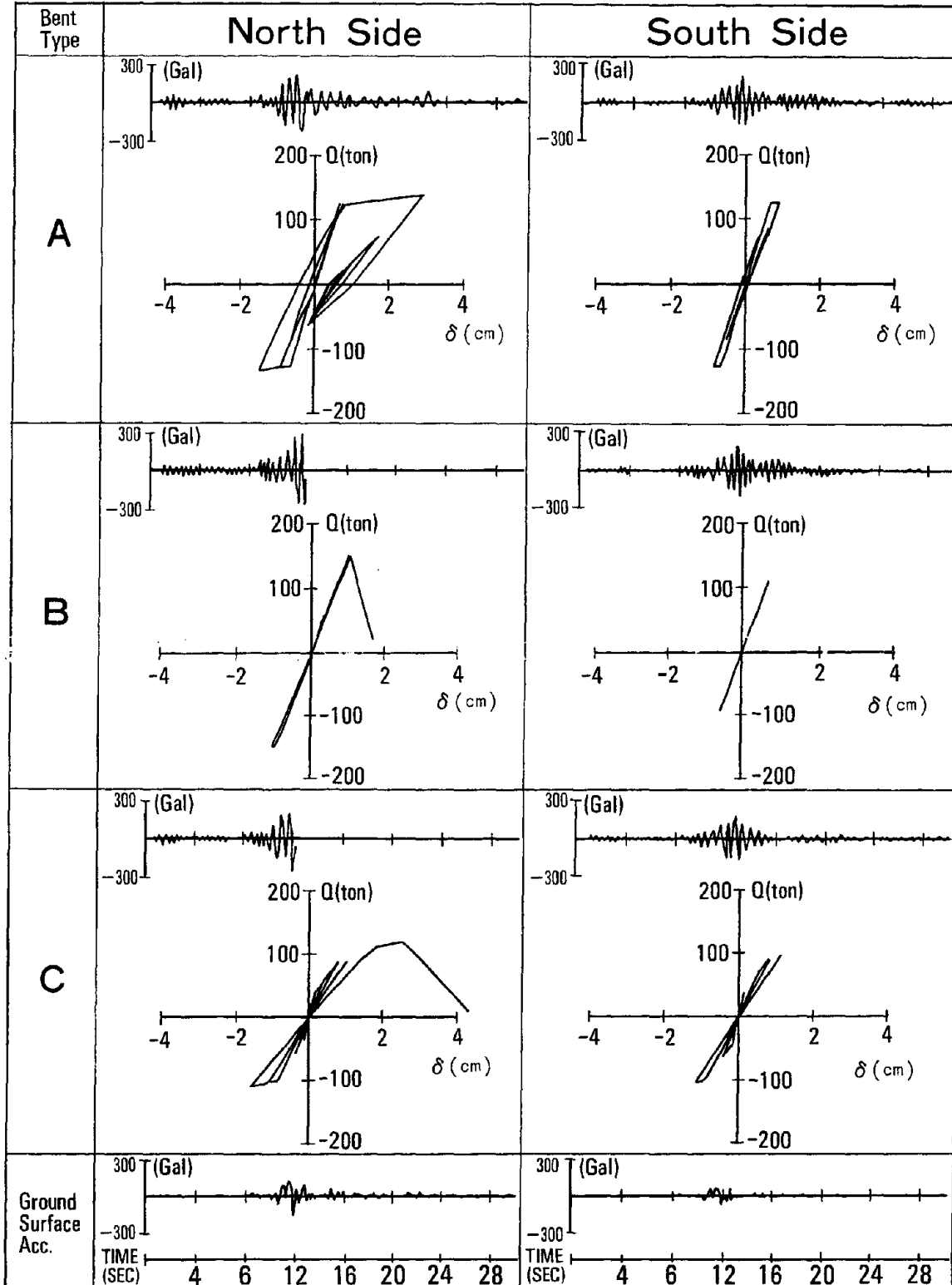
type bents, the upper story collapses immediately after the maximum ground surface acceleration attained. On the other hand in the south side, both type bents survive with some stiffness reduction appearance. The A type bent in the north side does not collapse with hysteretic damping effect due to flexural yielding. This analytical performance ensures survival of actual No.95 and No.96 bents despite considerable damages observed. It is considered that flexural yielding type hysteresis characteristics significantly contribute on preventing bent from catastrophic collapse.

SEISMIC PERFORMANCE SIMULATION OF RETROFITTED BENTS

Static Nonlinear Behavior of Retrofitted Bents   After comparison with the destructive test results to verify accuracy of the present numerical prediction, the analytical results for the following dynamic response analysis are to be discussed.

The first model for verification is the retrofitted No.46 bent[14], presently categorized as a B type bent. The jacking forces with prestressing rods for bent cap flexural strengthening are modeled by a pair of nodal forces and prestressing rods for column confinement and diagonal rock bolts in the beam column joint are respectively modeled as one of reinforcements. A Grade 40 steel is assumed for rock bolts and steel tubings to be combined with prestressing rods for column confinement.

Inadequate and insufficient anchorage effect of the bent cap lower reinforcement (D57) as described in the former section, should be considered. The insufficient anchorage directed depression is modeled by reducing yielding strength of D57 rebar in the joints based on the pull-out test results[15] which provided the developed tensile stress-bar size relationship of reinforcing bar. Material constants and another assumption in the analysis are similar with those provided in the former section.

A comparison between experimental and analytical load-displacement relationship is shown in Fig.17, where the analytical result generally predicts flexural type failure with fairly good agree-
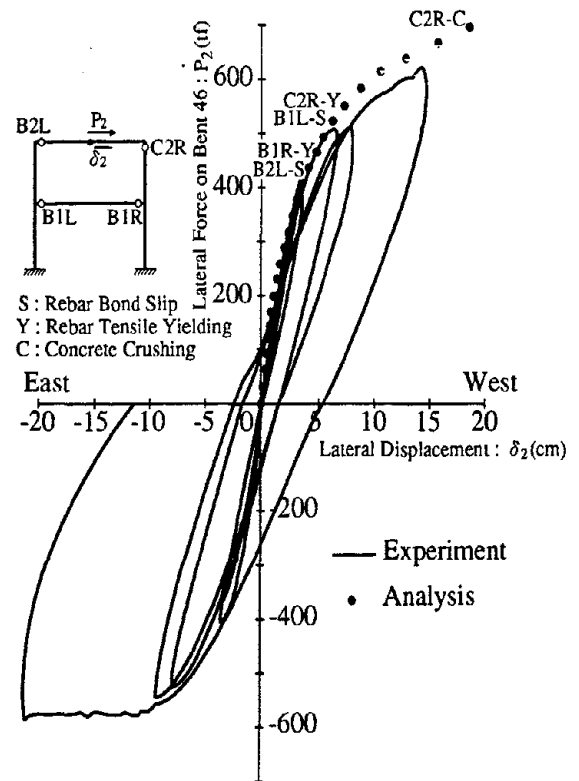

Fig.17 Load-Displacement Relationship (Retrofitted Bent-No.46)

466

ment with the experimental result.

Analytical load-displacement relationships, which are to be idealized for the hysteresis model in the following dynamic response analysis, are shown in Fig.18. This is the same type bent as that described above. The locations of yield hinges produced are also completely same as that. However, they appear in about 10% earlier load stage because of loading imposed on both upper and lower bent caps.
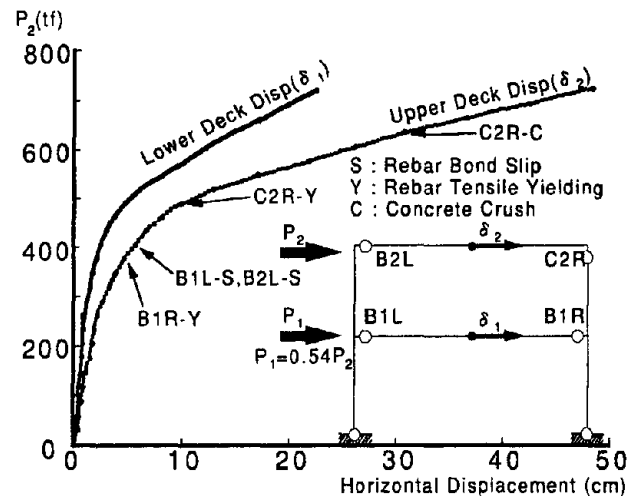

Fig.18 Load-Displacement Relationship (Retrofitted B Type Bent)

Design Response Spectrum and Input

Motion   Fig.19 illustrates elastic acceleration response spectrums by the previously predicted acceleration wave on the Cypress north side and the representative acceleration records in the past. The elastic seismic response spectrums for three soil types specified in the Seismic Design Guideline[16] are also shown. Design response fitted waves are respectively produced for three soil types by modifying acceleration amplitude of these waves with its phase angle unchanged.

Nonlinear Dynamic Response of Retrofitted Bents   A three degrees of freedom system model is used for both the Cypress wave and the modified Cypress wave, while a two degrees of freedom system model is used for another three modified waves because foundation and ground condition are not identified. The Takeda Model with tri-linear type enveloping is also idealized for both upper and lower stories.
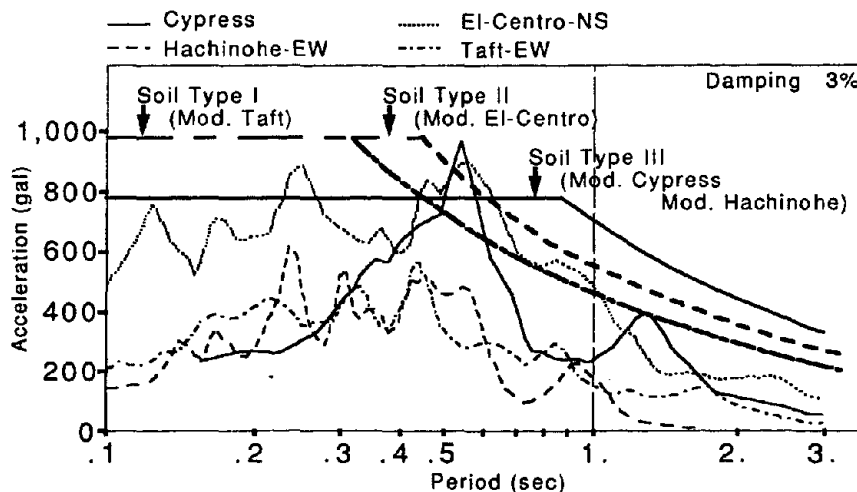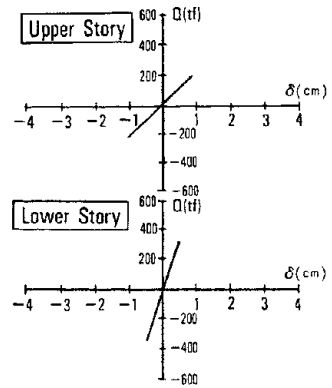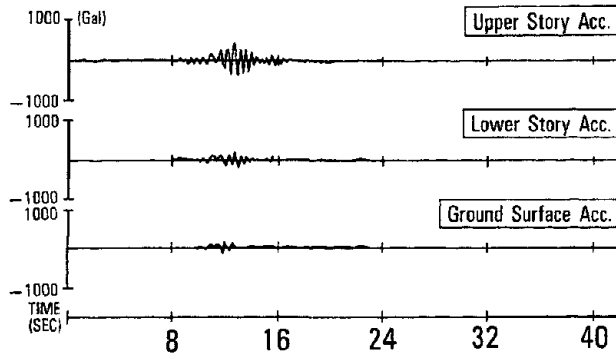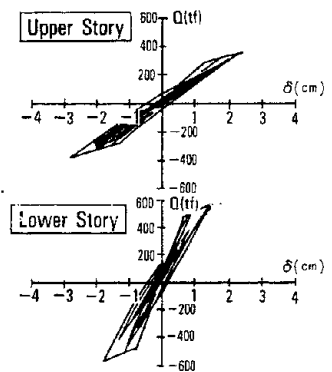

Fig.19 Elastic Acceleration Spectrum

467
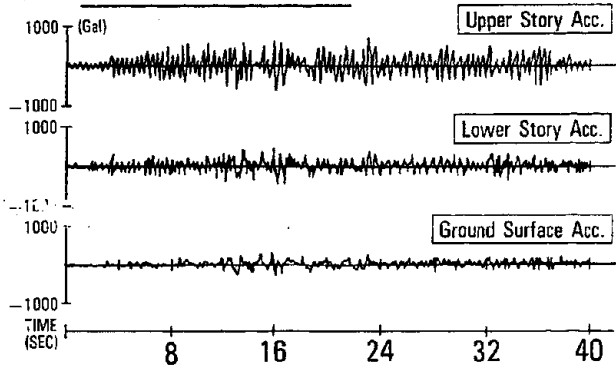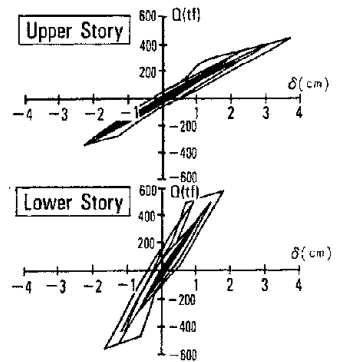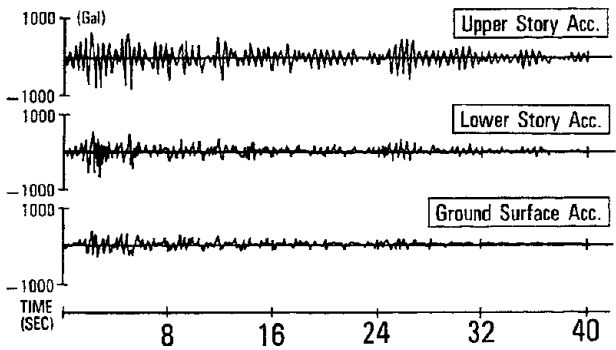
Fig.20 Seismic Response of Retrofitted Bent (B Type) - Acceleration Time History and Shear Force-Relative Displacement Hysteresis

468

Table 3 Seismic Performance of a Retrofitted Bent

Input Earthquake	Story	Input		Response			Safety Factor	
		y_{0max} Max. Vel. (cm/sec)	$\ddot{y}_{0max}$ Max. Acc. (gal)	$(y_0+\delta)_{max}$ Max. Acc (gal)	δ_{max} Max. Disp. (cm)	Q_{max} Max. Shear Force (tf)	Q_y/Q_{max} Strength	δ_u/δ_{max} Ductility
Cypress	2	24	173	398	1.00	222	2.23	16.30
	1			221	0.51	352	2.13	—
M.Cypress	2	68	345	635	2.33	349	1.42	7.00
	1			397	1.28	527	1.42	—
M.Hachinohe	2	49	310	680	2.84	383	1.29	5.74
	1			481	1.75	567	1.32	—
M.EL-Centro	2	47	383	810	3.65	437	1.13	4.47
	1			685	1.80	571	1.31	—
M.Taft	2	52	386	729	3.04	396	1.25	5.36
	1			491	1.52	547	1.37	—
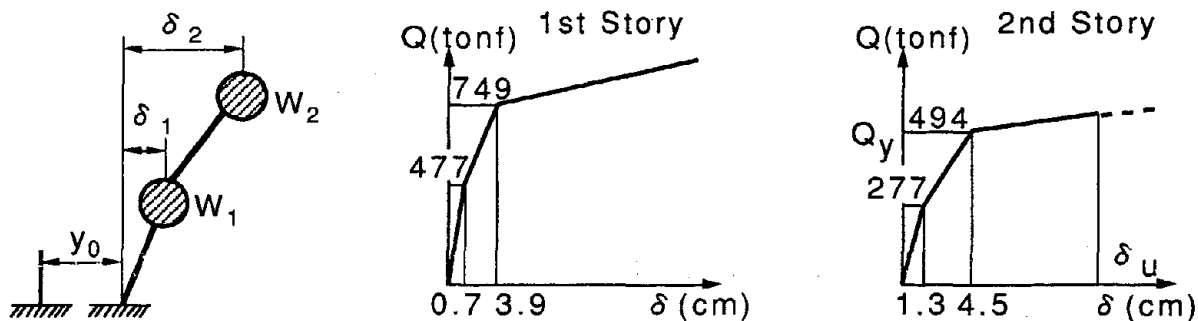
Analytical results are represented in Fig.20. For the original Cypress wave, both upper and lower story responses remain in elastic. Except this case, the shear force reaches beyond elastic limit but not yielding for any cases. The maximum response and the seismic performance evaluation in strength and ductility are provided in Table 3 for each input motion respectively, where the ultimate strength and the ultimate displacement are temporarily defined respectively by the yielding shear force Q_y and by the relative displacement δ_u when concrete crush initiates at the upper story column top. For all input waves, sufficient safety factor is assured in both strength and ductility. These results indicate that if the present type bent is strengthened in shear so that flexural-yielding-type performance be assured, sufficient margin in seismic performance can be provided against not only the Loma Prieta earthquake but the input motions consistent with the current seismic design guideline as well.

CONCLUDING REMARKS

Based on the results presented, a number of conclusions can be summarized as follows:
1) The one dimensional multiple reflection theory with an equivalent linearization method provided reasonable prediction in the amplified ground motion where shear strain ranges from 10^{-5} - 10^{-4}.
2) The two dimensional FE analysis predicted nonlinear behaviors of the existed bents and of the retrofitted bent up to the failure with good agreements in comparison with experimental results.
3) The multi degrees of freedom system nonlinear response analysis, on the basis of systematized analyses, i.e. on the amplified ground motion, on the soil-foundation interaction and on the nonlinear behavior of the bents up to the ultimate, provided rational explanation for the sequential collapse scenario of the Cypress Viaduct.
4) The present type of bent retrofitted provides sufficient seismic performance against input motions with acceleration amplitude consistent with the current seismic design guideline.

ACKNOWLEDGEMENT

REFERENCES

[1] The Earthquake Engineering Committee :Reconnaissance report on the Loma Prieta Earthquake of Oct.17,1989 2.2 Analysis on the Damage Features of the Cypress Viaduct Caused by the Loma Prieta Earthquake of 1989, Proc.JSCE, Vol.422/I-14,Oct.1990

[2] Caltrans:Log of Test Boring Concerning Cypress Viaduct

[3] Caltrans:Borehole Velocity Surveys at the Embarcadero in San Francisco and the Cypress Structure in Oakland, August 1990

[4] Seed,H.B.,et al.:Implication of Site Effects in the Mexico City Earthquake of Sept.1985 for

Earthquake Resistant Design Criteria in the San Francisco Bay Area of California, UCB/EERC / 03,Mar.1989

[5] Helly E.J. et al.:Flatland Deposits of the San Francisco Bay Region, California-Their Geology and Engineering Properties, and Their Importance to Comprehensive Planning, Geological Survey Professional Paper 943

[6] Ohmachi T. et al.:Ground Motion Characteristics in the San Francisco Bay Area Detected by Micro Tremor Measurements - A Preliminary Assessments -, Tokyo Institute of Technology No.800104, Nov.30, 1989

[7] Nims,D.K. et al.:Collapse of the Cypress Street Viaduct as a Result of the Loma Prieta Earthquake, UCB/EERC - 89/16, Nov.1989

[8] Moehle,J.P. and Mahin,S.A.:Implications of Nondestructive and Destructive Tests on the Cypress Street Viaduct Structure, 7th US-Japan Workshop on Bridge Structure,UJNR,May 1990

[9] Housner,G.W. et al.:Competing Against Time, Report to Governor George Deukmejian from the Governor's Board of Inquiry on the 1989 Loma Prieta Earthquake, May 1990

[10]Hibbit, Karlsson and Sorensen, Inc.:ABAQUS Theory Manual, Version 4.6, 1987

[11]Naganuma K.:Final User's Manual (Version 7), Technical Research Institute,Obayashi Co.Ltd.

[12]Caltrans: As Built Plans,10th to Distribution Structures,July 26,1957

[13]Takeda,T. et al.:Reinforced Concrete Response to Simulated Earthquakes, Jour. Structural, Div., ASCE,Vol.96, No.ST12, pp.2557-2573, 1970

[14]Caltrans:Cypress Street Viaduct Bent 45,46 and 47 Retrofit Detail - As Built Drawing,Dec.1989

[15]Park,R. and Paulay,T.:Reinforced Concrete Structures, John Wiley & Sons,pp.407-410,1975

[16]Applied Technology Council: Seismic Design Guideline for Highway Bridges, June 1986, 2nd Printing

SECOND U.S.-JAPAN WORKSHOP
ON SEISMIC RETROFIT OF BRIDGES

Developing a Mechanical Load-Transmission
Retrofit Device for Providing Integrity
to Structures During Earthquakes
*William Tanzo, Hiroshi Mutsuyoshi
and Akio Tsuzuki*
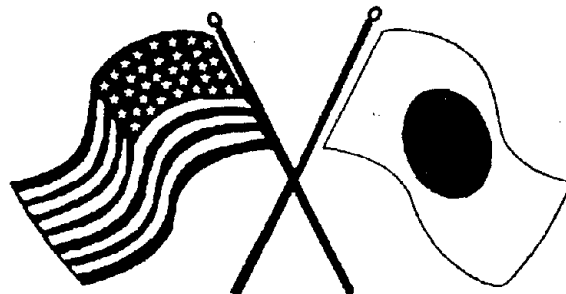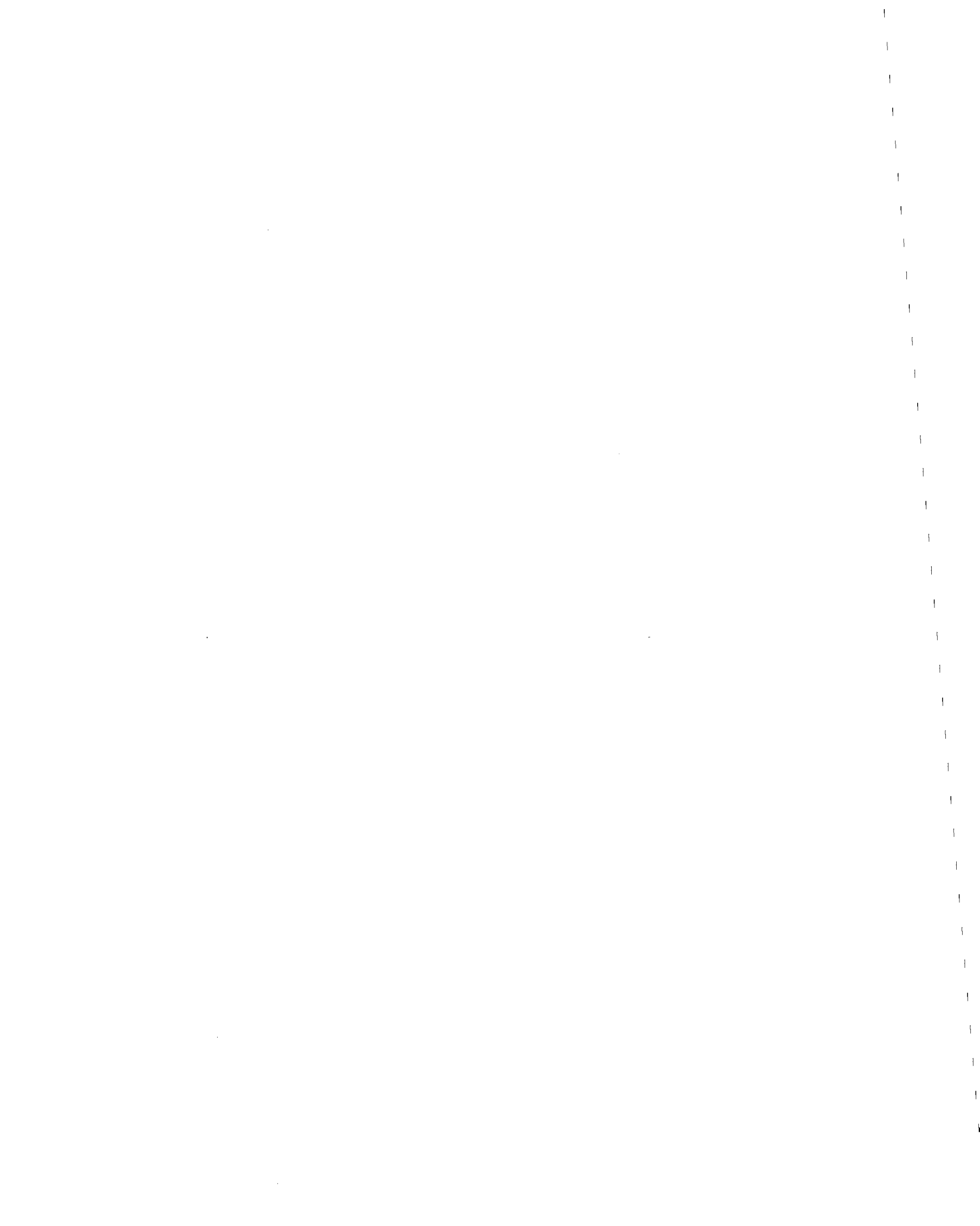
DEVELOPING A MECHANICAL LOAD-TRANSMISSION RETROFIT DEVICE FOR PROVIDING INTEGRITY TO STRUCTURES DURING EARTHQUAKES

William TANZO
Structural Materials Laboratory
Dept. of Civil & Environmental Engg.
Saitama University, Japan

Hiroshi MUTSUYOSHI
Structural Materials Laboratory
Dept. of Civil & Environmental Engg.
Saitama University, Japan

Akio TSUZUKI
Design First Section, Engineering Dept.
Kawaguchi Metal Industries Co., Ltd.
Kawaguchi, Saitama, Japan

ABSTRACT

A new mechanical load-transmission device is developed which enables transmission of lateral loads to piers with movable bearing supports when subjected to earthquake loadings while allowing unrestrained movement of deck during ambient temperature changes. The piston-cylinder housing is robust in construction and the silicone putty compound used is inert and stable which would make the device perform satisfactorily under adverse conditions while requiring minimum maintenance. Test results of the device under cyclic loadings are presented.

INTRODUCTION

It has been observed in many post-earthquake reconnaissance investigations that deck spans had fallen off in several damaged bridges during severe earthquakes. The falling off of the spans may be due to: (1) pull out of anchor bolts in fixed bearing supports or toppling of rocker bearing supports, (2) failures of the piers with the fixed supports, (3) rigid-body rotation of the piers due to liquefaction of the supporting soil. In all these cases of bridge failures, inherent strength and ductility of even properly designed bridge piers are not at all utilized due to inefficient transfer of the induced inertial forces from the heavy deck spans to the supporting piers and substructures.

The objective of this research program is to develop innovative mechanical devices that provides appropriate stiffening and damping mechanisms for effective transmission of loads between the superstructures and the substructures in bridge structures. A linear-type device for lateral load transmission is the subject of the initial phase of this research project, and a rotary-type device has big potential for preventing rigid-body rotation of the piers during soil liquefaction.

In this paper will be presented the preliminary development of such devices utilizing the frequency-dependent properties of silicone putty, a compound which easily deforms under slowly applied loads but will stiffen under shock or impulsive loads.

SEISMIC RETROFIT PROGRAMS

It is quite interesting to note that the seismic retrofit programs in the U.S. and Japan evolved in parallel to each other. Due to damages suffered during the 1964 Niigata Earthquake and the 1971 San Fernando Earthquake, the first stage of seismic retrofit program had focused on the development and installation of stoppers, restrainers [Selna and Malvar, 1984], seat extension, and other devices for preventing collapse of spans [Kawashima 1990]. The second stage of the seismic retrofit program is currently focusing on the improvement of column ductility based on experiences of the 1989 Loma Prieta Earthquake, 1978 Miyagi-ken-oki Earthquake, and the 1983 Nihon-kai-chubu Earthquake. Excellent reviews of the development of seismic retrofit philosophy are given by Kawashima [1990], Nutt and Cooper [1984], and Roberts [1991].

Current retrofit programs have been on component retrofitting. Kawashima [1990] noted that countermeasures made only to prevent damages suffered in past earthquakes may led to failures in the next weak points in future earthquakes. This has led to the revisions in the latest design specifications on highway bridges that requires the consideration of the total seismic safety of highway bridges [Kawashima et al, 1992].

Several newly developed devices (menshin bearings, damper-stoppers) have been used to distribute lateral forces among the piers. These have been used to retrofit simple span bridges in which the decks are made continuous and the existing bearings are replaced with menshin bearings [Naganuma et al, 1990]. In recent years, many newly constructed long-span bridges have avoided the use of bearings supports and instead used structural joints to transmit loads from the continuous girder to the piers [Tajima et al, 1990; 1982]. However, seismic behavior of joints is complex and the seismic design and analysis of such structures require extensive efforts. The girder-bearing-pier bridge structural system still offers simplicity, elegance, and generous accommodation for future expansion. Better seismic performance can be achieved through the utilization of mechanical load-transmission devices and possibly mechanical load-limiting devices to provide structural integrity.

NEW MECHANICAL LOAD-TRANSMISSION DEVICES

A few damper-stopper devices have been developed which function as fixed supports during earthquakes to enable lateral load distribution to piers with movable bearing supports while allowing movement of the deck due to ambient temperature changes. These developed devices

include a cylinder-type oil damper, viscous stopper, a viscous shear-type stopper, and a cable damper [cited in Kawashima et al, 1992].

The main objective of this research is to develop a device with similar functions, but possessing robustness that can better withstand adverse conditions and requiring minimum maintenance. In addition, a load-limiting function is considered as a possibility rather than just load transmission and displacement-limiting functions. The device uses a simple piston-cylinder unit (Fig. 1) similar in construction to oil damper and lead-extrusion damper [Skinner, Robinson, McVerry, 1993]. Unlike the other developed damper-stopper devices as mentioned above, the new device is mechanically simple and has no bypass valves nor other appendages that might malfunction or be rendered nonfunctional during severe shakings.
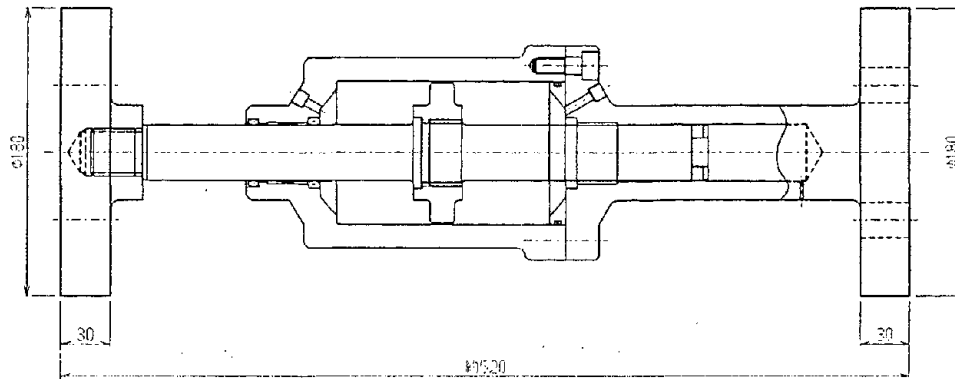
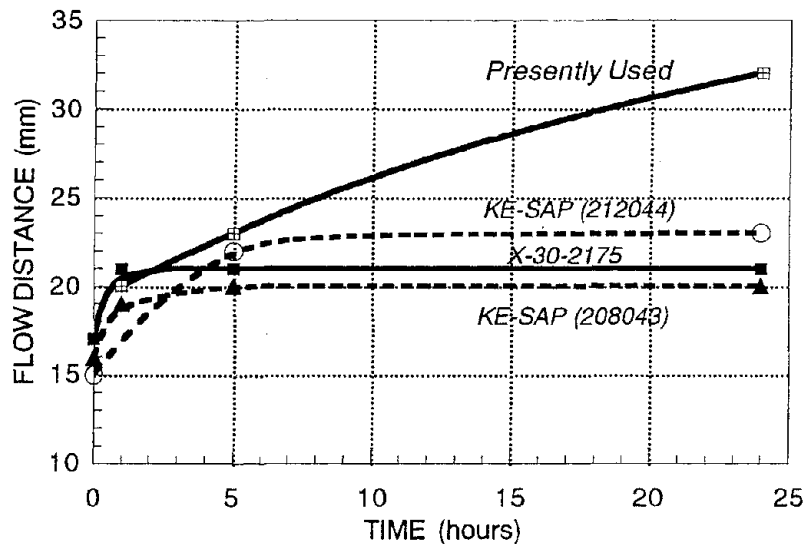Fig. 1   A New Mechanical Load-Transmission Device

Fig. 2   Flow Characteristics of Silicone Putty Used

The material used inside the cylinder is silicone putty, a compound which easily deforms under slowly applied loads but will stiffen under shock or impulsive loads. Silicones are polymer materials that are inert and greatly stable in both high and low temperatures. These silicone polymers are also available in other forms such as fluids, sealants, resins, and rubbers. The silicone putty compound can be manufactured with various 'flow' properties. Fig. 2 shows the flow properties as provided by the manufacturer. The results were obtained by measuring the increase in diameter of a fixed volume of putty placed in a circular area. The one that is presently used in the prototype device has the highest flow behavior.

The silicone putty is vacuum-packed into the piston-cylinder housing. Under applied loads, the putty compound is squeezed from one end of the cylinder to the other end through openings around or through the piston. With properly designed orifice opening and size of piston and cylinder, desired values of damping and stiffening can be obtained for the range of loading amplitude and frequency. The device is designed to be attached to the underside of the girder near a movable support and the top of the pier. In such manner, it allows movement of the movable support during ambient temperature gradients, but will fix the girder-pier connection during shock or earthquake loadings thereby transmitting a share of the lateral load to the piers with movable supports. Such devices are particularly suitable for seismic retrofit of simple span bridges and in newly constructed long-span bridges. Similar devices called STU has been used to relieve increasing traction and braking loads in the viaducts carrying London's Docklands Light Railway [Pritchard 1989].

TEST PROGRAMS

The preliminary objective is to investigate the basic mechanical behavior of prototype devices under cyclic loads. From these results, suitable putty compounds and piston-cylinder designs are evaluated and improvements are made to obtain the desired device performance. A 5-tonf capacity prototype (Photo 1) was first fabricated and tested.

Most recently, a 10-tonf capacity is fabricated (Fig. 1 and Photo 2) and subjected of repeated cycles of force-controlled and displacement-controlled loadings. Photo 3 shows the loading setup used in the tests.

The device is first tested under cyclic loading of different amplitudes and frequencies to investigate its basic mechanical properties. In the next phase of the investigation, a pier model with the device will be subjected to displacement-controlled cycling loadings for observing the load transmitted in a pier. Lastly, a simple span bridge prototype with the newly developed device will be tested under force-controlled cyclic loadings in which the lateral load distribution between the piers is investigated.

478
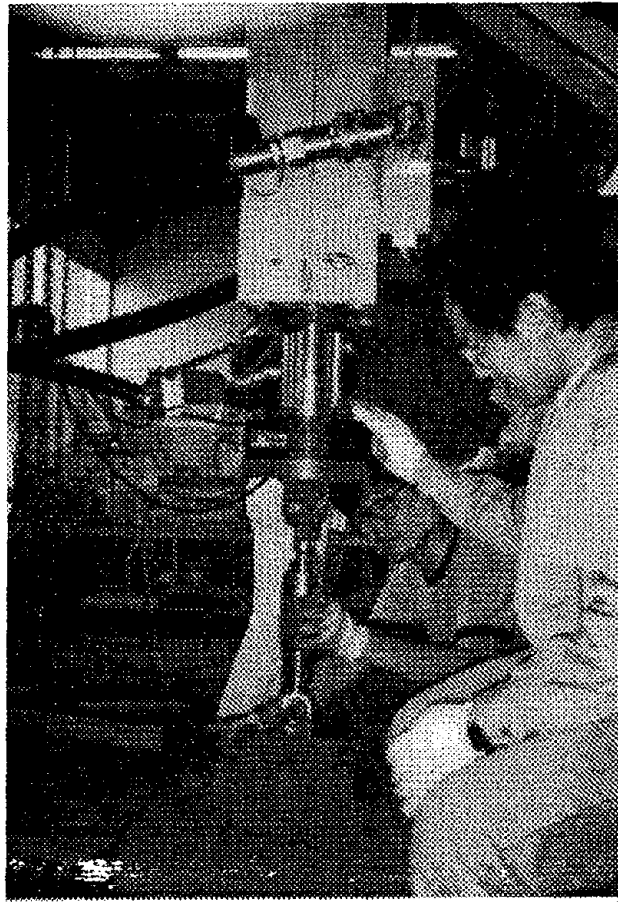
Photo. 1   The 5-tonf Capacity Prototype Used in Initial Investigation
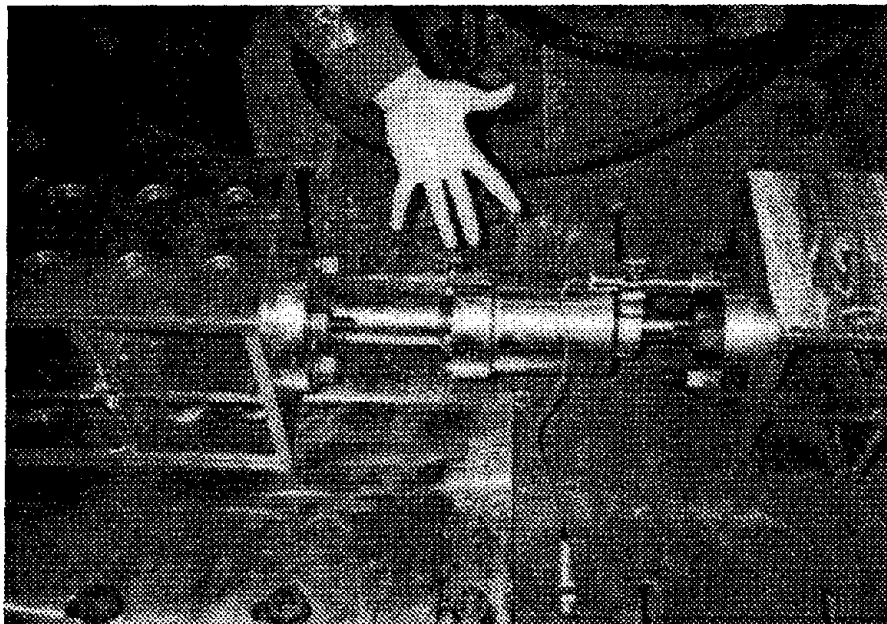
Photo. 2   The 10-tonf Capacity Prototype

Photo. 3   Setup for Testing Cyclic Mechanical Behavior

TEST RESULTS AND DISCUSSIONS

Test results under force-controlled loading under different frequencies are presented. Figs. 3(a) to 3(o) show the load-deformation behavior from 0.001 Hz (the slowest setting available in the loading actuator used) to 7 Hz under cyclic loading from -6. tonf to +6. tonf. It can be observed that the silicone putty readily allows deformation with significant hysteretic damping under low frequencies. It can be further observed that the device exhibits the stiffening effect at about 0.1 Hz as shown in Fig. 3(g). Beyond 0.1 Hz, no remarkable changes in the load-deformation behavior can be observed as shown in Figs. 3(h) to 3(o). That is above 0.1 Hz, the silicone putty has acted as almost a rigid body and stiffness is provided by the load-deformation characteristics of the end rod of the cylinder and the piston. Thus, it would be possible to design such mechanical load-transmission devices to have different stiffnesses to suitably distribute seismic lateral loads depending on the relative strengths of the piers. In addition, it seems possible to provide the end rod with a load-limiting mechanism (e.g., yielding element) after the load transmitted to the pier has reached the design capacity of the pier.

The load-deformation curves under two cases of displacement-controlled loading are shown in the plots in Fig. 4. It can be observed that load induced (from about 5. tonf for 5 Hz case) is significantly reduced (to less than 0.7 tonf for 0.001 Hz case) when subjected to slow loading. Under service loads due to temperature changes, a displacement-controlled cyclic loading with a period of 24 hours would probably induced almost no load resistance.

480
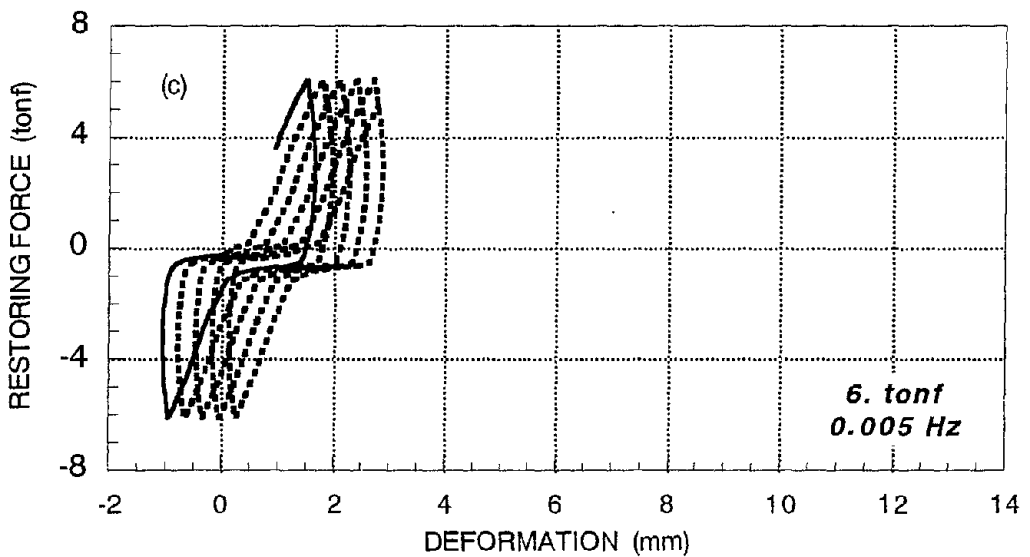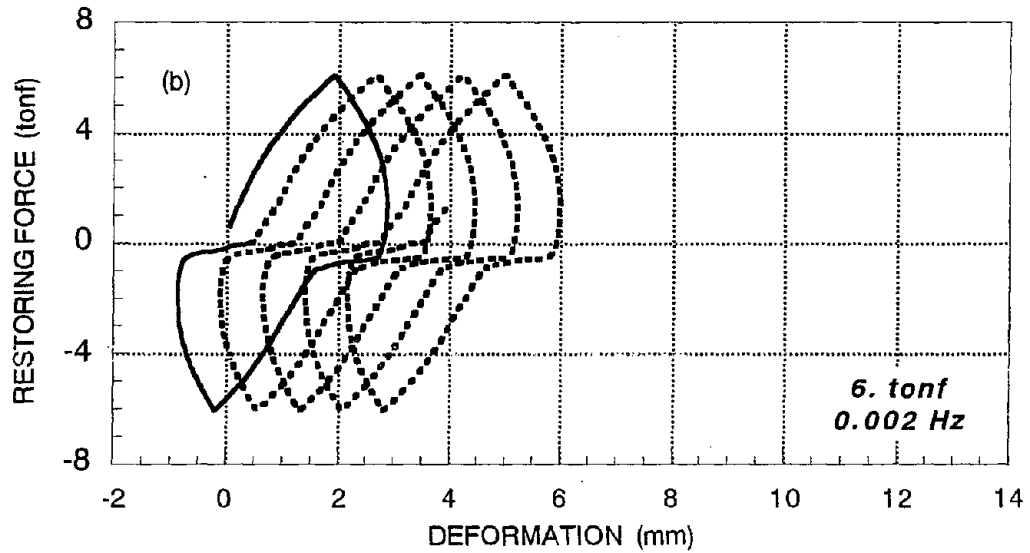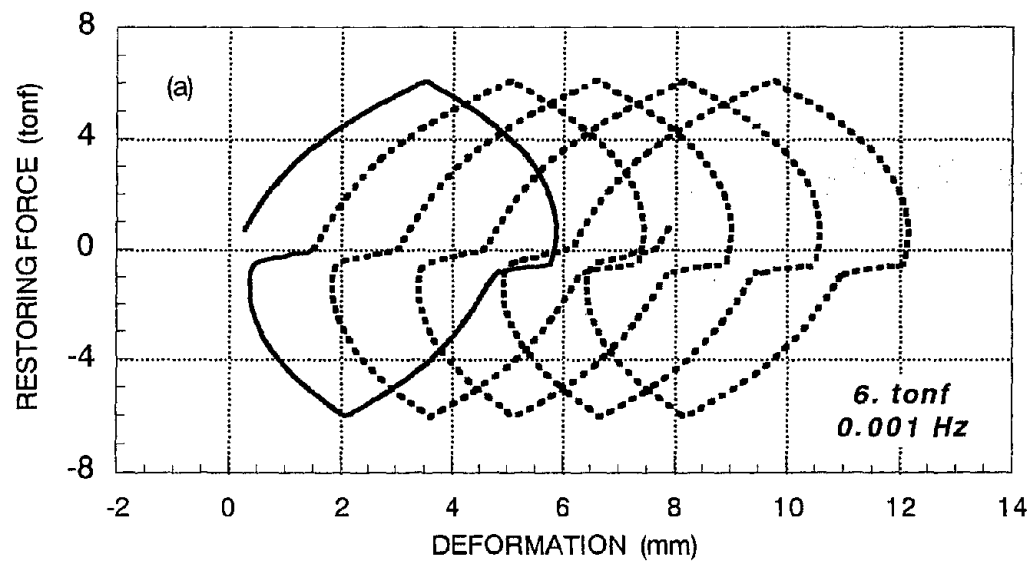
Fig. 3   Load-Deformation Behavior Under Load-Controlled Cyclic Loading

481
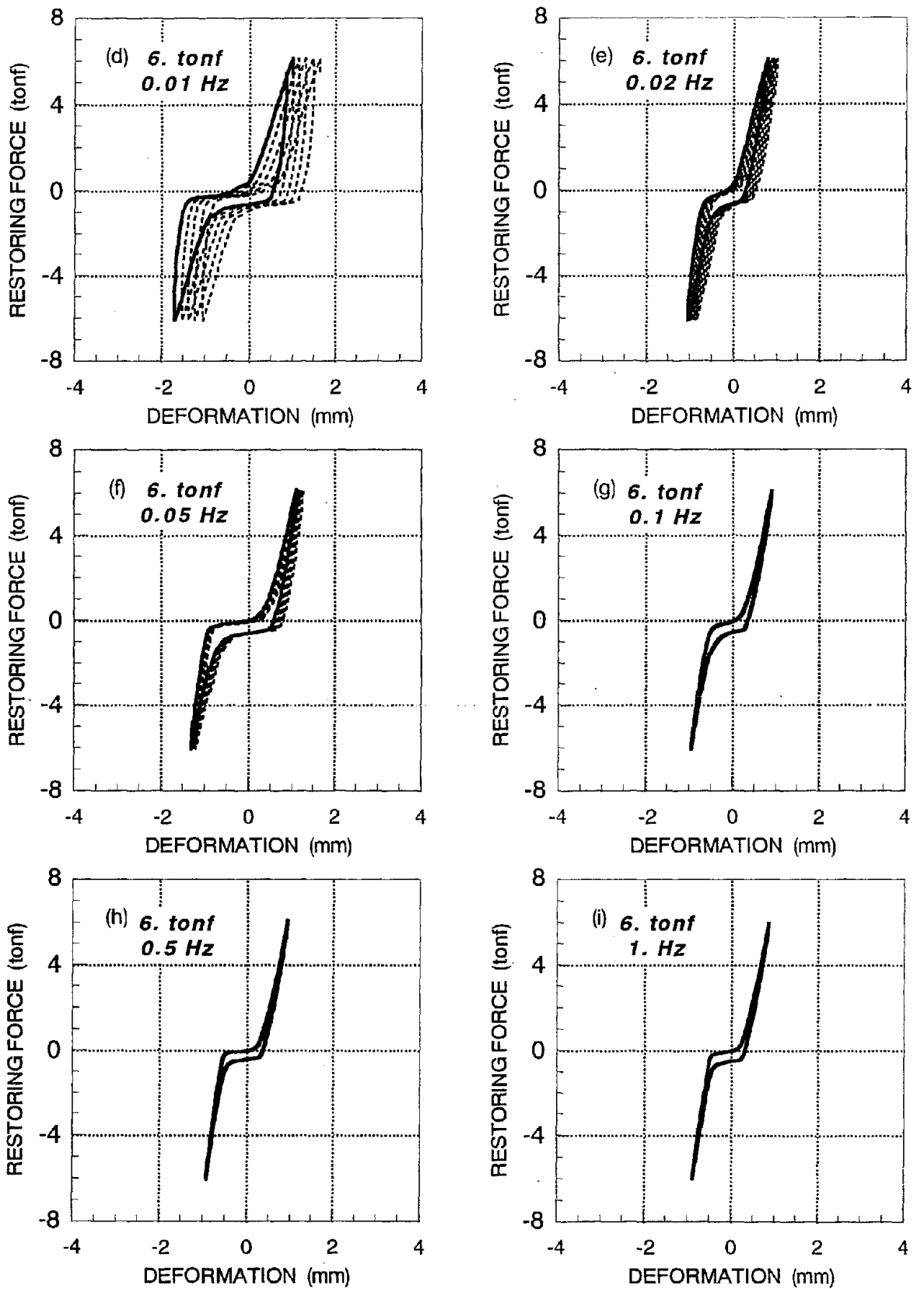
Fig. 3 cont'd   Load-Deformation Behavior Under Load-Controlled Cyclic Loading
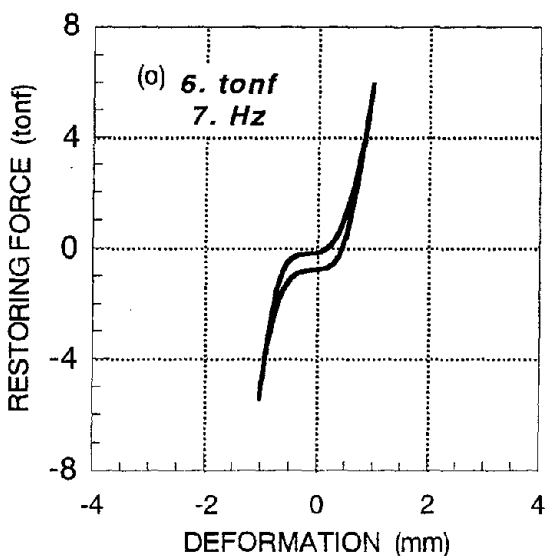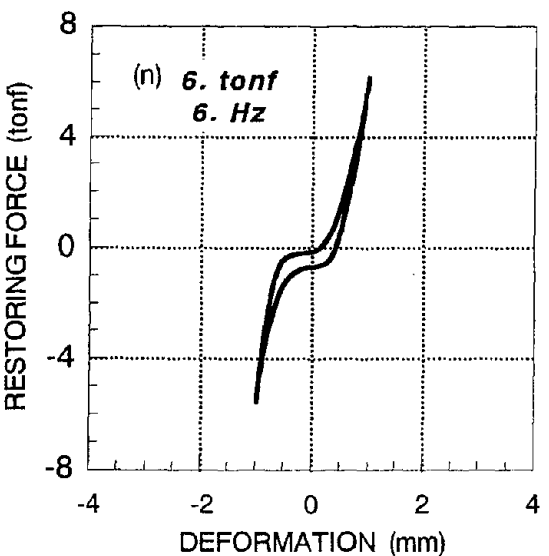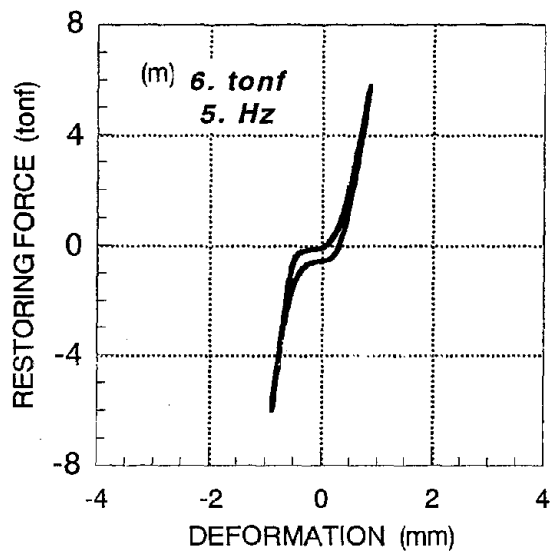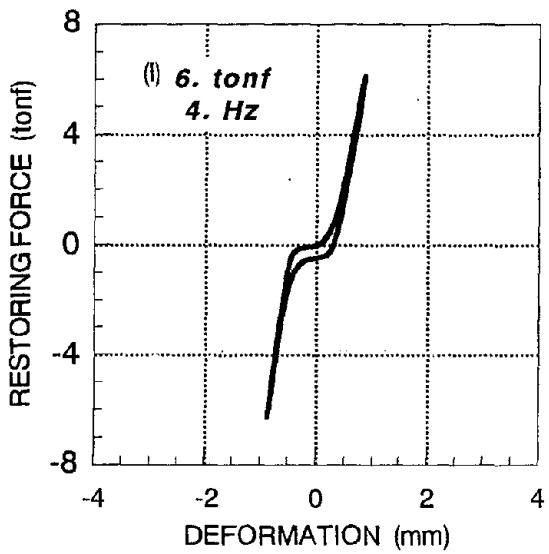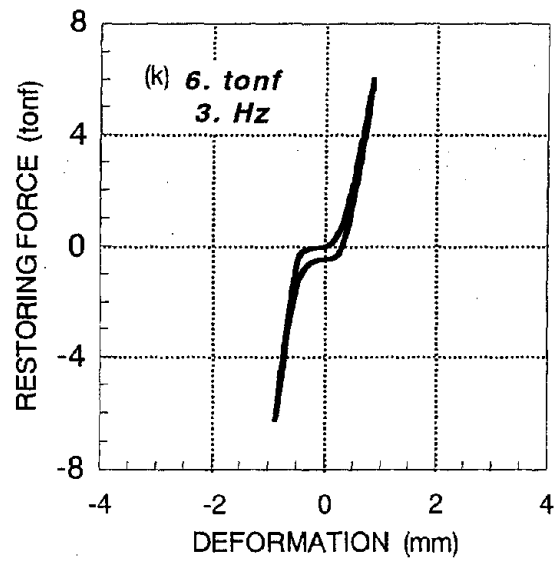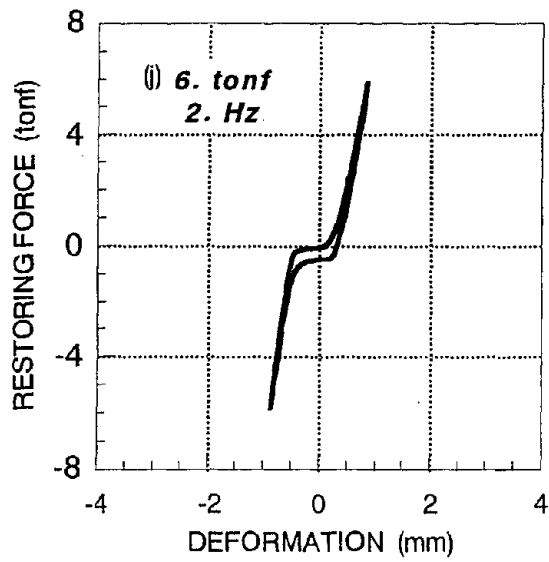
Fig. 3 cont'd   Load-Deformation Behavior Under Load-Controlled Cyclic Loading
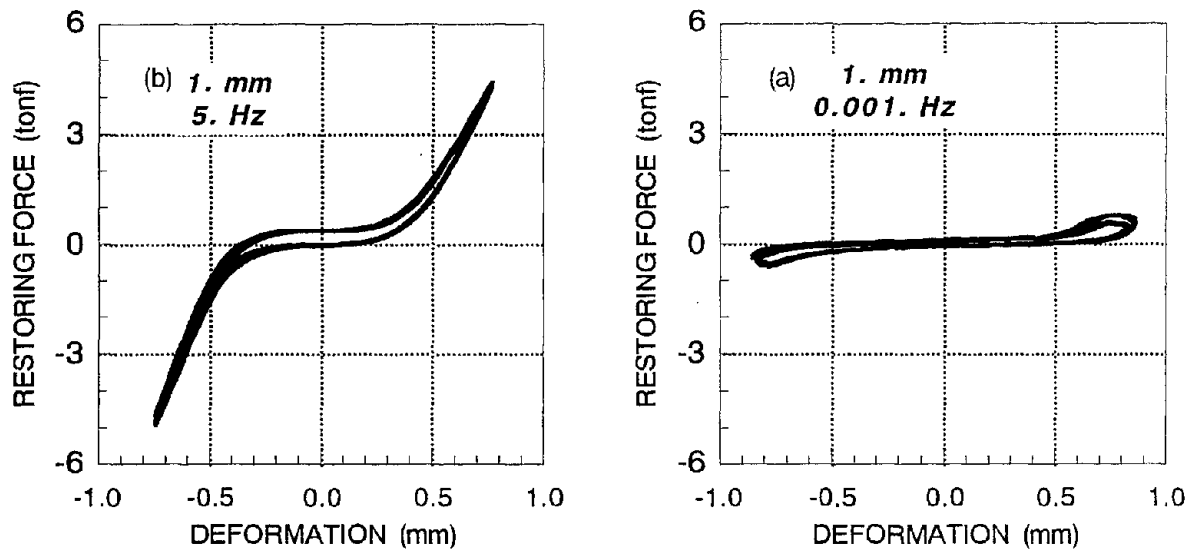
Fig. 4   Load-Deformation Behavior Under Displacement-Controlled Cyclic Loading

FURTHER CONSIDERATIONS AND CONCLUDING REMARKS

A research project is initiated on the development of a mechanical load transmission device that enables transmission of lateral loads to piers with movable bearing supports when subjected to earthquake loadings while allowing unrestrained movement of deck during ambient temperature changes. The piston-cylinder housing is of robust in construction and the silicone putty compound used is inert and stable which would make the device perform satisfactorily under adverse conditions while requiring minimum maintenance.

By effectively utilizing as a retrofit device, it would enable lateral load distribution among the piers. This avoids concentrated loads that would cause concentrated damage on certain piers, anchor bolts, and bearings. Moreover, structural integrity is provided which would greatly enhance seismic safety under adverse conditions such as severe shaking and soil liquefaction.

In this paper, test results of a preliminary investigation conducted to obtain basic load-deformation behavior of the mechanical load-transmission device under cyclic loadings are presented. The effect of packing, piston and cylinder sizes, putty material properties will be subjects of further investigations. Furthermore, it is necessary to have a simple analytical model of the devices in order to conduct earthquake response studies.

ACKNOWLEDGEMENTS

484

REFERENCES

K. Kawashima [1990]: "Seismic Design, Seismic Strengthening and Repair of Highway Bridges In Japan," *Proceedings, 1st U.S.–Japan Workshop on Seismic Retrofit of Bridges,* Tsukuba, Japan.

K. Kawashima, K. Oshima, K. Hasegawa, S. Unjoh, K. Okeda, Y. Maehara[1992]: *Computational Examples for Seismic Design of Highway Bridges,* Sankaido. (in Japanese)

D. Moore [1993]: *Viscoelastic Machine Elements: Elastomers and Lubricants in Machine System,* Butterworth-Heinemann Ltd.

T. Naganuma, S. Mizobuchi, H. Uno [1992]: "Development of Jointless System with Menshin Bearing for Existing Simple-Spanned Steel Bridges," *Proceedings, 2nd U.S.–Japan Workshop on Earthquake Protective Systems for Bridges,* Tsukuba, Japan.

R. Nutt, J. Cooper [1984]: "Seismic Retrofitting Guidelines for Highway Bridges," *8th World Conference on Earthquake Engineering,* San Francisco.

B. Pritchard [1989]: "Bridge Strengthening Using Load Relieving Techniques," *IABSE Symposium on Durability of Structures,* Lisbon.

J. Roberts [1991]: "Recent Advances in Seismic Design and Retrofit of California Bridges," *Proceedings, 4th U.S.-Japan Workshop on Earthquake Disaster Prevention for Lifeline Systems,* Los Angeles, Calif., pp. 125–136.

L. Selna, L. Malvar [1984]: "Box Girder Bridge Hinge Restrainer Test Program," *8th World Conference on Earthquake Engineering,* San Francisco.

R. Skinner, W. Robinson, G. McVerry [1993]: *An Introduction to Seismic Isolation,* John Wiley & Sons.

J. Tajima, A. Machida, H. Mutsuyoshi [1982]: "Behavior of Joints between Steel Members and Concrete Members," *Transactions of the Japan Concrete Institute,* vol. 4, pp.469–476.

J. Tajima, Y. Ito, A. Machida [1990]: "Joints in Hybrid Bridge of Steel Girder and Concrete Pier," *IABSE Symposium on Mixed Structures including New Materials,* Brussels, pp. 425–430.

I. Ward, D. Hadley [1993]: *Mechanical Properties of Solid Polymers,* John Wiley & Sons.

Second U.S.-Japan Workshop on Seismic Retrofit of Bridges

Abstracts
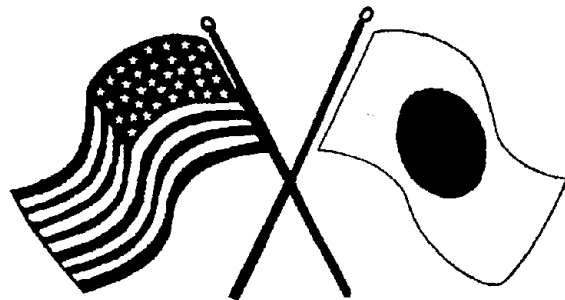
January 20 and 21, 1994
Berkeley Marina Marriott Hotel
Berkeley, California

STRUCTURAL IDENTIFICATION OF BRIDGES FOR CONDITION AND VULNERABILITY ASSESSMENT

by

A.E. Aktan, Professor
Director of Infrastructure Institute
University of Cincinnati, Ohio 45221-0071
Ph: 513-556-3689; Fax: -2599; email: aaktan@uceng.uc.edu

We should strive to successfully and *uniformly* mitigate our seismic risk exposure at different regions of the U.S. The first requirement for this is an understanding of the hazard, vulnerability and consequences of facility failure. Then, it would be possible to convince the public officials and politicians to develop region-specific infrastructure performance criteria and corresponding risk-reduction policies, followed by emergency response planning and longer-term hazard mitigation planning. It is interesting that an emergency response plan in the contemporary sense does not exist in many densely-populated urban areas in the U.S. This is due to the vast differences that exist in the public's awareness to seismic risk in different regions of the country. One consequence is that certain bridges in regions characterized as "low seismic zone" may be subjected to a much higher risk of lack-of-performance than what is considered acceptable in the Western regions of the country.

Within the above described global problem of seismic risk mitigation, seismic vulnerability evaluation of those bridges that are critical to emergency response and post-earthquake recovery have to be conducted through a comprehensive, facility-specific manner. We may consider the excellent efforts for evaluating the Bay and Golden Gate Bridges in this context. Meanwhile, type-specific evaluation procedures have to be developed for repeating bridge systems that may not fall into the critical category. One possible strategy for overcoming both the policy and the technical constraints that obstruct seismic research and implementation is to combine the seismic risk mitigation problem with the more general problem of infrastructure preservation. As part of this strategy, the writer has been exploring a structural-identification based method for structural condition and reliability evaluation. Modal testing is the principal experimental component of the method which leads to seismic vulnerability evaluation and retrofit design as a corollary. This method has been applied to seven bridges, three of which were tested to destruction. Two of the specimens were 80-year old steel through-truss bridges, with critical attributes corresponding to those of similar era monumental bridges which have to be reliably evaluated and preserved at all cost. The test bridges were subjected to retrofit, truck-load tests, modal tests and then to destructive testing by hydraulic actuators. One of the bridges also served as a real-life specimen for field exploration of an active-mass structural-control technique. The proposed paper will provide an overview of the structural condition/reliability/vulnerability evaluation procedure as exemplified on the two 80-year old truss bridges.

A COMPREHENSIVE METHOD FOR
BRIDGE SEISMIC RETROFIT PRIORITIZATION

Nesrin Basoz[1], Anne S. Kiremidjian[2]

Bridges are critical components in transportation systems. Damage to bridges by recent earthquakes has emphasized the need for seismic hazard mitigation. Seismic retrofitting, as a mean of hazard mitigation, must make efficient and effective use of available resources. Such retrofitting decisions under limited resources require that, a prioritization method be developed to rank the ensemble of existing bridges. The assessment of potential failures of existing bridges and of the socio-economic impact of such failure to a community are necessary for the ranking purposes.

A prioritization method is developed based on the importance and vulnerability of bridges. Seismic vulnerability is defined as the potential of a bridge to sustain significant damage or collapse when subjected to an earthquake. The vulnerability of a bridge depends on its seismic exposure, structural properties and design characteristics. For example, the material type, number of spans, continuity and seat width are some of the properties that play an important role on the structural performance of a bridge. ATC-13 (1985) defines earthquake engineering facility classes and corresponding damage probability matrices to represent possible damage levels that a bridge can sustain. Currently, ATC-13 defines only three bridge classes. These three classes do not provide adequate basis for effective assessment of vulnerability. Consequently, development of a more refined bridge classification is necessary. Such a classification will consider the basic attributes of a bridge's structural properties. In the proposed method, new bridge classes are defined based on structural properties. An expert system will be developed for classifying existing bridges into these bridge classes. A group of fragility function will be developed for each bridge class in order to define respective ground-motion damage relationships.

The failure of a bridge can impact the public safety and socio-economic well-being of a community. It can pose additional hazard and can delay post-earthquake disaster relief and restoration of community services. Thus, the prioritization must consider attributes relating consequences of failure of a bridge to public safety and socio-economic well-being of a community. Among the attributes that need to be considered are route type carried and crossed, average daily traffic and detour length. The importance of a bridge is closely related to its function within the transportation network system. The relative importance of bridges can be evaluated for emergency responses and long-term economic recovery conditions. The functionality of the transportation network should be preserved immediately after a major earthquake. Thus, connectivity network analysis is used to analyze the availability of bridges for emergency response purposes. For long-term economic recovery, however, a value model needs to be developed to properly determine the multi-attribute importance criterion.

The prioritization of bridges for seismic retrofitting and emergency planning purposes can be accomplished within the context of Geographic Information Systems (GIS) which integrates different types of information and procedures necessary for the overall ranking.

---

[1] Doctoral Candidate, The John A. Blume Earthquake Engineering Center, Department of Civil Engineering, Stanford University, Stanford, CA 94305-4020;

[2] Professor and Co-Director, The John A. Blume Earthquake Engineering Center, Department of Civil Engineering, Stanford University, Stanford, CA 94305-4020.

Seismic Vulnerability Evaluation of the Tacoma Narrows Bridge

by
David Brierley-Green, P.E.
Arvid Grant Associates, Olympia, Washington

Mark A. Ketchum, Ph.D., P.E
OPAC Consulting Engineers, Inc., San Francisco, California

J.P. Singh, Ph.D., P.E.
Geospectra, Inc., Richmond, California

The Tacoma Narrows Bridge, built in 1950 to replace an earlier structure in Washington State, has a main span of 2,800 ft (854 m) and total length (excluding viaducts) of 5,000 ft (1,524 m). This bridge, with the second-longest suspension span in the Western United States, is located in an area that is now known to be subjected to infrequent great earthquakes. Recognizing the potential vulnerability of the bridge, and with a desire to avoid damage in future earthquakes, the agency responsible for the bridge (the Washington State DOT) commissioned studies to evaluate its seismic vulnerability.

When the bridge was designed in the late 1940's, great care and detail were paid to its static design, as well as to wind loading and the dynamic influences of wind. Seismic design of the Tacoma Narrows Bridge, on the other hand, though forward looking for the era, is not in keeping with present day practice. The bridge towers are founded on caissons with maximum embedment of about 75 ft (23m) in 1000 ft (300 m) deep glacial till. The viaducts were built from the damaged remains of the previous, narrower bridge. Original seismic analysis was based on a static coefficient of 3.1% for the towers and 6.2% for the remainder of the bridge.

The scope of the studies included development of seismic performance criteria, geotechnical and seismic risk studies, synthesis of multi-support incoherent ground motions, soil-structure interaction analysis, response spectrum seismic analysis, linear and nonlinear dynamic structural analysis under multi-support incoherent ground motion input, field measurement of elastic and vibration properties, vulnerability assessment, plus identification of retrofitting concepts. Seismically interesting features of the bridge include its caisson foundations, its viaducts that are structurally coupled to the suspension spans, and its relatively deep and stiff suspended truss. This paper describes the scope, methods, and results of the seismic evaluation studies.
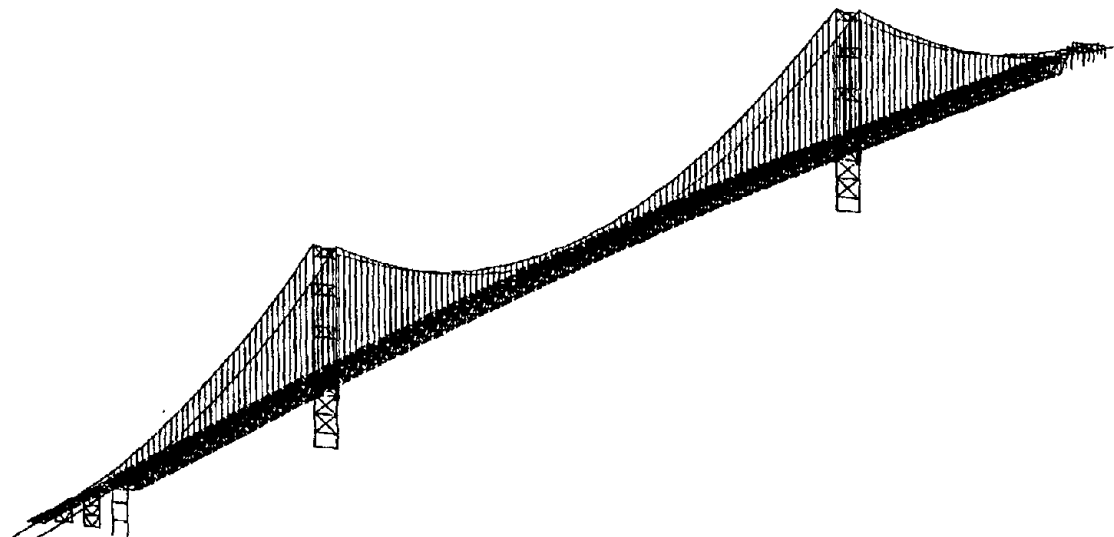
Seismic Retrofit of the University Bridge

Dimitrios P. Koutsoukos and John H. Clark

Abstract

The University Bridge was designed and constructed in the early 1930's over Lake Union in Seattle. The bridge is considered essential and carries four lanes of traffic and two side-walk/bicycle lanes on the north-south route of Eastlake Avenue. A seismic vulnerability assessment of the structure concluded that seismic retrofit of the bridge approaches is required if the bridge is to remain functional after the design seismic event.

The structure is divided into the south approach, the draw bridge and the north approach (Fig. 1). The south approach is a three-span truss bridge. Its superstructure is cast-in-place reinforced concrete slab on two 10 ft deep trusses. The north approach is a seventeen-span bridge with two 7.25 ft cantilevers. From the North Bascule Pier to Pier 10, the superstructure consists of reinforced concrete deck slab on two 12.5 ft deep steel deck trusses while from Pier 10 to the North Abutment it consists of reinforced concrete deck slab on four reinforced concrete haunched girders that are monolithic with integral crossbeams at the pier tops.

Although the preliminary seismic vulnerability assessment called for the strengthening and stiffening of the bridge approaches (improvement of linkage between sub- and super-structure, improvement of strength and ductility of piers, addition of superbents), additional analysis has shown that an improvement of the structural response with base isolation systems in the truss approach units will substantially lower the overall retrofit cost, resulting at the same time in a more reliable structural system for dissipating the seismic energy.

This paper describes the base isolation system that will be used in the truss approach units of the University Bridge. The isolation system design was challenging primarily because of the extremely limited space that was available for the installation of the seismic isolators and dampers. An innovative isolation system, consisting of specially fabricated lead-rubber bearings, was selected among several that satisfied the design specifications and requirements. Break-away expansion joints were designed at all locations where the isolated truss units border the bascule piers and the traditionally retrofitted concrete units. The bascule piers and the substructure members of the isolated units do not require additional retrofit measures and remain elastic during the design seismic event. In addition, implementation of the isolation system eliminates costly retrofit work on the piers' foundations that are under water in several locations.

492
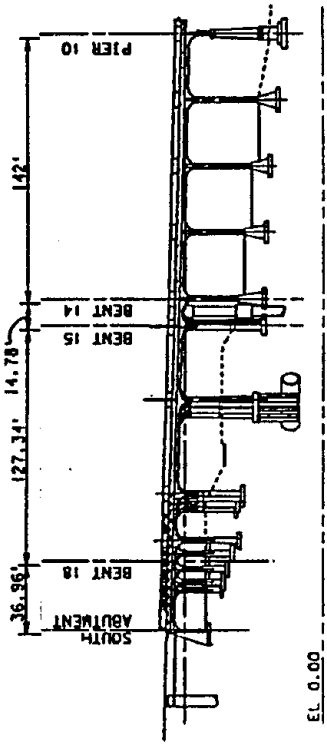
NORTH APPROACH CONCRETE UNITS
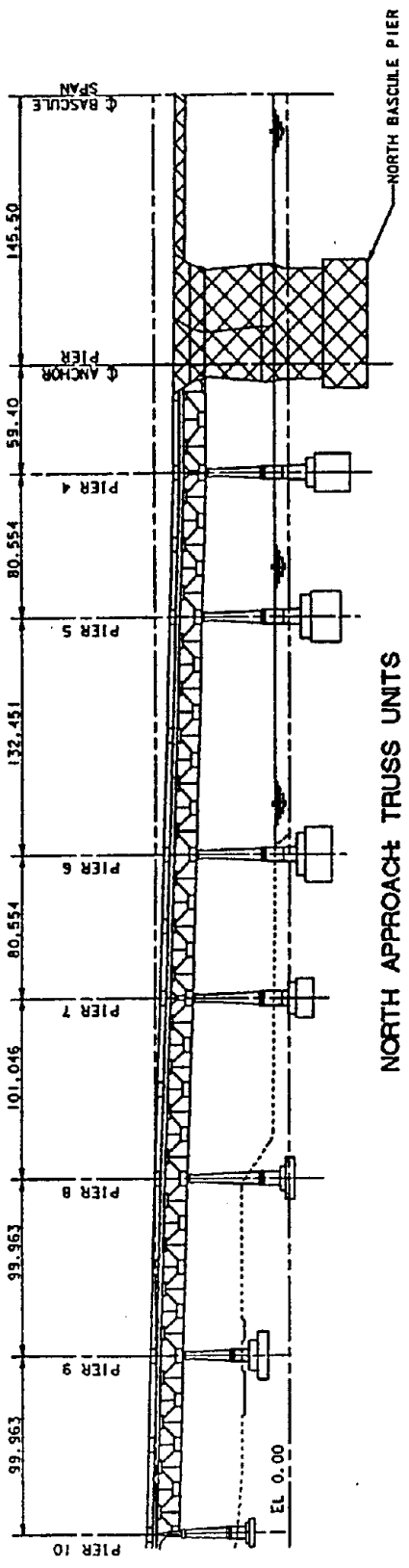
NORTH APPROACH TRUSS UNITS

SOUTH APPROACH
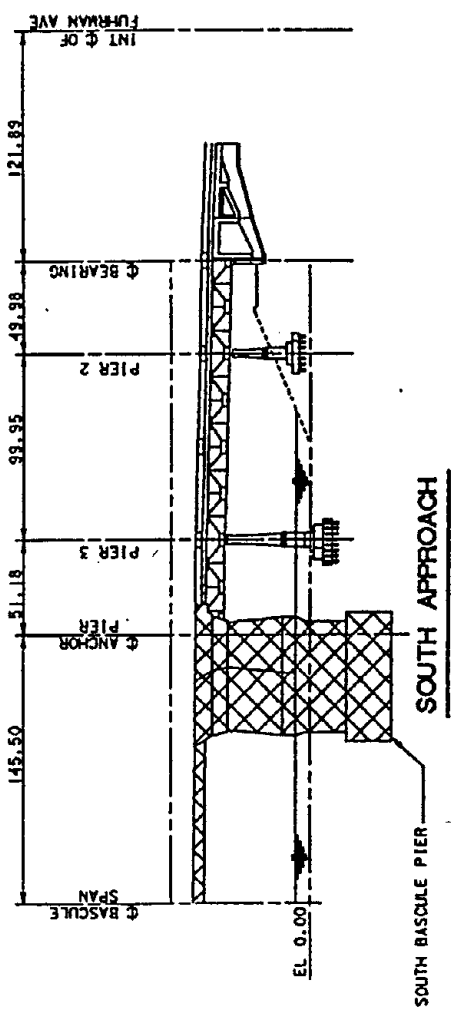
FIGURE 1 - UNIVERSITY BRIDGE

493

Seismic Retrofit of the San Francisco Central Viaduct at the Market Street Undercrossing

By Akın Özselçuk[1] , Mark S. Swatta[2] and Tomás A. Kompfner[3]

ABSTRACT: The San Francisco Central Viaduct is a double-deck, reinforced/prestressed concrete bridge similar to the Cypress Structure that collapsed during the 1989 Loma Prieta Earthquake. The California Department of Transportation, (Caltrans) has funded retrofit studies for the Central Viaduct and for the other double-deck structures. These studies resulted in a special type of retrofit called the *edge beam* concept. The edge beam retrofit concept consisted of removing and replacing columns and bent cap-column joints, and building longitudinal edge beams which span between the bents. The edge beam concept was impractical for the Market Street Undercrossing, because 1) it had a relatively long span (~145 ft.), 2) the edge beam dimensions would have been very large and 3) the existing post-tensioned superstructure made the bent cap retrofit extremely difficult. Therefore, a new type of retrofit scheme was developed.

The new concept provides independent transverse and longitudinal frames to transmit the dead, live and seismic forces into new foundations. The design objectives are 1) to change the structure's vertical and lateral load resisting system to a new configuration, 2) to maintain viaduct and city street traffic flow during construction and 3) to enhance the structure's seismic capacity.

The original Central Viaduct was designed in compliance with the 1950 AASHO Code and has a design base shear coefficient of 6.5% g. The retrofitted structure requires a minimum base shear coefficient of 25% g, and must be serviceable after a major earthquake. Therefore, in addition to static analyses, dynamic response spectrum analyses were carried out to calculate the force demands on the new columns and the maximum drift values, using appropriate Caltrans ARS curves. To prevent failure of the bearings and the superstructure both the minimum yield strength of the retrofitted structure and the maximum base shear (i.e. the plastic shear) were controlled.

The new structure consists of post-tensioned portal frames, which support the upper and lower cap beams and are also connected to each other in the transverse direction, resulting in a 3-D ductile framing system. The underpinning structure is designed to withstand several post-yield excursions at maximum ductility limits by using ductile reinforcing details. The portal frame columns are offset from the existing column locations to allow construction of the new cast-in-drilled-hole (CIDH) foundations, without interference with the existing pile caps. Apart from the ease of construction, CIDH shafts reduce the seismic force demands by increasing the fundamental period of the existing structure. Although the new structural system is conceptually clear, the complex geometry of the retrofitted structure results in biaxial shear, biaxial bending and torsion in the underpinning portal frames.

This paper will present Central Viaduct's design criteria and summarize: 1) the design of the new underpinning portal frames, 2) the interaction of the old structure and the new post-tensioned portal frames, 3) the flow of forces from the existing superstructure to the portal frames through bearings, and 4) the special considerations for construction. Several figures will be presented which illustrate the non-ductile existing details as well as the details of the retrofitted structure and of the bearings.

[1] Bridge Engineer, Richmond, CA 94805,

[2] Vice President, TUDOR Engineering Company,
1800 Harrison Street, Oakland, CA 94612.

[3] President, TK Engineering, El Cerrito, CA 94530

ASSESSMENT AND RETROFIT OF 3 MAJOR BRIDGES DAMAGED DURING RECENT EARTHQUAKES IN COSTA RICA AND THE PHILIPPINES.

Dr. Guillermo SANTANA

Research Engineer, University of California at Berkeley, 1301 South 46th Street, Bldg. 451, Richmond, CA 94804-4698.

SUMMARY

Three major bridges were selected for detailed study of their behavior and failure sequence as well as their collapse mechanisms when subjected to strong earthquakes both in the Philippines and in Costa Rica. Those bridges are: the Valle de la Estrella bridge in the Limón province in Costa Rica affected during the M7.6 earthquake of 1991 and the Magsaysay bridge in Dagupan City together with the Calvo bridge in Bayambang both in the province of Pangasinan in Luzon, Philippines damaged during the M7.8 earthquake of 1990.

The Valle de la Estrella bridge spans a total of 175 m and was designed in 1971 and constructed soon thereafter. The main structure consists of two steel through-truss spans that were unseated off their interior support, with unseating of one span at the end abutment as well. Liquefaction and slumping of the bridge embankment structures was extreme. The Magsaysay bridge is a 7-span, two-lane bridge over the Pantal River with an approximate total length of 120 meters. Three out of the seven spans utilized composite steel girders while the rest are reinforced concrete deck girder spans. The bridge was undergoing widening, some piles had already been driven, a sheet of pile cofferdam installed near the center of the river and parts of the sidewalk were being demolished to accommodate more piles when the earthquake struck. The Calvo bridge is a two lane, 4 span steel truss bridge with a total length, center-to-center of bearings on abutments, of 160 meters. The bridge spans the Agno River and links the towns of Bayambang and Bautista. During the earthquake, Pier no. 1 tilted and displaced towards the river by as much as 1 meter. The trusses on either side of the pier were completely unseated from the pier itself. The pier moved laterally under one truss, severely damaging one of the bottom chord members. As a result, the trusses affected were also laterally displaced from the adjoining Abutment A and Pier 2, the expansion type rocker bearings completely sliding off.

In all cases the ground motions are estimated based in the local geologic conditions, the soil characteristics and the strong motion records available. Based on the above, several of the leading current indicators of response were calculated, among them the maximum displacement demand. Furthermore, the obtained results were contrasted with the observed performance in each one of the structures. The analysis of the as-repaired facilities and their calculated seismic response is also presented.

SECOND U.S.-JAPAN WORKSHOP ON SEISMIC RETROFIT OF BRIDGES

Program
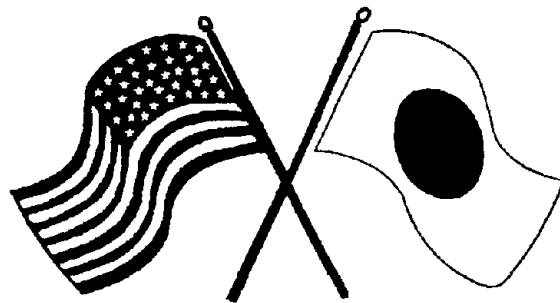
January 20 and 21, 1994
Berkeley Marina Marriott Hotel
Berkeley, California

U.S. - JAPAN WORKSHOP ON SEISMIC RETROFIT OF BRIDGES

January 20 and 21, 1994
Berkeley, California

Workshop Program

Thursday, January 20, 1994

7:45 AM   *Continental Breakfast* (outside of Angel Island and Belvedere Ballrooms)

8:00 AM   REGISTRATION (outside of Angel Island and Belvedere Ballrooms)

8:30 AM   OPENING SESSION (Angel Island and Belvedere Ballrooms)
        Co-Chairs: S. Mahin and K. Kawashima

        K. Kawashima, Japan Side Coordinator
        S. Mahin, U.S. Side Coordinator

        H.S. Lew, National Institute of Standards and Technology
        J. Cooper, Federal Highway Administration
        S.C. Liu, National Science Foundation
        J. Moehle, Earthquake Engineering Research Center, University of California at Berkeley

        J. Gates, California Department of Transportation, Division of Structures

8:50 AM   SESSION 1
        Co-Chairs: J. Gates and T. Iwasaki

        Seismic Strengthening of Bridges in Japan (K. Kawashima and S. Unjoh)
        A Brief History of Caltrans' Phase I Seismic Retrofit Program (M. Yashinsky)
        Seismic Retrofit of Reinforced Concrete Bridges in Northern Nevada (S. Saiidi and D. Sanders)

10:00 AM   *Break*

10:30 AM   SESSION 2
        Co-Chairs: S. Saiidi and W. Tanzo

        Damage of Bridges by Kushiro-oki Earthquake, January 1993, and Hokkaido nansei-oki Earthquake, July 1993 (K. Kawashima, S. Unjoh, T. Nakajima and J. Hoshikuma)
        Damage Analysis of Reinforced Concrete Bridge Piers by Kushiro-oki Earthquake, January 1993, and Hokkaido Nansei-oki Earthquake, July 1993 (K. Kawashima, J. Hoshikuma and S. Unjoh)

SESSION 2 (continued)

Methods of Restoring Bridges Damaged in the Kushiro Offshore
Earthquake of January 1993 and the Southwest Hokkaido Offshore
Earthquake of July 1993 (Y. Ono, M. Kaneko, T. Shirono, M. Sato
and T. Yamauchi)
An Experimental Study on the Behavior of a Large Model Pier after
Repair (Y. Adachi, K. Kousa and Y. Murayama)

12:00 PM   *Lunch* (Quarter Deck) *and Photo Session*

1:30 PM   SESSION 3
             Co-Chairs: J. Mander and H.Sugita

             Retrofit Strategies and Proof Tests for the Santa Monica Viaduct (N.
             Priestley, F. Seible and G. MacRae)
             Seismic Reinforcement of Existing Reinforced Concrete Piers (K.
             Amari, H. Hanno, K. Otsuka and Y. Fujimoto)
             Enhancement of the Seismic Design and Retrofit of Reinforced
             Concrete Bridge Piers in the United States (M. Haroun, G. Pardoen
             and R. Shepherd)
             Seismic Response Characteristics and Seismic Strengthening of
             Reinforced Concrete Bridge Piers subjected to Eccentric Loading (K.
             Kawashima, S. Unjoh and H. Mukai)

3:00 PM   *Break*

             SESSION 4
             Co-Chairs: S. Wood and Y. Yoshida

             Seismic Retrofit Procedures for Reinforced Concrete Bridge Piers in
             the Eastern United States (J. Mander and S. Chen)
             A Stress-Strain Model for Reinforced Concrete Bride Piers Confined
             by Hoop Reinforcement (J. Hoshikuma, K. Kawashima and K.
             Nagaya)
             Evaluation and Retrofitting of Existing Bridge Footings (Y. Xiao, N.
             Priestley and F. Seible)
             Seismic Evaluation and Retrofit of Major Steel Bridges (A. Astaneh-
             Asl, R. Donikian, R. Imbsen and C. Seim)

5:00 PM   Break

7:00 PM   *Reception hosted by U.S. Side*   (El Dorado Room - Second Floor)

7:30 PM   *Dinner hosted by U.S. Side*   (Amador and Mariposa Rooms - Second
             Floor)

500

Friday, January 21, 1994

7:45 AM   *Continental Breakfast* (outside of Angel Island and Belvedere Ballrooms)

8:30 AM   SESSION 5 (Angel Island and Belvedere Ballrooms)
               Co-Chairs: M. Haroun and J. Hoshikuma

               Tests and Research on Carbon Fiber Strengthening of Existing Bridges (N. Ogata, Y. Maeda and H. Ando)
               Shear Strengthening of Existing Reinforced Concrete Columns by Winding With Aramid Fiber (T. Okamoto, T. Noji, H. Yamanaka, M. Tanigaki and M. Oda)
               Increasing the Seismic Resistance of Highway Structures (A. Shirole and A. Malik)
               Seismic Retrofit of Ballard Bridge Approaches (U. Vasishth and J. Jacobsen)

10:00 AM   *Break*

10:30 AM   SESSION 6
               Co-Chairs: A. Malik and K. Toki

               Seismic Retrofit of Bridge Bearing supports by Mechanical Transmission Devices (T. William, H. Mutsuyoshi and Y. Tsuzuki)
               Bridge Retrofit Analysis and Earthquake Damage (L. H. Sheng, S. Mitchell and C.V. Ho)
               Collapse of the Cypress Viaduct and Seismic Performance of a Retrofitted Bent (H. Ohuchi, T. Tatsuda and Y. Goto)
               Seismic Vulnerability of the Alaskan Way Viaduct (M. Eberhard, S. Kramer, S. Wood, J. de la Colina and S. Ryter)

12:00 PM   *Lunch* (Quarter Deck)

1:00 PM   DEMONSTRATION (National Information Service for Earthquake Engineering On-line Computer Data Base) Optional activity located at Back of Angel Island Ballroom

1:30 PM   SESSION 7
               Co-Chairs: A. Astaneh-Asl and Y. Goto

               Behavior of As-built and Retrofit Column to Cap Connections (J. Moehle, C. Thewalt and S. Mahin)
               A Seismic Retrofitting Manual for Highway Bridges (I. Buckle, I. Friedland and J. Cooper)
               Special Reports on the January 17, 1994 Northridge, California, Earthquake

3:00 PM   *Break*

3:30 PM   PLENARY SESSION
                 Co-Chairs: S. Mahin and K. Kawashima

                 General Discussion
                 Development of example structure for possible future cooperative
                 seismic evaluation and retrofit studies
                 Formulation of Workshop Resolutions
                 Closing Ceremony

5:00 PM   *Workshop Adjourns*

Saturday, January 22, 1994

9:00 AM   STUDY TOUR (Busses leave from in front of Marriott Hotel)
                 Reservations Required

4:15 PM   *DINNER CRUISE hosted by Japanese Side*
                 (Ship leaves promptly at 4:30 PM)
                 Reservations Required

Sunday, January 23, 1994

8:30 AM   STUDY TOUR (Busses leave from in front of Marriott Hotel)
                 Reservations Required

Second U.S.-Japan Workshop
on Seismic Retrofit of Bridges

Appendix A
Workshop Participants
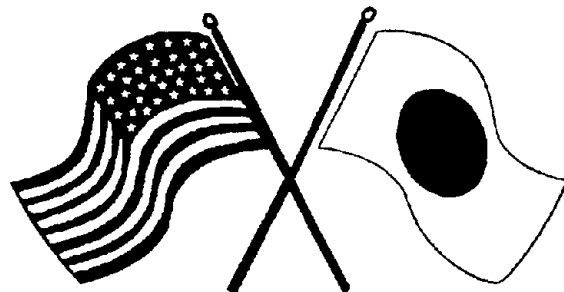
January 20 and 21, 1994
Berkeley Marina Marriott Hotel
Berkeley, California

THE SECOND U.S.-JAPAN WORKSHOP ON SEISMIC RETROFIT OF BRIDGES

Particpants From the Japan Side

Mr. Yukio Adachi
Design Section
Engineering Division
Hanshin Expressway Public Corporation
(Currently Graduate Student at
    University of California, Berkeley)
4-1-3, Kyutaro-cho, Chuo-ku
Osaka, JAPAN 541
TEL: 06-252-8121
FAX: 06-252-4583

Mr. Kazuo Endoh
Chief Engineer
Construction Materials Department
The Yokohama Rubber Co., Ltd.
2-1, Oiwake, Hiratsuka-shi
Kanagawa, JAPAN, 254
TEL: 0463-35-9681
FAX: 0463-35-9763

Dr. Yozo Goto
Manager
The 5th Civil Engineering Division
Technical Research Institute
Obayashi Corporation
4-640, Shimokiyoto, Kiyose-shi
Tokyo, JAPAN, 204
TEL: 0424-95-0951
FAX: 0424-95-0903

Mr. Junichi Hoshikuma
Research Engineer
Earthquake Engineering Division
Earthquake Disaster Prevention Department
Public Works Research Institute
Ministry of Construction
1, Asahi, Tsukuba-shi, Ibaraki
305 JAPAN
TEL: 0298-64-2211
FAX: 0298-64-0598

Dr. Toshio Iwasaki
Chairman of the Board
Construction Technology Research Institute
3-3-4, Kandakaji-cho, Chiyoda-ku
Tokyo, 101
JAPAN
TEL: 03-3254-9481
FAX: 03-3254-9448

Mr. Soichiro Kawahara
Manager
Development Section
Structural Equipment Division
Oiles Corporation
8, Kirihara-cho, Fujisawa-shi
Kanagawa, JAPAN, 252
TEL: 0466-44-4818
FAX: 0466-43-6059

Dr. Kazuhiko Kawashima
Head, Earthqauke Engineering Division
Earthquake Disaster Prevention Department
Public Works Research Institute
Ministry of Construction
1, Asahi, Tsukuba-shi, Ibaraki
305 JAPAN
TEL: 0298-64-2211
FAX: 0298-64-0598

Mr. Akihide Kubo
The 1st Technology Department
PS Corporation
3-20-6, Minami-Ohtsuka, Toshima-ku
Tokyo, JAPAN, 170
TEL: 03-5391-6091
FAX: 03-5391-6095

Mr. Yasuhito Morimoto
Consulting Engineer
Structural Second Division
Yokohama Branch
Pacific Consultants Co., Ltd.
3-8-8, Ohgi-machi, Naka-ku
Yokohama, JAPAN, 213
TEL: 045-664-4320
FAX: 045-651-5529

Professor Hiroshi Mutsuyoshi
Professor
Department of Civil and
    Environmental Engineering
Saitama University
225, Shimo-Okubo, Urawa
Saitama, 338
JAPAN
TEL: 048-858-3556
FAX: 048-855-9361

Mr. Keizo Ohtsuka
Maintenance Technology Division
Maintenance Facility Department
Metropolitan Expressway Public
  Corporation
(Currently Graduate Student at
  University of Texas)
1-4-1, Kasumigaseki, Chiyoda-ku
Tokyo, JAPAN, 100
TEL: 03-3502-7311
FAX: 03-3503-1806

Mr. Ikuo Shimoda
Manager
Development Section
Structural Equipment Division
Oiles Corporation
8, Kirihara-cho, Fujisawa-shi
Kanagawa, JAPAN, 252
TEL: 0466-44-4818
FAX: 0466-43-6059

Mr. Hideki Sugita
Research Engineer
Earthquake Engineering Division
Earthquake Disaster Prevention Department
Public Works Research Institute
Ministry of Construction
(Currently Visiting Researcher at
  University of California, Berkeley)
1, Asahi, Tsukuba-shi, Ibaraki
305 JAPAN
TEL: 0298-64-2211
FAX: 0298-64-0598

Mr. Isao Takatori
Director
Public Works Research Center
1-12-11, Daito, Daitoh-ku
Tokyo, JAPAN, 110
TEL: 03-3835-3609
FAX: 03-3832-7397

Mr. Tomio Tamura
Deputy Director-General
Technical Research Institute
Mistui Construction Corporation
518-1, Komaki, Nagareyama-shi
Chiba, JAPAN, 270-01
TEL: 0471-40-5201
FAX: 0471-40-5216

Dr. William Tanzo
Research Associate
Department of Civil and
  Environmental Engineering
Saitama University
225, Shimo-Okubo, Urawa
Saitama, 338
JAPAN
TEL: 048-858-3556
FAX: 048-855-9361

Professor Kenzo Toki
Professor
Department of Civil and Traffic Engineering
Kyoto University
Yoshida-hon-machi, Sakyo-ku
Kyoto, 606
JAPAN
TEL: 075-753-5111
FAX: 075-761-0646

Mr. Shigeki Unjoh
Senior Research Engineer
Earthquake Engineering Division
Earthquake Disaster Prevention Department
Public Works Research Institute
Ministry of Construction
1, Asahi, Tsukuba-shi, Ibaraki
305 JAPAN
TEL: 0298-64-2211
FAX: 0298-64-0598

Mr. Yoshitaka Yoshida
Manager
Bridge Design Division
Design Department
Trans-Tokyo Bay Highway Corp.
15-5 Ichibancho, Chiyoda-ku, Tokyo
JAPAN 102
TEL: 03-3239-6585
FAX: 03-3239-6586

SECOND U.S.-JAPAN WORKSHOP ON SEISMIC RETROFIT OF BRIDGES

U.S. Side Participants

George Amaro
Caltrans

Greg Fenves
U.C. Berkeley

Hassan Astaneh
U.C. Berkeley

Filip Filippou
U.C. Berkeley

Nesrin Basoz
Stanford University

Nick Forell
Forell/Elsesser Engineers, Inc.

Michel Benoit
Buckland & Taylor Ltd.

Ian Friedland
SUNY Buffalo

David Brierley-Green
Arvid Grant Associates

Jim Gates
Caltrans

Ian Buckle
SUNY Buffalo

Medhat Haroun
U.C. Irvine

Rob Chai
U.C. Davis

Chuong Ho
Caltrans

Jaime de la Colina
University of Washington, Seattle

Jay Jacobsen
Exeltech Engineering

Jim Cooper
FHWA

Kevin Keady
Caltrans

Ruben Donikian
Cygna Group Inc.

Mark Ketchum
OPAC Consulting Engineers

Marc Eberhard
University of Washington, Seattle

Anne Kiremidjian
Stanford University

Dimitrios Koutsoukos
Andersen Bjornstad Kane Jacobs, Inc.

Dawn Lehman
U.C. Berkeley

H.S. Lew
NIST

S.C. Liu
NSF

Wen David Liu
Roy Imbsen Associates

Jim MacIntyre
Caltrans

Greg MacRae
U.C. San Diego

Steve Mahin
U.C. Berkeley

Ayaz Malik
New York Dept. of Transportation

John Mander
SUNY Buffalo

Brian Maroni
Caltrans

Kurt McMullin
U.C. Berkeley

Steve Mitchell
Caltrans

Jack Moehle
U.C. Berkeley

Akin Ozselcuk
Bridge Engineer

Gerhard Pardoen
U.C. Irvine

James Ray
Waterways Experimental Station

Mike Rojanski
EQE International, Inc.

Karl Romstad
U.C. Davis

Said Saiidi
University of Nevada, Reno

David Sanders
University of Nevada, Reno

Guillermo Santana
U.C. Berkeley

Thomas Sardo
Caltrans

Ann Sardo
Caltrans

Pete Segenthaler
Caltrans

Chuck Seim
T.Y. Lin International

Rol Sharpe
Consultant

L.H. Sheng
Caltrans

Robin Shepherd
U.C. Irvine

J.P. Shing
Geospectra, Inc.

Bozibar Stojadinovic
U.C. Berkeley

Eric Straser
Stanford University

Mohsen Sultan
Caltrans

Andy Taylor
NIST

Chris Thewalt
U.C. Berkeley

Umesh Vasishth
Exeltech Engineering

John Wallace
Clarkson University

X.-F. Wang
Washington University

Andrew Whittaker
U.C. Berkeley

Sharon Wood
University of Washington, Seattle

Stan Woodson
Waterways Experimental Station

Yan Xiao
U.C. San Diego

Mark Yashinsky
Caltrans

Foued Zayati
U.C. Berkeley

EERC REPORTS

EERC reports are available from the National Information Service for Earthquake Engineering (NISEE) and from the National Technical Information Service (NTIS). To order EERC Reports, please contact the Earthquake Engineering Research Center, 1301 S. 46th Street, Richmond, California 94804-4698, ph 510-231-9468.

UCB/EERC-97/09: Second U.S.-Japan Workshop on Seismic Retrofit of Bridges, edited by K. Kawashima and S.A. Mahin, September, 1997. $57

UCB/EERC-97/08: Implications of the Landers and Big Bear Earthquakes on Earthquake Resistant Design of Structures, by Anderson, J.C. and Bertero, V.V., July 1997. $20

UCB/EERC-97/07: Analysis of the Nonlinear Response of Structures Supported on Pile Foundations, by Badoni, D. and Makris, N., July 1997. $20

UCB/EERC-97/06: Executive Summary on: Phase 3: Evaluation and Retrofitting of Multilevel and Multiple-Column Structures -- An Analytical, Experimental, and Conceptual Study of Retrofitting Needs and Methods, by Mahin, S.A., Fenves, G.L., Filippou, F.C., Moehle, J.P., Thewalt, C.R., May, 1997. $20

UCB/EERC-97/05: The EERC-CUREe Symposium to Honor Vitelmo V. Bertero, February 1997. $26

UCB/EERC-97/04: Design and Evaluation of Reinforced Concrete Bridges for Seismic Resistance, by Aschheim, M., Moehle, J.P. and Mahin, S.A., March 1997. $26

UCB/EERC-97/03: U.S.-Japan Workshop on Cooperative Research for Mitigation of Urban Earthquake Disasters: Learning from Kobe and Northridge -- Recommendations and Resolutions, by Mahin, S., Okada, T., Shinozuka, M. and Toki, K., February 1997. $15

UCB/EERC-97/02: Multiple Support Response Spectrum Analysis of Bridges Including the Site-Response Effect & MSRS Code, by Der Kiureghian, A., Keshishian, P. and Hakobian, A., February 1997. $20

UCB/EERC-97/01: Analysis of Soil-Structure Interaction Effects on Building Response from Earthquake Strong Motion Recordings at 58 Sites, by Stewart, J.P. and Stewart, A.F., February 1997. $57

UCB/EERC-96/05: Application of Dog Bones for Improvement of Seismic Behavior of Steel Connections, by Popov, E.P., Blondet, M. and Stepanov, L., June 1996. $13

UCB/EERC-96/04: Experimental and Analytical Studies of Base Isolation Applications for Low-Cost Housing, by Taniwangsa, W. and Kelly, J.M., July 1996. $20

UCB/EERC-96/03: Experimental and Analytical Evaluation of a Retrofit Double-Deck Viaduct Structure: Part I of II, by Zayati, F., Mahin, S. A. and Moehle, J. P., June 1996. $33

UCB/EERC-96/02: Field Testing of Bridge Design and Retrofit Concepts. Part 2 of 2: Experimental and Analytical Studies of the Mt. Diablo Blvd. Bridge, by Gilani, A.S., Chavez, J.W. and Fenves, G.L., June 1996. $20

UCB/EERC-96/01: Earthquake Engineering Research at Berkeley -- 1996: Papers Presented at the 11th World Conference on Earthquake Engineering, by EERC, May 1996. $26

UCB/EERC-95/14: Field Testing of Bridge Design and Retrofit Concepts. Part 1 of 2: Field Testing and Dynamic Analysis of a Four-Span Seismically Isolated Viaduct in Walnut Creek, California, by Gilani, A.S., Mahin, S.A., Fenves, G.L., Aiken, I.D. and Chavez, J.W., December 1995. $26

UCB/EERC-95/13: Experimental and Analytical Studies of Steel Connections and Energy Dissipators, by Yang, T.-S. and Popov, E.P., December 1995. $26

UCB/EERC-95/12: Natural Rubber Isolation Systems for Earthquake Protection of Low-Cost Buildings, by Taniwangsa, W., Clark, P. and Kelly, J.M., June 1996. $20

UCB/EERC-95/11: Studies in Steel Moment Resisting Beam-to-Column Connections for Seismic-Resistant

511

	Design, by Blackman, B. and Popov, E.P., October 1995, PB96-143243. $20
UCB/EERC-95/10:	Seismological and Engineering Aspects of the 1995 Hyogoken-Nanbu (Kobe) Earthquake, by EERC, November 1995. $26
UCB/EERC-95/09:	Seismic Behavior and Retrofit of Older Reinforced Concrete Bridge T-Joints, by Lowes, L.N. and Moehle, J.P., September 1995, PB96-159850. $20
UCB/EERC-95/08:	Behavior of Pre-Northridge Moment Resisting Steel Connections, by Yang, T.-S. and Popov, E.P., August 1995, PB96-143177. $15
UCB/EERC-95/07:	Earthquake Analysis and Response of Concrete Arch Dams, by Tan, H. and Chopra, A.K., August 1995, PB96-143185. $20
UCB/EERC-95/06:	Seismic Rehabilitation of Framed Buildings Infilled with Unreinforced Masonry Walls Using Post-Tensioned Steel Braces, by Teran-Gilmore, A., Bertero, V.V. and Youssef, N., June 1995, PB96-143136. $26
UCB/EERC-95/05:	Final Report on the International Workshop on the Use of Rubber-Based Bearings for the Earthquake Protection of Buildings, by Kelly, J.M., May 1995. $20
UCB/EERC-95/04:	Earthquake Hazard Reduction in Historical Buildings Using Seismic Isolation, by Garevski, M., June 1995. $15
UCB/EERC-95/03:	Upgrading Bridge Outrigger Knee Joint Systems, by Stojadinovic, B. and Thewalt, C.R., June 1995, PB95-269338. $20
UCB/EERC-95/02:	The Attenuation of Strong Ground Motion Displacements, by Gregor, N.J., June 1995, PB95-269346. $26
UCB/EERC-95/01:	Geotechnical Reconnaissance of the Effects of the January 17, 1995, Hyogoken-Nanbu Earthquake, Japan, August 1995, PB96-143300. $26
UCB/EERC-94/12:	Response of the Northwest Connector in the Landers and Big Bear Earthquakes, by Fenves, G.L. and Desroches, R., December 1994. $20
UCB/EERC-94/11:	Earthquake Analysis and Response of Two-Level Viaducts, by Singh, S.P. and Fenves, G.L., October 1994, PB96-133756 (A09). $20
UCB/EERC-94/10:	Manual for Menshin Design of Highway Bridges: Ministry of Construction, Japan, by Sugita, H. and Mahin, S., August 1994, PB95-192100(A08). $20
UCB/EERC-94/09:	Performance of Steel Building Structures During the Northridge Earthquake, by Bertero, V.V., Anderson, J.C. and Krawinkler, H., August 1994, PB95-112025(A10). $26
UCB/EERC-94/08:	Preliminary Report on the Principal Geotechnical Aspects of the January 17, 1994 Northridge Earthquake, by Stewart, J.P., Bray, J.D., Seed, R.B. and Sitar, N., June 1994, PB94203635(A12). $26
UCB/EERC-94/07:	Accidental and Natural Torsion in Earthquake Response and Design of Buildings, by De la Llera, J.C. and Chopra, A.K., June 1994, PB94-203627(A14). $33
UCB/EERC-94/05:	Seismic Response of Steep Natural Slopes, by Sitar, N. and Ashford, S.A., May 1994, PB94-203643(A10). $26
UCB/EERC-94/04:	Insitu Test Results from Four Loma Prieta Earthquake Liquefaction Sites: SPT, CPT, DMT and Shear Wave Velocity, by Mitchell, J.K., Lodge, A.L., Coutinho, R.Q., Kayen, R.E., Seed, R.B., Nishio, S. and Stokoe II, K.H., April 1994, PB94-190089(A09). $20
UCB/EERC-94/03:	The Influence of Plate Flexibility on the Buckling Load of Elastomeric Isolators, by Kelly, J.M., March 1994, PB95-192134(A04). $15
UCB/EERC-94/02:	Energy Dissipation with Slotted Bolted Connections, by Grigorian, C.E. and Popov, E.P., February 1994, PB94-164605. $26
UCB/EERC-94/01:	Preliminary Report on the Seismological and Engineering Aspects of the January 17, 1994 Northridge Earthquake, by EERC, January 1994, (PB94 157 666/AS)A05. $15
UCB/EERC-93/13:	On the Analysis of Structures with Energy Dissipating Restraints, by Inaudi, J.A., Nims, D.K. and Kelly, J.M., December 1993, PB94-203619(A07). $20
UCB/EERC-93/12:	Synthesized Strong Ground Motions for the Seismic Condition Assessment of the Eastern Portion of the San Francisco Bay Bridge, by Bolt, B.A. and Gregor, N.J., December

	1993, PB94-165842(A10). $26
UCB/EERC-93/11:	Nonlinear Homogeneous Dynamical Systems, by Inaudi, J.A. and Kelly, J.M., October 1995. $20
UCB/EERC-93/09:	A Methodology for Design of Viscoelastic Dampers in Earthquake-Resistant Structures, by Abbas, H. and Kelly, J.M., November 1993, PB94-190071(A10). $26
UCB/EERC-93/08:	Model for Anchored Reinforcing Bars under Seismic Excitations, by Monti, G., Spacone, E. and Filippou, F.C., December 1993, PB95-192183(A05). $15
UCB/EERC-93/07:	Earthquake Analysis and Response of Concrete Gravity Dams Including Base Sliding, by Chavez, J.W. and Fenves, G.L., December 1993, (PB94 157 658/AS)A10. $26
UCB/EERC-93/06:	On the Analysis of Structures with Viscoelastic Dampers, by Inaudi, J.A., Zambrano, A. and Kelly, J.M., August 1993, PB94-165867(A06). $20
UCB/EERC-93/05:	Multiple-Support Response Spectrum Analysis of the Golden Gate Bridge, by Nakamura, Y., Der Kiureghian, A. and Liu, D., May 1993, (PB93 221 752)A05. $15
UCB/EERC-93/04:	Seismic Performance of a 30-Story Building Located on Soft Soil and Designed According to UBC 1991, by Teran-Gilmore, A. and Bertero, V.V., 1993, (PB93 221 703)A17. $33
UCB/EERC-93/03:	An Experimental Study of Flat-Plate Structures under Vertical and Lateral Loads, by Hwang, S.-H. and Moehle, J.P., February 1993, (PB94 157 690/AS)A13. $26
UCB/EERC-93/02:	Evaluation of an Active Variable-Damping-Structure, by Polak, E., Meeker, G., Yamada, K. and Kurata, N., 1993, (PB93 221 711)A05. $15
UCB/EERC-92/18:	Dynamic Analysis of Nonlinear Structures using State-Space Formulation and Partitioned Integration Schemes, by Inaudi, J.A. and De la Llera, J.C., December 1992, (PB94 117 702/AS/A05. $15
UCB/EERC-92/17:	Performance of Tall Buildings During the 1985 Mexico Earthquakes, by Teran-Gilmore, A. and Bertero, V.V., December 1992, (PB93 221 737)A11. $26
UCB/EERC-92/16:	Tall Reinforced Concrete Buildings: Conceptual Earthquake-Resistant Design Methodology, by Bertero, R.D. and Bertero, V.V., December 1992, (PB93 221 695)A12. $26
UCB/EERC-92/15:	A Friction Mass Damper for Vibration Control, by Inaudi, J.A. and Kelly, J.M., October 1992, (PB93 221 745)A04. $15
UCB/EERC-92/14:	Earthquake Risk and Insurance, by Brillinger, D.R., October 1992, (PB93 223 352)A03.
UCB/EERC-92/13:	Earthquake Engineering Research at Berkeley - 1992, by EERC, October 1992, PB93-223709(A10). $13
UCB/EERC-92/12:	Application of a Mass Damping System to Bridge Structures, by Hasegawa, K. and Kelly, J.M., August 1992, (PB93 221 786)A06. $26
UCB/EERC-92/11:	Mechanical Characteristics of Neoprene Isolation Bearings, by Kelly, J.M. and Quiroz, E., August 1992, (PB93 221 729)A07. $20
UCB/EERC-92/10:	Slotted Bolted Connection Energy Dissipators, by Grigorian, C.E., Yang, T.-S. and Popov, E.P., July 1992, (PB92 120 285)A03. $20
UCB/EERC-92/09:	Evaluation of Code Accidental-Torsion Provisions Using Earthquake Records from Three Nominally Symmetric-Plan Buildings, by De la Llera, J.C. and Chopra, A.K., September 1992, (PB94 117 611)A08. $13
UCB/EERC-92/08:	Nonlinear Static and Dynamic Analysis of Reinforced Concrete Subassemblages, by Filippou, F.C., D'Ambrisi, A. and Issa, A., August, 1992. $20
UCB/EERC-92/07:	A Beam Element for Seismic Damage Analysis, by Spacone, E., Ciampi, V. and Filippou, F.C., August 1992, (PB95-192126)A06. $20
UCB/EERC-92/06:	Seismic Behavior and Design of Semi-Rigid Steel Frames, by Nader, M.N. and Astaneh-Asl, A., May 1992, PB93-221760(A17). $33
UCB/EERC-92/05:	Parameter Study of Joint Opening Effects on Earthquake Response of Arch Dams, by Fenves, G.L., Mojtahedi, S. and Reimer, R.B., April 1992, (PB93 120 301)A04. $15
UCB/EERC-92/04:	Shear Strength and Deformability of RC Bridge Columns Subjected to Inelastic Cyclic

513

Displacements, by Aschheim, M. and Moehle, J.P., March 1992, (PB93 120 327)A06. $20

UCB/EERC-92/03: Models for Nonlinear Earthquake Analysis of Brick Masonry Buildings, by Mengi, Y., McNiven, H.D. and Tanrikulu, A.K., March 1992, (PB93 120 293)A08. $20

UCB/EERC-92/02: Response of the Dumbarton Bridge in the Loma Prieta Earthquake, by Fenves, G.L., Filippou, F.C. and Sze, D.T., January 1992, (PB93 120 319)A09. $20

UCB/EERC-92/01: Studies of a 49-Story Instrumented Steel Structure Shaken During the Loma Prieta Earthquake, by Chen, C.-C., Bonowitz, D. and Astaneh-Asl, A., February 1992, (PB93 221 778)A08. $20

UCB/EERC-91/18: Investigation of the Seismic Response of a Lightly-Damped Torsionally-Coupled Building, by Boroschek, R. and Mahin, S.A., December 1991, (PB93 120 335)A13. $26

UCB/EERC-91/17: A Fiber Beam-Column Element for Seismic Response Analysis of Reinforced Concrete Structures, by Taucer, F., Spacone, E. and Filippou, F.C., December 1991, (PB94 117 629AS)A07. $20

UCB/EERC-91/16: Evaluation of the Seismic Performance of a Thirty-Story RC Building, by Anderson, J.C., Miranda, E., Bertero, V.V. and The Kajima Project Research Team, July 1991, (PB93 114 841)A12. $26

UCB/EERC-91/15: Design Guidelines for Ductility and Drift Limits: Review of State-of-the-Practice and State-of-the-Art in Ductility and Drift-Based Earthquake-Resistant Design of Buildings, by Bertero, V.V., Anderson, J.C., Krawinkler, H., Miranda, E. and The CUREe and The Kajima Research Teams, July 1991, (PB93 120 269)A08. $20

UCB/EERC-91/14: Cyclic Response of RC Beam-Column Knee Joints: Test and Retrofit, by Mazzoni, S., Moehle, J.P. and Thewalt, C.R., October 1991, (PB93 120 277)A03. $13

UCB/EERC-91/13: Shaking Table - Structure Interaction, by Rinawi, A.M. and Clough, R.W., October 1991, (PB93 114 917)A13. $26

UCB/EERC-91/12: Performance of Improved Ground During the Loma Prieta Earthquake, by Mitchell, J.K. and Wentz, Jr., F.J., October 1991, (PB93 114 791)A06. $20

UCB/EERC-91/11: Seismic Performance of an Instrumented Six-Story Steel Building, by Anderson, J.C. and Bertero, V.V., November 1991, (PB93 114 809)A07. $20

UCB/EERC-91/10: Evaluation of Seismic Performance of a Ten-Story RC Building During the Whittier Narrows Earthquake, by Miranda, E. and Bertero, V.V., October 1991, (PB93 114 783)A06. $20

UCB/EERC-91/09: A Preliminary Study on Energy Dissipating Cladding-to-Frame Connections, by Cohen, J.M. and Powell, G.H., September 1991, (PB93 114 510)A05. $15

UCB/EERC-91/08: A Response Spectrum Method for Multiple-Support Seismic Excitations, by Der Kiureghian, A. and Neuenhofer, A., August 1991, (PB93 114 536)A04. $15

UCB/EERC-91/07: Estimation of Seismic Source Processes Using Strong Motion Array Data, by Chiou, S.-J., July 1991, (PB93 114 551/AS)A08. $20

UCB/EERC-91/06: Computation of Spatially Varying Ground Motion and Foundation-Rock Impedance Matrices for Seismic Analysis of Arch Dams, by Zhang, L. and Chopra, A.K., May 1991, (PB93 114 825)A07. $20

UCB/EERC-91/05: Base Sliding Response of Concrete Gravity Dams to Earthquakes, by Chopra, A.K. and Zhang, L., May 1991, (PB93 114 544/AS)A05. $15

UCB/EERC-91/04: Dynamic and Failure Characteristics of Bridgestone Isolation Bearings, by Kelly, J.M., April 1991, (PB93 114 528)A05. $15

UCB/EERC-91/03: A Long-Period Isolation System Using Low-Modulus High-Damping Isolators for Nuclear Facilities at Soft-Soil Sites, by Kelly, J.M., March 1991, (PB93 114 577/AS)A10. $26

UCB/EERC-91/02: Displacement Design Approach for Reinforced Concrete Structures Subjected to Earthquakes, by Qi, X. and Moehle, J.P., January 1991, (PB93 114 569/AS)A09. $20

UCB/EERC-90/21: Observations and Implications of Tests on the Cypress Street Viaduct Test Structure, by

Bollo, M., Mahin, S.A., Moehle, J.P., Stephen, R.M. and Qi, X., December 1990, (PB93 114 775)A13. $26

UCB/EERC-90/20: Seismic Response Evaluation of an Instrumented Six Story Steel Building, by Shen, J.-H. and Astaneh-Asl, A., December 1990, (PB91 229 294/AS)A04. $15

UCB/EERC-90/19: Cyclic Behavior of Steel Top-and-Bottom Plate Moment Connections, by Harriott, J.D. and Astaneh-Asl, A., August 1990, (PB91 229 260/AS)A05. $15

UCB/EERC-90/18: Material Characterization of Elastomers used in Earthquake Base Isolation, by Papoulia, K.D. and Kelly, J.M., 1990, PB94-190063(A08). $15

UCB/EERC-90/17: Behavior of Peak Values and Spectral Ordinates of Near-Source Strong Ground-Motion over a Dense Array, by Niazi, M., June 1990, (PB93 114 833)A07. $20

UCB/EERC-90/14: Inelastic Seismic Response of One-Story, Asymmetric-Plan Systems, by Goel, R.K. and Chopra, A.K., October 1990, (PB93 114 767)A11. $26

UCB/EERC-90/13: The Effects of Tectonic Movements on Stresses and Deformations in Earth Embankments, by Bray, J. D., Seed, R. B. and Seed, H. B., September 1989, PB92-192996(A18). $39

UCB/EERC-90/12: Effects of Torsion on the Linear and Nonlinear Seismic Response of Structures, by Sedarat, H. and Bertero, V.V., September 1989, (PB92 193 002/AS)A15. $33

UCB/EERC-90/11: Seismic Hazard Analysis: Improved Models, Uncertainties and Sensitivities, by Araya, R. and Der Kiureghian, A., March 1988, PB92-193010(A08). $20

UCB/EERC-90/10: Experimental Testing of the Resilient-Friction Base Isolation System, by Clark, P.W. and Kelly, J.M., July 1990, (PB92 143 072)A08. $20

UCB/EERC-90/09: Influence of the Earthquake Ground Motion Process and Structural Properties on Response Characteristics of Simple Structures, by Conte, J.P., Pister, K.S. and Mahin, S.A., July 1990, (PB92 143 064)A15. $33

UCB/EERC-90/08: Soil Conditions and Earthquake Hazard Mitigation in the Marina District of San Francisco, by Mitchell, J.K., Masood, T., Kayen, R.E. and Seed, R.B., May 1990, (PB 193 267/AS)A04. $15

UCB/EERC-90/07: A Unified Earthquake-Resistant Design Method for Steel Frames Using ARMA Models, by Takewaki, I., Conte, J.P., Mahin, S.A. and Pister, K.S., June 1990, PB92-192947(A06). $15

UCB/EERC-90/05: Preliminary Report on the Principal Geotechnical Aspects of the October 17, 1989 Loma Prieta Earthquake, by Seed, R.B., Dickenson, S.E., Riemer, M.F., Bray, J.D., Sitar, N., Mitchell, J.K., Idriss, I.M., Kayen, R.E., Kropp, A., Harder, L.F., Jr. and Power, M.S., April 1990, (PB 192 970)A08. $20

UCB/EERC-90/03: Earthquake Simulator Testing and Analytical Studies of Two Energy-Absorbing Systems for Multistory Structures, by Aiken, I.D. and Kelly, J.M., October 1990, (PB92 192 988)A13. $26

UCB/EERC-90/02: Javid's Paradox: The Influence of Preform on the Modes of Vibrating Beams, by Kelly, J.M., Sackman, J.L. and Javid, A., May 1990, (PB91 217 943/AS)A03. $13

UCB/EERC-89/16: Collapse of the Cypress Street Viaduct as a Result of the Loma Prieta Earthquake, by Nims, D.K., Miranda, E., Aiken, I.D., Whittaker, A.S. and Bertero, V.V., November 1989, (PB91 217 935/AS)A05. $15

UCB/EERC-89/15: Experimental Studies of a Single Story Steel Structure Tested with Fixed, Semi-Rigid and Flexible Connections, by Nader, M.N. and Astaneh-Asl, A., August 1989, (PB91 229 211/AS)A10. $26

UCB/EERC-89/14: Preliminary Report on the Seismological and Engineering Aspects of the October 17, 1989 Santa Cruz (Loma Prieta) Earthquake, by EERC, October 1989, (PB92 139 682/AS)A04. $15

UCB/EERC-89/13: Mechanics of Low Shape Factor Elastomeric Seismic Isolation Bearings, by Aiken, I.D., Kelly, J.M. and Tajirian, F.F., November 1989, (PB92 139 732/AS)A09. $20

UCB/EERC-89/12: ADAP-88: A Computer Program for Nonlinear Earthquake Analysis of Concrete Arch

Dams, by Fenves, G.L., Mojtahedi, S. and Reimer, R.B., September 1989, (PB92 139 674/AS)A07. $20

UCB/EERC-89/11: Static Tilt Behavior of Unanchored Cylindrical Tanks, by Lau, D.T. and Clough, R.W., September 1989, (PB92 143 049)A10. $26

UCB/EERC-89/10: Measurement and Elimination of Membrane Compliance Effects in Undrained Triaxial Testing, by Nicholson, P.G., Seed, R.B. and Anwar, H., September 1989, (PB92 139 641/AS)A13. $26

UCB/EERC-89/09: Feasibility and Performance Studies on Improving the Earthquake Resistance of New and Existing Buildings Using the Friction Pendulum System, by Zayas, V., Low, S., Mahin, S.A. and Bozzo, L., July 1989, (PB92 143 064)A14. $33

UCB/EERC-89/08: Seismic Performance of Steel Moment Frames Plastically Designed by Least Squares Stress Fields, by Ohi, K. and Mahin, S.A., August 1989, (PB91 212 597)A05. $15

UCB/EERC-89/07: EADAP - Enhanced Arch Dam Analysis Program: Users's Manual, by Ghanaat, Y. and Clough, R.W., August 1989, (PB91 212 522)A06. $20

UCB/EERC-89/06: Effects of Spatial Variation of Ground Motions on Large Multiply-Supported Structures, by Hao, H., July 1989, (PB91 229 161/AS)A08. $20

UCB/EERC-89/05: The 1985 Chile Earthquake: An Evaluation of Structural Requirements for Bearing Wall Buildings, by Wallace, J.W. and Moehle, J.P., July 1989, (PB91 218 008/AS)A13. $26

UCB/EERC-89/04: Earthquake Analysis and Response of Intake-Outlet Towers, by Goyal, A. and Chopra, A.K., July 1989, (PB91 229 286/AS)A19. $39

UCB/EERC-89/03: Implications of Site Effects in the Mexico City Earthquake of Sept. 19, 1985 for Earthquake-Resistant Design Criteria in the San Francisco Bay Area of California, by Seed, H.B. and Sun, J.I., March 1989, (PB91 229 369/AS)A07. $20

UCB/EERC-89/02: Earthquake Simulator Testing of Steel Plate Added Damping and Stiffness Elements, by Whittaker, A., Bertero, V.V., Alonso, J. and Thompson, C., January 1989, (PB91 229 252/AS)A10. $26

UCB/EERC-89/01: Behavior of Long Links in Eccentrically Braced Frames, by Engelhardt, M.D. and Popov, E.P., January 1989, (PB92 143 056)A18. $39

UCB/EERC-88/20: Base Isolation in Japan, 1988, by Kelly, J.M., December 1988, (PB91 212 449)A05. $15

UCB/EERC-88/19: Steel Beam-Column Joints in Seismic Moment Resisting Frames, by Tsai, K.-C. and Popov, E.P., November 1988, (PB91 217 984/AS)A20. $39

UCB/EERC-88/18: Use of Energy as a Design Criterion in Earthquake-Resistant Design, by Uang, C.-M. and Bertero, V.V., November 1988, (PB91 210 906/AS)A04. $15

UCB/EERC-88/17: Earthquake Engineering Research at Berkeley - 1988, by EERC, November 1988, (PB91 210 864)A10. $26

UCB/EERC-88/16: Reinforced Concrete Flat Plates Under Lateral Load: An Experimental Study Including Biaxial Effects, by Pan, A. and Moehle, J.P., October 1988, (PB91 210 856)A13. $26

UCB/EERC-88/15: Dynamic Moduli and Damping Ratios for Cohesive Soils, by Sun, J.I., Golesorkhi, R. and Seed, H.B., August 1988, (PB91 210 922)A04. $15

UCB/EERC-88/14: An Experimental Study of the Behavior of Dual Steel Systems, by Whittaker, A.S., Uang, C.-M. and Bertero, V.V., September 1988, (PB91 212 712)A16. $33

UCB/EERC-88/13: Implications of Recorded Earthquake Ground Motions on Seismic Design of Building Structures, by Uang, C.-M. and Bertero, V.V., November 1988, (PB91 212 548)A06. $20

UCB/EERC-88/12: Nonlinear Analysis of Reinforced Concrete Frames Under Cyclic Load Reversals, by Filippou, F.C. and Issa, A., September 1988, (PB91 212 589)A07. $20

UCB/EERC-88/11: Liquefaction Potential of Sand Deposits Under Low Levels of Excitation, by Carter, D.P. and Seed, H.B., August 1988, (PB91 210 880)A15. $33

UCB/EERC-88/10: The Landslide at the Port of Nice on October 16, 1979, by Seed, H.B., Seed, R.B., Schlosser, F., Blondeau, F. and Juran, I., June 1988, (PB91 210 914)A05. $15

UCB/EERC-88/09: Alternatives to Standard Mode Superposition for Analysis of Non-Classically Damped

Systems, by Kusainov, A.A. and Clough, R.W., June 1988, (PB91 217 992/AS)A04. $15

UCB/EERC-88/08: Analysis of Near-Source Waves: Separation of Wave Types Using Strong Motion Array Recordings, by Darragh, R.B., June 1988, (PB91 212 621)A08. $20

UCB/EERC-88/07: Theoretical and Experimental Studies of Cylindrical Water Tanks in Base-Isolated Structures, by Chalhoub, M.S. and Kelly, J.M., April 1988, (PB91 217 976/AS)A05. $15

UCB/EERC-88/06: DRAIN-2DX User Guide, by Allahabadi, R. and Powell, G.H., March 1988, (PB91 212 530)A12. $26

UCB/EERC-88/05: Experimental Evaluation of Seismic Isolation of a Nine-Story Braced Steel Frame Subject to Uplift, by Griffith, M.C., Kelly, J.M. and Aiken, I.D., May 1988, (PB91 217 968/AS)A07. $20

UCB/EERC-88/04: Re-evaluation of the Slide in the Lower San Fernando Dam in the Earthquake of Feb. 9, 1971, by Seed, H.B., Seed, R.B., Harder, L.F. and Jong, H.-L., April 1988, (PB91 212 456/AS)A07. $20

UCB/EERC-88/03: Cyclic Behavior of Steel Double Angle Connections, by Astaneh-Asl, A. and Nader, M.N., January 1988, (PB91 210 872)A05. $15

UCB/EERC-88/02: Experimental Evaluation of Seismic Isolation of Medium-Rise Structures Subject to Uplift, by Griffith, M.C., Kelly, J.M., Coveney, V.A. and Koh, C.G., January 1988, (PB91 217 950/AS)A09. $20

UCB/EERC-88/01: Seismic Behavior of Concentrically Braced Steel Frames, by Khatib, I., Mahin, S.A. and Pister, K.S., January 1988, (PB91 210 898/AS)A11. $26

517